

AD-A091 078

AEROJET LIQUID ROCKET CO SACRAMENTO CA
LOW-THRUST BI-PROPELLANT ENGINE TECHNOLOGY. (U)
AUG 80 L SCHOENMAN, R L FRIEDMAN

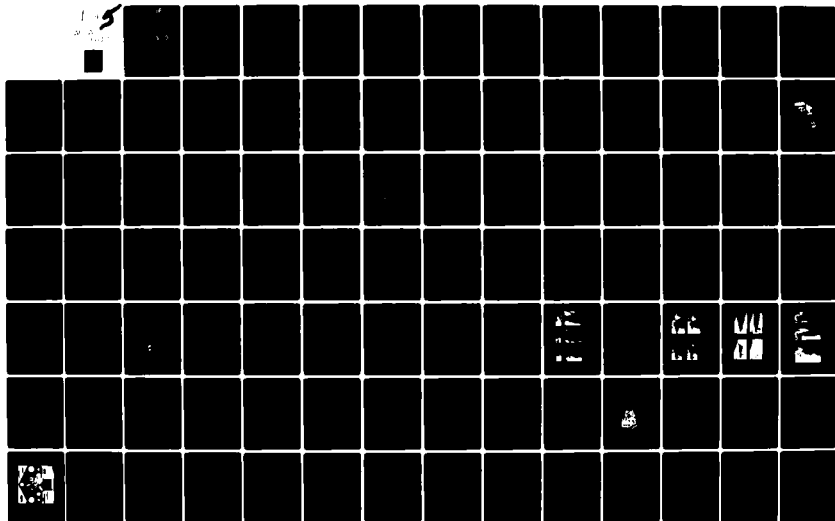
F/G 21/9.1

F04611-77-C-0053

UNCLASSIFIED

AFRPL-TR-80-47

NL





AFRPL-TR-80-47

LEVEL II

2

LOW-THRUST BI PROPELLANT ENGINE TECHNOLOGY

L. SCHOENMAN
R. L. FRIEDMAN

AEROJET LIQUID ROCKET COMPANY
SACRAMENTO, CALIFORNIA 95813

AUGUST 1980

DTIC
ELECTE
NOV 04 1980
S D
E

FINAL REPORT - SEPTEMBER 1977 - JULY 1980

APPROVED FOR PUBLIC RELEASE: DISTRIBUTION UNLIMITED

Prepared for:

AIR FORCE ROCKET PROPULSION LABORATORY
DIRECTOR OF SCIENCE AND TECHNOLOGY
AIR FORCE SYSTEMS COMMAND
EDWARDS AFB, CALIFORNIA 93523

AD A091078

DDC FILE COPY

80 10 27 126

NOTICES

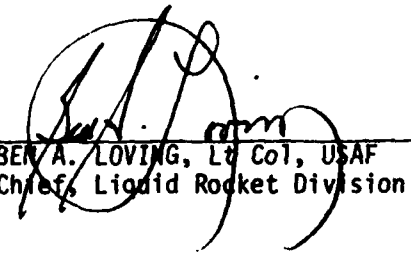
"When U.S. Government drawings, specifications, or other data are used for any purpose other than a definitely related government procurement operation, the government thereby incurs no responsibility nor any obligation whatsoever, and the fact that the government may have formulated, furnished, or in any way supplied the said drawings, specifications, or other data, is not to be regarded by implication or otherwise, or in any manner licensing the holder or any person or corporation, or conveying any rights or permission to manufacture, use or sell any patented invention that may in any way be related thereto."

This report was submitted by the Aerojet Liquid Rocket Company, P.O. Box 13222, Sacramento, California, 95813, under Contract NO. F04611-77-C-0053, Job Order Number 305811PT, with the Air Force Rocket Propulsion Laboratory, Edwards AFB CA 93523.

This report has been reviewed by the Information Office/TSP and is releasable to the National Technical Information Service (NTIS). At NTIS it will be available to the general public, including foreign nations. This technical report has been reviewed and is approved for publication; it is unclassified and suitable for general public release.


MELVIN V. ROGERS
Project Manager

FOR THE COMMANDER


BEN A. LOVING, Lt Col, USAF
Chief, Liquid Rocket Division


WALTER A. DETJEN
Chief, Satellite Propulsion Branch

UNCLASSIFIED

SECURITY CLASSIFICATION OF THIS PAGE (When Data Entered)

16 3058

(17) 11

REPORT DOCUMENTATION PAGE		READ INSTRUCTIONS BEFORE COMPLETING FORM
1. REPORT NUMBER AFRPL-TR-80-47	2. GOVT ACCESSION NO. AD-A091078	3. RECIPIENT'S CATALOG NUMBER
4. TITLE (and Subtitle) Low-Thrust Bipropellant Engine Technology.	5. TYPE OF REPORT & PERIOD COVERED Final Technical Report. September 1977-July 1980	6. PERFORMING ORG. REPORT NUMBER
7. AUTHOR(s) L. Schoenman R. L. Friedman	8. CONTRACT OR GRANT NUMBER(s) F04611-77-C-00537-1	
9. PERFORMING ORGANIZATION NAME AND ADDRESS Aerojet Liquid Rocket Company P.O. Box 13222 Sacramento, CA 95813	10. PROGRAM ELEMENT, PROJECT, TASK AREA & WORK UNIT NUMBERS P.E. 62302F Project 3058; Task 11 Work Unit AFRPL-305811PT	
11. CONTROLLING OFFICE NAME AND ADDRESS Air Force Rocket Propulsion Laboratory/- LKDM Edwards AFB, CA 93523	12. REPORT DATE August 1980	13. NUMBER OF PAGES
14. MONITORING AGENCY NAME & ADDRESS (if different from Controlling Office) (12) 428	15. SECURITY CLASS. (of this report) Unclassified	15a. DECLASSIFICATION DOWNGRADING SCHEDULE
16. DISTRIBUTION STATEMENT (of this Report) Approved for Public Release; Distribution Unlimited		
17. DISTRIBUTION STATEMENT (of the abstract entered in Block 20, if different from Report)		
18. SUPPLEMENTARY NOTES		
19. KEY WORDS (Continue on reverse side if necessary and identify by block number) Low-Thrust, 0.5 lbF, MIB, Platelet Injectors, N2O4/MMH, MON-X Oxidizers, High Performance, Bipropellant		
20. ABSTRACT (Continue on reverse side if necessary and identify by block number) The design, fabrication and hotfire test of a low-thrust, 0.5 lbF class bipropellant rocket engine, capable of providing very small, precisely repeatable impulse bits and long, high-performance, steady-state burns, was undertaken in a three-phase program. Phase I, Analysis and Design, consisted of detailed studies and tradeoff analyses of general mission/system requirements versus engine assembly parametrics and the development of the overall design approach. Phase II, Design Verification, consisted of		

DD FORM 1473 1 JAN 73 EDITION OF 1 NOV 65 IS OBSOLETE

UNCLASSIFIED

SECURITY CLASSIFICATION OF THIS PAGE (When Data Entered)

405880

UNCLASSIFIED

SECURITY CLASSIFICATION OF THIS PAGE(When Data Entered)

→ component (valve, injector and chamber) fabrication and development testing for the demonstration point design. Phase III, Demonstration, consisted of engine fabrication and demonstration of the point design.

While a 100% achievement of all contract goals was elusive within the resources provided, significant advancements in small engine technology were made that prove the feasibility of developing a 0.5 lbF class bipropellant engine.

Steady-state durability of 8 hours of firing without failure has been demonstrated, along with a small impulse bit of $20.005 \pm .0005$ lbF sec. It is reasonable to predict that the same engine that ran 8 hours steady-state will be able to accomplish the 10 hour life goal based on its excellent postfire condition. ←

The pulsing duty cycle limitations encountered early in the 10^6 pulse durability test of the Phase III engine may, in fact, have been artificially created by the selection of a duty cycle that is much more rigorous than would be required in actual use. Further testing is required to define the cause of hard engine starts which lead to gradual enlargement of the oxidizer orifice of this engine.

An engine performance (Isp) of 275 and 265 sec has been demonstrated in Phase II and III, respectively, of the program. These are lower than the program goal of 280 sec. Since the maximum chamber temperatures were 500°F less than allowable, further development could improve secondary mixing within the combustion chamber and raise performance. Improved secondary mixing might also attenuate the hard pulsing starts which could be caused by an accumulation of uncombusted propellant on the cold chamber wall.

Valve response, repeatability, life, engine minimum impulse bit requirements, and pulse repeatability were demonstrated on all configurations hot-fire tested.

All aspects of engine fabrication, i.e., platelets valves, chambers and metallurgical columbium-stainless steel assembly techniques, have been proven. Reproducibility of injectors and valves has been satisfactorily demonstrated to a degree commensurate with potential production requirements for these engines. The integration of the valve and injector, with the resultant low dribble volume required for the minimum plume contamination, has also been demonstrated. The selection valve and injector internal filtration system has been 100% successful in preventing clogging, flow decay, or other phenomena which could cause thrust reductions or mixture ratio shifts.

B
UNCLASSIFIED

SECURITY CLASSIFICATION OF THIS PAGE(When Data Entered)

TABLE OF CONTENTS

	<u>Page</u>
1.0 Introduction	1
1.1 Background	1
1.2 Objective	5
1.3 Technical Effort Organization	5
1.4 Report Organization	6
2.0 Program Accomplishments	7
2.1 Engine Design and Operating Characteristics	7
2.2 Improved Measurement Capabilities in Pulsing	10
2.3 Durability Testing Results	10
3.0 Flight Engine Design	11
4.0 Phase I - Analysis and Design	14
4.1 Industry Requirements	14
4.2 System-Mission-Engine Interactions and Oxidizer Blend Selections	17
4.2.1 Oxidizer Blends	17
4.2.2 Tank Blowdown Effects	17
4.2.3 Oxidizer Blends Versus Engine Performance	25
4.3 Engine Parameter Study	25
4.3.1 Chamber Pressure Optimization	25
4.3.2 Injector Design	33
4.3.3 Thrust Chamber Design	51
4.3.4 Valves	56
4.3.5 CONTAM Analyses	66
4.3.6 Thermal Design	84
4.4 Phase I - Conclusions and Recommendations	92
5.0 Phase II - Design, Fabrication, and Verification Testing	94
5.1 Engine Design and Fabrication	94
5.1.1 Valve Fabrication and Bench-Testing	94
5.1.2 Injector Fabrication and Flow Testing	101
5.1.3 Thrust Chamber Design and Fabrication	114

TABLE OF CONTENTS (cont.)

	<u>Page</u>
5.2 Hot-Fire Testing	115
5.2.1 Test Objectives	115
5.2.2 Test Specification and Goals	115
5.2.3 Test Hardware	121
5.2.4 Test Facility	122
5.2.5 Measurement and Data Processing	133
5.2.6 Phase II Test Program	137
5.3 Data Evaluation	148
5.3.1 Steady-State Performance	148
5.3.2 Pulse Repeatability	157
5.3.3 Pulse Performance	166
5.3.4 Steady-State Thermal Operation	173
5.3.5 Pulsing Thermal Characteristics	188
5.3.6 Blowdown and Stability	192
5.4 Phase II Conclusions	198
5.5 Phase II Recommendations	200
6.0 Phase III - Engine Demonstration	202
6.1 Special Hot Test Activities	204
6.2 Design Update	212
6.2.1 Detailed Thermal Update Analysis	212
6.2.2 Detailed Design	215
6.3 Engine Fabrication	227
6.3.1 Valves	227
6.3.2 Injector Fabrication	227
6.3.3 Chamber Fabrication	231
6.3.4 Chamber and Engine Assembly	231
6.4 Phase III - Demonstration Testing	234
6.4.1 Test Instrumentation and Facility Modifications	234
6.4.2 Phase III Demonstration Testing of Engines	237

TABLE OF CONTENTS (cont.)

	<u>Page</u>
6.4.3 Durability Test Results	248
6.5 Test Data Evaluation	249
6.5.1 Engine Response	249
6.5.2 Pulse Repeatability	257
6.5.3 Engine Specific Impulse	272
6.5.4 Thermal Data Evaluation	281
7.0 Test 512 Data Evaluation	292
7.1 Test Objectives	292
7.2 Test Results	292
7.3 Test Data Evaluation	292
7.4 Test Data Interpretation	296
7.5 Conclusions	297
8.0 Program Conclusions and Recommendations	299
8.1 Conclusions	299
8.2 Recommendations	300
<u>Appendices</u>	
A Industry Requirements Survey	A-1
B Supporting Valve Cycle Life Analysis	B-1
C Injector Dimensional and Flow Data	C-1
D Phase III Valve Acceptance Test Data, MOOG Model 51E112, SN 004 and 005	D-1
E Phase III Steady-State Durability Test Data	E-1
F Phase III Pulse Data, Tests 698-512-1 Through -11, Impulse Bit and Repeatability	F-1
G Phase III Pulsing Thermal Data	G-1

Accession For	
NTIS GRA&I	<input checked="" type="checkbox"/>
DDC TAB	<input type="checkbox"/>
Unannounced	<input type="checkbox"/>
Justification	
By _____	
Distribution/ _____	
Availability Codes	
Dist	Avail and/or special
A	

LIST OF TABLES

<u>Table No.</u>		<u>Page</u>
1-I	General Assembly Design Goals Contract F04611-77-C-0053	4
2-I	Program Accomplishments	9
3-I	Flight Design Characteristics	13
4-I	Small Thruster Key Issues	15
4-II	Contract Goal versus System Requirements	16
4-III	Low-Thrust Rocket Engine Survey	52
4-IV	CONTAM Model Case Variables	70
4-V	CONTAM Model Case Results	71
4-VI	Injector Heat Balance and Temperature Summary	90
5-I	Response Mapping of 177 Ohm Bench-Test Valve	98
5-II	Life Cycle Test Results of 51E112 Prototype Valve	100
5-III	SN 1 to 9 Coaxial Swirler Cold Flow Data	108
5-IV	"V" Doublet Swirler Injector Cold Flow Data	109
5-V	Splash Plate Injector Cold Flow Data	110
5-VI	Multiple Mode Propellant Delivery System Characteristics	132
5-VII	Phase II Instrumentation	134
5-VIII	Typical Pulse Performance Data Computer Output	136
5-IX	Phase II Injector Fabrication and Test Results	139
5-X	Pulse Duty Cycle Definition	141
5-XI	Phase II Block I Testing, 1-CAS SN 9 Injector, Flanged Chamber	142
5-XII	Phase II Block I Testing, 3-SPA Injector, Flanged Chamber	143
5-XIII	Phase II Block II Testing, 1-CAS Injector, SN 9 Welded Chamber and SN 10A Flanged Chamber	144
5-XIV	Phase II Testing with MON 10 Oxidizer	146
5-XV	Additional Phase II Testing with Modified 1-CAS Injector (10 AM = 10B)	147
6-I	Steady-State Performance Summary, 1-CAS SN 10A MOD C Injector 2 in. L' Steel Chamber	208
6-II	Time/Temperature Table (°F) -Short Sleeve	217

LIST OF TABLES (cont.)

<u>Table No.</u>		<u>Page</u>
6-III	1-CAS Injector Flow History	228
6-IV	1-CAS Injector Flow History	230
6-V	Phase III Engine Instrumentation	236
6-VI	Test Fixture History	239
6-VII	Phase III Test History, Engine SN 21	241
6-VIII	Phase III, Block I Duty Cycle	243
6-IX	Phase III Test History, Engine SN 22	245
6-X	Phase III, 5 Pulse Impulse Bit Average and Temperature Summary	258
6-XI	Engine 22 Thermal Data	283
6-XII	Postfire Heat Soak Following Test 528, Full-Thrust Insulated Chamber	287
6-XIII	Postfire Heat Soak at Various Operating Conditions	289

LIST OF FIGURES

<u>Figure No.</u>		<u>Page</u>
2-1	ALRC 0.5 lbF Bipropellant Engine - Phase III Configuration	8
3-1	0.5 lb Thruster Engine Envelope for 143:1 Area Ratio Chamber	12
4-1	MON - Oxidizer Freezing Temperature, Vapor Pressure and Engine Blowdown Capability versus NO Content	18
4-2	Tank Pressure vs Temperature for Various MON Oxidizers	19
4-3	MON-1 vs MON-10 MR Shifts at Off Nominal Temperatures for Various Ullages	20
4-4	Higher MON Oxidizers and MR Shift Variations During Blowdown	22
4-5	Propellant Tank Level vs Tank Pressure for Various MON Oxidizer Ullage Selections	23
4-6	Minimum and Maximum Propellant Temperatures versus NO %	24
4-7	Theoretical Specific Impulse for Various MON Oxidizers	26
4-8	Theoretical Specific Impulse versus Engine Mixture Ratio	27
4-9	Performance Improvement vs Chamber Pressure	28
4-10	Initial Chamber Pressure Selection vs Tank Blowdown Ratio	30
4-11	Engine Chug Stability versus Blowdown	31
4-12	Low Propellant Inlet Temperature and Low Chamber Pressure vs Ignition Delay Time	32
4-13	Area Ratios vs Isp	34
4-14	Perfect Injector Specific Impulse versus Mixture Ratio and Area Ratio	35
4-15	Injection Element Design Objective	37
4-16	Cold Flow of Loose Superscale (10 x Geometric) Platelets	39
4-17	Three Element Splash Plate Injector Design	40
4-18	Fuel Swirler Three Element "V" Doublet Oxidizer Injector Design	41

LIST OF FIGURES (cont.)

<u>Figure No.</u>		<u>Page</u>
4-19	Coaxial Swirler Injector Design	42
4-20	Symmetrically-Cooled versus Bias-Cooled Splash Plate	43
4-21	Splash Plate Modifications for Optimum Spray Distribution	44
4-22	Modifications to "V" Doublet to Eliminate Oxidizer Penetration	45
4-23	Initial Vortex Designs at Reduced Flowrate	46
4-24	Modifications to Vortex Designs	47
4-25	Modified Splash Plate Distribution	48
4-26	Modified Vortex "V" Doublet Spray Distribution	49
4-27	The Coaxial Injector; Oxidizer-Rich Core and Fuel-Rich Barrier	50
4-28	JANNAF BLIMP Model - Engine Boundary Layer Performance Efficiency Prediction Compared to Other Models and Experimental Data	53
4-29	Nozzle Contour versus Boundary Layer Thickness	54
4-30	Modified CONTAM Quenching Prediction	55
4-31	Combustion Gas Velocity vs Propellant Injection Velocity	57
4-32	Injection Element Density versus Injector Face Operating Temperature	58
4-33	Chamber Contour vs Head End Heat Flux	59
4-34	MOOG Bipropellant Torque Motor Valve	61
4-35	Torque Motor Cross Section and Functional Parts	63
4-36	Integrated Valve/Injector Seals Configuration	64
4-37	Photo-Etched Valve Seats are Part of the Injector	65
4-38	Valve/Injector Interface Bolt Pattern	67
4-39	Chamber Length vs Performance and Contaminant Fraction	72
4-40	Computer Plots of CONTAM Transient Responses (Variable Propellant Inlet Temperatures)	73
4-41	CONTAM Modeling of Warm Propellant Ignition Characteristics in Small Bipropellant Engines	74
4-42	Dribble Volumes vs Firing Rates for Hot or Cold Engines (Unlimited Duty Cycle)	75

LIST OF FIGURES (cont.)

<u>Figure No.</u>		<u>Page</u>
4-43	Computer Plots of CONTAM Transient Responses (Variable Pulse Width)	76
4-44	CONTAM Model Predicts Pulse Performance Goals	77
4-45	Dribble Volumes vs Response, Pulse Performance, and Plume Contaminants	78
4-46	Computer Plots of CONTAM Transient Responses (Variable Tank Blowdown Pressures)	79
4-47	Performance vs Propellant Temperature (MON-1) Over a 5:1 Blowdown Ratio	80
4-48	CONTAM Performance Predictions in a Blowdown Mode	81
4-49	MON Content vs Pulsing Performance and Engine Blowdown Capability	82
4-50	Oxidizer Manifold Fill Time vs Total Impulse Repeatability for Increased Oxidizer MON Content at Lower Tank Pressures	83
4-51	Estimated Thermal Cycle Life of Columbian Stainless Steel Joint	85
4-52	Chamber Thermal Model NODAL Network	87
4-53	Injector-Chamber Adapter Employed in Thermal Analysis	88
4-54	Injector NODAL Network	88
4-55	Chamber Wall Thickness vs Heat Soak and Operating Temperature	91
5-1	Torque Motor Valve Model 51E112 Assembly and Interface Drawing	95
5-2	Opening Response Time of 177 Ohm Bench-Test Valve at 28 Volts	97
5-3	Repeatability of Three Valves and Sensitivity to Line Pressure and Voltage	99
5-4	Phase II Injector Screening and Verification Testing	102
5-5	Photo-Etched Injector Fabrication Arrays	103
5-6	Three-Element "V" Doublet-Swirler Injector V-VDS	104
5-7	Coaxial Swirler Injector (1-CAS)	105
5-8	Backside of Typical Photo-Etched Injector Containing Integral Valve Seats and Seal Glands	106

LIST OF FIGURES (cont.)

<u>Figure No.</u>		<u>Page</u>
5-9	Coaxial Swirler Injector Kw-dimensional Sensitivity	111
5-10	Coaxial Swirler Kw- ΔP Sensitivity for 3 Injectors	112
5-11	"V" Doublet Swirler Kw- ΔP Sensitivity for 3 Injectors	113
5-12	Phase II Chamber Design and Dimensions	116
5-13	Phase II Flanged Chamber Configuration	117
5-14	Phase II Columbiu Chamber Photographs Before Coating	118
5-15	Phase II Engine Assemblies with 1 inch and 2 inch Chamber L's	119
5-16	Comparison of Goals and Phase II Accomplishments	120
5-17	Phase II Thrust Stand with the 0.5 lb Thrust Engine in Place	124
5-18	0.5 lb Thrust Test Stand Load Paths	126
5-19	Dual-Tuned Thrust Measurement System Calibration Test Results	127
5-20	Multiple Mode Propellant Delivery System	129
5-21	Micro-PDFM Electro-Optical Flow Measurement	131
5-22	Thermal Instrumentation, Flanged Engine Assembly	135
5-23	Phase II Test Activities Logic Chart	138
5-24	Thrust and Chamber Pressure Measurements	149
5-25	Steady-State Performance, 3-SPA Injector with 1" L' Chamber	150
5-26	Steady-State Performance, 3-SPA Injector with 2" L' Chamber	151
5-27	Steady-State Performance, 1-CAS Injector Series with 2" L' Chamber	152
5-28	Phase II Injectors, Performance Comparison	153
5-29	Experimental C_f Data	154
5-30	Comparison of C_f Data and BLIMP Model Predictions	156
5-31	1-CAS Injector Thrust Pulse Traces	158
5-32	Repeatable Electrical Pulses of 0.005 Sec and Impulse Bits of 0.0015 lbF-Sec	160
5-33	1-CAS Injector 0.010 Sec EPW Impulse Bits and Repeatability	161
5-34	Impulse Bit Repeatability, CAS SN 10A	162

LIST OF FIGURES (cont.)

<u>Figure No.</u>		<u>Page</u>
5-35	Environmental Temperature and Oxidizer NO Content vs Delivered Impulse Bits	163
5-36	Impulse Bit versus EPW as a Function of Tank Pressure and Oxidizer NO Content	164
5-37	Impulse Bit versus EPW	165
5-38	Chamber Wall Temperature vs Pulse Performance (EPW = 0.1 sec)	167
5-39	Chamber Wall Temperature vs Pulse Performance (EPW = 0.05, .010 and .030 sec)	168
5-40	1-CAS Injector, Cold Chamber Pulse Performance	169
5-41	1-CAS Injector, Hot Chamber Pulse Performance Estimation	170
5-42	3-SPA Injector Pulse Performance L' = 2.0" Cold Chamber	171
5-43	3-SPA Injector Pulse Performance L' = 2.0" Hot Chamber	172
5-44	3-Element Splash Plate and Coaxial Swirler Injector Pulse Predictions	174
5-45	Pulse Performance vs CONTAM Model Predictions	175
5-46	Thermal Management for Steady State Capability and Pulsing	176
5-47	Steady-State Thermal Response Test 118	177
5-48	Chamber Thermal Profiles, 3-SPA Injector End	178
5-49	Comparison of Thermal Transients of Coaxial Injector SN 9 and 10A with Flanged and Welded Chambers	180
5-50	Postfire Heat Soak on Flanged and Welded Chamber Configurations	181
5-51	Shorter Wide Angle Premix Cup Length vs Chamber Head End Temperature	182
5-52	Thermal Steady-State at .37 lb Thrust	183
5-53	Postfire Heat Soak After Steady-State Burn	184
5-54	Thermal Steady-State Temperatures with 1-CAS Mod B Injector at 65 PSIA, 0.25 lb Thrust	185
5-55	Steady-State Thermal Conditions at .37 lb Thrust	186
5-56	Steady-State Chamber Temperature Axial Profiles as a Function of Chamber Pressure	187

LIST OF FIGURES (cont.)

<u>Figure No.</u>		<u>Page</u>
5-57	Phase III Options to Resolving the Hot Joint Limitations in Long Duration Burns	189
5-58	Pulsing Thermal Transients, "B" Duty Cycle	190
5-59	Pulsing Thermal Transients Following a Long Burn	191
5-60	The 1-CAS Injector Configuration MOD B Blowdown Capability	193
5-61	1-CAS SN 9 Injector Engine Start and Shutdown Transients at Maximum Thrust	194
5-62	1-CAS SN 9 Injector Engine Transients at 30% Thrust	195
5-63	Comparison of Combustion Roughness for Injectors Tested in Phase II	196
5-64	Injector 1-CAS MOD B Dynamic Thrust Trances at 0.49 and 0.17 lb Thrust	197
6-1	1-CAS 10A MOD C Injector Configuration	205
6-2	Stainless Steel Heat Transfer Chamber Design	206
6-3	Stainless Steel Heat Transfer Chamber	207
6-4	Performance of 1-CAS MOD A, B, & C Injector	209
6-5	Shorter Premix Cup vs Chamber Head End Temperature	210
6-6	1-CAS Injector, 2" L', Thrust versus Chamber Pressure	211
6-7	Thermal Map, Modified Chamber Head End Design	213
6-8	Thermal Model Input	214
6-9	Phase III Chamber NODAL Network	216
6-10	Predicted Temperature vs Time Heat Soakback	219
6-11	Phase III Engine	220
6-12	Phase III 1-CAS Injector	223
6-13	Phase III Combustion Chamber	232
6-14	Phase III Engine	233
6-15	Phase III Test Instrumentation Locations	235
6-16	0.5 lbF Test Fixture Adapted for 0.5 lbF Phase III Testing	238
6-17	0.5 lbF Engine, Typical Pulse	250
6-18	Engine Pulse, EPW = .120 Sec	252

LIST OF FIGURES (cont.)

<u>Figure No.</u>		<u>Page</u>
6-19	Engine Pulse, EPW = .030 Sec, Pulse #1	253
6-20	Engine Pulse, EPW = .030 Sec, Pulse #2	254
6-21	Engine Pulse, EPW = .100 Sec	255
6-22	Test 512, Pulse Data Composite	262
6-23	I-Bit versus EPW, First 3 Groups of 5	264
6-24	I-Bit versus EPW, Continuous Pulsing	265
6-25	I-Bit Versus EPW, First 3 Groups of 5	266
6-26	Bit Impulse Repeatability of .60 Sec EPW	267
6-27	Bit Impulse Repeatability of 0.30 Sec EPW	268
6-28	Test Data for .010 Sec EPW - First 15 Pulses	269
6-29	Impulse Bit Repeatability	270
6-30	Effect of Coast Time on Impulse Bit	271
6-31	Specific Impulse versus Firing Time Engine SN 22	273
6-32	Vacuum Thrust versus Steady-State Isp	274
6-33	Vacuum Thrust versus Isp and C*	276
6-34	Engine SN 22 MR Sensitivity	277
6-35	Nozzle C_f Correlation	278
6-36	Chamber Contour Changes to Improve Mixing	280
6-37	Axial Temperature Profile, Engine SN 21	282
6-38	Axial Temperature Profile, Engine SN 22	284
6-39	Wall Temperatures versus P_c , Engines SN 2 and SN 33	285
6-40	Temperatures versus Pulse Number	290
7-1	Test No. 512 Thrust Traces from Various Pulses of Each Group	293

GLOSSARY

ACS	Attitude Control System
AFRPL	Air Force Rocket Propulsion Laboratory
BLIMP	A Computer Program Title for Boundary Layer
BLL	Boundary Layer Loss
BPV	Bipropellant Valve
C*	Characteristic Exhaust Velocity ft/sec
CAS	Coaxial Swirler Injector
Cb-SS	Columbium - Stainless Steel
C_F	Thrust Coefficient
CONTAM	A Computer Program Title for Performance and Plume
EB	Electron Beam
E	Nozzle Expansion Ratio
EC	Nozzle Contraction Area Ratio
EDM	Electrical Discharge Machining
EPW	Electrical Pulse Width
EP	Electrical Pulse
FFC	Fuel Film Cooling
FS	Fire Switch
HEATLQ	Liquid Film Cooling Model
Isp	Specific Impulse Performance
JANNAF	Joint Army Navy NASA Air Force
Kw	Flow Coefficient
Lbm	Pounds Mass
MIB	Minimum Impulse Bit
MMH	Monomethylhydrazine
MMIII PSRE	Minuteman III Propulsion System Rocket Engine
MON-X	Propellant Blend N_2O_4 + NO (% By Weight)
MR	Mixture Ratio = O/F Ratio By Weight
ms (msec)	Millisecond
NO	Nitric Oxide (additive to N_2O_4)
NDT	Non-Destructive Testing
OD	Outside Diameter

GLOSSARY (cont.)

ODE	One Dimensional Equilibrium
ODK	One Dimensional Kinetics
Pc	Thrust Chamber Pressure
PDFM	Positive Displacement Flow Meter
PPS/PPM	Pulses per Second/Minute
psid	Pounds per Square Inch Differential ΔP
RCS	Reaction Control System
ROM	Rough Order of Magnitude
SINDA	A Computer Program Title for Heat Transfer
3-SPA	3-Element Splash Plate Injector Model A
Tg	Gas Temperature
TJB	Injector Backside Temperature
TL	Stainless Steel Structural Support Temperature
TPC	Pressure Tap Boss Temperature
TS	Stainless Steel Thermal Standoff Temperature
TT	Throat Temperature
TVB	Valve Body Temperature
T Weld	Bimetallic Interface Temperature
VDS	V-Doublet Swirler Injector

SECTION I

INTRODUCTION

1.0 INTRODUCTION

1.1 BACKGROUND

Prior to 1963, few spacecraft missions required the injection of a payload into orbit. Furthermore, there was little need or room for an on-board propulsion system as part of the orbiting package. However, as mission goals became more ambitious, and in view of increased payload weights during the period from 1963 to 1968, the necessity of developing station-keeping systems became apparent. Reaction control systems employing catalytic decomposition of hydrogen peroxide and/or cold gas jets were utilized, but the instability of the hydrogen peroxide under storage, along with the need for pressure relief valves, made the reliability of the peroxide systems inherently low. Cold gas systems, although much more reliable, provided very low performance.

Monopropellant reaction control systems utilizing hydrazine were evaluated for station-keeping missions starting in 1967. By 1973, such systems had performed well in a wide range of applications and enjoyed an undisputed industry acceptance.

In general, the systems of the 70's employed solid kick stages or on-board solid motors for high-thrust functions, such as initial orbit insertion. Monopropellant hydrazine systems of various thrust level combinations ranging from approximately 300 down to 0.1 lbf provided for the remaining control functions.

In contrast, systems of the 80's, designed for space shuttle launch and low orbit deployment, dictate larger payload diameters and reduced overall lengths. The net effect is that high-thrust solid motors do not package as efficiently as lower thrust (100 to 1000 lbf) bipropellant ΔV type engine systems which deliver the required high total impulse via multi-hour burns. Furthermore, integration of a bipropellant ΔV and RCS propellant system provides further weight savings and propellant utilization advantages.

In addition, current and future demands being identified for propulsion in military space applications are rapidly approaching the limits of monopropellant hydrazine propulsion. Wide-ranging propulsion demands result from missions requiring orbit insertion, injection error correction, orbit maintenance, momentum wheel unloading, orbit adjust, orbit change, etc.

1.1, Background (cont.)

Mission functions have become more ambitious due to new demands made on position accuracy, mission duration, on-station maneuvering capability, and volume constraints. Under these circumstances, the capabilities of monopropellant hydrazine systems are approached or exceeded, while the flexibility, improved performance, and lower system weight of fully integrated storable bipropellant systems become advantageous.

Other potential advantages of a bipropellant RCS compared to monopropellant units include

- ° Longer life and nearly unlimited thermal cycling, with performance loss and attendant monopropellant catalyst bed degradation entirely eliminated;
- ° Higher pulse mode performance, with particular performance advantages obtained during cold starts;
- ° More predictable response and lower power consumption, resulting from an ability to operate without catalyst bed heaters;
- ° Lower propellant freezing temperatures; and
- ° Improved handling and reliability, resulting from the ability to clean and flush a fully integrated spacecraft control system after ground checkout without fear of catalyst bed contamination or damage.

Storable bipropellant propulsion systems have been used extensively for more than 20 years in high-thrust applications. However, the technology required for highly reliable, long-life, high-performance pulsing engines in the 0.5 to 100 lb thrust range has been put into place only recently.

The development and demonstration of the required technology for low-thrust bipropellant engines was initiated by ALRC in 1973 under AFRPL Contract F04611-73-C-0061. This initial work produced a high-performance, clean-burning 5 lb thrust class engine, capable of both pulse mode and steady-state operation.

1.1, Background (cont.)

The award of Contract F04611-77-C-0053 to ALRC in 1977 provided for the extension of the storable bipropellant technology to engines in the 0.5 lb thrust classification. A successful demonstration of this device would complete the engine technology required for a fully integrated bipropellant satellite propulsion system. The general design goals for this program are defined in Table 1-I.

The key technical challenges of this program resulted from the relatively minute sizing of the hardware (in particular, the injector manifold and elements) and the multiplicity of requirements as displayed in Table 1-I. Secondly, the complexity of test measurements of pulsed flow and impulse bit for the very low level parameters of an engine of this size presented new challenges.

Those areas which have historically proved troublesome to small engines were addressed in the new technology work accomplished on this program. They included:

- ° Poor combustion efficiency and performance due to very low propellant flowrates and a limited number of injection elements;
- ° Failure to achieve uniform and axisymmetric propellant combustion free from wall-damaging hot streaks;
- ° Inadequate nozzle cooling and unacceptable coast period heat soaks over a wide range of duty cycles;
- ° A relatively high volume of residual propellants within the injector, degrading performance, aggravating ignition spike problems, and increasing plume contamination levels; and
- ° Exhaust plume contamination resulting from ejection of propellant droplets due to incomplete combustion.
- ° Fabricability of small components; i.e., injector passages, orifices, etc.

GENERAL ASSEMBLY DESIGN GOALS CONTRACT F04611-77-C-0053

4

1.0, Introduction (cont.)

1.2 OBJECTIVE

The objective of this program was to develop and demonstrate the technology required for a high-performance, long-lived, fast-response 0.5 lb thrust class bipropellant engine capability for future Air Force requirements. The propellants to be employed in the demonstration were nitrogen tetroxide (N_2O_4) and monomethylhydrazine (MMH). The ability to operate at reduced propellant temperatures with MON oxidizer blends was to be determined.

Table 1-I indicates the design goals established for this program. Most noteworthy are the two-hour steady-state burn, 280 sec steady-state specific impulse, impulse bits of less than .005 lb-sec, the 4:1 tank pressure ratio for a blowdown system, the 20 to 120°F range of propellant supply temperatures, and the general life (750,000 pulses) and reliability requirements.

1.3 TECHNICAL EFFORT ORGANIZATION

The program structured for this technology development and demonstration consisted of three phases: Phase I - Requirements Definition and Engine Design Analysis; Phase II - Design and Verification Testing; and Phase III - Demonstration Testing. The scope of each phase was as follows.

Phase I conducted studies and tradeoff analyses of general mission/system requirements versus engine parameters. Typical representative mission duty cycles were identified by literature search, review of current specifications, and consultation with spacecraft manufacturers, users, and selected government agencies.

Phase II developed point designs against the selected mission requirements based upon the relationships established in Phase I. Design verification hot-fire testing, using the N_2O_4 /MMH and MON-10/MMH propellant combinations, was conducted to provide supportive data. Three injector designs and several thermal management systems were evaluated. The best of these approaches became the basis for the design of demonstration test engines for use in Phase III.

Phase III consisted of finalizing the selected engine designs and the fabrication and demonstration hot-fire testing of two engines. Testing was accomplished under simulated altitude conditions with 143:1 geometric area ratio nozzles.

1.0, Introduction (cont.)

1.4 REPORT ORGANIZATION

This final report consists of three parts. The first, Introduction, provides a background to the program, along with a description of the program's objectives and structure. This is followed by a summation of the program's accomplishments and a description of flight engine designs based on the units tested.

The second part, Experimental Results and Discussions, is a chronological exposition of the program's three phases.

The final section, Conclusions and Recommendations, summarizes the technology improvements and collorary information resulting from the review of the program's data. The recommendations describe the manner in which this data should be utilized: either to further develop small thruster technology or to facilitate the application of the technology to current and/or anticipated spacecraft needs.

SECTION 2.0

PROGRAM ACCOMPLISHMENTS

2.0 PROGRAM ACCOMPLISHMENTS

2.1 ENGINE DESIGN AND OPERATING CHARACTERISTICS

The engine developed during this program is shown in Figure 2-1. The combined requirements of long duration (>2 hours), short pulses (10 ms) with an MIB of 0.005 lb-sec, and relatively high performance (280 sec steady-state, 220 sec pulsing) have not yet been collectively achieved, but should be obtainable with further development activities. Those goals that were attained are indicated in Table 2-I.

This program demonstrated that precisely controlled injector manifolds and orifices can be fabricated from photo-etched platelets. The injectors were thin and had the valve seats etched into their back surface, providing an integrated valve and injector with low dribble volume. This, in turn, assures pulse-to-pulse repeatability and minimum plume contamination due to unburned, post-pulse residual propellant. The entire engine assembly has been made with metallurgical joints, thereby avoiding hot gas seals.

The bipropellant torque motor valve, supplied by MOOG, Inc., has been well demonstrated by 10^6 bench-test cycles and a multitude of hot-fire tests. Opening and closing times at all conditions (24-32 vdc and 0-400 psia inlet) have been faster than the minimum response time goals. Repeatability has also been demonstrated for bench-test and hot-fire test valves. Response and hydraulic repeatability has been demonstrated on the two Phase III valves tested.

Engine thermal management has been defined by thermocouple measurements during hot test firing. Maximum chamber temperatures were less than 2100°F with an insulated chamber. The valve and injector remained under 300°F during duration tests as long as 5 hours in Phase III testing, and post-fire heat soak was acceptable. Engine pulse repeatability and MIB were demonstrated with impulse measurements of ≈ 0.0026 lbF-sec (± 0.0003 lbF-sec) obtained during a .010 sec EPW burn.

In Phase II, engine blowdown capability of 5:1 was demonstrated with stable engine operation to 80 psia inlet pressure. The engine proved to be relatively insensitive to propellant inlet temperatures or high (Mon 10) NO content in the oxidizer. Unfortunately, minor injector design changes, required to improve the head end thermal margin for the Phase III design,

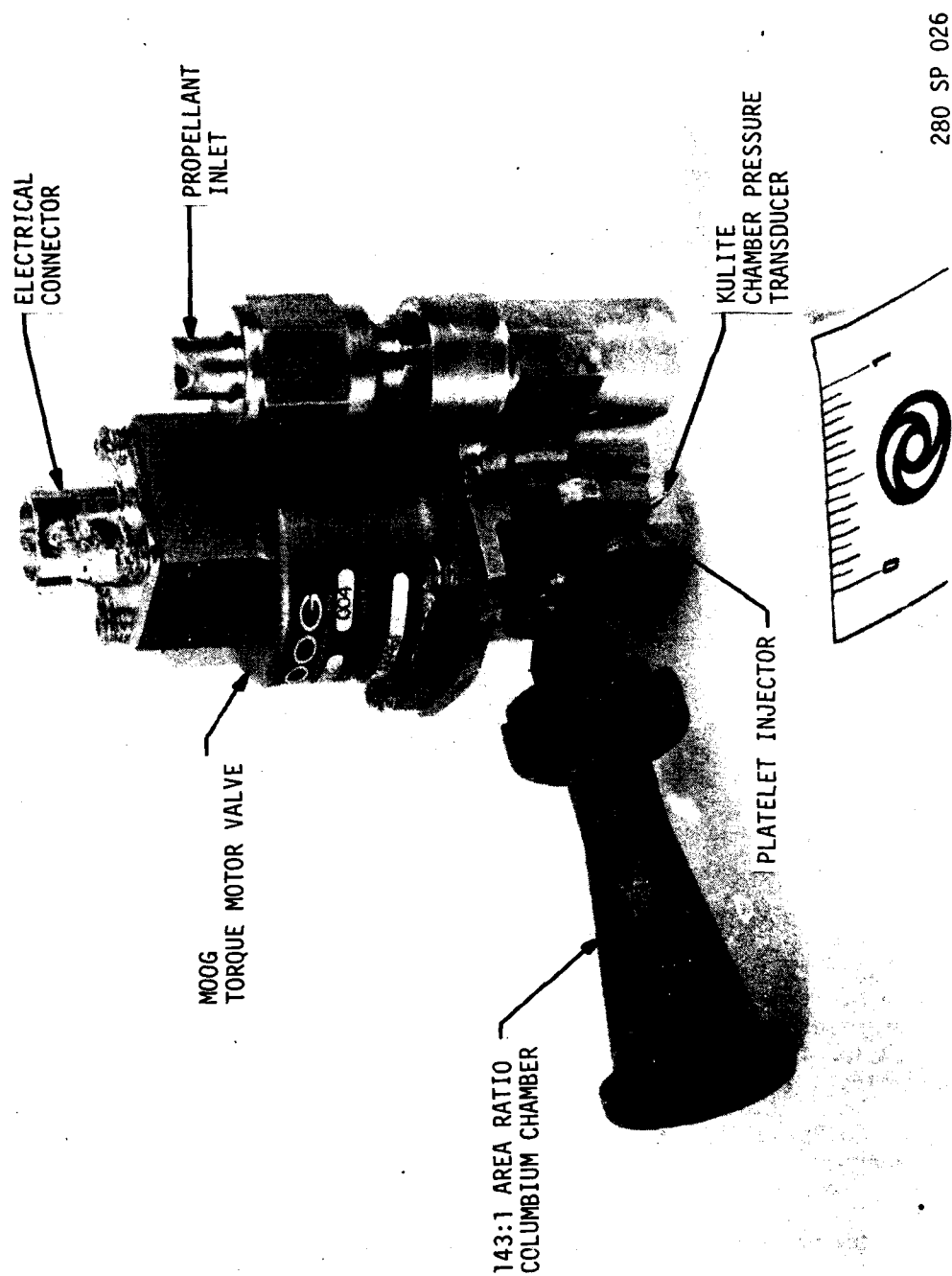


Figure 2-1. ALRC 0.5 lbF Bipropellant Engine - Phase III Configuration

TABLE 2-I

PROGRAM ACCOMPLISHMENTS

PARAMETER	GOAL	PHASE II	PHASE III
Nominal Vacuum Full Thrust	0.5 lbf	0.17 to 0.49	0.2 to .52
Chamber Pressure	Not Evaluated	40 to 125 psia	50 to 135 psia
Maximum Feed System Pressure	400 psia	420	450
Minimum Feed System Pressure	Not Evaluated	108 psia (Not Lower Limit)	200 psia
Expansion Ratio		143.1 Geometric	Same
Nominal Isp (at Full Thrust)			
Steady-state	280 sec	275	265
Pulsing (10 ms)	220 sec	180 (Cold Engine)	Not Evaluated
Nominal Minimum Impulse Bit (at Full Thrust)	0.005 lb-sec + 0.0005 lb-sec	0.002 + 5% 1 Sigma	.004 + 0.0005
Number of Maximum Thermal Cycles	>1000	Not Evaluated	Not Evaluated
Total Number of Starts	>750,000	1,000,000 Valve Only Bench Test H ₂ O	2500
Single Burn Duration	>2 hr	260 sec at .38 lb Thrust	5.5 hrs
Total Firing Life	>10 hr	Not Evaluated	Not Evaluated
Valve Response			8 hrs demonstrated
Signal to Full Open	<0.005 sec (<5.0 ms)	< .003 sec Open	.004
Signal to Full Close	<0.005 sec (<5.0 ms)	≈ .001 sec Close	Same
Valve Leakage	<2.3 scc/hr	< 2.3 SCC/hr	None
(GN ₂ @ ΔP = Max Feed System Press)			
Propellants			
Oxidizer	Nitrogen Tetroxide (MON-1) (99% N ₂ O ₄ -0.8% NO)	MON 1 & Mon 10	MON-1
Fuel	Monomethylhydrazine (N ₂ H ₃ CH ₃)	N ₂ H ₃ CH ₃	N ₂ H ₃ CH ₃
Mixture Ratio	1.64, nominal at 70°F	1.2 to 1.7	1.45 - 2.16
Propellant Inlet Temperature Range	20-120°F	30 to 125	50 - 70
Storage Life	10 Yr	Not Evaluated	Not Evaluated
Flightweight Assembly Reliability	0.999	Not Evaluated	Not Evaluated
Flightweight Assembly Maintainability	Zero Maintenance Over Storage Life	Not Evaluated	Not Evaluated
Flightweight Assembly Weight	Not Evaluated	0.7 lbm	0.6 lbm

2.1, Engine Design and Operating Characteristics (cont.)

reduced the engine stability and blowdown capabilities. Recommended changes in the chamber contour in future development work could restore the blowdown capabilities to the Phase II condition and also improve the performance.

2.2 IMPROVED MEASUREMENT CAPABILITIES IN PULSING

Thrust measurement during pulse testing required an improvement of the techniques generally in use with higher thrust engine programs. A test fixture with combined steady-state and pulse thrust measurement, including inplace calibration capabilities, was provided by ALRC. The force measurement fixture incorporated 3-point-mount, high-response load cells mounted on a critically damped seismic mass for impulse measurements. This three-crystal load cell measurement system, when coupled with a charge amplifier, provided accurate pulse/thrust measurements during 10 ms EPWs. The load cell is capable of a rise time of $<6\mu$ sec to full scale (5.5 lbf), with a resolution capability of .0006 lbf. The steady-state load measuring system utilized a standard-strain, gage-type flexure load cell with a force range of 1.0 lbf, dampened by a viscous fluid bed. The series-loaded dynamic and static measuring systems were simultaneously calibrated by a piston/ standard cell system, applying the calibrated load directly to the engine mount. This inplace calibration therefore accounted for flexure, propellant line, and instrumentation cabling restraints. The accuracies are evidenced by the repeatability of pulses, discussed elsewhere in this report, and the linear relationship displayed by plotting chamber pressure and thrust.

2.3 Durability Testing Results

Steady-state, long-duration capability has been demonstrated in Phase III. Engine 1 was tested for 9000 sec total, of which 5000 sec was in a single burn. Engine 2 has accumulated 30,000 sec, of which 18,000 sec was a single burn. No steady-state thermal limitations were encountered.

Engine S/N 21's injector failed in pulse limits testing either due to repeated hard starts or backflow of fuel into the oxidizer manifold. Further testing is required to isolate the exact cause of the failure.

SECTION 3.0

FLIGHT ENGINE DESIGN

3.0 FLIGHT ENGINE DESIGN

This section describes the anticipated characteristics of a flight type 0.5 lb thruster based upon the work completed under this contract. Weight, envelope, and performance data are provided for the actual designs tested, along with estimates of improvements which should be attainable with additional development work.

Figures 2-1 and 3-1 provide a photograph of the flight weight engine configuration and the engine envelope for a 143:1 area ratio nozzle. Slightly higher performance could be obtained by increasing the nozzle length by 1 inch. This would increase the area ratio to approximately 200:1 and provide a 1% Isp improvement based on analysis.

The engine weight is 0.6 lb, but this could probably be reduced approximately 10% by removing some material from the valve body and chamber.

Other features of the design are itemized in Table 3-1.

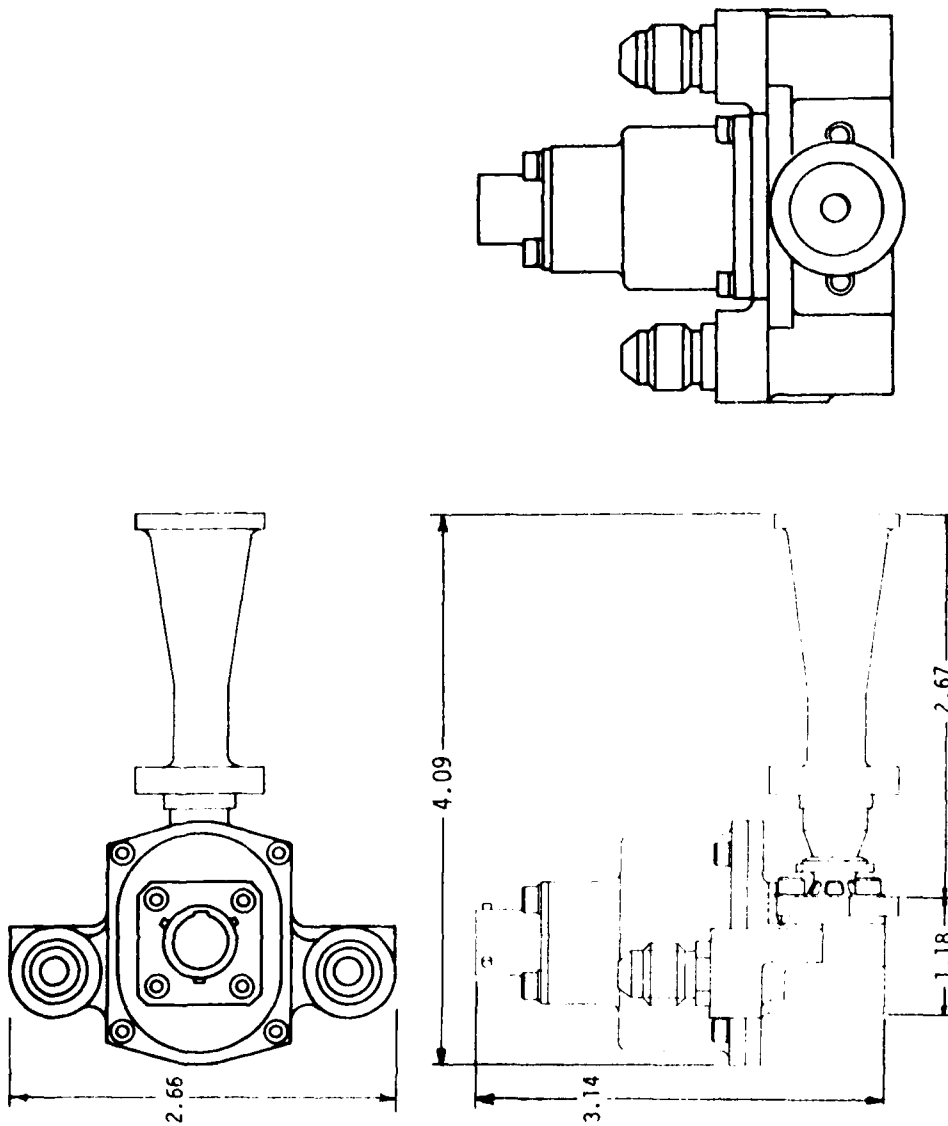


Figure 3-1. 0.5 lb Thruster Engine Envelope for 143:1 Area Ratio Chamber

TABLE 3-1
FLIGHT DESIGN CHARACTERISTICS

<u>Parameter</u>	<u>Phase III</u>	<u>Flight Potential</u>
Thrust Min/Max lbF	.2/.5	.2/.5
Length, in.	4.09	4.09
Width, in.	2.66	2.66
Height, in.	3.14	3.14
Weight, lb.	.6	~.54
Valve Voltage, Volts	24-32 (28 nom)	24-32 (28 nom)
Valve Power, Watts	4.4	4.4
Performance $\epsilon = 143:1$		
Steady-State, sec	265	>280
Pulse, sec	Not Evaluated	Not Evaluated
Burn Times		
Max Single, hours	>5	>10
Min Pulse, sec	.010	.005
Total Life, hours	>8	>10
Impulse bit (min.) lb-sec	.004	.002
Propellants		
Fuel	MMH	MMH
Oxidizer	N ₂ O ₄ , MON 1-to MON-10	N ₂ O ₄ , MON-1 to MON-10
Tank Pressure		
Max, psi	400	400
Min, psi	150	100
Temperature		
Max, °F	120 MON-1, 100 MON-10	120 MON-1, 100 MON-10
Min, °F	20 MON-1 0 MON-10	20 MON-1 0 MON-10

SECTION 4.0

PHASE I - ANALYSIS AND DESIGN

4.0 PHASE I - ANALYSIS AND DESIGN

4.1 INDUSTRY REQUIREMENTS

Phase I began with an industry-wide survey of potential users of the 0.5 lb thrust class bipropellant (N₂O₄/MMH) engine programmed for development. A questionnaire, consisting of four technical categories (mission aspects, spacecraft system, propulsion subsystem, and thruster requirements) and a business category, was submitted to ten Aerospace companies. Eighteen users representing eight companies responded. Appendix A provides a copy of the questionnaire and a tabulation of the technical category results.

The business category explored the key issues for selection of a 0.5 lb class engine for a flight system. A ranking of issues (from 1 as most to 10 as least important) was obtained. An index of total points divided by total response was developed as shown in Table 4-I. Reliability and cost were considered most important, followed by performance and duty cycle flexibility which were allotted nearly equal weight. All other factors were considered secondary. The cost, in 1978 dollars, showed the apparent value to be approximately \$20,000 per engine.

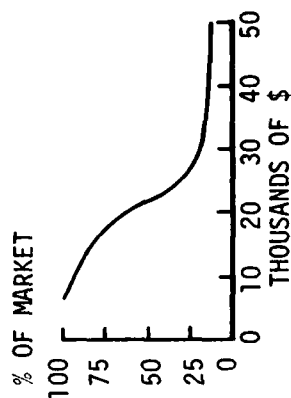
After obtaining the survey data, the multiplicity of requirements were evaluated and compared to the goals defined in the statement of work, Table 4-II. These were generally consistent, except for the following:

- ° Tank Blowdown 4:1 with a maximum tank pressure of 360 psia
- ° Temperature Range 0 to 100°F preferred by 50% of users over the specified 20 to 120°F. (Note MON-1 oxidizer freezes at 11°F; MON-10 is required for 0°F operation).
- ° Minimum Impulse Bit 0.002 lbF-sec desired at start of mission (i.e., .005 lbF-sec not small enough).
- ° Life 10 hour total may not be sufficient.

TABLE 4-I

SMALL THRUSTER KEY ISSUES

PROGRAM	POINTS	NO.	AVG.
1. RELIABILITY	41	18	2.28
2. COST	48	18	2.67
3. & 4. { SPECIFIC IMP.	57	18	3.17
{ DUTY CYCLE FLEX	51	16	3.19
5. IMPULSE REPEATABILITY	86	17	5.06
6. WEIGHT	103	18	5.72 \approx 1 1/2 TO 1 1/2 LB
7. BLOWDOWN CAPABILITY	94	16	5.88 3:1 OK
8. FAMILIARITY	98	16	6.12
9. THERMAL /POWER REQ'MTS	113	17	6.65
10. ENVELOPE /PACKAGING	123	16	7.69



*FROM ALRC's SURVEY QUESTIONNAIRE TO SATELLITE PRIMES

TABLE 4-II

CONTRACT GOAL VS SYSTEM REQUIREMENTS

PARAMETER	GOAL	RECOMMENDED VALUE
Nominal Vacuum Full Thrust	0.5 lbF	No change
Chamber Pressure	780 psia	125
Maximum Feed System Pressure	400 psia	360
Minimum Feed System Pressure	780 psia	90
Expansion Ratio	780	4:1 Blowdown
		100:1
Nominal Isp (at Full Thrust)	280 sec	No Change
Steady-State Pulsing (10 ms)	220 sec	
Nominal Minimum Impulse Bit (at Full Thrust)	0.005 lb-sec \pm 0.0005 lb-sec	.001 to .003
Number of Maximum Thermal Cycles	1000	
Total Number of Starts	750,000	
Single Burn Duration	2 hr	No Change, However Firing Life > 10 Hours May be Required
Total Firing Life	10 hr	
Valve Response		
Signal to Full Open	0.005 sec	
Signal to Full Close	0.005 sec	
Valve Leakage (GN ₂ @ P = Max Feed System Press)	2.3 sec/hr	No Change Valve Redundancy is Desired
Propellants		
Oxidizer	Nitrogen Tetroxide (MON-1) (99% N ₂ O ₄ -0.8% NO)	MON 10 Alternate Oxidizer
Fuel	Monomethylhydrazine (N ₂ H ₃ CH ₃)	
Mixture Ratio	1.64, nominal at T _{cof}	1.64 To 1.74 for Blowdown for Alternate Oxidizer
Propellant Inlet Temperature Range	23-125°F	0-100°F
Storage Life	10 yr	
Flightweight Assembly Reliability	0.999	No Change
Flightweight Assembly Maintainability	Zero Maintenance Over Storage Life	
Flightweight Assembly Weight	780 lbm	Less than 1 lb

4.0, Phase I - Analysis and Design (cont.)

4.2 SYSTEM-MISSION-ENGINE INTERACTIONS AND OXIDIZER BLEND SELECTIONS

This task considered engine operational variations resulting from the interaction of pressurant gases, propellant vapor pressure, and environmental temperatures of tanks and propellant feed lines for a locked-up system operating in the blowdown mode. Freezing limits for various MON blends and the effect of supply pressure on the engine mixture ratio were major factors of concern.

4.2.1 Oxidizer Blends

Inasmuch as MMH has a freezing point of -63°F , compared to 11°F for N_2O_4 , the use of NO to depress the N_2O_4 freezing point would minimize the need for heaters to preclude propellant freezing in orbiting satellites.

Consequently, the use of higher MON oxidizer mixtures was analyzed. Nominal N_2O_4 (MON-1) is $\sim 1\%$ NO by weight. It was determined that MON-10 could be interchanged with MON-1 and yet retain similar operational characteristics if the maximum propellant temperature limit were simultaneously reduced from 120°F for MON-1 to 100°F for MON-10. This MON change depresses the oxidizer freezing point from $+9^{\circ}\text{F}$ for MON-1 to -10°F for MON-10. Ignition characteristics of MON-10 with cold propellants at low P_c 's corresponding to the end of the blowdown mission needed to be experimentally verified.

Figure 4-1 shows the relationship between vapor pressure and freezing temperature as NO is added to the oxidizer N_2O_4 . The X in MON-X represents the weight % of NO in solution. Addition of NO increases the vapor pressure of the oxidizer. In comparison the fuel vapor pressure remains low (3 psia at 120°F).

4.2.2 Tank Blowdown Effects

The difference in propellant vapor pressure will influence the tank pressurization as the tanks empty or as the tank temperature changes.

The pressure of locked-up tanks, initially loaded at 400 psia and 70°F at 20% ullage, is shown in Figure 4-2 with temperature variations from -60 to $+120^{\circ}\text{F}$. The differential vapor pressure between fuel and oxidizer is extended as the MON level increases, causing a mixture ratio shift bounded by the limits for MON-1 and MON-10 shown in Figure 4-3.

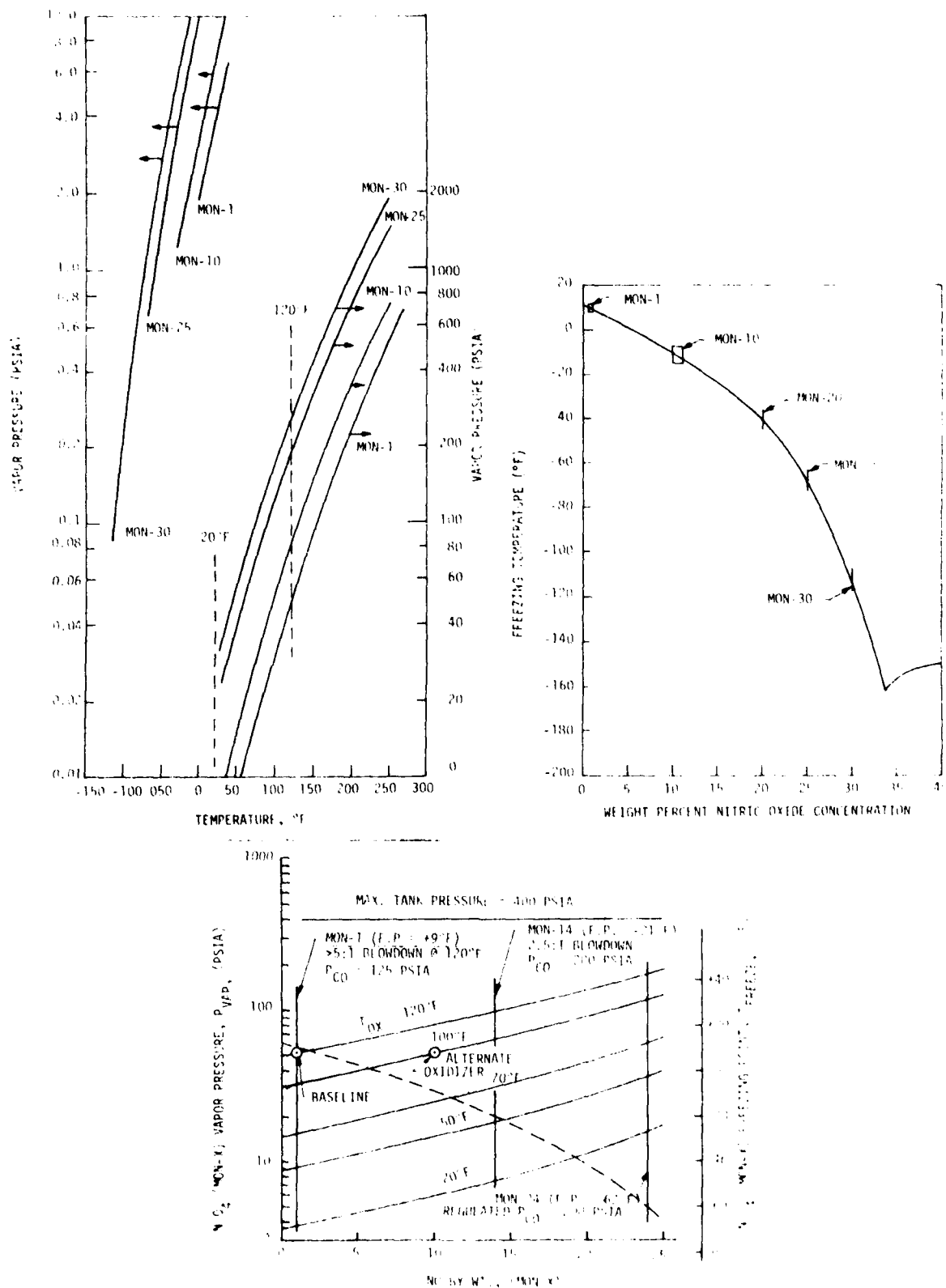


Figure 4-1. MON-Oxidizer Freezing Temperature, Vapor Pressure and Engine Blowdown Capability versus NO Content

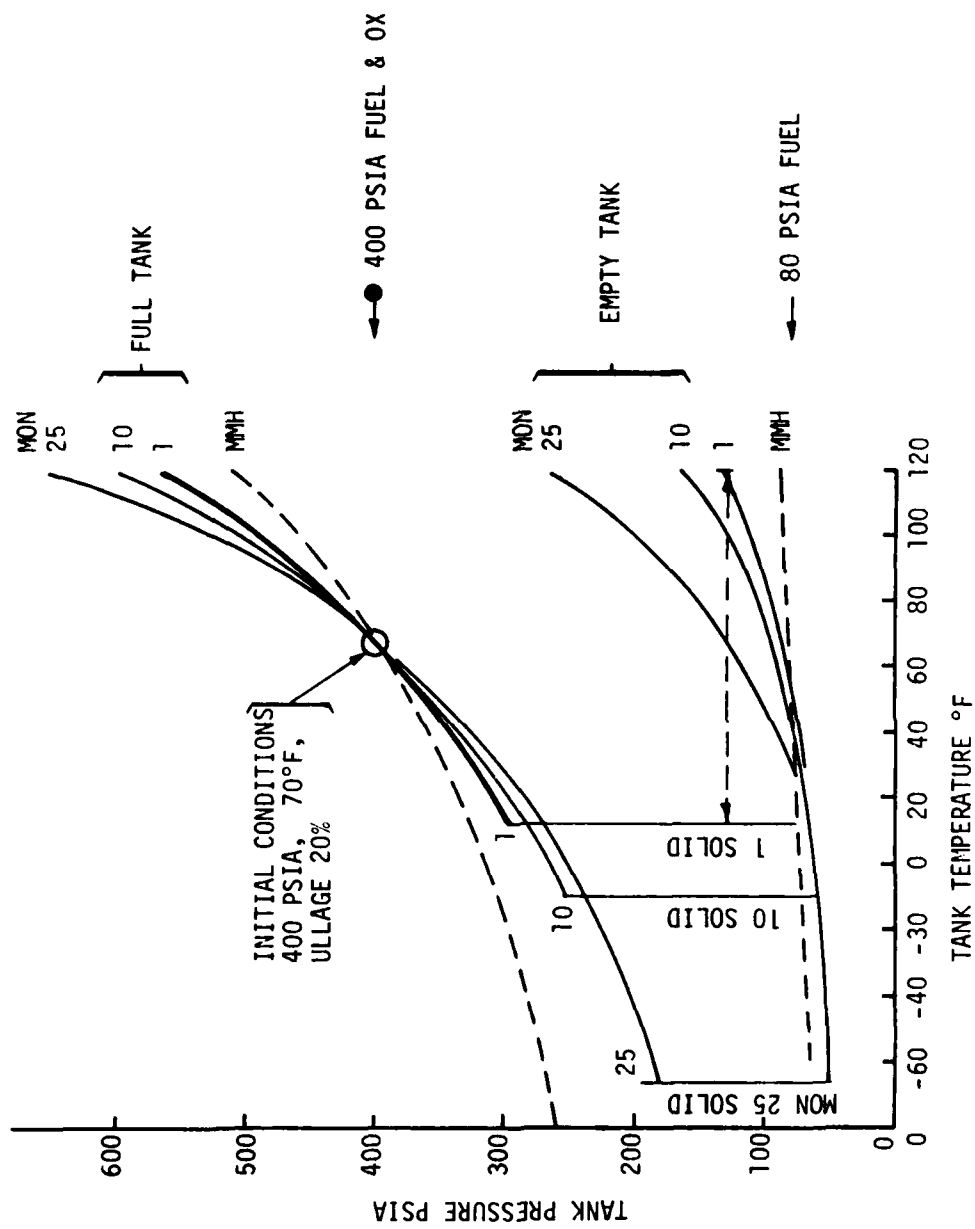


Figure 4-2. Tank Pressure vs Temperature for Various MON Oxidizers

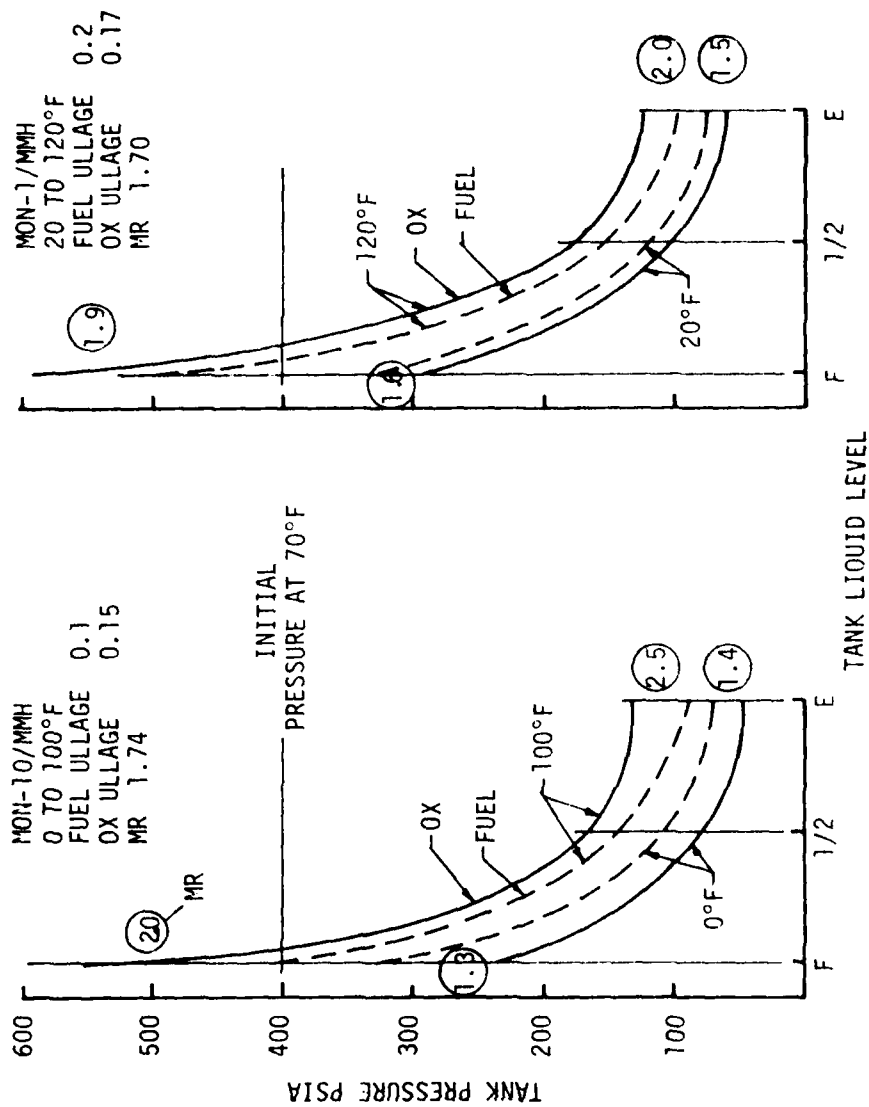


Figure 4-3. MON-1 vs MON-10 MR Shifts at Off Nominal Temperatures for Various Ullages

4.2, System-Mission-Engine Interactions and Oxidizer Blend Selections (cont.)

With constant tank temperatures, the higher vapor pressure of high MON oxidizers results in differential tank pressures as propellant is consumed (see Figure 4-4).

This situation can be compensated for by the proper selection of the initial ullage in each tank, resulting in a life-averaged acceptable condition of mixture ratio and propellant utilization (see Figure 4-5). For example, if the oxidizer tank (assuming equal size tanks) has less ullage at the start, it compensates for the faster depletion rate when the tanks are nearly empty and the oxidizer tank has a higher pressure than the fuel tank. This situation becomes more significant as the NO percentage is increased.

The conclusion reached from this task was that the freezing temperature of the propellants could be reduced below 0°F by the use of 10% NO (MON-10). In order to prevent excessive overpressure in a locked-up tank or shifts in mixture ratio, it would be necessary to reduce the upper allowable temperature, i.e.:

- ° MON-1 should be employed between 20°F and 120°F
- ° MON-10 should be employed between 0°F and 100°F

The survey indicated that most users would be satisfied with a 3:1 blowdown capability as compared to the 5:1 blowdown goal. Others expressed a willingness to reduce the maximum propellant temperature from 120°F to 100°F, if this would lower the minimum from 20°F to 0°F. This suggests the selection of MON-10 as an alternate oxidizer over the range from 0°F to 100°F, since it has similar performance characteristics as MON-1 within the 20°F to 120°F range.

Tank blowdown effects on the Low-Thrust Bipropellant Engine for MON-1 and higher MON-X oxidizers were evaluated over ranges of propellant inlet temperatures up to 120°F (Figure 4-6). The analysis investigated the effects of (1) propellant temperature, (2) tank ullage volume, and (3) MON content upon the fuel and oxidizer propellant tank pressures and resultant engine mixture ratios. The resulting conclusions were:

(1) Hot propellant tanks result in higher oxidizer tank pressures, leading to the engine being driven progressively oxidizer rich as

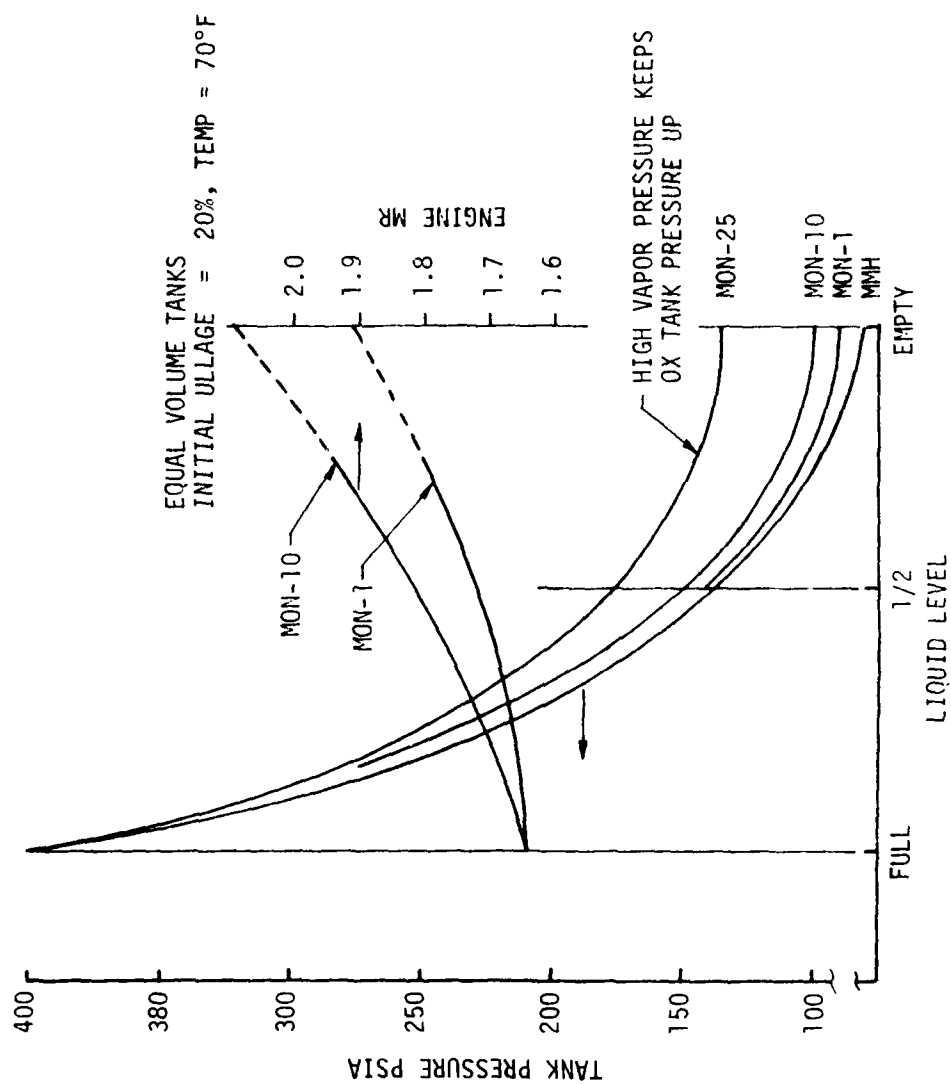


Figure 4-4. Higher MON Oxidizers and MR Shift Variations During Blowdown

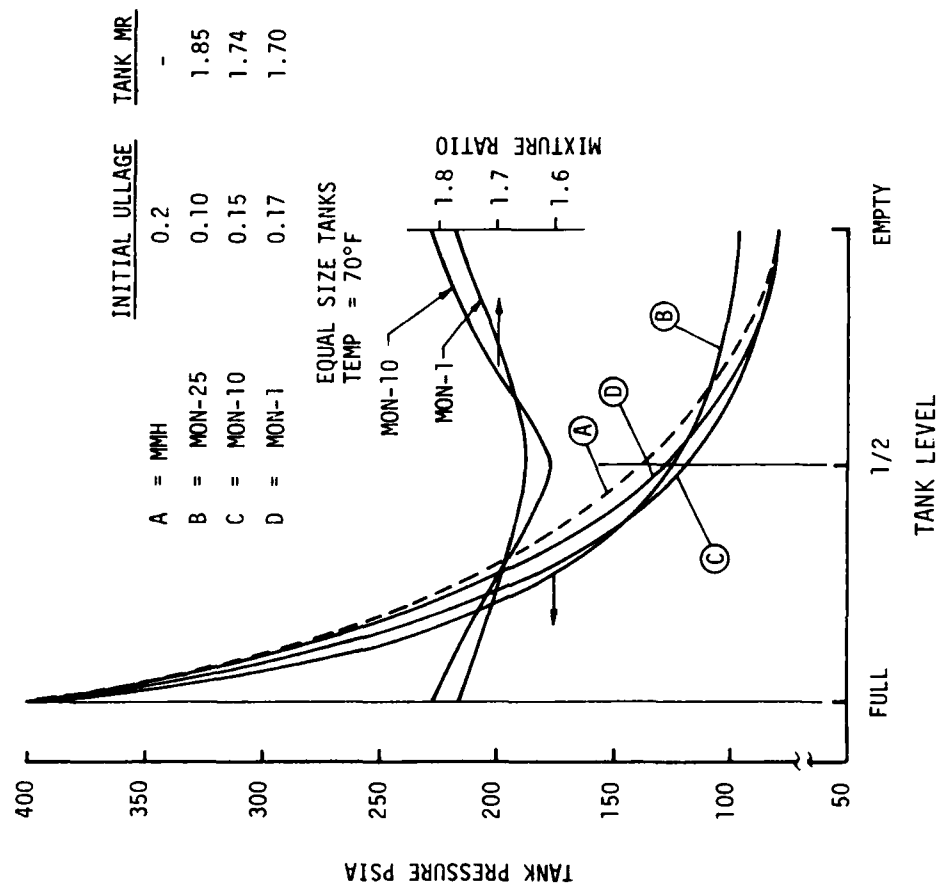


Figure 4-5. Propellant Tank Level vs Tank Pressure for Various MON Oxidizer Ullage Selections

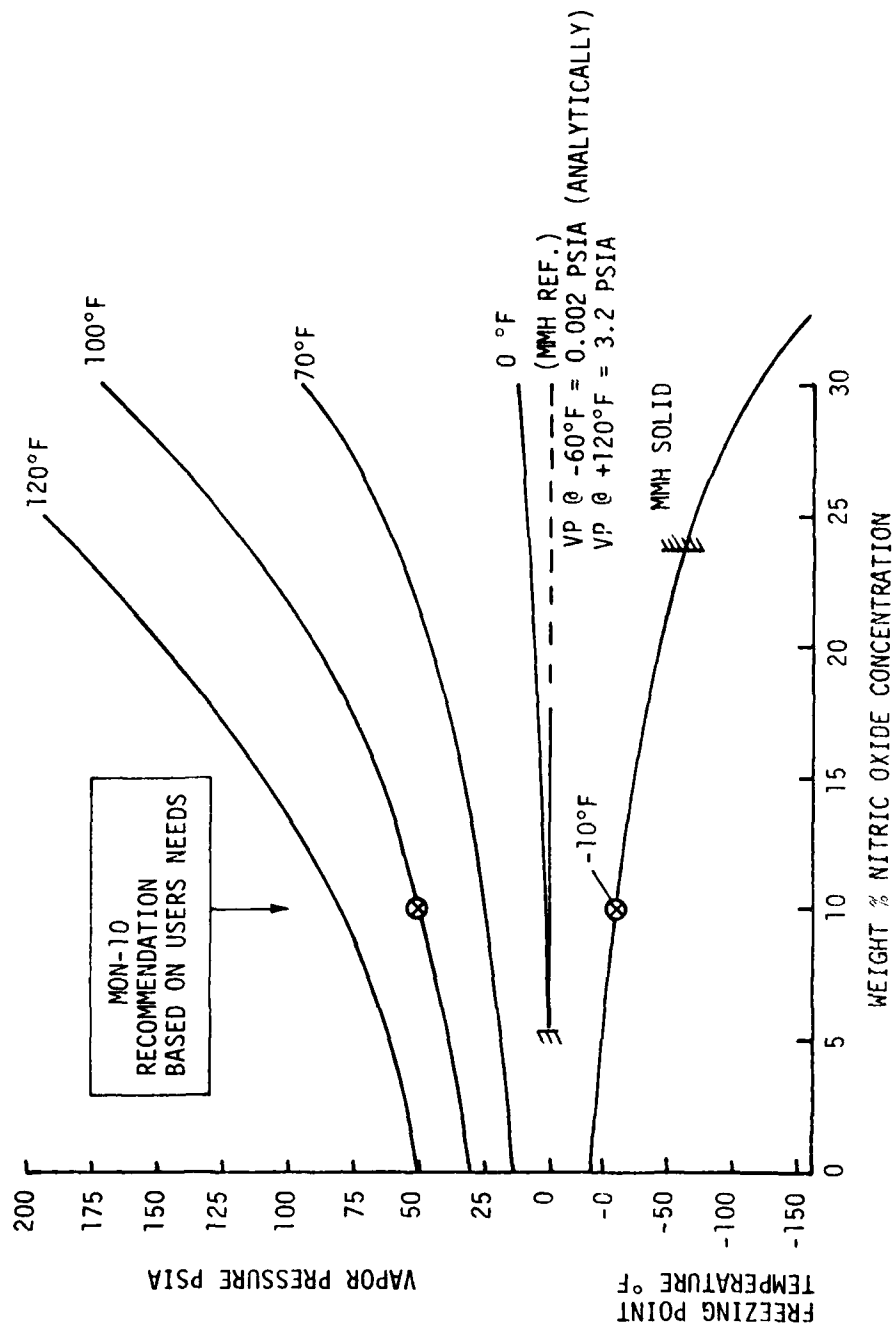


Figure 4-6. Minimum and Maximum Propellant Temperatures Versus NO %

4.2, System-Mission-Engine Interactions and Oxidizer Blend Selections (cont.)

the mission proceeds. This could result in reduced engine cycle life, engine thermal failure, increased plume contaminants, or premature oxidizer tank depletion. The problem is further aggravated as MON content is increased and propellant tank depletion is accelerated.

(2) Even with MON-1 at 70°F, the higher oxidizer partial pressure maintains the oxidizer tank at a higher pressure than the fuel as blowdown progresses. This results in a shift to higher engine O/F and oxidizer tank depletion for equal volume tankage starting with equal ullage volumes. This problem can be alleviated by offloading the fuel tank at start of the mission (slightly larger fuel ullage and reduced fuel blowdown ratio) to compensate for a slower rate of oxidizer tank pressure decay. This maintains engine O/F nearly constant throughout the mission, resulting in nearly simultaneous depletion; however, the engines must be balanced for an engine O/F > 1.64.

4.2.3 Oxidizer Blends Versus Engine Performance

Figure 4-7 provides a comparison of the theoretical specific impulse versus nozzle area ratio. Considering MON-1 and MON-20 oxidizer blends, the effect of the oxidizer blend on the theoretical performance is noted to be small even at nozzle area ratios up to 400:1. The influence of nozzle kinetics (i.e., equilibrium versus frozen flow and ODK) are noted to be a much more significant factor. The predicted change in performance due to the addition of 10% NO to the oxidizer was less than 1/2 of one percent. However, testing with MON-10 was recommended for Phase II to verify these conclusions.

4.3 ENGINE PARAMETER STUDY

4.3.1 Chamber Pressure Optimization

Engine performance, blowdown capability, ignition delay times, and chamber cooling are controlled by the chamber geometry and chamber pressure. This section provides the analytical basis for the selection of the nominal design chamber pressure used in the Phase II verification tests.

Figures 4-8 and 4-9 show that performance improves at high P_c due to reduction of nozzle kinetic losses. If this were the only consideration, a high value of P_c would be suggested; however, there are at least three other factors which strongly influence the design P_c selection.

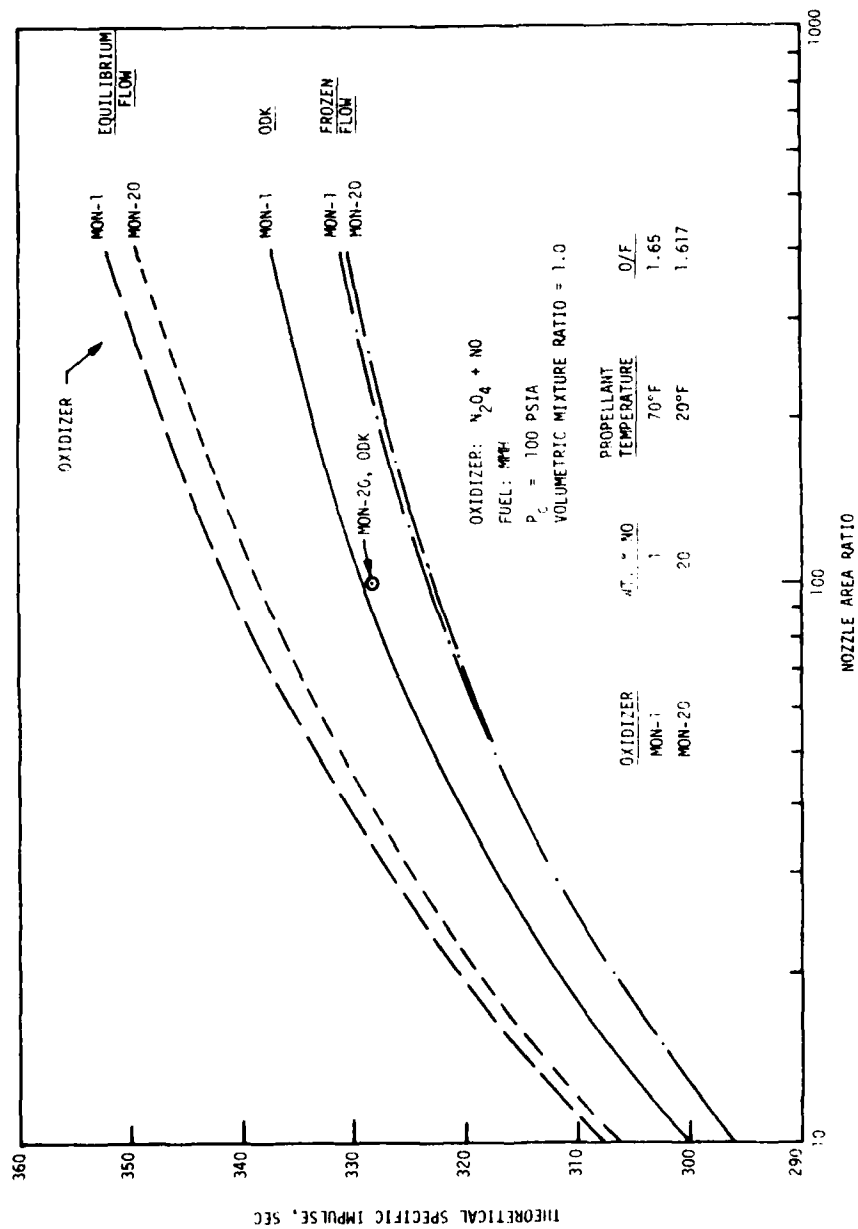


Figure 4-7. Theoretical Specific Impulse for Various MON Oxidizers

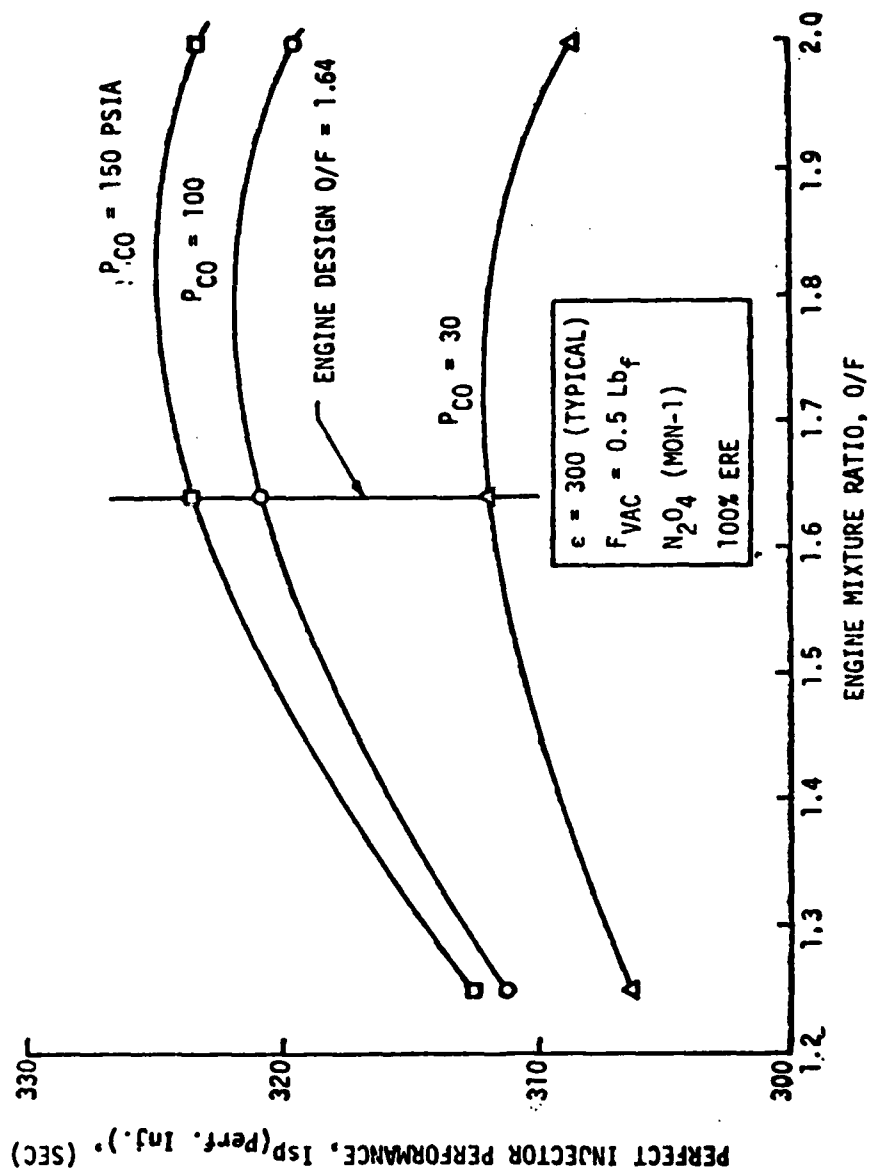


Figure 4-8. Theoretical Specific Impulse Versus Engine Mixture Ratio

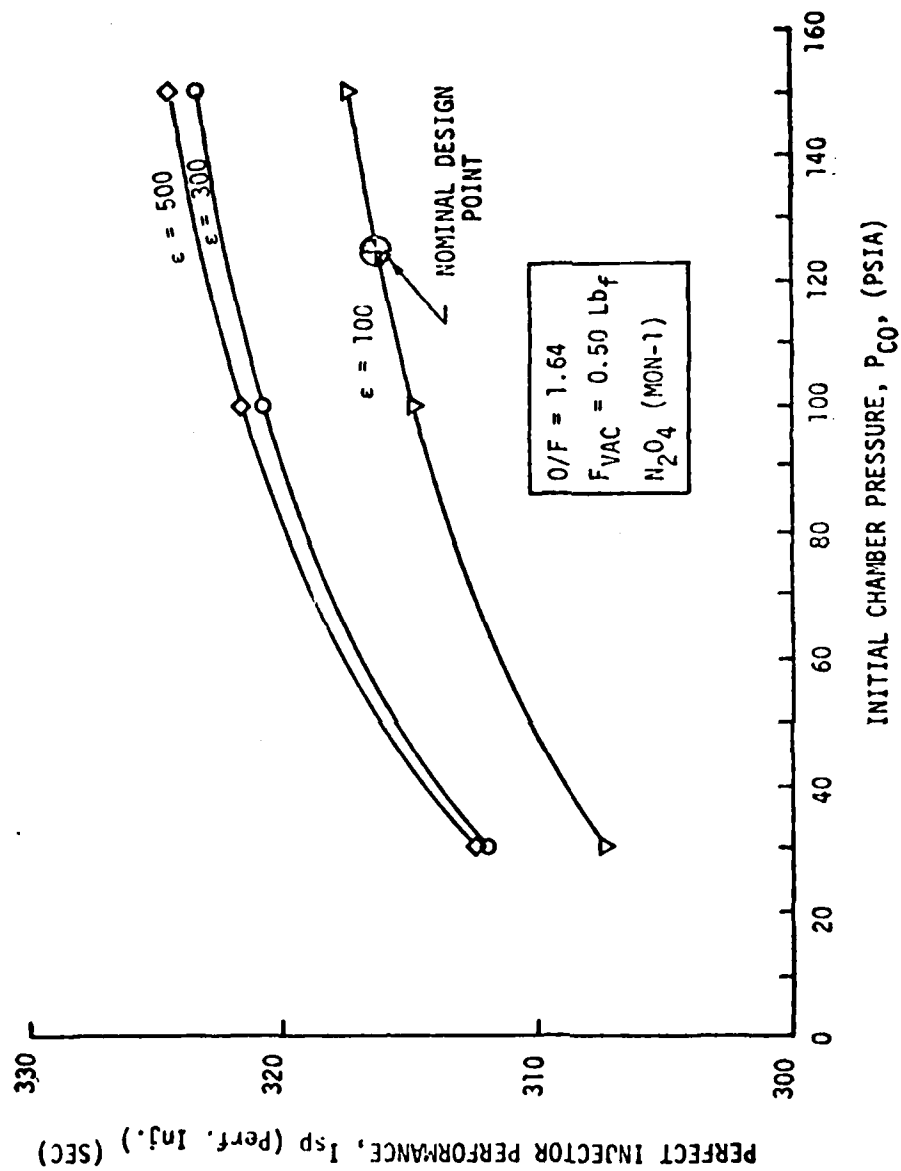


Figure 4-9 Performance Improvement vs Chamber Pressure

4.3, Engine Parameter Study (cont.)

First, in order to operate satisfactorily in a blowdown mode, adequate injection ΔP must always be available to suppress chugging. Since injector ΔP is proportional to P_c^2 , high initial ΔP must be incorporated at the maximum initial tank pressure to provide engine blowdown capability. Prior experience from many ALRC storable engines have repeatedly demonstrated that approximately 20 psid minimum injector ΔP is required to suppress chugging. Thus Figure 4-10 shows, for various initial design P_c 's starting from 400 psia maximum tank pressure, the final blowdown P_c and tank pressure at which the injection element ΔP is reduced to 20 psid. This suggests that a lower value of initial P_c increases the tank blowdown ratio capability before the 20 psid injector ΔP threshold is reached. Based on this first order analysis, a design $P_c < 125$ psia was selected in order to achieve the 5:1 tank blowdown ratio. A more detailed chugging analysis of the low-thrust bipropellant engine was conducted, using calculated combustion time lags representative of 0.5 lbf thrust class engines. The results from this chugging analysis, shown in Figure 4-11, confirmed the preliminary ROM (20 psid minimum ΔP) stability criterion. Thus 0.5 lbf engines with initial design $P_c < 125$ psia are predicted to have chug stability throughout the 5:1 blowdown ratio.

Second, propellant ignitability diminishes at low P_c 's. Thus it was analyzed for representative conditions at the end of the 5:1 blowdown ratio. In particular, ignition margin is reduced with cold (20°F minimum) propellants and reduced chamber L^* volume (minimum anticipated chamber length = 1.0 in.). These results, shown in Figure 4-12, indicate that ignition is predicted above 50 psia minimum P_c , which is the lowest P_c achieved at the end of the 5:1 blowdown ratio when starting from an initial P_c of 125 psia.

Third, two phase (vapor/liquid) injection must be avoided in the oxidizer manifold. The oxidizer vapor pressure increases for hot propellants. At the 120°F maximum inlet temperature, MON-1 oxidizer has a vapor pressure of 53 psia. While this is slightly higher than the 50 psia minimum P_c at the end of the 5:1 blowdown mission, it is still well below the 70 psia (50 psia P_c + 20 psid ΔP) oxidizer manifold pressure. Thus, although some slight oxidizer flashing may occur within the chamber, the oxidizer manifold should be entirely within the liquid state, assuring uniform injection distribution.

From the standpoint of oxidizer manifold vapor lock, MON-10 at 100°F maximum behaves similarly to MON-1 at 120°F maximum. Thus chug stability and blowdown capability are not expected to be compromised by

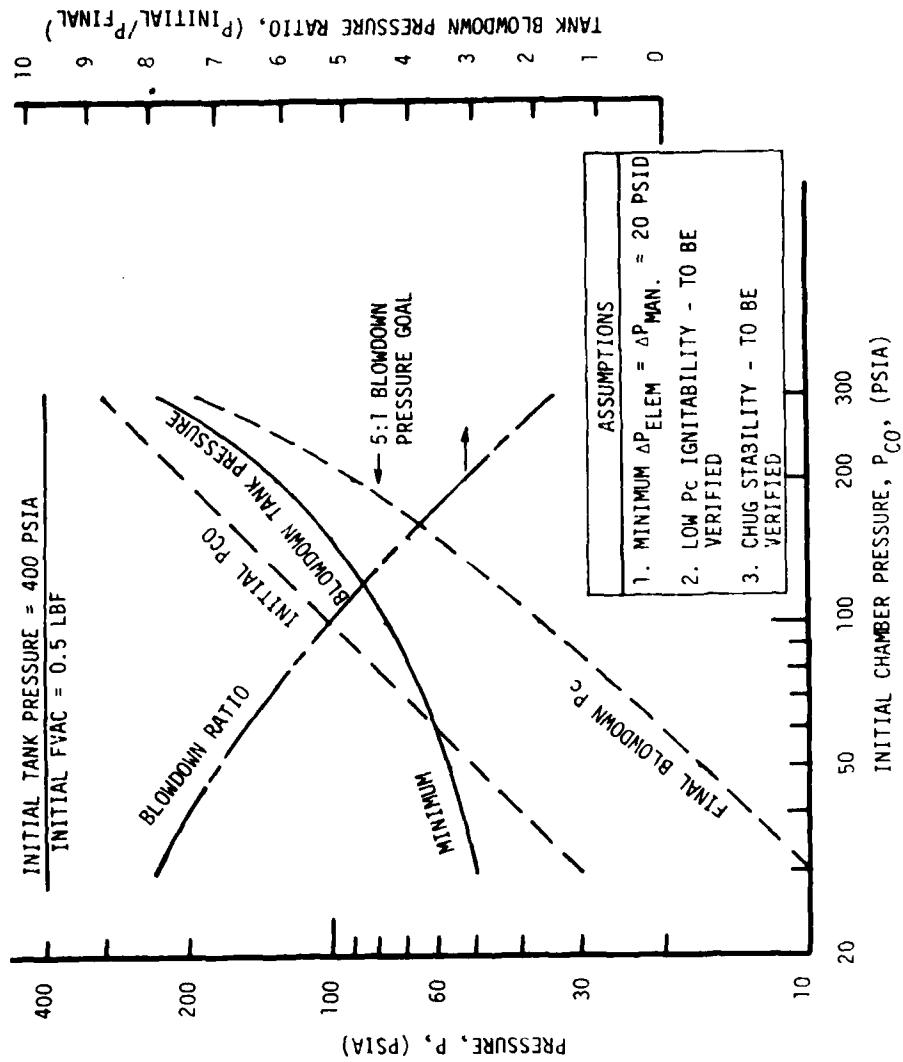


Figure 4-10. Initial Chamber Pressure Selection vs Tank Blowdown Ratio

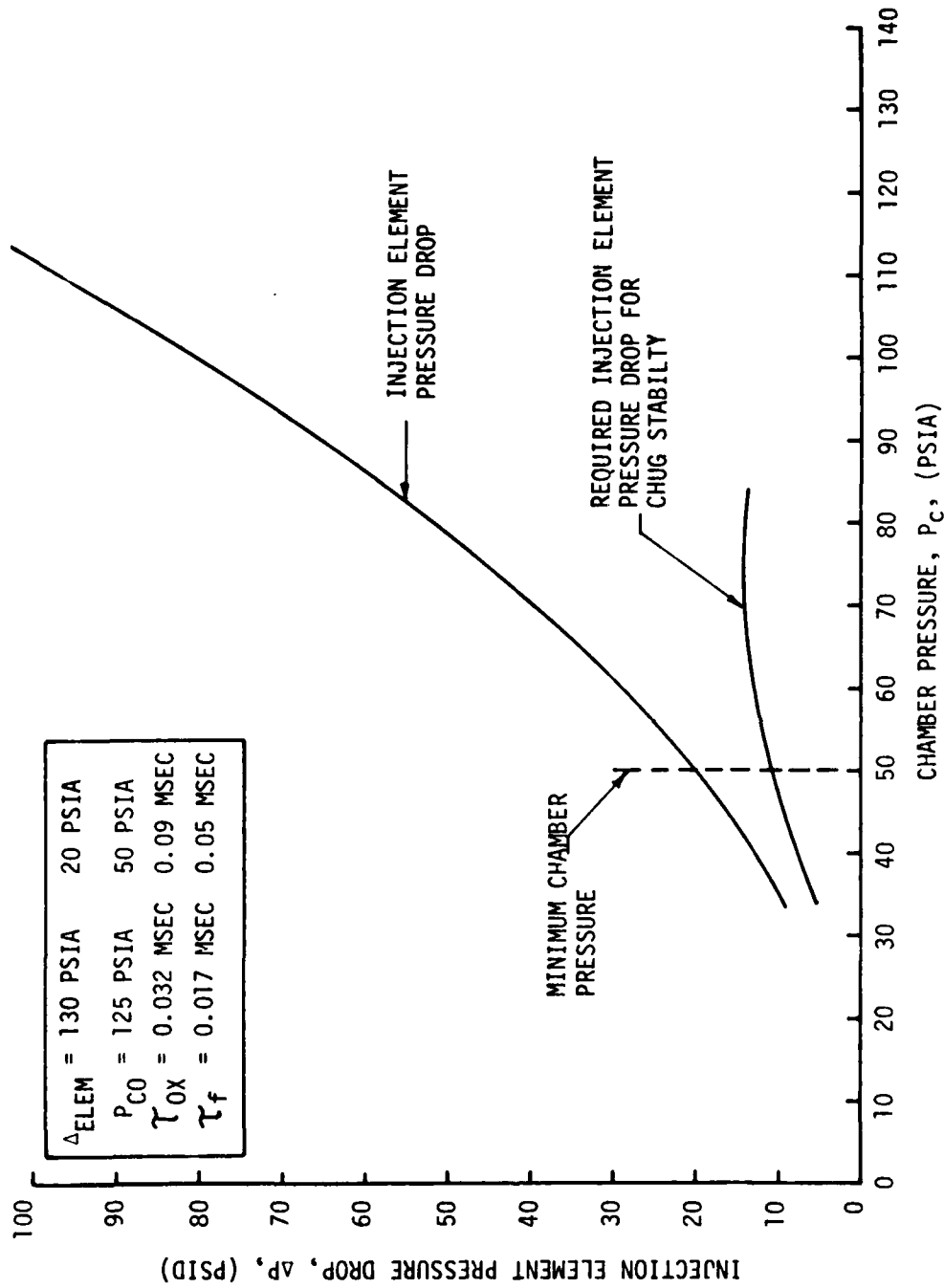


Figure 4-11. Engine Chug Stability Versus Blowdown

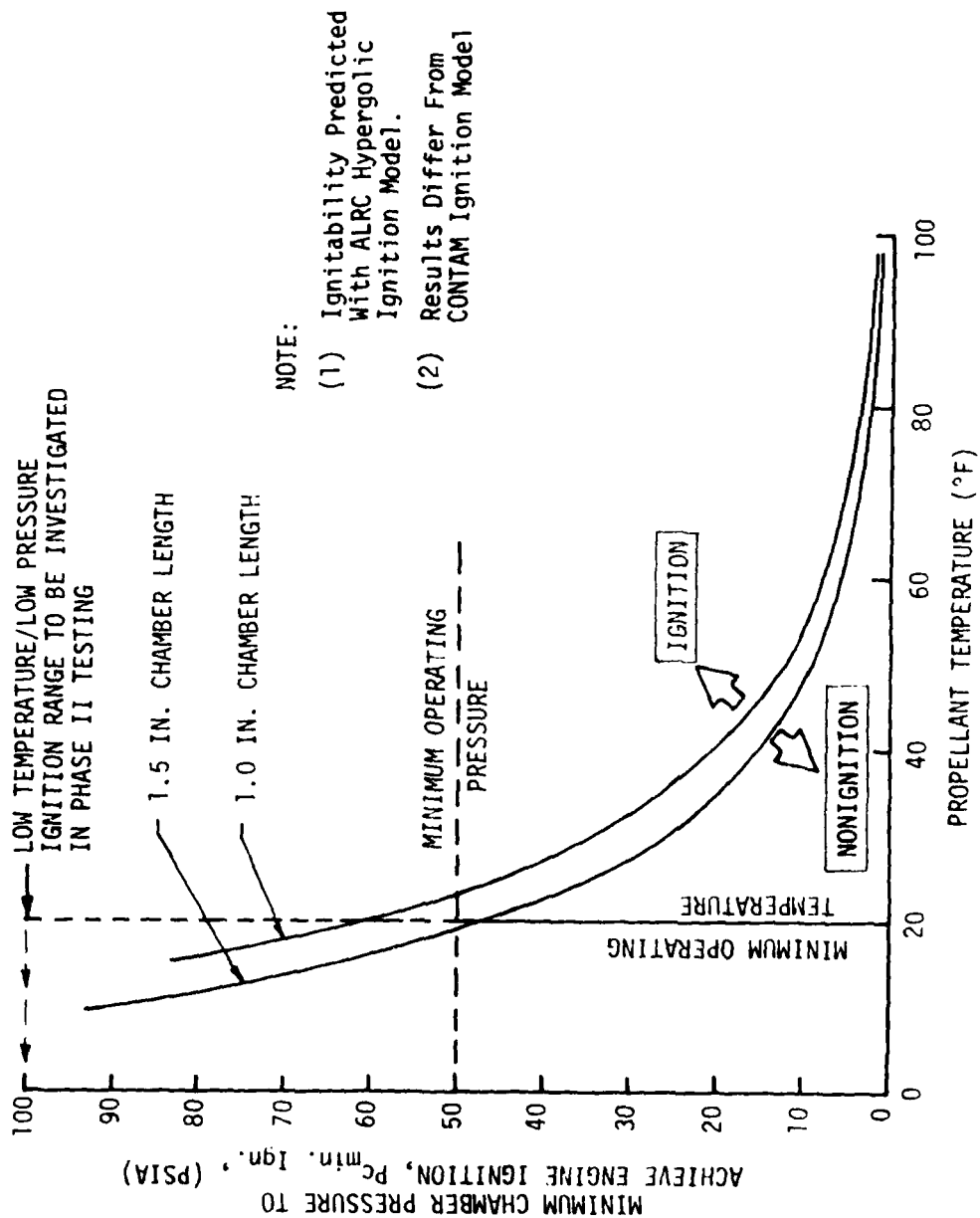


Figure 4-12. Low Propellant Inlet Temperature and Low Chamber Pressure vs Ignition Delay Time

4.3, Engine Parameter Study (cont.)

the alternate MON-10 oxidizer. Ignition of MON-10 at 0°F minimum, compared to MON-1 ignition at 20°F minimum, may present another story, however (see Figure 4-12). Although both oxidizers have comparable vapor pressures at the above conditions, the MMH vapor pressure is lower at 0°F than it is at 20°F. Thus low temperature ignition, particularly at the end of the blowdown mission, at low (50 psia) P_c may present a problem. Minimum propellant temperature ignition, especially at low P_c , needed to be verified experimentally during Phase II.

4.3.2 Injector Design

The predicted success of the 0.5 lbF engine was heavily dependent upon achieving a satisfactory injector design to yield the desired spray characteristics necessary for achieving high combustion performance and uniformly benign chamber thermal compatibility. Thus, in recognition of the criticality of the injector design, 10:1 supersonic injector spray pattern experiments were conducted in order to empirically complement the extensive analytical design predictions.

Figures 4-8, 4-9, 4-13 and 4-14 show the perfect injector performance prediction cross-plotted as functions of chamber pressure, engine mixture ratio, nozzle exit area ratio, and nozzle length. The perfect injector performance corresponds to the theoretical One Dimensional Equilibrium (ODE) specific impulse reduced for (1) nozzle kinetic loss, (2) nozzle divergence loss, and (3) nozzle boundary layer loss (predicted by the BLIMP model). Thus, while the perfect injector performance does account for real nozzle inefficiencies, it does not account for injector performance losses attributable to (1) incomplete propellant vaporization, (2) non-homogeneous gas mixing, or (3) cooling losses required to maintain chamber compatibility.

Figures 4-9 and 4-13 show that perfect injector performance maximizes at high P_c 's and high ϵ (500:1). Rationale for the selection of $P_c = 125$ psia was described in an earlier section. The selection of nominal $\epsilon = 143$ was based on the test facility vacuum capability (Ref. Subsection 4.3.3.1). Under these conditions, the perfect injector performance potential for the 0.5 lbF engine is 316 sec Isp. The nozzle losses are based on the BLIMP Model analyses discussed in Section 4.3.3.1.

Based upon extrapolation of previous ALRC 5 lbF bipropellant engine and 100 lbF MIB experience, it was estimated that a 20 sec

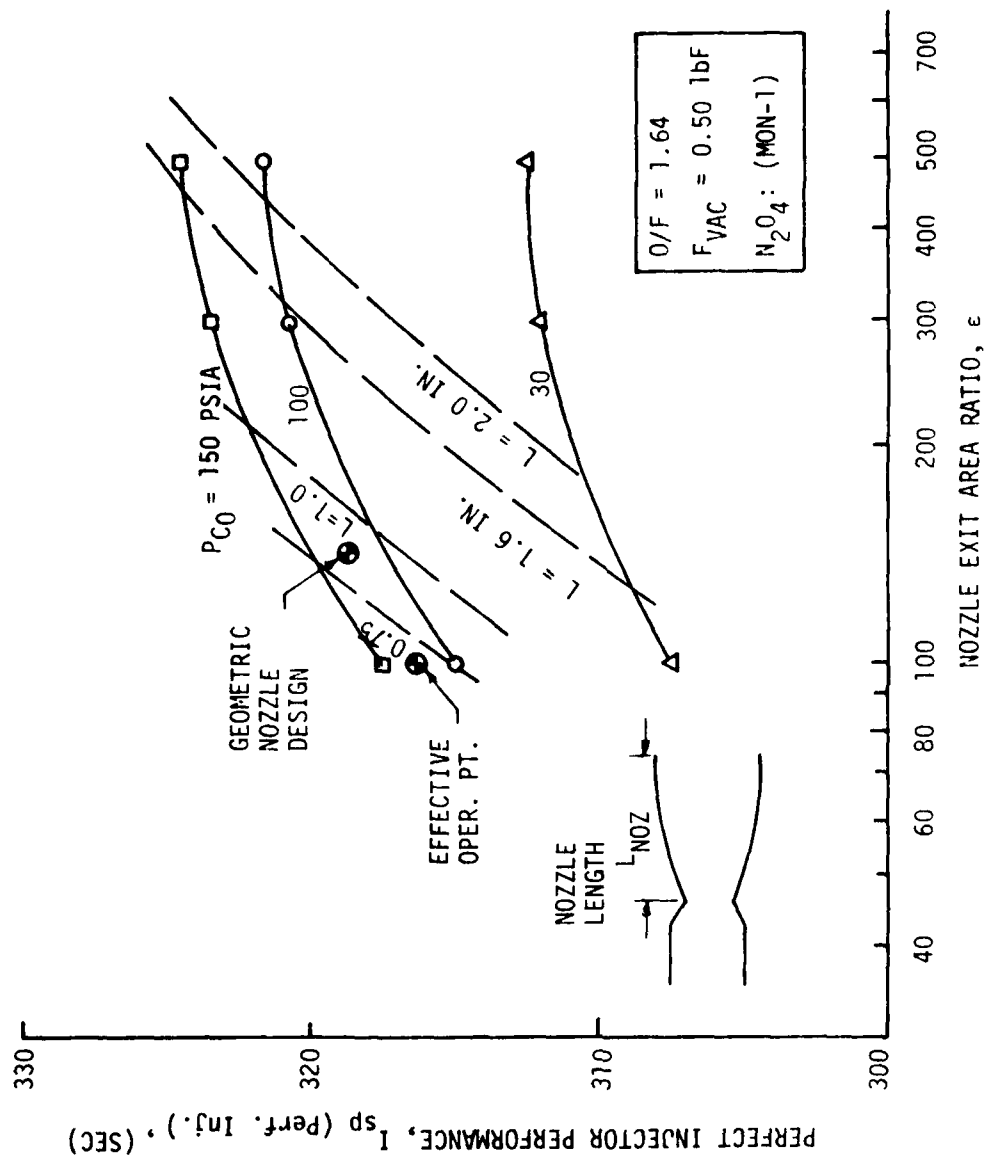


Figure 4-13. Area Ratios vs I_{sp}

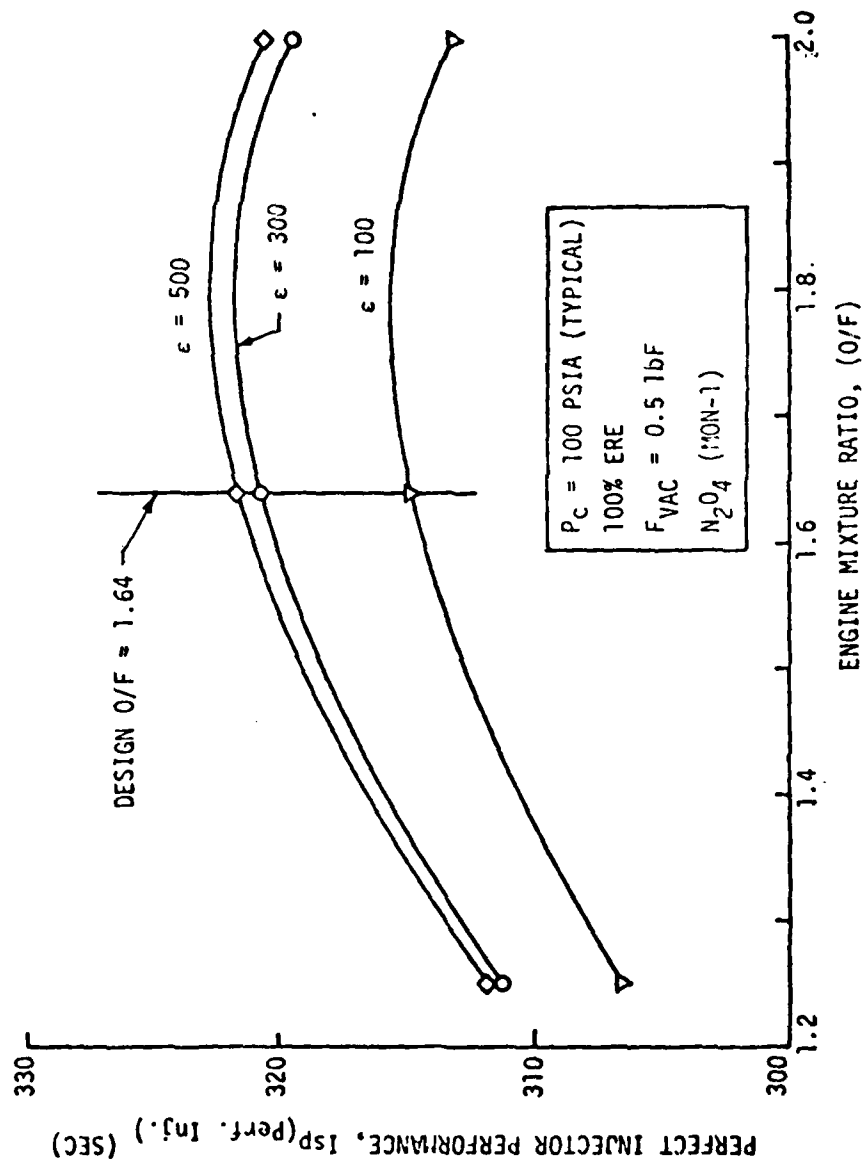


Figure 4-14. Perfect Injector Specific Impulse Versus Mixture Ratio and Area Ratio

4.3, Engine Parameter Study (cont.)

performance penalty would be associated with achieving the necessary chamber thermal compatibility for a >2 hr single burn, >1000 thermal cycles, and >750,000 pulse firings. This reduces the engine performance from 316 sec to 296 sec Isp. It was further estimated that an additional injector inefficiency of approximately $2\% \pm 2\%$ Isp should be anticipated as the result of either incomplete propellant vaporization or core mixing inefficiency. This leaves a predicted engine Isp capability of $290 \text{ sec} \pm 5 \text{ sec}$, exceeding the 280 sec contract performance goal by 5 to 15 sec. However, this was predicated on achieving the desired optimized injector spray pattern characteristics. In fact, the critical importance of this requirement was the basis for ALRC including superscale injector experiments in their design data predictions.

Therefore, the 0.5 lbf engine design requirements could be predicated upon achieving an injector design fulfilling the following criteria:

- ° Small injector manifold dribble volumes conducive to rapid pulsing response, high-pulse performance and low-plume contaminants.
- ° Compatible injection spray distribution.

In regard to the first requirement, it was possible to design platelet injector manifolds with dribble volumes equivalent to approximately 1 msec of propellant fill time at the nominal rated flowrates. Although the contract pulse performance goal permitted larger dribble volumes, extensive effort was taken to reduce dribble volume to an absolute minimum. This was done in recognition of the fact that the 0.5 lbf engine would quench almost immediately after valve closure due to its small chamber diameter, with the propellant contained in the dribble volume upon shutdown a potential plume contaminant source.

Figure 4-15 demonstrates the objective of the injection element/pattern design visually, displaying that the ideal injection element and pattern characteristic, whether it be achieved by a single- or multi-element injector, is one whose sprays are reasonably well-atomized and whose core is well-mixed and mildly oxidizer rich ($O/F \approx 2.5 \pm 0.3$), with a symmetrical fuel-rich periphery adjacent to the wall. This combination will provide high steady-state combustion performance and provide the chamber wall thermal environment necessary for achieving the engine life goals. Chamber compatibility is also essential for achieving rapid pulsing response, high-pulse performance, and low-plume contaminants, since moderate chamber temperatures reduce postfire heat soakback into the injector and valve between firings.

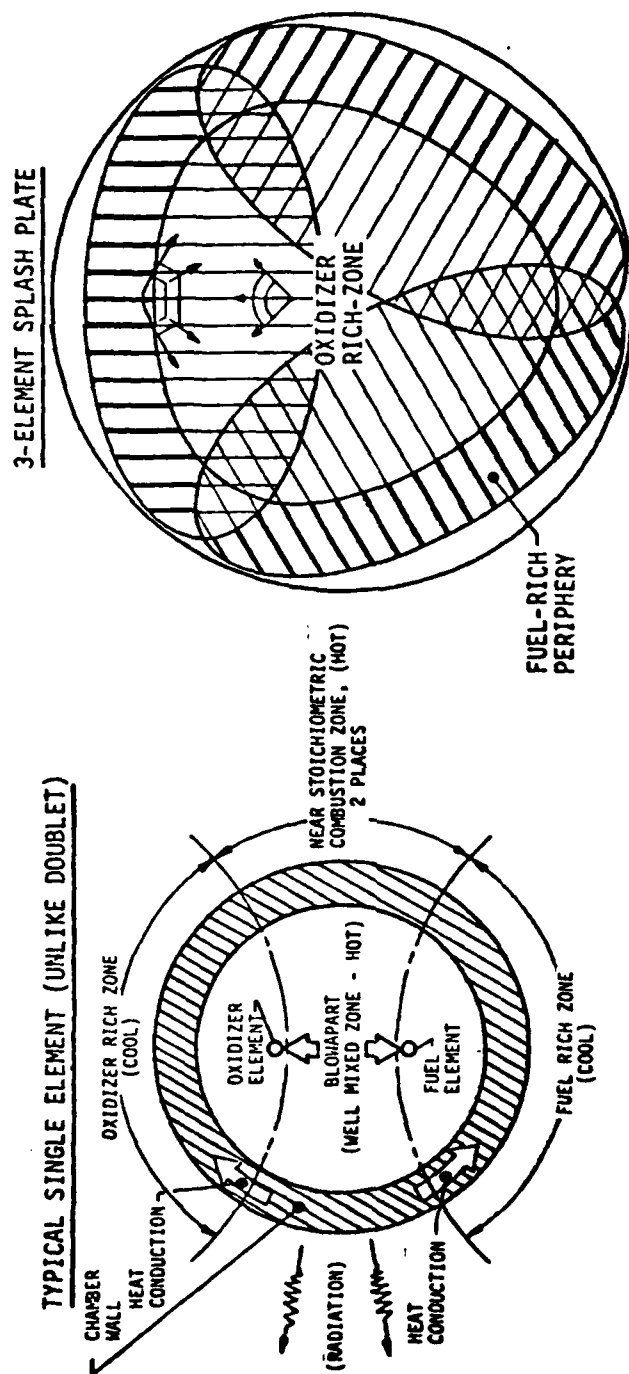


Figure 4-15. Injection Element Design Objective

4.3, Engine Parameter Study (cont.)

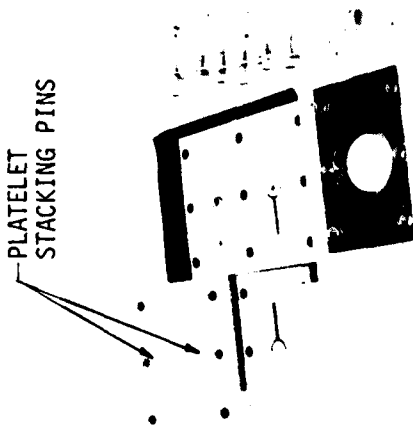
To verify the desired injector pattern objective, 10:1 diameter (100:1 flowrate) superscale platelet injectors were designed, fabricated, cold-flow tested, and evaluated during Phase I. These superscale injectors were produced from the prototype platelet art work, photo-enlarged to 10:1 scale. To further enhance usefulness, the cold-flow fixture shown in Figure 4-16 was fabricated to permit flow testing of loose unbonded platelets representing a significant breakthrough in injector development state-of-the-art.

Three basic injector concepts shown in Figures 4-17, 4-18 and 4-19 were experimentally evaluated in two iterations. Two film-coolant variations of the splash plate injector, shown in Figure 4-20, were evaluated during the first test series, as the result of which the symmetrical FFC design was found to be superior. A total of 4 superscale patterns were cold-flowed and evaluated in the first test series. On the basis of these tests, it was concluded that none of the patterns designed on the basis of analysis alone were acceptable for actual hot-fire testing. Thus all injector pattern concepts were modified. Two variations each of the Vortex/V-Doublet and Co-Axial Vortex/Swirl Cup designs and one modified splash plate design, for a total of 5 injector patterns, were tested in the second cold-flow series.

Design deficiencies resulting in undesirable spray characteristics for each of the 3 initial injector concepts are shown in Figures 4-21, 4-22 and 4-23. The required design modifications to improve spray characteristics incorporated prior to the second test series are shown in Figures 4-21, 4-22 and 4-24. The resultant spray distribution improvements achieved with the modified injector designs are shown in Figures 4-25, 4-26 and 4-27. At least 4 of the 5 patterns evaluated in the second series appeared satisfactory for hot-fire testing, and one each of the 3 basic element concepts were recommended for prototype fabrication and Phase II verification hot-fire testing.

In addition to the spray pattern/compatibility improvements noted, the injector manifold dribble volumes were reduced by 20% to 35% from first to second injector series. This significant design improvement was made possible by flowing the loose platelet manifold in segments to ascertain manifold pressure drop and injection distribution sensitivity to manifold volume in order to calibrate the manifold hydraulic model. Obtainment of this hydraulic sensitivity data was possible due to the capability to flow loose platelets in varying combinations and stacking sequences.

PLATELET
STACKING PINS



FRONT VIEW

BACK VIEW

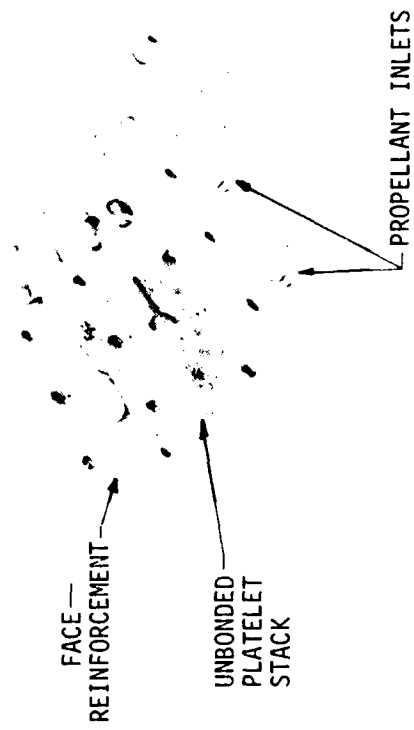


Figure 4-16. Cold Flow of Loose Superscale (10 X Geometric) Platelets

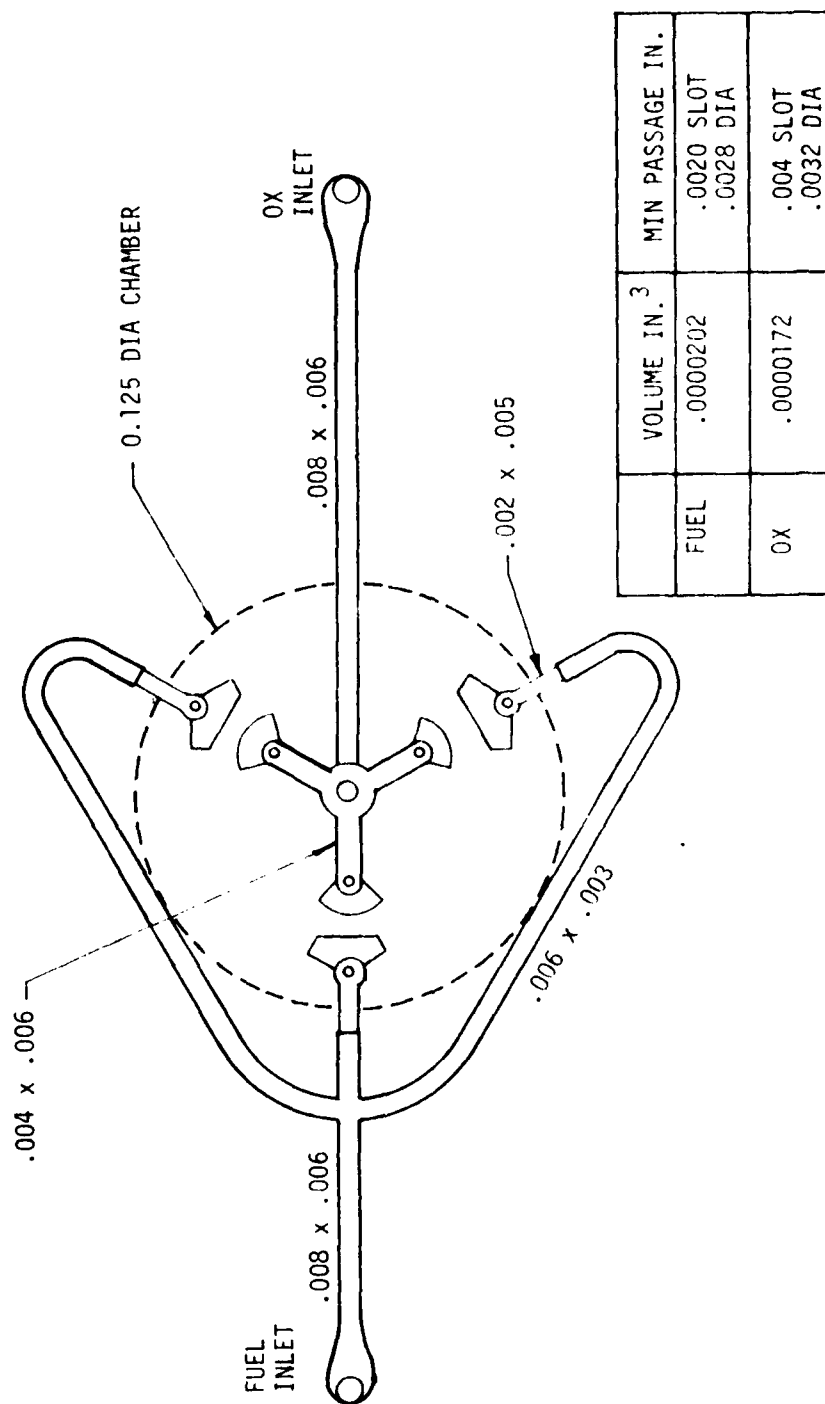
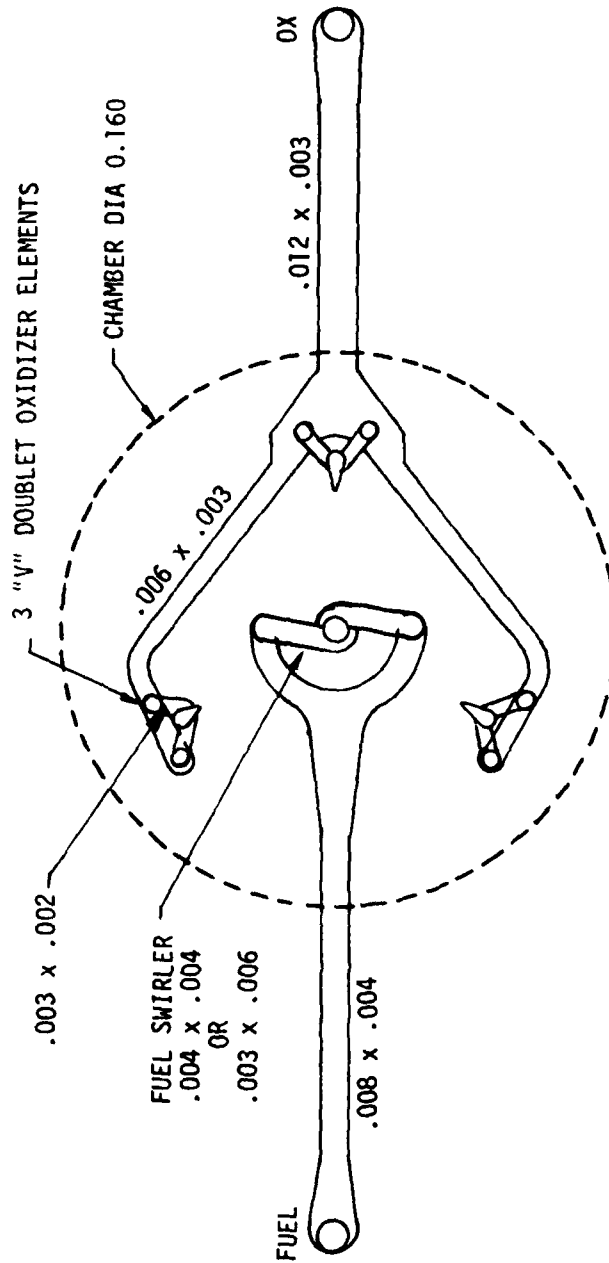


Figure 4-17. Three Element Splash Plate Injector Design



	VOLUME IN. ³	MIN PASSAGE IN.
FUEL	.0000191	.004/.003 SLOT .007 DIA
OX	.0000216	.002 SLOT .003 DIA

Figure 4-18. Fuel Swirler Three Element "V" Doublet Oxidizer Injector Design

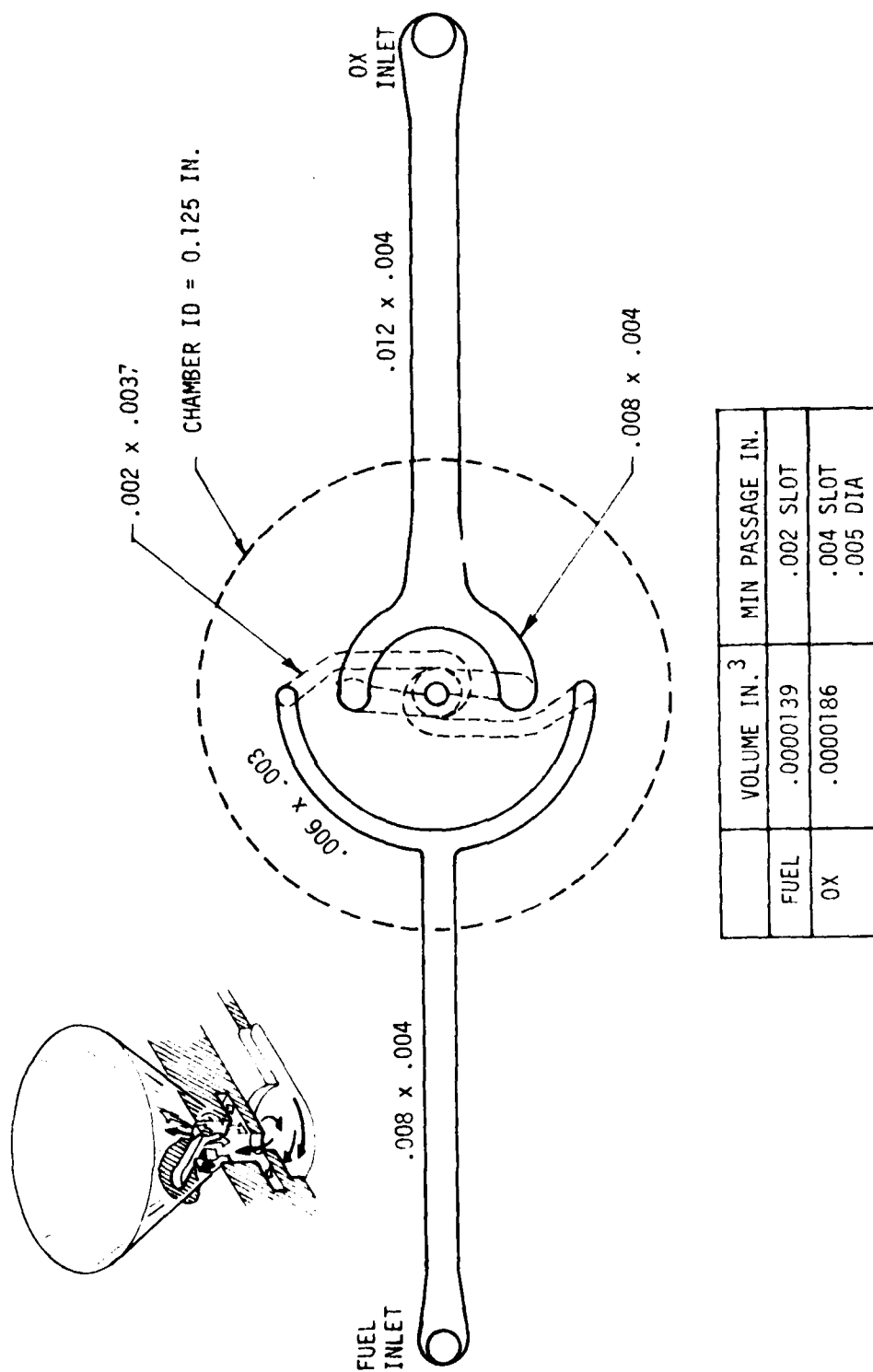


Figure 4-19. Coaxial Swirler Injector Design

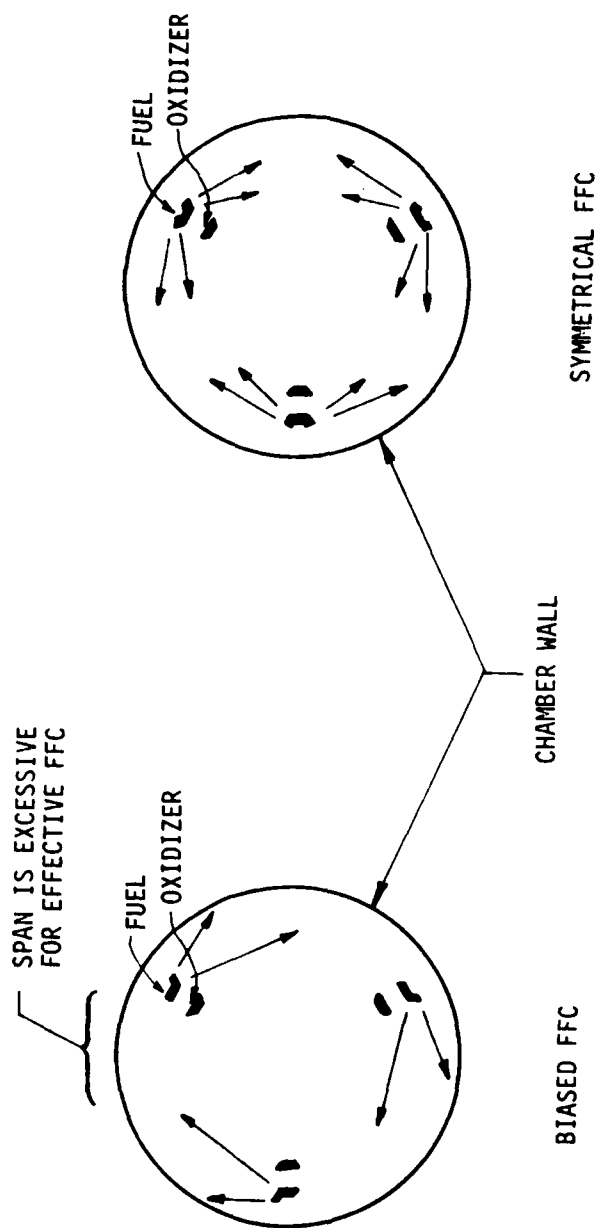


Figure 4-20. Symmetrically Cooled Versus Bias Cooled Splash Plate

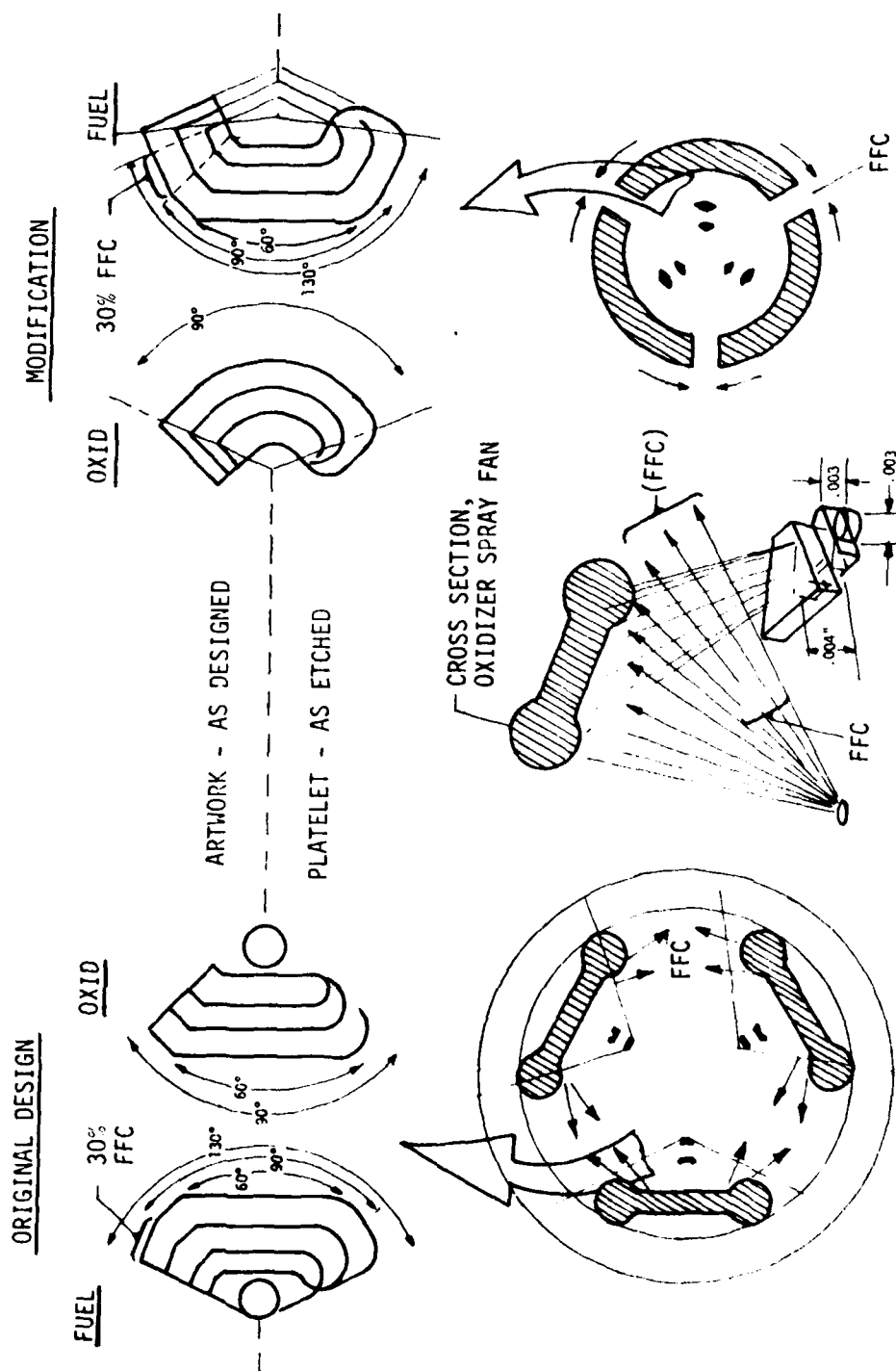


Figure 4-21. Splash Plate Modifications for Optimum Spray Distribution

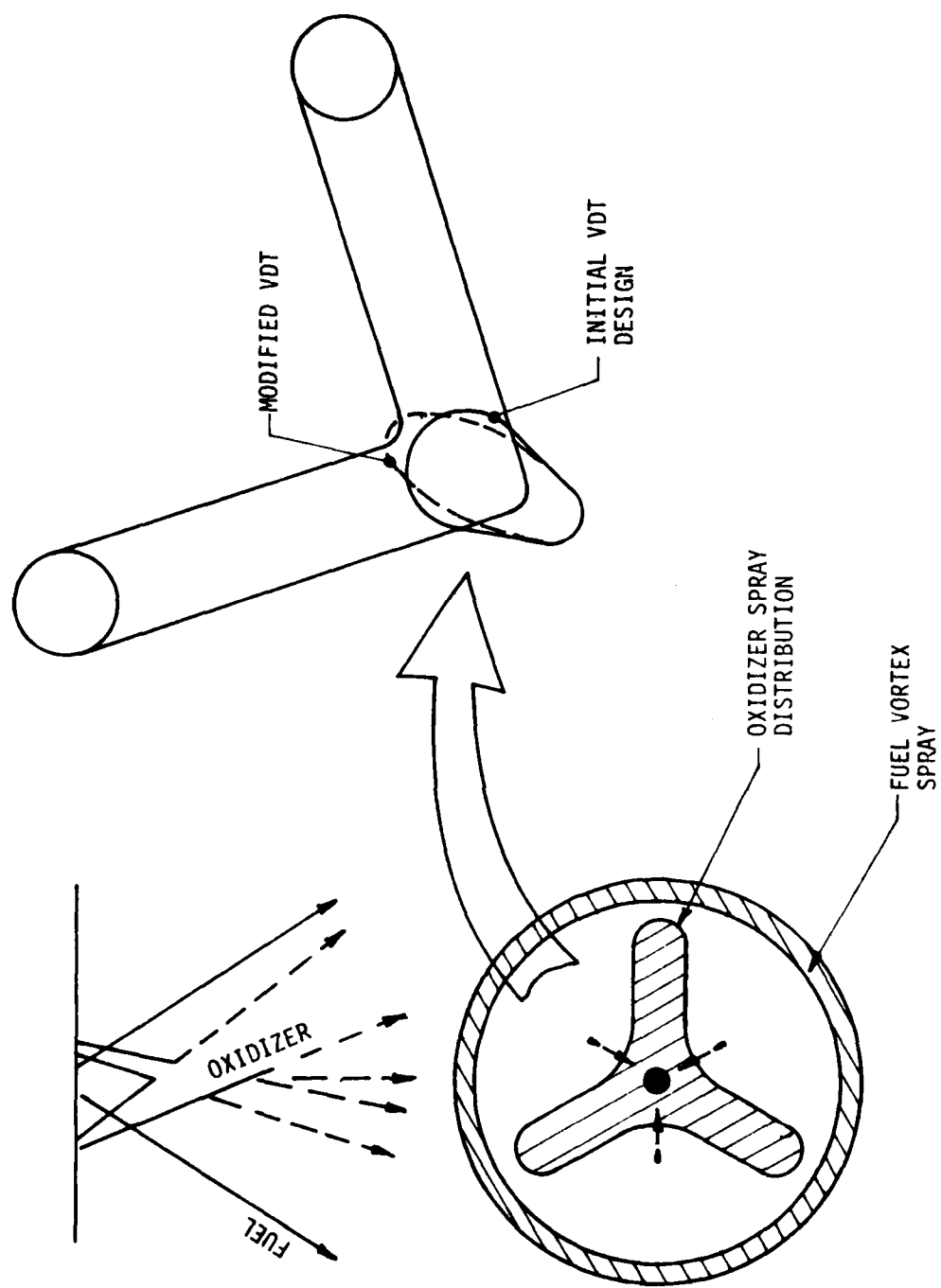
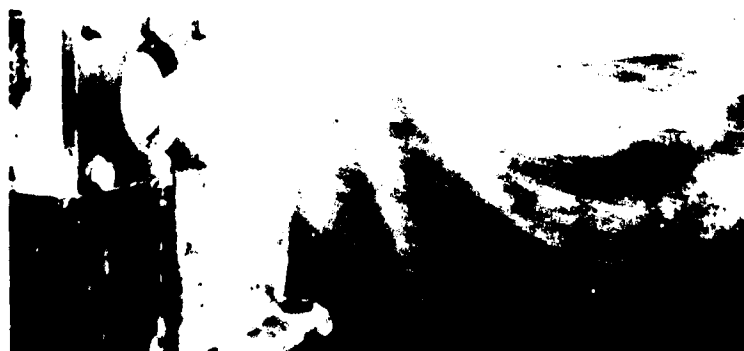


Figure 4-22. Modifications to "V" Doublet to Eliminate Oxidizer Penetration

INJECTOR: VORTEX/V-DOUBLET - MOD "O"



$\Delta P_f = 30$ PSID



$\Delta P_f = 100$ PSID



$\Delta P_f = 200$ PSID

Figure 4-23. Initial Vortex Designs at Reduced Flowrate

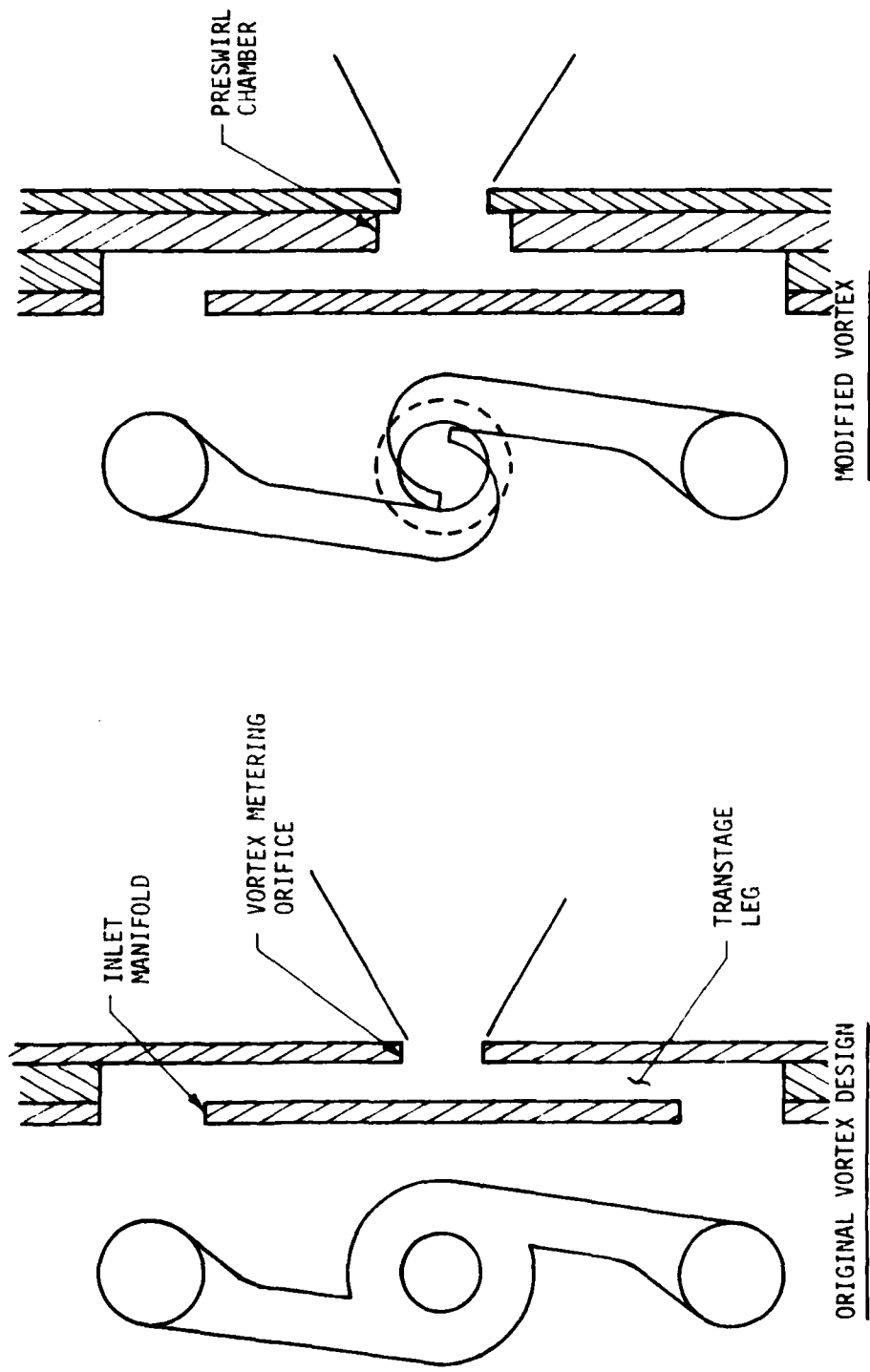


Figure 4-24. Modifications to Vortex Designs

3 SP-MOD "0"



$\Delta P_{ox} = 200 \text{ PSID}$



$\Delta P_{ox} = \Delta P_f = 200 \text{ PSID}$

3 SP-MOD A



$\Delta P_{ox} = 200 \text{ PSID}$



$\Delta P_{ox} = \Delta P_f = 200 \text{ PSID}$

Figure 4-25. Modified Splash Plate Distribution

VORTEX/VDT-MOD A



$\Delta P_f = 200 \text{ PSID}$

VORTEX/VDT-MOD B



$\Delta P_{ox} = \Delta P_f = 200 \text{ PSID}$



$\Delta P_f = 50 \text{ PSID}$



$\Delta P_{ox} = \Delta P_f = 50 \text{ PSID}$

Figure 4-26. Modified Vortex "V" Doublet Spray Distribution

INJECTOR: CO-AXIAL VORTEX/SWIRL CUP - MOD B



$\Delta P_f = 100 \text{ PSID}$



$\Delta P_{ox} = 50 \text{ PSID}$



$\Delta P_{ox} = \Delta P_f = 100 \text{ PSID}$

Figure 4-27. The Coaxial Injector; Oxidizer-Rich Core and Fuel-Rich Barrier

4.3, Engine Parameter Study (cont.)

4.3.3 Thrust Chamber Design

4.3.3.1 Nozzle Contour and Boundary Layer Loss

Preliminary performance estimates determined that considerable analytical uncertainty existed in the prediction of Boundary Layer Losses (ΔBLL) for 0.5 lb thrust class engines.

A literature survey to determine experimental nozzle efficiencies of small engines is summarized in Table 4-III. The empirical correlation of nozzle C_F efficiency plotted vs throat Reynolds number for these engines is shown in Figure 4-28. Also shown thereon are the 3 ranges of ΔBLL predicted by the candidate models. The JANNAF-recommended BLIMP program appeared to provide the best correlation and hence was used to provide the performance prediction. The $\epsilon = 100:1$ nozzle contour corrected for displacement boundary layer thickness, based upon the BLIMP model, is shown in Figure 4-29.

The 0.5 lbF engines were scheduled for testing in the ALRC Research Physics Laboratory with a vacuum test cell capability of < 0.1 psia. The 0.5 lbF engine was designed for a nozzle geometric ϵ of 143:1, as shown in Figure 4-29. When corrected for the assumed displacement of the boundary layer, this 143:1 geometric ϵ is calculated to result in an aerodynamic ϵ of 100:1. This nozzle ϵ was selected because it is the maximum ϵ , resulting in near optimum expansion to the cell back pressure at full thrust, and because it is overexpanded but still flows attached without separating at the minimum P_c .

4.3.3.2 Chamber Diameter

The minimum chamber diameter was based on ignition quenching considerations. The original CONTAM model formulation did not accurately predict cold engine performance on the 5 lbF engine program, although hot engine pulse characteristics were adequately modeled. It was hypothesized that the adiabatic quenching criterion during shutdown was in error. The formulation was consequently modified by using wall-temperature-dependent quenching criteria, which resulted in an excellent correlation of the 5 lbF test data and 100 lbF MIB engine pulsing characteristics. The original adiabatic quenching model results and the modified wall-temperature-dependent quenching model results, using the modified wall-temperature-dependent quenching criteria, are compared in Figure 4-30. Since previous design experience had established that the small 0.5 lbF engine would quench rapidly following valve closure, it is advantageous to maximize the chamber

TABLE 4-III

LOW THRUST, ROCKET ENGINE SURVEY

NO.	MANUFACTURER ¹	THRUST ¹	NOZZLE ¹	LOW THRUST, ROCKET ENGINE SURVEY			IDEAL ³ THRUST COEFFICIENT	THRUST EFFICIENCY ⁴
				PROPELLANT ¹	THROAT ² REYNOLDS NUMBER	ACTUAL ¹ THRUST COEFFICIENT		
1	Bell	1.0	Conical	Peroxide	59,200	1.640	1.751	0.936
2	Bell	1.5	Conical	Peroxide	79,600	1.675	1.751	0.956
3	Bell	1.0	Bell	H ₂ O ₄ -UDMH	8,510	1.765	1.872	0.943
4	Walter-Kidde	2.5	Conical	Peroxide	110,900	1.627	1.762	0.923
5	Marquardt	5.0	Bell	H ₂ O ₄ -UDMH	13,500	1.770	1.845	0.932
6	RRC	0.5	Conical	Hydrazine	44,000	1.758	1.831	0.960
7	RRC	1.0	Conical	Hydrazine	65,000	1.756	1.788	0.982
8	Hughes	1.5	Bell	Peroxide	48,000	1.760	1.845	0.921

LARGER ENGINES

9	Bell	50	Conical	Peroxide	535,000	1.690	1.744	0.969
10	Bell	24	Conical	Peroxide	288,000	1.675	1.744	0.960
11	Bell	100	Bell	N ₂ O ₄ /UDMH	222,000	1.743	1.845	0.945
12	RRC	25	Bell	Hydrazine	277,000	1.756	1.851	0.949

1. Taken directly from Reference (2); Survey of Liquid Rocket Space Propulsion Engines, AERCO Doc. No. 731176 (F. S. James).

2. $Re = \frac{\rho V_e D}{\mu}$; properties estimated at throat conditions.

3. Taken from thrust coefficient tables of Reference 1 and 2.

4. Actual thrust coefficient/ideal thrust coefficient.

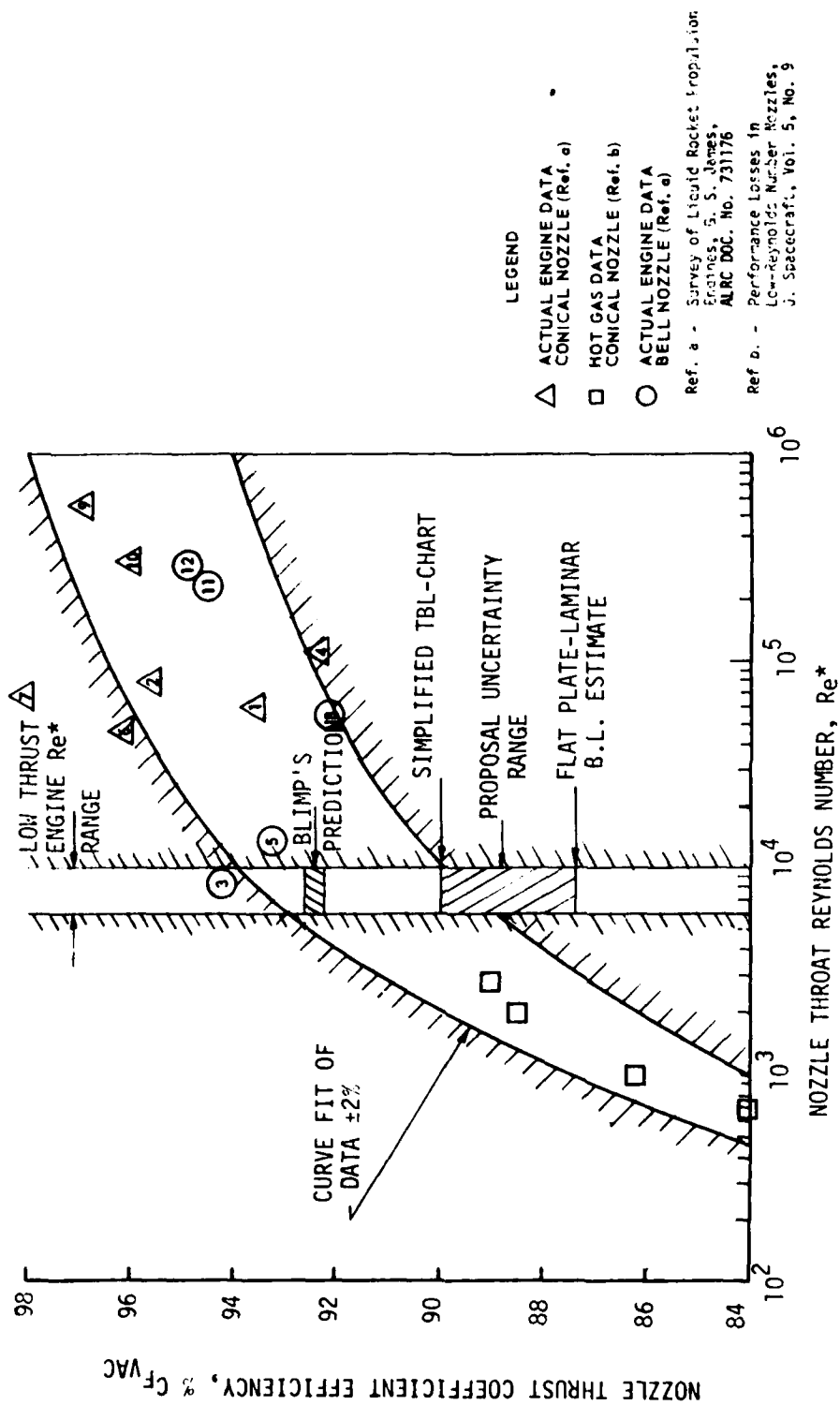


Figure 4-28. JANNAF BLIMP Model - Engine Boundary Layer Performance Efficiency Prediction Compared to Other Models and Experimental Data

NOZZLE CONTOUR COMPARISON

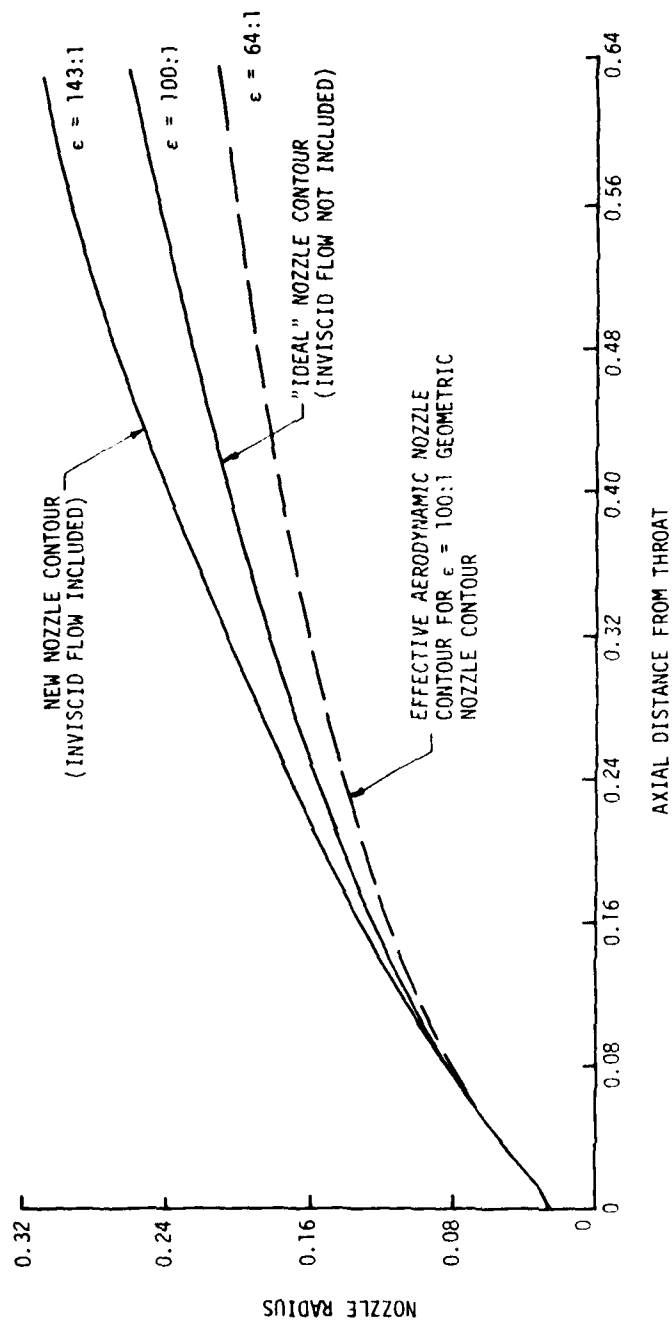


Figure 4-29. Nozzle Contour vs Boundary Layer Thickness

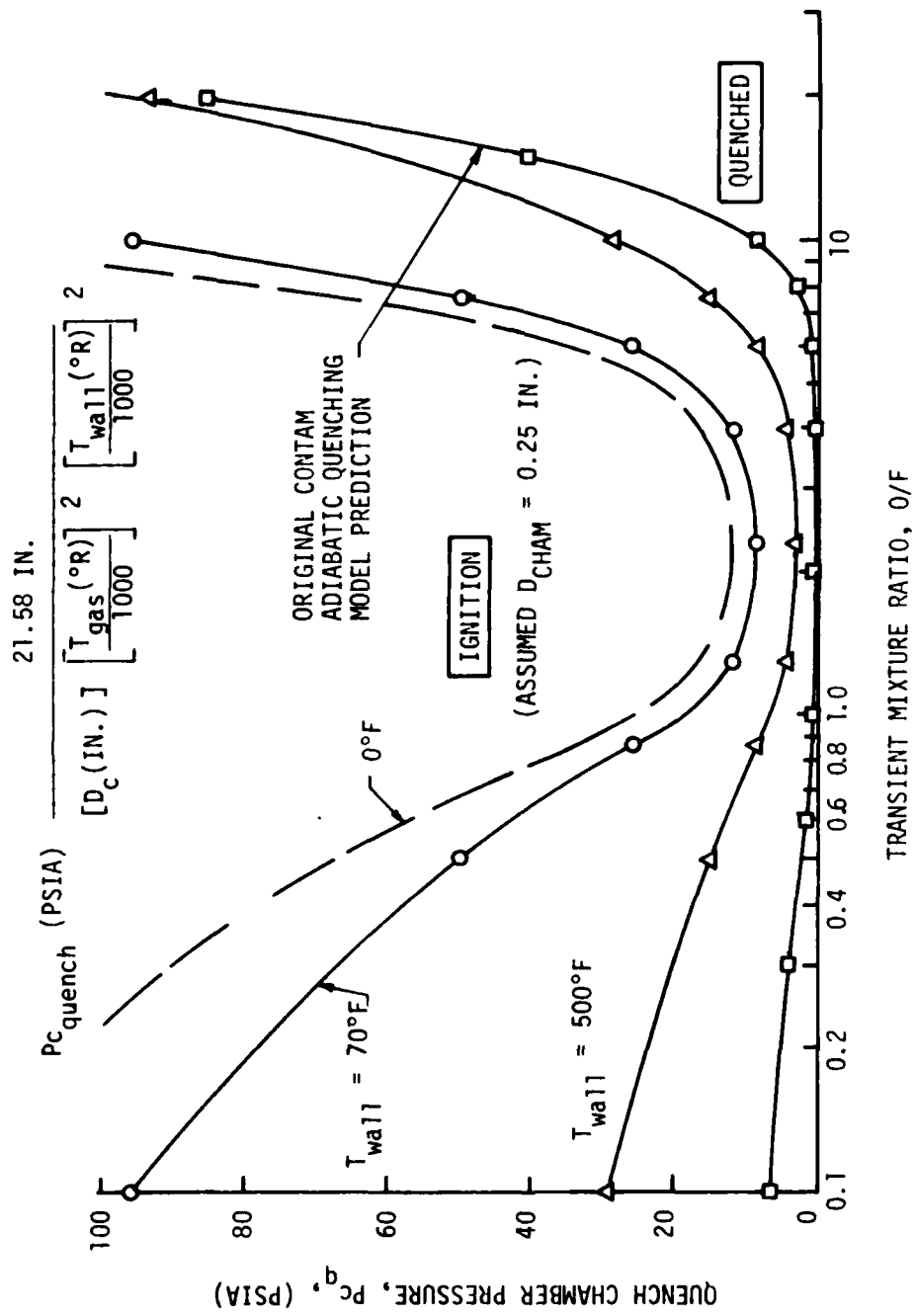


Figure 4-30. Modified CONTAM Quenching Prediction

4.3, Engine Parameter Study (cont.)

diameter to delay quenching as long as possible in order to maximize cold engine pulse performance. However, based on the analysis summarized on Figure 4-31, it would not be desirable to exceed the 16:1 chamber contraction ratio since the propellant injection velocity would then exceed the one-dimensional combustion gas velocity. This would likely give rise to hot-gas recirculation patterns within the chamber which degrade compatibility. Thus a maximum allowable chamber diameter of .225 in. was selected for the $P_c = 125$ psia engine.

Previous correlations of the injector face operating temperature for the baseline splash plate elements showed it to be pattern-density-dependent (Figure 4-32). This implied that even though a 16:1 chamber contraction ratio was desirable for ignition, a smaller diameter at the injector face is needed to reduce face temperature and minimize heat soakback into the valves. The chamber insert providing this function is shown in Figure 4-33. Based upon the calculated axial energy release profile, its contour was designed to achieve a nearly constant gas velocity profile throughout.

The modified Priem vaporization analysis for 0.5 lbf class engines predicted reasonable vaporization efficiencies in chamber lengths ≤ 1.0 in. Based on combined vaporization and mixing/cooling considerations, it was estimated that a nominal chamber length ~ 1.5 in. would be required. Consequently, chamber lengths of 1.0 in. and 2.0 in. were planned for testing during Phase II. The final chamber length for the Phase III demonstration engine could then be interpolated from the resulting Phase II performance and thermal data.

4.3.4 Valves

4.3.4.1 Valve Selection

Valve response time and dribble volume are critical for successful attainment of the desired minimum impulse bits. The size, weight and cost of the valve are also very important in terms of potential total engine size, weight, and cost.

The performance requirements for the valve were determined to be within the current state-of-the-art for both the torque motor and the solenoid-actuated valves of the required size.

Valve designs currently produced combine valve elements in different ways, with 3 basic types dominant. One is solenoid-actuated, using a conventional cylindrical armature with sliding motion of

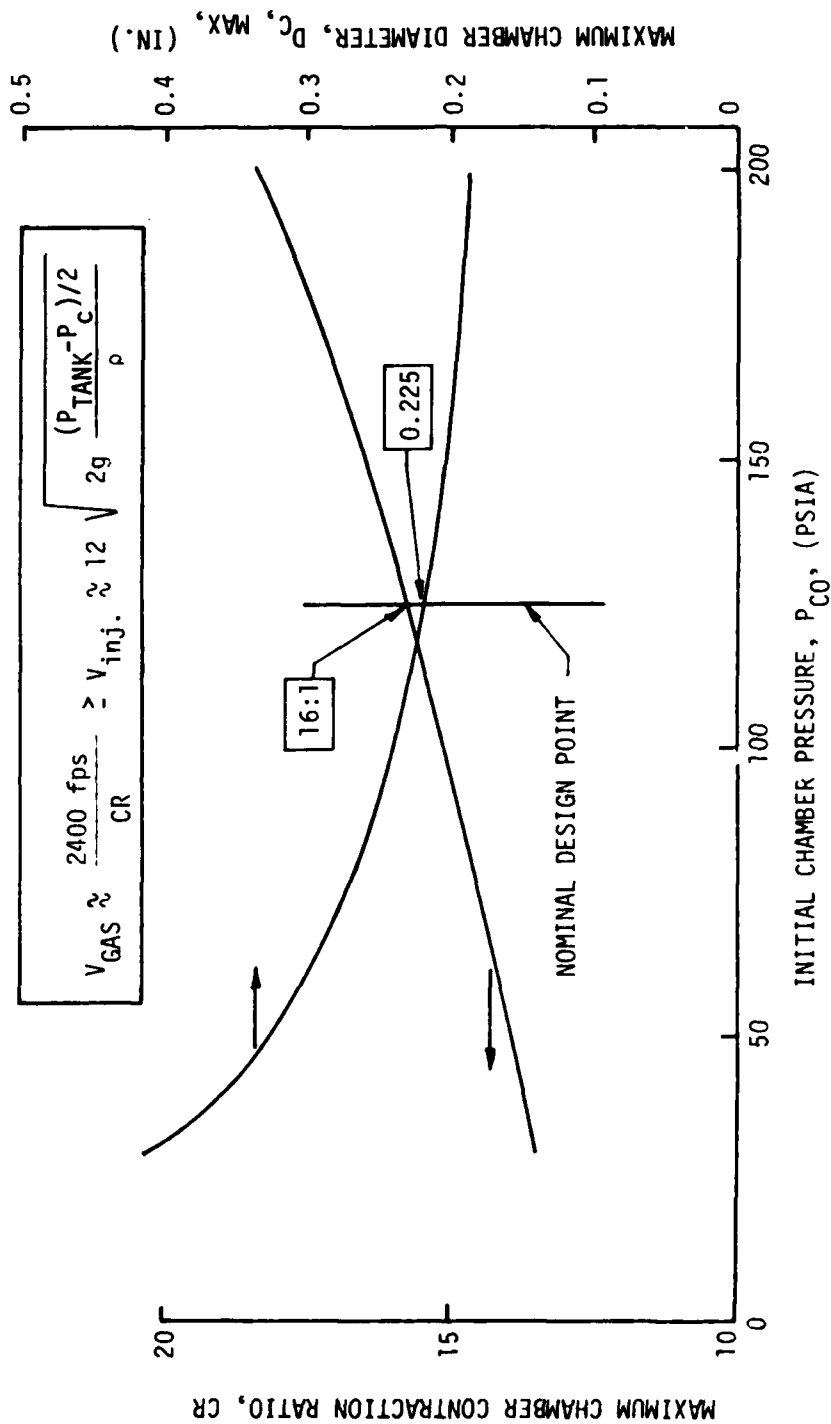


Figure 4-31. Combustion Gas Velocity vs Propellant Injection Velocity

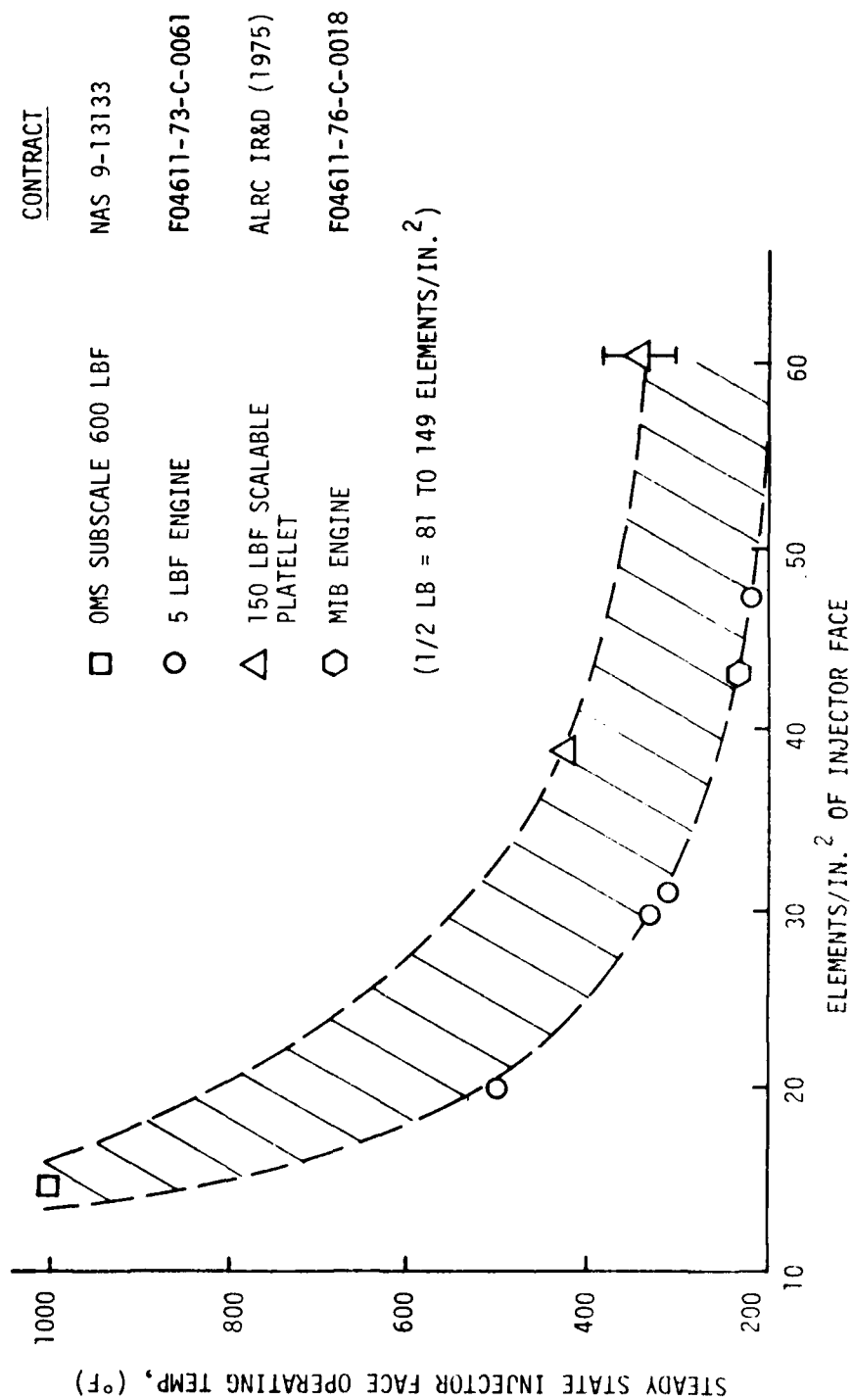


Figure 4-32. Injection Element Density Versus Injector Face Operating Temperature

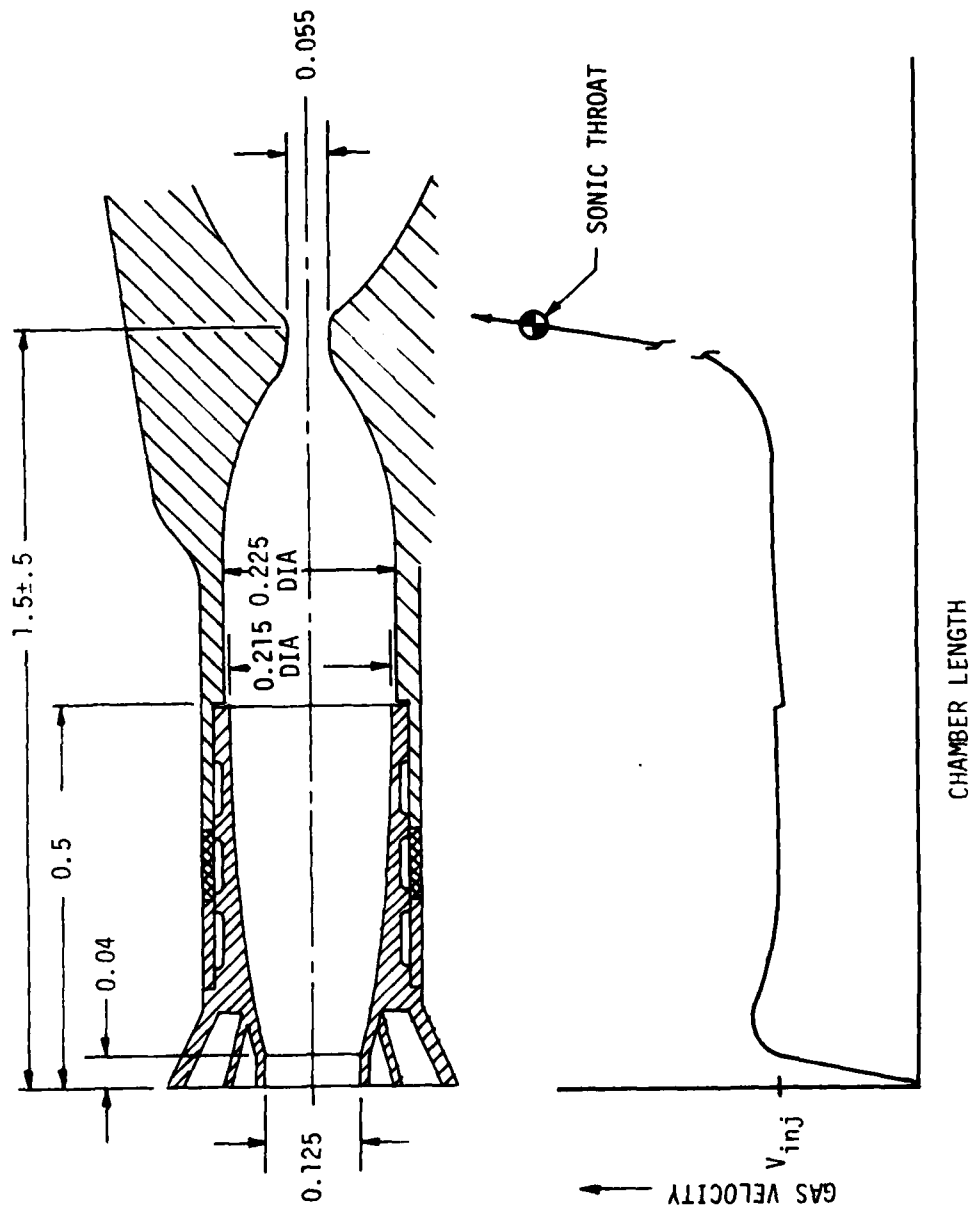


Figure 4-33. Chamber Contour vs Head End Heat Flux

4.3, Engine Parameter Study (cont.)

the armature and poppet as the driver. This approach is typical of valves made by vendors such as Carleton Controls, Circle Seal, Eckel, Futurecraft, Marquardt, Marotta, Pyronetics, Valcor and Wright Components. A second solenoid type, made by MOOG, Inc., Marquardt, and the Systems Division of Parker Hannifin, uses a flat face armature as the driver and eliminates relative sliding motion. The third basic design, typical of valves made by Hydraulic Research and MOOG, Inc., uses a double air gap torque motor with pivoting armature and flexure sleeves. Since current production valves of this type were capable of meeting the performance requirements for the 0.5 lbF thruster program, additional valve technology work was not necessary. Selected for use was a MOOG mechanically linked, bipropellant torque motor valve with soft-on-hard shutoff sealing (Figure 4-34). It was selected based on the following factors:

- The basic mechanically linked concept has demonstrated high reliability in similar applications.
- The valves are flight-qualified and have been produced in quantity.
- Torque motor valves have been successfully integrated with an injector/thruster at both the 5 lb and 100 lb thrust levels.
- The valve has no rubbing seals or sliding parts.
- The construction materials have been demonstrated to be fully compatible with the propellants.
- Minor modifications to the design would allow for reduced weight and power consumption while still achieving the required performance.

4.3.4.2 Valve Design and Interfaces

The Phase I valve design and Phase II and III fabrication was performed under subcontract by MOOG, Inc., East Aurora, New York. The selected design was a smaller version of that produced for the MMIII PSRE. Scaleability had been proven earlier on the 5 and 100 lb thrust class bipropellant engine contracts. Minimum dribble volume is achieved by bolting

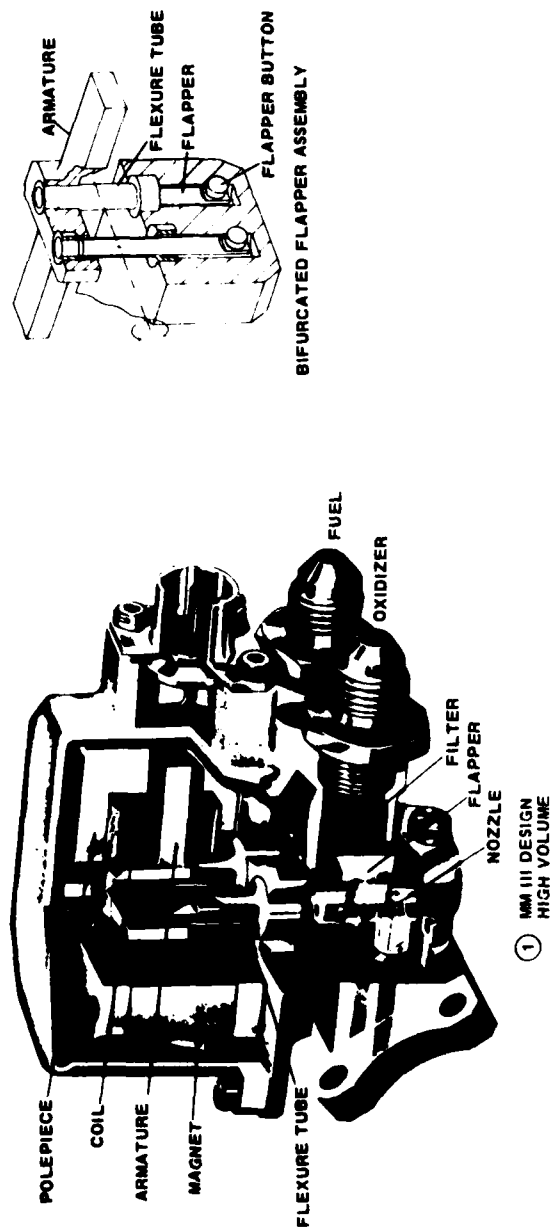


Figure 4-34. M00G Bipropellant Torque Motor Valve

4.3, Engine Parameter Study (cont.)

the valve directly to the injector. The basic torque motor design, materials, connector, cover, and inlet filter type were unchanged from the flight-qualified design. This 0.5 lb thrust version of the MOOG valve has been designated Model 51E112.

Figure 4-35 shows a section view of a typical MOOG bi-propellant torque motor valve. These direct-acting valves use a torque motor to provide simultaneous opening and closing of a pair of control orifices. Each orifice is formed by the peripheral opening between a nozzle and a flapper.

The flappers are located in separate, fluid-sealed chambers to give complete isolation of the fuel and oxidizer circuits. The flappers are mounted on separate flexure tubes which are arranged side by side. A common armature member provides torque to the flapper assembly to provide simultaneous actuation of the fuel and oxidizer.

Valve operation is as follows. When an electrical step input is applied, the resultant coil flux produces a torque tending to open the nozzle orifices. The electrical input saturates the magnetic circuit of the torque motor, providing a high driving force which fully opens the flappers against the stops.

Removal of the electrical signal permits the flappers to return to the closed position. Symmetrical on-and-off transient characteristics are obtained by matching the magnetic bias force to the net driving force from the electrical signal input. The bias force is established by initial setup of the torque motor so that no adjustments or separate bias springs are needed.

Torque motor valves have been made in a range of sizes for 0.3 to 300 lb thrusters. The 5 msec response times are attainable for the 0.5 lbF application without the use of special electrical drive circuits or changes in materials from those used previously.

The required close coupling is achieved by mounting the valve directly to the backside of the injector (Figures 4-36 and 4-37), thereby forming the valve seating between the valve flapper buttons (soft) and the polished seating surface.

The valve-to-injector interface seals are a spring-energized Teflon seal design fabricated by Fluorocarbon, Inc. Each of the annular seal grooves is vented, thereby requiring the failure of both seals

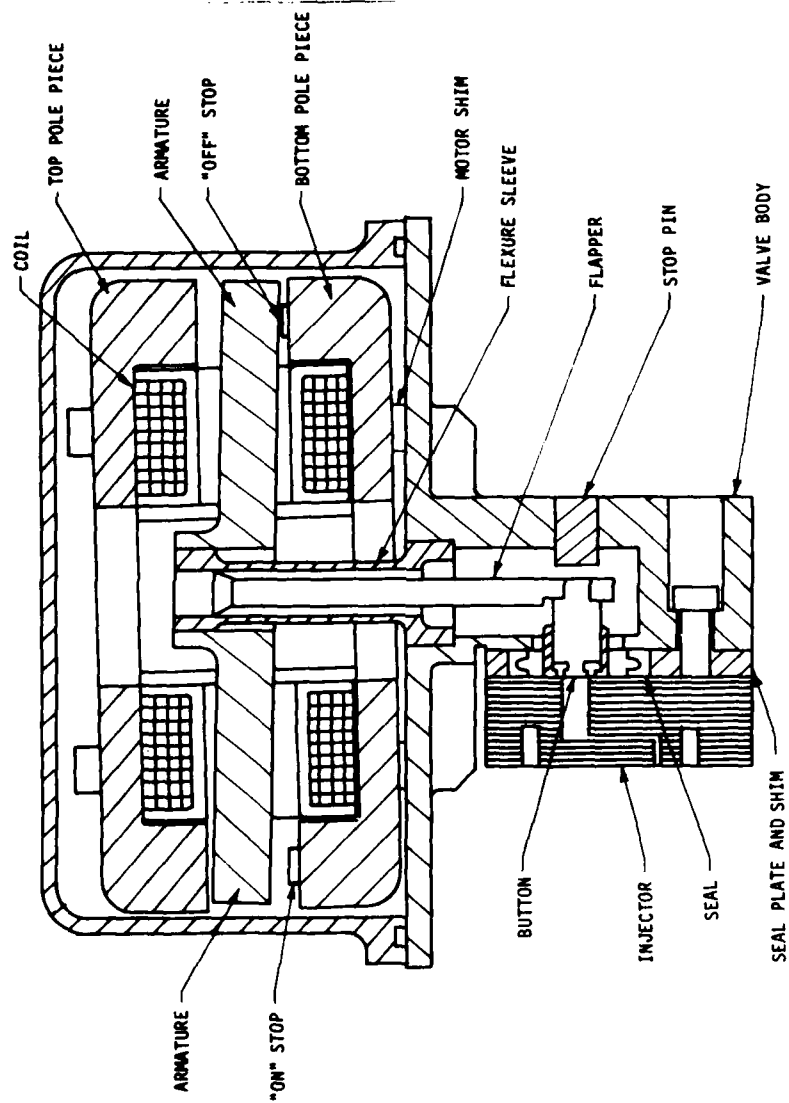


Figure 4-35. Torque Motor Cross Section and Functional Parts

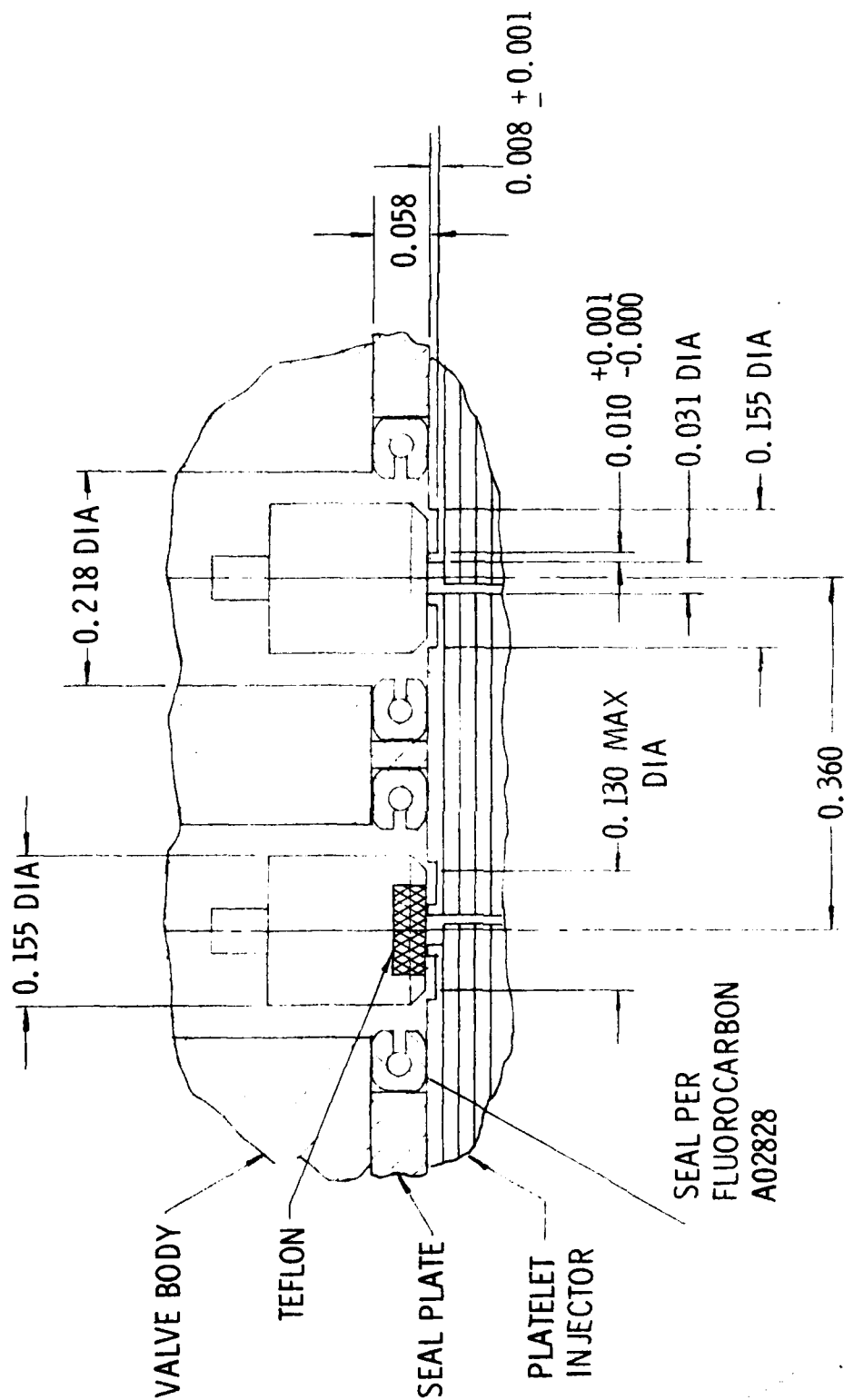


Figure 4-36. Integrated Valve/Injector Seals Configuration

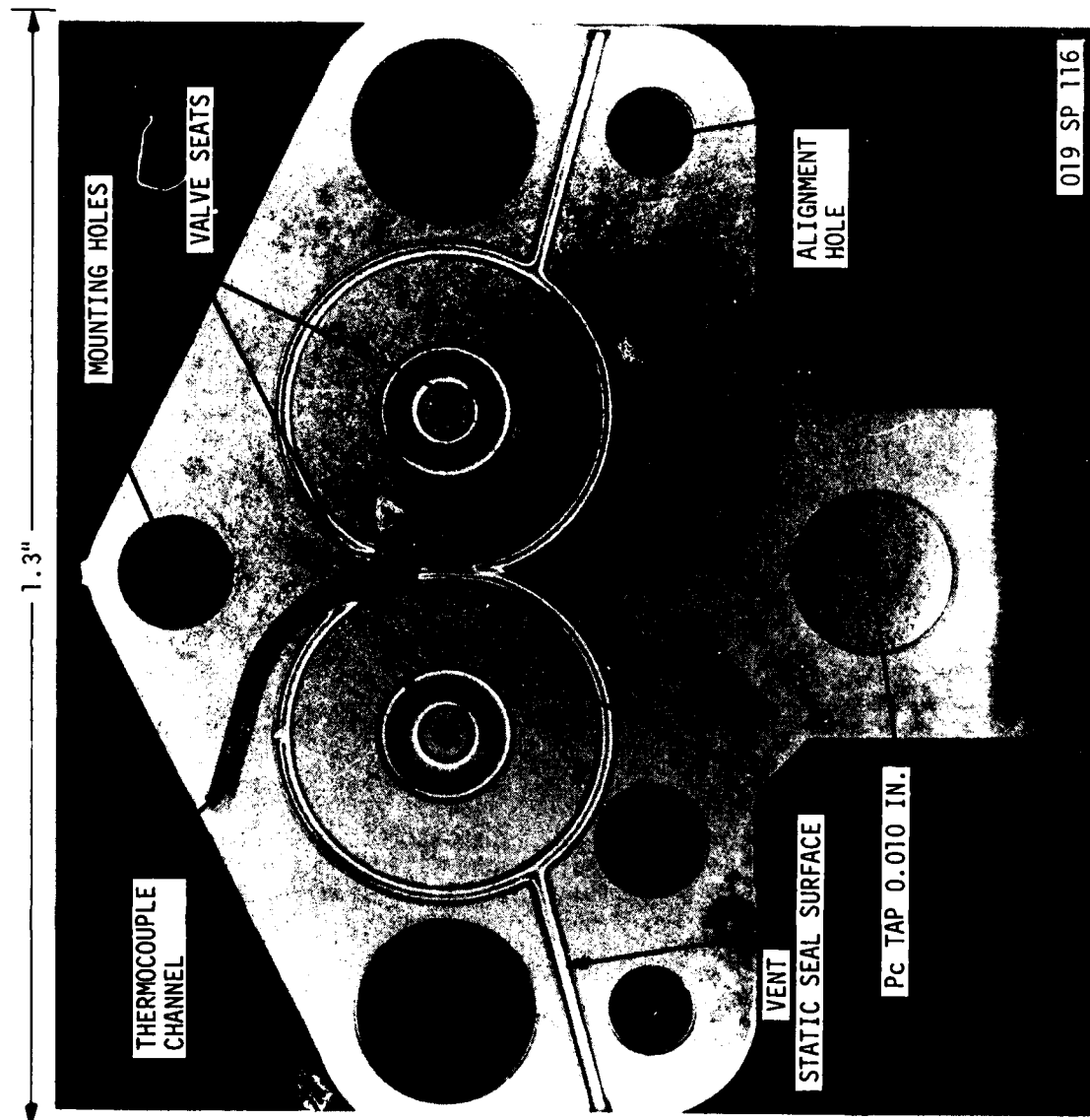


Figure 4-37. Photo-etched Valve Seats Are Part of the Injector

4.3, Engine Parameter Study (cont.)

to create an inter-propellant leak. The seals are retained by a seal plate, sandwiched between the injector and the MOOG valve (Figure 4-36). The valve/injector assembly is held together by 3 #4-40 bolts which pass through the injector and into threaded holes in the valve (Figure 4-38).

For this engine application, the in-line propellant inlet ports common to MOOG valves have been rotated 90° to the vertical (Figure 4-38). This change to the baseline MOOG valve was designed to shorten the overall engine length and provide for ease of mounting to the thrust takeout of the test fixture. The propellant inlets are MS 33656-4 fittings with integral filters, sized for 10 nominal filtration. The valve employs a 2 pin Bendix electrical connector, PTO 2H-8-2P.

MOOG, Inc. conducted analyses to optimize the flexure tubes, valve flappers and shutoff elements in order to provide the 10⁶ cycle life capability. The button design used was similar to that of the MOOG Model 52E163 (5 lbF Engine AJ10-181) bipropellant valve. This valve demonstrated a cycle life greater than one million cycles.

Analyses indicated that, under normal operating conditions, the flexure sleeves operate at a stress level which is considerably less than the fatigue strength of the flexure sleeve material (85 Ksi vs 110 Ksi). Details of these analyses are provided in Appendix A.

Valve response was considered critical in terms of achieving the desired engine pulsing performance. The response characteristics of the selected valve were estimated at the time of valve selection by comparing it with similar valves for which response data existed. Response data for Model 51 x 101 shows that the selected valve will readily meet the 0.005 second opening and closing response requirements. For example, the opening response of Model 51 x 101 is 0.0017 sec at 200 psi and 28 vdc. The unbalance pressure area of Model 51 x 101 is about 30% larger than that of Model 51E112. This minimizes the effect of the difference in operating pressures. The pull-in current for the Model 51 x 101 valve at 300 psi is 0.081 amps, demonstrating that Model 51E112 will have a very high force margin for this application.

4.3.5 CONTAM Analyses

This section documents the parametric analysis conducted for the 0.5 lbF bipropellant engine with the CONTAM program. The program used was CONTAM II, "Plume Contamination Effects Prediction," as described in AFRPL TR 73-46. The purpose of this analysis was to determine the

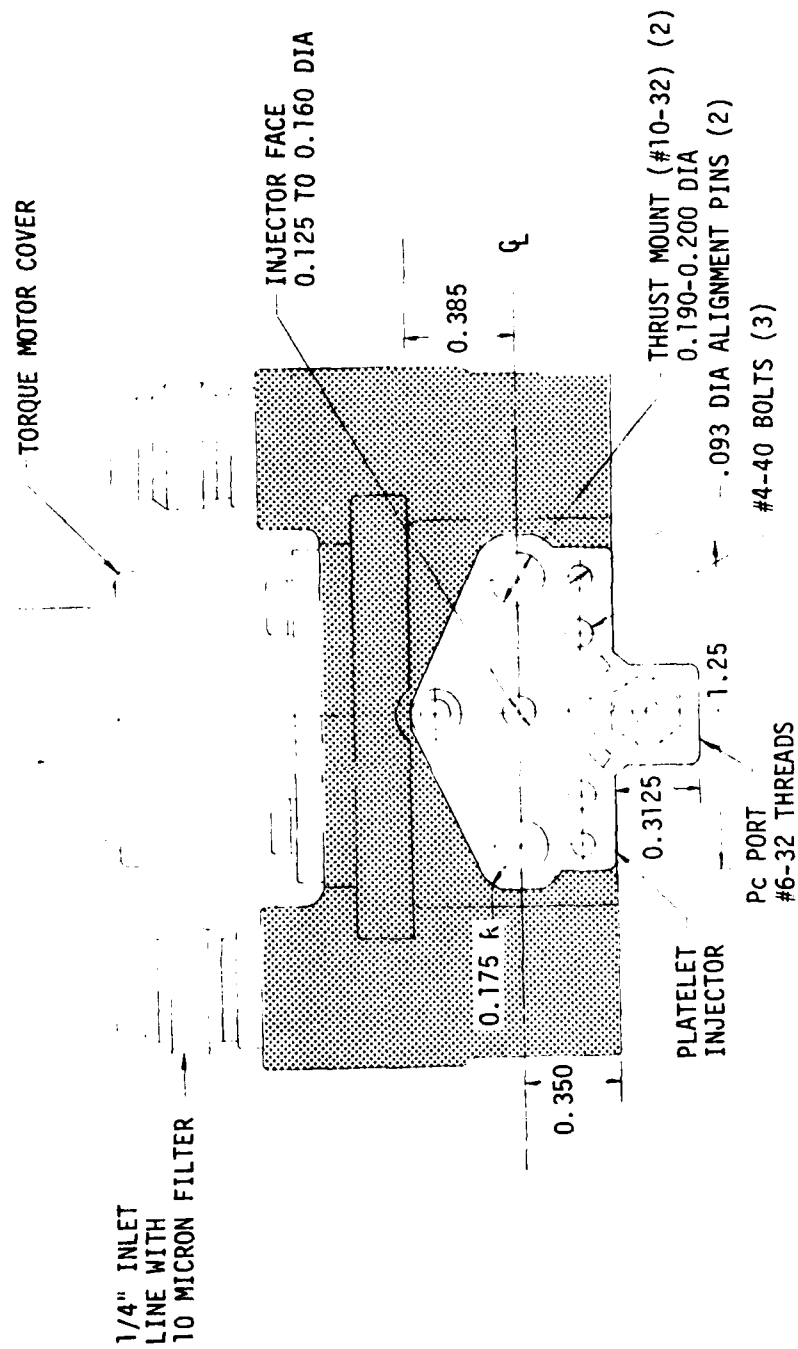


Figure 4-38. Valve/Injector Interface Bolt Pattern

4.3, Engine Parameter Study (cont.)

interaction of several engine design parameters on the pulsing and contamination performance. Prior to the parametric study, the CONTAM model had to be fine-tuned in order to match the previously predicted results of the steady-state propellant vaporization analyses (Priem generalized length model).

The standard atomization model predicted the droplet diameter to be on the order of 5 microns for both the fuel and oxidizer. To obtain the same diameters in the CONTAM prediction, the droplet size factors for the fuel and oxidizer were selected to be 0.087 and 0.130, respectively. Subsequent use of these droplet size factors, however, resulted in the vaporization efficiency predictions of CONTAM being significantly lower than predicted by the Priem analysis and being independent of the fuel and oxidizer burning rates. Because this was inconsistent with anticipated results, problems with the combustion model within CONTAM were suspected.

Examination of the droplet model within CONTAM revealed that the driving force on the droplets was simply the aerodynamic drag of the vaporized propellants accelerating the droplets out of the chamber. Because this aerodynamic drag is a function of the droplet diameter squared while the droplet mass varies inversely with diameter cubed, a strong influence exists between droplet diameter and droplet acceleration rates. The droplet model indicates that this acceleration rate becomes very high as the diameters become very small (<10 microns). Likewise, the Priem model predicts high acceleration rates for small droplets, but predicts the burning rate increases more rapidly, resulting in higher vaporization efficiencies. Inasmuch as the ALRC application of the Priem model for prediction of percent vaporization had been proven in use, and since it was in disagreement with the linearized burning rate approximation built into CONTAM II (for small element size), the droplet size factors were increased in CONTAM II to agree with the Priem model. This timesaving factor eliminated the need to reprogram the CONTAM II small droplet model. Doubling the droplet size factors for both the fuel and oxidizer (to 0.174 and 0.260, respectively) resulted in the normal behavior of the CONTAM vaporization calculations.

The standard Priem model analysis predicted the propellant vaporization efficiency to be 99% for the oxidizer and 95% and 96%, respectively, for the single and double fuel flame. (The latter includes monopropellant burning of the fuel.) To obtain these same propellant vaporization rates within the CONTAM model, the corresponding burning rates were:

4.3, Engine Parameter Study (cont.)

Oxidizer Burning Rate, K'_{ox} , DDD1 (145)	=	0.0116
Fuel Burning Rate, K'_{fu} , DDD1 (125)	=	0.0063
Monopropellant Burning Rate, DDD1 (126)	=	0.471
DDD1 (127)	=	0.00942
DDD1 (128)	=	0.66

The modeling of the higher NO level (MON-X) oxidizers would have required the modification of the oxidizer property data input to CONTAM. However, these data for the MON-X oxidizers are not readily available, thus the decision was made to simulate the MON-X oxidizers by using the MON-1 property data. A review of existing data yielded conflicting results as to the ignition of the MON-X oxidizers. The primary difference between the MON-1 and MON-X oxidizers under transient combustion characteristics is the vapor pressure/temperature relationship. The vapor pressure increases with an increase of the % NO in the oxidizer. This increased vapor pressure of the MON-X oxidizers was simulated with the MON-1 oxidizer by adjusting the MON-1 inlet temperature to a higher value in order to yield the desired vapor pressure.

A total of 30 different cases (not including the 23 calibration pre-runs) were identified in order to completely model the 0.5 lbf engine parameters. Table 4-IV is a case-by-case description of each of the 30 valid cases modeled with the CONTAM program. The major parameters varied in this analysis are L' , propellant temperature, electrical pulse width (EPW), injector dribble volume, tank blowdown pressures, and MON-X content.

The timing of significant events and primary outputs of the CONTAM parametric study are tabulated in Table 4-V, and are illustrated graphically in Figures 4-39 through 4-50. The significant conclusions of this study are listed below.

- ° CONTAM predicted that the ignition delay times were greatly increased with higher propellant inlet temperatures. It is not believed, however, that this prediction is indicative of a real engine.

TABLE 4-IV

CONTAM MODEL CASE VARIABLES

CASE	DESCRIPTION						
1	Baseline Design*, Cold Start ($T_p = T_{JO} = T_{co} = T_{ambient}$)						
2	Baseline Design, Hot Start ($T_p = 70^{\circ}\text{F}$, $T_{JO} = 150^{\circ}\text{F}$, $T_{co} = 500^{\circ}\text{F}$)						
3	$L' = 1.0''$, Cold						
4	$L' = 2.0''$, Cold	L' Variation - Hot and Cold Engines					
22	$L' = 1.0''$, Hot						
23	$L' = 2.0''$, Hot						
5	$T_p = 20^{\circ}\text{F}$, $T_{JO} = T_{co} = 20^{\circ}\text{F}$						
6	$T_p = 50^{\circ}\text{F}$, $T_{JO} = T_{co} = 50^{\circ}\text{F}$						
7	$T_p = 100^{\circ}\text{F}$, $T_{JO} = T_{co} = 100^{\circ}\text{F}$	T_p Variation					
8	$T_p = 120^{\circ}\text{F}$, $T_{JO} = T_{co} = 120^{\circ}\text{F}$						
9	$T_p = 120^{\circ}\text{F}$, $T_{JO} = 150^{\circ}\text{F}$, $T_{co} = 500^{\circ}\text{F}$						
10	EPW = 0.005 sec, Hot						
11	EPW = 0.020 sec, Hot						
12	EPW = 0.040 sec, Hot	EPW Variation Hot and Cold Engines					
20	EPW = 0.005 sec, Cold						
21	EPW = 0.020 sec, Cold						
14	Dribble Volume = 0.000015 in. ³ , Cold	Dribble Volume Variation					
15	Dribble Volume = 0.000030 in. ³ , Cold						
16	$P_T = 200$ psia, Cold						
17	$P_T = 133$ psia, Cold	Tank Blowdown Variation					
18	$P_T = 100$ psia, Cold						
19	$P_T = 80$ psia, Cold						
24	$P_T = 80$ psia, $T_{JO} = 150^{\circ}\text{F}$, $T_{co} = 500^{\circ}\text{F}$, $T_p = 120^{\circ}\text{F}$						
25	$P_T = 80$ psia, $T_{JO} = T_{co} = T_p = 20^{\circ}\text{F}$	Temp. Sensitivity at end of 5:1 blowdown					
30	$P_T = 80$ psia, $T_{JO} = T_{co} = T_p = 120^{\circ}\text{F}$						
	<u>MON Level</u>	<u>T_{ox}</u>	<u>T_F</u>	<u>P_T</u>	<u>T_{JO}</u>	<u>T_{co}</u>	
26	10	139°F	120°F	400 psia	150°F	500°F	
27	10	139°F	120°F	100 psia	150°F	500°F	
28	14	140°F	120°F	133 psia	150°F	500°F	Ox-MON Level Variation
29	24	176°F	120°F	400 psia	150°F	500°F	

*Baseline Design

 $P_T = 400$ psia $L' = 1.5''$

EPW = 0.0010 sec

Ox Drib. Vol. = .000020 in.³Fuel Drib. Vol. = .000020 in.³ $T_{ox} = T_f = 70^\circ\text{F}$

TABLE 4-V

1. The first step is to identify the problem or question that needs to be answered. This involves understanding the context and the specific requirements of the task.

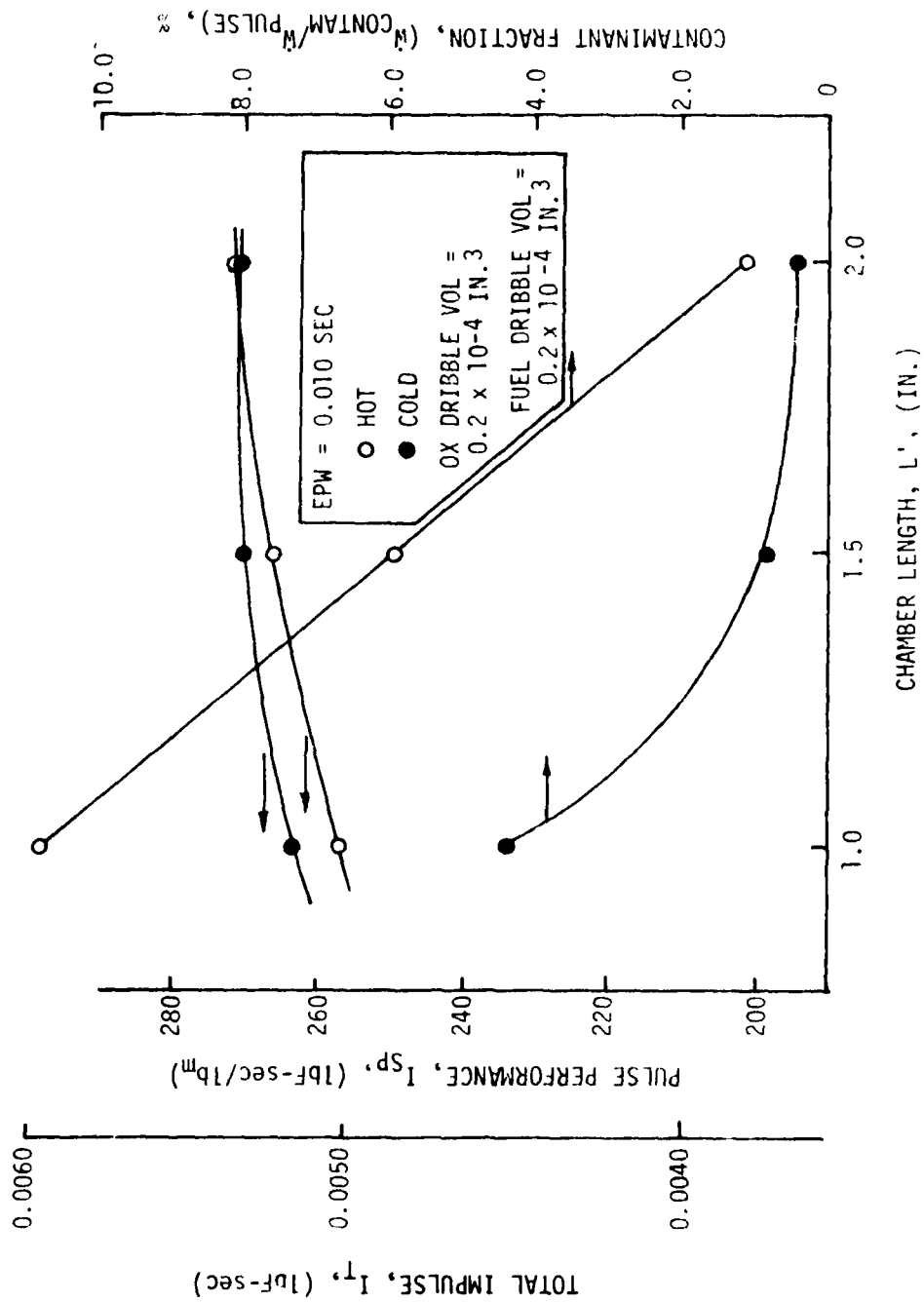


Figure 4-39. Chamber Length vs Performance and Contaminant Fraction

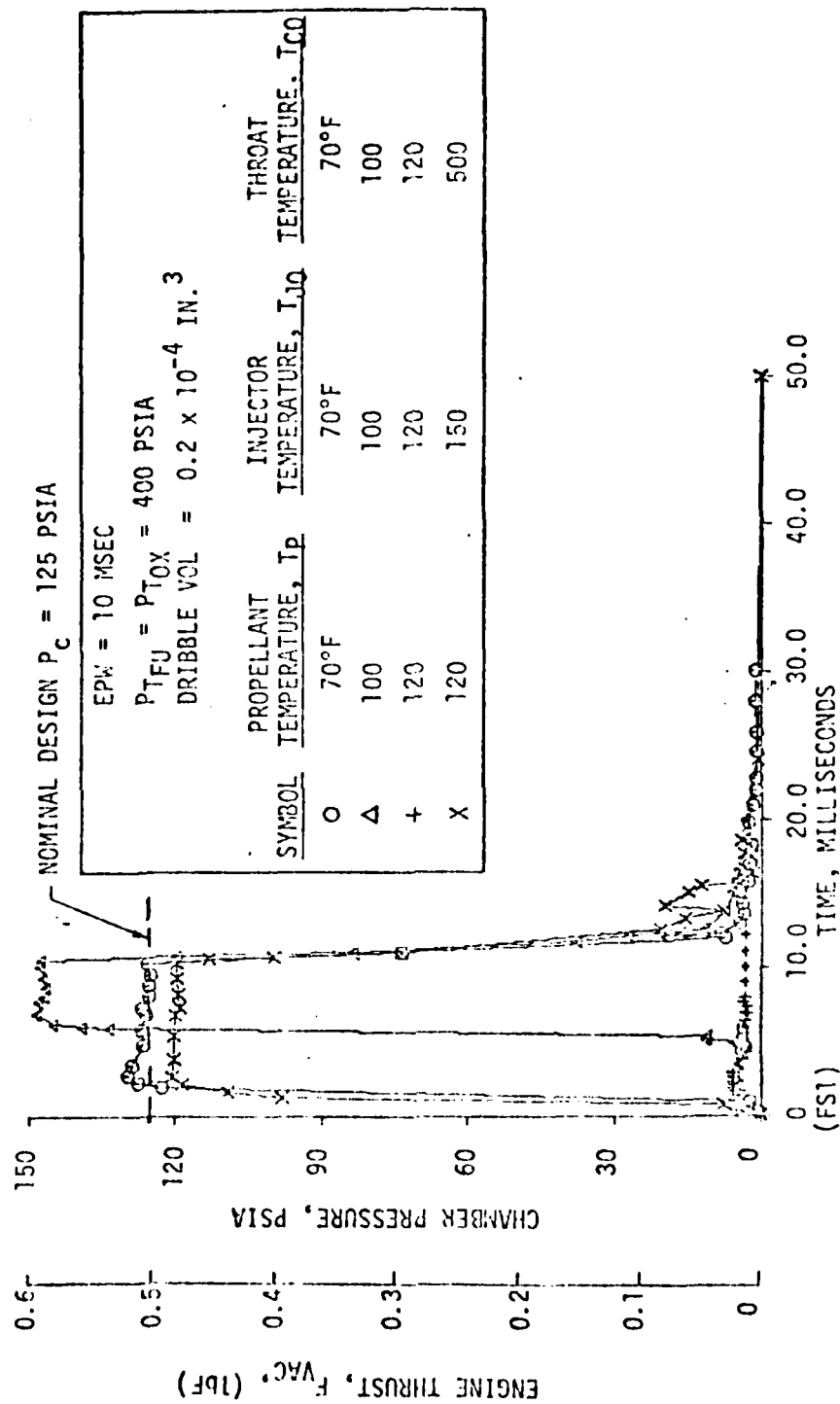


Figure 4-40. Computer Plots of CONTAM Transient Responses (Variable Propellant Inlet Temperatures)

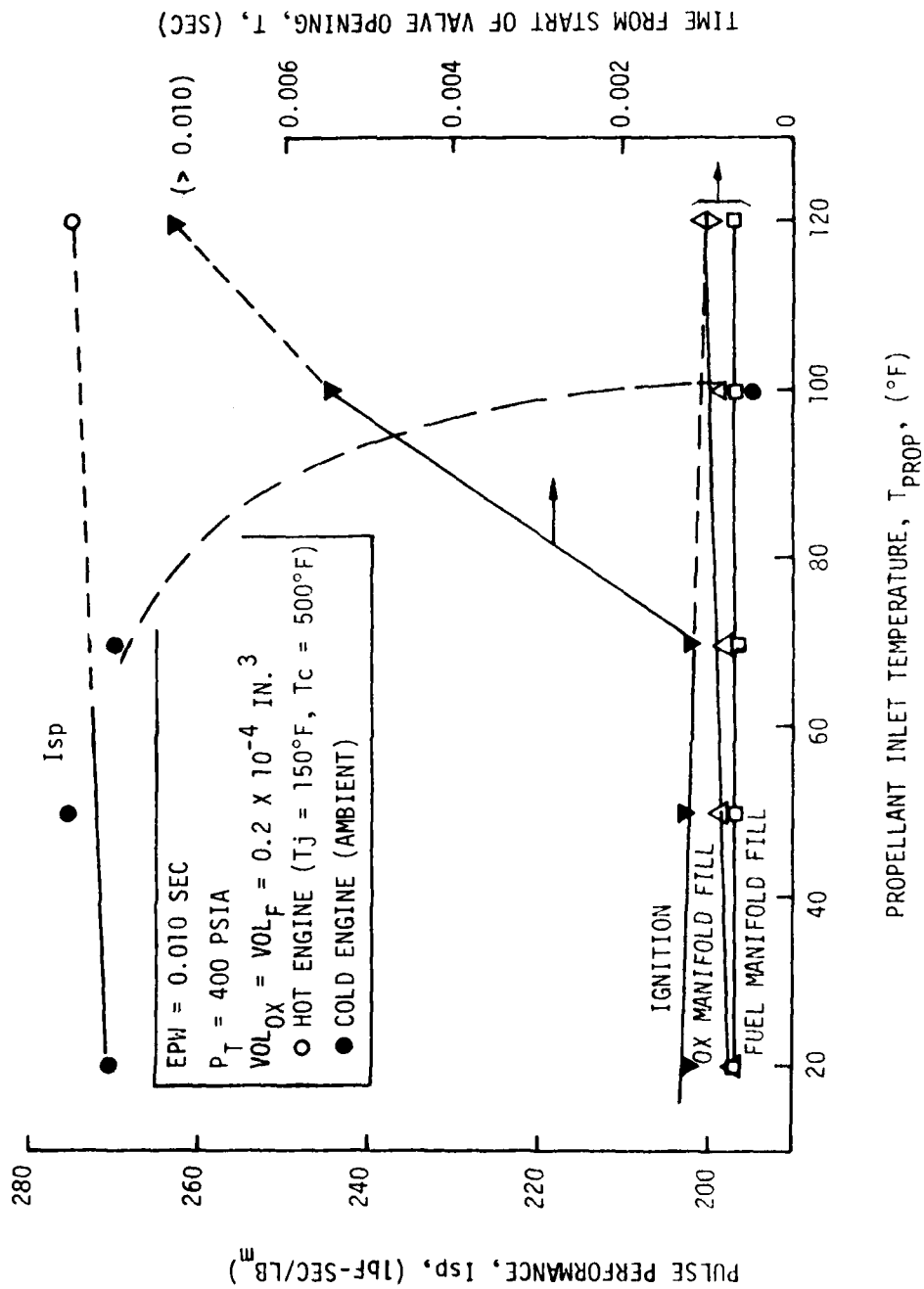


Figure 4-41. CONTAM Modeling of Warm Propellant Ignition Characteristics in Small Bipropellant Engines

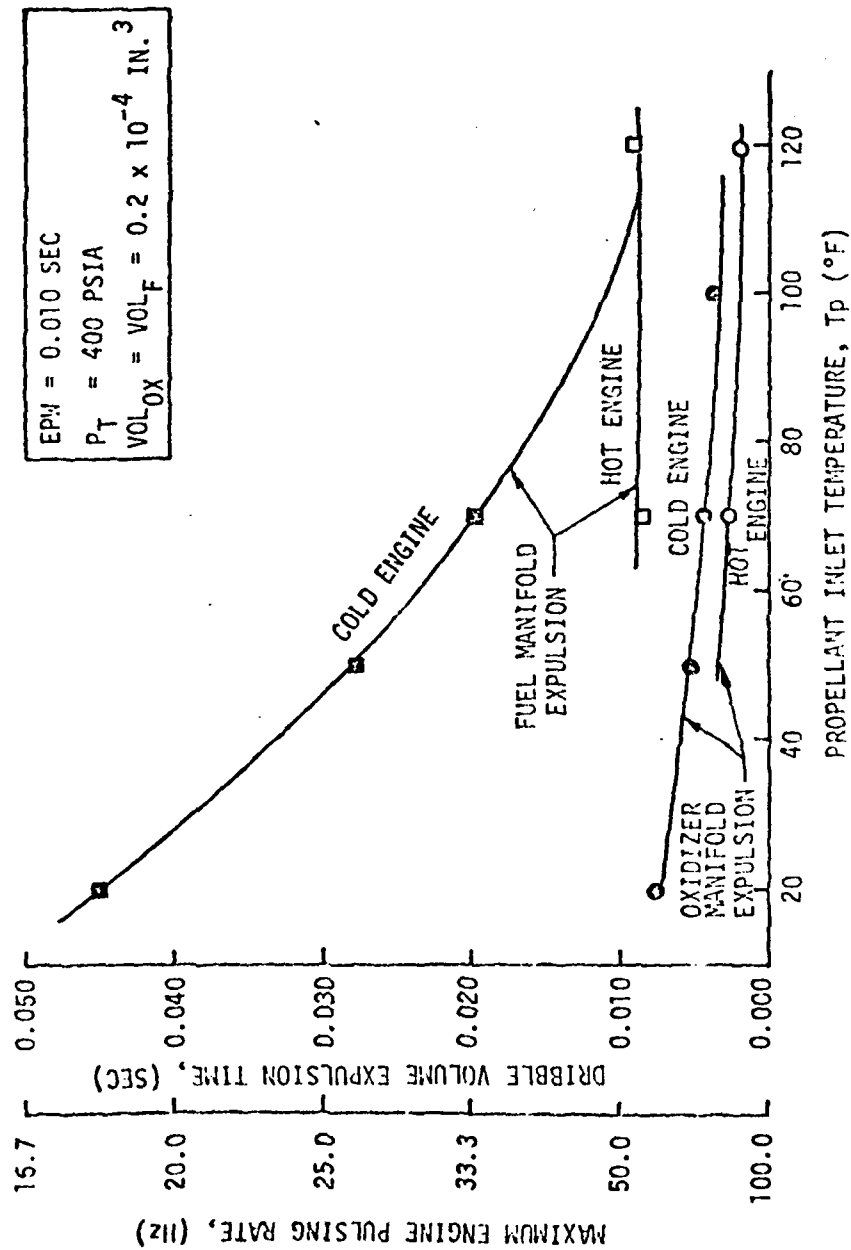


Figure 4-42 Dribble Volumes vs Firing Rates for Hot or Cold Engines (Unlimited Duty Cycle)

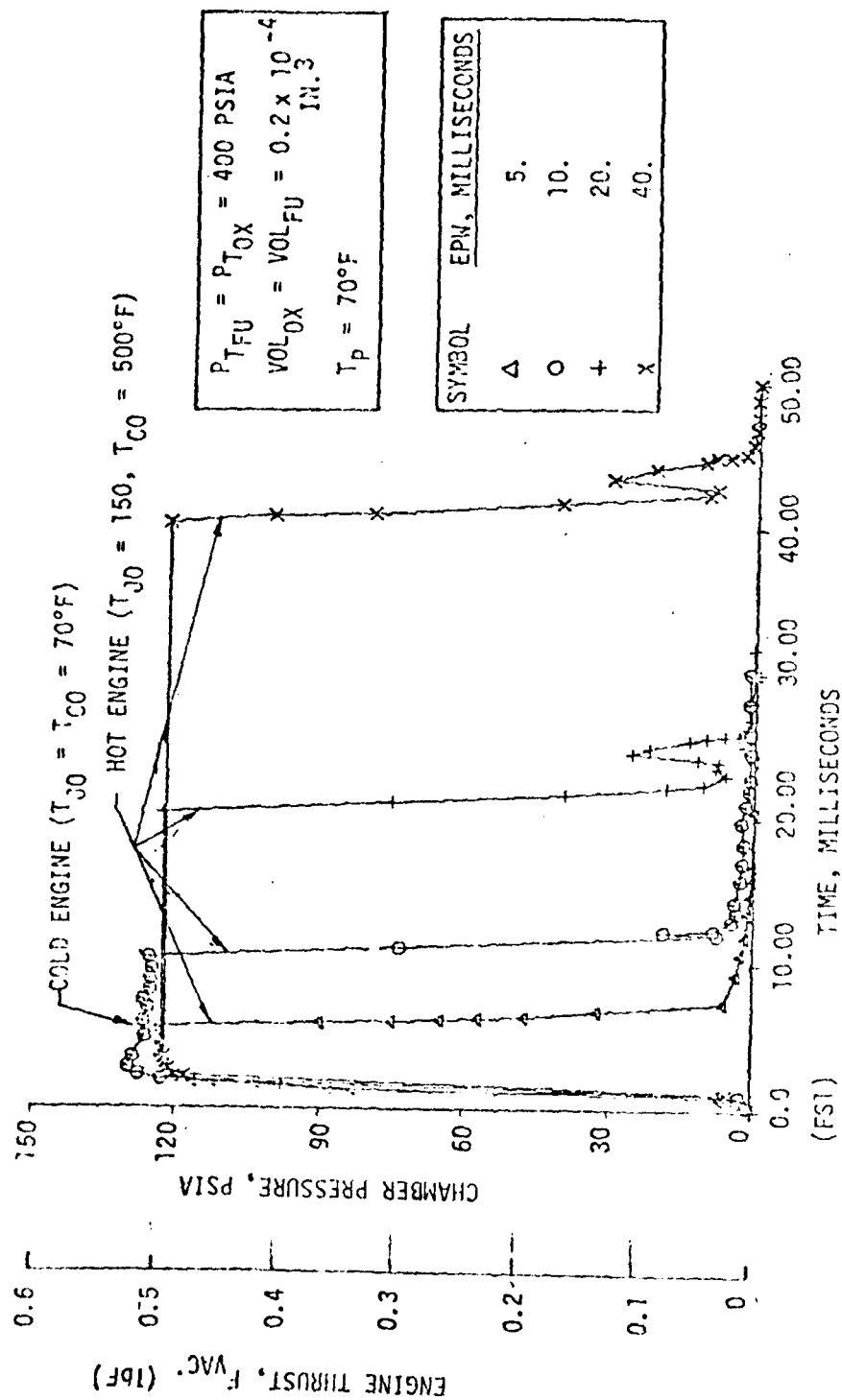


Figure 4-43. Computer Plots of CONTAM Transient Responses (Variable Pulse Width)

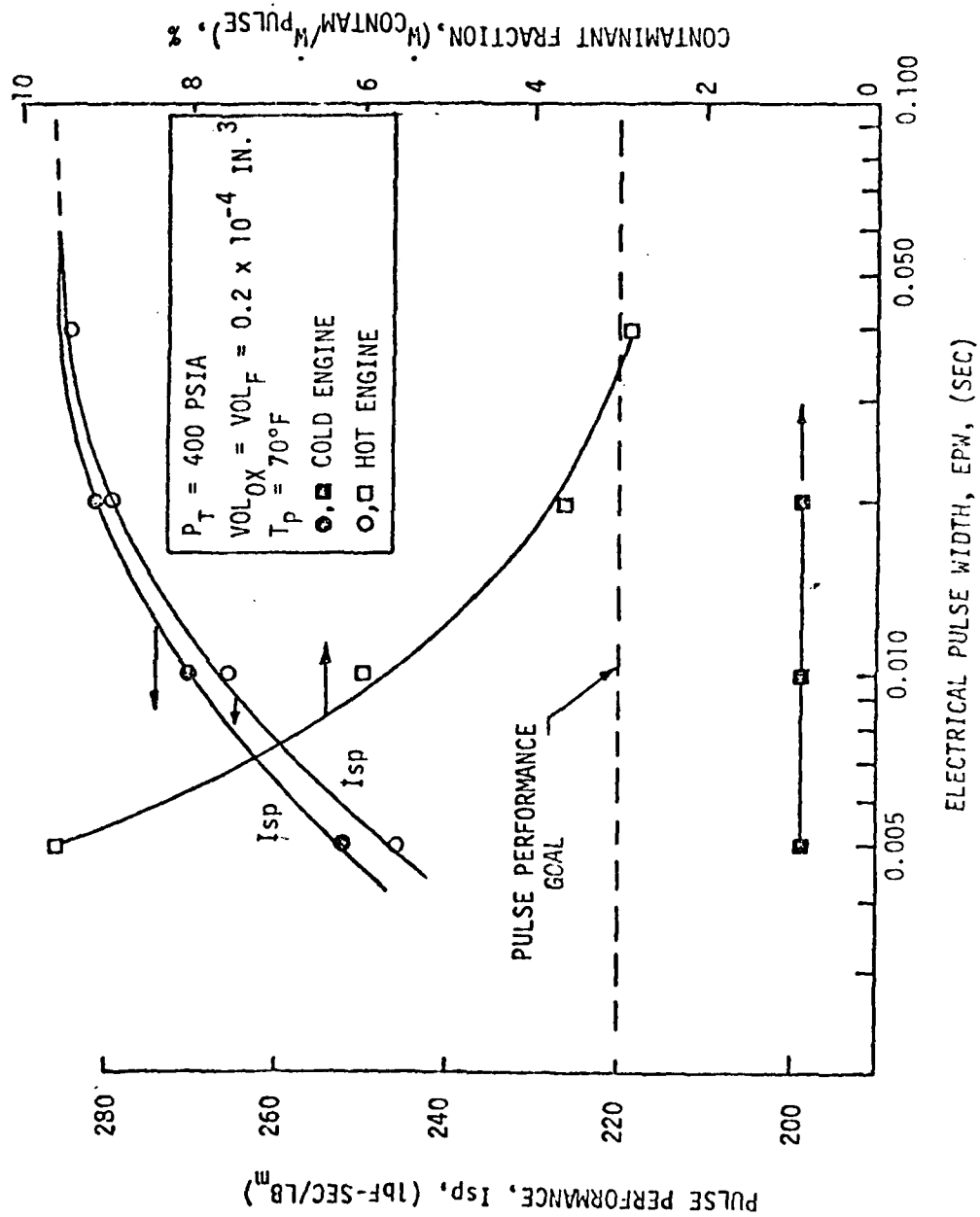


Figure 4-44. CONTAM Model Predicts Pulse Performance Goals

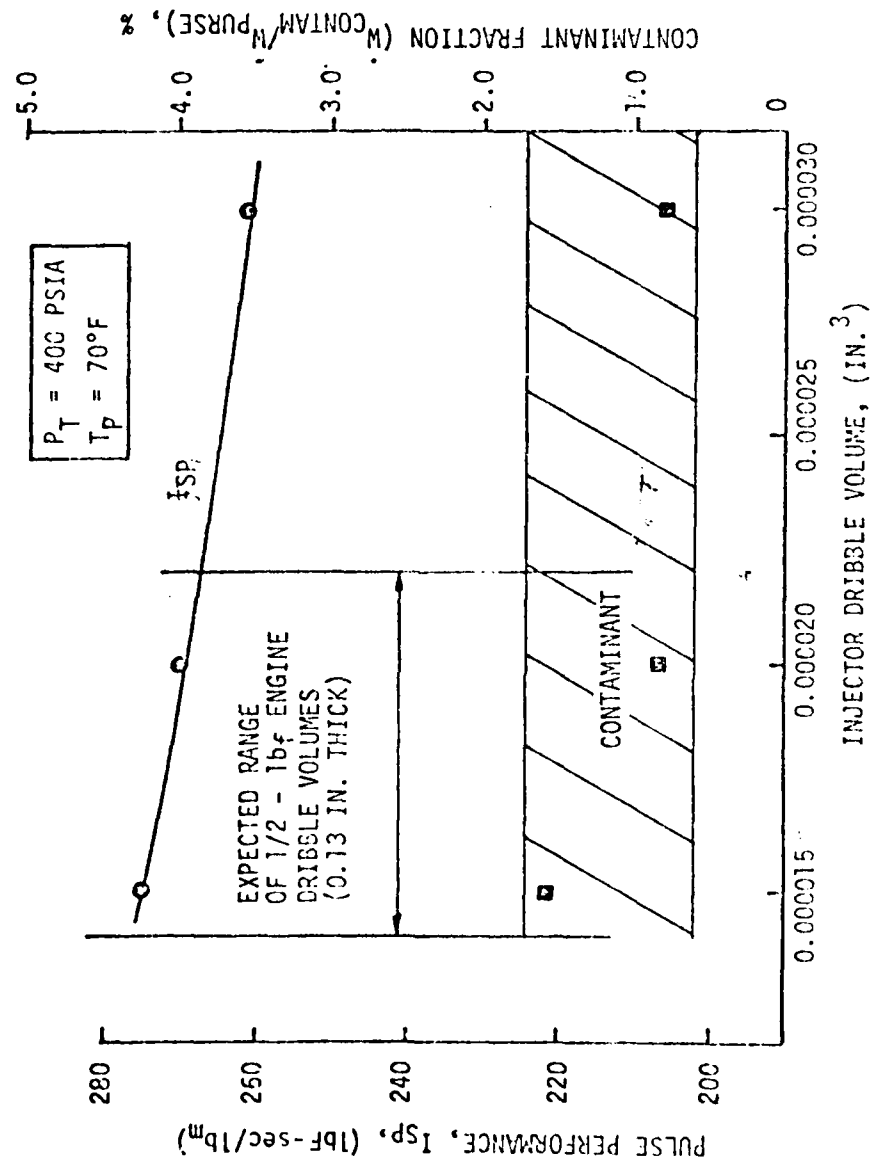


Figure 4-45. Dribble Volumes vs Response, Pulse Performance, and Plume Contaminants

AD-A091 078

AEROJET LIQUID ROCKET CO SACRAMENTO CA
LOW-THRUST BIPROPELLANT ENGINE TECHNOLOGY.(U)
AUG 80 L SCHOENMAN, R L FRIEDMAN

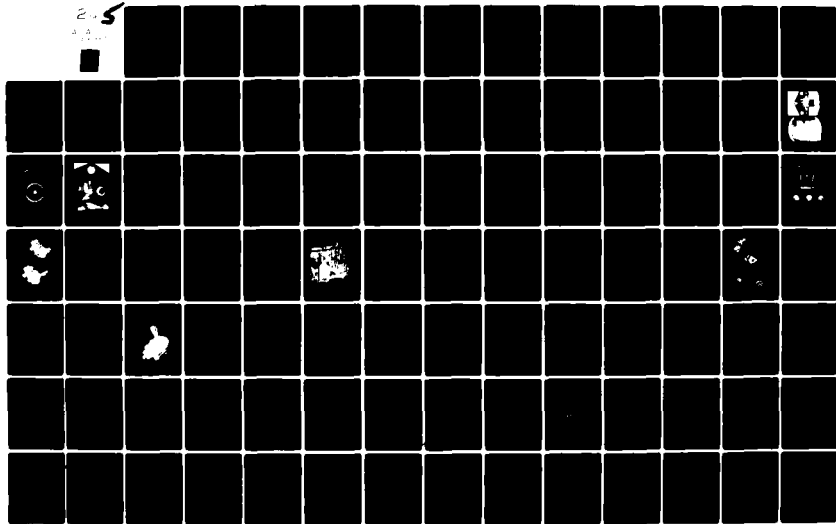
F/G 21/9.1

F04611-77-C-0053

UNCLASSIFIED

AFRPL-TR-80-47

NL

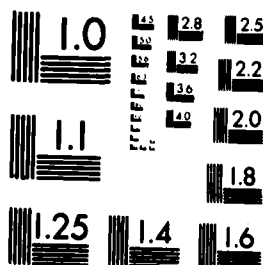


551F1E

2 OF 5

AD. A

091078



MICROCOPY RESOLUTION TEST CHART
NATIONAL BUREAU OF STANDARDS-1963-A

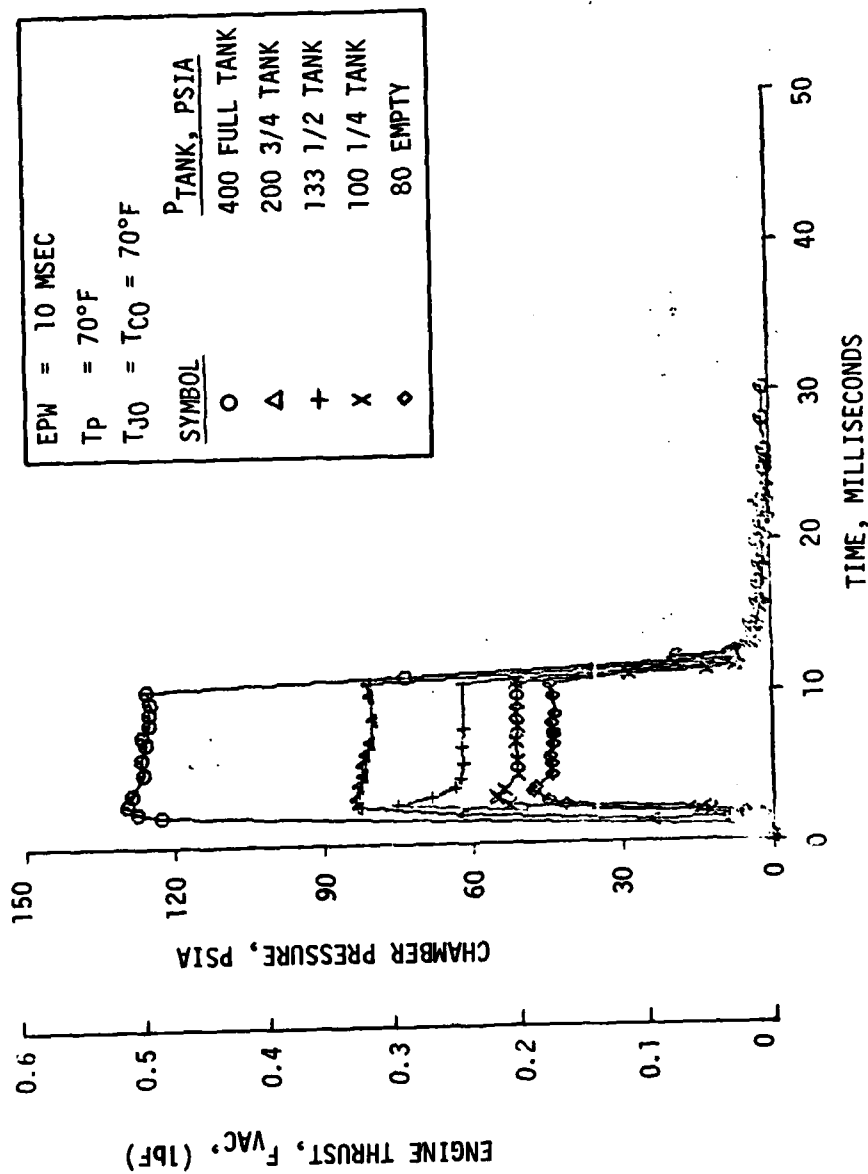


Figure 4-46. Computer Plots of CONTAM Transient Responses (Variable Tank Blowdown Pressures)

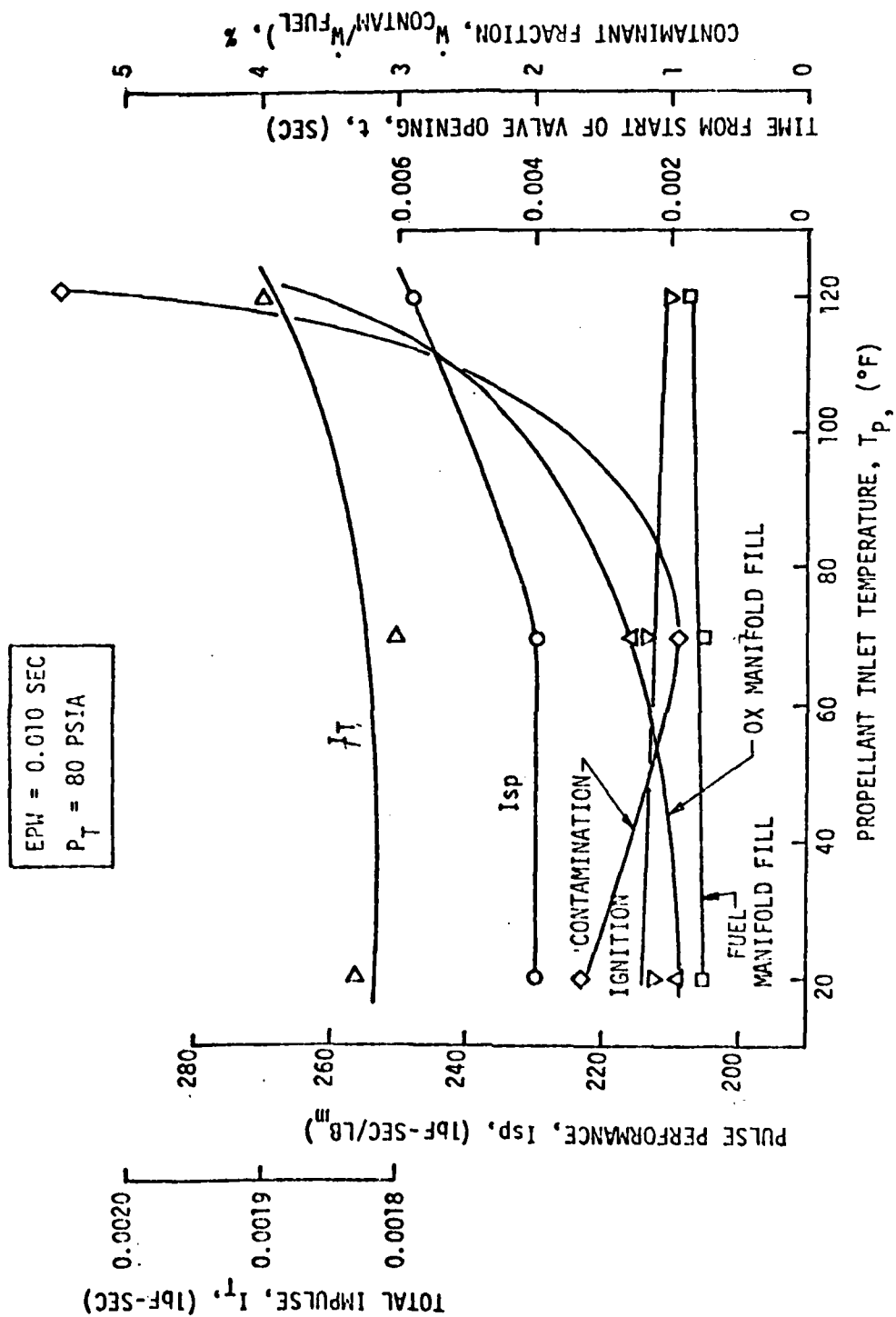


Figure 4-47. Performance vs Propellant (MON-1) Over a 5:1 Blowdown Ratio

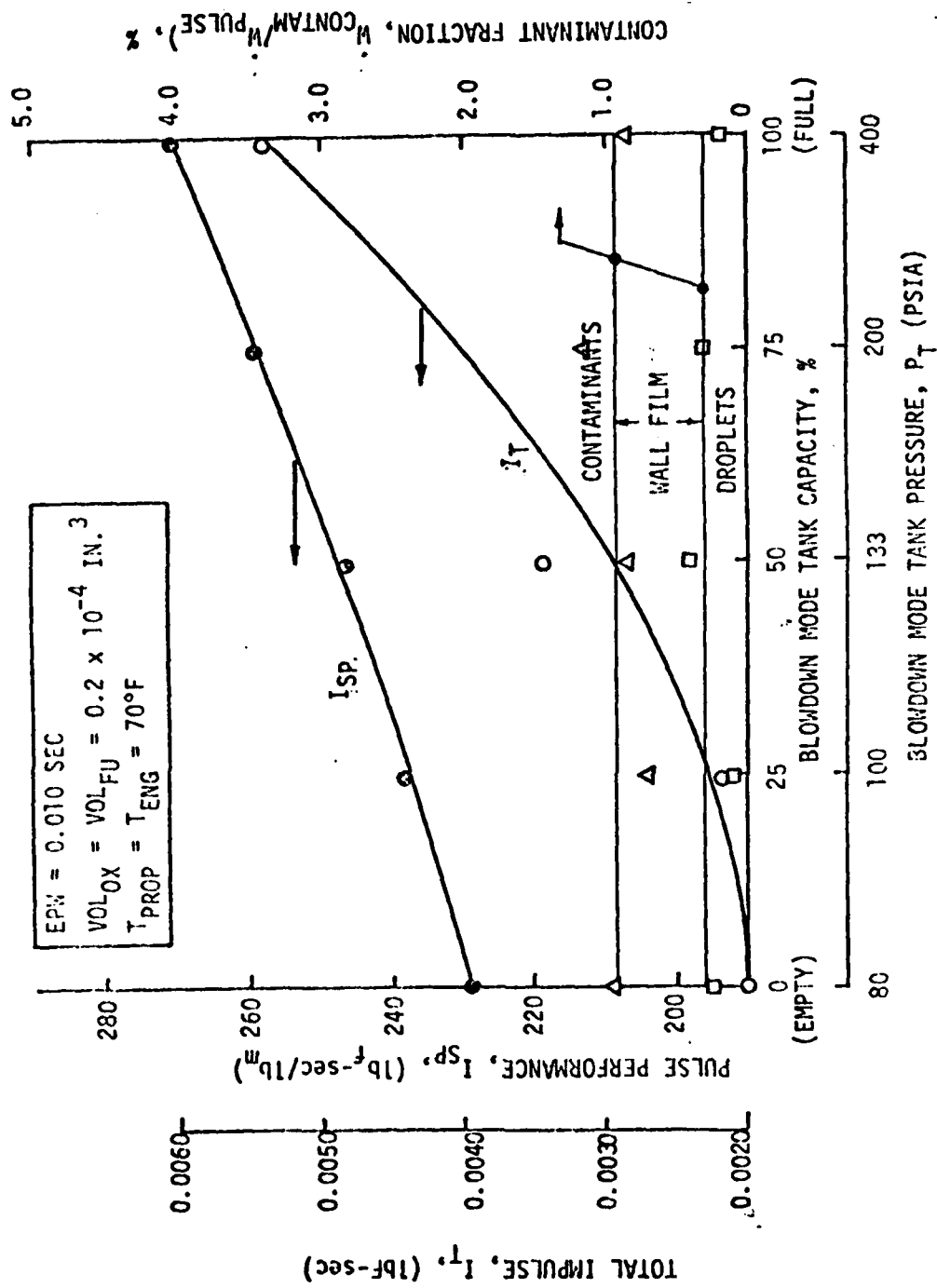


Figure 4-48. CONTAM Performance Predictions in a Blowdown Mode

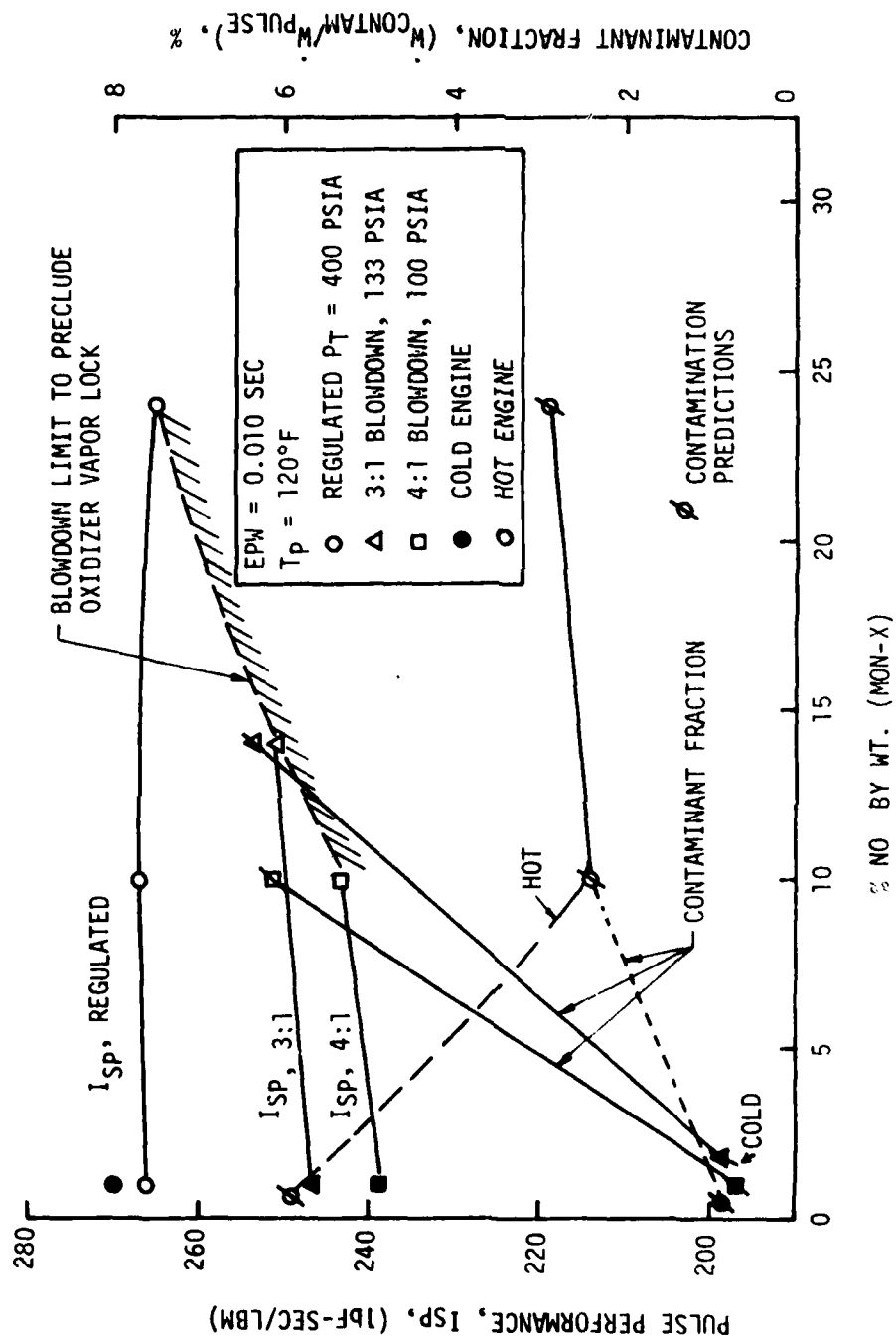


Figure 4-49. MON Content vs Pulsing Performance and Engine Blowdown Capability

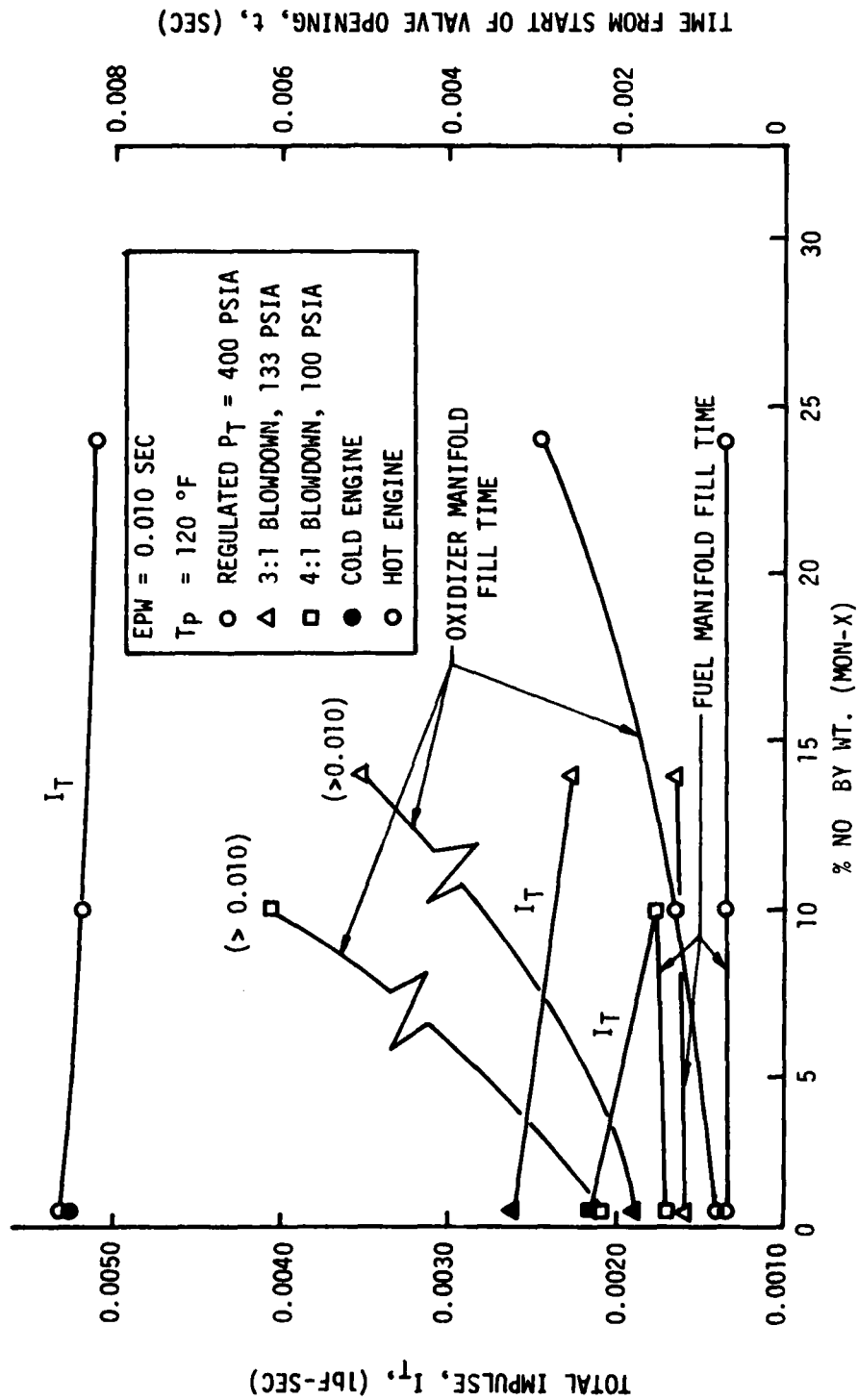


Figure 4-50. Oxidizer Manifold Fill Time vs Total Impulse Repeatability for Increased Oxidizer MON Content at Lower Tank Pressures

4.3, Engine Parameter Study (cont.)

- ° CONTAM predicted that the oxidizer manifold fill times are increased with the higher MON level oxidizers. This increase in fill time is a result of the increased vapor pressure of the MON-X oxidizers.
- ° No serious pressure overshoots were predicted by CONTAM. A maximum of ~1000 psia was observed in a hot propellant case. The ignition delay which resulted in this pressure overshoot is not believed to be real (as mentioned above). Otherwise, maximum spike pressures of approximately 200 psia were predicted.
- ° The amount of the maximum engine contamination was predicted to be approximately 5%, with nominal contaminants of 1% to 2%.
- ° CONTAM predicted the pulsing specific impulse to be well above the contractual goal of 220 seconds. CONTAM predicted a pulsing Isp of 250 -270 seconds.

Based upon the results of the CONTAM parametric study, no significant design deficiencies or performance anomalies were found.

4.3.6 Thermal Design

The objective of the thermal design task was to configure the engine heat storage and heat conduction paths in order to provide acceptable steady-state operating temperature and heat soaks following long burns. The design criteria for these analyses were as follows:

- ° The columbium chamber should be under 2500°F in the silicide-coated region and under 800°F in regions where coating is not practical (head end weld).
- ° The bimetallic Cb-SS interface should be under 800°F in order to achieve the 1000 full thermal cycle goal. This temperature is based on the life cycle prediction data shown in Figure 4-51. The predicted failure of the joint is based on the differential expansion rates between the columbium and stainless steel.
- ° The backside of the injector which forms the valve seats should not exceed the boiling temperature of the N_2O_4 at the

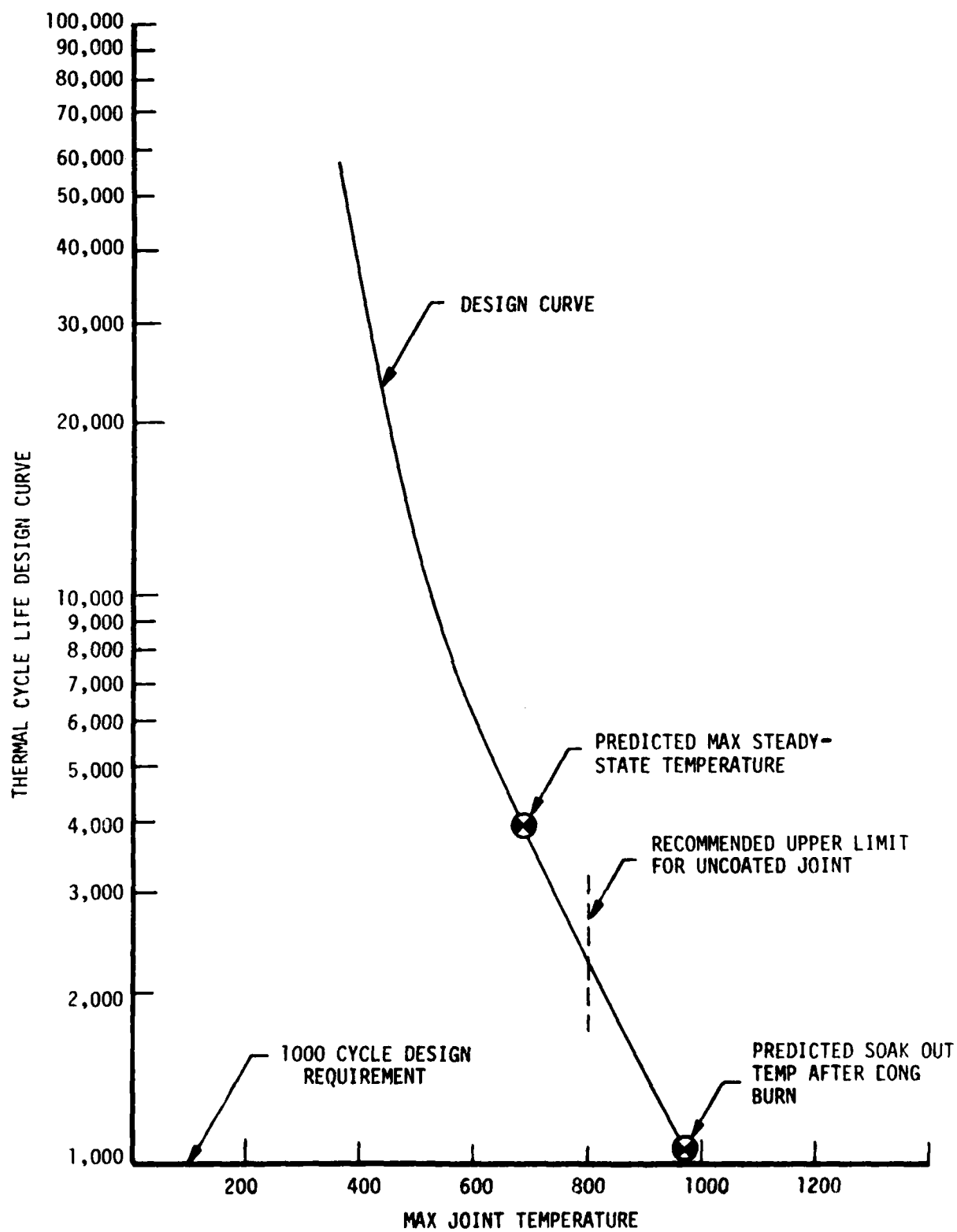


Figure 4-51. Estimated Thermal Cycle Life of Columbian Stainless Steel Joint

4.3, Engine Parameter Study (cont.)

valve inlet pressure during steady-state and should not soak out to a temperature higher than 300°F after shutdown. This is required to protect the Teflon buttons in the valve when it closes.

- ° The total heat transferred to the spacecraft should be minimized.

During Phase I, thermal analyses of the thrust chamber assembly were made to evaluate various thermal control configurations. The SINDA computer program was employed to establish optimum wall thickness profiles and to aid in understanding the heat transfer characteristics. An evaluation of the engine-to-spacecraft heat shunt effects and the injector steady-state and soakout temperature was also included.

The SINDA computer program was used to solve a thermal network representation of the 0.5 lbf engine using the node locations shown in Figure 4-52. This configuration illustrates a relatively thick wall section near the throat region to take advantage of the heat flux transformation benefits.

A thinner wall (.030") is represented for the somewhat cooler chamber forward end to limit thermal capacitance and conduction of heat into the injector during the engine coast periods. Further reduction of heat conduction into the injector is effected through a stainless steel insert at the chamber forward end. This portion of the chamber was expected to be relatively cool as a result of a liquid film deposited by the injector in this region. Dimensional details of the forward section which were utilized in the SINDA model are shown in Figure 4-53.

The chamber nodal resistance-capacitance network shown in Figure 4-52 includes heat radiation to space from the chamber exterior surface and the nozzle interior surface where appropriate view factors are utilized. An emissivity value of 0.8 was considered for both the exterior and interior surfaces.

Adiabatic wall temperature and wall mixture ratio profiles were predicted using the HEATLQ liquid film cooling model. They are based on an energy release efficiency of 94 percent, with 30 percent of the fuel acting as film cooling. Based on previous cold flow data for similar injection elements, the film cooling flow was estimated to be 25-30 percent.

The injector nodal network is shown in Figure 4-54. In the injector, model heat conduction into the propellants, spacecraft, and

CHAMBER NODAL NETWORK

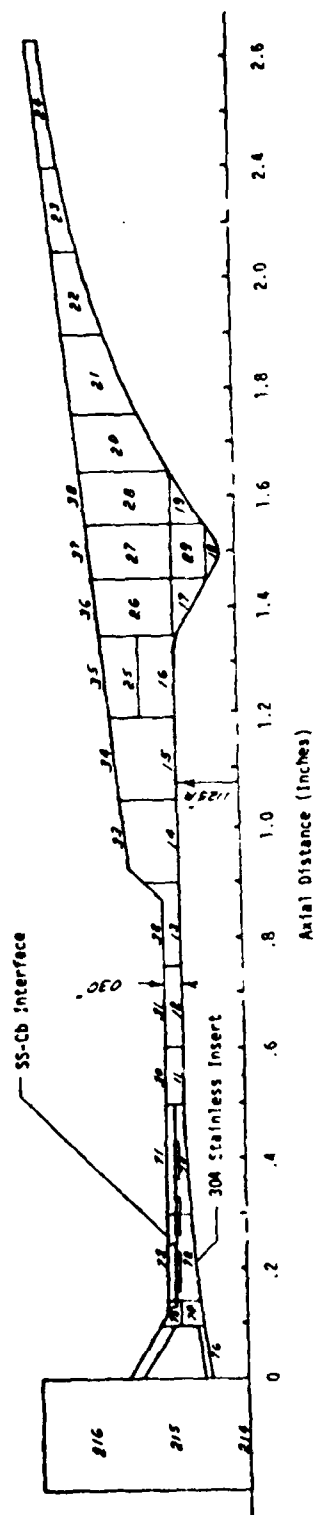
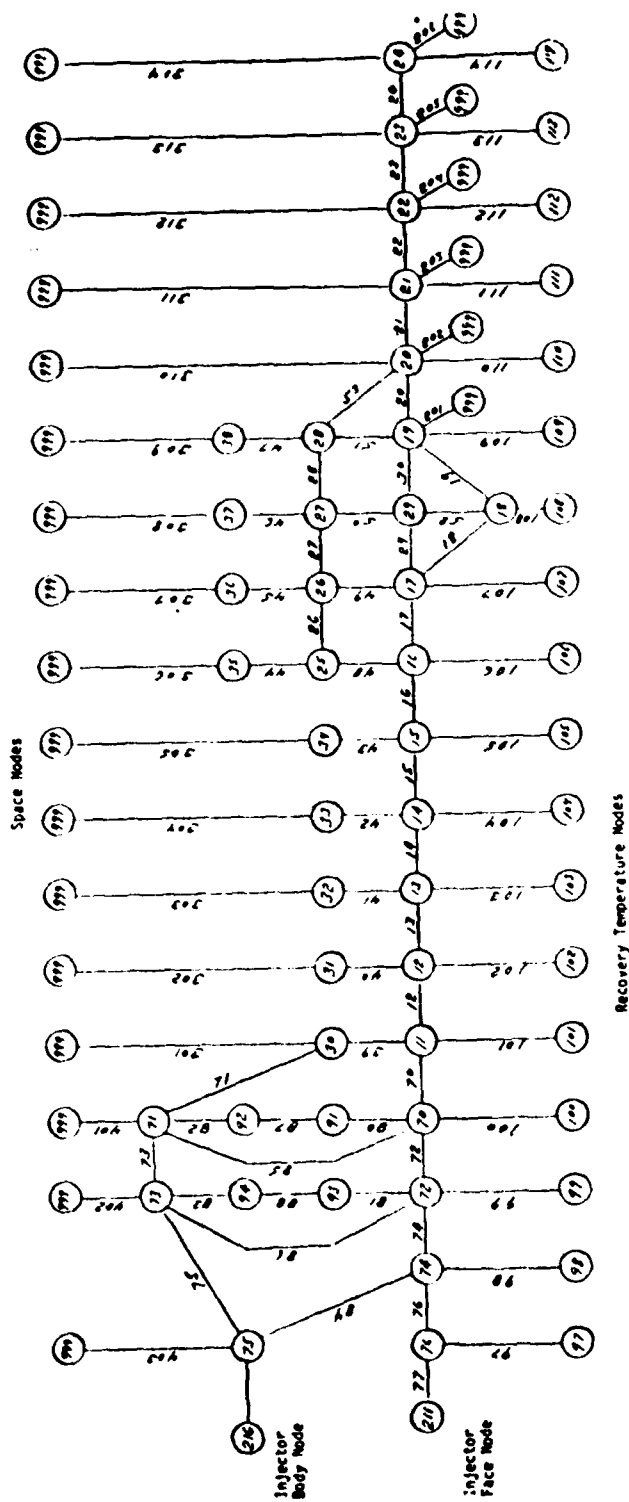


Figure 4-52. Chamber Thermal Model NODAL Network

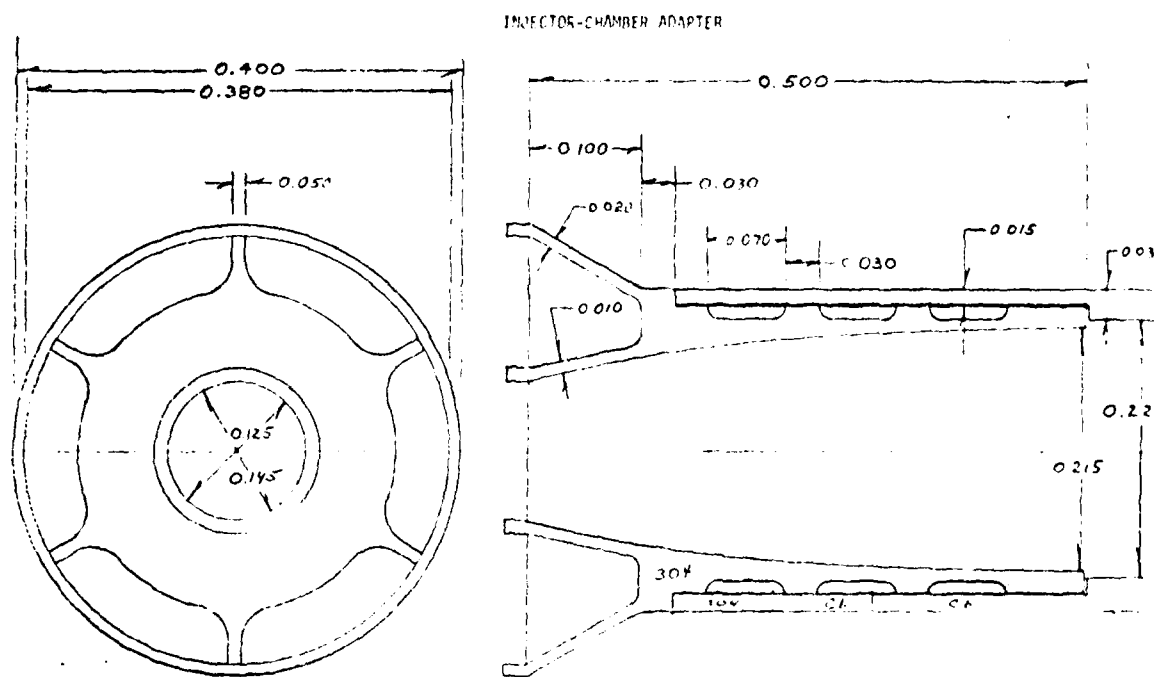


Figure 4-53. Injector-Chamber Adapter Employed in Thermal Analysis

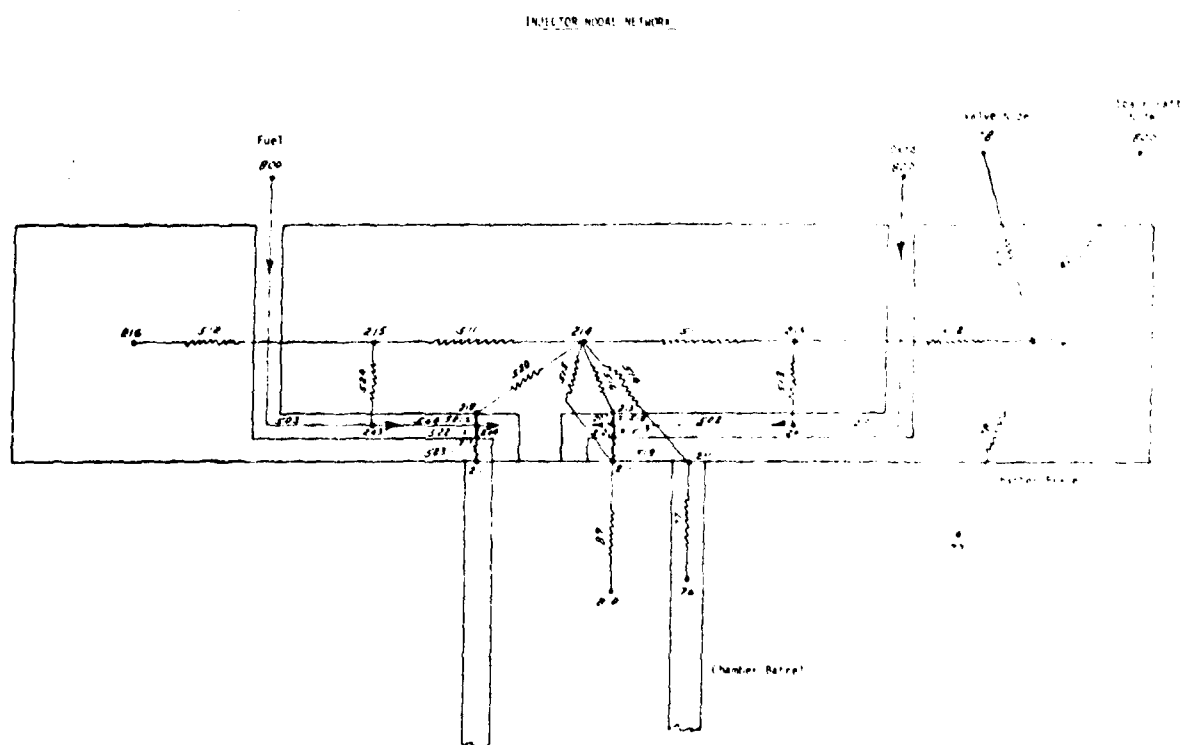


Figure 4-54. Injector NODAL Network

4.3, Engine Parameter Study (cont.)

valve was considered. Previous platelet injector small engine test data showing injector face temperature versus element quantity per square inch of face indicated injector face temperatures near 300°F. This was considered as one boundary condition during steady-state modeling of the 0.5 lbF engine. During coast periods, this temperature was allowed to soak to values as calculated by the SINDA Program.

An injector heat balance summary for various heat conduction rates into the spacecraft is presented in Table 4-VI. This includes injector steady-state and soakout temperatures for the corresponding configurations.

As a result of the small manifold surface area, comparatively little heat is absorbed by the propellants. This becomes more pronounced as heat conduction into the spacecraft is increased. For example, when the injector-to-spacecraft conductance is .00015 Btu/sec-°F, the total steady-state heat input to the injector is 12.21 watts. Of this total, 8.00 watts is conducted into the spacecraft while a total of 4.21 watts is absorbed by the propellants. A large portion of the total heat input during firing is conducted directly across the injector face and ultimately diffuses into the injector body. Some of this heat input can be reduced by constructing an insulator platelet (voided area) within the injector stack. To evaluate the effect of this, an insulator plate was considered. The results, presented for a spacecraft conductance of .00015 Btu/sec-°F, are shown in Table 4-VI. For this case, a spacecraft heat load of 7.26 watts is predicted, which compares with 8.00 watts for the non-insulated face.

The resulting steady-state and soakout temperatures of the injector and valve were included in Table 4-VI for the above configurations. These temperatures decrease to some extent with increased conductance to the spacecraft. The temperatures given are based on 100°F spacecraft and propellant inlet temperatures.

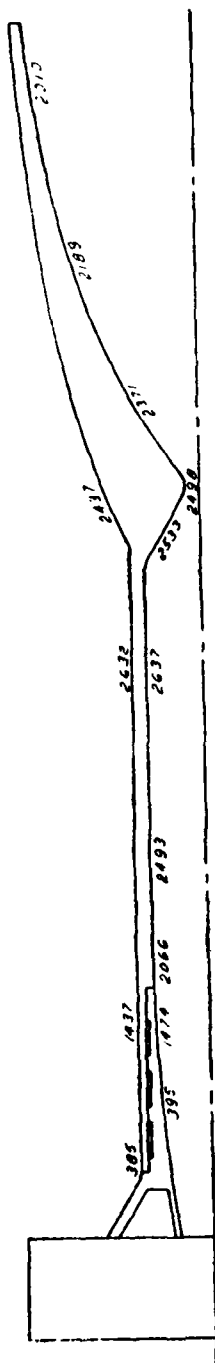
Computed temperature distributions for chambers of various configurations are illustrated in Figure 4-55. The medium wall chamber design, as illustrated, represents the optimum configuration in that the maximum chamber temperature is within acceptable material limits. For this configuration, a maximum temperature of 2412°F is predicted for the throat. Immediately after shutdown, cooling of the chamber occurs, except in the forward section where the termination of film cooling results in some increase in temperature as indicated by the parenthesized values. For

TABLE 4-VI

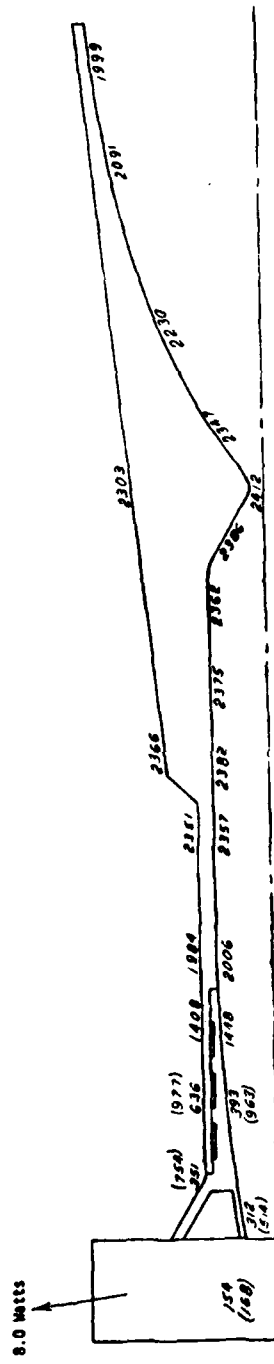
INJECTOR HEAT BALANCE AND TEMPERATURE SUMMARY

(Spacecraft and Propellant Inlet Temperature = 100°F)

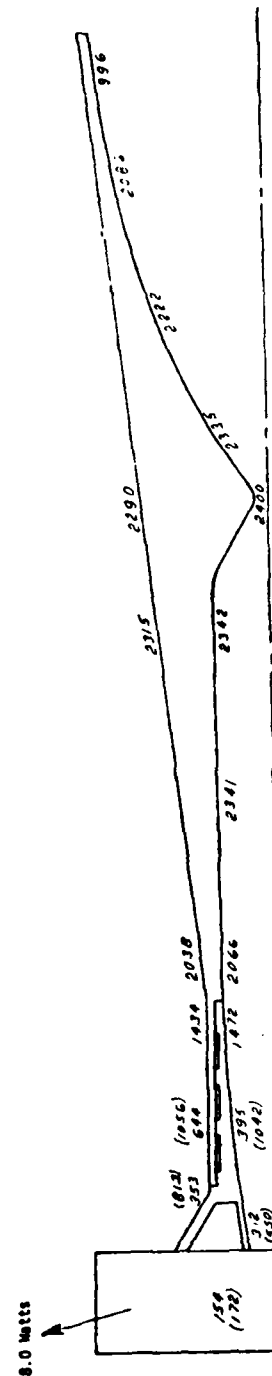
	NON-INSULATED FACE		INSULATED FACE	
INJECTOR-TO SPACECRAFT-CONDUCTANCE (Btu/sec-°F)	.0001	.00015	.00020	.00015
STEADY-STATE HEAT LOSS (WATTS)				
Conduction to Spacecraft	6.91	8.00	8.68	7.26
Heat Absorbed by Oxidizer	1.33	1.25	1.20	1.23
Heat Absorbed by Fuel	3.15	2.96	2.83	2.89
TOTAL	11.39	12.21	12.71	11.38
STEADY-STATE HEAT INPUT (WATTS)				
Conduction Across Injector Face	5.26	5.74	6.04	4.81
Conduction Along Chamber Wall	3.17	3.28	3.34	3.31
Conduction Along Chamber Brace	2.96	3.19	3.33	3.26
TOTAL	11.39	12.21	12.71	11.38
Injector Steady-State Temperature (°F)	168	154	144	149
Injector Body Maximum Soakout Temperature (°F)	188 @ 34 sec.	168 @ 30 sec.	157 @ 26 sec.	165 @ 30 sec.
Valve Steady-State Temperature (°F)	166	151	141	146
Valve Maximum Soakout Temperature (°F)	166 @ 40 sec.	151 @ 34 sec.	142 @ 32 sec.	147 @ 36 sec.
Steady-State Oxidizer Temperature Rise (°F)	2.75	2.59	2.48	2.53
Steady-State Fuel Temperature Rise (°F)	6.20	5.71	5.57	5.68



Temperature shown in °F



Temperature shown in °F
Maximum soakout temperatures are shown in parenthesis.



Temperature shown in °F
Maximum soakout temperatures are shown in parenthesis.

Figure 4-55. Chamber Wall Thickness vs Heat Soak and Operating Temperature

4.3, Engine Parameter Study (cont.)

example, at the extreme forward end, the temperature increases from 351°F during steady-state to a maximum soakout temperature of 757°F. Near the stainless steel/ columbium joint, a maximum soakout temperature of 979°F is predicted. The medium wall thickness design was recommended for Phase II fabrication.

4.4 PHASE I CONCLUSIONS AND RECOMMENDATIONS

The Phase I analysis of the issues described in the "User's Survey" and the resultant hardware selection/designs concluded that:

- ° 4:1 blowdown appeared to be adequate
- ° Engine design needed to be tolerant of mixture ratio excursions
- ° MON-10 would provide lower temperature operation but would reduce the elevated temperature capabilities
- ° Minimum impulse bits of .001-.003 \pm 10% were of interest
- ° >10 hr life needed demonstration
- ° Valve redundancy needed to be addressed.

Phase II hardware needs, based on the anticipated test program and performance requirements, were evaluated and resulted in the following recommendations:

- ° Fabricate 2 torque motor model 51E112 valves
- ° Fabricate and cold-flow 3 injector designs
 - ° 1 coaxial swirler
 - ° 1 fuel swirler - 3 "V" doublet oxidizer
 - ° 1 - 3 element splash plate

4.4, Phase I Conclusions and Recommendations (cont.)

- Fabricate flanged columbium chambers $L' = 1$ and 2 in.
- Continue to evaluate methods of bimetallic joint fabrication.
- Proceed with development of dual mode thrust stand.

The Phase II test program was recommended to proceed as proposed in the baseline program plan. The test program and associated design and analysis activities recommended were:

- Verify predicted steady-state and pulse mode performance
- Test at vacuum with 143:1 geometric nozzle
- Evaluate chamber L' of 1.0 to 2.0 in.
- Use MON-1 as baseline oxidizer (20 to 120°F)
- Use MON-10 as alternate oxidizer (0 to 100°F)
- Verify identical performance and verify 0°F ignition with MON-10
- Verify variable mixture ratio operation
- Determine minimum impulse of injector designs
- Instrument chamber and injector to verify calculated boundary conditions and predicted temperatures
- Design engine-to-test stand mount simulating spacecraft conduction paths
- Instrument engine mounts to verify heat load
- Verify thermal soakback predictions
- Verify deficiencies in CONTAM predictions.

SECTION 5.0

PHASE II - DESIGN, FABRICATION, AND VERIFICATION TESTING

5.0 PHASE II - DESIGN, FABRICATION AND VERIFICATION TESTING

The design conditions and criteria for the Phase II verification test hardware were based on the Phase I analysis and design activities.

Phase II thus consisted of (1) detailed analyses and the development of design configurations which would satisfy the design requirements; (2) fabrication of the components (valve, injectors and chambers) required to obtain data; (3) systematic bench- and hot-fire testing of each of the components over the range of parameters of interest in order to verify and upgrade the analyses and to establish feasibility of the concepts; and (4) the generation of designs for Phase III demonstration testing.

5.1 ENGINE DESIGN AND FABRICATION

5.1.1 Valve Fabrication and Bench Testing

5.1.1.1 Valve Fabrication

Fabrication of the valves was done by MOOG, Inc. The top assembly drawing for the valve is shown in Figure 5-1.

Two hot-fire test valves and one bench-test valve were fabricated during Phase II. No fabrication difficulties were encountered.

5.1.1.2 Valve Bench Testing

MOOG, Inc. bench-tested one valve, Model 51E112, at their facility. The bench-test valve was proof-tested at 800 psia with GN₂ for 3 minutes. Visual observations disclosed no deformation or other anomalies.

Internal and external leak checks were performed with an integrated valve and injector at 50 and 400 psia. The external leakage was checked by using "Leaktec" bubble solution, whereas the internal checks were made using a water displacement method. There was no leakage.

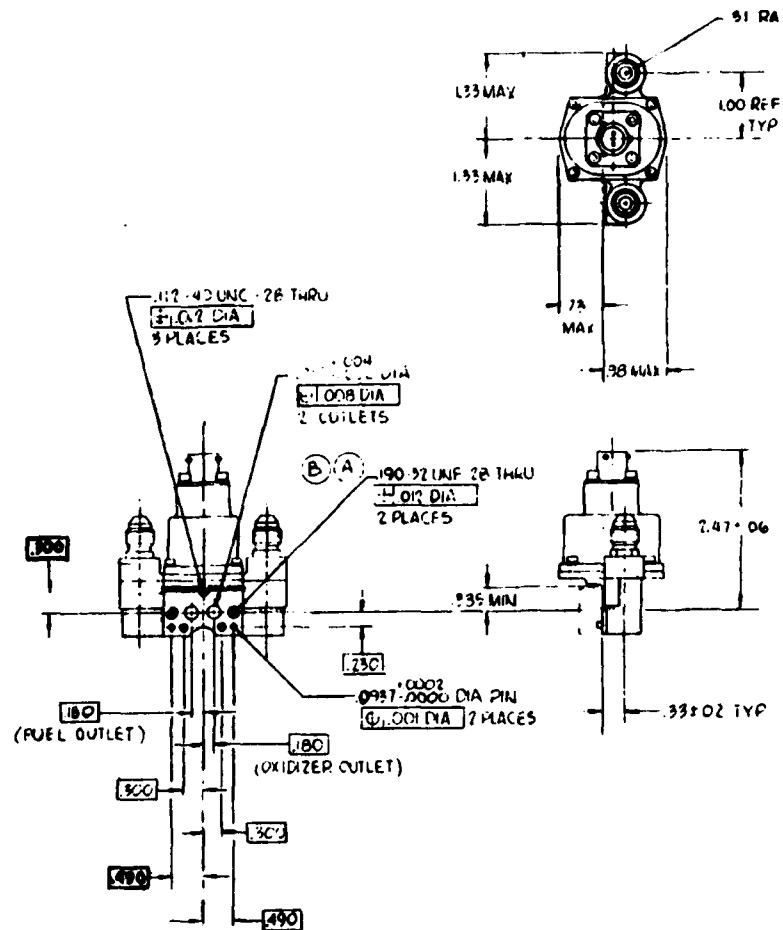


Figure 5-1. Torque Motor Valve Model 51E112 Assembly and Interface Drawing

5.1, Engine Design and Fabrication (cont.)

The valve response was initially measured with both a 100 ohm coil and a 170 ohm coil. The 100 ohm coil gave the following results:

Coil	Voltage	GN ₂ Pressure psia	Open Time ms	Close Time ms
100 Ω	20	400	3.6	0.6
100 Ω	25	400	3.2	0.6
100 Ω	28	400	2.6	0.5
100 Ω	31	400	2.4	0.5
100 Ω	28	400	3.6	0.5

The use of a 16.4 volt voltage clipping Zener diode increased the close time from 0.5 to 1.2 ms.

The 100 ohm coil generated a 7.8 watt heat load and power drain, whereas the 170 ohm coil required only 4.6 watts. Both designs met the design goals (i.e., a valve response time of less than 5 ms). A selection of the 170 ohm coil was made to minimize the system heat load.

When the final bench test coil was wound, it had a resistance of 177 ohms. Response data obtained with this coil are provided in Figure 5-2 and Table 5-I. Compared to the design goal of 5.0 ms maximum, the nominal opening response time at 400 psia, 28 volts was 3.2 ms and the closing time was 1.0 ms.

The two deliverable contract valves were assembled with injectors. Figure 5-3 shows a comparison of their opening response times with that of the bench-test valve.

The bench-test valve was also subjected to a 1,000,000 cycle test with 400 psia water inlet. No mechanical or leakage problems were encountered during this testing. A life cycle test history is provided in Table 5-II.

Both circuits of all delivered injector/valve assemblies were flowed with demineralized water for K_w * determination when received at ALRC. These data were generally in good agreement with the ALRC injector/valve pre-assembly flow data.

$$*K_w = \dot{w} / \sqrt{PS.g.}$$

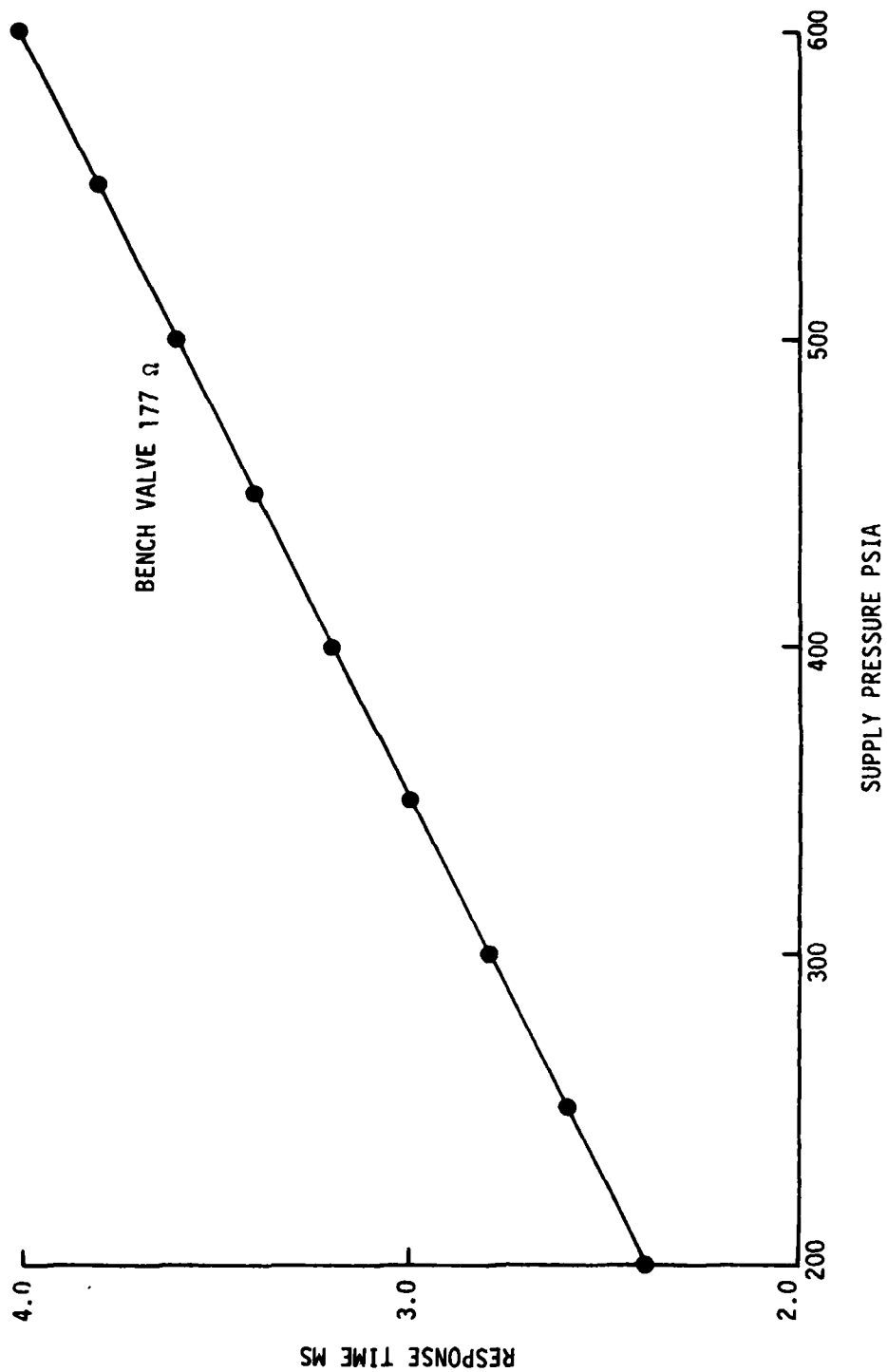


Figure 5-2. Opening Response Time of 177 Ohm Bench Test Valve at 28 Volts

TABLE 5-I

RESPONSE MAPPING OF 177 OHM BENCH-TEST VALVE

Inlet Pressure (psi)	Opening Response Time (ms)	
	<u>25VDC</u>	<u>28VDC</u>
200	2.8	2.4
250	3.0	2.6
300	3.2	2.8
350	3.4	3.0
400	3.6	3.2
450	3.9	3.4
500	4.2	3.6
550	4.4	3.8
600	5.1	4.0

The valve closing Response Time was 1.0 ms at all conditions of supply pressure and voltage.

DRY vs. WET RESPONSE TIMES

	Response Times at 400 psig (Open/Close) (ms)			
	20V	25V	28V	32V
GN ₂ -16.4 V Diode	4.9/1.5	3.6/1.5	3.3/1.5	2.8/1.5
GN ₂ -30 ohm Series Resistor 16.4 V Diode	5.6/1.4	4.0/1.4	3.5/1.5	3.0/1.5
H ₂ O-No Diode	4.8/1.0	3.8/1.0	3.3/1.1	2.9/1.1
H ₂ O-16.4 V Diode	-	-	3.3/2.5	-

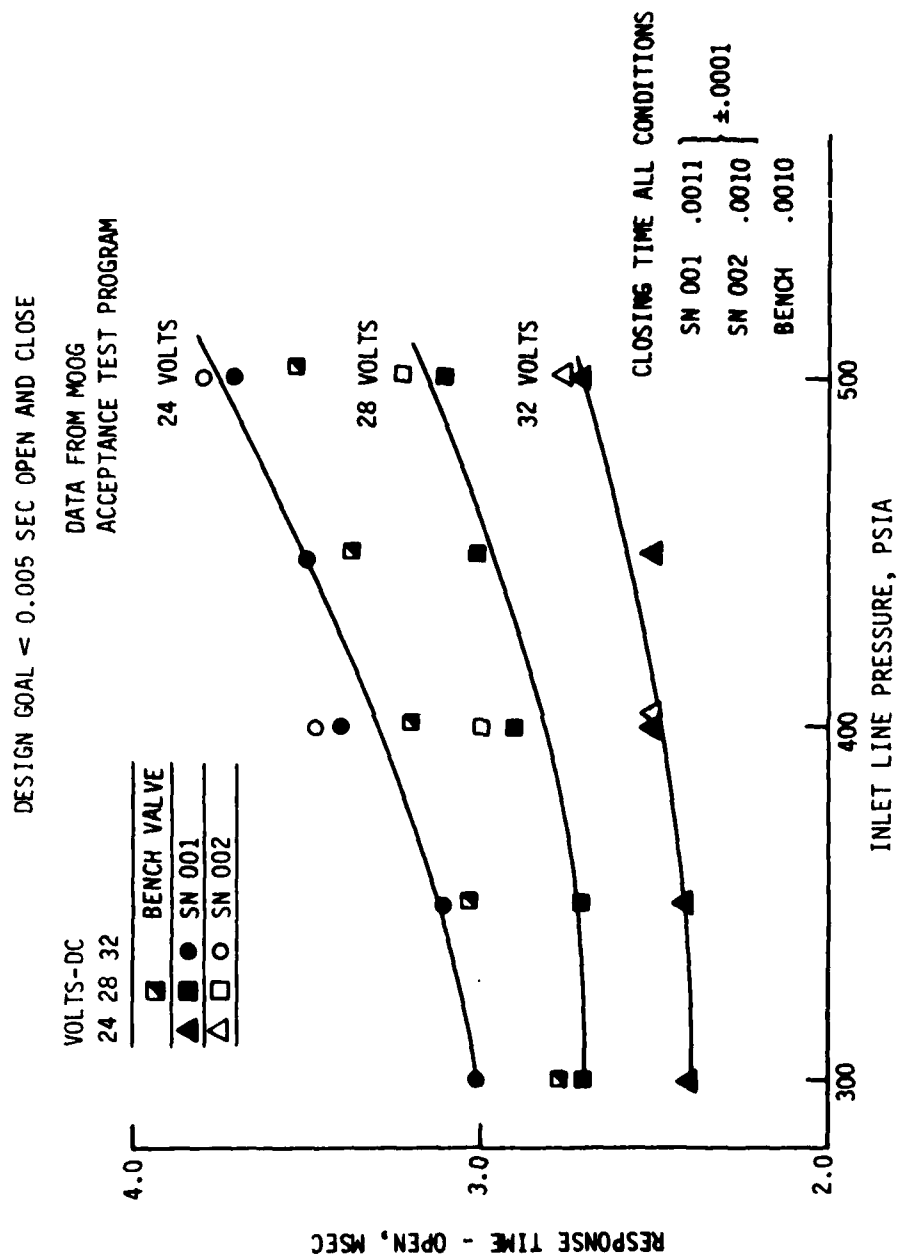


Figure 5-3. Repeatability of Three Valves and Sensitivity to Line Pressure and Voltage

TABLE 5-II

LIFE CYCLE TEST RESULTS OF 51E112 PROTOTYPE VALVE

Cycles 400 psi	Pull-In Current @ 400 psig GN ₂ (mA)	Drop-Out Current @ 400 psig GN ₂ (mA)	Response Times @ 400 psig GN ₂ (Open/Close) Amb. Temp. (MS)			Internal Leakage Fuel Oxidizer 50 psig 400 psig (scc/hr)	Δ P Fuel Oxidizer (lb/sec) H ₂ O
			20V	25V	28V	32V	
0	60 (1)	50 (1)	4.9/1.5*	3.6/1.5*	3.3/1.5*	2.8/1.5*	-
2,400 (GN ₂)	63.5 (1)	54 (1)	4.9/1.5	3.6/1.5	3.2/1.5	2.8/1.5	-
7,400 H ₂ O	57	27	4.8/1.0	3.8/1.0	3.3/1.1	2.9/1.1	.00119/.00124
20,773	57	27	-	3.6/0.9	3.2/0.9	-	-
40,773	56	27	-	3.7/0.9	3.2/1.0	-	-
67,440	58	27	-	3.7/1.0	3.3/1.0	-	-
100,773	60	27	-	3.7/1.0	3.3/1.0	-	-
134,106	60	27	-	3.7/0.9	3.2/1.0	-	-
167,439	60	27	-	3.7/0.9	3.3/0.9	-	-
200,772	60	27	-	3.8/0.9	3.4/0.9	-	-
300,000	61	27	-	3.7/0.9	3.3/0.9	-	-
400,000	62	27	-	3.7/0.9	3.3/0.9	-	-
500,000	60	27	-	3.7/0.9	3.3/0.9	-	.00119/.00124
600,000	60	27	-	3.7/1.0	3.3/1.0	-	-
700,000	61	27	-	3.7/1.0	3.3/1.0	-	-
800,000	57	27	-	3.8/1.0	3.3/1.0	-	-
900,000	58	27	-	3.7/1.0	3.2/1.0	-	-
1,000,000	65	27	4.6/0.9	3.5/0.9	3.1/0.9	2.7/0.9	.00119/.00124

1) No downstream orifices. All wet cycles were run with 0.007 in. orifices downstream of the valve.

* 16.4V Diode

0-500,000 Cycles @ 20 Hz
500,000-800,000 Cycles @ 40 Hz
800,000-1,000,000 Cycles @ 80 Hz

5.1, Engine Design and Fabrication (cont.)

The injector/valve assemblies were cold-flowed again at ALRC following final braze assembly of the injector and chamber. No changes in flow characteristics or plugging were experienced during this assembly process.

5.1.2 Injector Fabrication and Flow Testing

5.1.2.1 Design Selection

Based on the results of the Phase I superscale cold flow results, three injector designs were selected for fabrication. These designs were:

- ° A one element coaxial swirler (1-CAS)
- ° A pattern consisting of 3 0x V-doublets impinging on a single central fuel swirler (3-VDS)
- ° A 3 element splash plate (3-SPA)

Schematic drawings of the element and spray patterns were shown in Figures 4-17 to 4-27 of Section 4. The fabrication, cold-flow and hot-fire test history of these three designs is summarized in Figure 5-4.

5.1.2.2 Fabrication

Nine units of each injector design were fabricated, using the photo-etched platelet array shown in Figure 5-5. Figures 5-6, 5-7, and 5-8 show close-up photographs of a finished 3-VDS and 1-CAS injector. Alignment problems encountered in the stacking of the "9 unit" arrays resulted in SN 3 and SN 7 of each design being rejected as atypical of the lot and fabrication process. Following this, the injectors were stacked and bonded one unit at a time. The alignment problem was subsequently traced to a human error in the photographic reduction and corrected, starting with SN 11.

The manufacturing experience showed that, of the three designs, the 1-CAS injector was the easiest to fabricate. This design required fewer total parts, the minimum platelet thickness was .002 in. compared to a .001 in. for the other designs, and the passage sizes were larger and easier to inspect.

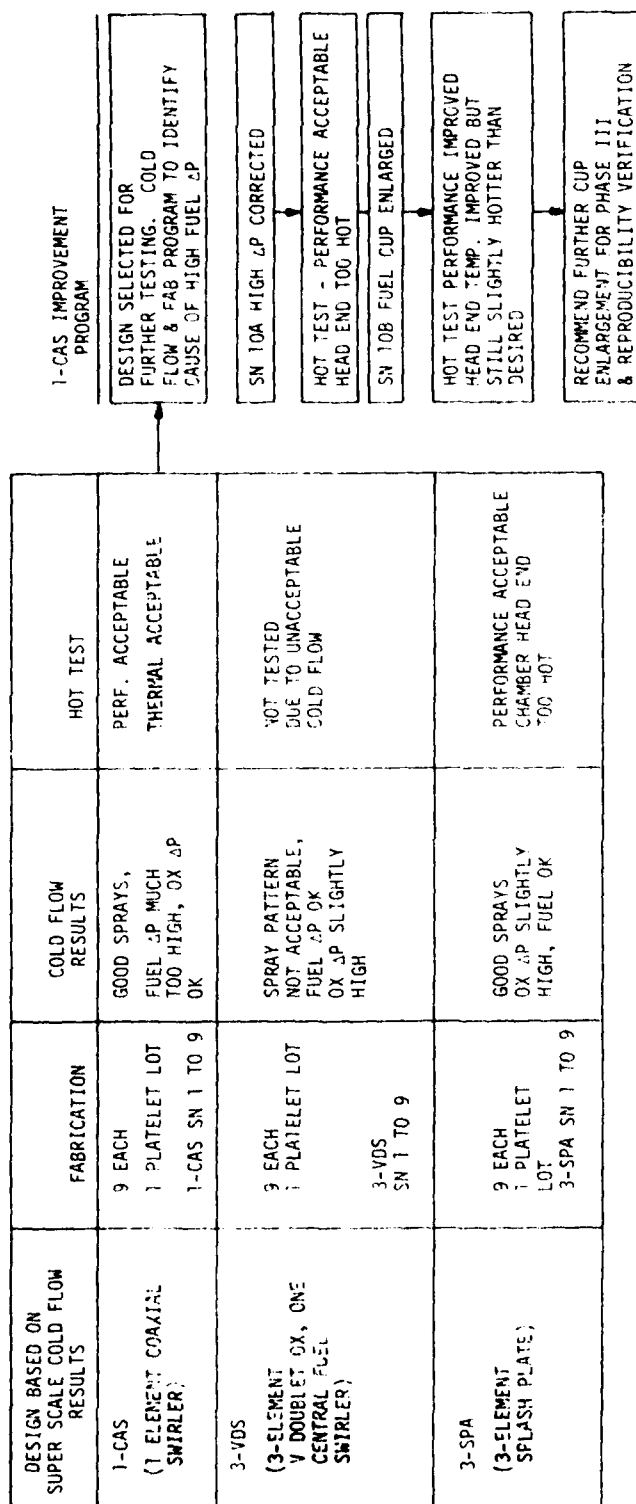


Figure 5-4. Phase II Injector Screening and Verification Testing

0478 SP 079

Aerofel Liquid Rocket Company

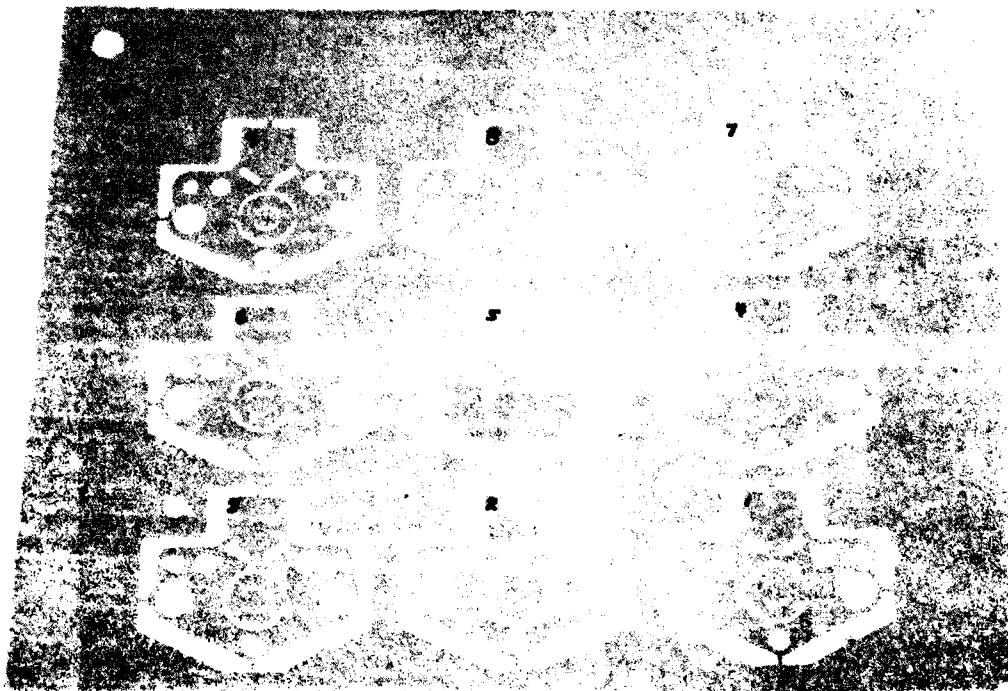


Figure 5-5. Photo-etched Injector Fabrication Arrays

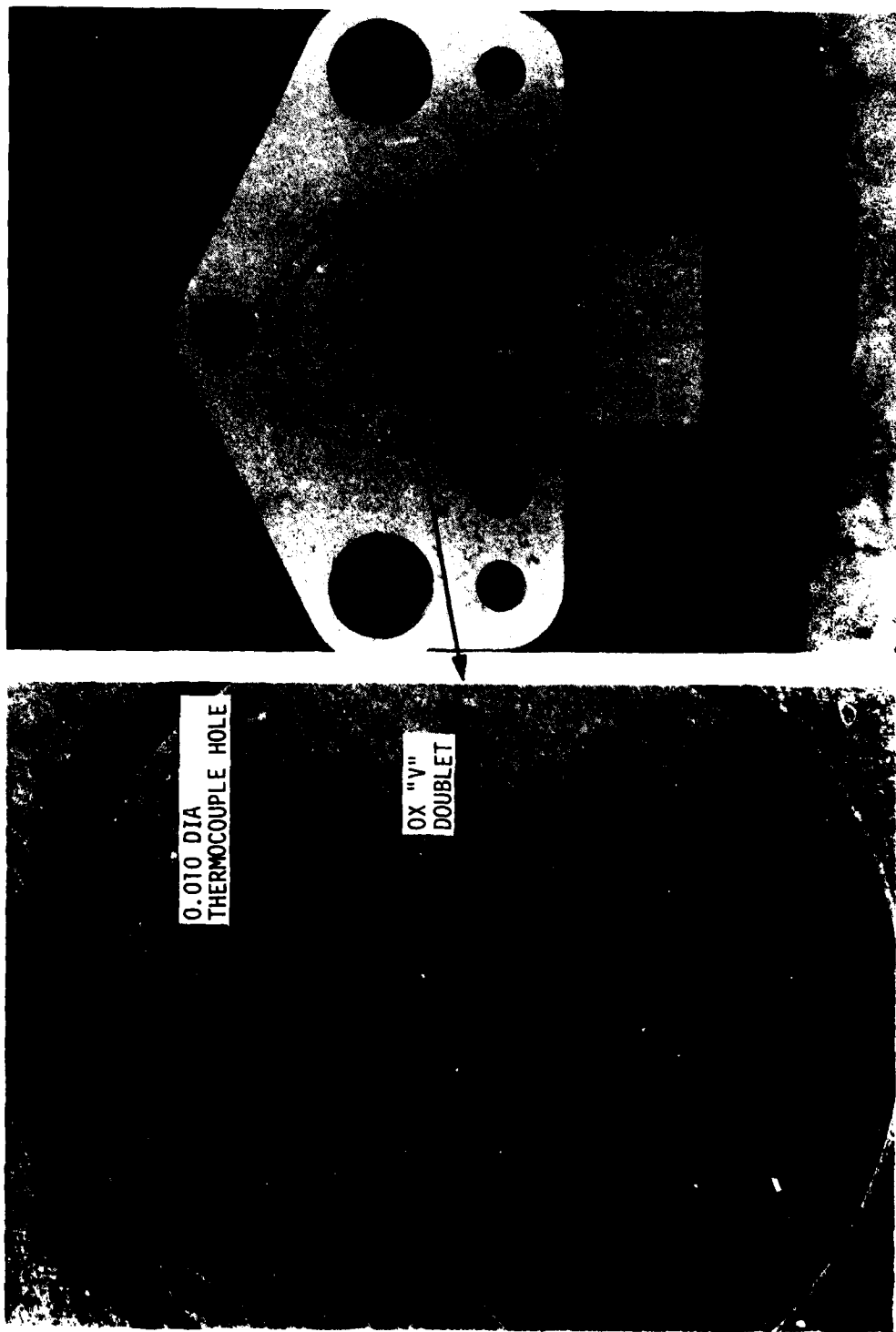


Figure 5-6. Three-Element V Doublet-Swirler Injector 3-VDS

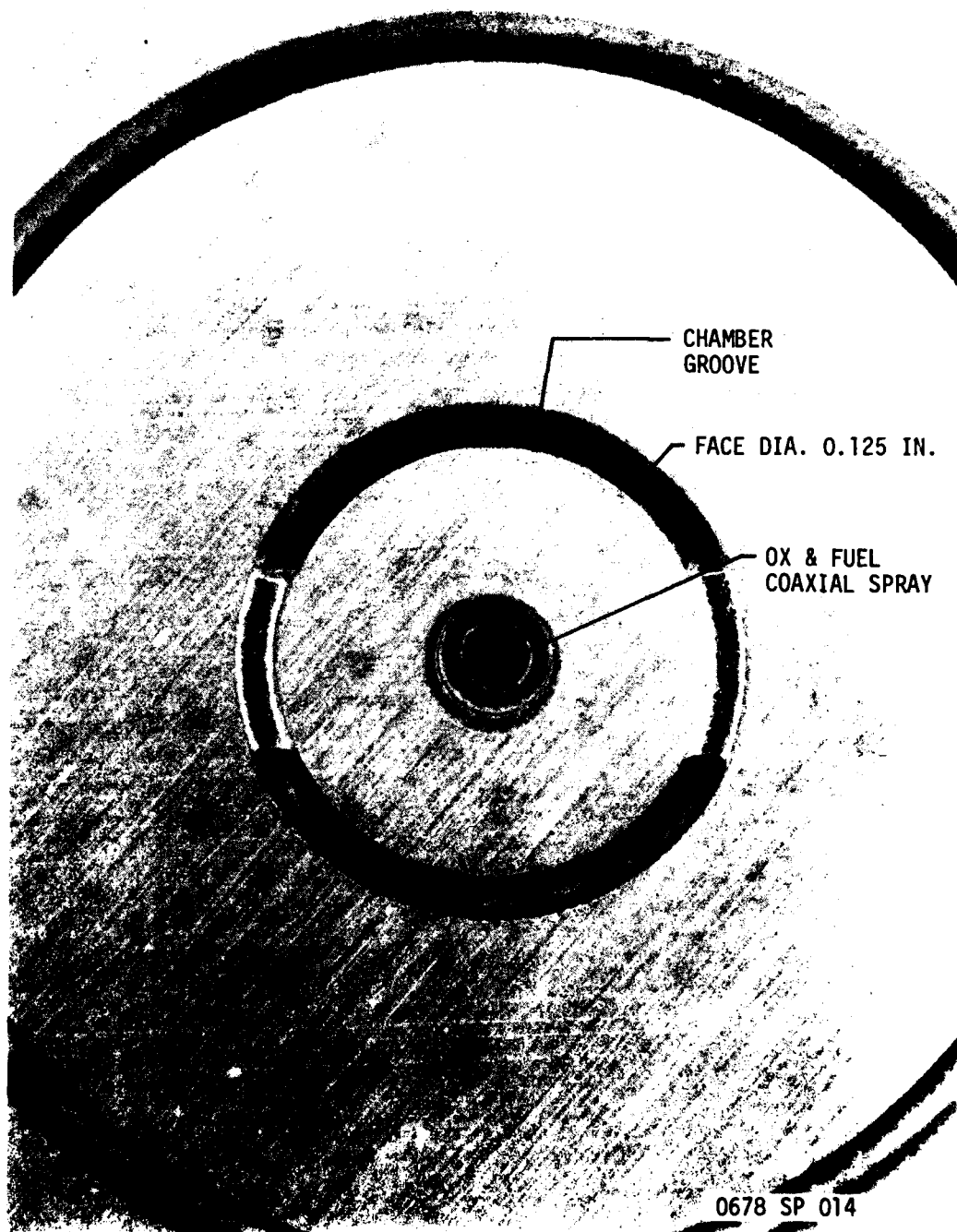


Figure 5-7. Coaxial Swirler Injector (1-CAS)

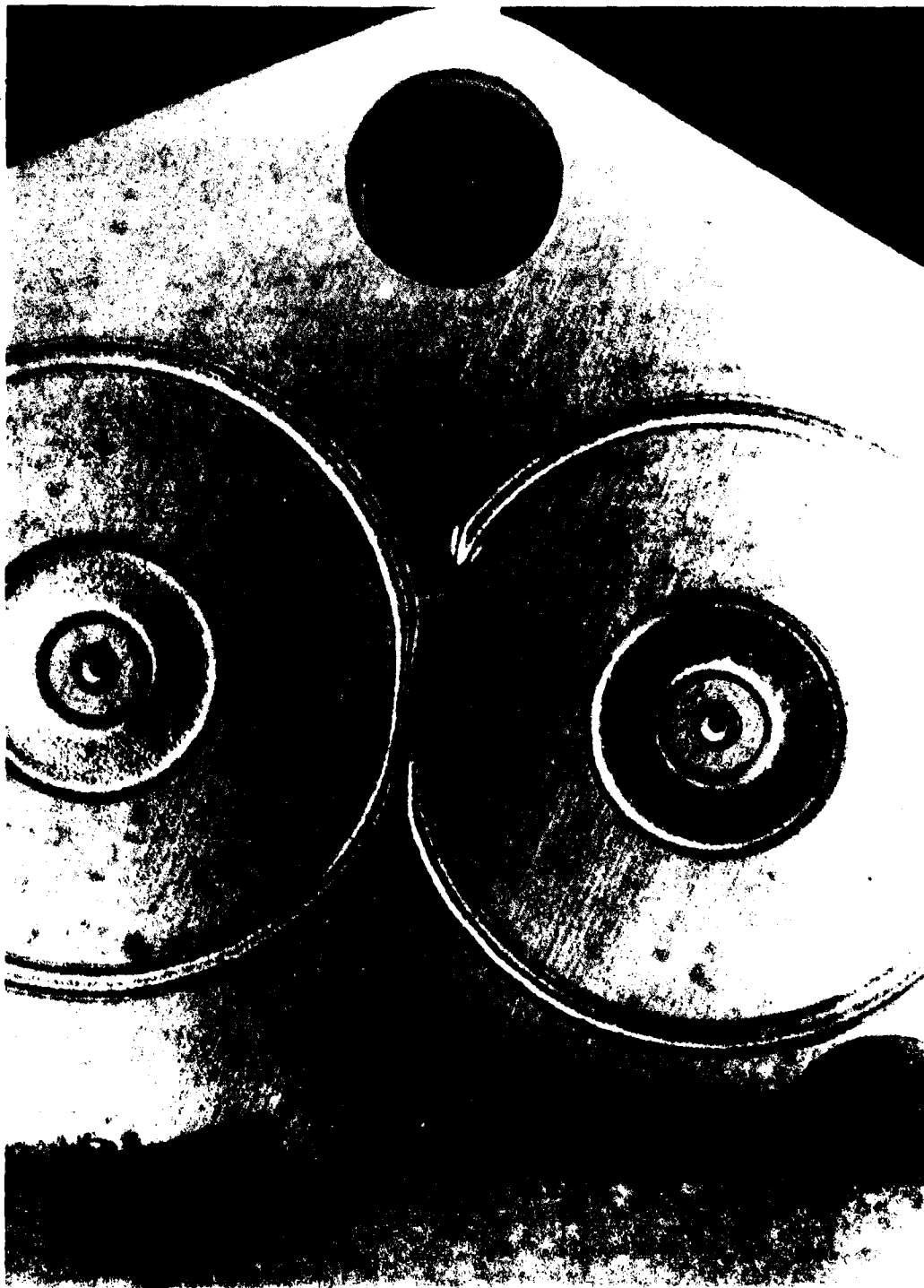


Figure 5-8. Backside of Typical Photo-etched Injector Containing Integral Valve Seats and Seal Glands

5.1, Engine Design and Fabrication (cont.)

After the selection of the 1-CAS design as superior in terms of performance, cooling, and fabrication considerations, a series of tests were conducted to correct the high fuel circuit pressure drop. These tests consisted of sectioning one of the injectors and measuring the actual post-bond passage sizes. They also included cold-flowing a series of nonbonded platelets to identify the actual pressure drops in the various elements, i.e., inlet, filter plates, manifold plates, etc. This work is documented in Appendix C.

The result of these tests indicated that no deformation during bonding occurred and that the addition of several additional plates of existing designs would provide the desired pressure drop.

5.1.2.3 Cold Flow

Units SN 1 through SN 9 of the 1-CAS design, SN 4, 8, and 9 of the 3-VDS design, and SN 1, 4, 8 and 9 of the 3-SPA design were flowed to examine the pressure drop and spray pattern. The injector Kw data are provided in Tables 5-III, 5-IV and 5-V, and Figures 5-9, 5-10 and 5-11.

Figure 5-9 shows the sensitivity of Kw to small differences in fabrication tolerances for each circuit. The 1-CAS fuel circuit flow area and Kw were found to be more repeatable. The fuel circuit utilizes the plate thickness and slot width to provide metering, while the oxidizer circuit utilizes the relative diameters of the vortex cups.

Figures 5-10 and 5-11 display the variation of Kw with pressure drop for each of the two design circuits. The drop in Kw at the low flowrates (low ΔP) is due to a laminar flow condition. The 3 data points of the CAS-1 SN 9 injector assembled into the first valve can be fit by the following combined laminar and turbulent flow equation:

$$\Delta P = K_1 \mu V + K_2 S_g V^2$$

where:

- ΔP = pressure drop (psi, fuel circuit)
- μ = viscosity (Cp)
- V = volumetric flowrate (cc/sec)
- S_g = specific gravity
- K_1, K_2 = empirical constants

TABLE 5-III

SN 1 TO 9 COAXIAL SWIRLER COLD FLOW DATA

SN	ΔP psi	Oxidizer				Fuel			
		n sec	Q cc	T °C	$\frac{Q}{n} \sqrt{\frac{\rho}{\Delta P}}$ lb/sec/ $\sqrt{\text{psi}}$	n sec	Q cc	T °C	$\frac{Q}{n} \sqrt{\frac{\rho}{\Delta P}}$ lb/sec/ $\sqrt{\text{psi}}$
1	500					200	70.4	-	0.0000347
	500	200	102.6	21.6	0.0000505	200	70.8	21.0	0.0000349
	100	200	45.3	-	0.0000499	200	29.2	20.0	0.0000372
	25	84	9.4	20.4	0.0000493	150	10.0	20.1	0.0000294
	500					200	70.9	-	0.0000349
2	500	90	63.5	-	0.0000695	200	70.0	23.0	0.0000345
	100	200	58.5	-	0.0000644	200	29.2	-	0.00003216
	25	60	8.7	-	0.00006388	120	7.8	-	0.00002863
3	500					200	64.0	-	0.0000315
	500	180	74.2	19.0	0.0000406	200	63.0	19.8	0.0000310
	100	200	36.7	-	0.0000404	200	26.0	-	0.0000286
	25	106.6	9.60	18.6	0.0000397	120	6.6	-	0.0000247
	500					200	63.0	-	-
4	500	120	66.0	-	0.00005418	200	71.5	24.0	0.0000352
	100	200	50.0	-	0.00005507	200	30.0	-	0.00003304
	25	60	7.6	-	0.0000558	120	7.9	-	0.000029
5	500	160	96.0	23.0	0.00005909	200	71.5	24.0	0.00003522
	100	200	53.0	-	0.00005837	200	31.0	-	0.00003414
	25	60	8.1	-	0.00005947	120	7.8	-	0.00002863
6	500	180	120	23.0	0.00006567	200	69.0	23.6	0.00003398
	100	200	59.5	-	0.00006553	200	29.0	-	0.00003194
	25	60	8.5	-	0.00006241	120	7.6	-	0.0000279
7	500	120	60.0	21.0	0.00004925	200	70.5	21.0	0.0000347
	100	200	45.5	-	0.00005011	200	29.5	-	0.00003249
	25	80	8.2	-	0.000045154	120	7.0	-	0.00002570
8	500	120	78.0	23.0	0.00006402	200	73.0	-	0.00003595
	100	200	57.0	-	0.00006278	200	32.5	-	0.00003579
	25	60	8.8	-	0.0000646	120	8.15	-	0.00002992
9	500	120	68.2	17.2	0.0000560	200	71.2	18.8	0.0000351
	100	200	50.0	16.9	0.0000551	65.5	9.70	-	0.0000326
	25	75	9.69	-	0.0000569	141.2	9.57	-	0.0000292

Water Flow for KW; Flow Facility: Trailer (Filtration = 1, ea 5 μ milipore)

TABLE 5-IV

"V" DOUBLET SWIRLER INJECTOR COLD FLOW DATA

Injector SN	ΔP	Ox Circuit		Fuel Circuit	
		\dot{W} lb/sec 10^{-4}	K_w 10^{-5}	\dot{W} lb/sec 10^{-4}	K_w 10^{-5}
4	25	2.42	4.85	2.06	4.11
	100	5.21	5.21	4.41	4.41
	500	12.04	5.39	10.13	4.53
	500	12.00	5.37	9.93	4.47
8	25	2.28	4.58	2.20	4.41
	100	4.85	4.85	4.70	4.70
	500	11.12	4.98	10.50	4.73
	500	11.01	4.93	10.90	4.89
9	25	1.93	3.86	2.13	4.26
	100	4.70	4.04	4.55	4.55
	500	9.36	4.19	10.50	4.70
	500	9.43	4.22	10.50	4.70

Design ΔP Ox = .00112
Fu = .00068

TABLE 5-V
SPLASH PLATE INJECTOR COLD FLOW DATA

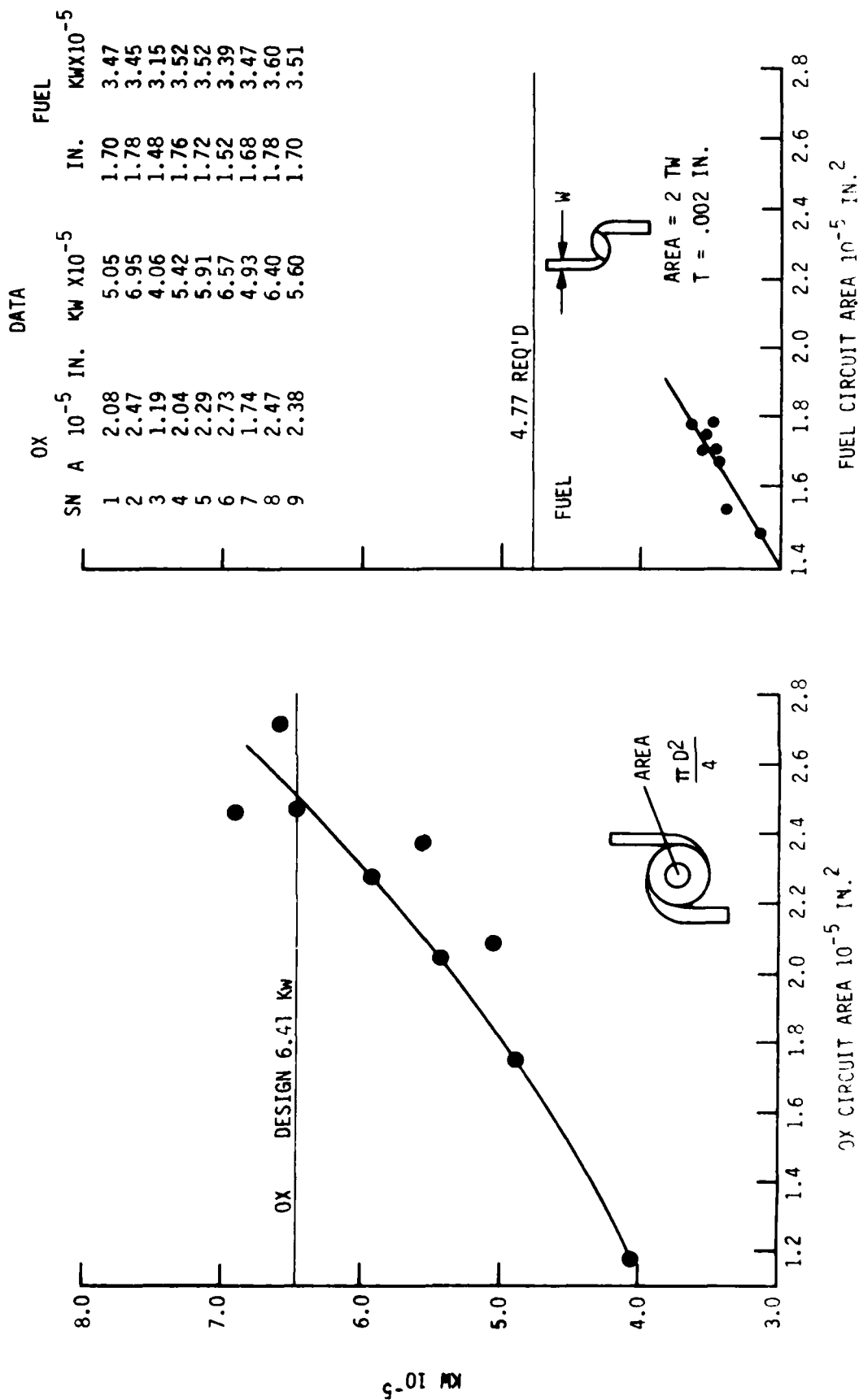
SN	Pressure, psia	Ox K _w ¹⁰⁻⁵	Fuel K _w ¹⁰⁻⁵
1	100	5.09	4.74
	500	5.24	4.71
4	100	5.26	5.02
	500	5.39	4.83
8	100	5.16	4.57
	500	5.20	4.89
9	100	4.60	4.52
	500	4.56	4.51

DESIGN VALUE	6.41	4.77
AVERAGE DATA	5.06	4.72
% DIFFERENCE	21%	.8%

$$K_w = \frac{\dot{W}}{\sqrt{\Delta p \cdot sg}} = \frac{(\text{lb/sec})}{\sqrt{\text{psi} (\text{spec. grav.})}}$$

INJECTOR KW-AREA SENSITIVITY 1-CAS DESIGN

$\Delta P = 500$ PSIA WATER



- 7 PLATELET

- 10 PLATELET

Figure 5-9. Coaxial Swirler Injector Kw-Dimensional Sensitivity

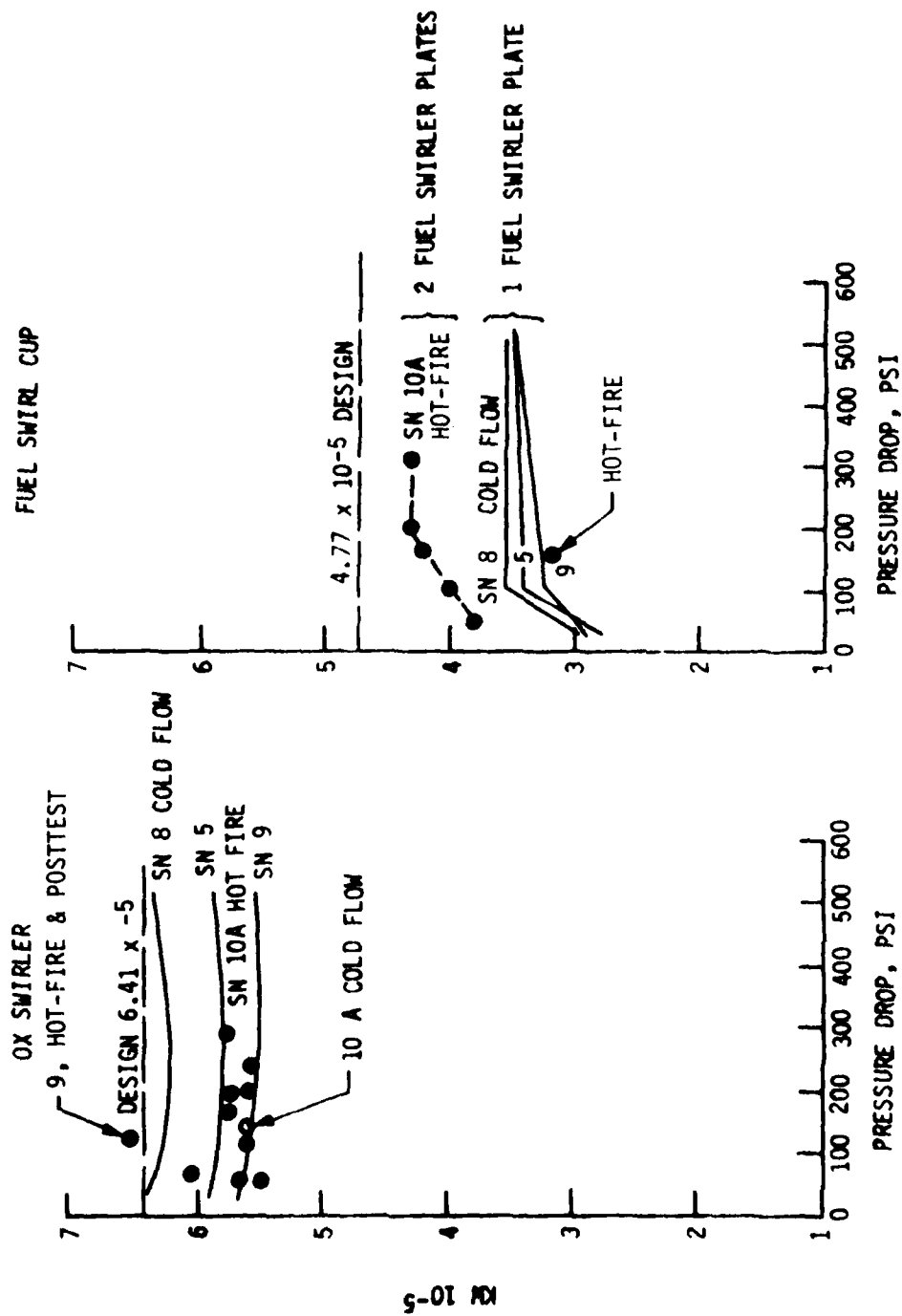


Figure 5-10. Coaxial Swirler Kw-AP Sensitivity for 3 Injectors

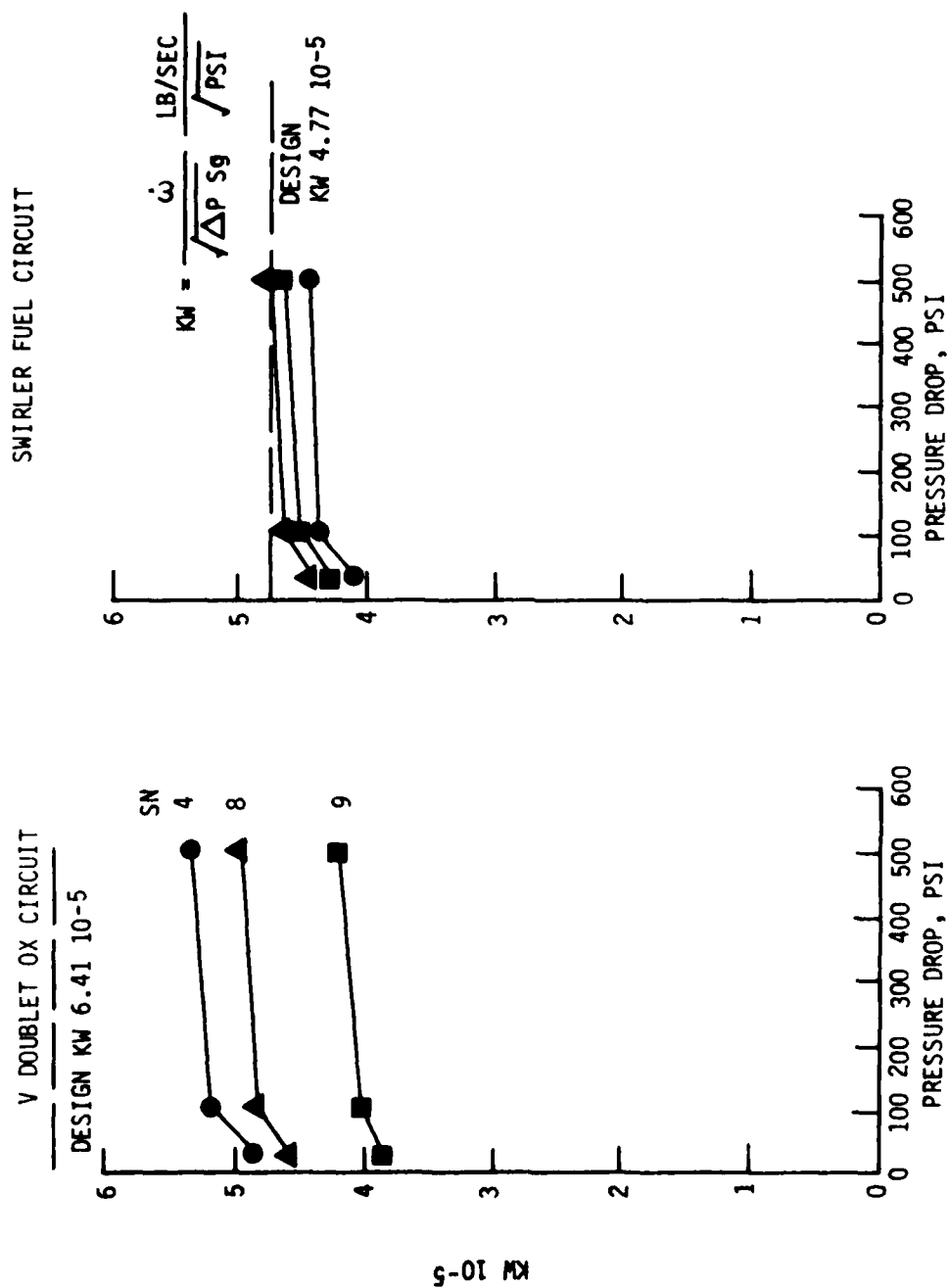


Figure 5-11. "V" Doublet Swirler Kw-P Sensitivity for 3 Injectors

5.1, Engine Design and Fabrication (cont.)

This equation indicates that, at 500 psi, 11% of the pressure drop is associated with laminar flow and 89% with turbulence, while, at 25 psi, 40% is laminar and 60% turbulent.

The larger unit-to-unit differences in the V-doublet ox circuit pressure drop are due to this design's sensitivity to stacking alignment since both the inlet and discharge ends of the "V" are controlling. The superior reproducibility of the fuel swirler on the 3-VDS design is due to the larger .008 in. control orifice versus the .0055 diameter for the similar ox swirler of the 1-CAS design.

The three 3-VDS design injectors that were considered to have the best alignment were cold-flowed and visually inspected for pattern uniformity. The swirler fuel circuits were found to be symmetric, repeatable, and finely atomized. Visual inspection of the 3 V-doublet elements showed that the 3 oxidizer streams did not impinge as predicted, with the result that 3 unatomized oxidizer streams passed completely through the fuel vortex cone. Since this condition is predicted to result in poor compatibility and low performance, work on this design was discontinued at this point in the program.

The cold-flow spray and pressure drop data from the 3-SPA designs, shown in Table 5-V, were found to be acceptable, and units 1 and 9 were selected as candidates for hot-fire testing.

5.1.3 Thrust Chamber Design and Fabrication

5.1.3.1 Design

Thrust chambers were designed for Phase II verification testing to meet the following test requirements:

- 1) Aerodynamic area ratio of 100:1 (geometric area ratio of 143:1) to allow the nozzle to flow full at chamber pressures as low as 50 psia
- 2) Chamber lengths which permit performance and thermal data to be obtained at $L^* = 1$ and 2 in.
- 3) A flanged assembly such that each injector could be tested at the two chamber lengths
- 4) A chamber wall thickness and internal contour which conform to the Phase I thermal and performance analyses.

5.1, Engine Design and Fabrication (cont.)

The chambers designed to meet these test requirements are shown in Figure 5-12. The steel head end, which is brazed to the injector, and the clamps, which hold the flanges together, are shown schematically in Figure 5-13. One additional chamber was fabricated without a flange to explore the potential problems of an all-welded configuration.

5.1.3.2 Fabrication

The 143:1 area ratio thrust chambers discussed in the previous section were fabricated from C-103 columbium bar and coated with an R 512-E, silicide diffusion coating by Hitemco, Inc. A photo of these chambers prior to coating is shown in Figure 5-14. No fabrication problems were encountered in the chamber machining, brazing, coating, or engine assembly. Figure 5-15 shows engine assemblies with 1" and 2" chamber lengths.

5.2 HOT-FIRE TESTING

5.2.1 Test Objectives

The objective of this test activity was to verify (1) the forecast steady-state and pulsing mode performance, (2) dynamic and response characteristics, and (3) thermal characteristics of components for a 0.5 lb thrust class bipropellant engine.

5.2.2 Test Specification and Goals

The program goal was to demonstrate a steady-state specific impulse of 280 sec and a bit impulse capability of 0.005 lb sec (0.01 sec pulse) for which the pulse performance was 220 sec. The Phase II testing was intended to verify the capabilities of the anticipated Phase III designs. Testing was conducted over the following range of conditions:

Pc	40 - 125 psia
Thrust	0.2 - 0.5 lb
MR	1.65 (nom. range 1.2 - 1.7)
Prop. Temp	20 - 120°F

Figure 5-16 provides a comparison of the design goal versus actuals. The propellants employed in testing were Green N₂O₄ (99.0 + % N₂O₄, 0.8% NO) per MIL-P-26539 and MMH (CH₃N₂H₃, 98% purity) per MIL-P-27404. Certification of all propellants was provided.

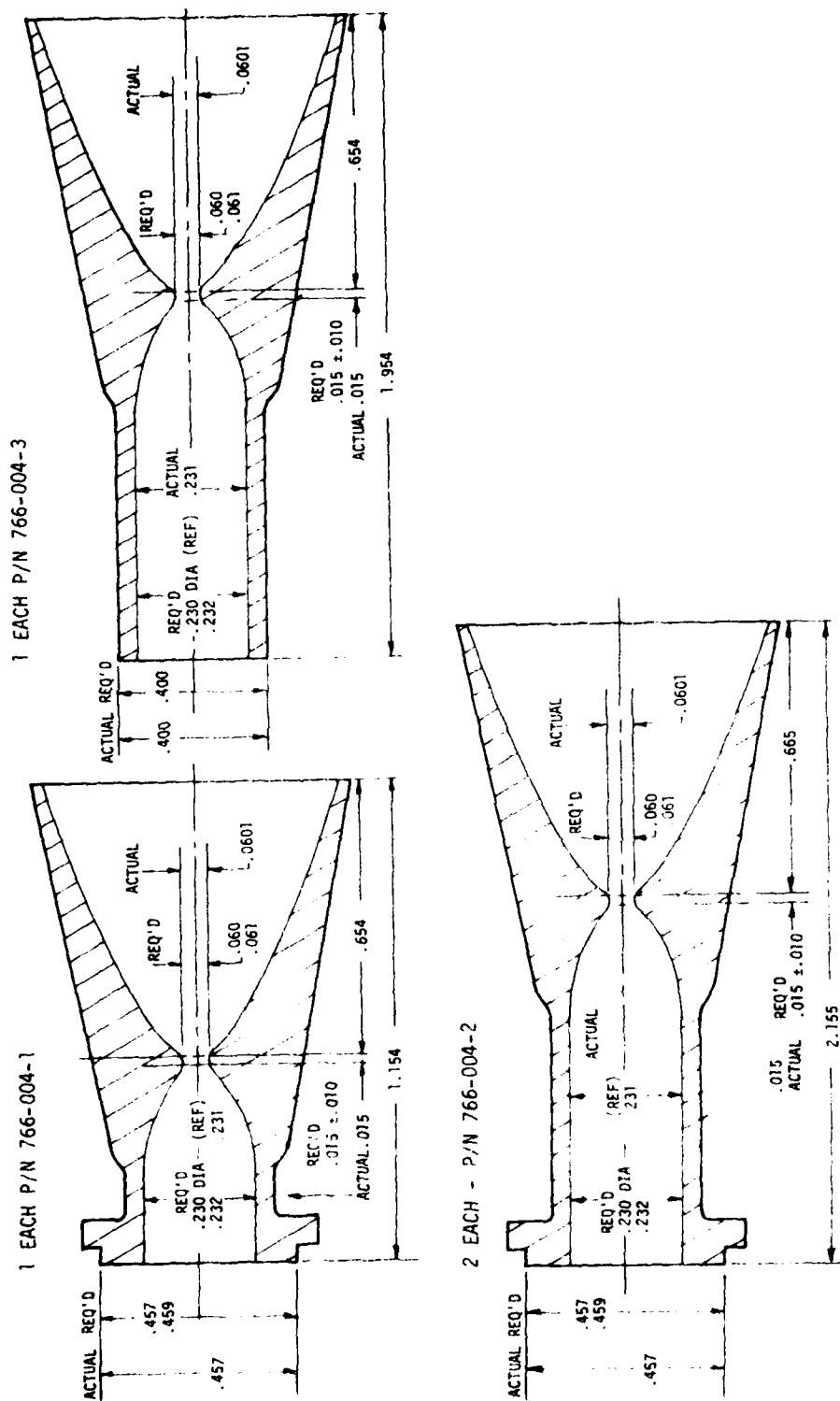


Figure 5-12. Phase II Chamber Design and Dimensions

FLANGED DESIGN FOR PHASE II VERIFICATION AND L' OPTIMIZATION TESTING

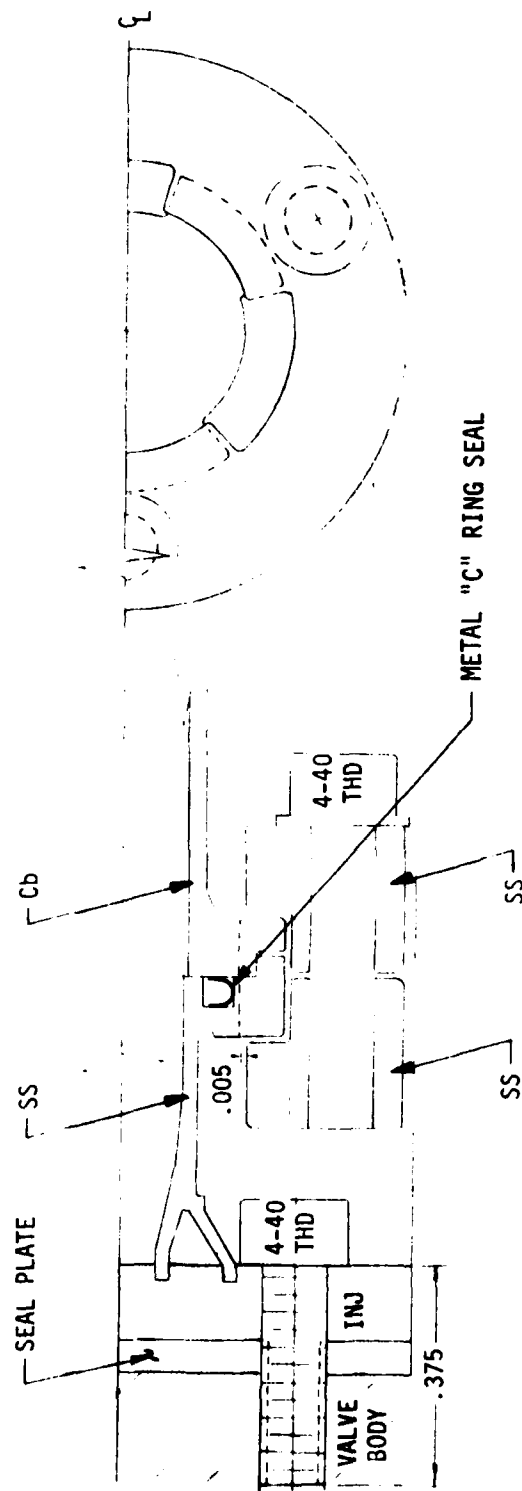


Figure 5-13. Phase II Flanged Chamber Configuration

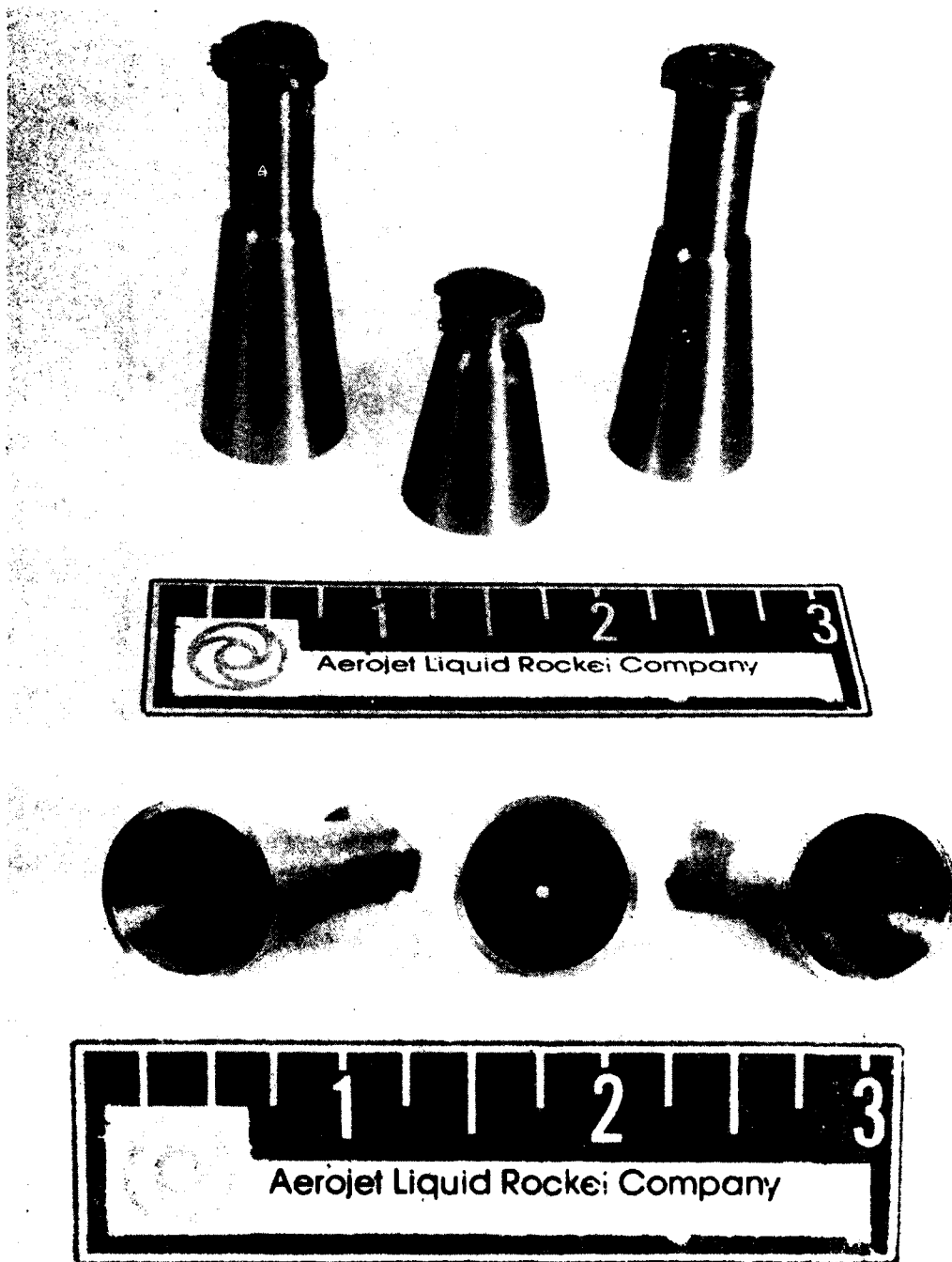
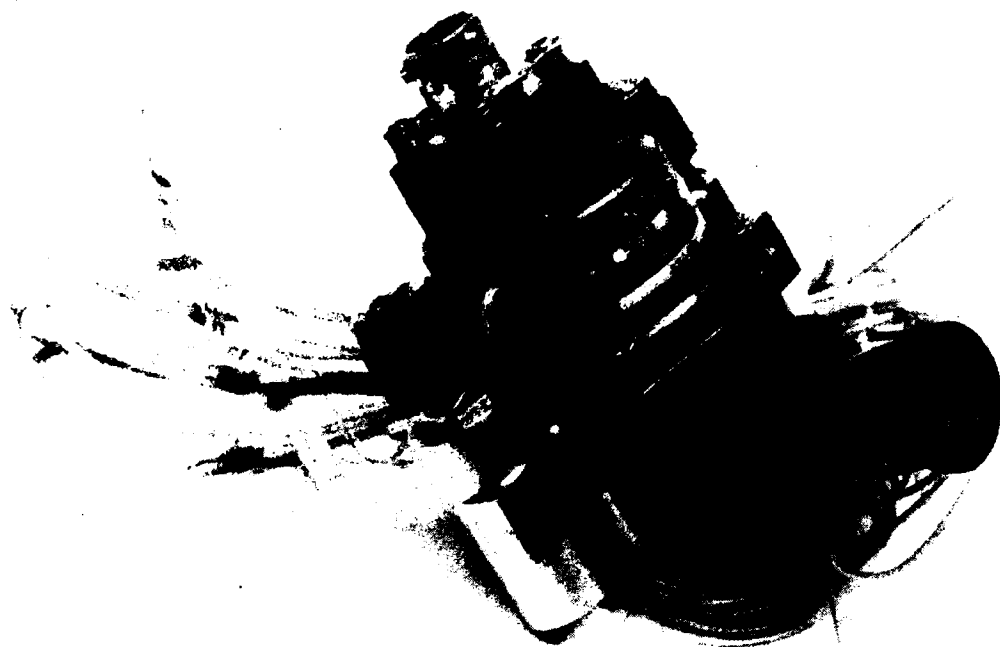
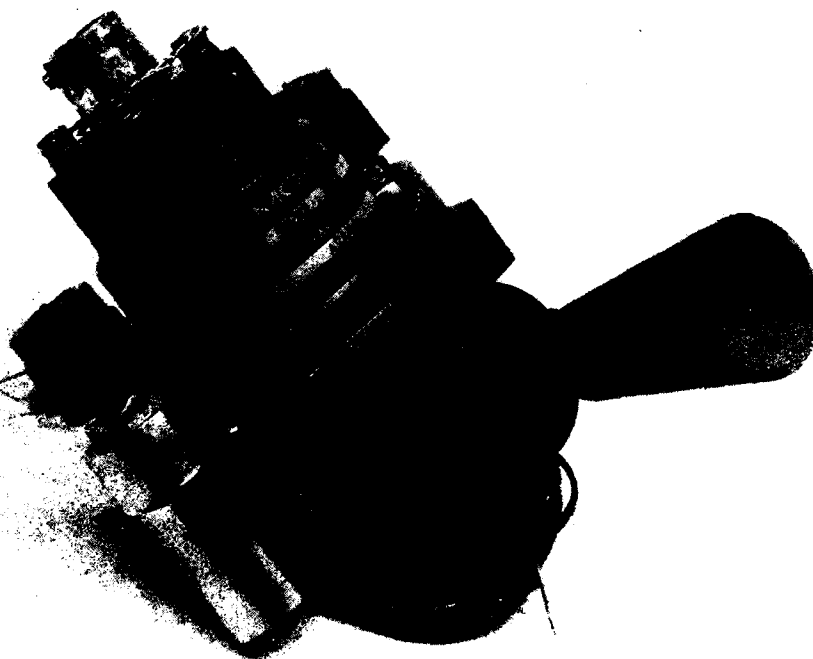


Figure 5-14. Phase II Columbum Chamber Photographs before Coating



$L' = 1''$



$L' = 2''$

Figure 5-15. Phase II Engine Assemblies with 1 inch and 2 inch Chamber L 's

GENERAL ENGINE ASSEMBLY DESIGN GOAL

PARAMETER	GOAL	ACTUAL TEST RANGE
Nominal Vacuum Full Thrust	0.5 lbf	0.17 to 0.49
Chamber Pressure	TBD psia	40 to 125
Maximum Feed System Pressure	400 psia	420
Minimum Feed System Pressure	TBD psia	108 (Not Lower Limit)
Expansion Ratio	TBD	100:1 Aerodynamic
Nominal Isp (at Full Thrust)		
Steady-state	280 sec	275
Pulsing (10 ms)	220 sec	180 (Cold Engine)
Nominal Minimum Impulse Bit (at Full Thrust)	0.005 lb-sec \pm 0.0005 lb-sec	0.002 \pm 5% 1 Sigma
Number of Maximum Thermal Cycles	>1000	Not Evaluated
Total Number of Starts	>750,000	1,000,000 Valve Only Bench Test H_2
Single Burn Duration	>2 hr	260 sec at .38 lb Thrust
Total Firing Life	>10 hr	TBD
Valve Response		
Signal to Full Open	< 0.005 sec (< 5.0 ms)	< .003 sec Open
Signal to Full Close	< 0.005 sec (< 5.0 ms)	\approx .001 sec Close
Valve Leakage	< 2.3 scc/hr	< 2.3 SCC/hr
(GN ₂ @ ΔP = Max Feed System Press)		
Propellants		
Oxidizer	Nitrogen Tetroxide (MON-1) (99% N ₂ O ₄ -0.8% NO)	Mon 1 & Mon 10
Fuel	Monomethylhydrazine (N ₂ H ₃ CH ₃)	N ₂ H ₃ CH ₃
Mixture Ratio	1.64, nominal at 70°F	1.2 to 1.7
Propellant Inlet Temperature Range	20 to 200°F	30 to 125
Storage Life	10 Yr	Not Evaluated
Flightweight Assembly Reliability	0.999	Not Evaluated
Flightweight Assembly Maintainability	Zero Maintenance Over Storage Life	Not Evaluated
Flightweight Assembly Weight	TBD lbm	0.7

Figure 5-16. Comparison of Goals and Phase II Accomplishments

5.2, Hot-Fire Testing (cont.)

5.2.3 Test Hardware

The hardware employed in Phase II hot-fire testing included the following:

PHASE II HARDWARE SUMMARY

	<u>Part Designation</u>	<u>Material</u>	<u>Quantity Built</u>
Flanged Sleeve (3SPA)	PC-766-001	CRES 304L	1
Flanged Sleeve (3VDS)	PC-766-002	CRES 304L	1
Flanged Sleeve (1CAS)	PC-766-003	CRES 304L	1
Flanged Chamber $\epsilon = 143:1$ $L' = 2"$	PC-766-004-2	C-103	2
Flanged Chamber $\epsilon = 143:1$ $L' = 1"$	PC-766-004-1	C-103	1
Chamber Weld Blank $\epsilon = 143:1$	PC-766-004-3	C-103	1
Flange Clamp	PC-766-005	CRES 304	2
Pressure Seal	PC-766-006	CRES 304	3
Pressure Port	PC-766-007	CRES 304	5
Injector 3SPA 3 Element Splashplate	PC-766-008	CRES 347	9
Injector 3VDS 3 Element V-Doublet Swirler	PC-766-009	CRES 347	9
Injector 1-CAS 1 Element Coaxial Swirler	PC-766-010	CRES 347	10

5.2, Hot-Fire Testing (cont.)

	<u>Part Designation</u>	<u>Material</u>	<u>Quantity Built</u>
Valve Simulator (Injector cold flow)	PC-766-011	Aluminum	1
Purchased Items			
4-40 Capscrews		A286	12
Seal, Spring Energized Teflon Fluorocarbon PN A02828			24
Seal, Metal C Ring Pressure, Science Corp. PN 612 RS-0004-2			24
Valve, Torque Motor Bipropellant, Moog PN A24462, Model 52F112			2

5.2.4 Test Facility

Development of the 0.5 lb thrust engine required an extensive altitude test program consisting of pulses and steady-state burns. Consequently, accurate thrust stand and propellant metering systems were required to provide total impulse and specific impulse data. Extensive test experience from specially developed test systems had been obtained at ALRC with 100 and 5 lbf pulse engines. Based on this, a pulse engine test stand and a propellant delivery system for use with the 0.5 lb thrust bipropellant engine was developed at ALRC with company funding. It included component temperature control and propellant temperature conditioning and was designed to operate at vacuum.

A number of thrust measurement techniques were considered, such as impulse measuring pendulum stands, conventional force measurement stands with strain gage load cells, and conventional stands with crystal load cells. Pendulum-type stands were eliminated since they provide no direct measurement of pulsed thrust versus time and are not suited for impulse or thrust measurements of continuous firings. Strain gage load

5.2, Hot-Fire Testing (cont.)

cells of special design had been successfully used in similar applications (e.g., 5 lb thruster, Contract F04611-73-C-0061) and the resulting stand natural frequency (500 to 800 Hz) was near the desired value for good pulse and transient measurements. However, stands of this type have very small load cell deflections and as a result the systems are very sensitive to small changes in temperature. These temperature effects can become very significant in long duration firings, making the stand unsuitable for accurate steady thrust measurements for durations over a few seconds.

The selected thrust measuring system employs a dual thrust measurement with separate instrumentation for steady-state thrust measurement and for pulse and transient measurement. The basic components of the selected system are a high frequency section with a thruster mounting plate, a low frequency section, and a load cell calibrator. The dual thrust concept had been developed for the Small Impulse Bit ACS Engine (Contract F04611-76-C-0018) and was being refined under Contract F04611-77-C-0019, Design and Fabrication of a Thrust Measuring System for a 100 lb Thrust Attitude Control System.

° THRUST MEASUREMENT

The thrust stand shown in Figure 5-17 consists of 1) a dynamic section to measure thrust for durations of zero to 2 sec and 2) a critically damped steady-state section for measuring thrust for durations of 0.5 sec and longer. The dynamic cell has very high frequency response, but, being a crystal device, is subject to exponential signal decay when measuring a constant force.

The steady-state cell gives accurate readings of relatively slowly changing forces. However, its lack of stiffness (0.01 in. full-scale deflection) prevents it from having high frequency response. The relatively large deflection of the steady-state measurement system reduces the error potential due to small temperature changes.

The engine assembly is attached to a temperature-conditioned mounting plate which, in turn, is mounted to the dynamic load cell. The dynamic load cell, a BLH Model LPB-1 with a dynamic range of ± 1 lbf, is temperature-conditioned by the shroud that surrounds it.

A seismic mass isolates the dynamic section from the steady-state force system, limiting the rate at which load is applied to the steady-state load cell and the acceleration of the dynamic system. The seismic mass, in conjunction with a fluid damper, provides steady force readings

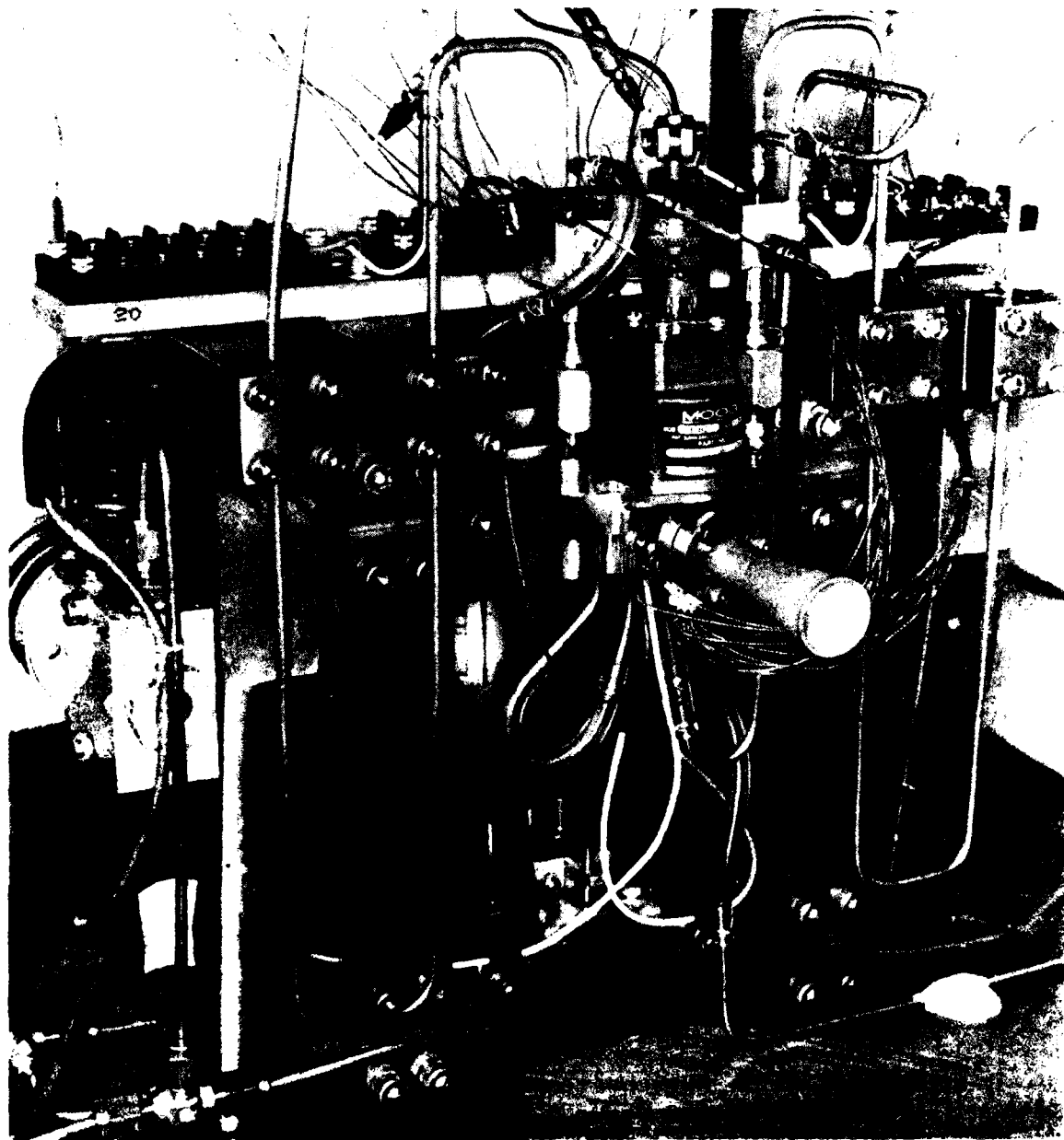


Figure 5-17. Phase II Thrust Stand with the 0.5 lb Thrust Engine in Place

5.2, Hot-Fire Testing (cont.)

in ≈ 0.5 sec. This assembly is mounted on leaf flexures. The stiffness of these flexures balances the destabilizing force due to the deflected mass of the stand, thereby maintaining the test bed in a neutral, vertical position.

Figure 5-18 is a schematic drawing showing the load paths in the system. For thrust measurement, the engine forces are applied through the dynamic load cell to the seismic mass and into the measuring load cell to ground. For calibration of both load cells, an external force is applied through a calibrator load cell. This cell is connected to the engine side of the crystal load cell by means of a calibrator pull rod which engages the engine mounting plate as the calibrator load cell rotates on a flexure mount during loading. This calibrator system is used to measure the unavoidable restraints of the flexures supporting the seismic mass, instrumentation lines, and plumbing.

The steady-state thrust stand measurements shown in Figure 5-19 indicated good repeatability and constant stand bias.* The thrust stand calibration is routinely rechecked prior to and after testing. During long coasts, a computer-controlled automatic thrust calibration program is used.

The single washer style load cell was used because of the low engine mass and to reduce the overall complexity of the system. However, the resulting structure had a 300 Hz natural frequency in the transverse bending mode when the relatively large, overhung mass of the columbium throat/exit assembly was in place.

The axial natural frequency was 800 to 1200 Hz. Some coupling between the axial force and the transverse mode (or some amount of non-axial force) excited the 300 Hz transverse mode during force transients, producing a ring which persisted for relatively long times. However, through a combination of electrical filtering and choice of proper integration period, accurate measurements of pulse impulse were achieved even in the presence of the ringing.

° PROPELLANT MEASURING SYSTEM

Propellant flowrates for a 0.5 lbf engine are in the range of 0.001 lbm per second. Since covering the wide range of total propellant delivery (0.010 sec pulse to steady-state) with a single measuring

$$*Bias = \left[\frac{\text{Applied Force}}{\text{Measured Force}} - 1 \right]$$

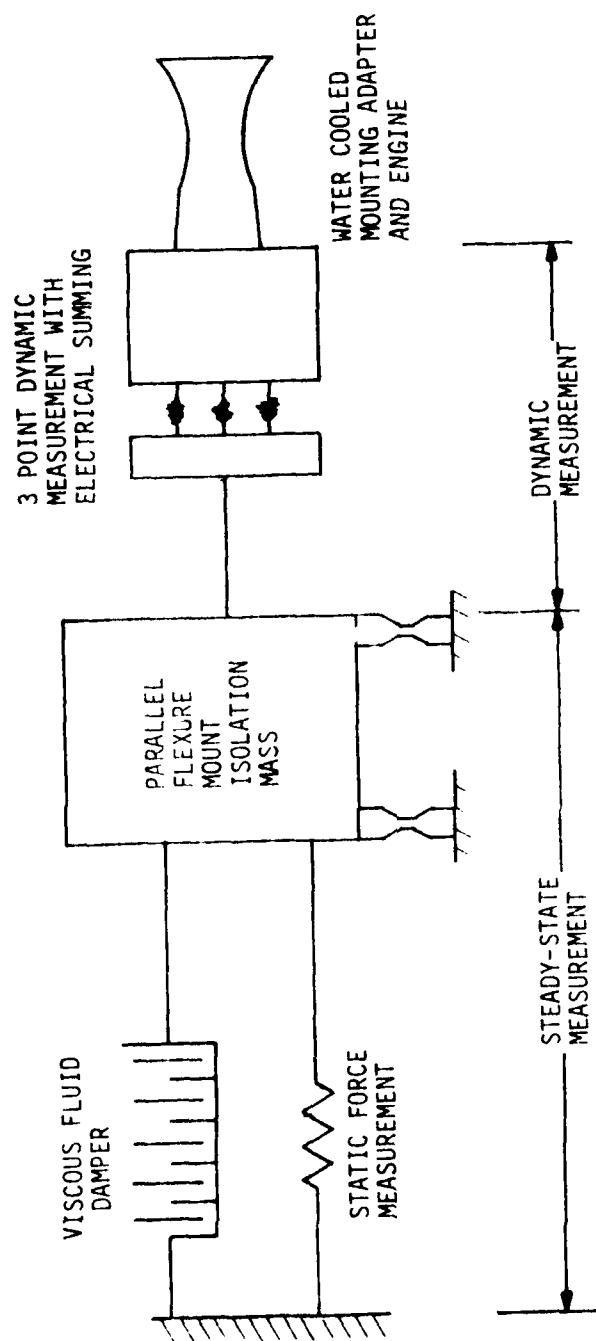


Figure 5-18. 0.5 lb Thrust Test Stand Load Paths

11 REPEAT CALIBRATIONS

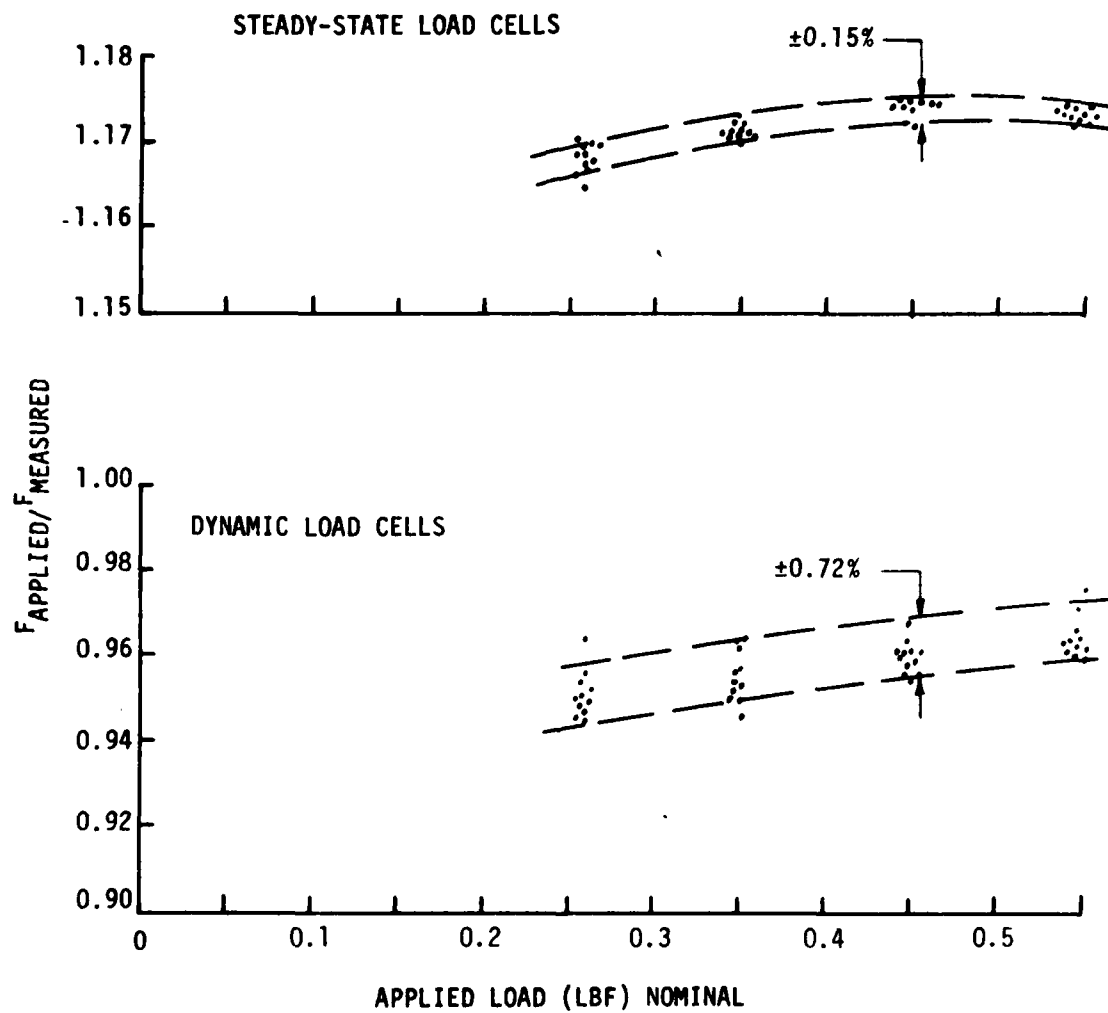


Figure 5-19. Dual-Tuned Thrust Measurement System Calibration Test Results

5.2, Hot-Fire Testing (cont.)

device would have been impractical, three flow measuring systems were incorporated. Paddle wheel flow meters were used for long duration tests, large positive displacement (piston) flow meters (PDFM) were used for intermediate durations, and specially developed gas displacement meters (micro-PDFM) were used for durations under one second. The general arrangement of the three different flow measuring systems used for both fuel and oxidizer is shown in Figure 5-20.

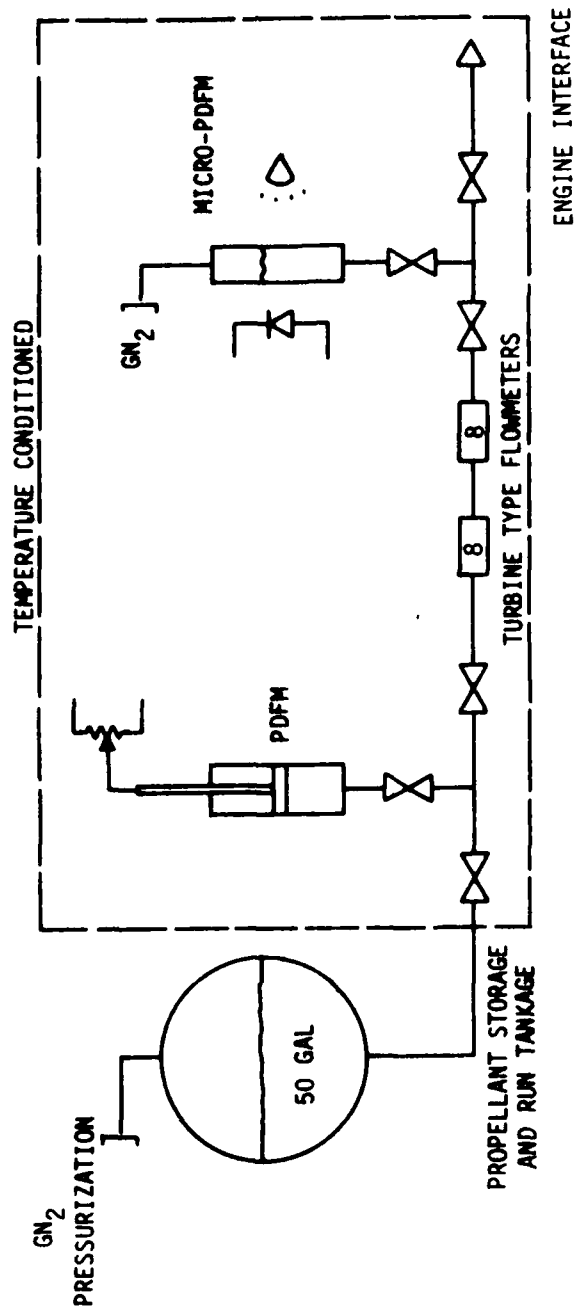
During pulsing and short duration tests, the line volumes were large relative to the small amount of propellant delivered. As a result, the feed system temperature needed to be accurately controlled since even small temperature changes introduce large errors caused by propellant volume changes. Therefore, all critical propellant system components and lines were either jacketed and conditioned with temperature-controlled fluid or mounted in temperature-controlled enclosures. Removal of all non-condensable gases from the micro-PDFM propellant feed system was essential for accurate pulse propellant delivery measurements.

The Flow Technology paddle wheel flow meters utilized were a variation of the turbine meter used routinely in rocket flow measurements, with modifications to permit operation in the .001 lbm/sec flow range. The relatively slow response of these meters limited them to steady-state flow measurements. They were calibrated against the large PDFM in each test where the 2 systems were run in series.

For intermediate total durations (in the 10 to 200 second range), either pulse or continuous positive displacement flow meters (PDFM) were used. Measurement of the displacement of a precision piston/cylinder assembly provided accurate propellant volume delivery data. The PDFM's used have a volume of about 0.025 gal, providing a maximum run capability of about 200 sec at full thrust. They have a 13 μ gal resolution when measured with a linear potentiometer. Because they provide the integral of flowrate, or total propellant delivered, they are ideal for providing flow data for total impulse measurements in pulsed mode operation.

The measurement of pulsed and short duration propellant flows was recognized to be a serious problem in characterizing low thrust engines. For example, fuel delivery for one 10 ms pulse is about 5 microliters in volume. The frictional resistance of a small diameter sliding piston measurement system was calculated to be excessive and would result in a significant drop in line pressure each time the valve is opened.

- DELIVERY SYSTEM CONCEPT



- FEATURES

- STEADY STATE - LONG BURN DURATION
- MIB
- REDUNDANT MEASUREMENT

Figure 5-20. Multiple Mode Propellant Delivery System

5.2, Hot-Fire Testing (cont.)

It became apparent that a minimum contact gas pressurization system using optical measurement techniques for fluid level measurement might be suitable for this application. Reticon, a subsidiary of EG&G, makes such optical devices. Their product consists of accurate arrays of photo diodes spaced as close as 16 microns and up to an inch in length, along with the electronics necessary to operate the device. Two special units were built by Reticon for Aerojet's application. These had 1728 diodes each, spaced 16 microns apart over a length of about one inch. This assembly is displayed in Figure 5-21.

These devices, with their associated electronics, provided both analog and digital measurement of the number of light or dark diodes in the array. The total diode array was scanned electronically 1000 times per second, providing the capability of one millisecond time resolution.

The diode array was used to measure the propellant level in a glass capillary precision bore tube. The tube bore was chosen to give a continuous test duration of about one second (equivalent to 100 pulses of 10 ms duration each). This results in about an 18 diode level change per pulse, or a minimum resolution of about 5% of one 10 ms pulse. Considering the maximum scan rate available (10 scans per 10 ms pulse), this is a reasonable choice.

A critical feature of the micro-PDFM design is the optical arrangement of the propellant level tube and optical sensor array. The fluid level in the tube cannot be used to attenuate the light reaching the diodes for a clear liquid topped with a clear vapor space. To make the level system practical, the propellant and tube operate as a lens system which focuses parallel light on the diode array; the focal point of the empty tube is not on the array. This effect provides a strong light level difference at the array in correspondence to presence or absence of fluid. This, plus the digital nature of the optical sensor, also makes the system highly immune to errors caused by any small droplets on the tube above the liquid level; since the light reaching the diode at any level is focused from the whole diameter of the tube, one or a few opaque drops do not block sufficient light to give a false reading.

Table 5-VI summarizes the multiple mode propellant delivery characteristics.

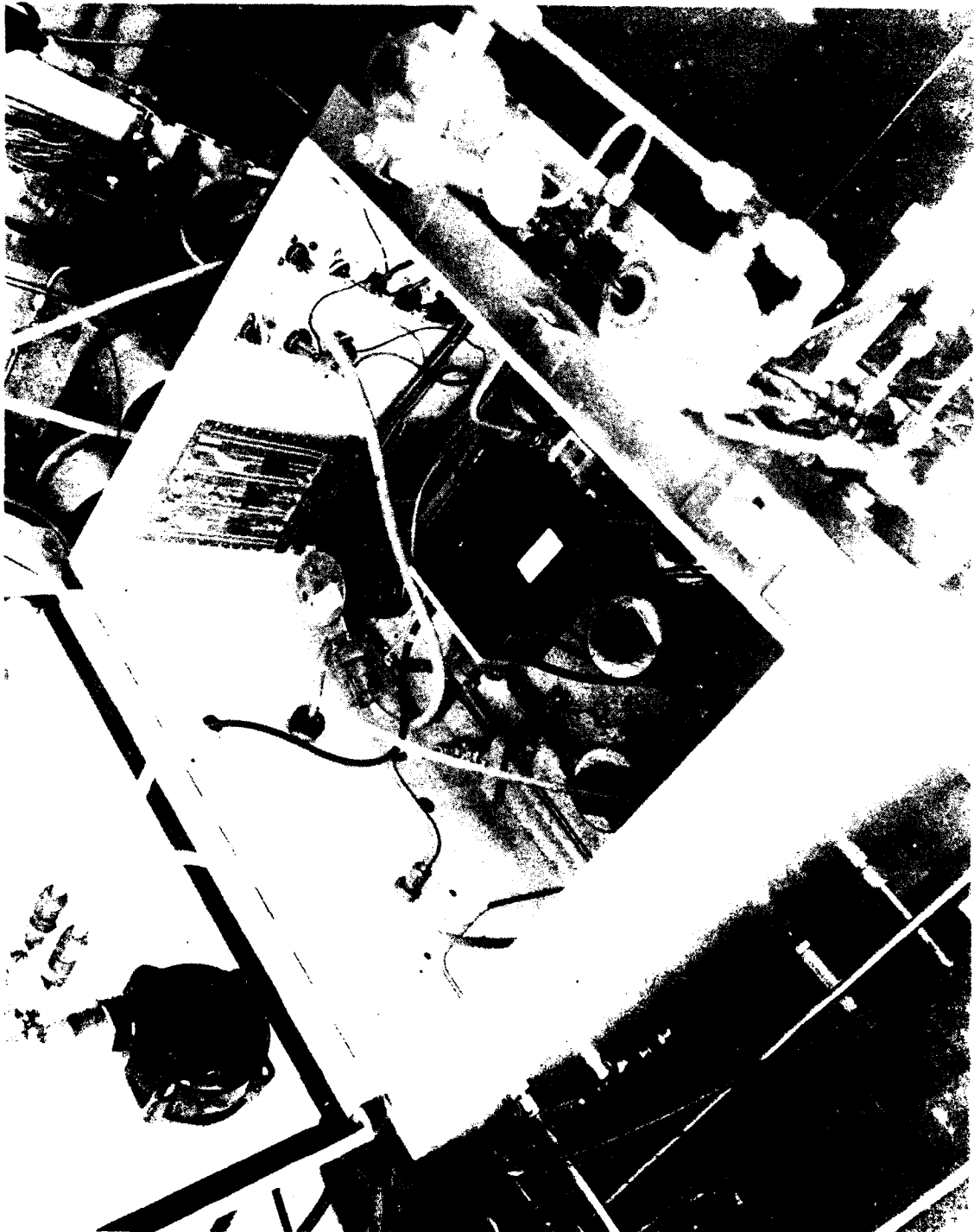


Figure 5-21. Micro PDFM Electro-Optical Flow Measurement

TABLE 5-VI

MULTIPLE MODE PROPELLANT SYSTEM CHARACTERISTICS

° Run Tank Capacity 1.50 Gallons

PDFM

- ° Capacity: 0.025 gallon
- ° Resolution: 13 microgallon
- ° Accuracy: $\pm 1/2\%$

° Micro PDFM

- ° Capacity: 105 microgallon
- ° Resolution: 0.06 microgallon
- ° Accuracy: $\pm 1\%$

° Turbine Flowmeters

- ° Flow Range: 60 microgallon to 0.04 gallon/sec
- ° Accuracy: $\pm 0.5\%$

5.2, Hot-Fire Testing (cont.)

5.2.5 Measurement and Data Processing

Table 5-VII documents the measurements and instrumentation nomenclature employed throughout Phase II of the test program. Figure 5-22 shows the location of the thermal instrumentation on the test engines. Steady-state performance is calculated from the bias-corrected, time-averaged thrust and from the total propellant consumed during the data time summary period, as indicated by the PDFM's.

Typical computer analysis of the pulse data is shown in Table 5-VIII. Columns 1 and 2 designate the pulse numbers in the sequence. Column 3 (EPW) indicates the duration the 28 volt power was applied to the valve. The Bit Impulse (BI, column 4) is measured by:

$$BI = \int_{FS1}^{FS2 + .025} F_d dt$$

where the dynamic thrust (F_d) is sampled 11,000 times per second. The coast impulse (Column 5) data shown is defined as follows:

$$CI = \int_{FS2 + .025}^{FS2 + .050} F_d T$$

All times are in seconds. Additional diagnostic data on the dynamic load cell measure return to zero following each pulse (F post).

$$F \text{ post} = F \text{ avg} (FS2 + .050 \text{ to } FS2 + .065) - F \text{ avg} (FS1 - .005 \text{ to } FS1)$$

Columns designated Ox Coast and Fu Coast indicate changes in the micro-PDFM levels in micro lbs (10^{-6}) of propellant when the engine is not firing. These level changes indicate engine or facility valve leakage, propellant volume changes due to line pressure or temperature drifts, or other malfunctions of the propellant supply and measurement system. Large changes in this measurement following pulses 20 and 25 reflect the micro-PDFM refills. Each series of pulses is examined for flow changes between pulses and the actual propellant consumption during the firing (WOT and WFT). Invalid flow readings are corrected, where possible, or the data for the pulse are rejected.

Columns 13, 14, and 15, BC LIN, OC LIN, and FC LIN, indicate the impulse and flow linearity obtained by dividing the impulse, Ox

TABLE 5-VII
PHASE II INSTRUMENTATION

<u>Parameter</u>	<u>Units</u>	<u>Symbol</u>
Time of Day	Hr Min	--
Valve Voltage	Volts	EP
Ox Paddle Wheel Flow	lb/sec	QOFM
Fuel Paddle Wheel Flow	lb/sec	QFFM
Large PDFM Ox	lb	LoPDFM
Large PDFM Fuel	lb	LFPDEM
Valve Power	Ambs	IP
Vacuum Cell Press.	psia	PVAC-1
Ox Line Press.	psia	Pol
Fuel Line Press.	psia	PfL
Ox Line Press. High freq.	psia	PolH
Fuel Line Press. High freq.	psia	PfLH
Chamber Pressure	psia	Pc
Steady-State Thrust	lb	F stat
Calibration Load Cell	lb	F cal
Dynamic Force Meas.	lb	F dyn
Ox Line Temp.	°F	ToL
Fuel Line Temp.	°F	TfL
Oxidizer Temp. at Valve	°F	ToVI
Fuel Temp. at Valve	°F	TFVI
Valve Body Temp.	°F	TVB
Valve Cover Temp.	°F	TVc
Flange or Transition Joint Temp.	°F	T flg or T Weld
Throat Temp.	°F	TT
Pressure Port Temp.	°F	TPc
Leg Temp.	°F	TL
Steel Temp.	°F	TS
Cell Temp.	°F	T Amb

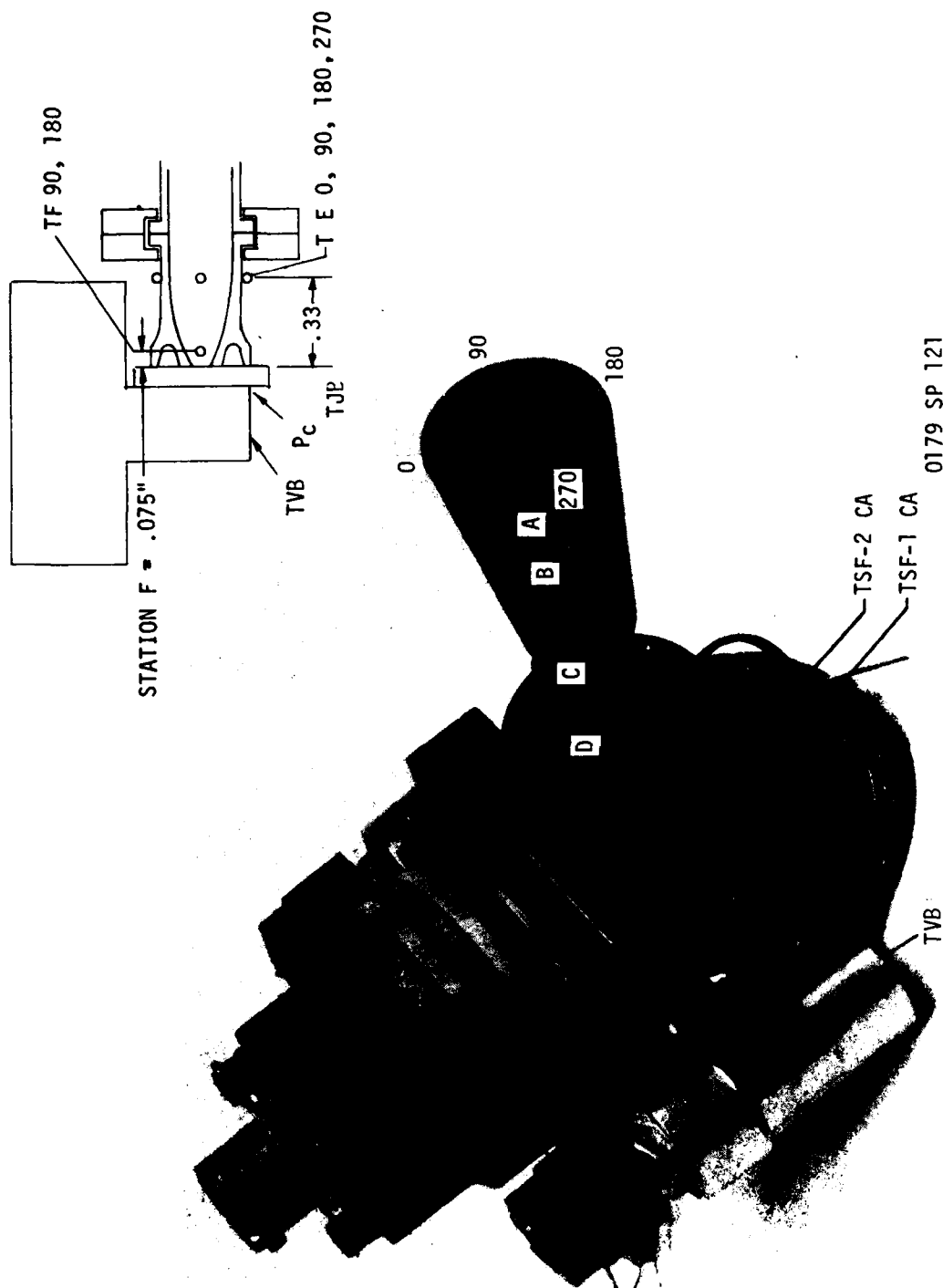


Figure 5-22. Thermal Instrumentation, Flanged Engine Assembly

TYPICAL PULSE PERFORMANCE DATA COMPUTER OUTPUT

136

5.2, Hot-Fire Testing (cont.)

Flow and Fuel Flow, by the EPW. The last column indicates the time of the pulse as measured from the start of the sequence. Major downtimes correspond to micro-PDFM refills.

Columns 9 and 12 provide the pulse specific impulse and mixture ratio based on the propellant consumption per pulse.

5.2.6 Phase II Test Program

Phase II testing was conducted in two blocks. Block I involved comparative testing of the two candidate injector and L' sections. Block II testing demonstrated steady-state and pulse mode performance and the effects of high MON content oxidizer on the selected configuration. All Phase II testing was performed at simulated altitudes in the facility previously described. This section will address the test program. Subsequent sections will present the test results.

The logic chart, Figure 5-23, summarizes the testing events and resulting design modification and selection activities which occurred during Phase II. Valve bench-testing had been discussed in Section 5.1.1.2 of this report. The V-Doublet Swirler (VDS) was eliminated during cold flow testing due to its poor atomization qualities, thereby leaving the Coaxial Swirler (CAS) and the 3-element splash plates (3-SPA) for demonstration testing during Phase II. Flanged combustion chambers of both 1 and 2 in. L' sections and welded chambers of 2 in. L' were tested. Testing proceeded with the following goals:

- ° Verify predicted steady-state and pulse mode performance
- ° Test at vacuum with 143:1 geometric nozzle (100:1 aerodynamic)
- ° Evaluate chamber L' of 1.0 to 2.0 in.
- ° Identify deficiencies in CONTAM predictions and modify inputs.
- ° Investigate low temperature and pressure ignition delay with MON-1 and with MON-10 oxidizer

Table 5-IX identifies the injectors tested and summarizes the operating characteristics evidenced by the Phase II test program.

TABLE 5-IX

PHASE II INJECTOR FABRICATION AND TEST RESULTS

PARAMETER	1-CAS BASELINE			SN 10A	SN 10 MOD B
	SPA	SN 9			
MIN FUEL PASSAGE IN.	0.0028	0.002 x 0.004	0.004 x 0.004 0.003 x 0.007		NO CHANGE
MIN OX PASSAGE IN.	0.0032	0.0055	0.0057		NO CHANGE
FUEL Kw % OF GOAL	99	73	90		90
OX Kw % OF GOAL	79	88	96		90
% PLATES REQUIRED	34	31	33		33
Is AT MAX THRUST (SEC)	275	275	275		275
TANK BLOWDOWN RANGE	4:1	4:1	4:1		>4:1
PULSE Is AT 0.005 LB F- SEC COLD/HOT	205/220	190/235	190/235		Not Evaluated
DURATION LIMIT BY TEMP. SEC					
Pc PSIA	Flange	Flange	WELD	Flange	Flange
115	5	17		4	24
90	8	35	23	18	260
60	20	-	60	275	>334 (NO LIMIT)
50	250	-	-	-	NO LIMIT

5.2, Hot-Fire Testing (cont.)

Table 5-X defines the pulse train of 2 standard duty cycles used in the screening tests. Steady-state operations during this phase were limited to 200-300 sec burns, based on the propellant capacity limitations of the large PDFM, and the engine temperature limits selected to preclude hardware damage.

° Block I Testing

Phase II, Block I testing was initiated with the SN 9 CAS injector. A total of 30 tests (#101-130) were performed, including 1900 starts and a maximum single burn of 30 sec. Test durations were limited by high temperatures at the hot gas seal in the chamber flange. This test data is summarized in Table 5-XI. The first 10 tests were facility checkout tests. Extensive modifications to the micro-PDFM were made between Tests 107 and 108.

The second series of Block I tests evaluated a 3-SPA injector for 18 tests (#201-218) that included 1188 starts with a maximum single burn of 259 seconds at reduced Pc. Test durations at full Pc were limited by head end temperatures. This data is summarized in Table 5-XII.

° Block II Testing

Data review of the Block I test series resulted in the CAS-type injector being selected as the baseline. A welded assembly was tested with the SN 9 CAS injector to determine if the duration limitations imposed by the hot gas seal temperature could be overcome through elimination of the flange and to obtain comparative performance and thermal data resulting from the change.

These tests (#301 to 309) are summarized in Table 5-XIII. The welded configuration demonstrated the same performance characteristics and thermal limitations as the flanged configuration. The bimetallic transition joint performed well; however, the temperatures were considerably higher than the Phase I predictions.

A second CAS injector, SN 10A, was assembled (flanged) in a manner to correct the mismatched (O/F) AP indicated in the cold- and hot-fire tests of SN 9. Tests #310-322, summarized in Table 5-XIII, document the results of these tests. Correcting the injector pressure drop unbalance had little effect on performance and aggravated the hot head end condition. The total Block II testing of SN 9 and 10A injectors included 22 tests with 262 starts.

TABLE 5-X

PULSE DUTY CYCLE DEFINITION

A DUTY CYCLE = 10 PULSES OF 0.010 SEC EPW AT 1 PER SEC
10 PULSES OF 0.030 SEC EPW AT 1 PER SEC
10 PULSES OF 0.100 SEC EPW AT 1 PER SEC, OR 0.080 AT 1 PER SEC

B DUTY CYCLE = 30 PULSES OF 0.005 SEC AT 4 PER MIN
20 PULSES OF 0.010 SEC AT 4 PER MIN
10 PULSES OF 0.030 SEC AT 4 PER MIN
10 PULSES OF 0.080 SEC AT 4 PER MIN

50 PULSES OF 0.005 SEC AT 1 PER SEC
50 PULSES OF 0.010 SEC AT 1 PER SEC
20 PULSES OF 0.030 SEC AT 1 PER SEC
10 PULSES OF 0.080 SEC AT 1 PER SEC

50 PULSES OF 0.005 SEC AT 1.718 PER SEC
50 PULSES OF 0.010 SEC AT 1.705 PER SEC
20 PULSES OF 0.030 SEC AT 1.647 PER SEC
10 PULSES OF 0.080 SEC AT 1.522 PER SEC

330 TOTAL

TABLE 5-XI

PHASE II BLOCK I TESTING, 1-CAS SN 9 INJECTOR, FLANGED CHAMBER

Line	Rate	Injector Type	Valve	Pressure	Flow	Temp	Pressure	Flow	Temp	Pressure	Flow	Temp	Pressure	Flow	Temp	Pressure	Flow	Temp	Pressure	Flow	Temp	Pressure	Flow	Temp	Pressure	Flow	Temp	Pressure	Flow	Temp	Pressure	Flow	Temp	Pressure	Flow	Temp	Pressure	Flow	Temp	Pressure	Flow	Temp	Pressure	Flow	Temp	Pressure	Flow	Temp	Pressure	Flow	Temp	Pressure	Flow	Temp	Pressure	Flow	Temp	Pressure	Flow	Temp	Pressure	Flow	Temp	Pressure	Flow	Temp	Pressure	Flow	Temp	Pressure	Flow	Temp	Pressure	Flow	Temp	Pressure	Flow	Temp	Pressure	Flow	Temp	Pressure	Flow	Temp	Pressure	Flow	Temp	Pressure	Flow	Temp	Pressure	Flow	Temp	Pressure	Flow	Temp	Pressure	Flow	Temp	Pressure	Flow	Temp	Pressure	Flow	Temp	Pressure	Flow	Temp	Pressure	Flow	Temp	Pressure	Flow	Temp	Pressure	Flow	Temp	Pressure	Flow	Temp	Pressure	Flow	Temp	Pressure	Flow	Temp	Pressure	Flow	Temp	Pressure	Flow	Temp	Pressure	Flow	Temp	Pressure	Flow	Temp	Pressure	Flow	Temp	Pressure	Flow	Temp	Pressure	Flow	Temp	Pressure	Flow	Temp	Pressure	Flow	Temp	Pressure	Flow	Temp	Pressure	Flow	Temp	Pressure	Flow	Temp	Pressure	Flow	Temp	Pressure	Flow	Temp	Pressure	Flow	Temp	Pressure	Flow	Temp	Pressure	Flow	Temp	Pressure	Flow	Temp	Pressure	Flow	Temp	Pressure	Flow	Temp	Pressure	Flow	Temp	Pressure	Flow	Temp	Pressure	Flow	Temp	Pressure	Flow	Temp	Pressure	Flow	Temp	Pressure	Flow	Temp	Pressure	Flow	Temp	Pressure	Flow	Temp	Pressure	Flow	Temp	Pressure	Flow	Temp	Pressure	Flow	Temp	Pressure	Flow	Temp	Pressure	Flow	Temp	Pressure	Flow	Temp	Pressure	Flow	Temp	Pressure	Flow	Temp	Pressure	Flow	Temp	Pressure	Flow	Temp	Pressure	Flow	Temp	Pressure	Flow	Temp	Pressure	Flow	Temp	Pressure	Flow	Temp	Pressure	Flow	Temp	Pressure	Flow	Temp	Pressure	Flow	Temp	Pressure	Flow	Temp	Pressure	Flow	Temp	Pressure	Flow	Temp	Pressure	Flow	Temp	Pressure	Flow	Temp	Pressure	Flow	Temp	Pressure	Flow	Temp	Pressure	Flow	Temp	Pressure	Flow	Temp	Pressure	Flow	Temp	Pressure	Flow	Temp	Pressure	Flow	Temp	Pressure	Flow	Temp	Pressure	Flow	Temp	Pressure	Flow	Temp	Pressure	Flow	Temp	Pressure	Flow	Temp	Pressure	Flow	Temp	Pressure	Flow	Temp	Pressure	Flow	Temp	Pressure	Flow	Temp	Pressure	Flow	Temp	Pressure	Flow	Temp	Pressure	Flow	Temp	Pressure	Flow	Temp	Pressure	Flow	Temp	Pressure	Flow	Temp	Pressure	Flow	Temp	Pressure	Flow	Temp	Pressure	Flow	Temp	Pressure	Flow	Temp	Pressure	Flow	Temp	Pressure	Flow	Temp	Pressure	Flow	Temp	Pressure	Flow	Temp	Pressure	Flow	Temp	Pressure	Flow	Temp	Pressure	Flow	Temp	Pressure	Flow	Temp	Pressure	Flow	Temp	Pressure	Flow	Temp	Pressure	Flow	Temp	Pressure	Flow	Temp	Pressure	Flow	Temp	Pressure	Flow	Temp	Pressure	Flow	Temp	Pressure	Flow	Temp	Pressure	Flow	Temp	Pressure	Flow	Temp	Pressure	Flow	Temp	Pressure	Flow	Temp	Pressure	Flow	Temp	Pressure	Flow	Temp	Pressure	Flow	Temp	Pressure	Flow	Temp	Pressure	Flow	Temp	Pressure	Flow	Temp	Pressure	Flow	Temp	Pressure	Flow	Temp	Pressure	Flow	Temp	Pressure	Flow	Temp	Pressure	Flow	Temp	Pressure	Flow	Temp	Pressure	Flow	Temp	Pressure	Flow	Temp	Pressure	Flow	Temp	Pressure	Flow	Temp	Pressure	Flow	Temp	Pressure	Flow	Temp	Pressure	Flow	Temp	Pressure	Flow	Temp	Pressure	Flow	Temp	Pressure	Flow	Temp	Pressure	Flow	Temp	Pressure	Flow	Temp	Pressure	Flow	Temp	Pressure	Flow	Temp	Pressure	Flow	Temp	Pressure	Flow	Temp	Pressure	Flow	Temp	Pressure	Flow	Temp	Pressure	Flow	Temp	Pressure	Flow	Temp	Pressure	Flow	Temp	Pressure	Flow	Temp	Pressure	Flow	Temp	Pressure	Flow	Temp	Pressure	Flow	Temp	Pressure	Flow	Temp	Pressure	Flow	Temp	Pressure	Flow	Temp	Pressure	Flow	Temp	Pressure	Flow	Temp	Pressure	Flow	Temp	Pressure	Flow	Temp	Pressure	Flow	Temp	Pressure	Flow	Temp	Pressure	Flow	Temp	Pressure	Flow	Temp	Pressure	Flow	Temp	Pressure	Flow	Temp	Pressure	Flow	Temp	Pressure	Flow	Temp	Pressure	Flow	Temp	Pressure	Flow	Temp	Pressure	Flow	Temp	Pressure	Flow	Temp	Pressure	Flow	Temp	Pressure	Flow	Temp	Pressure	Flow	Temp	Pressure	Flow	Temp	Pressure	Flow	Temp	Pressure	Flow	Temp	Pressure	Flow	Temp	Pressure	Flow	Temp	Pressure	Flow	Temp	Pressure	Flow	Temp	Pressure	Flow	Temp	Pressure	Flow	Temp	Pressure	Flow	Temp	Pressure	Flow	Temp	Pressure	Flow	Temp	Pressure	Flow	Temp	Pressure	Flow	Temp	Pressure	Flow	Temp	Pressure	Flow	Temp	Pressure	Flow	Temp	Pressure	Flow	Temp	Pressure	Flow	Temp	Pressure	Flow	Temp	Pressure	Flow	Temp	Pressure	Flow	Temp	Pressure	Flow	Temp	Pressure	Flow	Temp	Pressure	Flow	Temp	Pressure	Flow	Temp	Pressure	Flow	Temp	Pressure	Flow	Temp	Pressure	Flow	Temp	Pressure	Flow	Temp	Pressure	Flow	Temp	Pressure	Flow	Temp	Pressure	Flow	Temp	Pressure	Flow	Temp	Pressure	Flow	Temp	Pressure	Flow	Temp	Pressure	Flow	Temp	Pressure	Flow	Temp	Pressure	Flow	Temp	Pressure	Flow	Temp	Pressure	Flow	Temp	Pressure	Flow	Temp	Pressure	Flow	Temp	Pressure	Flow	Temp	Pressure	Flow	Temp	Pressure	Flow	Temp	Pressure	Flow	Temp	Pressure	Flow	Temp	Pressure	Flow	Temp	Pressure	Flow	Temp	Pressure	Flow	Temp	Pressure	Flow	Temp	Pressure	Flow	Temp	Pressure	Flow	Temp	Pressure	Flow	Temp	Pressure	Flow	Temp	Pressure	Flow	Temp	Pressure	Flow	Temp	Pressure	Flow	Temp	Pressure	Flow	Temp	Pressure	Flow	Temp	Pressure	Flow	Temp	Pressure	Flow	Temp	Pressure	Flow	Temp	Pressure	Flow	Temp	Pressure	Flow	Temp	Pressure	Flow	Temp	Pressure	Flow	Temp	Pressure	Flow	Temp	Pressure	Flow	Temp	Pressure	Flow	Temp	Pressure	Flow	Temp	Pressure	Flow	Temp	Pressure	Flow	Temp	Pressure	Flow	Temp	Pressure	Flow	Temp	Pressure	Flow	Temp	Pressure	Flow	Temp	Pressure	Flow	Temp	Pressure	Flow	Temp	Pressure	Flow	Temp	Pressure	Flow	Temp	Pressure	Flow	Temp	Pressure	Flow	Temp	Pressure	Flow	Temp	Pressure	Flow	Temp	Pressure	Flow	Temp	Pressure	Flow	Temp	Pressure	Flow	Temp	Pressure	Flow	Temp	Pressure	Flow	Temp	Pressure	Flow	Temp	Pressure
------	------	---------------	-------	----------	------	------	----------	------	------	----------	------	------	----------	------	------	----------	------	------	----------	------	------	----------	------	------	----------	------	------	----------	------	------	----------	------	------	----------	------	------	----------	------	------	----------	------	------	----------	------	------	----------	------	------	----------	------	------	----------	------	------	----------	------	------	----------	------	------	----------	------	------	----------	------	------	----------	------	------	----------	------	------	----------	------	------	----------	------	------	----------	------	------	----------	------	------	----------	------	------	----------	------	------	----------	------	------	----------	------	------	----------	------	------	----------	------	------	----------	------	------	----------	------	------	----------	------	------	----------	------	------	----------	------	------	----------	------	------	----------	------	------	----------	------	------	----------	------	------	----------	------	------	----------	------	------	----------	------	------	----------	------	------	----------	------	------	----------	------	------	----------	------	------	----------	------	------	----------	------	------	----------	------	------	----------	------	------	----------	------	------	----------	------	------	----------	------	------	----------	------	------	----------	------	------	----------	------	------	----------	------	------	----------	------	------	----------	------	------	----------	------	------	----------	------	------	----------	------	------	----------	------	------	----------	------	------	----------	------	------	----------	------	------	----------	------	------	----------	------	------	----------	------	------	----------	------	------	----------	------	------	----------	------	------	----------	------	------	----------	------	------	----------	------	------	----------	------	------	----------	------	------	----------	------	------	----------	------	------	----------	------	------	----------	------	------	----------	------	------	----------	------	------	----------	------	------	----------	------	------	----------	------	------	----------	------	------	----------	------	------	----------	------	------	----------	------	------	----------	------	------	----------	------	------	----------	------	------	----------	------	------	----------	------	------	----------	------	------	----------	------	------	----------	------	------	----------	------	------	----------	------	------	----------	------	------	----------	------	------	----------	------	------	----------	------	------	----------	------	------	----------	------	------	----------	------	------	----------	------	------	----------	------	------	----------	------	------	----------	------	------	----------	------	------	----------	------	------	----------	------	------	----------	------	------	----------	------	------	----------	------	------	----------	------	------	----------	------	------	----------	------	------	----------	------	------	----------	------	------	----------	------	------	----------	------	------	----------	------	------	----------	------	------	----------	------	------	----------	------	------	----------	------	------	----------	------	------	----------	------	------	----------	------	------	----------	------	------	----------	------	------	----------	------	------	----------	------	------	----------	------	------	----------	------	------	----------	------	------	----------	------	------	----------	------	------	----------	------	------	----------	------	------	----------	------	------	----------	------	------	----------	------	------	----------	------	------	----------	------	------	----------	------	------	----------	------	------	----------	------	------	----------	------	------	----------	------	------	----------	------	------	----------	------	------	----------	------	------	----------	------	------	----------	------	------	----------	------	------	----------	------	------	----------	------	------	----------	------	------	----------	------	------	----------	------	------	----------	------	------	----------	------	------	----------	------	------	----------	------	------	----------	------	------	----------	------	------	----------	------	------	----------	------	------	----------	------	------	----------	------	------	----------	------	------	----------	------	------	----------	------	------	----------	------	------	----------	------	------	----------	------	------	----------	------	------	----------	------	------	----------	------	------	----------	------	------	----------	------	------	----------	------	------	----------	------	------	----------	------	------	----------	------	------	----------	------	------	----------	------	------	----------	------	------	----------	------	------	----------	------	------	----------	------	------	----------	------	------	----------	------	------	----------	------	------	----------	------	------	----------	------	------	----------	------	------	----------	------	------	----------	------	------	----------	------	------	----------	------	------	----------	------	------	----------	------	------	----------	------	------	----------	------	------	----------	------	------	----------	------	------	----------	------	------	----------	------	------	----------	------	------	----------	------	------	----------	------	------	----------	------	------	----------	------	------	----------	------	------	----------	------	------	----------	------	------	----------	------	------	----------	------	------	----------	------	------	----------	------	------	----------	------	------	----------	------	------	----------	------	------	----------	------	------	----------	------	------	----------	------	------	----------	------	------	----------	------	------	----------	------	------	----------	------	------	----------	------	------	----------	------	------	----------	------	------	----------	------	------	----------	------	------	----------	------	------	----------	------	------	----------	------	------	----------	------	------	----------	------	------	----------	------	------	----------	------	------	----------	------	------	----------	------	------	----------	------	------	----------	------	------	----------	------	------	----------	------	------	----------	------	------	----------	------	------	----------	------	------	----------	------	------	----------	------	------	----------	------	------	----------	------	------	----------	------	------	----------	------	------	----------	------	------	----------	------	------	----------	------	------	----------	------	------	----------	------	------	----------	------	------	----------	------	------	----------	------	------	----------	------	------	----------	------	------	----------	------	------	----------	------	------	----------	------	------	----------	------	------	----------	------	------	----------	------	------	----------	------	------	----------	------	------	----------	------	------	----------	------	------	----------	------	------	----------	------	------	----------	------	------	----------

TABLE 5-XII

PHASE II BLOCK I TESTING, 3-SPA INJECTOR FLANGED CHAMBER

Run	Date	Injector Type	L' in.	P _o psia	P _f psia	P _{vac} psia	Valve Inlet Or Fuel Temp. °F	P _c psia	F _{vac} lb-F	MP	t _s sec	Duty Cycle	K _{wo} 10 ⁻⁵	K _{wf} 10 ⁻⁵
201	1-24-79	3-SPA	1	343	305	.014	53	98	.42			0.8		
202	1-24-79			359	305	.007	58	100	.43	1.64	263	5.0	5.28	4.67
203	1-25-79			363	300	.009	53	99	.44	1.64	268	6.3 +	5.20	4.69
204	1-25-79			275	203	.004	48	80	.35	No Flow Data	A + 8.3 +	5.32	5.32	3.76
204R	1-25-79			277	197	.004	50	80	.354	2.05	261	A + 20 + A	5.34	4.39
205	1-25-79			166	143	.004	48	58	.25	2.06	254	A + 20 + A	5.32	3.76
206	1-25-79			105- 115	109- 118	.008	49	44	.19	1.59	228	A + 100 + A	5.27	4.32
207	1-25-79			176	189	.003	49	65	.29	1.40	254	79.4	5.20	4.54
208	2-1-79		2	369	316	.010	47	54	.44			5.0		
209	2-1-79			119	122	.017	52	54				A + 259 + A		
210	2-1-79			180	154	.010	53	68				A + 45 + A		
211	2-1-79			179	180	.012	52	70				A + 58 + A		
212	2-1-79			93	97	.012	55	40				A + 20 + A		
213	2-2-79			226	196	.018	52	82	.34	1.54	270	A + 31 + A	5.19	4.58
214	2-2-79			325	283									
215	2-2-79													
216				76	75	.0068			.134			2 Sec Chugg Test	.037	1b P/P
217				49	52	.0066			.084			2 Sec Chugg	.037	1b P/P
218				253	196	.035	54	82	.338	1.84	271	B + 18 + B		

FLANGED

PHASE II BLOCK II TESTING, 1-CAS INJECTOR, SN 9 WELDED CHAMBER
AND SN 10A FLANGED CHAMBER

[illegible]

5.2, Hot-Fire Testing (cont.)

° MON-X Testing

All Phase II testing to this point had been conducted with NTO/MMH. The scheduled Block II program was then completed with a high MON oxidizer and CAS injector SN 10A.

A nominal MON-10 blend was formulated by dissolving a known pressurized volume of NO into a known weight of N_2O_4 . Because of the high vapor pressure of this blend, the tank was maintained in a locked-up condition at all times except when transferring the blend from the storage tank. Because lowering the pressure or venting allows NO to come out of solution, a sample for analysis was not extracted until after the completion of Test 330, the final test in the MON-10 series.

The micro-PDFM measurement system could not be employed for the MON-10 pulse testing as the large gas volume above the liquid level indicator would result in the depletion of the dissolved NO during the propellant transfer operation. Large piston-drive flowmeter tanks were employed for all tests in this series.

The results of the MON-X testing are summarized in Table 5-XIV. This series included 8 tests with 128 starts and a maximum duration of 30 seconds. The last test with MON-X oxidizer, Test 330, experienced a number of flame-outs and relights during the course of the 30 sec burn. Analysis of flowrates, line and chamber pressure measurements revealed that these flame-outs resulted from "bubbles" in the oxidizer feed line, with the data indicating increasing "hardness" after each relight. The composition of the gas in the line was not determined; however, air, nitrogen and NO were possible candidates, based on propellant loading techniques and the temperature cycling which occurred prior to the tests.

° Additional Phase II Testing

Higher than desired front end temperatures resulting from the SN 10A CAS tests led to a modification of the fuel cone angle of the swirler cup to provide more fuel film cooling closer to the front end. This design change is further discussed in Section 6.1 following. A total of 9 tests with 39 starts and a maximum single burn of 334 seconds were performed. The test configuration consisted of a flanged chamber and utilized N_2O_4 oxidizer. This injector, initially designated SN 10A-M, was later referred to as SN 10B. The test results, summarized in Table 5-XV, indicated reduced head end temperatures, with no loss in performance.

PHASE II TESTING WITH MON 10 OXIDIZER

Comdizer flow rate and I_{sp} calculated from injector Kw data

quate. All pulses 0.01, 0.03, 0.00 sec [FW in groups of 16 at one sec sec-

W.M. : Not Measured

ADDITIONAL PHASE II TESTING WITH MODIFIED 1-CAS INJECTOR
(10 AM = 10B)

TEST	DATE	TIME	10	11	12	13	14	15	16	17	18	19	20	VAC DATA P%	SUMMARY P% TIME, SEC	F TIME, SEC	10-F SEC	10-F IMPULSE
331	8-08-79	10AM	275	1.25	115	316	457	516	4	1.23	-	144	1004	1012	5 10 143.990		466	
332	8-08-79	10AM	275	1.25	115	316	457	516	4	1.23	-	144	1002	1012	5 10 143.990		466	
333	8-08-79	10AM	275	1.25	115	316	457	516	4	1.23	-	144	1002	1012	5 10 143.990		466	
334	8-08-79	10AM	275	1.25	115	316	457	516	4	1.23	-	144	1002	1012	5 10 143.990		466	
335	8-08-79	10AM	275	1.25	115	316	457	516	4	1.23	-	144	1002	1012	5 10 143.990		466	
336	8-08-79	10AM	275	1.25	115	316	457	516	4	1.23	-	144	1002	1012	5 10 143.990		466	
337	8-08-79	10AM	275	1.25	115	316	457	516	4	1.23	-	144	1002	1012	5 10 143.990		466	
338	8-08-79	10AM	275	1.25	115	316	457	516	4	1.23	-	144	1002	1012	5 10 143.990		466	
339	8-08-79	10AM	275	1.25	115	316	457	516	4	1.23	-	144	1002	1012	5 10 143.990		466	
340	8-08-79	10AM	275	1.25	115	316	457	516	4	1.23	-	144	1002	1012	5 10 143.990		466	
341	8-08-79	10AM	275	1.25	115	316	457	516	4	1.23	-	144	1002	1012	5 10 143.990		466	
342	8-08-79	10AM	275	1.25	115	316	457	516	4	1.23	-	144	1002	1012	5 10 143.990		466	
343	8-08-79	10AM	275	1.25	115	316	457	516	4	1.23	-	144	1002	1012	5 10 143.990		466	
344	8-08-79	10AM	275	1.25	115	316	457	516	4	1.23	-	144	1002	1012	5 10 143.990		466	
345	8-08-79	10AM	275	1.25	115	316	457	516	4	1.23	-	144	1002	1012	5 10 143.990		466	
346	8-08-79	10AM	275	1.25	115	316	457	516	4	1.23	-	144	1002	1012	5 10 143.990		466	
347	8-08-79	10AM	275	1.25	115	316	457	516	4	1.23	-	144	1002	1012	5 10 143.990		466	
348	8-08-79	10AM	275	1.25	115	316	457	516	4	1.23	-	144	1002	1012	5 10 143.990		466	
349	8-08-79	10AM	275	1.25	115	316	457	516	4	1.23	-	144	1002	1012	5 10 143.990		466	
350	8-08-79	10AM	275	1.25	115	316	457	516	4	1.23	-	144	1002	1012	5 10 143.990		466	

PROPELLANT = H_2O_2 / MMH

5.0, Phase II - Design, Fabrication and Verification Testing (cont.)

5.3 DATA EVALUATION

This section presents the performance data (steady-state, pulse and MON-X) of the injectors and L' sections tested during Phase II.

5.3.1 Steady-State Performance

Figure 5-24 displays steady-state thrust versus chamber pressure. These data reveal the linearity to be anticipated from internally consistent measurements and the expected instrument/facility accuracies.

5.3.1.1 3-SPA Testing

Test results of the 3-element Splash Plate Injector, using 1" and 2" L' sections, are displayed in Figures 5-25 and 5-26. These data clearly indicate an increase in performance of ~ 10 sec of specific impulse as the L' increases from 1" to 2". A significant decrease in performance is noted as chamber pressure decreases below 50 psia. This is due to reduced combustion efficiency and the increasing importance of chamber heat losses at lower pressures. As a result of these tests, use of the 1" L' section was discontinued and all subsequent Phase II and III tests were conducted with 2" L' sections.

5.3.1.2 CAS Testing

Coaxial swirler injector (CAS) testing was performed in the flanged and welded configuration (SN 9) and, subsequently, on 2 modifications (SN 10A and SN 10B), both in the flanged configuration. A further injector modification (SN 10C) was tested at the onset of Phase III; results are covered in Section 6 of this report. The steady-state test results of the Phase II testing are presented in Figure 5-27. It should be noted that both the SPA injector and CAS injectors (2 modifications) provide the same performance at full P_c . The CAS injectors exhibited the same performance drop-off (~ 30 sec) at the 40 psia P_c level as did the SPA unit.

A direct comparison of the SPA/CAS injector performance at 1" and 2" L' is shown in Figure 5-28. The estimated performance loss due to heat transfer to the chamber wall is noted to be significant at low thrust.

As displayed in Figure 5-29, the nozzle C_f data for both CAS and SPA injectors are consistent. The performance loss due to residual combustion in the nozzle is evident in the C_f data, plotted on the same figure for the 1" L' section.

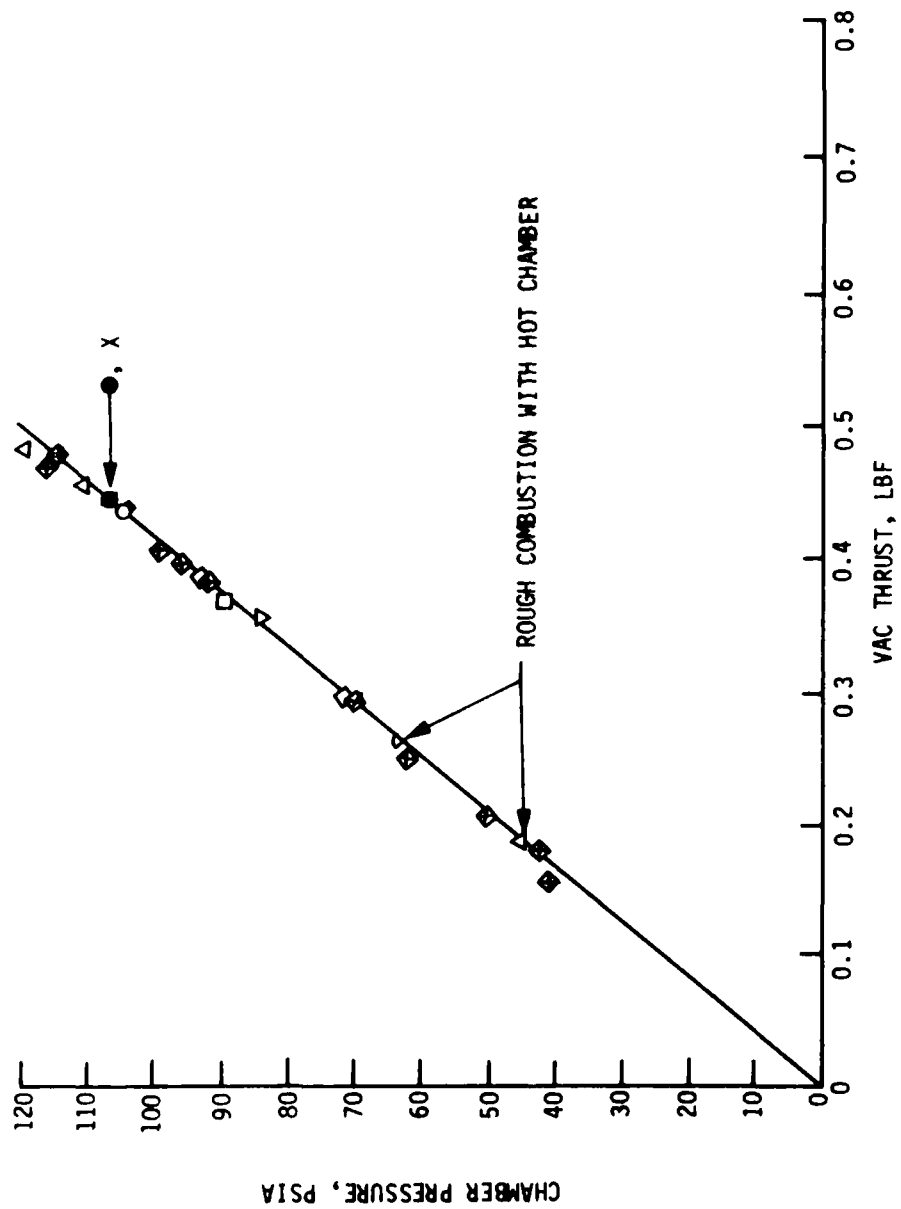


Figure 5-24. Thrust and Chamber Pressure Measurements

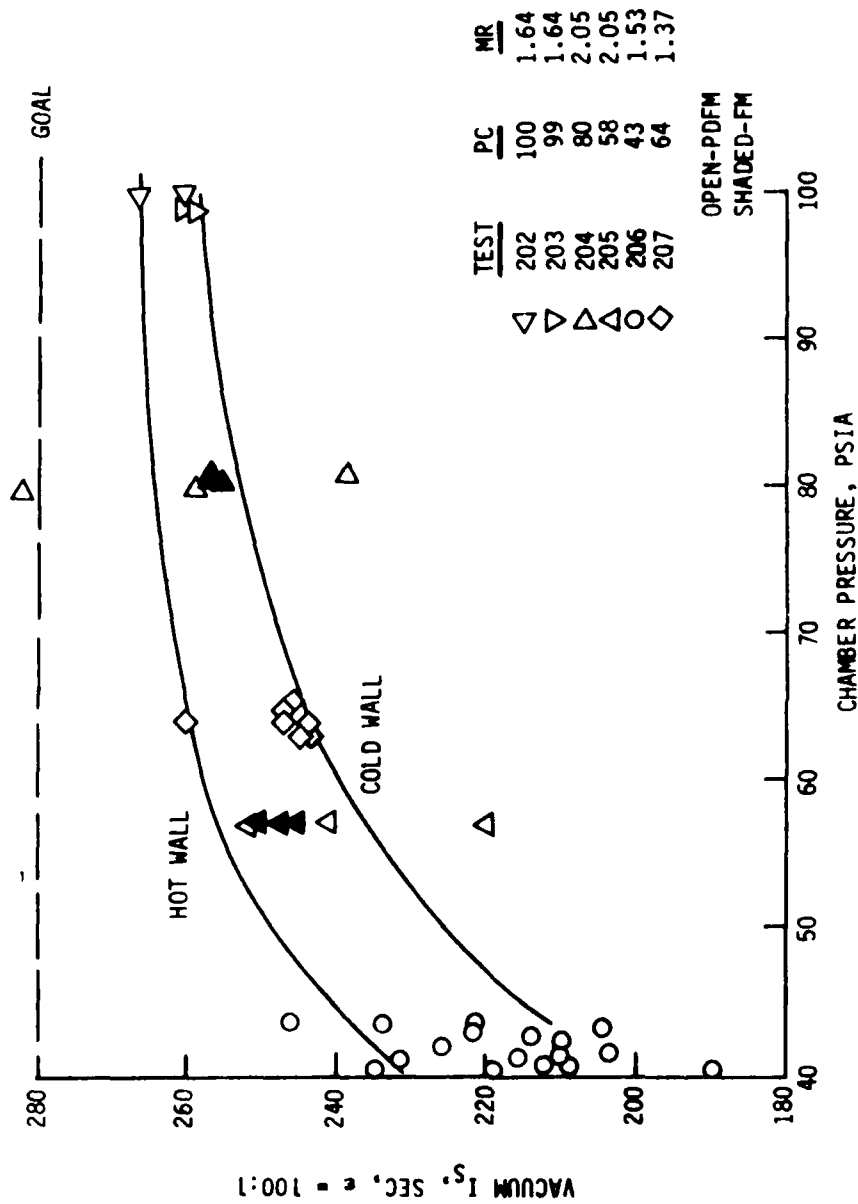


Figure 5-25. Steady-State Performance, 3-SPA Injector with 1" L' Chamber

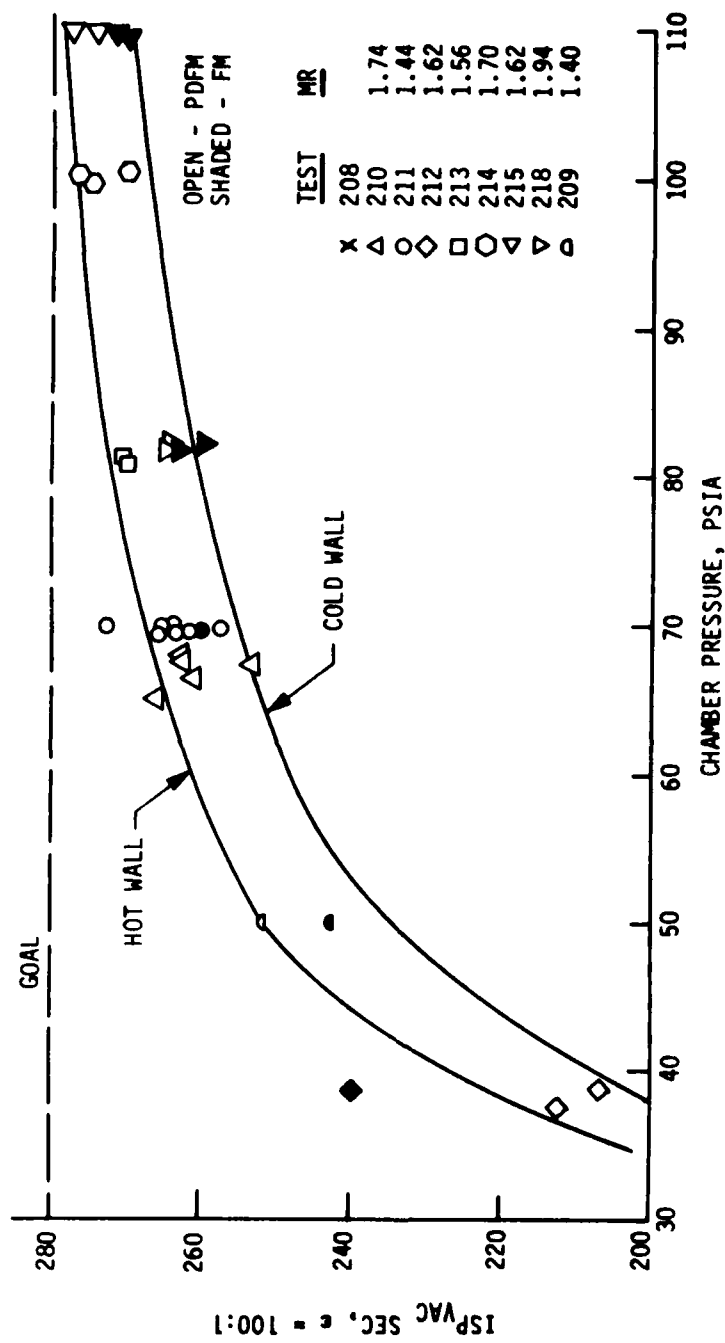


Figure 5-26. Steady-State Performance, 3-SPA Injector with 2" L' Chamber

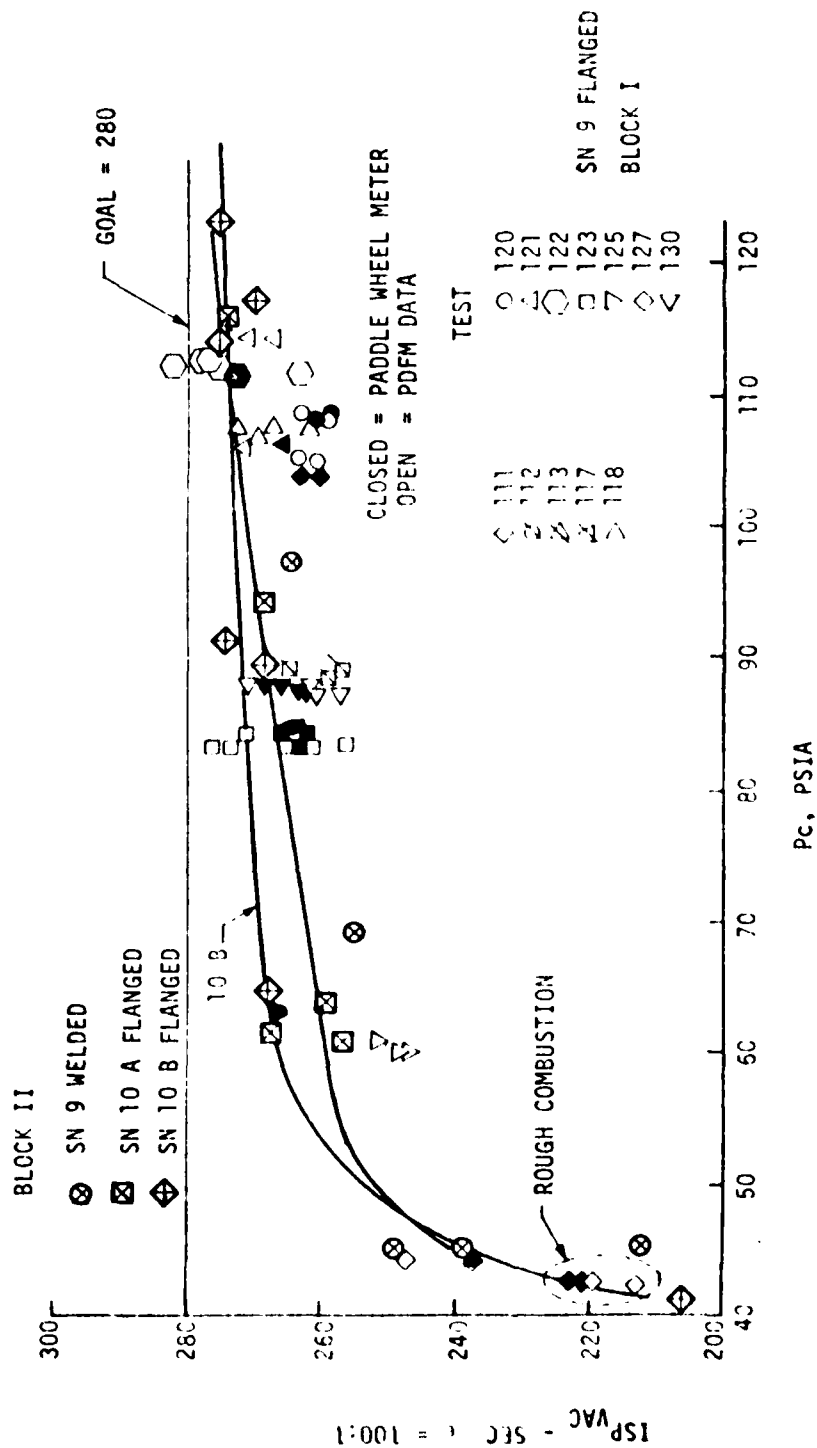


Figure 5-27. Steady-State Performance, 1-GAS Injector Series with 2' L' Chamber

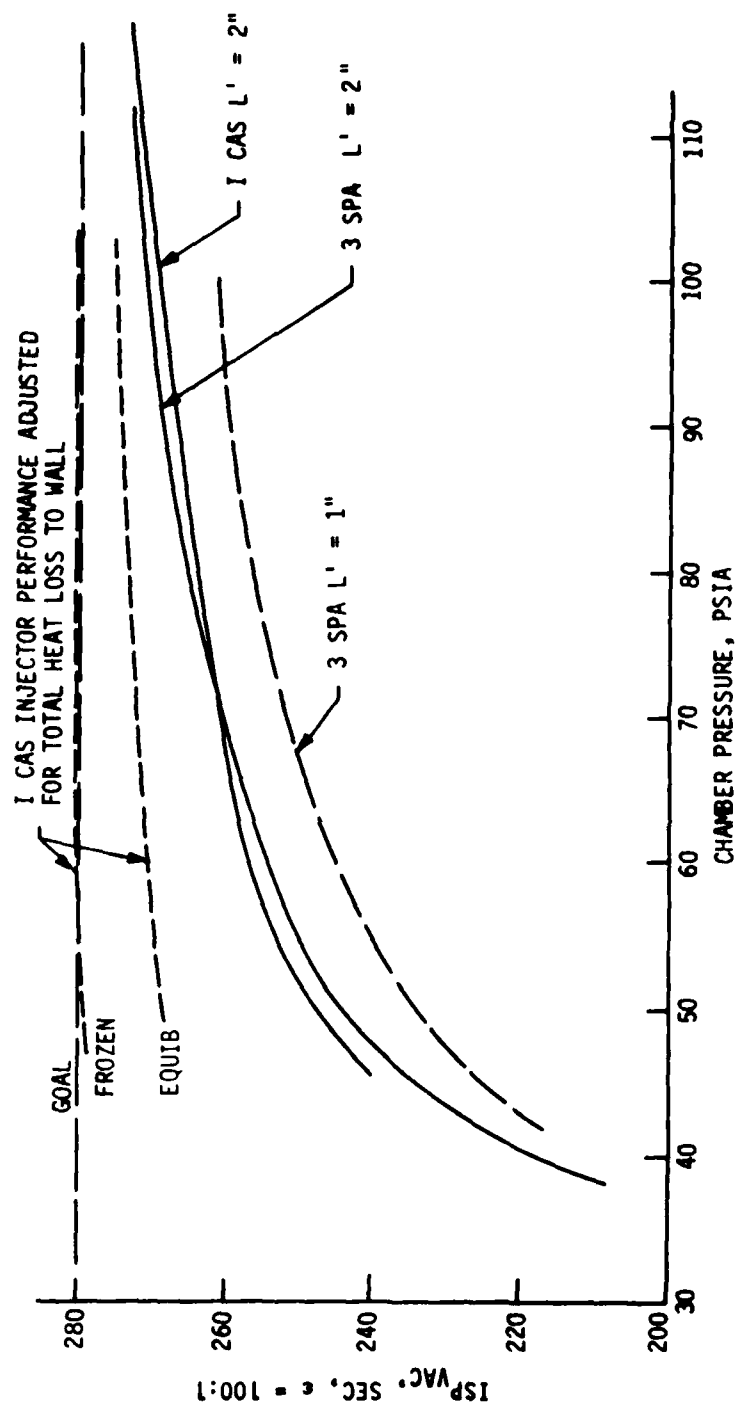


Figure 5-28. Phase II Injectors, Performance Comparison

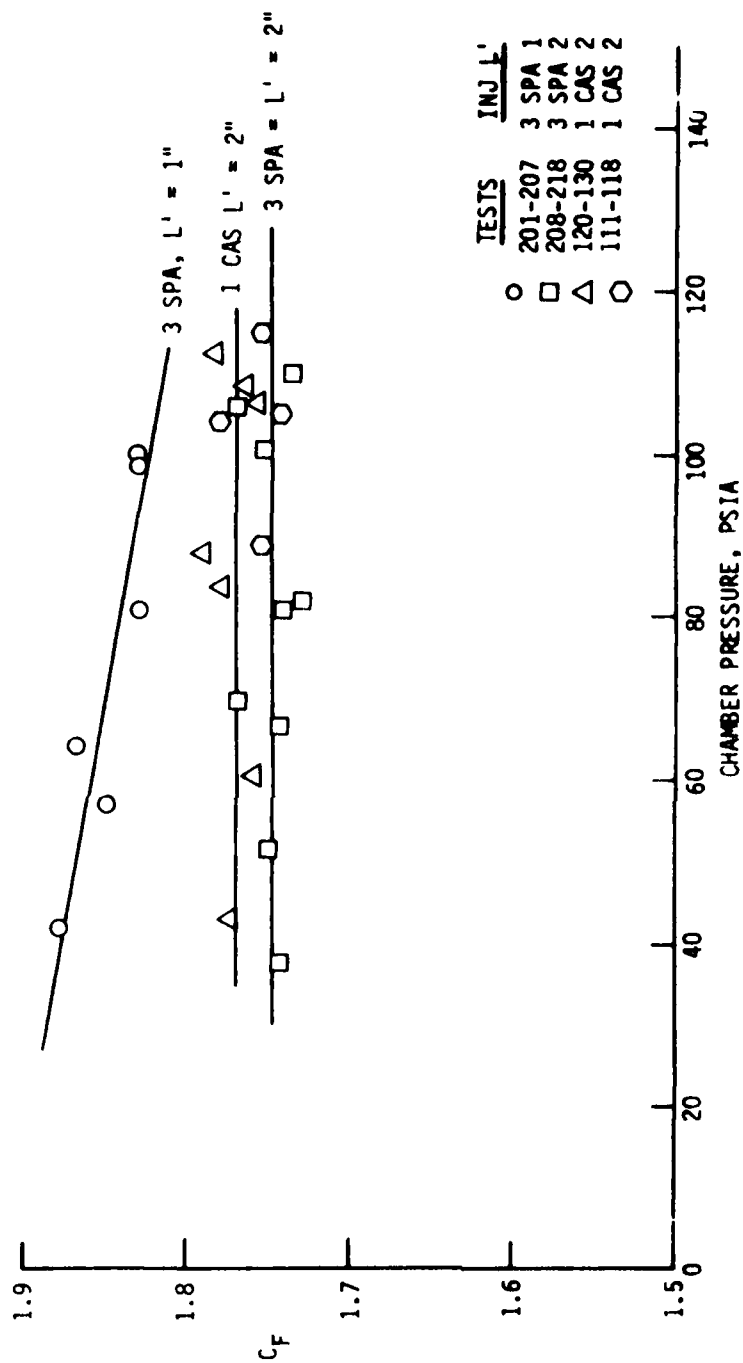


Figure 5-29. Experimental C_F Data

5.3, Data Evaluation (cont.)

5.3.1.3 BLIMP Predictions

A plot of the Phase I, BLIMP Model predictions versus test-derived nozzle thrust coefficient (C_f) data is displayed in Figure 5-30. The BLIMP predictions of nozzle efficiency fall above the bulk of the test data points. Review of the Phase II and subsequent Phase III experimental data indicates a ηC_f (vacuum) of 90%; this is 2% below the BLIMP prediction. The same test data are in good agreement with the ALRC simplified TBL-chart predictions which were previously proven accurate at the 2 to 5 lb thrust level.

The exact reasons for the 2% difference in BLIMP predictions are not known; however, they could be a combination of the following:

- 1) Chamber wall roughness resulting from the coating.
- 2) Improper definition of heat losses.
- 3) Effective nozzle area ratio is different from the predicted 100:1 value.
- 4) Throat area errors due to dimensional changes in the throat are not predicted by normal thermal expansion of uniformly heated cylinders.
- 5) Experimental measurement errors.

5.3.1.4 Steady-State Performance Conclusions

Evaluation of the preceding sections may be summarized in the following conclusions:

° An increase in L' from 1 to 2 in. provides a performance increase of 10 sec of specific impulse. Increases over $L' = 2$ " are not advised due to high heat losses.

° Testing with both the coaxial swirler and 3-element splash plate injector designs resulted in equal performance, i.e., 275 sec of specific impulse at $L' = 2$ in. and $P_c = 120$ psia.

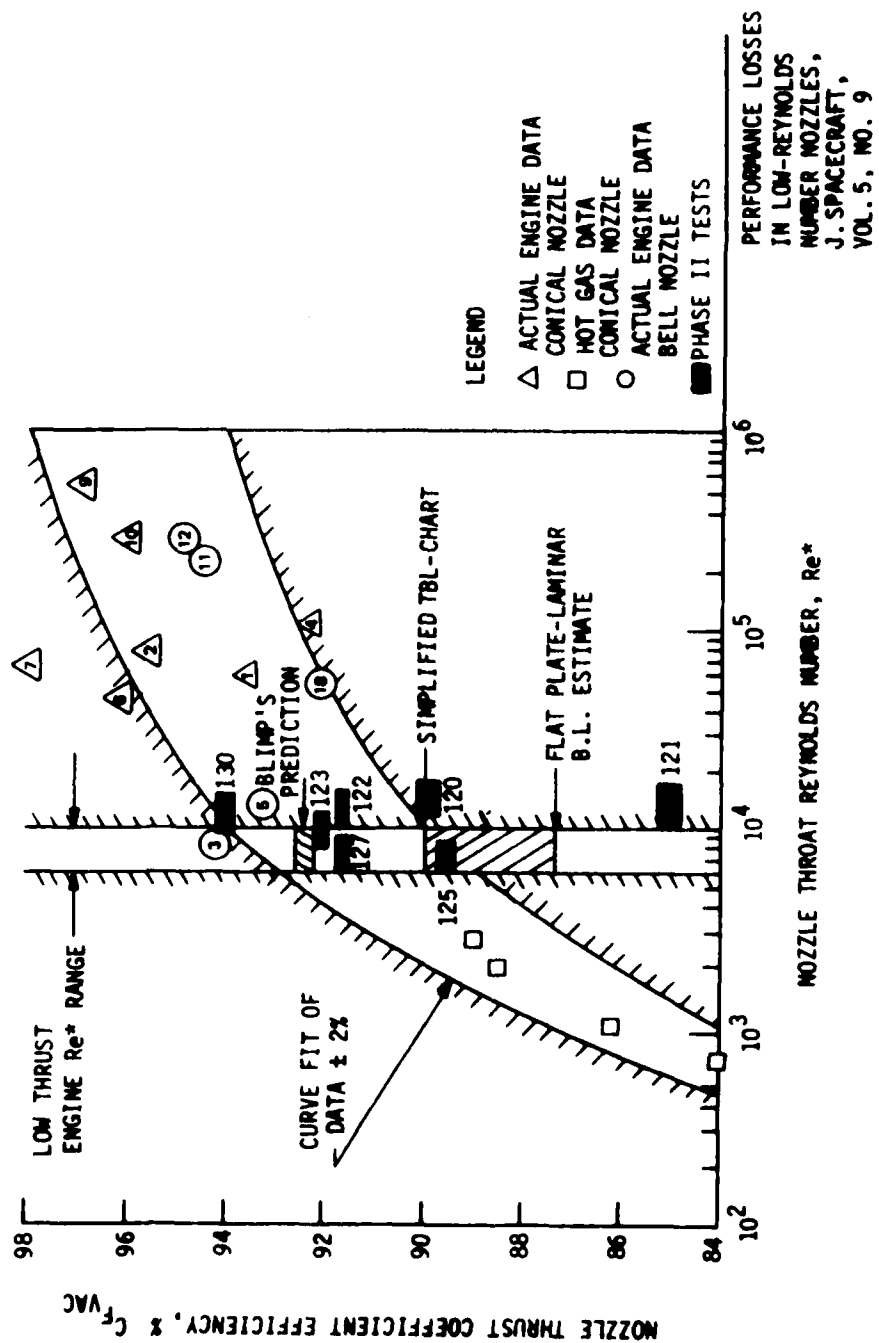


Figure 5-30. Comparison of C_f Data and BLIMP Model Predictions

5.3, Data Evaluation (cont.)

- ° Heat losses significantly affect performance as chamber pressure is decreased, i.e., ~30 sec of specific impulse loss at $P_c = 50$ psia.

- ° Nozzle C_f data indicates that the BLIMP Modeling predictions may be 2% high.

- ° Higher MON content oxidizers (MON-10) provide the same performance as N2O4.

In summary, injector design selection for Phase III verification testing should be based on criteria other than steady-state performance, i.e., pulse performance, thermal management, fabricability, etc.

5.3.2 Pulse Repeatability

The "A" duty cycle identified earlier consisted of 2 trains of 30 pulses each, with a long steady-state burn between the 2 groups of pulses. The objective of this type of testing was to identify impulse repeatability and pulse performance differences between cold and hot chamber restarts. Due to difficulties in switching from the large PDFM to the micro-PDFM, and the reloading time, the second group of pulses did not always start up when the chamber was at a maximum temperature. The second group was, however, representative of an engine which had recently fired and soaked out to an elevated temperature. A similar situation applies to the longer "B" duty cycle.*

Pulse test variables included electrical on time (EPW), pulse rates (PPS or PPM), and propellant supply system pressure. Figure 5-31 displays typical successive engine pulses of .010, .03, and .08 sec EPW at an intermediate tank pressure setting. The traces shown were taken from the filtered dynamic force trace channel of the online oscillograph. These pulses are noted to be highly repeatable.

*The computer data uses A and B to designate the first and second pulse groups of a single test (i.e., 130A and 130B). This should not be confused with the "A" and "B" duty cycle.

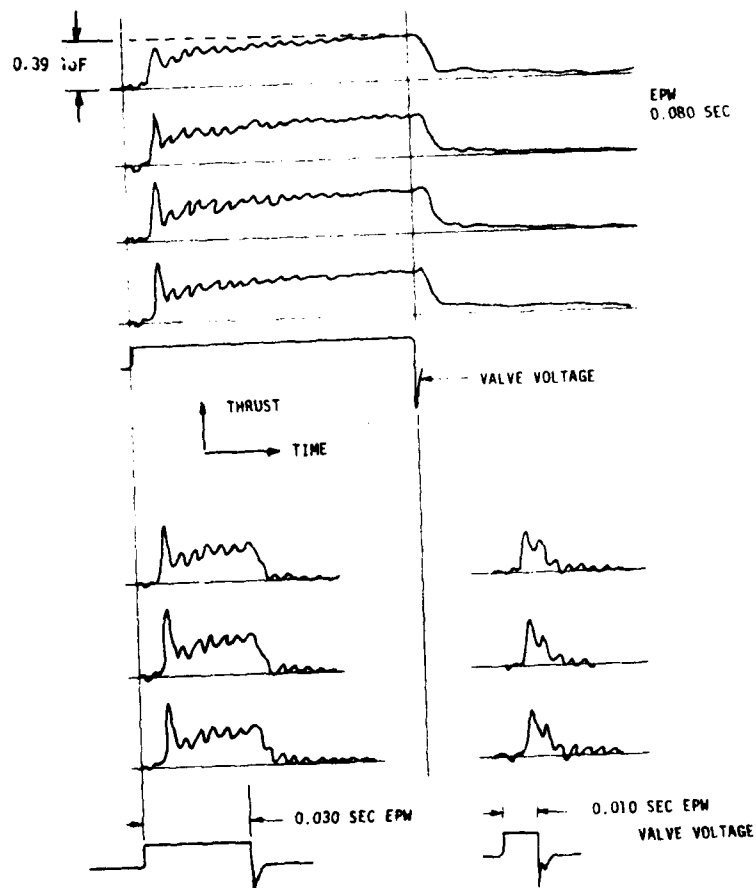


Figure 5-31. 1-CAS Injector Thrust Pulse Traces

5.3, Data Evaluation (cont.)

Figure 5-32 shows similar force time traces for 0.005 sec EPW in Test 130. These were executed at a rate of 1.7 pulses per second, with the maximum tank pressure at 372 psi.

The impulse bit is computer-calculated from the digital data which defines the area under the thrust time trace. A display of individual .010 second EPW pulse Impulse bits from Test 130 (B duty cycle) are shown in Figure 5-33. These data cover pulse rates of 4 pulses per minute to 1.7 pulses per second. The "A" and "B" on this figure correspond to the pre- and post-steady-state pulses. In this test, the engine temperature was approximately the same on the repeat pulse series. The minimum impulse bit and pulse repeatability of this series demonstrated the contractual goals of $I \text{ bit} < .005 \text{ lbf-sec}$ by providing $.0026 \pm .0003 \text{ lbf-sec}$.

The pulse repeatability is computed as the 1 sigma standard deviation of the 10 pulse average for each test condition considering all pulses. The repeatability versus I bit, displayed in Figure 5-34, considers the following variables: propellant temperature, chamber pressure (based on tank settings), EPW, and oxidizer blend (N2O4 and MON-10). The impulse bit of the first pulse is always lower than that of subsequent pulses. The I-bit repeatability was found to be within $\pm 5\%$ for I-Bits greater than .0025. The reduction in propellant temperature is noted to have an adverse effect on pulse repeatability. No significant differences were noted when the oxidizer was changed from N2O4 to the higher MON oxidizer (MON-10).

Figure 5-35 shows the relation between impulse bit for the 1-CAS SN 10A injector as a function of environmental and propellant temperature, for EPW values of .010, .030, and .080 seconds with N2O4 and MON-10 oxidizer. Each data point represents the average of 10 successive pulses. These tests were conducted at a low chamber pressure (62 psia) because it represents worst case conditions, i.e., vapor lock at high temperature and longer ignition delays at low temperatures. The poorer repeatability indicated at low temperatures in Figure 5-34 is probably due to the changes in ignition delay times.

Environmental temperatures between 30°F and 120°F were found to have only small effects on the statistical I-Bit values.

Figure 5-36 maps the relation between EPW, I-Bit, and tank pressure settings for 2 oxidizers and a range of propellant supply temperatures. Each data point represents the average of 10 successive pulses. Figure 5-37 provides the same I-Bit data, normalized by dividing the I-Bit

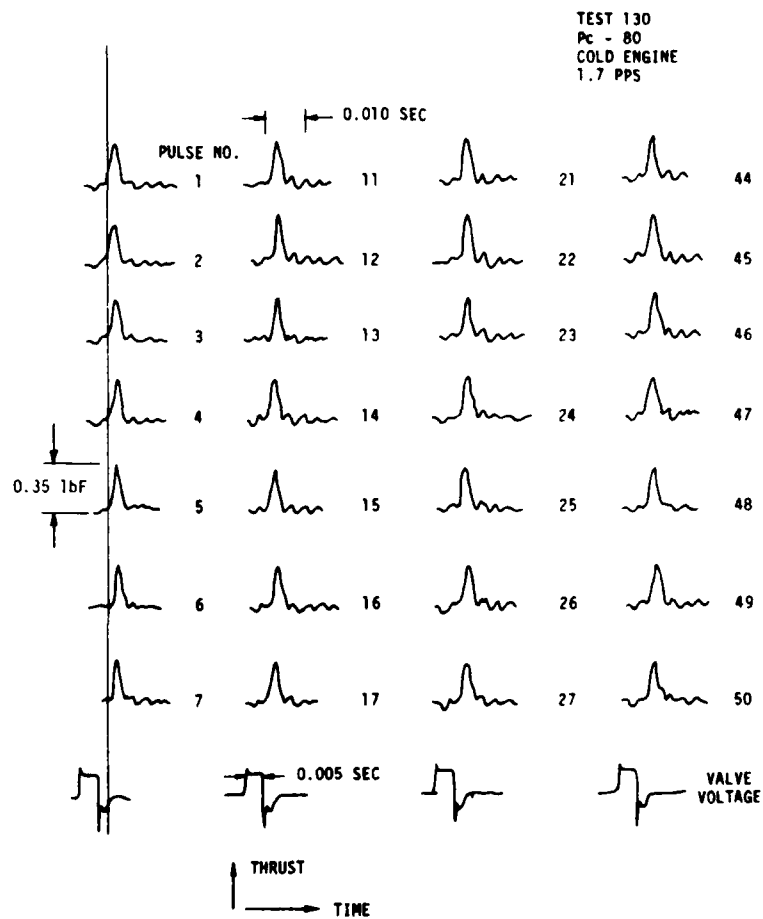


Figure 5-32. Repeatable Electrical Pulses of 0.005 Sec and Impulse Bits of 0.0015 1bF-Sec

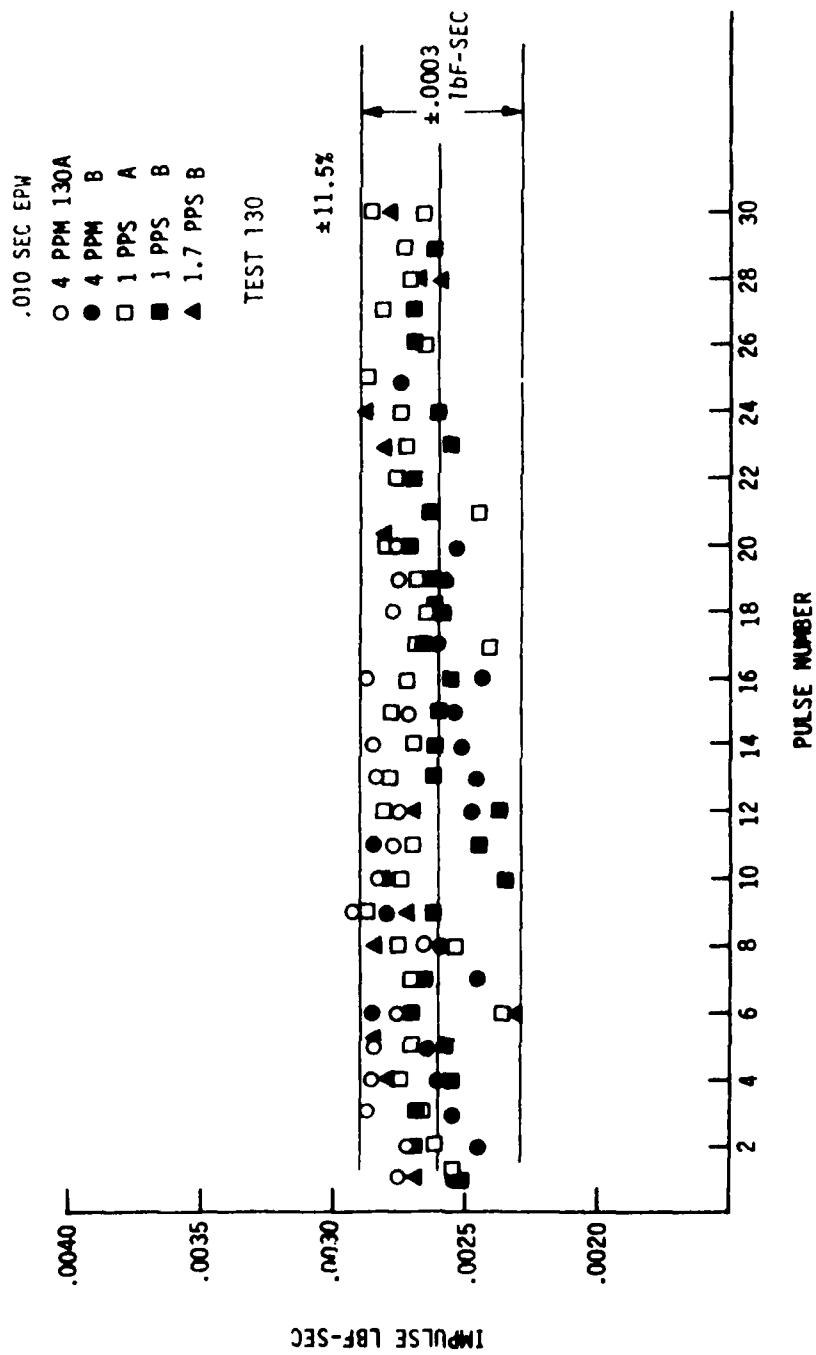


Figure 5-33. 1/CAS Injector 0.0015 Sec EPW Impulse Bits and Repeatability

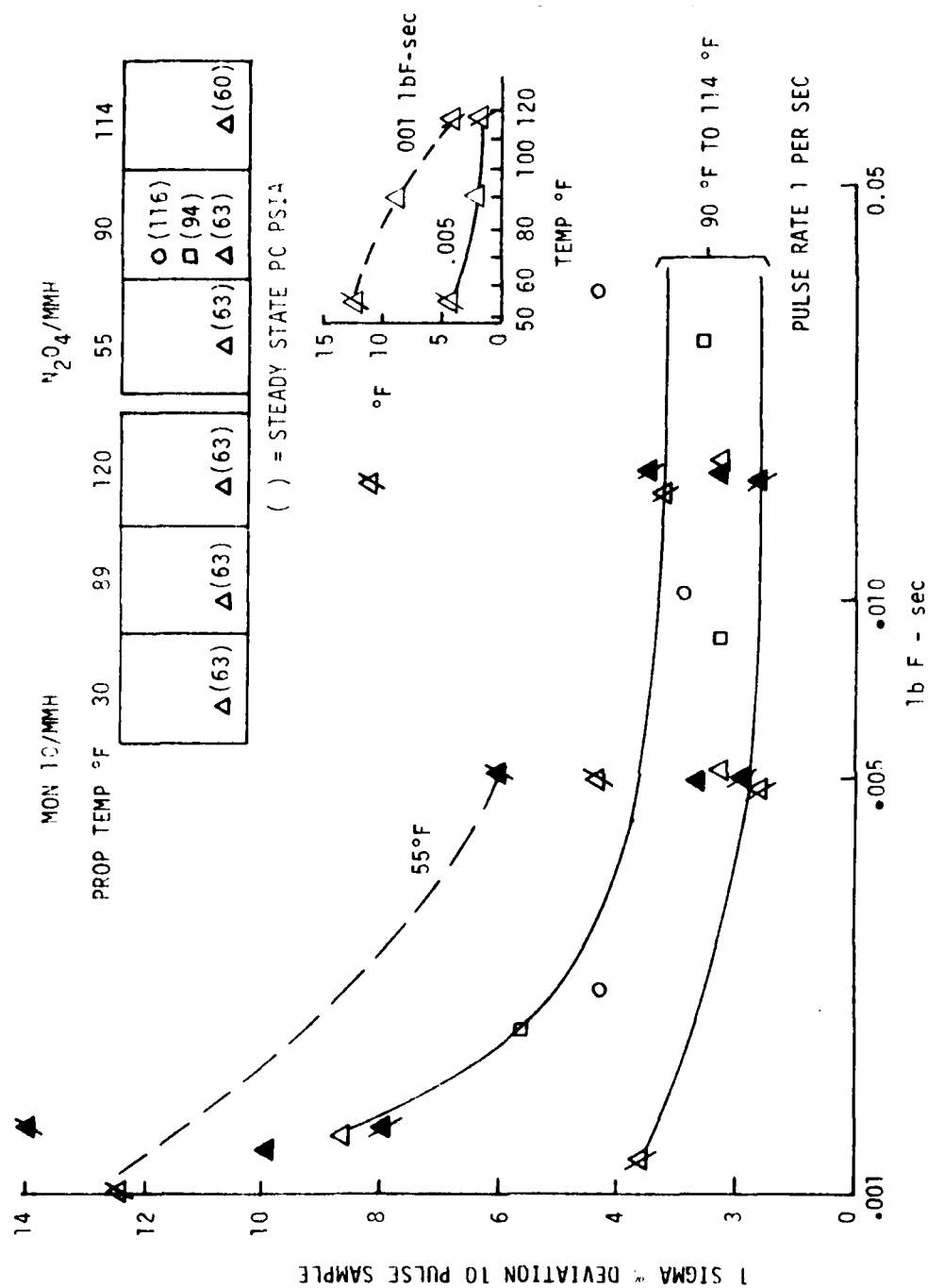


Figure 5-34. Impulse Bit Repeatability, CAS SN 10A

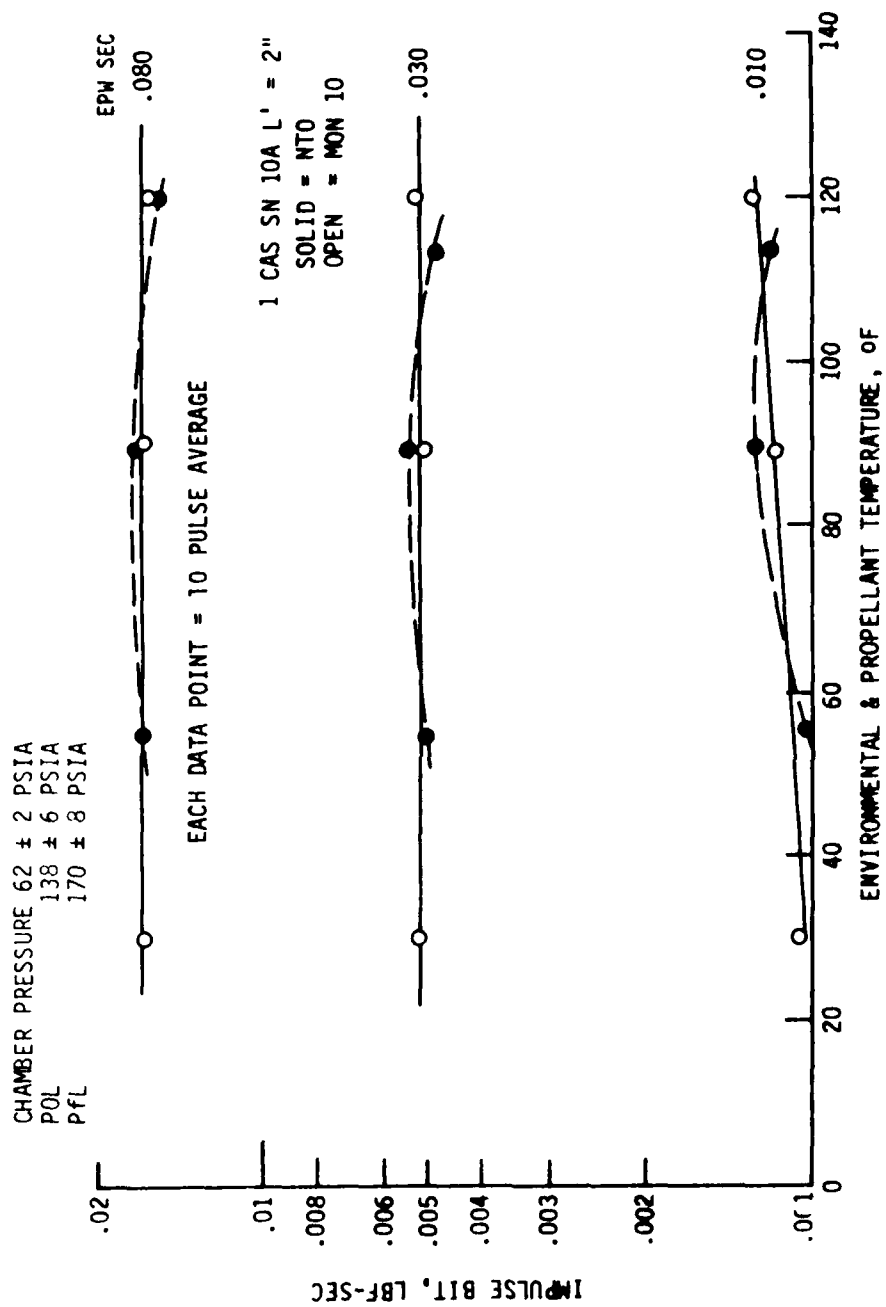


Figure 5-35. Environmental Temperature and Oxidizer NO Content vs Delivered Impulse Bits

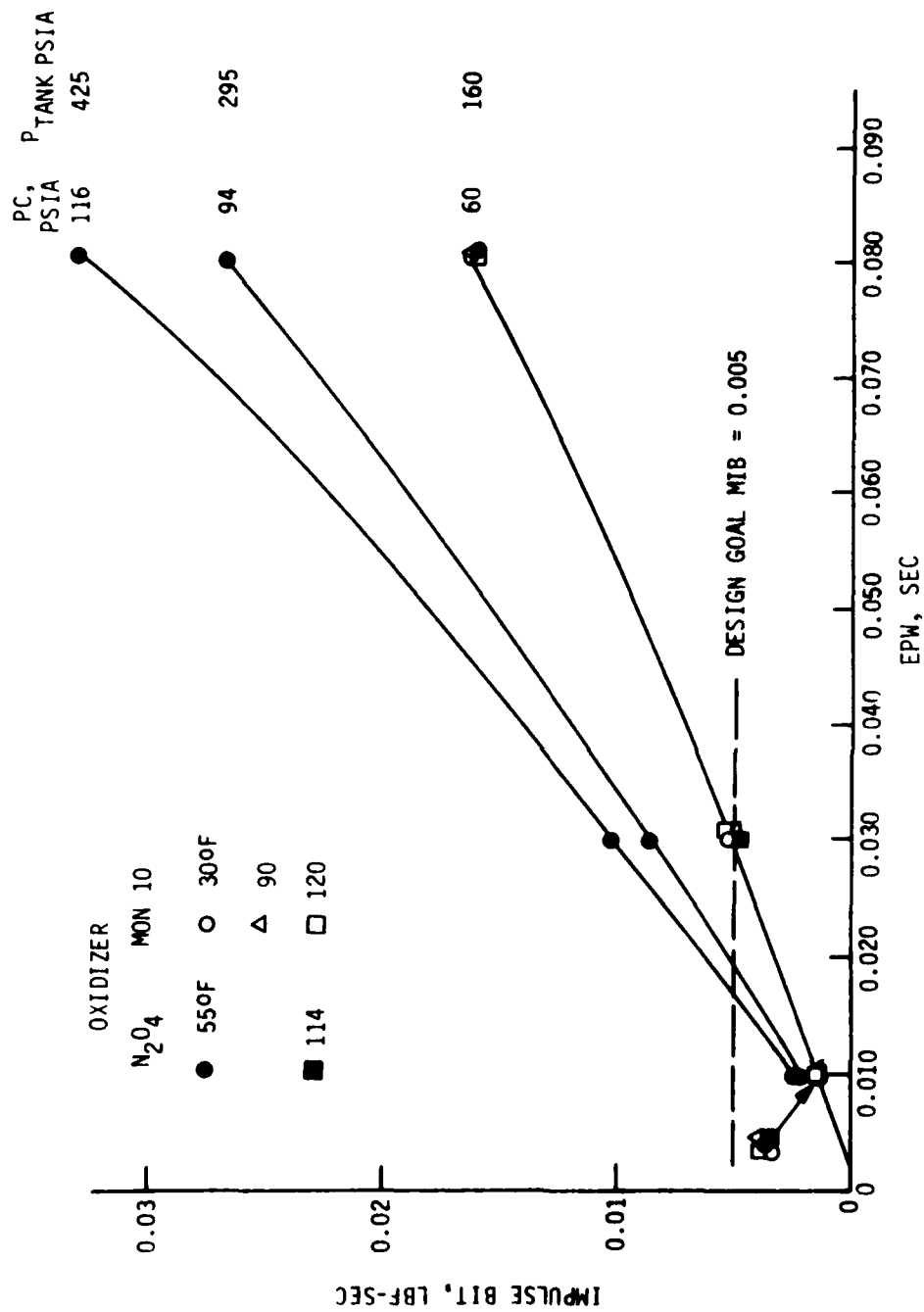


Figure 5-36. Impulse Bit versus EPW as a Function of Tank Pressure and Oxidizer NO Content

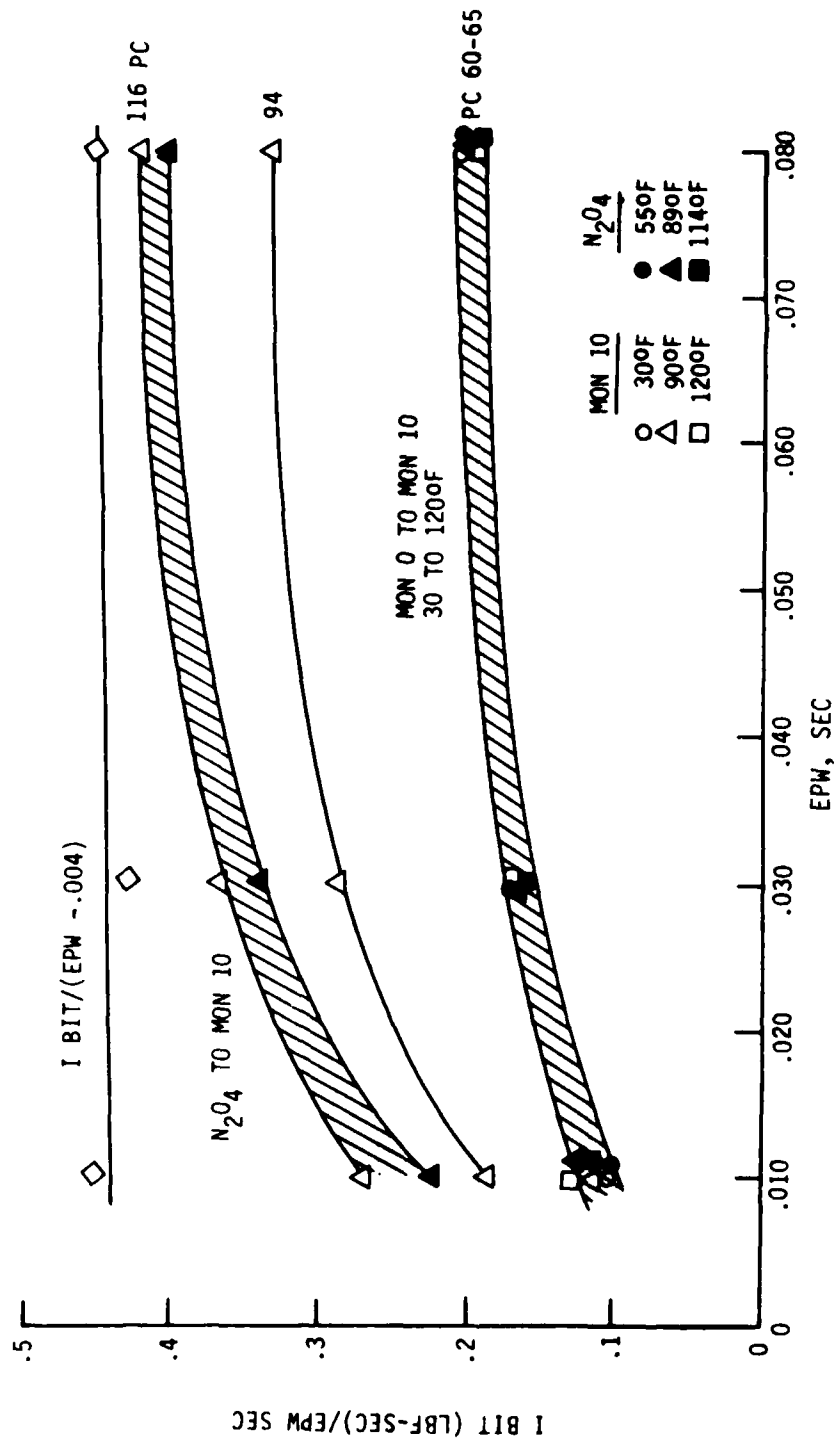


Figure 5-37. Impulse Bit versus EPW

5.3, Data Evaluation (cont.)

by the EPW. In the perfect system, this relation would be a constant which is a function only of the tank pressure setting. The value of the constants would be equal to the steady-state thrust for the particular tank pressure setting.

In reality, the time delay in valve opening and the inertia in filling the injector manifold volume reduces the effective engine firing time relative to the EPW time. The diamond symbols of the top curve of Figure 5-37 show the effect of subtracting .004 second from EPW before normalizing the data for the 116 Pc condition. The .004 second corresponds approximately to the valve electrical delay and manifold fill time. The resulting nearly horizontal line through the 3 data points shows the tested configuration to provide nearly perfect 1-Bit linearity for EPW values greater than .010 second.

5.3.3 Pulse Performance

Since the flow measurement for single pulses is not reliable, pulse performance is computed for the average of 10 pulses.

Figures 5-38 and 5-39 show the effect of chamber wall temperature on the pulse Isp for a variety of test conditions. The hot wall results in better utilization of the propellant. The dark data points in Figure 5-38 show, pulse by pulse, the improvement in Isp as the chamber heats from 80°F to 200°F. The resolution of the micro-PDFMs was sufficiently good to develop these data for the series of 0.1 second EPW pulses. Pulse performance is significantly higher when the pulses follow a steady-state burn ($T_w = 450^\circ\text{F}$), as displayed by the open data points in Figure 5-38.

The cold chamber pulse performance data for the two 1-CAS injector assemblies tested in Block II are shown in Figure 5-40. These data are superimposed on the original Block I data. The Block I and II test data are noted to be in good agreement. The correction of the high fuel circuit pressure drop did not alter the pulse performance. The validity of the pulse performance in Figure 5-40 is questionable at an EPW of .005 second because of the very low propellant consumption.

Figure 5-41 provides the performance data obtained from the pulse series following steady-state burn. The higher pulse Isp is due to the hot chamber walls.

Figures 5-42 and 5-43 provide similar pulse performance data for the 3-SPA injector for pulses with a cold and hot chamber.

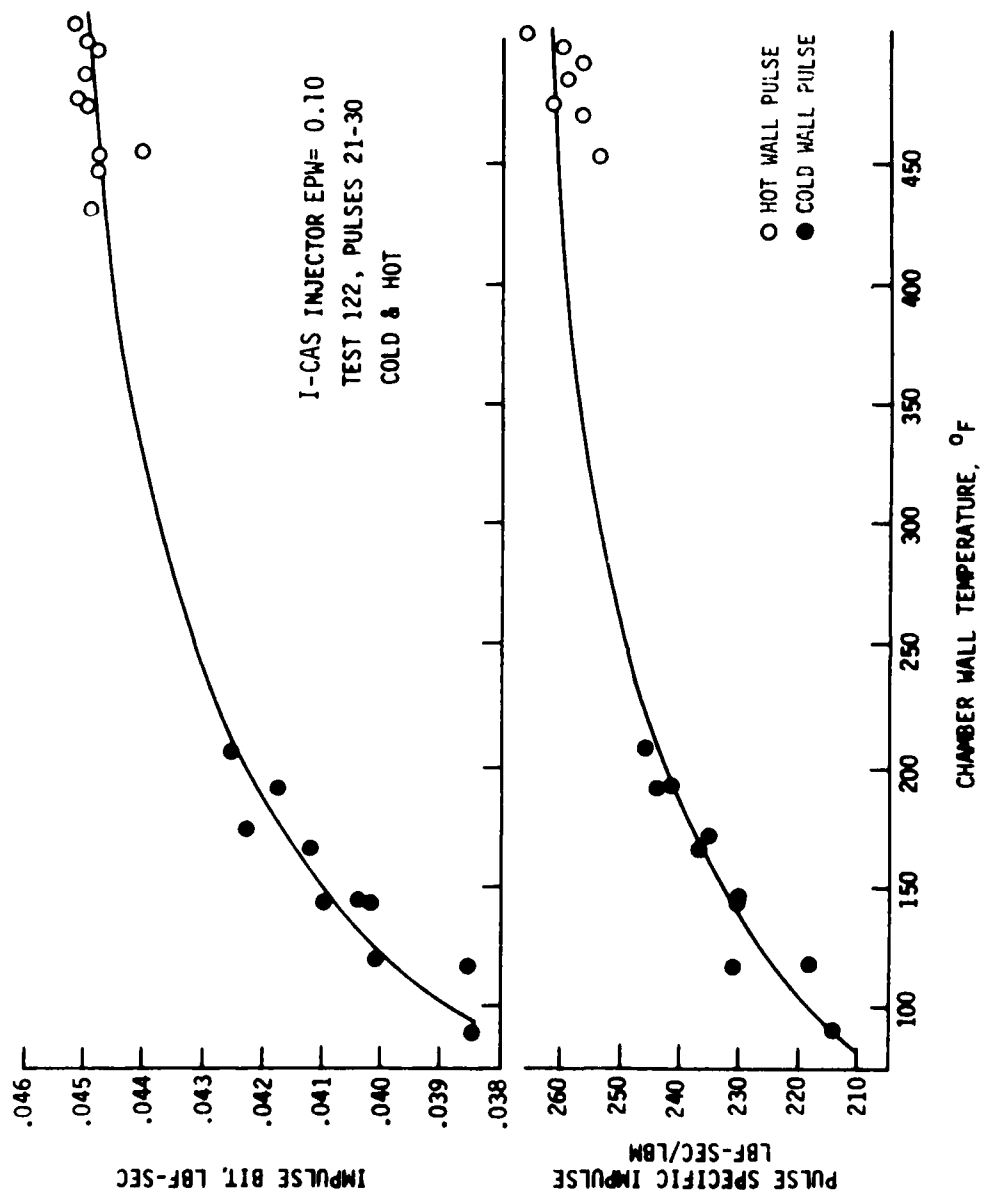


Figure 5-38. Chamber Wall Temperature vs Pulse Performance
(EPW = 0.1 sec)

BLOCK I

SS THRUST LBF	0.44	0.37	0.45	0.48	0.35
RATE 4 PPM		○			
1 PPS	◇	□	○	▽	△
2 PPS		△			

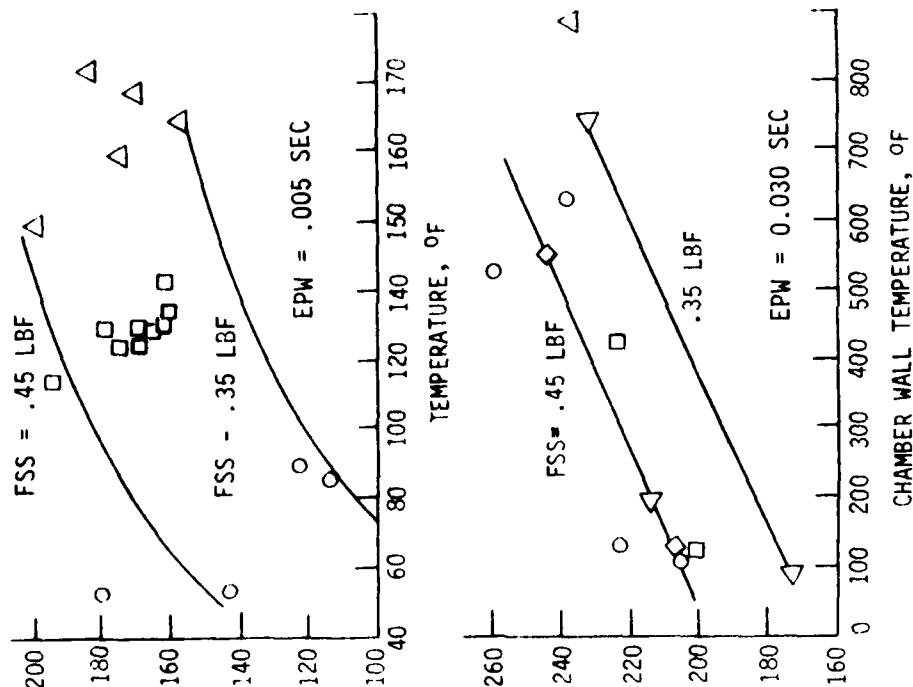
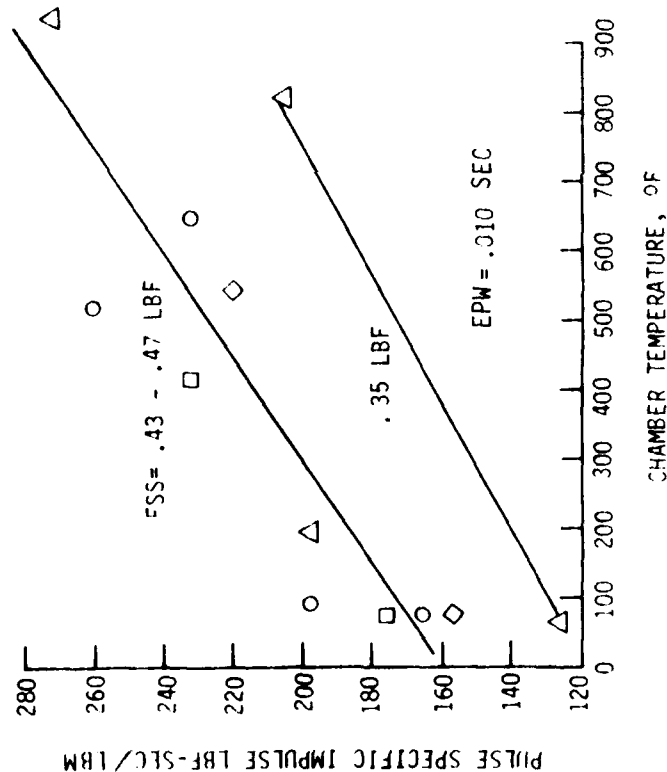


Figure 5-39. Chamber Wall Temperature vs Pulse Performance
(EPW = .005, .010 and .030 sec)

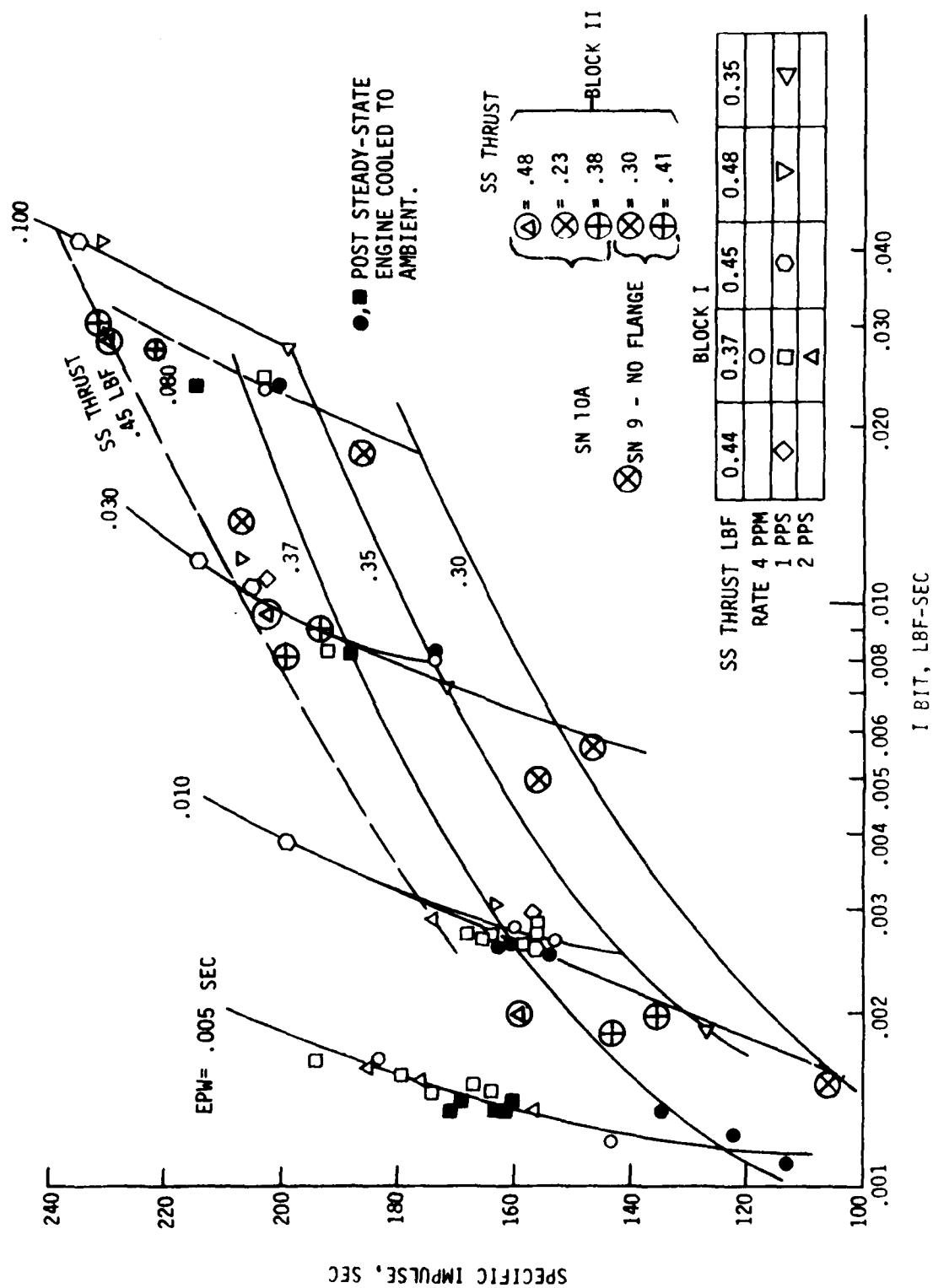


Figure 5-40. 1-CAS Injector, Cold Chamber Pulse Performance

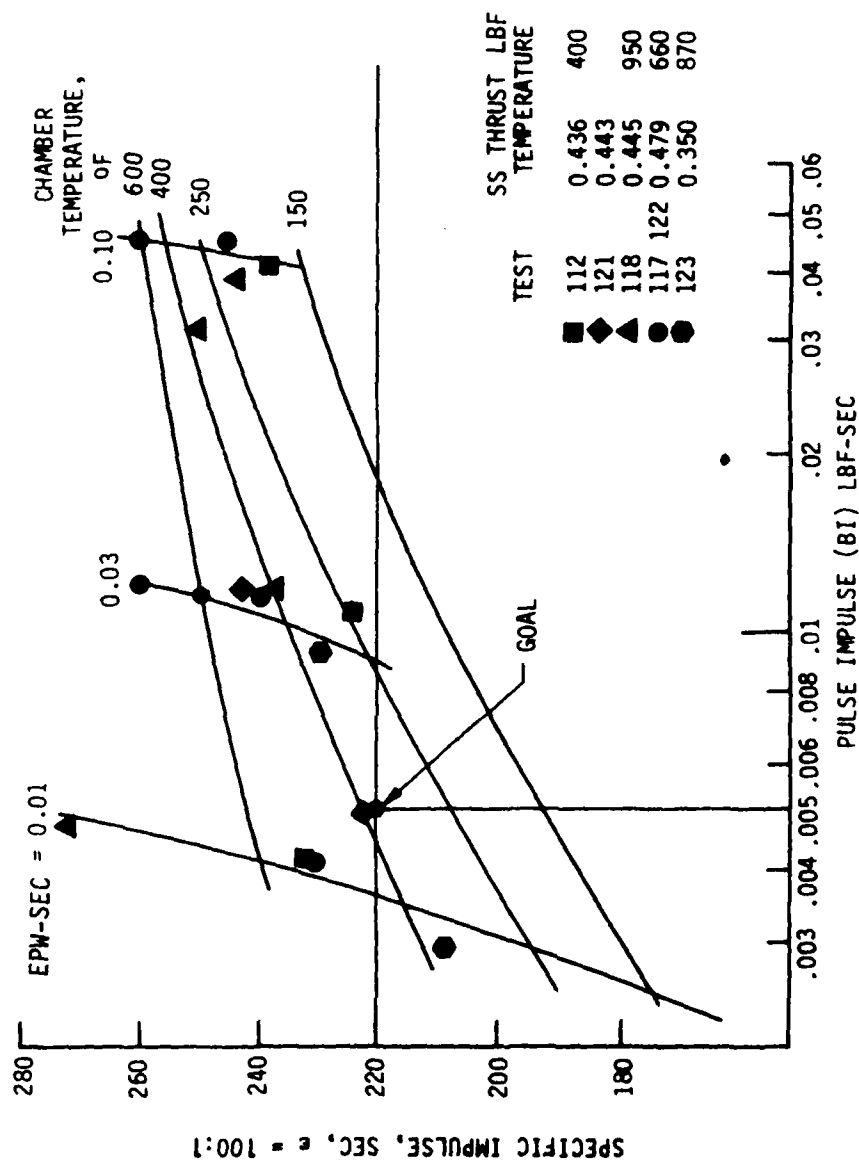


Figure 5-4]. 1-CAS Injector, Hot Chamber Pulse Performance Estimation

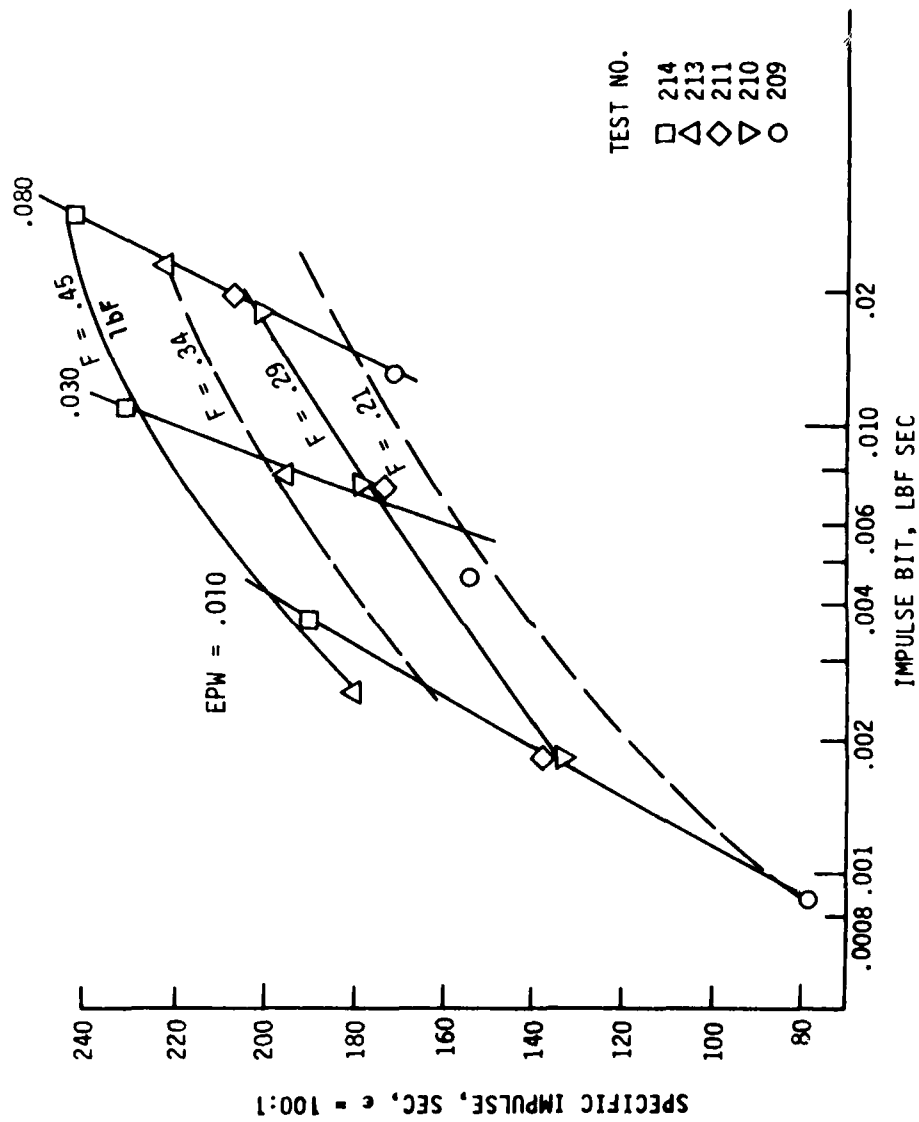


Figure 5-42. 3-SPA Injector Pulse Performance, $L' = 2.0$ " Cold Chamber

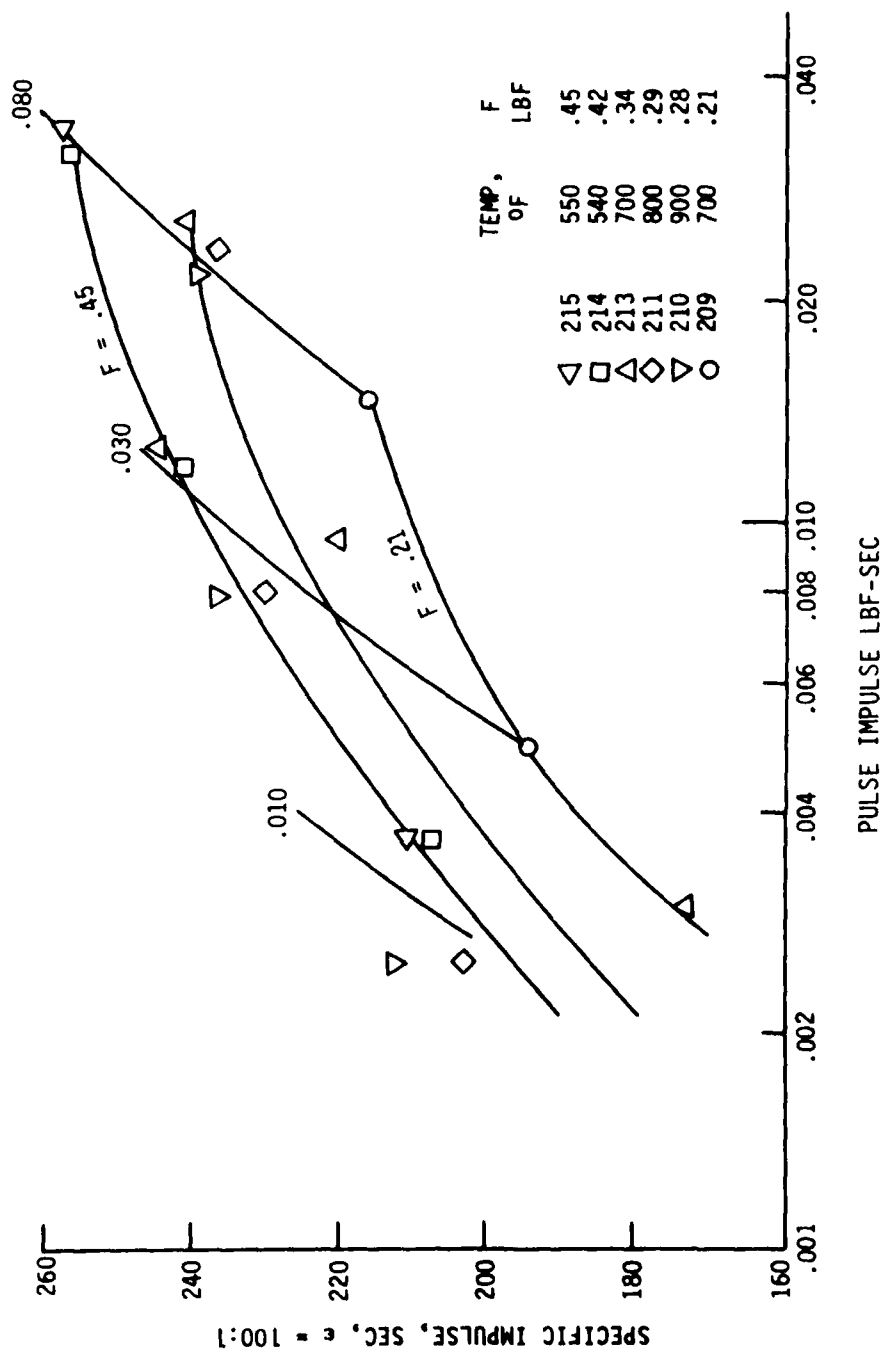


Figure 5-43. 3-SPA Injector Pulse Performance, L' = 2.0" Hot Chamber

5.3, Data Evaluation (cont.)

Figure 5-44 provides a comparison of the 2 injector designs tested, as well as the various modifications to the 1-CAS design. Data are presented for hot walls and cold walls at nominal (~ 125 psia) as well as 60% chamber pressure.

The pulse performance of the 3-element splash plate is higher than that of the 1-CAS SN 9 and SN 10A design when the walls are cold; when the chamber walls are hot the reverse is true. The 1-CAS SN 10B design performed the same as the 3-SPA at the single cold wall, 60% P_c test condition evaluated.

The selection of an injector for Phase III was not based on pulsing performance because the units tested were all about the same.

Figure 5-45 compares the measured hot and cold wall pulse performance with the Phase I CONTAM model predictions. The actual performance was about 10% lower than the predicted values. No effort was made to resolve this difference.

5.3.4 Steady-State Thermal Operation

The design criteria and thermal limitations of the engine are identified in Figure 5-46. This figure schematically illustrates the cross section of the chamber head end and valve for the flanged and welded configuration. A liquid fuel film and the thin wall stainless steel sleeve minimize the heat flow to the injector and valve during steady-state firing and postfire heat soak.

Figure 5-47 shows a typical set of thermal transients for the first design tested (1-CAS SN 9 injector, flanged 2" L' chamber). All temperatures appeared to be as predicted, except at the seal location. The temperature at the head end of the chamber (Station F) was 250°F, and the columbium throat region wall was approaching 2000°F. Testing in this series was limited by the hot gas seal which was approaching the 1800°F limit about 35 sec into the test.

Figure 5-48 provides a comparison of the engine axial temperature profiles for the 2 injectors tested (1-CAS and 3-SPA).

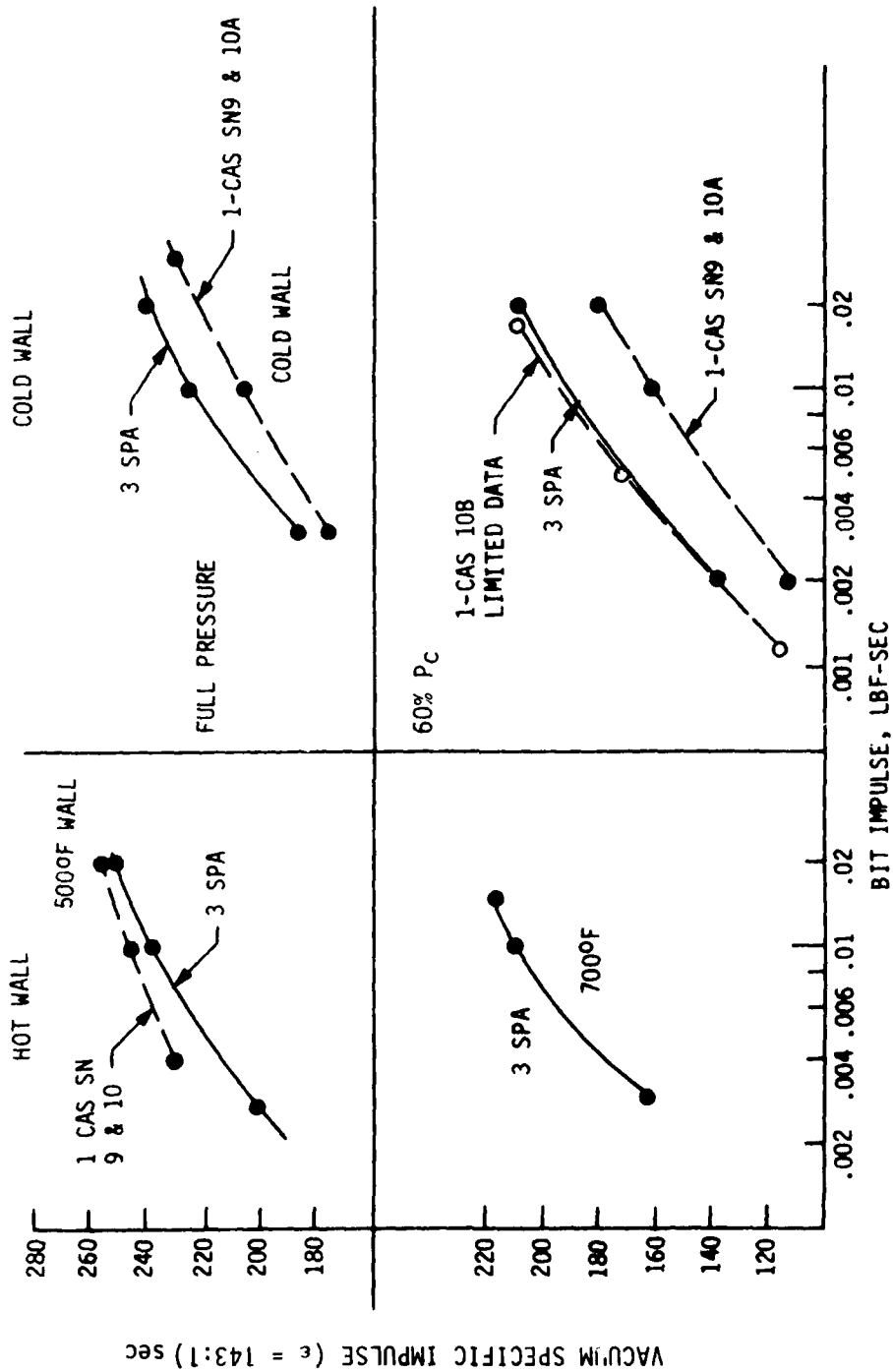


Figure 5-44. 3-Element Splash Plate and Coaxial Swirler Injector Pulse Predictions

AD-A091 078

AEROJET LIQUID ROCKET CO SACRAMENTO CA
LOW-THRUST BI-PROPELLANT ENGINE TECHNOLOGY, (U)
AUG 80 L SCHOENMAN, R L FRIEDMAN

F/6 21/9.1

F04611-77-C-0053

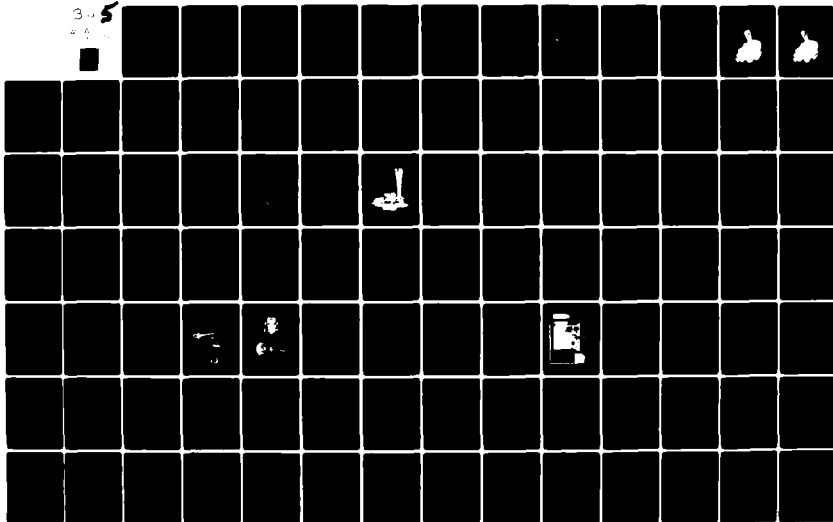
UNCLASSIFIED

AFRPL-TR-80-47

NL

3-4

4-4

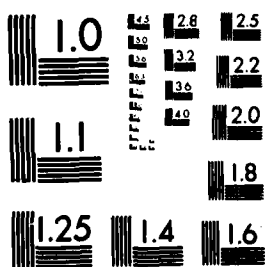


1551F1E

3 OF 5

AD. A

091078



MICROCOPY RESOLUTION TEST CHART
NATIONAL BUREAU OF STANDARDS-1963-A

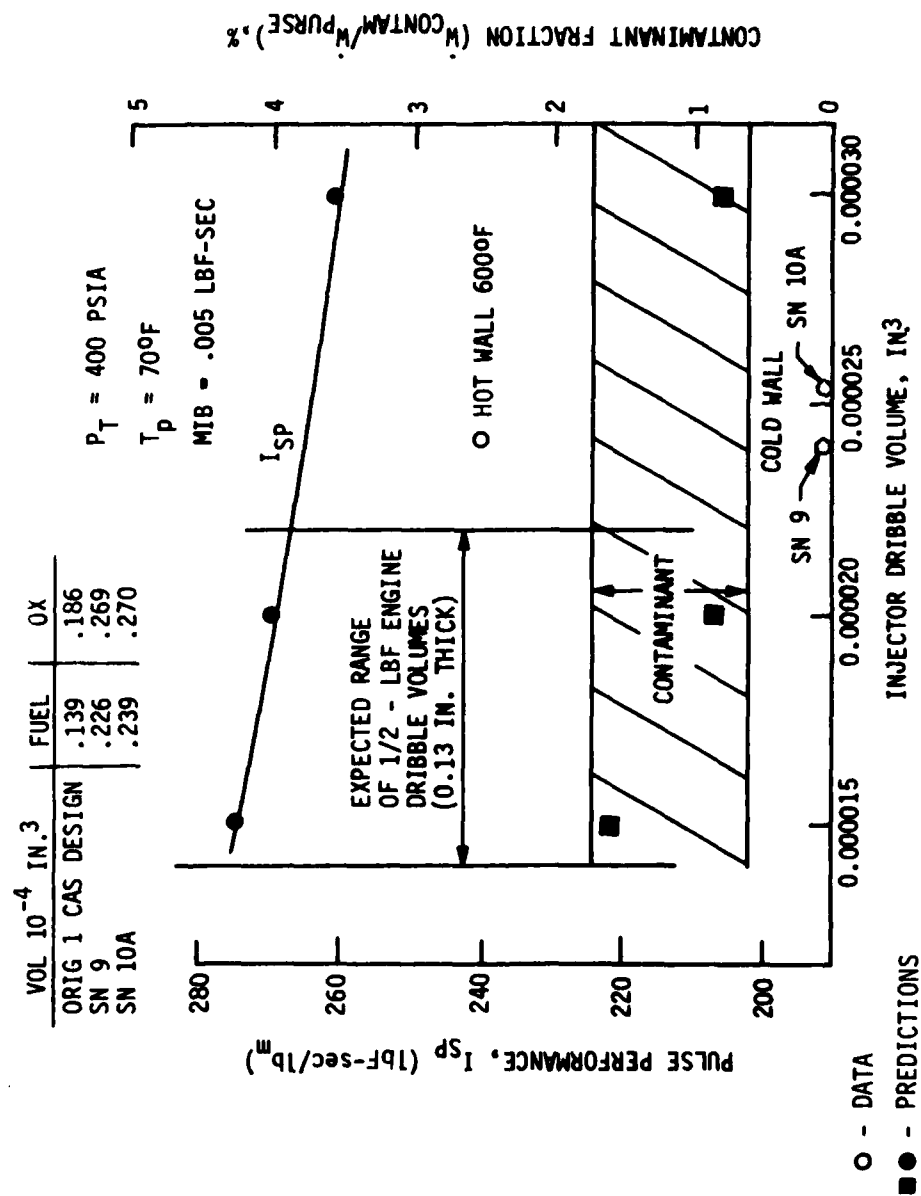


Figure 5-45. Pulse Performance vs CONTAM Model Predictions

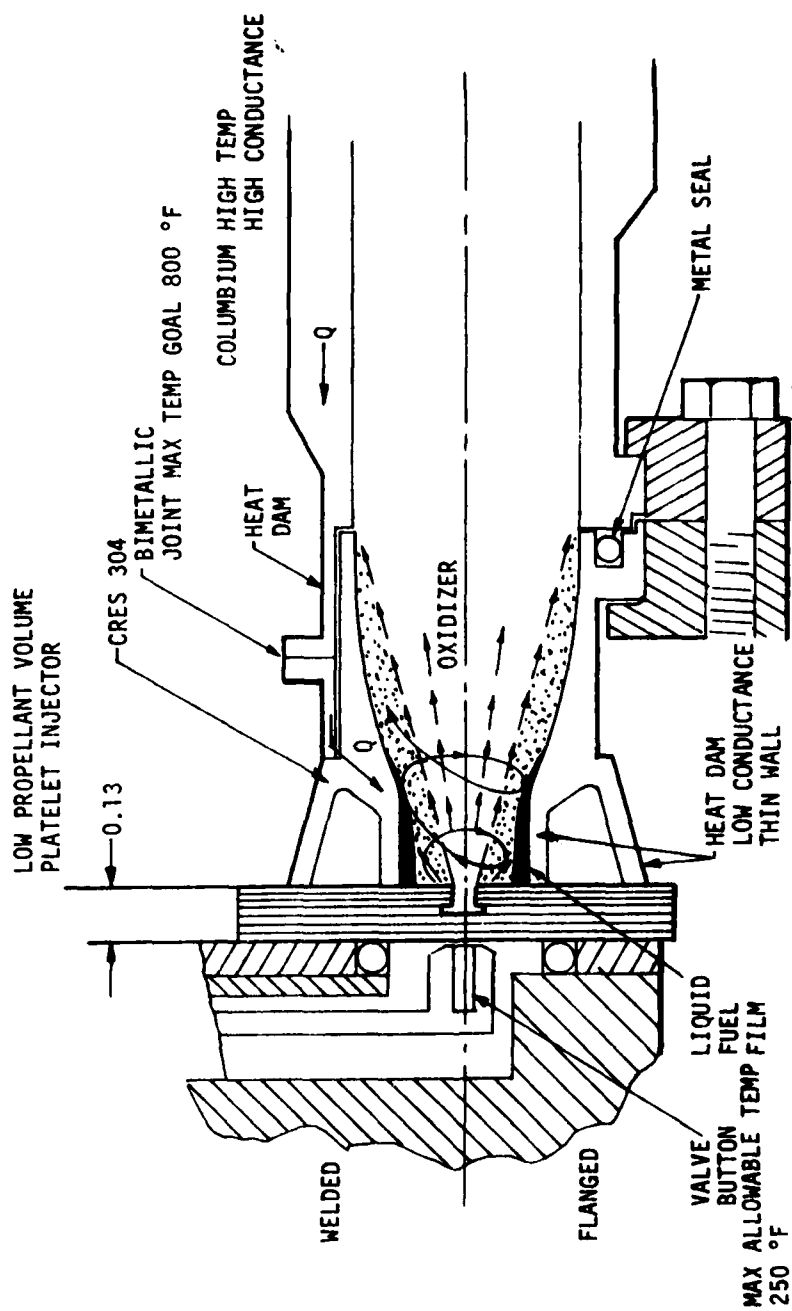


Figure 5-46. Thermal Management for Steady-State Capability and Pulsing

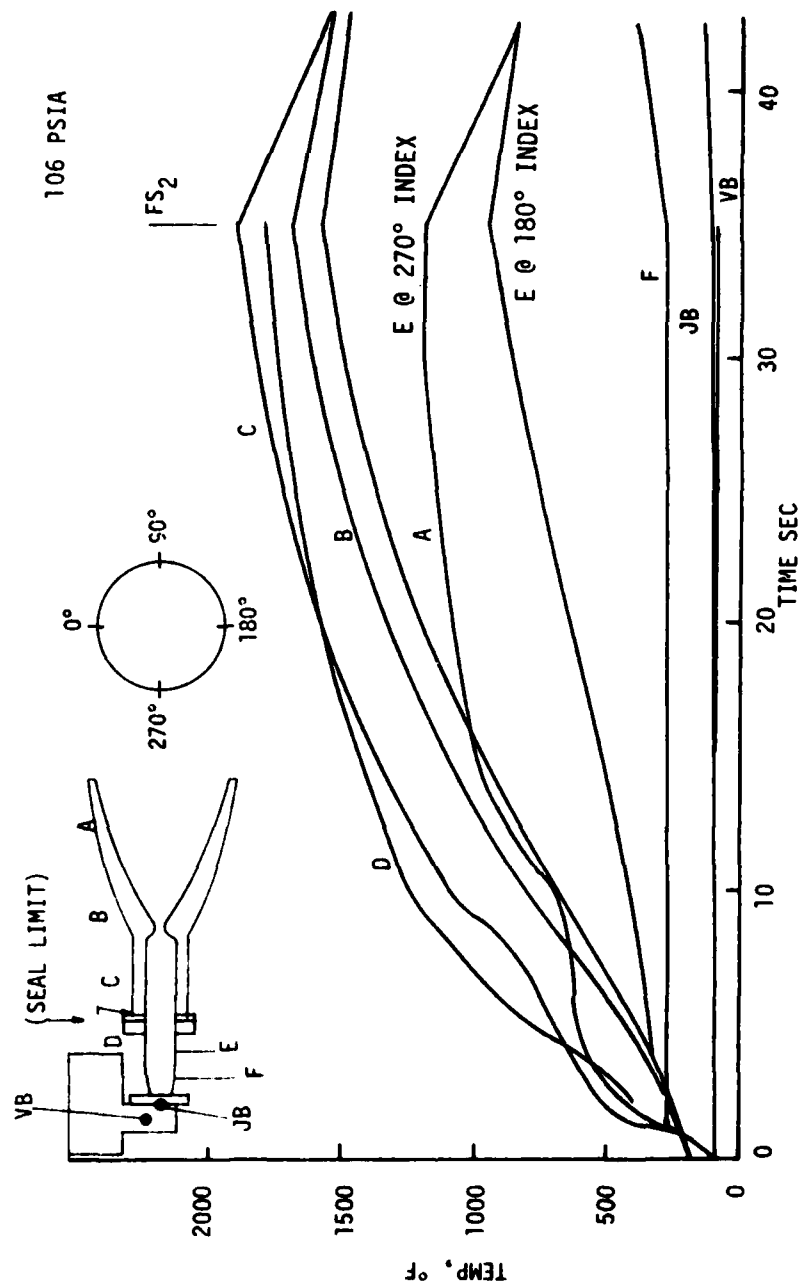


Figure 5-47. Steady-State Thermal Response Test 118

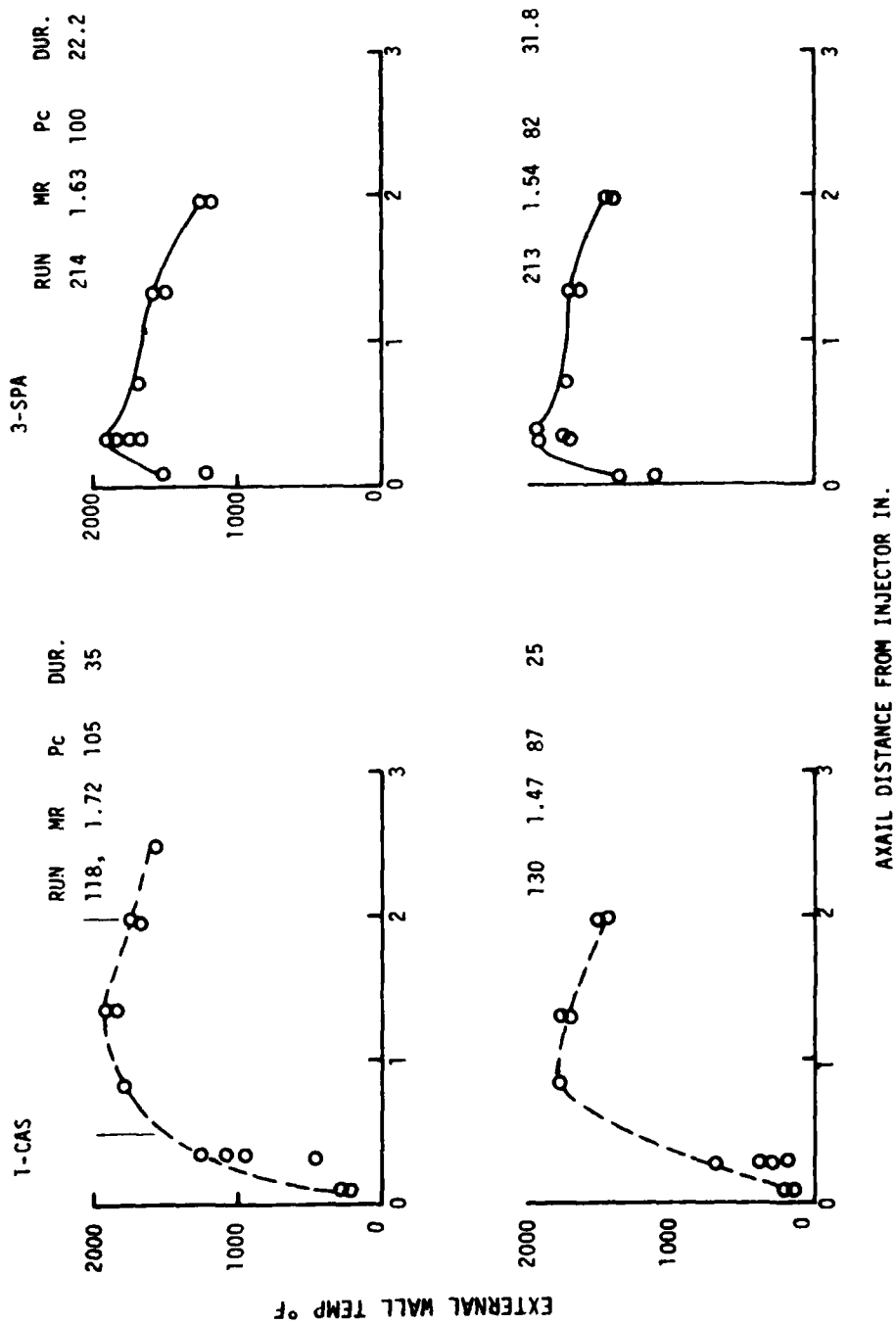


Figure 5-48. Chamber Thermal Profiles, 3-SPA Injector End

5.3, Data Evaluation (cont.)

The temperatures at the head end of the splash plate injector/chamber were approaching 2000°F and were unacceptable for steady-state operation. Those of the CAS design were considerably lower, but still higher than desired. Since both designs provided about the same specific impulse, attention was placed on reducing the head end temperatures and correcting the fuel circuit ΔP of the CAS design.

Figure 5-49 provides comparative Station E and F thermal response data for flanged and welded chambers for the 1-CAS SN 9 configuration and the SN 10A flanged configuration. Data are presented for chamber pressures between 60 and 120 psia. SN 9 in the welded flight-type configuration was found to run cooler at the seal location than the flanged version. The reduction in fuel injection velocity incorporated in SN 10A also caused the front end to run hotter. This was expected since decreased fuel injection velocity reduces the swirl forces which deposit the fuel on the chamber wall. The data indicate that the cooling becomes more effective as the propellant supply pressure and thrust and P_c are reduced.

Figure 5-49 also shows that SN 10A achieved steady-state thermal operation in a 250 sec continuous test at a P_c of 63 psia. The maximum throat temperature was noted to be 1800°F.

Figure 5-50 provides a comparison of the postfire soak following these long burns. The welded configuration is soaked out at higher temperatures than the flanged design.

Because of the high chamber temperatures, the injector head end was subsequently modified, as shown in Figure 5-51, to allow more of the fuel in the outer swirl cone to impinge on the wall before combusting with the oxidizer. This simple change allowed test durations of 250 sec (the facility flow limit for the large PDFM) to be accomplished at chamber pressures up to 90 psia. Thermal maps and transient data for this assembly are provided in Figures 5-52 through 5-55. The postfire heat soak, shown in Figure 5-53, is considered acceptable; however, the flange is operating near the upper limit temperature for the gold plating on the seal (1800°F).

Figure 5-56 provides a thermal map of the assembly at chamber pressures between 65 and 115 psia. The vertical arrows on several of the high pressure data points indicate that these locations have not achieved steady-state and that temperatures were still climbing at the end of the test.

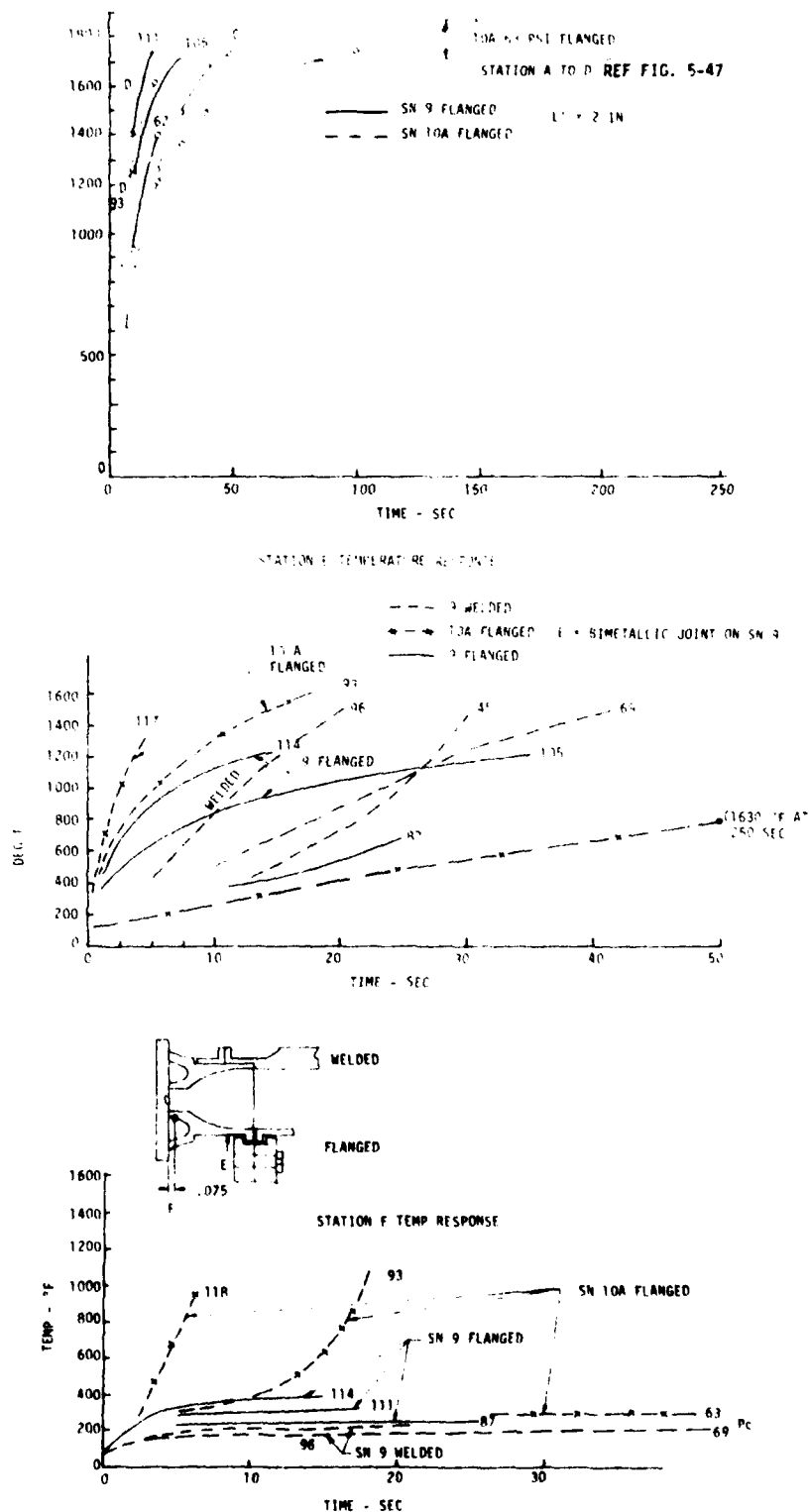


Figure 5-49. Comparison of Thermal Transients of Coaxial Injector SN 9 and 10A with Flanged and Welded Chambers

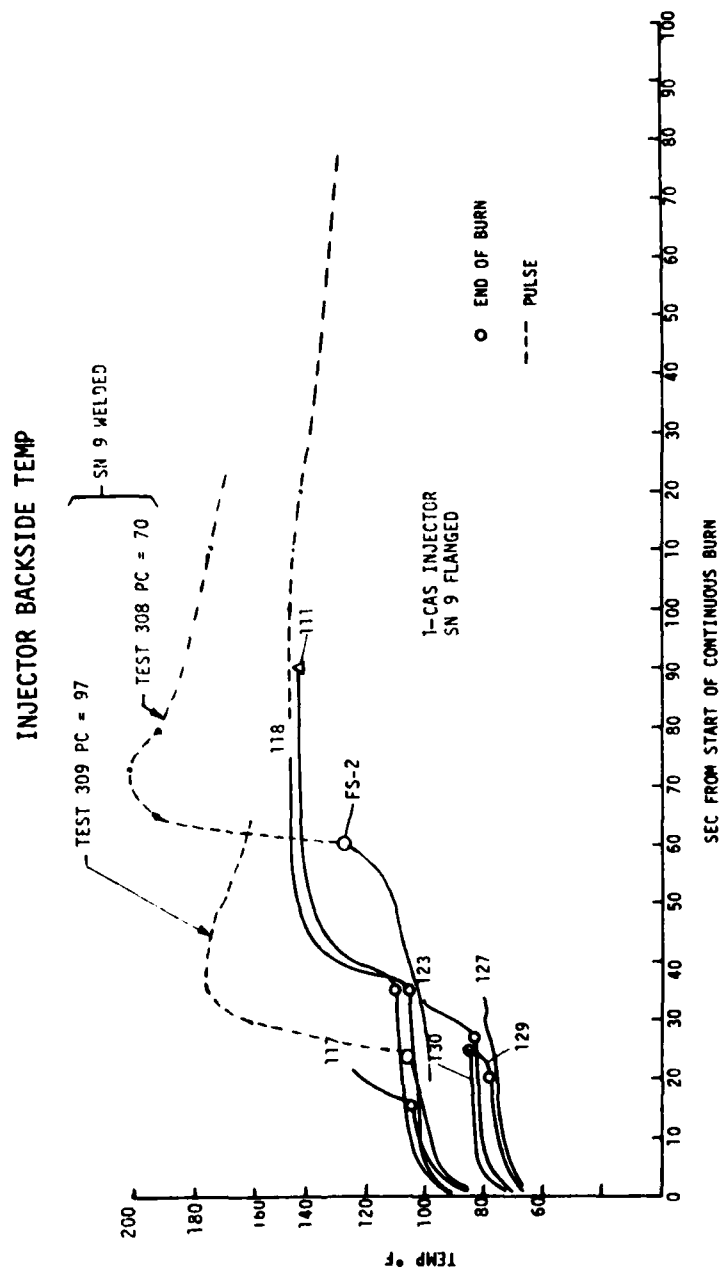


Figure 5-50. Postfire Heat Soak on Flanged and Welded Chamber Configurations

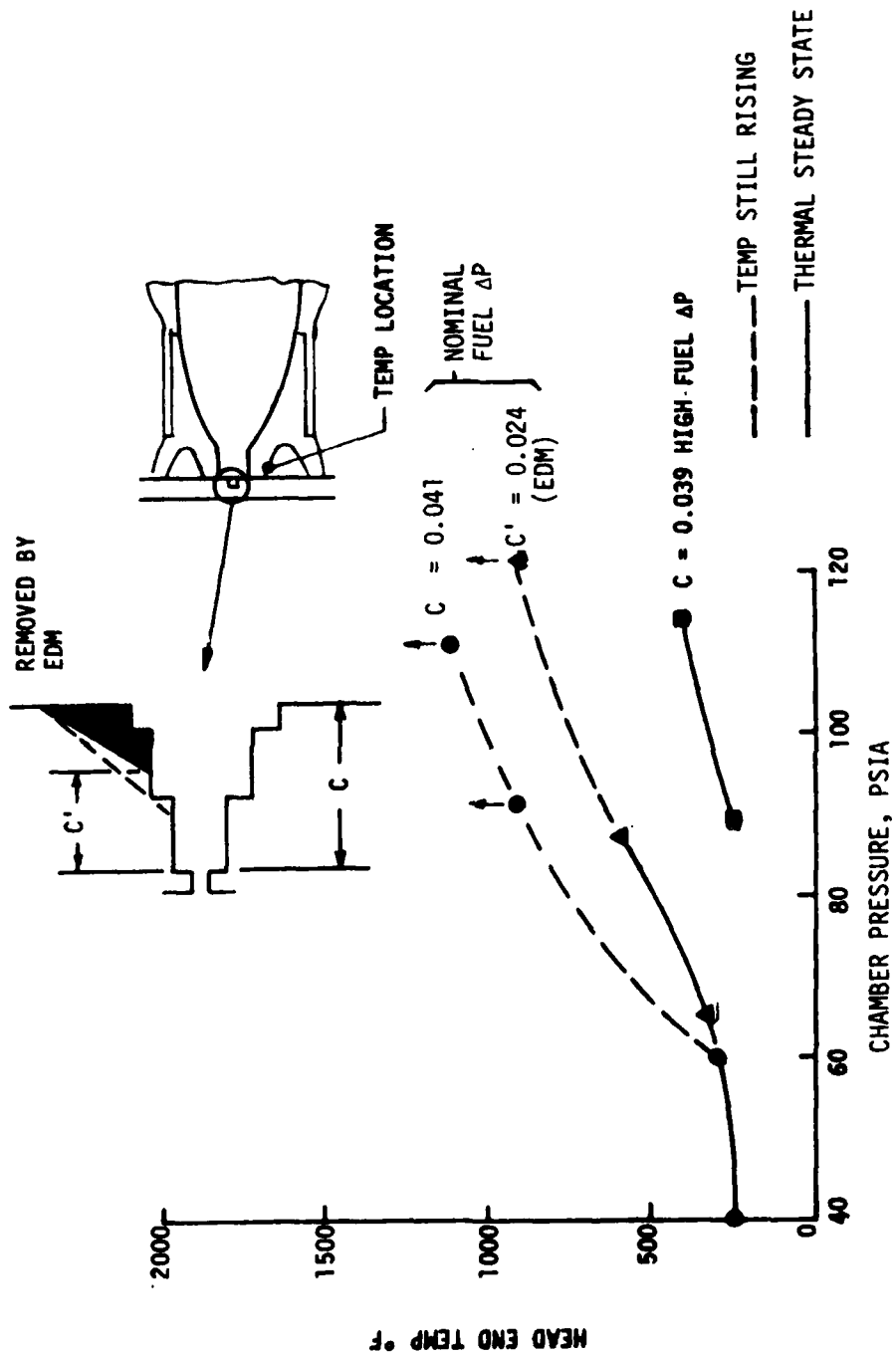


Figure 5-51. Shorter Wide Angle Premix Cup Length vs Chamber Head End Temperature

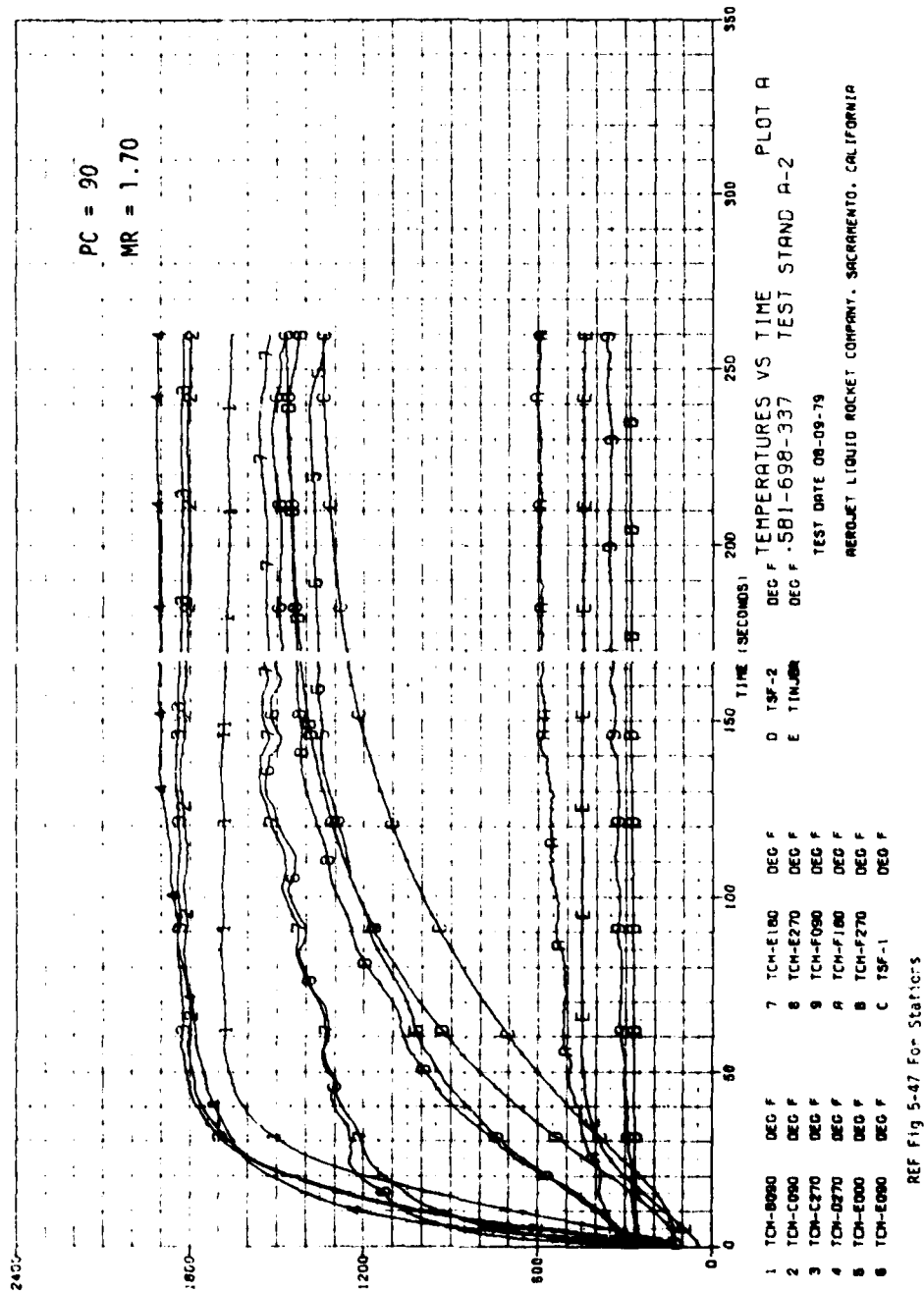


Figure 5-52. Thermal Steady-State at .37 lb Thrust

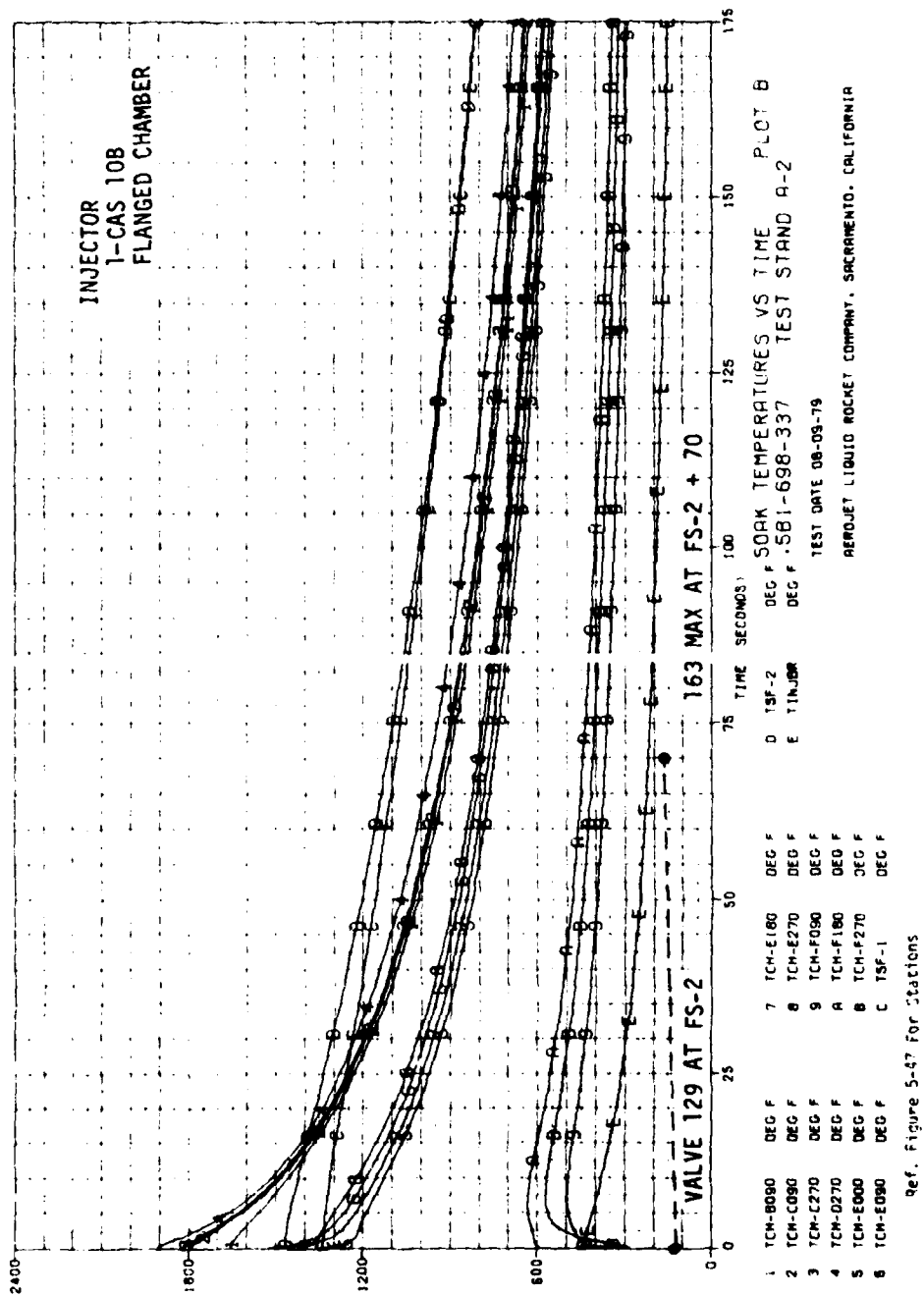


Figure 5-53. Postfire Heat Soak After Steady-State Burn

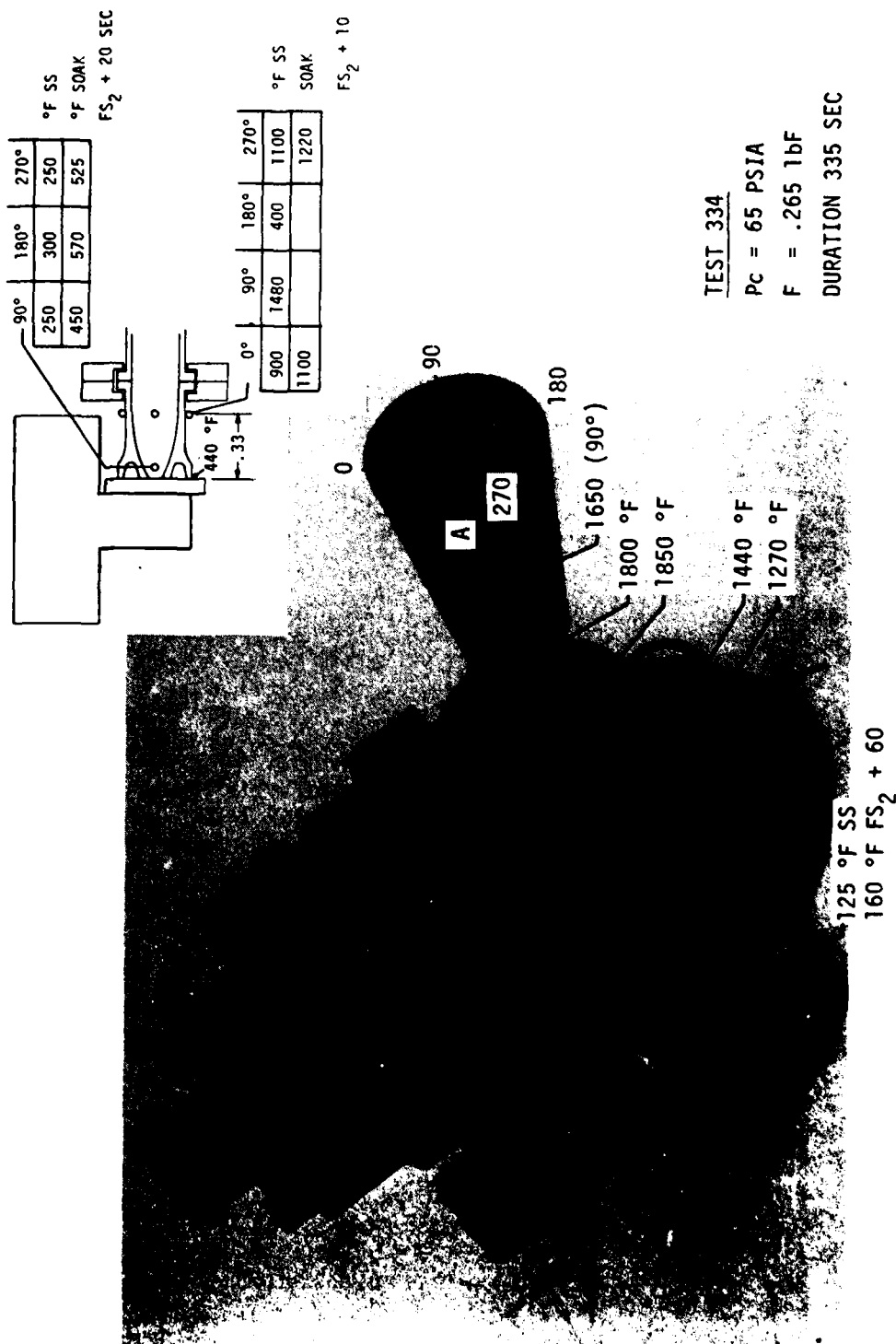


Figure 5-54. Thermal Steady-State Temperatures with 1-CAS Mod B Injector at 65 Psia, 0.25 lb Thrust.

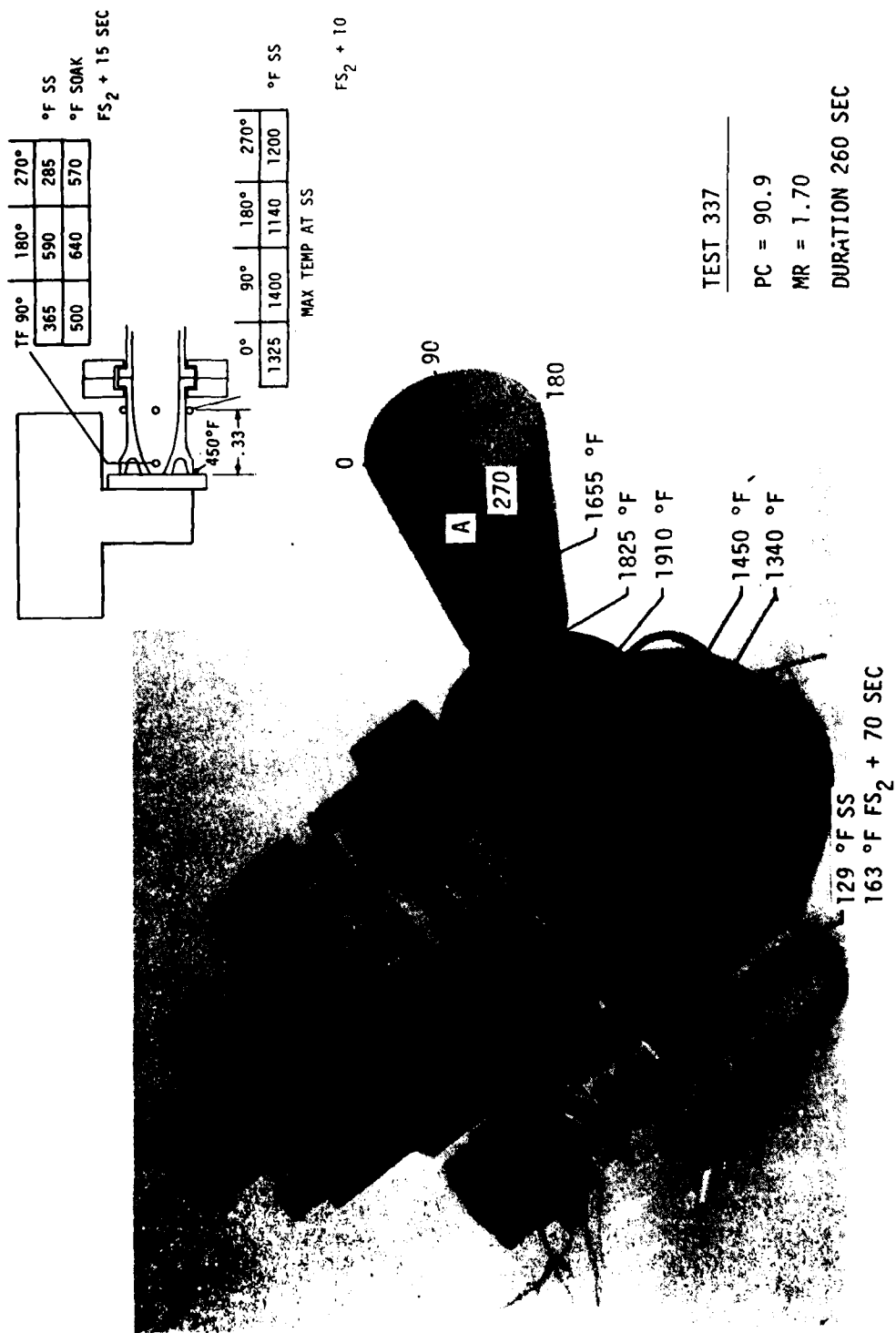


Figure 5-55. Steady-State Thermal Conditions at .37 lb Thrust

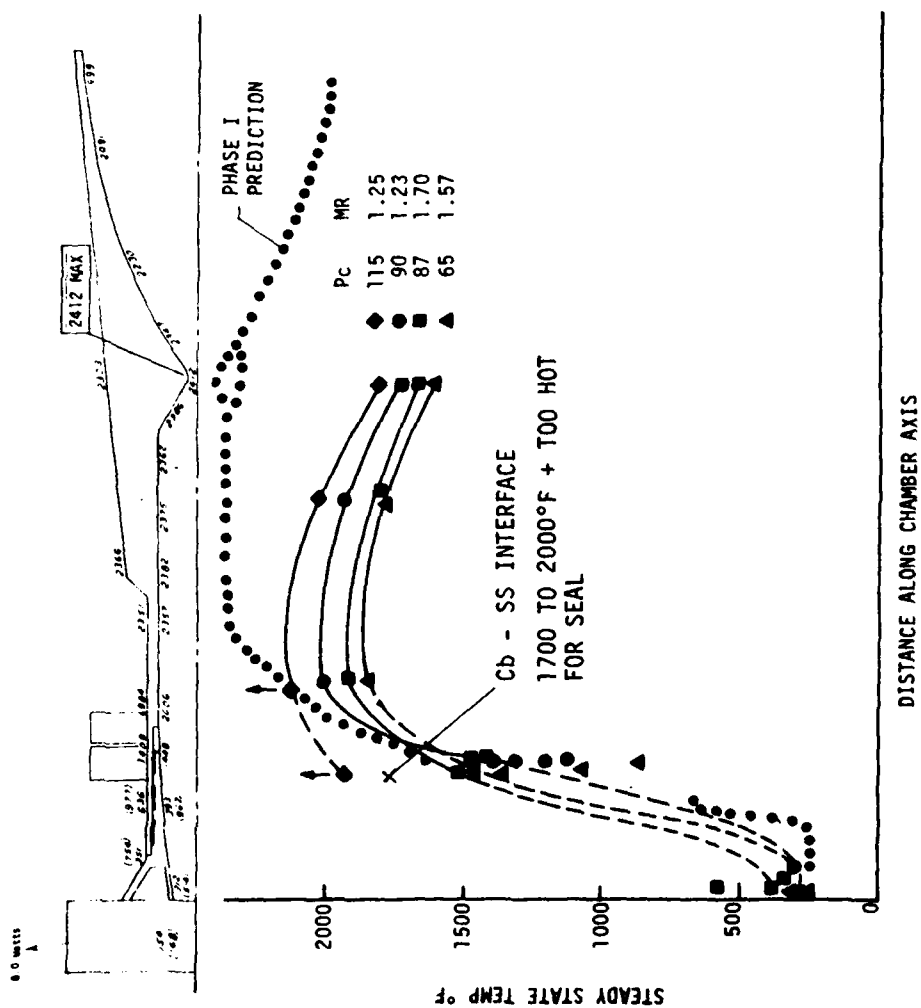


Figure 5-56. Steady-State Chamber Temperature Axial Profiles as a Function of Chamber Pressure

5.3, Data Evaluation (cont.)

Figure 5-51 summarizes the ability of the film-cooled steel head end to remove the heat being conducted along the chamber. Data are presented for the various test configurations as a function of operating pressure.

Figure 5-57 documents the approaches which could be employed to further reduce the head end temperature and extend the operating range. A decision was made to investigate further enlargement of the cup angle and depth to the "C" configuration, as shown in Figure 5-51.

5.3.5 Pulsing Thermal Characteristics

No thermally limiting conditions were noted during any of the pulse test series conducted in Phase II. However, the pulse testing conducted in Phase II was not of sufficient duration (continuous pulsing at fixed conditions) to achieve equilibrium thermal conditions under all duty cycles. The duty cycles were designed mainly to provide impulse bit and pulse performance data.

Figure 5-58 provides thermal transients at two chamber locations: on the steel sleeve adjacent to the injector (ISL) and on the thin wall portion of the columbium close to the flange (TCH-90). These data for test 130 correspond to the "B" duty cycle consisting of the 330 pulses as was defined in Table 5-X, page 141.

The temperatures indicated in these figures correspond to the value at the end of each pulse. The * indicates a single pulse, while numbers 2 through 5 define the quantity of successive pulses having the same temperature. When these numbers approach 4 or 5, one can conclude that this is the equilibrium thermal condition for the pulse sequence. Many of the pulse groups did reach an equilibrium value. The sudden drop in temperature between successive pulses is caused by a hold in the pulse sequence to refill the microPDEFM flow meters.

The maximum temperatures of the head end and columbium did not exceed 240°F and are considerably less than the steady-state operating value for these locations.

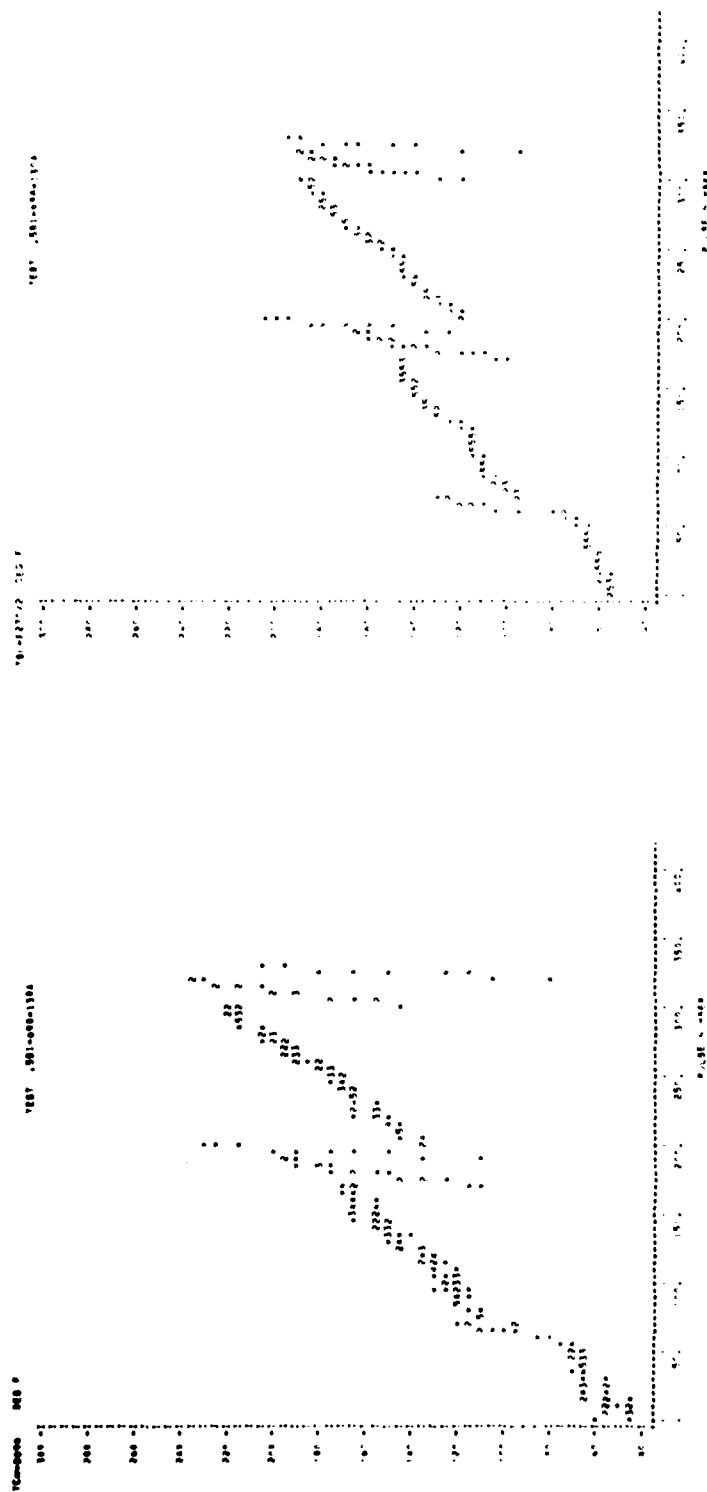
Figure 5-59 shows "A" duty cycle pulse thermal data from test 123B following a 27 sec continuous firing. (The "B" after the test number indicates the pulses following the long burn.) Pulsing was initiated when the chamber head end soaked out to 530°F (the maximum soakout temperature). At the time pulsing resumed the columbium was at 720°F. These data indicate that chamber temperatures drop during the pulsing and that

APPROACH

DISADVANTAGE

Use Existing Flange and Injector Design. Limit Pc to \approx 70 to 90 Psi \approx 0.3 lb Thrust.	Joint is still hot \approx 1500°F. Blowdown Capability is Reduced.
Modify Injector Cup to Obtain More Head End Wall Cooling.	Approach is Empirical. More Than One Iteration Could Be Required.
Heat Sink Seal Area \approx 40 Watts.	Heat Load Not Desirable for Space Craft. 15 W goal.
Separate Valve and Injector. Move Seal Behind Injector.	Increased Holdup Volume. Poor Pulsing and Higher Contamination in Pulse Mode Operation
Seek an Alternate Chamber Design Approach While Maintaining Same Thermal Management.	Solution may be Dependent on Injector Design Change.
Evaluate Alternate Chamber Materials and Fabrication Approaches.	Could Result in Need for New Process Development Work.

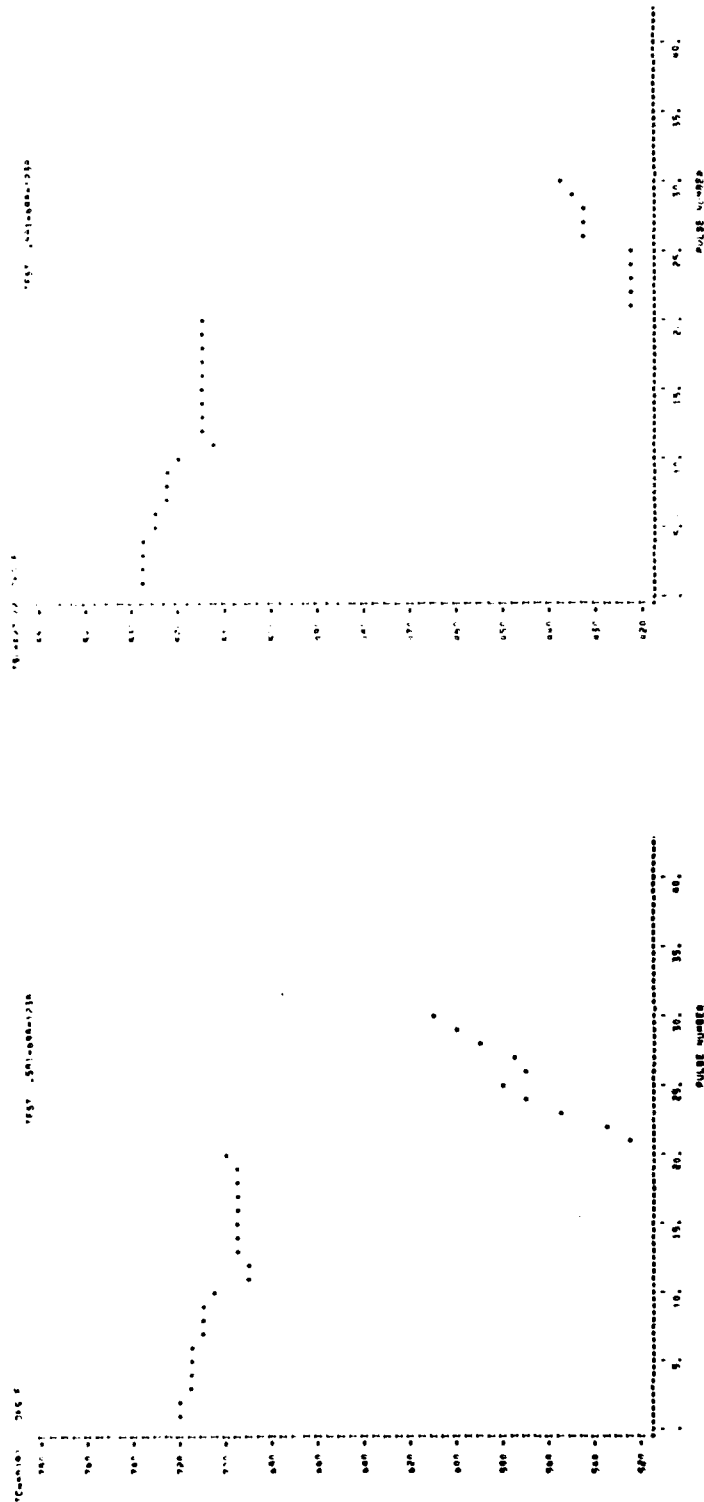
Figure 5-57. Phase III Options to Resolving the Hot Joint Limitations in Long Duration Burns



*Single Pulse

2,3,4,5 Successive Pulses with the same Temp.
Ref. Page 128

Figure 5-58. Pulsing Thermal Transients, "B" Duty Cycle



Ref Page 138 for Locations

Figure 5-59. Pulsing Thermal Transients Following a Long Burn

5.3, Data Evaluation (cont.)

there are no adverse effects on engine restarts when the chamber had soaked out to its maximum head end temperature.

5.3.6 Blowdown and Stability

The testing of each injector included obtaining data at tank pressures between 80 and 400 psi where ever possible. The relationship between tank pressure and chamber pressure for the 1-CAS SN 10B injector is shown in Figure 5-60.

As the supply pressure is reduced, the stability of the engine is measured by the output of the following parameters: dynamic thrust, chamber pressure, and feed line pressures. Of all measurements, the dynamic thrust measurement was found to be the most sensitive in recording combustion roughness.

Figure 5-61 provides a reproduction of these traces for the 1-CAS SN 9 injector at full thrust. The initial dynamic stand ringing is noted to damp out in $\approx .05$ sec while the highly damped static measurement responds very slowly. The overshoot in P_c is believed to be a result of having a small drop of fuel in the .010 dia pressure port. As the injector heats, the Liquid in the passage boils and increases the pressure until the passage is dried out.

Figure 5-62 shows similar data for the same assembly operating at 30% thrust.

The start transients are slower at reduced thrust, and maximum P_c is not achieved for several tenths of seconds. In addition, the combustion roughness, as measured by the peak-to-peak variation in the dynamic force measurement divided by the mean thrust, becomes greater as the chamber wall heats. This effect was noted on both injectors tested.

Figure 5-63 provides a comparison of the vibrational amplitude measured in lbF peak-to-peak as recorded on the F dyn trace. Data are shown for the 3-element splash plate and the coaxial swirler designs. The effect of duration and operating pressure are noted. Mod B of the 1-CAS design provided the most consistently stable operation of all test configurations. Data for the 1-CAS 10B injector at 122 P_c and 42 P_c are shown in Figure 5-64. This supported the selection of 1 CAS Mod B design for further optimization.

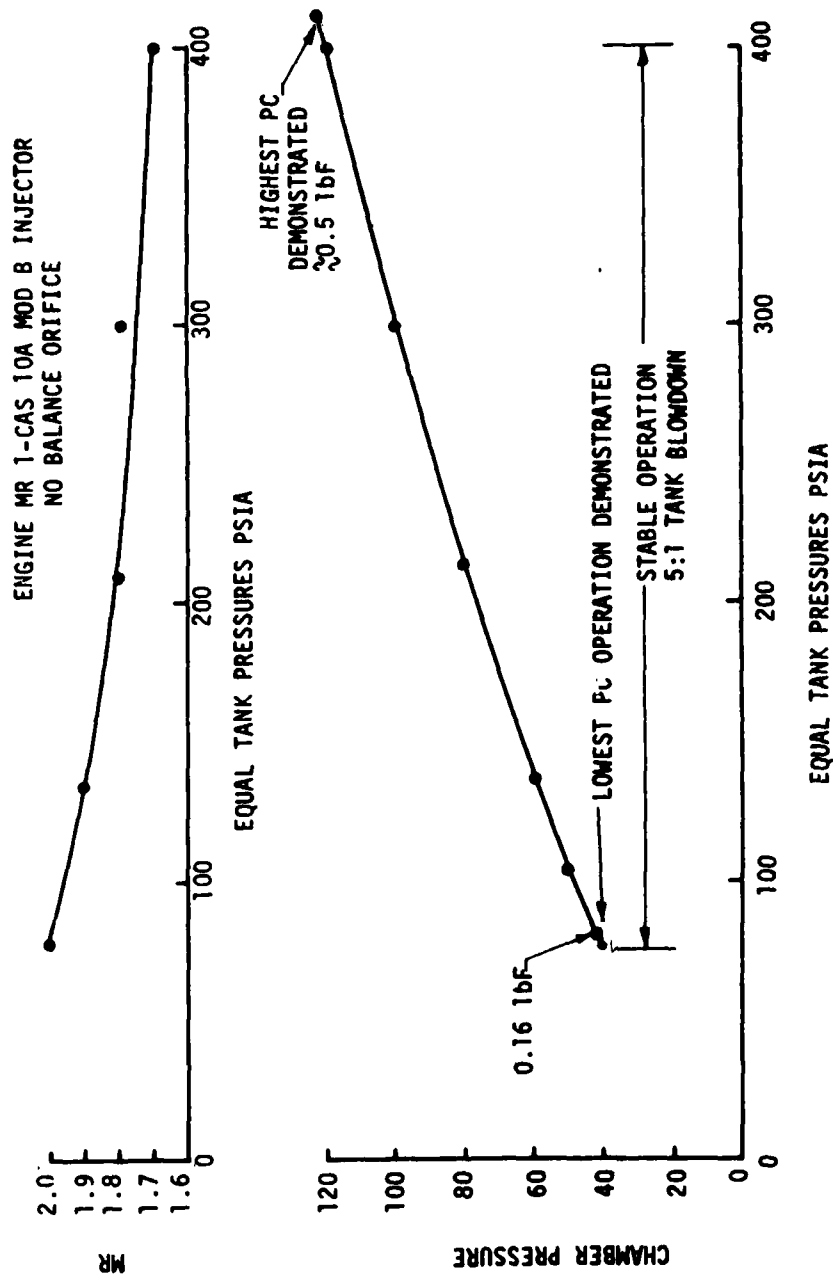


Figure 5-60. The 1-CAS Injector Configuration MOD B Blowdown Capability

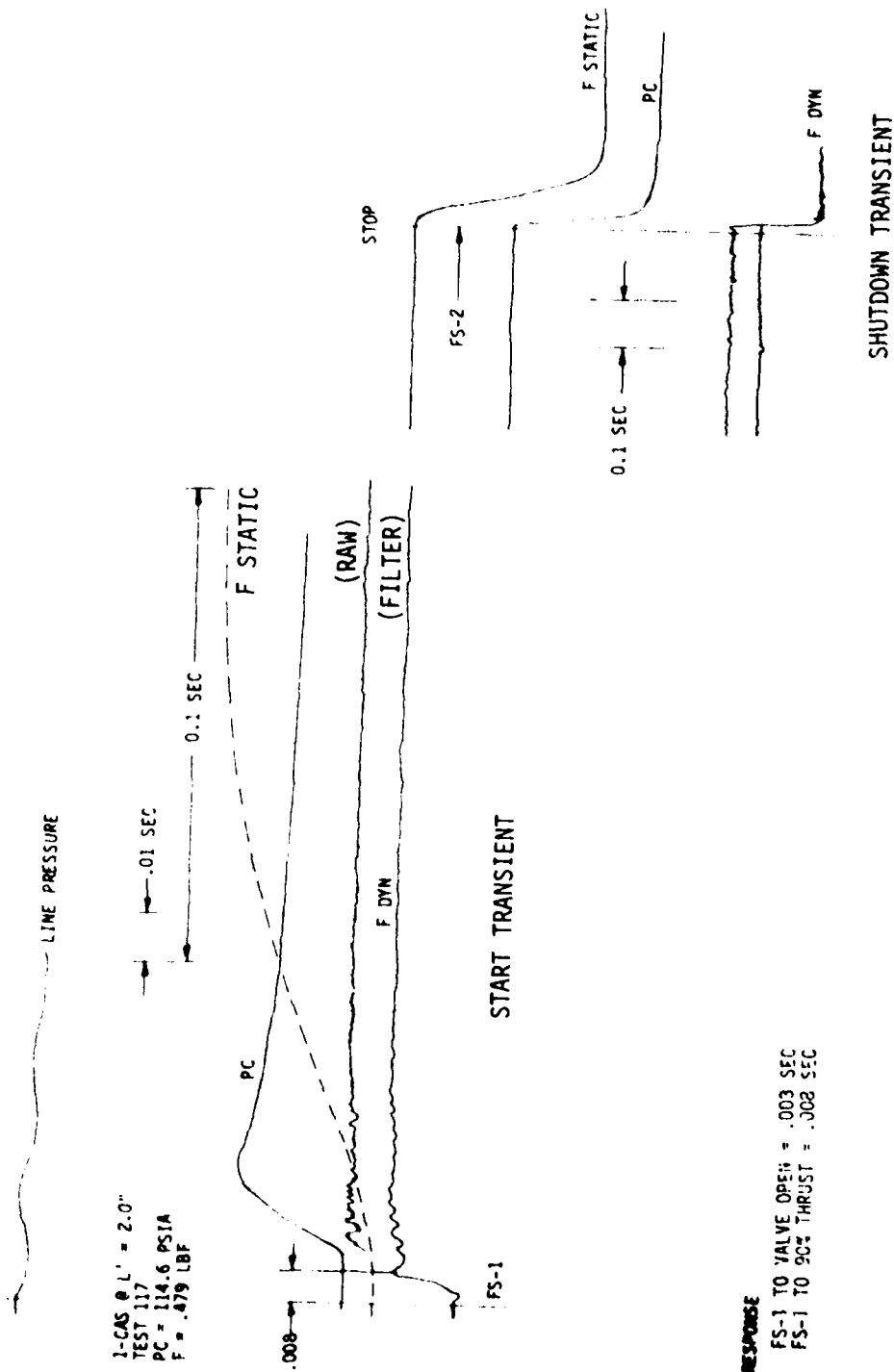


Figure 5-61. 1-CAS SN-9 Injector Engine Start and Shutdown Transients at Maximum Thrust

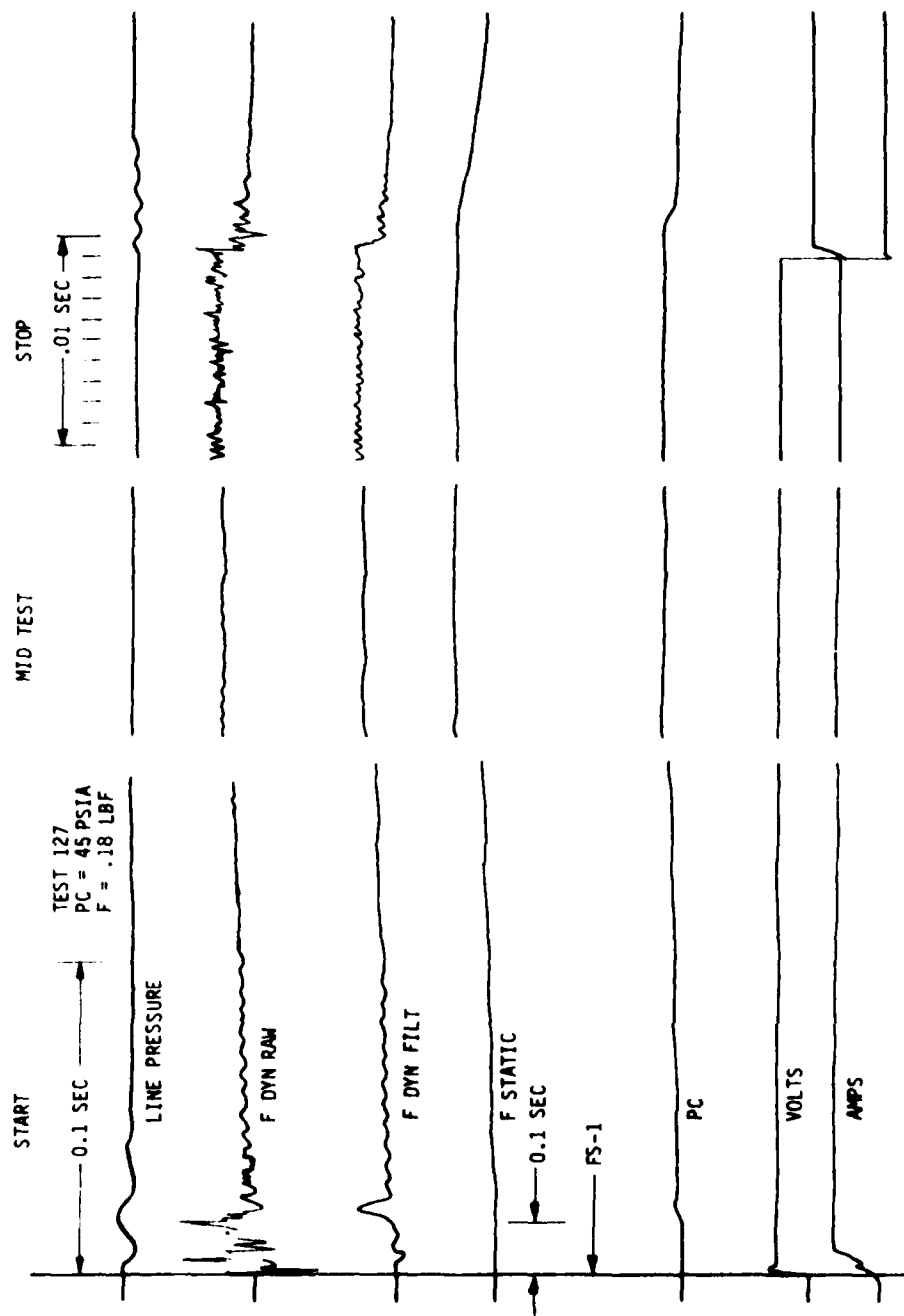


Figure 5-62. 1-CAS SN 9 Injector Engine Transients at 30% Thrust

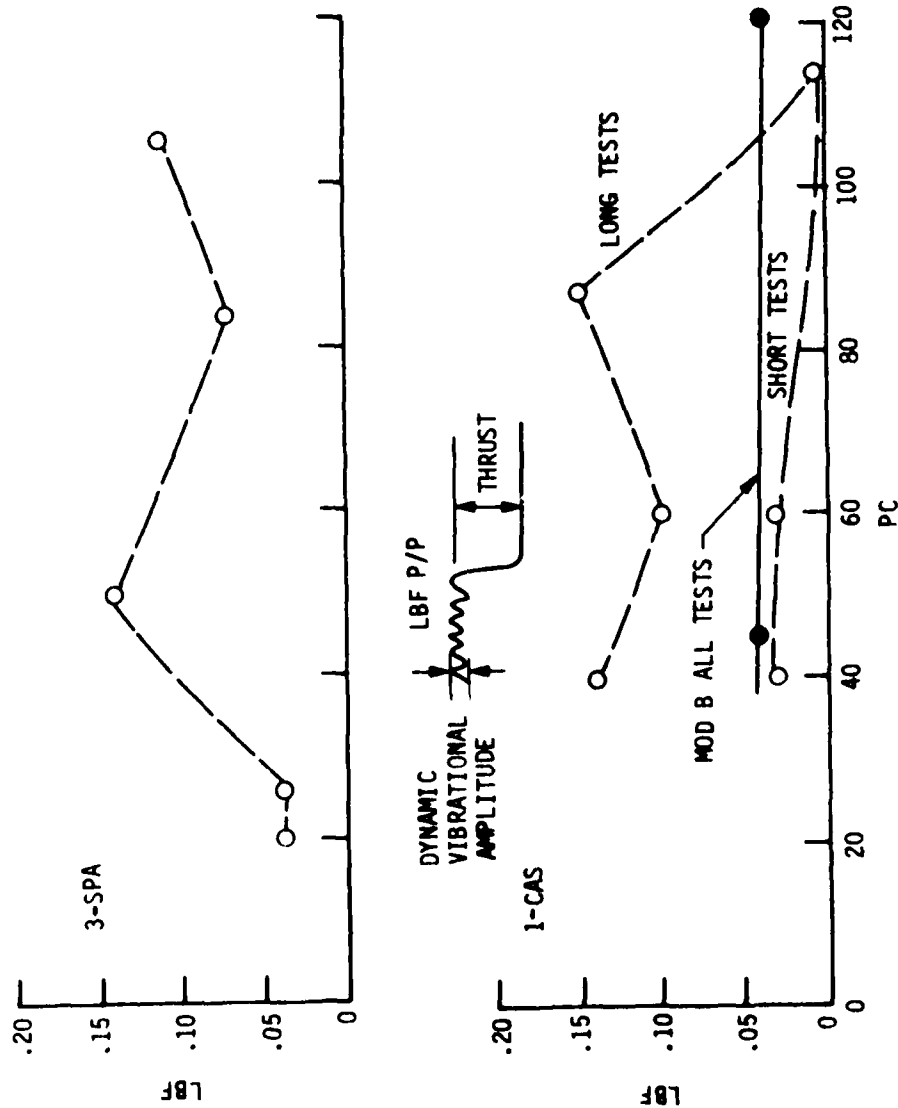


Figure 5-63. Comparison of Combustion Roughness for Injectors Tested in Phase II

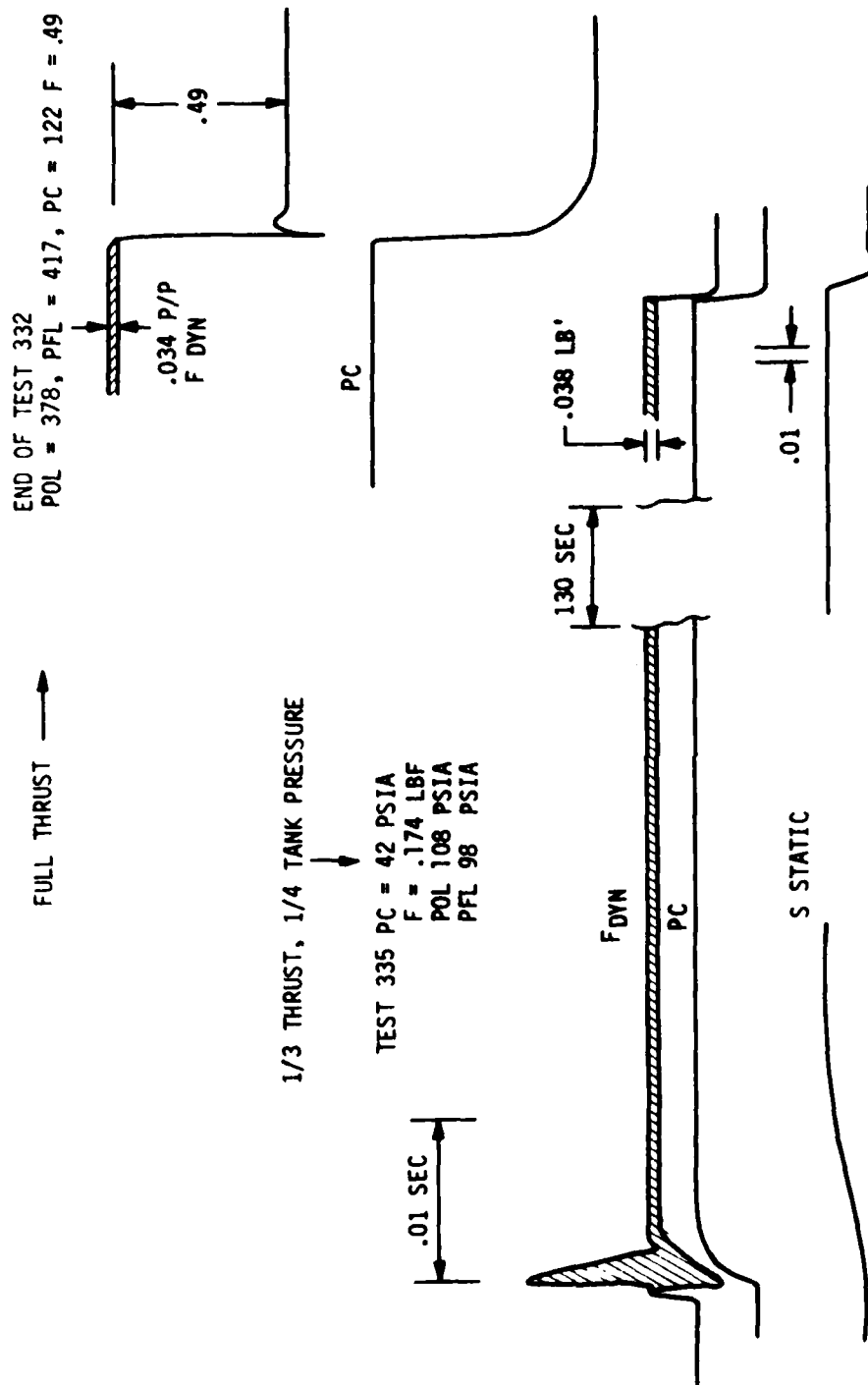


Figure 5-64. Injector 1-CAS Mod B Dynamic Thrust Traces at 0.49 and 0.17 lb Thrust

5.3, Data Evaluation (cont.)

The cause for the increase in roughness with burn duration was not precisely identified but appears to be a thermally induced effect. Two possibilities exist: one is that the heated chamber wall causes the fuel droplets to undergo mono-propellant decomposition; the second is that the heat addition to the oxidizer passing through the injector causes two phase flow injection.

The thermal instrumentation placed on the injector face and backside failed in the braze assembly of the injector and chamber and was not available to identify the injector temperature at the time the combustion roughness started. Further testing is required to provide data to relate temperature effects to the onset of combustion roughness. This roughness appears to start between 10 and 30 sec after FSI.

On the basis of the test results with one design, it appears possible to attain a 5:1 tank blowdown ratio, as shown in Figure 5-64.

5.4 PHASE II CONCLUSIONS

Phase II fabrication activities resolved several problems resulting from the small size of the components of the 0.5 lbf engine. These are summarized as:

- Valve fabrication techniques were put in place with no problems encountered.
- Initial problems in etching small injector passages were resolved.
- Methods of improving platelet stacking alignment were resolved by an ALRC sponsored program.
- No problems were encountered in the fabrication of columbium chambers.
- No problems were encountered in weld assembling a chamber with a stainless/columbium explosively bonded transition joint.
- Methods of joint NDT needed development.

Bench-testing of the fabricated hardware was performed with the following results:

5.4, Phase II Conclusions (cont.)

- ° Valve response and repeatability was satisfactory for Phase III demonstration.
- ° Required valve cycle life was achieved.
- ° Injector fabrication and pressure drop for the 1-CAS Mod A injector is acceptable.
- ° Hydraulic reproducibility of injector SN 10A configuration needs to be verified by fabrication of additional parts in Phase III.

The hot-fire test program of Phase II was evaluated by steady-state performance results, pulse mode operation, and general observations as follows:

Steady-State Performance Conclusions

- ° Increasing chamber L' from 1 to 2 in. increased performance by 10 sec.
- ° Coaxial swirler & splash plate injectors both delivered 275 sec of specific impulse at $L' = 2$ in., $P_c = 120$ psia.
- ° Heat losses became significant (~ 30 sec of Isp) at lower chamber pressure (50 psia).
- ° Increasing L' beyond 2 in. was not advised because of the high heat losses.
- ° MON-10 oxidizer provided the same performance as N_2O_4 .
- ° Nozzle C_f data indicated BLIMP model predictions were acceptable.
- ° Injector design selection would be based on factors other than steady-state performance.

Pulse Mode Conclusions

- ° The minimum impulse bit goal, $0.005 \text{ lbf-sec} \pm 0.0005$, was demonstrated.

5.4, Phase II Conclusions (cont.)

- Impulse was not dependent on oxidizer blend, MON-1 to MON-10.
- Impulse was not sensitive to environmental temperature, 20 to 120°F.
- Cold engine MIB Isp performance, 190 sec, was less than program goal, 220 sec at 0.005 lbF-sec.
- Pulse performance program goal was attained when chamber wall was ~400°F, 220 sec at 0.005 lbF-sec.

General Observations

- The Phase II design was within 1 3/4% of performance goal.
- 106 cycle valve was successfully bench-tested.
- Minimum impulse bit goals and pulse repeatability were demonstrated.
- 4:1 tank pressure blowdown was demonstrated.
- Pulsing-only operation had no observable thermal limitations.
- Steady-state head end and throat temperatures were acceptable.
- Stainless steel to columbium chamber interface was hotter than desired at full thrust operation (0.5 lbF).
- Interface cooling problem became manageable at reduced thrust and P_c (0.25 lbF).

5.5 PHASE III RECOMMENDATIONS

Phase III recommendations, based on an in-depth data review and the above summarized Phase II conclusions, were:

5.5, Phase III Recommendations (cont.)

- ° Fabricate and assemble two engines for Phase III durability testing as planned (1-CAS injectors with 2" L' chambers).
- ° Conduct one additional design iteration test on coaxial swirler cup L/D as a parallel activity.
- ° Select optimum dimension for maximum durability and operational versatility and incorporate results in Phase III assembly.
- ° Utilize explosive-bonded bimetallic plate to join injector and chamber; modify joint design to provide greater cooling margin.
- ° Conduct Phase III demonstration testing with NTO/MMH as proposed.

SECTION 6.0

PHASE III - ENGINE DEMONSTRATION

6.0 PHASE III - ENGINE DEMONSTRATION

BACKGROUND AND SUMMARY

Phase II activities provided data on valve fabrication, response and leakage for 3 valves, and cold-flow, and hot-fire test data on 3 injector designs and chambers of 2 different lengths. The data showed that valve response was acceptable, but changes in the flexure tube stiffness and seal surface area were recommended for the Phase III design to eliminate a marginal sealing condition. In the injector area, one of the 3 injector designs was found to be superior to the others, using ease of fabrication and hot-fire test results as selection criteria. Two modifications of the selected injector design were produced and hot-fire tested in Phase II in order to provide sensitivity data for the injection element. The selected coaxial swirler element was a new concept that is particularly applicable to low flowrates.

The first modification of the element design corrected a high fuel pressure drop. The second modification, "Mod B", altered the spray angle of the outer cone by opening the swirl cup angle. This resulted in a significant improvement in chamber head-end cooling and improved operation at low propellant tank pressures, increasing tank blowdown capability. The data available at the conclusion of Phase II tests indicated that the design came close to meeting the program goals, with one exception: namely, long duration burns could be accomplished only at up to 75% of nominal thrust.

Phase III was initiated with one modification of the original program plan. This provided for one additional hot-fire data point -- a further-increased swirl cup angle -- prior to finalizing the injector design for Phase III.

The proposed "C" injector modification was completed, and the engine was then reassembled with a specially designed stainless steel chamber which facilitated analysis of the thermal data by limiting the axial heat conduction.

The engine was subjected to eight steady-state tests, with inlet pressures varying between 100 and 400 psia. The results of the tests showed an improvement in cooling margin as predicted. However, this was accompanied by reduced performance and rougher combustion at all operating conditions. This

6.0, Phase III - Engine Demonstration (cont.)

prompted a reanalysis of the Mod B design. It was determined that an improved head end thermal condition could be achieved with the Mod B injector if the chamber design were changed. The expected maximum thrust for sustained operation with this configuration would be between 0.4 lbF and 0.5 lbF.

Two Phase III engines were assembled, incorporating the modified valve design, the 1-CAS injector with the Mod B cup configuration, and the 143:1 area ratio, all-welded stainless steel/columbium chambers employing a redesigned head end thermal standoff. These engines were identified by the injector serial number (i.e., 21B and 22B), with B denoting the cup configuration.

Engine 21B was subjected to 14 steady-state tests of durations from 5 to 5000 sec over a chamber pressure range from 79 to 124 psia, corresponding to a thrust range of 0.31 to 0.45 lbF. No thermally limiting operating conditions were encountered. Maximum thrust was limited by the facility/propellant supply pressure of \sim 400 psia.

Subsequently, a series of pulse limit tests were conducted, during which the on-and-off times were systematically adjusted to explore the duty cycle capabilities (expressed as time percentages). Testing was initiated at a .017% duty cycle and increased up to 30%. A total of 2535 pulses were conducted in this series.

The test data indicated a change in the injector hydraulic characteristics starting at the 2% duty cycle. Postfire inspection revealed that the oxidizer orifice had been enlarged, either from the mechanical forces of start transients or from combustion in the injector cup during start or shutdown transients.

The second unit, 22B, was then subjected to a series of 15 steady-state engine durability tests, providing single burn durations of 5 to 18,000 sec at chamber pressures from 55 to 124 psia and thrust levels from .22 to .52 lb. Mixture ratios were varied from 1.5 to 1.9. No limiting thermal conditions were encountered during the 8 hours of firing time accumulated on Engine 22B, nor were there any changes in hydraulic characteristics or measurable throat diameter changes during that time period.

6.0, Phase III - Engine Demonstration (cont.)

6.1 SPECIAL HOT TEST ACTIVITIES

Phase III hot-fire testing began with the 1-CAS 10A Mod C injector configuration. This design incorporated the increased EDM'd cup depth as shown in Figure 6-1. The unit was welded to a stainless steel heat transfer chamber shown in Figures 6-2 and 6-3.

Circumferential grooves were cut into the outer surface of the chamber wall to prevent axial heat conduction. This allowed a better determination of the local heat transfer coefficient and hot-gas or liquid fuel film temperature at each of the axial stations. Multiple backside temperature measurements were made on the calorimeter sections as well as the stations shown in Figure 6-2.

The test conditions are summarized in Table 6-I along with the test results. Figure 6-4 shows the resulting steady-state performance relative to the A and B configurations. Two curves are shown for the "C" configuration data; one corresponds to a 5 to 10 sec data summary, the other is the average from 5 sec to the end of the test. The online oscillograph recorded development of significant combustion roughness as the chamber wall heated. This problem was more pronounced at lower pressures. The lower performance of the full test duration data summary resulted from the rough combustion in the latter part of the test.

All tests were characterized by a significant increase in combustion roughness as the chamber wall heated. Although the magnitude of this roughness does not appear to be a structural problem, it does result in reduced performance.

The tests were terminated when the 2150°F kill limit was reached (generally in the midsection of the steel chamber). Since this region would be columbium in the flight design, this limitation was not considered a problem. The head end of the chamber, which previously ran hot at full thrust, was now considerably cooler at all test conditions, as shown in Figure 6-5.

There was continued excellent measurement consistency between thrust and chamber pressure, as displayed in Figure 6-6.

The results of this special test activity indicated that the Mod B injector provided a better cup configuration and that methods of head end thermal control other than injector design should be considered for additional thermal margin and operating range.

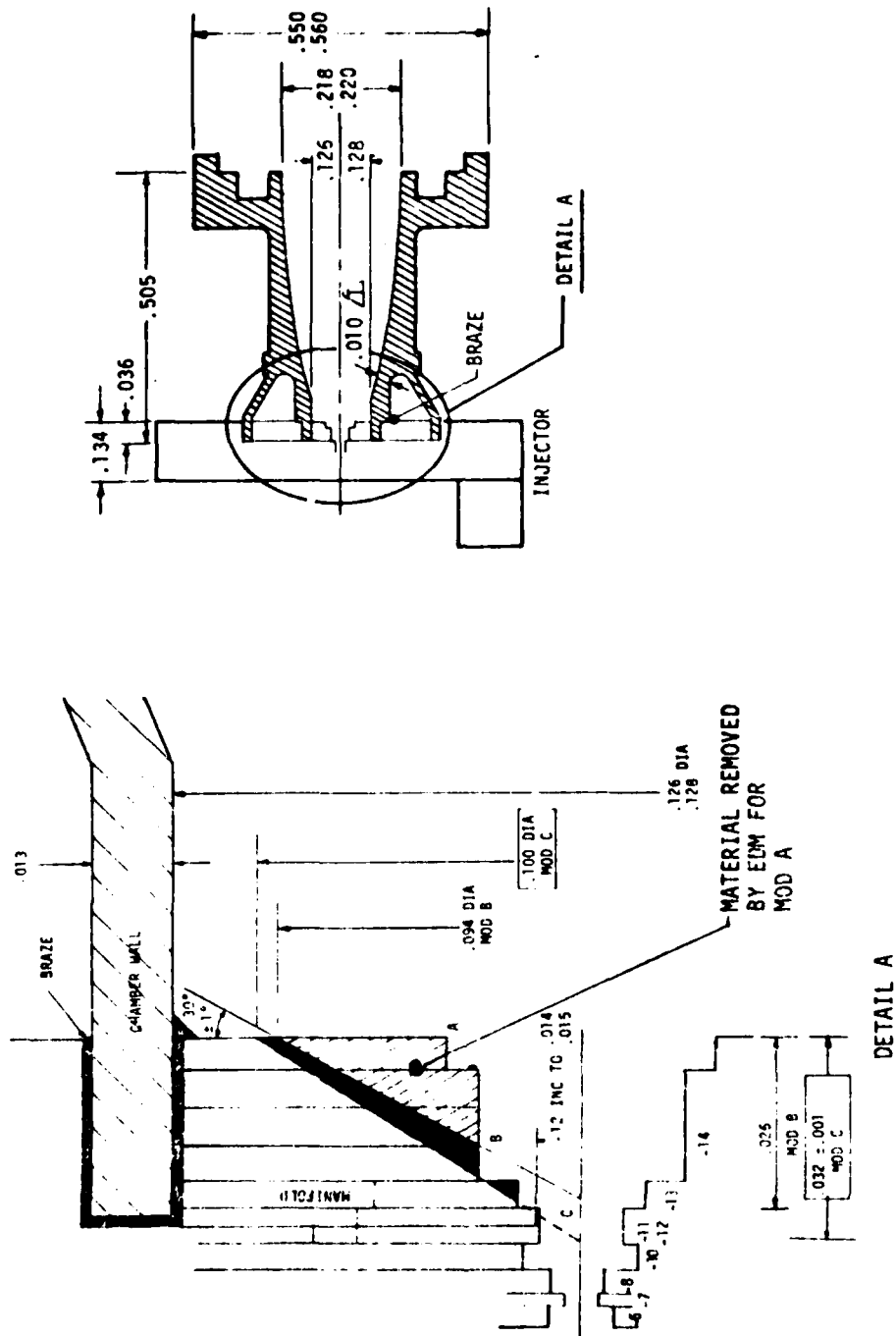


Figure 6-1. 1-CAS 10A Mod C Injector Configuration



•

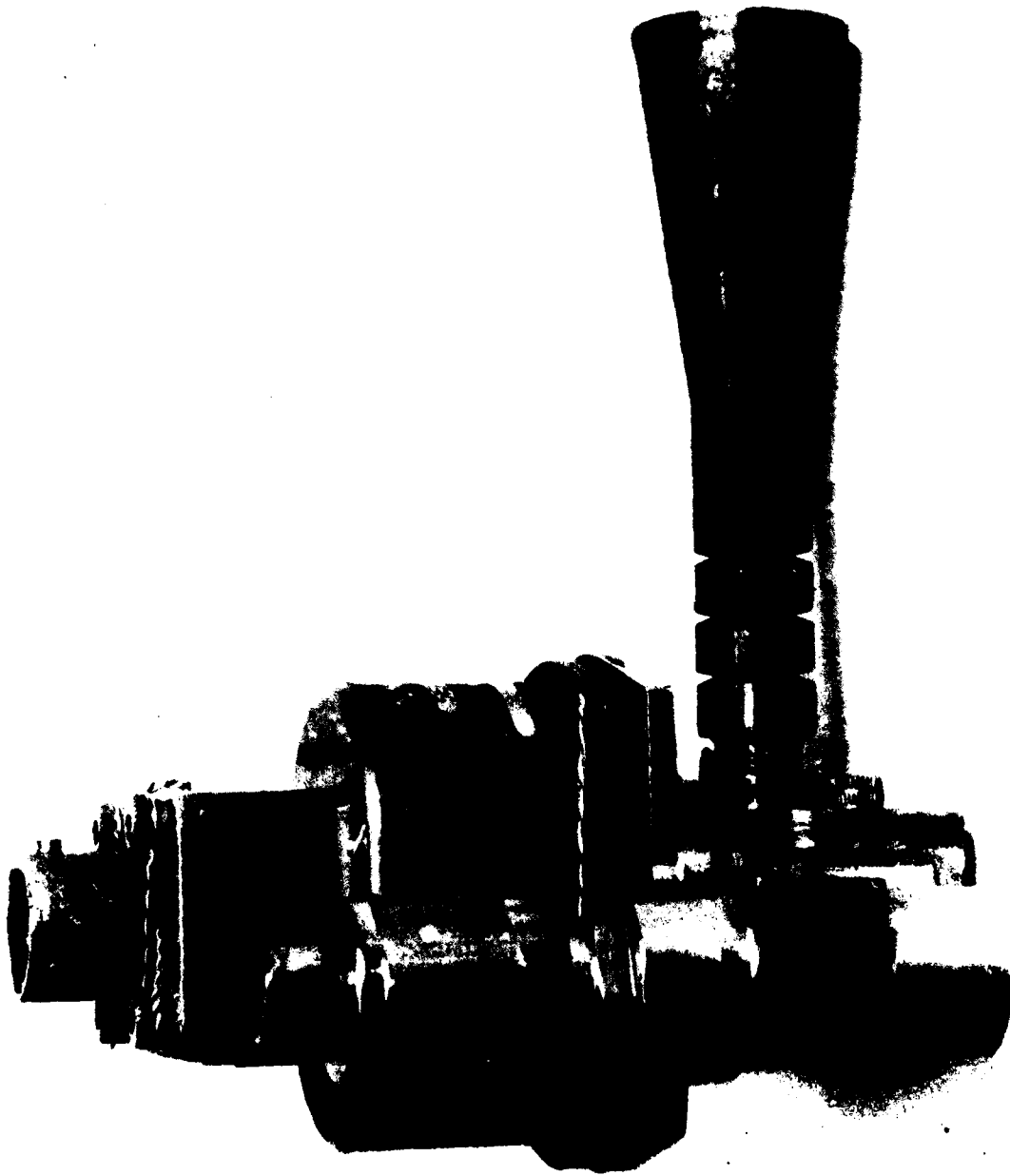


Figure 6-3. Stainless Steel Heat Transfer Chamber

TABLE 6-I

STEADY-STATE PERFORMANCE SUMMARY, 1-CAS
SN 10A MOD C INJECTOR 2 IN L' STEEL CHAMBER

Test No.	Date	Duration, sec	Summary Pd sec	Pol. psia	PFL psia	P _c psia	Thrust, lb	MR	C _f	K _{wo} 10-5 CF (5.97)	K _{wf} 10-5 CF (4.41) Bias	Stand Temp Ox	Propellant Temp Ox	I _{sp} sec	P _{vac} psia
401a	10/18/79	1	Checkout	370	420	121	0.49	1.59			1.32				
b	10/18/79	1	Checkout												
c	10/18/79	5	Checkout												
402	10/19/79	81	5-10 5-81	96 103	85 85	36 38	0.150 0.146	2.01 2.2	1.844 1.695	6.10 6.33	4.18 4.59	38 42	39 50	176 161	0.0081 0.0086
403	10/19/79	84.7	5-10 5-84	134 135	153 155	55 55	0.222 0.205	1.76 1.65	1.764 1.719	6.42 6.17	4.25 4.35	47 50	56 58	203 187	0.0085 0.0092
404	10/19/79	58	5-10 5-58	240 241	251 251	87 89	0.348 0.347	1.63 1.66	1.742 1.688	6.04 6.15	4.61 4.62	55 57	61 62	239 236	0.0087 0.0095
405	10/19/79	43.3	5-10 5-43	229 231	303 303	93 94	0.372 0.366	1.36 1.38	1.74 1.708	6.76 6.14	4.62 4.64	59 61	61 62	250 245	0.0090 0.0097
406	10/19/79	27.4	5-10 5-27	308 308	439 439	117 118	0.463 0.460	1.30 1.30	1.719 1.697	6.13 6.14	4.66 4.68	65 65	64 64	257 255	0.0103 0.0102
407	10/19/79	22.7	5-10 5-22	383 383	401 400	126 130	0.498 0.503	1.64 1.65	1.719 1.691	6.11 6.18	4.63 4.67	65 65	65 65	262 264	0.0096 0.0098
408	10/19/79	21.9	5-10 5-21	413 413	402 403	131 134	0.510 0.515	1.72 1.74	1.702 1.673	6.11 6.19	4.64 4.67	66 66	66 65	261 262	0.0092 0.0097

Notes: Throat diameter pretest (401) 0.054 in.
Posttest (408) 0.053 in.

CF = Cold Flow at ΔP = 200 psi

ALL TESTS WITH N_2O_4

$L' = 2$ IN.

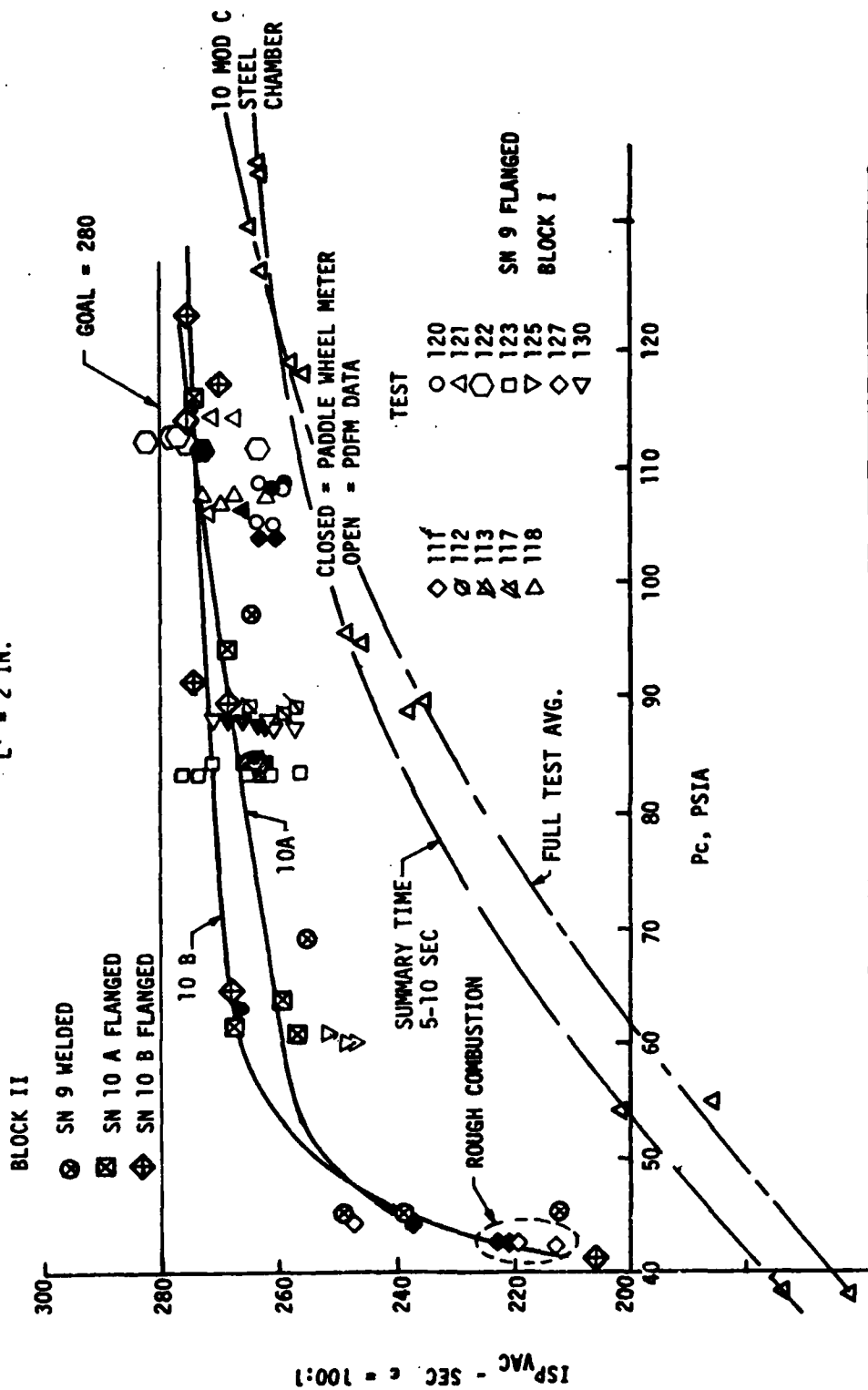


Figure 6-4. Performance of 1-CAS Mod A, B, & C Injector

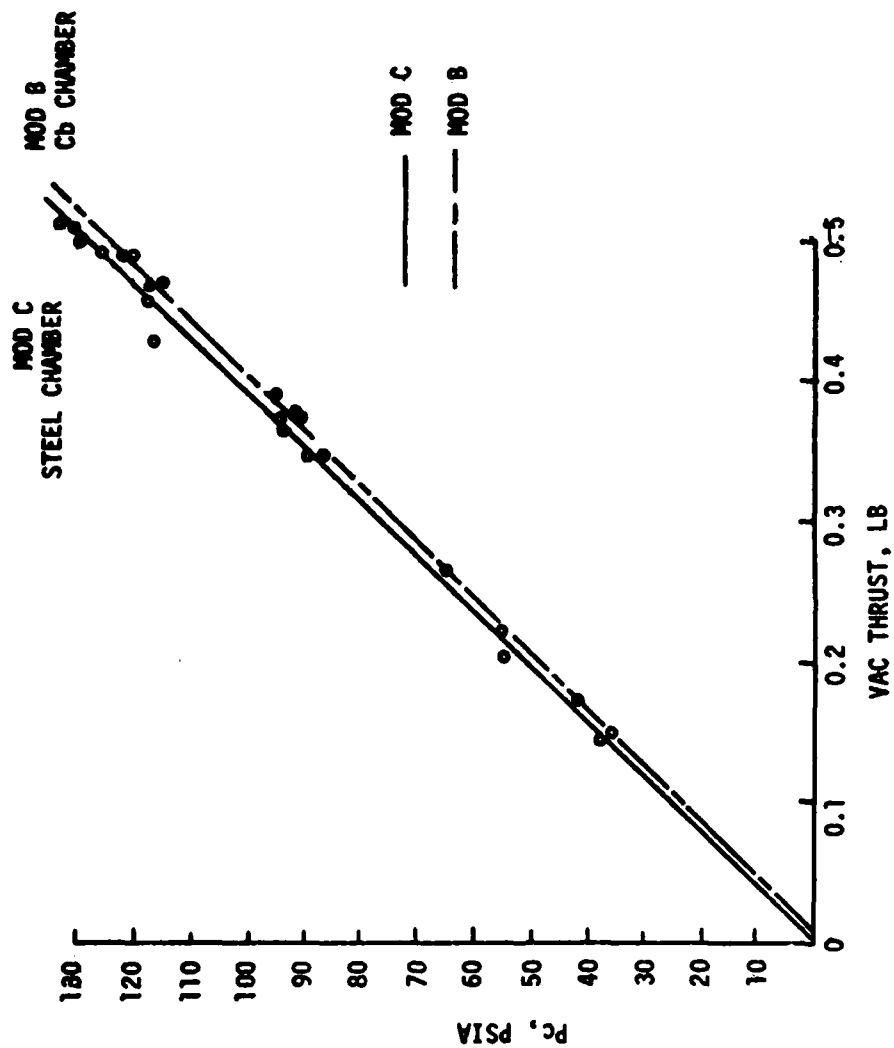


Figure 6-6. 1-CAS Injector, 2 in L', Thrust vs Chamber Pressure

6.0, Phase III - Engine Demonstration (cont.)

6.2 DESIGN UPDATE

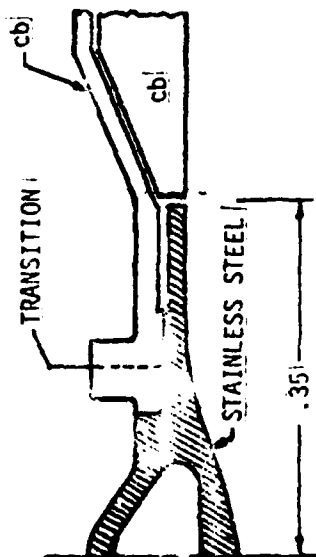
The thermal data obtained during the test series with the Mod B and C cup configurations were reviewed to determine the actual gas side thermal environment at the chamber head end. This data was then used for input in a SINDA model analysis to evaluate potential changes in the chamber design for reducing the head end temperatures. These changes involve moving the columbium/stainless steel interface closer to the injector while increasing the thermal resistance path between the chamber and injector. The results of the two most promising configurations are shown in Figure 6-7. The .25 and .35 inch liner lengths are both less than the 0.5 inch length employed in Phase II tests. The temperatures in the thermal model nodal boxes correspond to the long liner configuration (.35 in.). The underlined temperatures provide comparative predictions for the short liner. The short liner design has a predicted 2300°F maximum Cb temperature and 616°F maximum stainless steel and transition joint temperature at steady-state. The maximum transition temperature in postfire soak was predicted to be 834°F. These values were all acceptable for the required life goals. The engine assembly configuration having the 0.25 in. long steel section was selected for the Phase III design, and the detailed design drawings were updated to reflect the new head end configuration.

6.2.1 Detailed Thermal Update Analysis

The computer model of the half pound engine* was initially modified to include a bimetallic flange and thickened chamber wall to more closely simulate the Phase II engine that had been tested. The temperature at the columbium weld joint from Test 309 was plotted and compared with the temperatures from the computer model. The original temperature predictions did not match the data very closely. New thermal boundary conditions matching the data were obtained by a trial and error procedure. It was not possible to match the curves closely during the thermal transient, but the steady-state temperatures did match fairly well. It was suspected that the early time temperature mismatch resulted from the regression of the liquid fuel film length as the chamber walls became hotter, a behavior not simulated in the computer model. The resulting boundary conditions obtained from the Mod B and Mod C injector are compared with the pre-test predictions in Figure 6-8. The steady-state liquid fuel film length inferred from the test data was approximately 0.1 in. less than the original predictions. The remainder of the thermal boundary conditions required only slight modification.

*Reference: [a] Memorandum 9752:0068, D.H. Saltzman to L. Schoenman, Subject: "Half Pound Engine Thermal Analysis," dated 21 February 1978.

LONG LINER CONFIGURATION



SHORT LINER CONFIGURATION

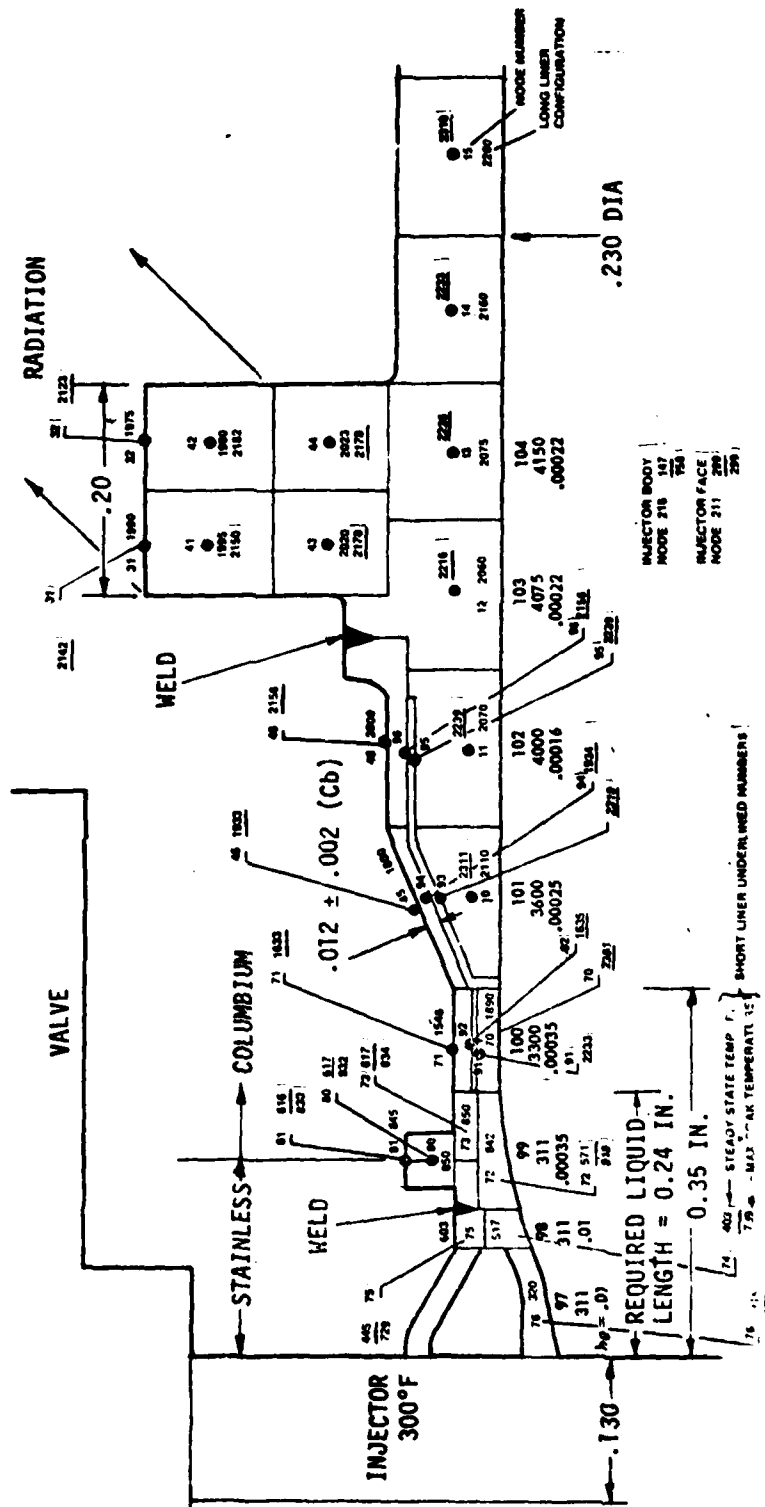
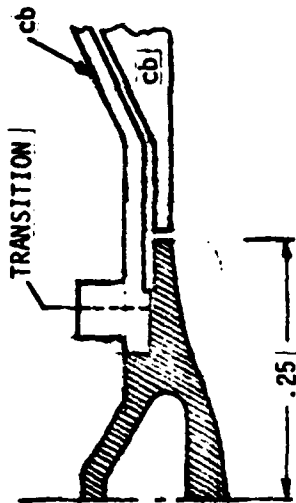


Figure 6-7. Thermal Map, Modified Chamber Head End Design

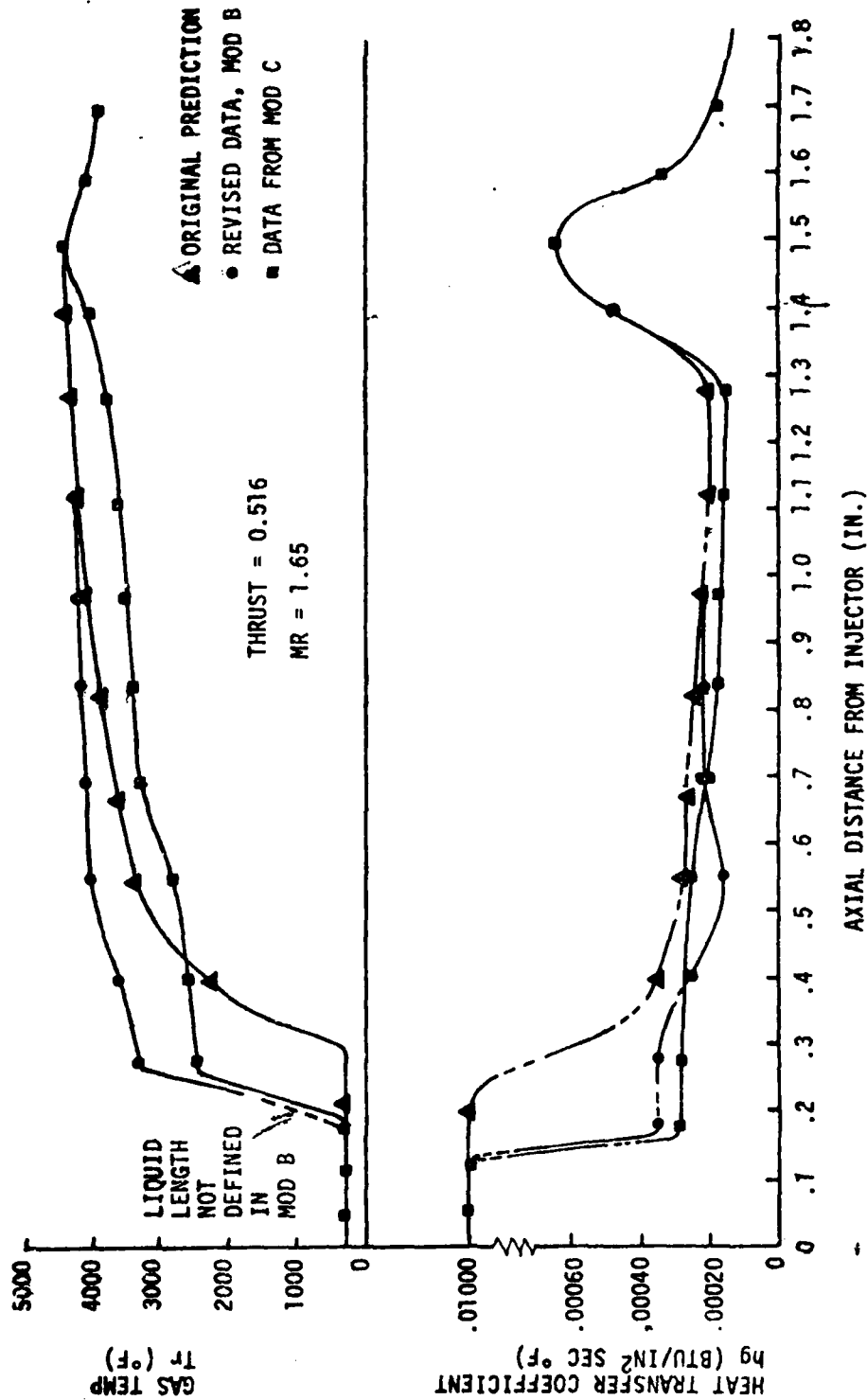


Figure 6-8. Thermal Model Input

6.2, Design Update (cont.)

Several changes were made in the chamber wall design in an attempt to lower the temperatures at the bimetallic joint and the stainless steel sleeve while maintaining the columbium temperature at an acceptable level as was shown in Figure 6-7. A fin was added to radiate heat out of the columbium, and a long gap was put in to force the heat through a long conduction path to the bimetallic joint. The computer model was modified to fit the new design, with the new boundary conditions being those derived from the Mod B injector cup configuration. A modified nodal network and heat flows corresponding to a .35 in. liner configuration were evaluated. This configuration resulted in lower head end temperatures; however, the temperature at node 70 was near 1900°F, higher than desirable for stainless steel. A further design modification was made by connecting node 70 to 10 and leaving a gap between nodes 70 and 72. This change extended the columbium surface upstream (node 70 was now made of columbium), and conduction was not allowed between nodes 70 and 72. Figure 6-7 showed the physical meaning of this change. Figure 6-9 shows the nodal network with the new heat flows for the 0.25 in. long liner. The calculated results of this change are documented in the time/temperature transients in Table 6-II. This change raised the temperature of node 70, but it lowered the temperatures of the bimetallic joint and the stainless steel sleeve. During firing, the maximum predicted stainless steel temperature now occurs at the bimetallic joint and is only 616°F, which is an acceptable value.

Using this configuration, a heat soakback simulation was performed to evaluate temperature rises resulting from combustion stopping and fuel ceasing to cool the chamber and injector. The results at several nodes are shown in Figure 6-10. These heat soak values were considered acceptable.

6.2.2 Detailed Design

The Phase III test hardware incorporated minor design changes in the valve flapper and valve seats to control the stress on the Teflon button. Reducing the stiffness of the flappers and the seal surface area allowed the sealing force on the Teflon to remain nearly constant, even when the Teflon cold-flows with time.

The head end of the chamber was modified, as shown in the detailed drawings of Figures 6-11 and 6-12, to incorporate the results of the previously described thermal analyses. Other minor design changes are defined in the drawings.

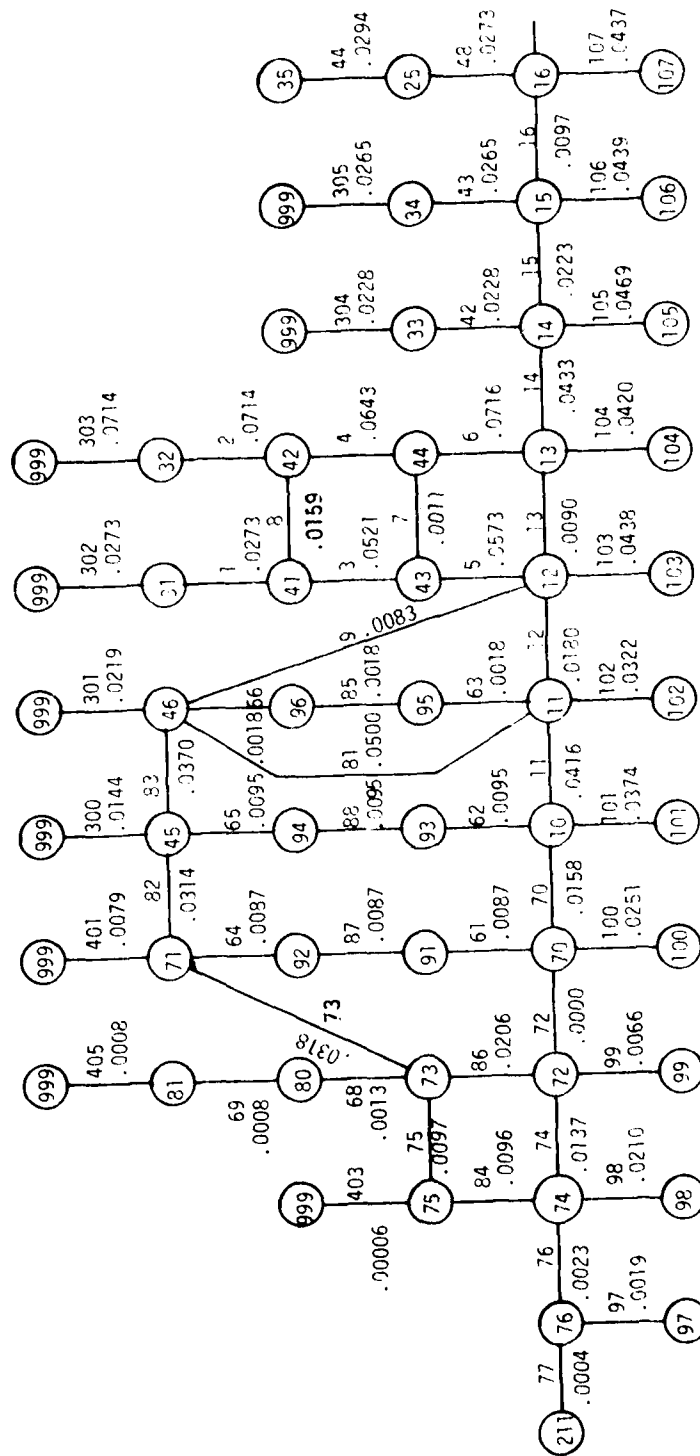


Figure 6-9. Phase III Chamber Node1 Network

TABLE 6-II

TIME/TEMPERATURE TABLE (°F) - SHORT SLEEVE

TIME

TIME= 2.00000+00 DTIME= 2.00000+00 CSEMIN(211)= 1.02991+05 TEMPC(70)= 7.41541+02 HELKCC(71)= 9.35304+03											

TIME	TEMP.	TIME	TEMP.	TIME	TEMP.	TIME	TEMP.	TIME	TEMP.	TIME	TEMP.
112	470.65	12	376.00	13	373.21	14	463.62	15	484.34	16	477.72
113	557.12	19	619.00	18	523.04	17	447.62	20	460.53	21	481.30
114	567.76	22	531.96	25	452.70	24	450.17	26	451.65	27	448.10
115	425.21	28	641.54	31	292.79	30	196.30	32	189.28	33	251.14
116	218.67	34	303.75	37	100.01	36	100.00	38	100.02	39	101.78
117	109.04	40	104.95	43	299.09	42	130.20	44	107.19	45	104.84
118	102.57	46	620.02	49	278.63	48	278.45	50	307.11	51	306.52
119	347.47	52	417.03	55	182.95	54	278.60	56	278.33	57	303.95
120	444.10	58	452.95	61	459.06	60	451.52	62	447.99	63	441.10
121	292.49	64	620.77	67	347.50	66	470.04	68	417.03	69	103.00
122	183.07	70	106.01	73	182.90	72	311.00	74	311.00	75	311.00
123	330.00	76	390.00	79	400.00	78	4075.0	80	4150.0	81	4203.0
124	425.00	82	430.00	85	430.00	84	4389.0	86	4050.0	87	3400.0
125	1825.0	88	3900.0	91	3800.0	90	3600.0	92	100.00	93	300.00
126	70.000	94	3800.0	97	3800.0	96	3600.0	98	100.00	99	300.00

2 SEC

TIME= 4.00000+00 DTIME= 2.00000+00 CSEMIN(211)= 1.02991+05 TEMPC(24)= 3.44051+02 HELKCC(71)= 9.23020+03																	

1	11	743.16	Y	12	621.20	Y	13	618.02	Y	14	739.35	Y	15	786.01	Y	16	790.97
1	17	472.34	Y	18	930.77	Y	19	840.92	Y	20	770.62	Y	21	785.30	Y	22	810.16
1	23	442.16	Y	24	876.81	Y	25	769.66	Y	26	779.34	Y	27	773.74	Y	28	770.70
1	29	643.64	Y	30	1162.5	Y	31	712	Y	32	263.61	Y	33	264.21	Y	34	284.59
1	35	266.00	Y	36	309.07	Y	37	78	Y	38	100.02	Y	39	100.04	Y	40	102.05
1	42	100.07	Y	43	2642	Y	44	78	Y	45	100.00	Y	46	110.02	Y	47	107.50
1	49	105.30	Y	50	912.69	Y	51	211	Y	52	134.44	Y	53	110.02	Y	54	107.50
1	56	905.91	Y	57	102.69	Y	58	412	Y	59	502.60	Y	60	539.63	Y	61	537.90
1	63	945.23	Y	64	681.67	Y	65	602	Y	66	502.44	Y	67	501.96	Y	68	714.83
1	70	745.21	Y	71	769.47	Y	72	362	Y	73	773.25	Y	74	770.15	Y	75	1162.0
1	77	143.12	Y	78	914.52	Y	79	914	Y	80	743.13	Y	81	661.69	Y	82	103.97
1	84	493.23	Y	85	102.69	Y	86	812	Y	87	311.00	Y	88	311.00	Y	89	311.00
1	91	330.00	Y	92	390.00	Y	93	400.00	Y	94	4075.0	Y	95	4150.0	Y	96	4203.0
1	98	425.00	Y	99	430.00	Y	100	430.00	Y	101	4389.0	Y	102	4050.0	Y	103	3400.0
1	105	1825.0	Y	106	3900.0	Y	107	3800.0	Y	108	3600.0	Y	109	100.00	Y	110	300.00
1	112	70.000	Y	113	3800.0	Y	114	3800.0	Y	115	3600.0	Y	116	100.00	Y	117	300.00
1	119	70.000	Y	120	3800.0	Y	121	3800.0	Y	122	3600.0	Y	123	100.00	Y	124	300.00

4 SEC

TIME= 1.00000+01 DTIME= 2.00000+00 CSEMIN(211)= 1.02991+05 TEMPC(27)= 2.00401+02 HELKCC(92)= 9.26200+03											
TIME	TEMP.	TIME	TEMP.	TIME	TEMP.	TIME	TEMP.	TIME	TEMP.	TIME	TEMP.
112	1335.6	12	1239.0	13	1245.7	14	1380.9	15	1457.0	16	1487.2
113	1570.9	18	1621.0	19	1548.5	20	1491.6	21	1497.4	22	1505.0
114	1511.8	22	1519.4	25	1474.9	24	1493.3	26	1493.9	27	1492.7
115	1511.2	28	1670.5	31	966.76	30	394.66	32	414.29	33	337.55
116	342.47	34	311.65	37	100.11	36	100.01	38	100.00	39	102.18
117	100.14	40	104.84	43	299.99	42	135.19	44	117.32	45	114.92
118	112.82	46	1495.2	49	1133.4	48	1132.6	50	1167.4	51	1168.5
119	113.5	52	1270.9	55	410.01	54	1132.4	56	1130.0	57	1377.9
120	1452.4	58	1470.4	61	1460.7	60	1460.6	62	1468.7	63	1666.9
121	947.34	64	1470.4	67	1138.6	66	1335.4	68	1270.9	69	105.45
122	143.24	70	113.74	73	410.53	72	311.00	74	311.00	75	311.00
123	330.00	76	390.00	79	400.00	78	4075.0	80	4150.0	81	4203.0
124	425.00	82	430.00	85	430.00	84	4389.0	86	4050.0	87	3400.0
125	1825.0	88	3900.0	91	3800.0	90	3600.0	92	100.00	93	300.00
126	70.000	94	3800.0	97	3800.0	96	3600.0	98	100.00	99	300.00

10 SEC

TABLE 6-II (cont.)

.....

TIME 2.0000+01 DTPLUM 2.00000+00 CSMIN(211)= 1.02991+05 TEMPC(41)= 9.00130+01 RELKCC(72)= 9.47571+03

1	112	10.9.9	1	12	1800.8	1	13	1873.0	1	14	1972.7	1	15	2031.6	1	16	2056.3
1	112	21.4.0	1	18	2157.1	1	18	2092.9	1	20	2031.2	1	21	2011.5	1	22	1979.4
1	23	183.4	1	24	1879.9	1	25	2042.9	1	26	2055.7	1	27	2051.6	1	28	2044.1
1	23	2130.4	1	70	2126.6	1	71	1395.3	1	72	505.03	1	73	541.69	1	74	561.66
1	75	105.15	1	76	313.73	1	78	100.37	1	79	100.04	1	201	100.16	1	202	102.32
1	203	107.25	1	204	105.12	1	211	299.49	1	212	135.31	1	214	126.90	1	215	124.60
1	216	127.64	1	10	2004.0	1	41	1781.3	1	42	1777.5	1	43	1810.7	1	44	1812.2
1	52	167.32	1	48	1836.5	1	80	535.71	1	31	1777.4	1	32	1767.3	1	33	1963.6
1	34	261.5	1	35	2039.3	1	36	2044.9	1	37	2043.1	1	38	2033.4	1	39	2123.6
1	42	156.4	1	43	207.2	1	44	144.8	1	45	190.6	1	46	1836.6	1	47	187.24
1	217	183.41	1	218	126.65	1	81	536.19	1	47	311.00	1	48	311.00	1	49	311.00
1	100	93.9	1	101	360.0	1	102	400.0	1	103	4075.0	1	104	4150.0	1	105	4200.0
1	106	425.0	1	107	4600.0	1	108	4350.0	1	109	4369.0	1	110	4050.0	1	111	3400.0
1	112	3475.0	1	113	3400.0	1	114	3800.0	1	115	3800.0	1	800	100.00	1	810	300.00
1	998	76.303															

20 SEC

.....

TIME 3.0000+01 DTPLUM 2.00000+00 CSMIN(211)= 1.02991+05 TEMPC(41)= 3.11073+01 RELKCC(72)= 9.84192+03

1	112	2135.7	1	12	2104.9	1	13	2116.0	1	14	2188.2	1	15	2227.2	1	16	2240.3
1	112	287.2	1	18	2319.7	1	18	2256.4	1	20	2188.5	1	21	2156.6	1	22	2107.4
1	23	2041.8	1	24	1963.4	1	25	2223.0	1	26	2239.6	1	27	2220.3	1	28	2208.3
1	23	227.1	1	70	2355.3	1	71	1558.3	1	72	545.13	1	73	592.41	1	74	349.42
1	75	431.86	1	76	314.5	1	78	100.74	1	79	100.07	1	201	100.23	1	202	102.43
1	203	100.35	1	204	105.34	1	211	299.49	1	212	135.40	1	214	133.58	1	215	131.46
1	216	124.57	1	10	2055.8	1	41	2034.4	1	42	2028.2	1	43	2063.1	1	44	2063.7
1	45	184.1	1	46	2215.6	1	80	591.13	1	31	2028.4	1	32	2012.7	1	33	2175.4
1	34	220.5	1	35	2218.6	1	36	2220.2	1	37	2299.3	1	38	2190.6	1	39	2301.4
1	42	159.7	1	43	2214.6	1	44	1865.0	1	45	2135.2	1	46	2050.0	1	47	2135.4
1	217	183.54	1	218	125.49	1	81	590.48	1	47	311.00	1	48	311.00	1	49	311.00
1	100	310.0	1	101	3600.0	1	102	4000.0	1	103	4075.0	1	104	4150.0	1	105	4200.0
1	106	425.0	1	107	4600.0	1	108	4350.0	1	109	4369.0	1	110	4050.0	1	111	3400.0
1	112	3475.0	1	113	3400.0	1	114	3800.0	1	115	3800.0	1	800	100.00	1	810	300.00
1	998	76.100															

30 SEC

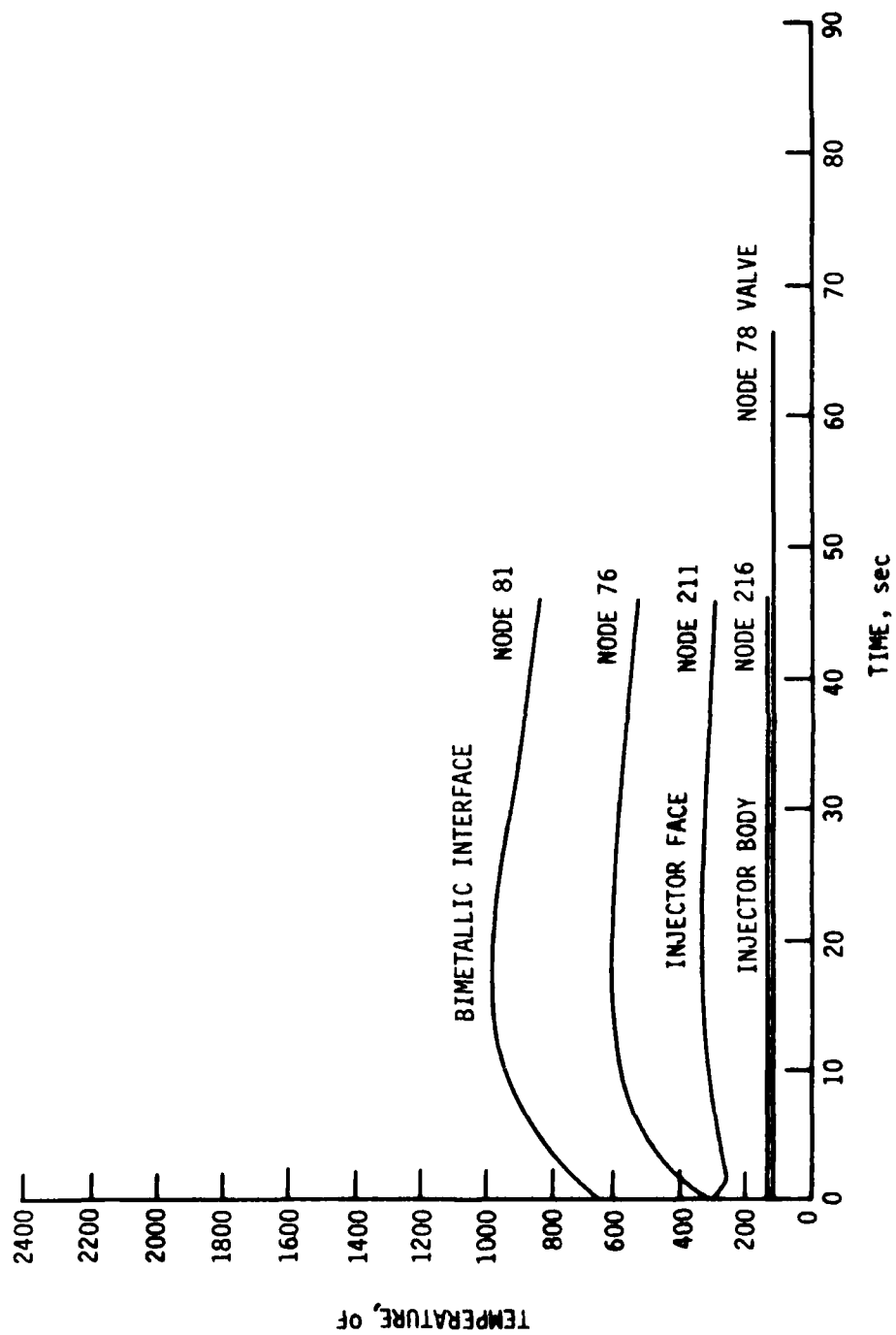
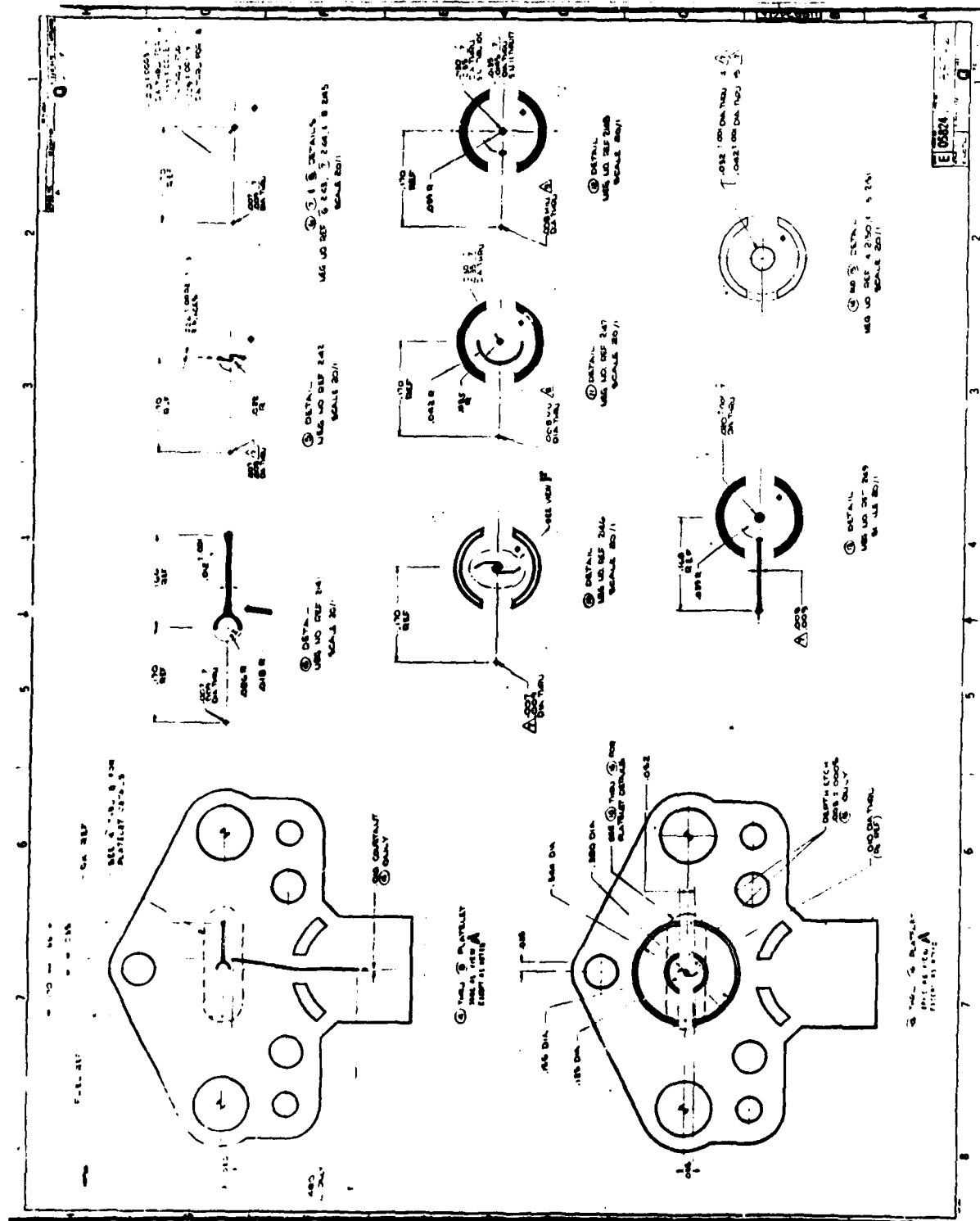


Figure 6-10. Predicted Temperature vs Time Heat Soakback



6.0, Phase III - Engine Demonstration (cont.)

6.3 ENGINE FABRICATION

6.3.1 Valves

Two Phase III valves mated to ALRC platelet injectors were delivered by MOOG, Inc. Acceptance data for these valves are provided in Appendix D. Both units met the program response and leakage goals. A curve of response versus voltage and feed system pressure is provided in the Appendix. Valve-to-valve repeatability is within $\pm .0001$ sec for the two units. The Phase III valves were slower than the Phase II valves by .001 sec (at 400 psi and 28 volts) due to the reduced flapper tube stiffness and the increased torque motor windup. These changes were incorporated in the Phase III valves to eliminate the internal leakage problems encountered in the early Phase II designs. Both Phase II valves showed "zero" leakage.

6.3.2 Injector Fabrication

Using improved etching techniques, platelets for 12 injectors were etched. None of the etching problems experienced during Phase II were evident in these new parts. Alignment on the first set of 6 units bonded in a sheet was acceptable; however, further improvements are possible. The cold-flow data history for the 1-CAS design, beginning with SN 10A, is documented in Table 6-III. (Note: SN 1-9 had smaller fuel passages.)

The cold-flow results of SN 12, 14, 15 and 16, shown in Table 6-III, indicate a highly repeatable flow coefficient; however, the magnitude is below that of the SN 10A and the required value. Injector SN 17 was subsequently cold-flowed as a loose stack and found to be acceptable. It was bonded as a single unit, using the same process parameters as for SN 10A. The results showed a significant reduction in flow coefficient following bonding. The oxidizer circuit proved to be the same as for SN 12 to 16. The fuel circuit also showed a reduced Kw, but it was similar to that of SN 10A when flowed on the simulator and therefore was considered acceptable.

Injectors SN 15 and 16 were sectioned and examined under 100X magnification. The measurements showed the passage sizes had been reduced by 0.001 in. (25 to 30% in area) by the bonding process. The cause of the excessive creep was due to an improper combination of load and temperature.

At this point, two parallel courses of action were undertaken. One involved assembling and cold-flowing as loose stacks all

TABLE 6-III
1-CAS INJECTOR FLOW HISTORY

<u>SN</u>	<u>Configuration</u>	<u>Test</u>	<u>ΔP psi</u>	<u>Oxidizer Kw 10^{-5}</u>	<u>Fuel Kw 10^{-5}</u>
10A	Loose Stack Simulator	Cold	150	6.10	4.80
			200	6.06	4.85
	Post Bond Simulator	Cold	150	5.50	4.07
			200	5.20	
	On Valve	Cold	150	5.63	4.19
10B	On Valve	Hot Fire	Range	5.6 to 5.8	4.0 to 4.2
	On Valve	Hot Fire	Range	5.6 to 5.8	4.0 to 4.3
10C	On Valve	Cold Flow	200	5.97	4.41
	On Valve	Hot Test	Range	6.1 to 6.3	4.6
12	Bonded Simulator	Cold	200	4.52	3.12
14	Bonded Simulator	Cold	200	4.67	3.37
15	Bonded Simulator	Cold	200	4.57	3.01
16	Bonded Simulator	Cold	200	4.31	-
Set of 6 Bonded Together					
17	Loose Stack, Simulator	Cold	50	6.23	5.29
			100	5.87	5.29
			200	5.97	5.55
	Bonded Single Simulator	Cold	200	4.67	3.99
			100		3.74
18	Loose Stack - Simulator Bonded, Simulator	Cold	100	5.51	5.14
			200	5.61	5.29
			200	5.45	4.57
19	Loose Stack, Simulator	Cold	100	6.38	5.21
		Cold	200	6.23	5.55
20	Loose Stack, Simulator	Cold	100	5.58	5.14
			200	5.71	5.34
21	Loose Stack, Simulator	Cold	100	5.87	5.14
			200	5.87	5.30
	Bonded, Simulator Bonded, Valve	Cold	200	4.77	3.94
			200	4.53	3.82*
22	Loose Stack, Simulator	Cold	100	5.87	5.07
			200	5.81	5.30

*MOOG Data

6.3, Engine Fabrication (cont.)

remaining injector parts (SN 19 through 22). These results are shown in the lower part of Table 6-III. The hydraulic reproducibility of these parts was acceptable; however, the fuel-to-oxidizer Kw ratio in the loose stack configuration is too high to provide equal pressure drops. Since the fuel circuit Kw normally drops slightly during the bond operation, this was not a problem.

The second activity was company-sponsored and directed at further refining the bonding process parameters on small parts. This work consisted of the following activities:

- ° Thermocouple calibration in vacuum applications
- ° Bonding adequacy at reduced temperatures
- ° Load calibration

A bond run on parts of injector SN 21 using reduced temperatures was conducted after completion of the above activities. The Kw's resulting from SN 21 were nearly identical to those of SN 17.

SN 17 Bonded Kw OX = 4.67×10^{-5} ; Fuel = 3.99×10^{-5}

SN 21 OX = 4.77×10^{-5} ; Fuel = 3.94×10^{-5}

A second bond run on SN 18 was conducted using reduced load. These conditions closely reproduced the baseline SN 10 Kw's.

SN 18 Bonded Kw Kw OX = 5.45×10^{-5}
 Kw Fuel = 4.57×10^{-5}

SN 10 Bonded Baseline Kw OX = 5.20×10^{-5}
 Kw Fuel = 4.07×10^{-5}

Injector SN 21 was supplied to MOOG, Inc. for assembly to the first valve. The second valve was assembled with SN 22 (a slightly higher Kw injector). A second high and low Kw injector was bonded to have two of each type available for Phase III.

Four injectors were thus completed for use in Phase III, two having a slightly higher pressure drop and two having approximately the same pressure drop as the selected Phase II design. The history of these parts is documented in Table 6-IV.

TABLE 6-IV

1-CAS INJECTOR FLOW HISTORY

Phase	1-CAS Injector SN	Configuration	Test	ΔP Psi	$K_w \times 10^{-5}$	
					Oxidizer	Fuel
II	10B	On Valve	Hot Fire	Full Range	5.6 to 5.8	4.0 to 4.3
III High ΔP	17	Loose Stack Simulator	Cold	50	6.23	5.29
				100	5.87	5.29
				200	5.97	5.55
		Bonded, Simulator	Cold	200	4.67	3.99
				100		3.74
				200	4.30	3.54
	21	Loose Stack Simulator	Cold	100	5.87	5.14
				200	5.87	5.30
		Bonded, Simulator	Cold	200	4.77	3.94
				200	4.53	3.82
	21B	Bonded, Simulator After Braze	Cold	100	4.92	3.74
				200	4.67	3.84
	21B	Final Assembly on Valve	Cold	200	4.60	3.94
III Low ΔP	20	Loose Stack, Simulator	Cold	100	5.58	5.14
				200	5.71	5.34
		Bonded, Simulator Seats not Finished	Cold	100	5.58	4.55
				200	5.56	4.67
	22	Loose Stack, Simulator	Cold	100	5.87	5.07
				200	5.81	5.30
		Bonded, Simulator	Cold	200	5.80	4.62

B Config. = EDM Cup

6.3, Engine Fabrication (cont.)

6.3.3 Chamber Fabrication

Two 143:1 geometric area ratio columbium combustion chambers and the columbium portion of the thermal standoff were machined from C-103 bar stock as shown in Figure 6-13.

Discussion of coating process R 512 with the subcontractor indicated that the entire welded assembly could be coated as a single unit, rather than first coating and welding the parts and then recoating the weld area. Two each of the chambers and thermal standoffs were electron-beam-welded and coated. The coated chamber assemblies were returned to ALRC for mating with the bimetallic transition joint spools which had been readied for welding.

6.3.4 Chamber and Engine Assembly

Final engine assembly required the following operational steps:

- 1) Brazing of Pc boss and chamber liner;
- 2) EDM machine face to B cup configuration;
- 3) Conduct flow and leak checks;
- 4) EB weld Cb-Cb interface on bimetallic ring;
- 5) Inspect weld and machine stainless interface to mate with chamber liner;
- 6) EB weld stainless interface of bimetallic ring to stainless chamber liner-injector;
- 7) Assemble injector-chamber assembly to valve;
- 8) Conduct leak and flow checks.

Except for Step 4, all operations were successful on the first attempt. Step 5 uncovered cracks in the weld joint on 3 successive weld attempts attributed to two possible factors: 1) flow of the silicide coating into the weld and 2) insufficient allowance for weld shrinkage on cool-down.

The weld joint design was subsequently modified to allow for weld shrinkage, and the silicide coating was dressed back away from the weld. A new bimetallic transition ring was then machined and successfully welded to the chamber. Photographs of the assembled engine are shown in Figure 6-14.

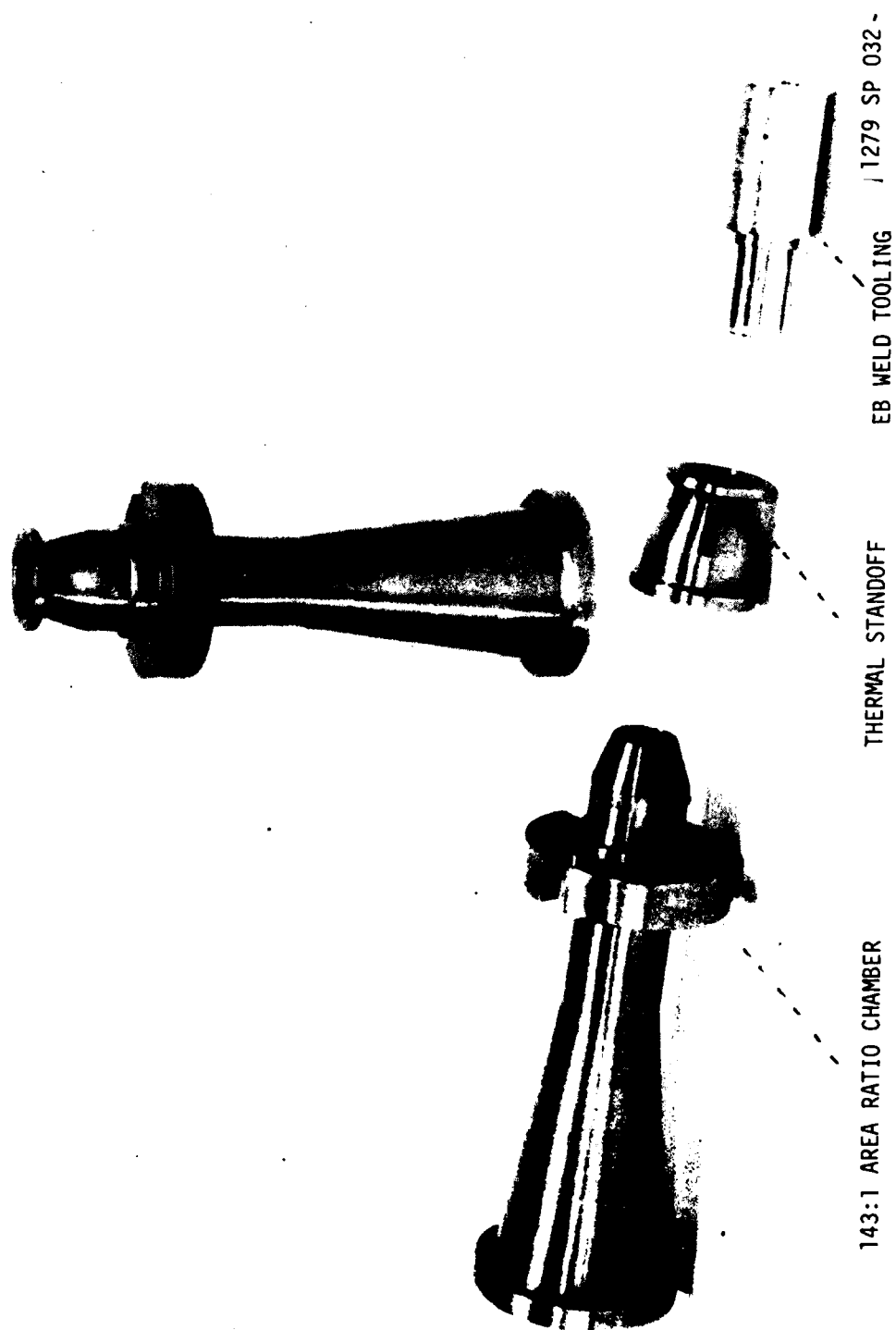


Figure 6-13. Phase III Combustion Chamber

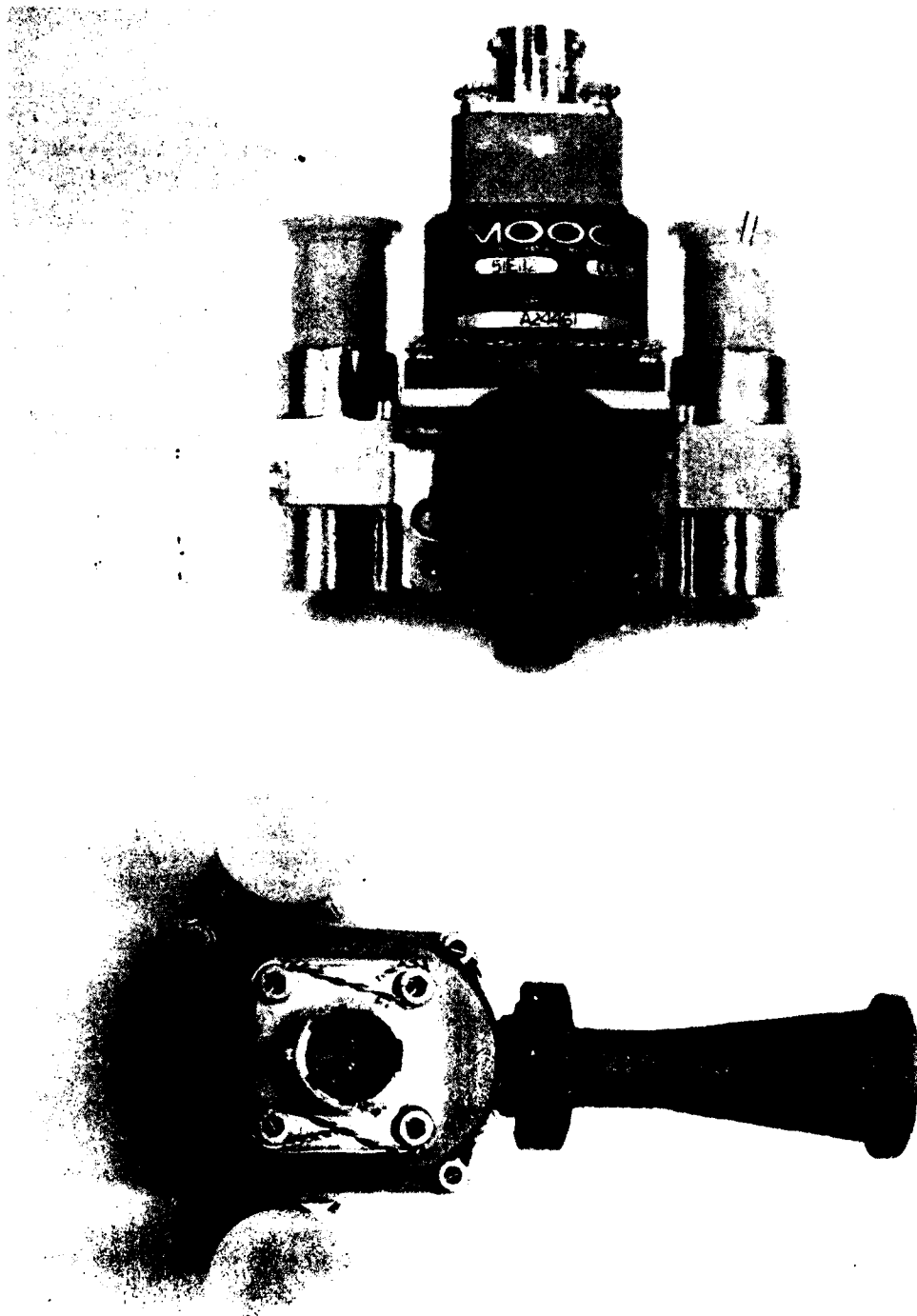


Figure 6-14. Phase III Engine

6.3, Engine Fabrication (cont.)

Both engines were subjected to leak checks of the welded and brazed joints and high-pressure (400 psia) GN₂ leak checks of the valve injector interface seals. No leakage was noted in either engine.

6.4 PHASE III - DEMONSTRATION TESTING

6.4.1 Test Instrumentation and Facility Modifications

6.4.1.1 Phase III - Test Instrumentation

The facility instrumentation used in Phase III was the same as for Phase II. The location of the thermocouples on the Phase III test engine assemblies is shown in Figure 6-15 and Table 6-V.

The throat temperature measurement was added following Test 506. This thermocouple was located between the chamber OD and the insulation. The T_g measurement was added following Test 526. This was a tension-loaded .003 in. diameter (Type K) wire junction, contacting the Cb - Cb uncoated weld area.

Following Test 527, the feed system Kulite pressure transducers were replaced with Kistler transducers to provide a higher degree of sensitivity in the feed system.

6.4.1.2 Phase III Test Facility Modifications

Hot-fire test operations during Phase II revealed several facility inadequacies which, while providing reliable test data, resulted in significant test delays. The test fixture initially fabricated for this program proved to have several limitations, described as follows:

- ° Washer type load cell - This concept, while providing accurate pulse measurements, required delicate engine alignment due to its single point mount. The crystal load cell described in Phase II was proven accurate; however, previously used (100 and 5 lbf test fixtures) 3 point-mount crystal cells with electrical summing had been operationally more efficient.

- ° In-place calibration - The pneumatic, diaphragm-type load application technique used for calibration resulted in oscillations and drift that made calibrations complex and time-consuming. The load application pull rod proved to be very difficult and time-consuming to align and "hung up" when returned to zero.

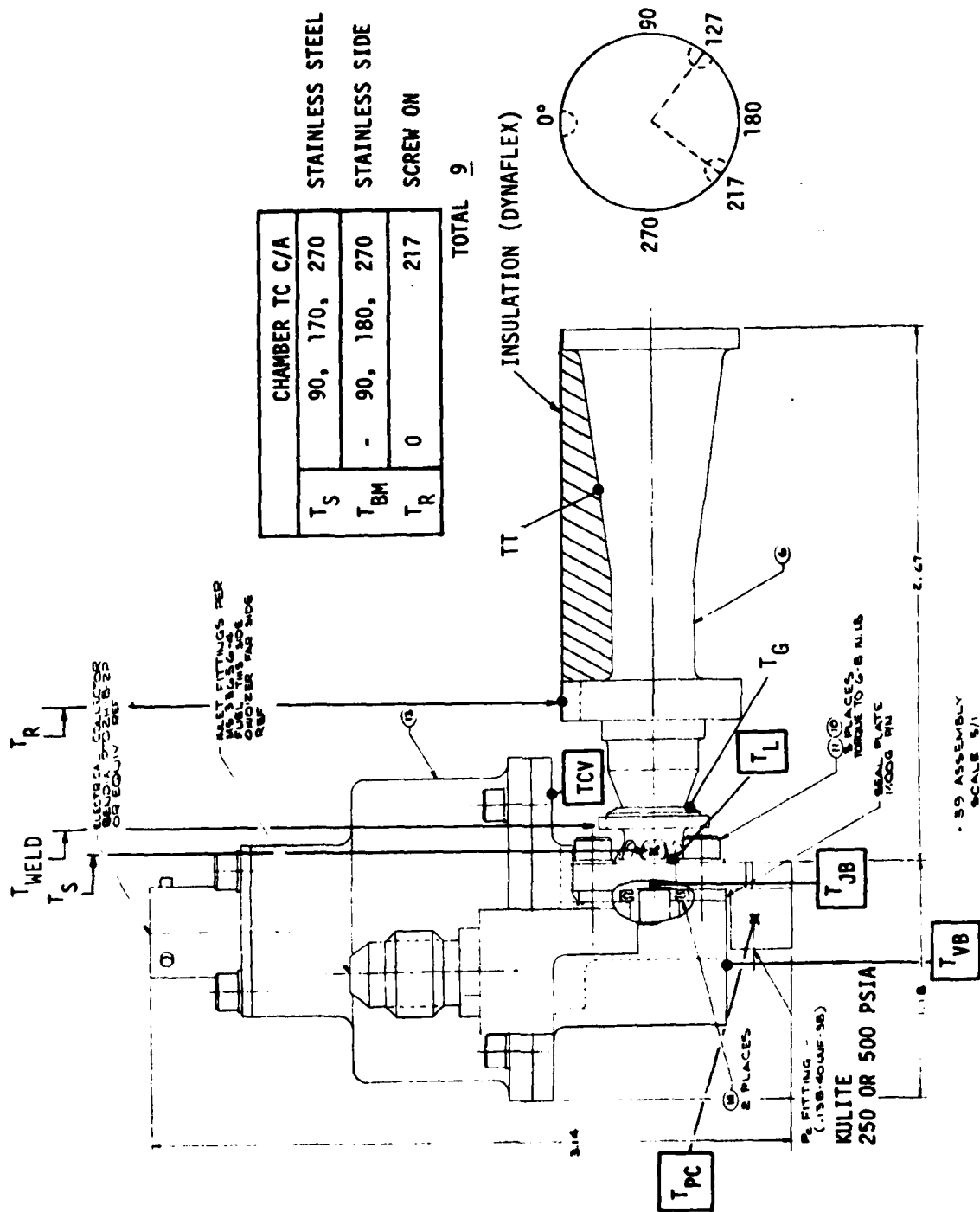


Figure 6-15. Phase III Test Instrumentation Locations

TABLE 6-V
 PHASE III ENGINE INSTRUMENTATION

<u>TEMPERATURE</u>		<u>QUANT.</u>	<u>THERMOCOUPLE RANGE (TYPE K) °F</u>	<u>DESIRED MAX</u>	<u>KILL</u>
Valve					
Body	TVB	1	0-300	< 250	Visual Auto
Cover	TVC	1	0-300	< 250	Visual
Injector					
Backside	TJB	1	0-400	< 200	300
P _c Tap	TPC	1	0-400	< 200	
Chamber					
Support Leg	TL	1	0-500	< 350	500
Steel Sleeve	TS	3	0-1500	< 500	1000
Bimetallic Joint	Tweld	3	0-2000	<1000	1500
Cb-Cb weld	Tg	1	0-2000	<1500	None
Radiator	TR	2	0-2400	<2400	2400
Throat	TT	1	0-2400	2400	2600
<u>PRESSURE</u>			Kulite		
Chamber	P _c	1	0-200 psi		

6.4, Phase III - Demonstration Testing (cont.)

A review of the operation techniques and design responses of the 5 lbF test fixture used during the ALRC test program was made. This indicated that use of this fixture in lieu of the 0.5 lbF unit would allow for a more efficient test operation. Replacement of the load cells (static, dynamic and calibrate) with those sized for the 0.5 lbF engine would be required.

This fixture was of the same basic design as the one in Phase II, except for:

- ° 3-point dynamic load cell mount for pulse measurements.
- ° Pull cable versus pull rod for calibration force application, thereby allowing self-alignment and return to zero. The pull cable went slack after removal of the calibration load.
- ° Hydraulic piston load application for calibration, thereby eliminating drift and oscillations during calibrations.

The 5 lbF test fixture, Figure 6-16, was therefore installed and used in the significantly improved Phase III test program. A comparison of test fixtures from proposed baseline through Phase II and into Phase III testing is summarized in Table 6-VI.

6.4.2 Phase III Demonstration Testing of Engines

This test series was given the identification number
Test .5B-698-5XX.

Two engines were assembled for Phase III testing as follows:

Engine 21: Valve SN 004, injector SN 21, 143:1 e
chamber

Engine 22: Valve SN 005, injector SN 22, 143:1 e
chamber

Valves and chambers were identical on both engines. The injectors were of the same design; however, they had different pressure drops, with the SN 21 unit having a higher pressure drop than SN 22. The engines were serialized in accordance with the injector serial number.

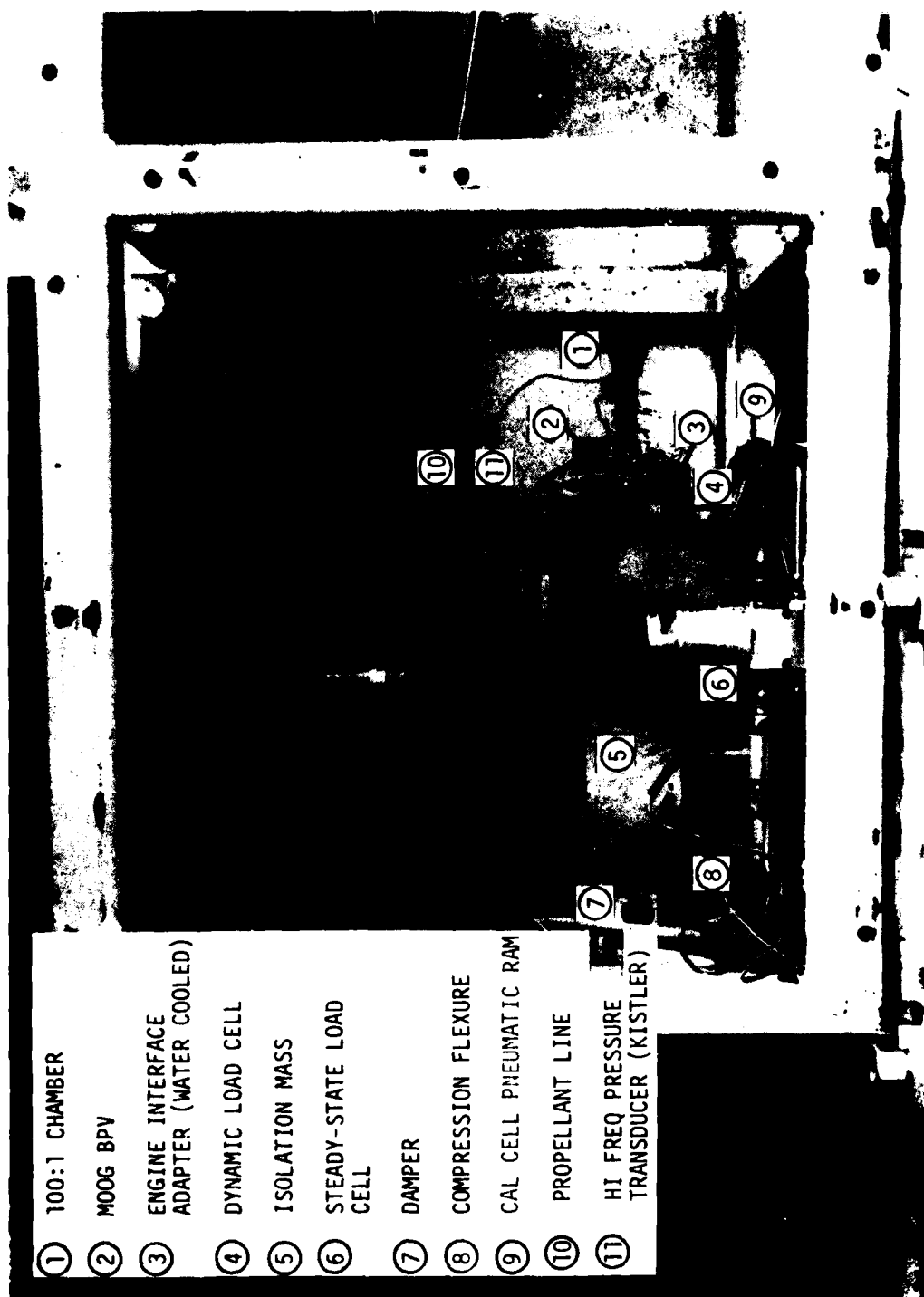


Figure 6-16. 5.0 lbf Test Fixture Adapted for
0.5 lbf Phase III Testing

TABLE 6-VI

TEST FIXTURE HISTORY

	<u>BASELINE</u>	<u>.5 LBF TESTS</u>	<u>MODIFICATION TO 5 LBF STAND</u>
1. STEADY-STATE LOAD CELL FORCE RANGE RESOLUTION	BLH LPB-1 1.0 LBF FULL SCALE .0005 LBF	BLH LPB-1 1.0 LBF .0005 LBF	BLH LPB-1 1.0 LBF .0005 LBF
2. DYNAMIC LOAD CELL FORCE RANGE RESOLUTION	PCB 201A 10 LBF .0004 LBF	PCB 201A-WASHER 10 LBF SAME	KISTLER 922 F1-3 POINT 5.5 LBF .0006 LBF
3. DAMPER	EDDY CURRENT	VISCOUS FLUID	VISCOUS FLUID
4. SEISMIC MASS	30 LBM	30 LBM	50 LBM
5. FLEXURES	CRITICALLY LOADED IN COMPRESSION	SAME	SAME
6. CALIBRATOR	INTEGRAL SIMULTANEOUS FORCE CALIBRATOR FOR BOTH STEADY-STATE AND DYNAMIC LOAD CELLS	PULL ROD LOAD APPLI- CATION-DIAPHRAGM LOAD APPLICATOR	PULL CABLE LOAD APPLI- CATION-PISTON LOAD APPLICATOR
7. TEMPERATURE CONTROL	PROPELLANT LINES AND DYNAMIC LOAD CELL TEMP- ERATURE CONDITIONED	SAME	SAME

6.4, Phase III - Demonstration Testing (cont.)

6.4.2.1 Engine 21 Testing - Test Series 698, Runs 501-514

The test history of this engine is summarized in Table 6-VII. Fourteen series were conducted, starting with a 5 sec checkout. Tests 502 through 506 were conducted with a radiation-cooled chamber, with propellants supplied by the positive displacement flow meters with run durations (200 to 300 sec) limited by their capacity. Testing started at low pressure (50 psia). The operating pressure was increased in each successive test to determine the maximum safe operating pressure up to the nominal 400 psi propellant supply. The series also provided data relating tank pressure to performance and temperature. Test 502 was terminated early due to rough combustion. The data showed the mixture ratio to be slightly low. Test 506, a repeat of 502 but at proper mixture ratio, showed an improvement in the combustion roughness. All tests showed some degree of "popping" (to be discussed in greater detail later in this report). The fuel flow data (presented in Table 6-VII) of Test 504 was adjusted, using the injector Kw, due to a slow closing facility bleed valve. Test 504 also ended with a significant drop in thrust and flow, caused by oxidizer depletion. No damage was encountered.

The chamber was insulated with Johns-Manville Dynaflex starting with Test 507 (4 lb/ft³ density), from the radiation fin to the exit plane. All subsequent tests were conducted in this configuration. Test 507 and 508 were repeats of earlier test conditions to establish performance improvement due to reduction in heat loss. A significant improvement was noted in each case.

Tests 509 through 511 were engine durability tests using propellant tanks in lieu of the PDFMs. Flow measurements were monitored by small paddle wheel flow meters. Flow calibration for these tests was made by using PDFM-paddle wheel relationships developed on the previous two tests. These test durations were 53.9, 2295, and 4954 sec, respectively. Facility instrumentation malfunction was responsible for termination of Tests 509 and 510. Thrust, flowrate and Pc or Kw were changed during these tests, as was shown in Table 6-VII. The throat temperature drifted upward during testing. This is believed to be a result of alloying of the thermocouple junction with the silicide chamber coating. Similar long-term instrumentation drifts have been reported in industry literature.

Test 512 was a block 1 pulse series, itemized in Table 6-VIII. Duty cycles up to 2% were completed as planned. The engine was unable to complete the total pulse series, starting with group 8, 10% duty cycle, because the head end of the chamber exceeded the 450°F limitation imposed. The actual number of pulses completed for each group is also

TABLE 6-VII

SN 21

1. The first part of the report is a general introduction to the subject of the study.

TABLE 6-VIII

PHASE III BLOCK I DUTY CYCLE

Planned Test Program										Actual Test and Results and Number of Pulses Completed	
Pulse Group	% DC	Number of Pulses	Cumulative Pulse Total	On Time	Off Time	Cycle Time	Total On Time	Lapsed Time	Cumulative On Time	Date	
1	.017	15	15	.01	59.99	60.00	0.15	900.	.15	Feb. 8	All 445 pulses completed. No limiting conditions encountered.
2	.050	15	30	.03	59.97	60.00	0.30	900.	.45		
Stop to switch to large PDFM's											
3	.200	15	45	.12	59.88	60.00	1.80	900.	2.25		Pulse 200 hard start.
4	.200	200	245	.01	4.99	5.00	2.00	1000.	4.25		Hard starts on some pulses
5	.600	200	445	.03	4.97	5.00	6.00	1000.	10.25		
6	2.00	200	645	.10	4.90	5.00	20.00	1000.	30.25	Feb. 11	Group 6 conducted 2 times, 400 total pulses. Some bilevel operation noted in first 15 pulses. Repeat test did not reproduce problems
7	2.00	300	945	.02	0.98	1.00	6.00	300.	36.25	Feb. 11	Group 7 300 pulses of group 7 completed satisfactorily.
8	10.00	300	1245	.10	0.90	1.00	30.00	300.	66.25	Feb. 11	Group 8 stopped after 155 pulses $T_S 90 = 450^\circ F$
9	10.00	3000	4245	.015	0.135	0.150	45.00	450.	111.25	Feb. 11	Group 9 stopped after 962 pulses $T_S 90 = 450$
10	20.00	3000	7245	.030	0.120	0.150	90.00	450.	201.25	Feb. 11	Group 10 stopped after 171 pulses $T_S 90 > 450$
Stop to fill large PDFM's											
11	30.00	3000	10245	.045	0.105	0.150	135.00	450.	336.25	Feb. 11	Group 11 stopped after 81 pulses
Stop to fill large PDFM's											
12	30.00	300	10545	.60	1.400	2.000	180.00	600.	516.25	Feb. 11	Group 12 stopped after 21 pulses
Stop to fill large PDFM's											
13	100.00	1	10546	300.00	-	-	300.00	300.	816.25	Feb. 11	Group 13 steady state 4.75 sec. head end too hot
Total pulses 2535											

NOTE: Only the first and last 15 pulses of each of pulse groups 4 through 12 are to be recorded. All pulses of pulse groups 1, 2, 3 and 13 are to be recorded.

NOTE: Only the first and last 15 pulses of each of pulse groups 4 through 12 are to be recorded. All pulses of pulse groups 1, 2, 3 and 13 are to be recorded.

6.4, Phase III - Demonstration Testing (cont.)

provided in Table 6-VIII. Details of the pulse testing results are discussed in Section 7.

The final run of Test 512, scheduled for a 300 sec continuous burn, was terminated at 4.75 sec when the chamber head end exceeded the 500°F limitation. Tests 513 and 514 were conducted to verify the test results. Analysis of the data showed a significant reduction in the resistance of the injector oxidizer circuit. A leak check with GN₂ showed no internal or external leaks.

Visual inspection of the injector revealed erosion of the oxidizer metering orifice and a portion of one of the oxidizer swirler legs. A subsequent cold flow of the injector confirmed the change in the oxidizer circuit Kw obtained in Tests 512 through 514.

Inspection of the valve and columbium portion of the chamber showed no signs of wear after the approximately 9000 seconds of burn time accumulated on this unit. Further testing of engine SN 21 was discontinued.

6.4.2.2 Engine 22 Testing - Test Series 698, Runs 515-526

The test history of this engine is summarized in Table 6-IX. Tests 515 through 520 repeated Tests 501 to 506 to obtain direct comparison of the two engines. Propellant was supplied by the positive displacement flow system, and the chamber was radiation cooled. Testing was again started at low pressure (52 psia) and increased to the maximum nominal; no thermal limits were encountered. The second engine, having a lower pressure drop injector, proved to be more prone to chugging at the lowest operating pressure. All tests except 516 were terminated by the exhaustion of propellant in the positive displacement feed system. Test 516 was terminated manually after 59 sec due to excessive chugging.

The chamber was insulated in a similar manner as Engine 21 for all tests subsequent to 520. Tests 522, 523 and 524 examined the influence of mixture ratio at full thrust. Acceptable temperatures were obtained at MR = 1.84. Testing was terminated at 45 sec at a MR of 1.97 when the head end chamber temperature exceeded 500°F.

Propellant for Test 525, the 2-hour durability test, was supplied from the large propellant tanks with paddle wheel meters for flow measurement. This test was terminated at 744 sec by a facility instrumentation malfunction. Test 526, a continuation of 525, was 8114 sec in

PHASE III TEST HISTORY

SN 22

[illegible]

of Δ based on profile zero position of loaded cell.

Δ = Difference between pre- and posttest load cell reading (bf).

PHASE III TEST HISTORY

[illegible]

PHASE III TEST HISTORY

[illegible]

6.4, Phase III - Demonstration Testing (cont.)

duration and was terminated at the end of the work shift. Thrust, flow, Pc, etc. was unchanged during this burn. The throat thermocouple behaved in a manner similar to that of Engine S/N 21 (Ref. Table 6-VII).

Test 527 was a 185 sec burn at .5 lb thrust using the PDFM supply. Prior to this test, a .003 in. diameter thermocouple (Tg) was added to the uncoated Cb-Cb weld joint at the bimetallic splice. The temperature reached a steady-state value of 1640°F. The objective of the additional measurement, in addition to determining potential life limitations, was to try to relate the onset of popping to changes in temperature in the thermal isolation slot. Following this test, the two Kulite transducers at the valve inlet were replaced by Kistler transducers to provide increased feed system measurement sensitivity.

Test 528 utilized tank propellant supply to continue steady-state durability testing. The duration of Test 528 was 2563 sec. No change in operation was noted during this period.

Test 529 was a continuation of Test 528 for a duration of 18,000 seconds. Testing was terminated at the end of the work shift. Posttest hardware inspection showed no visible changes. Cold flow of the assembly showed no significant change in pressure drop or throat diameter, i.e.:

	<u>Kw at 200 psid water</u>	
	<u>Ox Circuit</u>	<u>Fuel Circuit</u>
Pretest	5.92 x 10 ⁻⁵	4.88 x 10 ⁻⁵
Posttest after 8.5 hours burn	6.00 x 10 ⁻⁵	4.60 x 10 ⁻⁵

6.4.3 Durability Test Results

A total of 14 full thermal cycles and 2535 partial thermal cycles were applied to Engine SN 21. No loss of coating or signs of weld failure were noted. The firing life of this unit was approximately 9000 sec. The failure of the oxidizer orifice of this engine -- as noted by the change in magnitude of the impulse bit -- is discussed in Section 7. It was not obvious that damage had occurred until the final steady-state burn of the series was undertaken. Details of this activity are covered in Section 7.0, "Test 512 Data Evaluation," of this report.

6.4, Phase III - Demonstration Testing (cont.)

A total of 15 full thermal cycles was applied to Engine SN 22. Hardware inspection following eight hours of total burn showed no change in hydraulic or dimensional characteristics. The longest single burn on this engine was 18,000 continuous seconds at full thrust. No operating limitations were encountered in steady-state firing at thrusts between .3 and .5 lb.

A complete record of the durability tests is provided in Appendix E.

6.5 TEST DATA EVALUATION

6.5.1 Engine Response

The engine response data in this section is based on Test 512 (pulsing limits testing, Engine SN 21).

Figure 6-17 shows an online oscillograph trace of a typical pulse. All quoted response data are based on measurements taken from these records.

The sequence of start transient events is as follows:

- ° 28 volts is applied to the valve at time zero.
- ° An immediate rise in current and movement of the torque motor armature is observed. The movement of the torque motor is detected as vibration by the three crystal load cells which form the dynamic thrust measurement system. The filtered dynamic thrust trace shows the net force on the stand to be zero due to valve movement.
- ° Flow into the injector is detected by the drop in feed line pressures, using fast-response Kulite pressure transducers located at the valve inlets.
- ° The completion of valve travel is noted by the spike in F dynamic (unfiltered) as the torque motor armature hits the mechanical stops.
- ° Ignition is sensed by F dynamic (filtered) and Pc rise. The Pc rise is highly damped by the .004 by .010 in. sensing passage in the injector, leading from the injector face to the transducer boss, approximately 0.5" away.

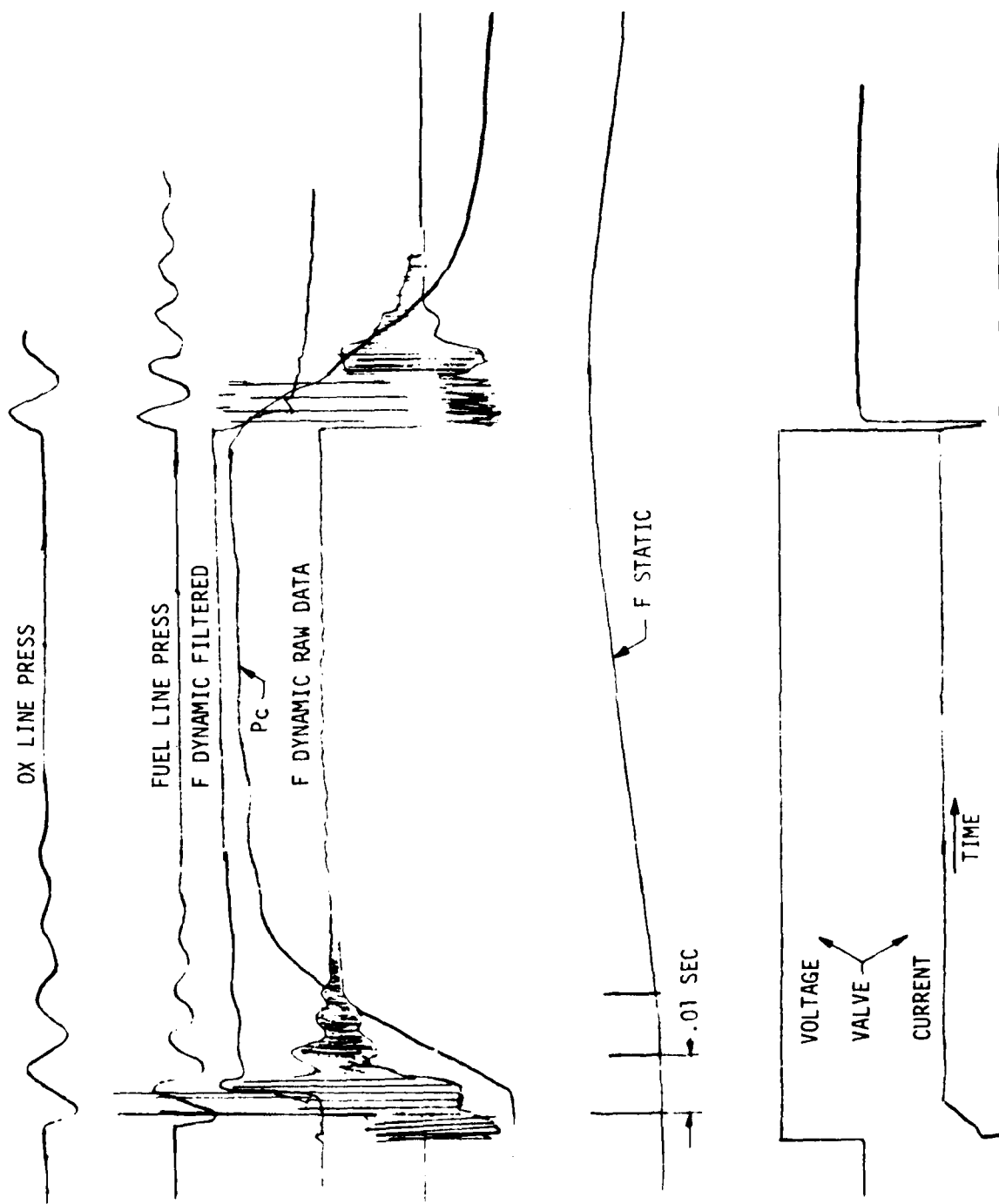


Figure 6-17. 0.5 lbF Engine, Typical Pulse

6.5, Test Data Evaluation (cont.)

- ° The rise in F dynamic (filtered) is delayed and rounded slightly by the electronic filter.

The slow responding static thrust measurement does not provide data.

The sequence of events in the shutdown transient is as follows:

- ° The voltage drops when power to the valve is removed.

- ° Valve motion is detected first by the drop in F dynamic and then by the rise in feed line pressure as the valve ports are closed. These events take place within .001 sec of each other.

- ° The feed system pressure rings at the natural frequency of the lines. The dynamic force rings at the very high stand frequency. The spikes in F dynamic are due to the torque motor returning to the mechanical stops in the closed position.

- ° The decay in the filtered dynamic thrust measurement is delayed slightly because of the electronic filter.

- ° The drop in P_c is highly damped because of the volume of gas and liquid propellant trapped in the cavity between the transducer diaphragm and the end of the threaded boss. This volume of fluid must be discharged via the .004 x .010 port.

The start and shutdown response can best be observed from a relatively long pulse where there is sufficient time to completely damp out the start transient effects before encountering the shutdown transients.

Figures 6-18 through 6-21 show typical engine pulses under varying operating conditions.

Figure 6-18 is the 14th .120 sec pulse of a sequence conducted at 1 pulse per minute.

GROUP 3 PULSE 14

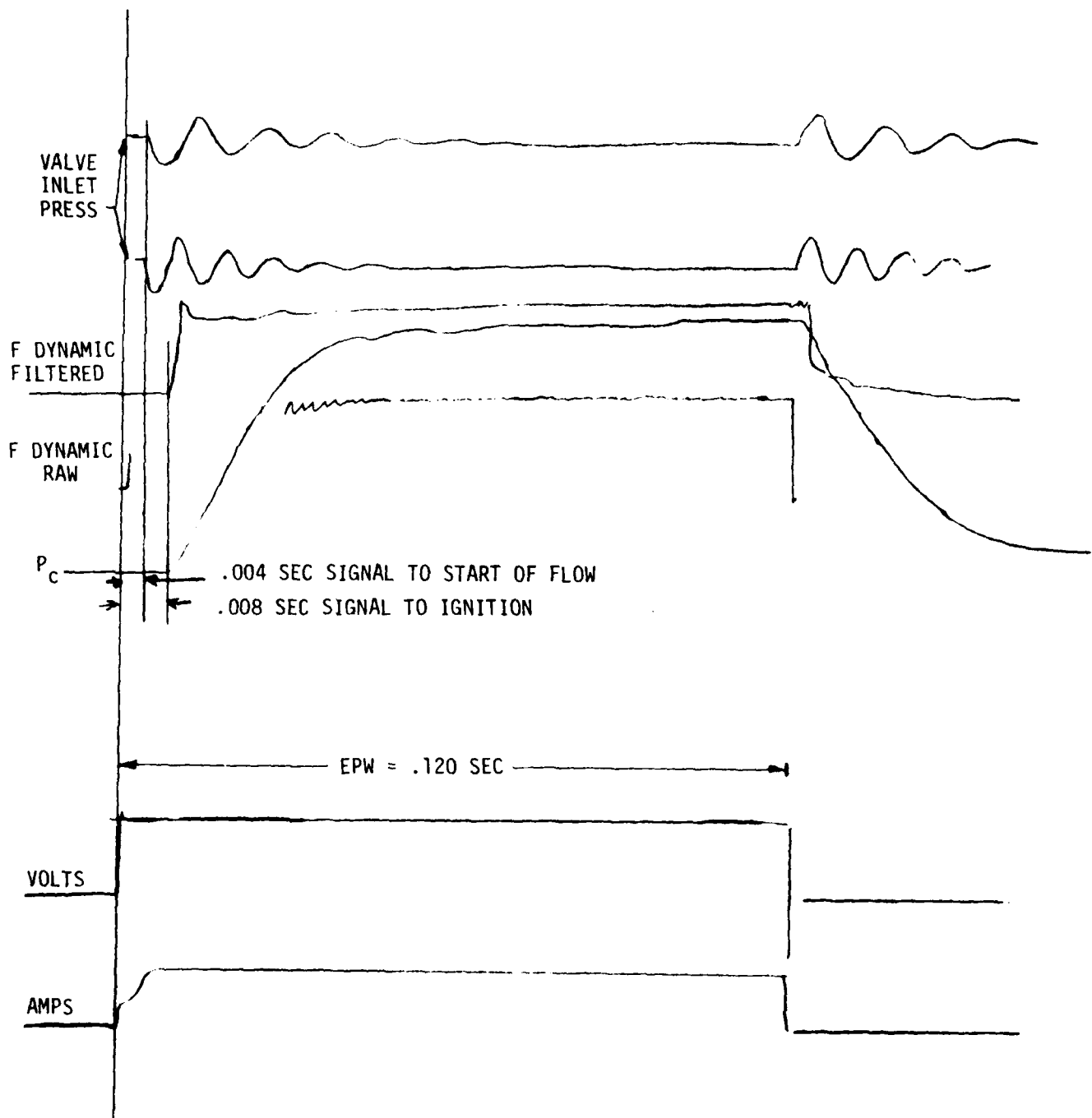


Figure 6-18. Engine Pulse - EPW = .120 sec

GROUP 5 PULSE 1

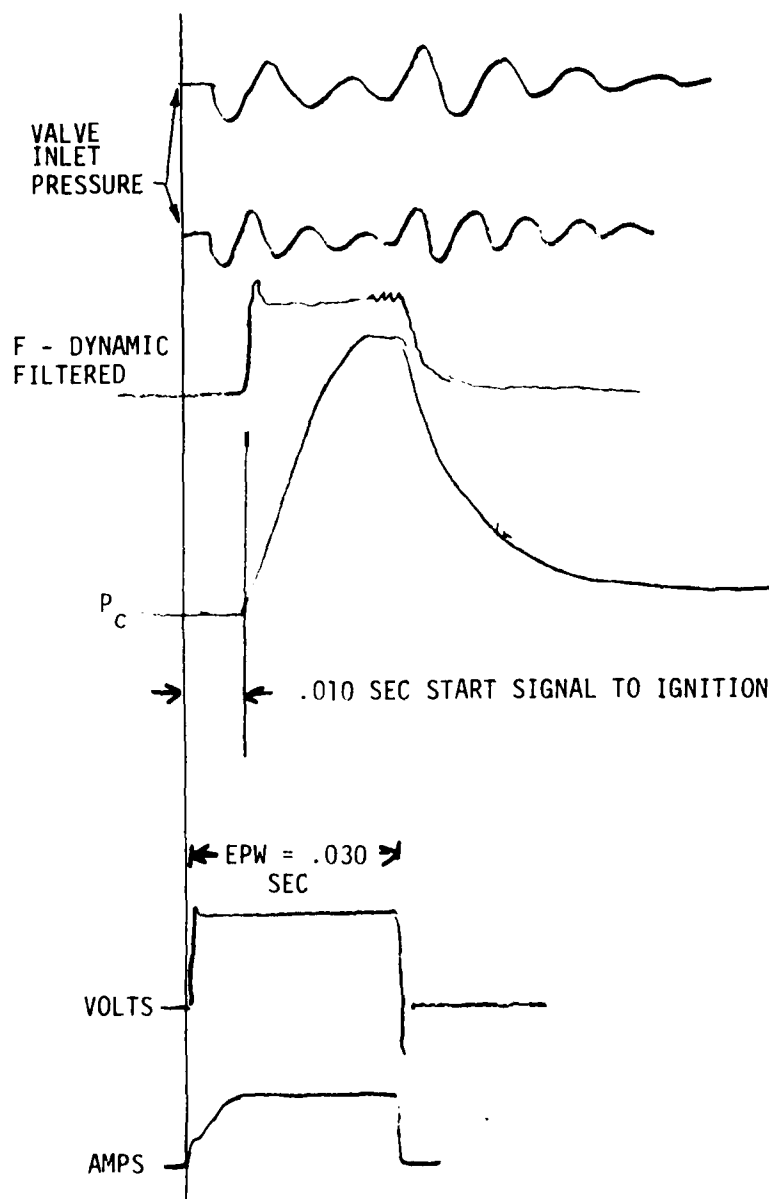


Figure 6-19. Engine Pulse, EPW - .030 sec, Pulse #1

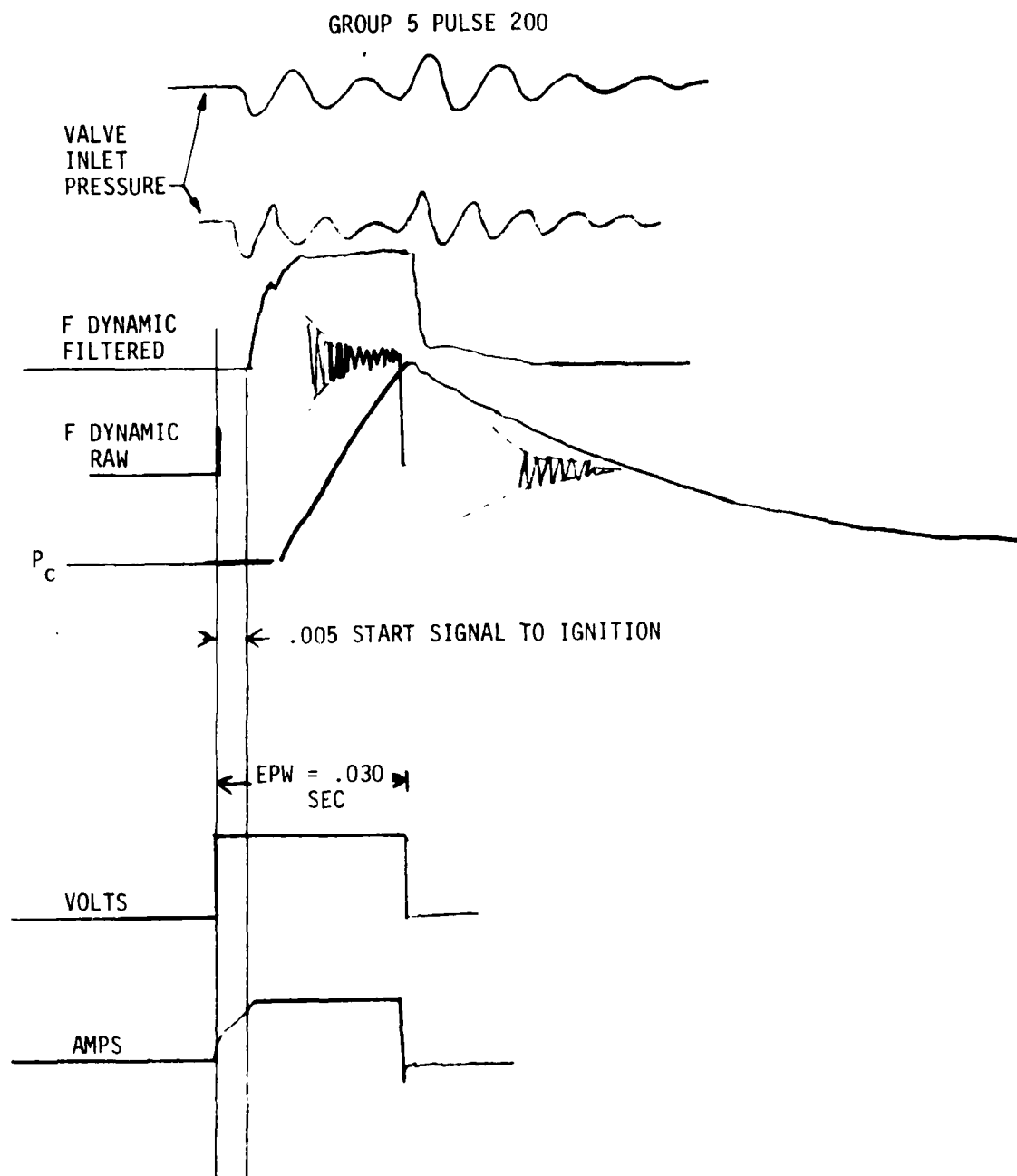


Figure 6-20. Engine Pulse, EPW = .030 sec, Pulse #2

COLD ENGINE .100 SEC PULSE

GROUP 6 PULSE 2

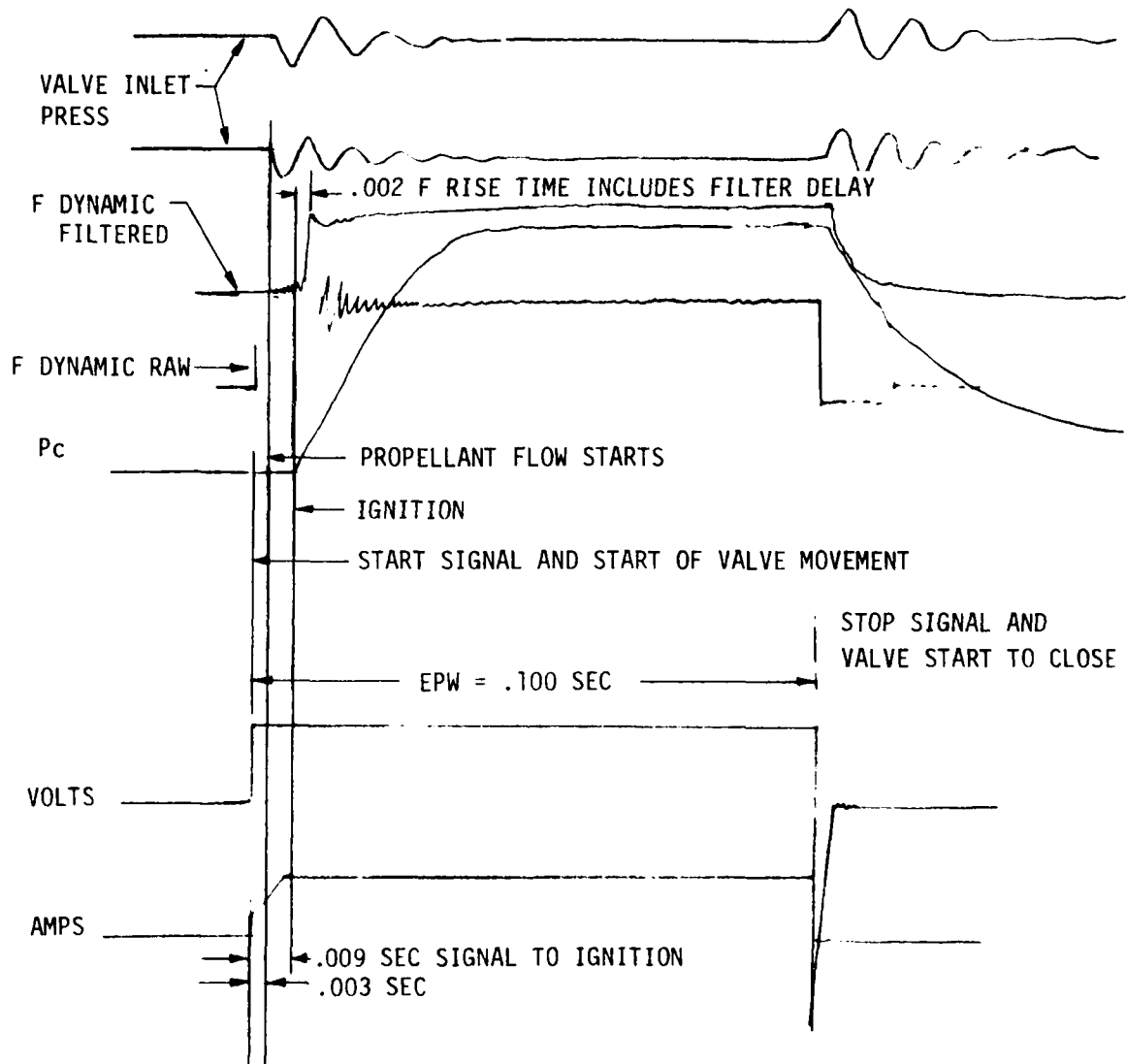


Figure 6-21. Engine Pulse, EPW = .100 sec

6.5, Test Data Evaluation (cont.)

Figure 6-19 is the first .030 sec pulse of a sequence conducted at 1 pulse per 5 sec.

Figure 6-20 is the 200th .030 sec pulse of the same series.

Figure 6-21 is the 2nd .100 sec pulse of a sequence having 5 sec between pulses. These data provide the following results:

- 1) Time from start signal to start of flow is .003 to .004 sec.
- 2) Time from start signal to ignition is .009 to .010 sec for a cold engine and .005 sec for a warm engine (i.e., pulse 200 of duty cycle 5).
- 3) The thrust rise rate is very rapid (less than .002 sec) but cannot be determined exactly because the filtration alters the rise rate of the thrust measurement. The raw signal cannot be interpreted due to the interference of the valve vibration.

The shutdown transients cannot be based upon chamber pressure measurement due to the highly damped response.

- ° Valve closure follows the signal to close by less than .001 sec.
- ° The thrust decay is delayed by about .002 sec. This could be influenced by the filter electronics, and the decay in thrust may actually start within .001 sec.
- ° The final tail-off in thrust is noted to last up to .030 sec after FS-2 when the engine is warm, as was shown in Figure 6-17. This is due to flow from the Pc tap and residual propellant boiling off the chamber wall, as well as the residual propellant contained in the manifold.

The response demonstrated by the Phase III design was found to meet the contract goals.

6.5, Test Data Evaluation (cont.)

6.5.2 Pulse Repeatability

Pulse testing consisted of a series of pulses having the burn and coast times defined in Table 6-VIII. Because of the large volume of data, only selected pulses were recorded and processed.

Data were recorded on an on-line oscillograph and a digital recording system. The digitized recording rate was 11,000 samples per second. Impulse bits were obtained by numerical integration of the force-time measurement from the start of each pulse to 0.025 sec after the valve voltage drops from "28" to "0" volts. The impulse developed between 0.025 and 0.050 sec after voltage termination is reported as the coast impulse.

Representative data traces from the analog recorder are shown in Figures 6-18 through 6-21. The I-Bit repeatability appears to be more consistent for the initial pulses when the engine is cold. The 200th pulse in group 5 of Figure 6-20 produced a hard start, probably due to an accumulation of unreacted propellant on the chamber wall, and also produced a higher impulse bit.

The number of pulses in each pulse train were selected to provide a reasonable compromise between pulse quantity, total facility utilization time, and the data storage limits of the data discs. The initial series pulsed at 1 pulse per minute. Data for 15 successive pulses were recorded. These data were processed to define single pulse I-Bits and also the average of 5 successive pulses.

Pulse trains of 200 to 3000 pulses were planned at the faster pulse rates. Data were recorded for the first and last 15 pulses of the group. Appendix C documents some of the individual pulse data recorded, indicating the I-Bit integral and coast impulse as well as representative hardware temperatures. The 5 pulse average data is summarized in Table 6-X. Figure 6-22 is a composite of all data obtained on Test 512, which was run in 11 parts and contained 12 different combinations of pulsing rates. The data of Figure 6-22 show a nearly linear relationship between EPW (Electrical Pulse Width measured in sec) and I-Bit (in lbf-sec). The 3 data bands consider only the first 15 pulses of each group. The offsets in the bands reflect the pulsing rate. The lowest impulse bit for a given EPW is developed at slow pulse rates, 1 to 12 per min, where the chamber remains cold and the manifolds are completely empty at the start of each pulse. The highest impulse bits are obtained at a given EPW at a pulse rate of 500 PPM, with the 1000 PPM predictably falling in between. Higher chamber wall temperatures, providing a more effective utilization of the residual propellants, also allow for the faster pulsing rates.

TABLE 6-X

PHASE III, 5 PULSE IMPULSE BIT

AVERAGE AND TEMPERATURE SUMMARY

Pulse Group	% DC	Pulse No.	EPW Sec	Off		TL-2 °F	Ts-90 °F	Tw
				Sec.	I Bit lbF Sec			
1	.017	15*	.01	59.99				
a		1-5			.00445	55	55	
b		6-10			.00398	56	56	
c		11-13			.00386	56	57	
2	.05	15*	.03	59.97				
a		2-5			.0103	57	57/62	
b		6-10			.0106	58	59/62	
c		11-15			.0110	58	61/64	
3	.20	15*	.12	59.88				
a		1-5			.0421	58/63	60/123	
b		6-10			.0435	64/67	71/133	
c		11-15			.0441	67/69	76/132	
4	.20	200*	.01	4.99				
a		1-5			.00412	64/64	69/69	
b		6-10			.00412	65/65	70/71	
c		11-15			.00447	65/66	71/73	84
d		185-190			.00462	74/74	86/87	108
e		191-195			.00479	74/74	85/86	108
f		196-200			.00511	74/74	86/87	108

*Total Pulses

TABLE 6-X (cont.)

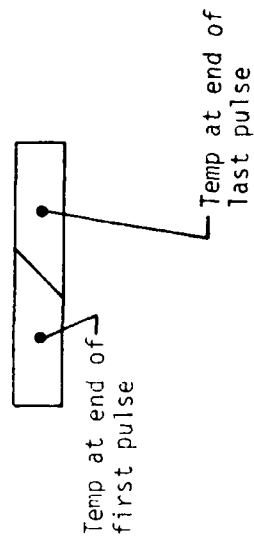
Pulse Group	DC	Pulse No.	EPW Sec	Off Sec	I Bit 1bF Sec	TL-2 °F	Ts-90 °F	Tw
5	.60	200*	.03	4.97				
a		1-5			.01125	66/68	70/76	77/86
b		6-10			.01162	67/70	75/82	88/95
c		11-15			.01205	70/72	80/86	95/103
d		185-190			.01390	109/110	145/147	211/213
e		191-195			.01471	110/110	146/150	214/215
f		196-200			.01419	111/112	147/151	216/218
6	2.00	200*	.10	4.90				
		1-5			.0363			
		6-8			.0384			
6 Repeat		1-5			.0351	57/68	59/118	62/99
		6-10			.0367	70/75	82/132	106/126
		11-15			.0370	77/79	96/140	130/143
		185-190			.0421	134/134	190/209	295/296
		191-195			.0419	134/135	191/210	297/296
		196-200			.0422	135/135	191/209	296/298

TABLE 6-X (cont.)

Pulse Group	% DC	Pulse No.	On Sec.	Off Sec.	I Bit 1bF Sec.	TL-2 °F	Ts-90 °F	Tw
7	2.00	300*	.02	.90	.00973	135/136	192/194	298/302
		1-5			.00962	136/137	194/196	305/307
		6-10			.00961	136/138	197/198	309/311
		11-15			.01066	165/165	244/244	394/395
		285-290			.01063	165/165	244/244	395/396
		291-295			.01075	165/166	244/244	397/396
8	10.0	155*	.10	.90	.04640	165/174	244/275	397/422
		1-5			.04630	176/183	265/285	428/450
		6-10			.04656	185/189	275/294	456/477
9	10.0	450*	.015	.135	.00739	90/92	98/125	118/120
		1-5			.00749	92/96	127/138	121/128
		6-10			.00754	97/100	140/148	130/138
		11-15						
10	20.0	171*	.03	.120	.0151	94/96	103/182	125/127
		1-5			.0157	98/105	194/209	130/141
		6-10			.0163	106/112	215/221	143/158
		11-15						

TABLE 6-X (cont.)

Pulse Group	DC	Pulse No.	On Sec.	Off Sec.	1 Bit 1bF Sec.	TL-2 °F	TS-90 °F	Tw
11	30.0	81*	.045	.105				
		1-5			.0228	103/107	118/259	152/156
		6-10			.0239	109/120	274/320	158/174
		11-15			.0231	122/131	322/366	178/203
12	30.0	21*	.600	2.0				
		1-5			.295	102/187	115/633	149/465
		6-10			.298	205/260	395/802	318/738
		11-15			.299	276/325	527/896	774/929



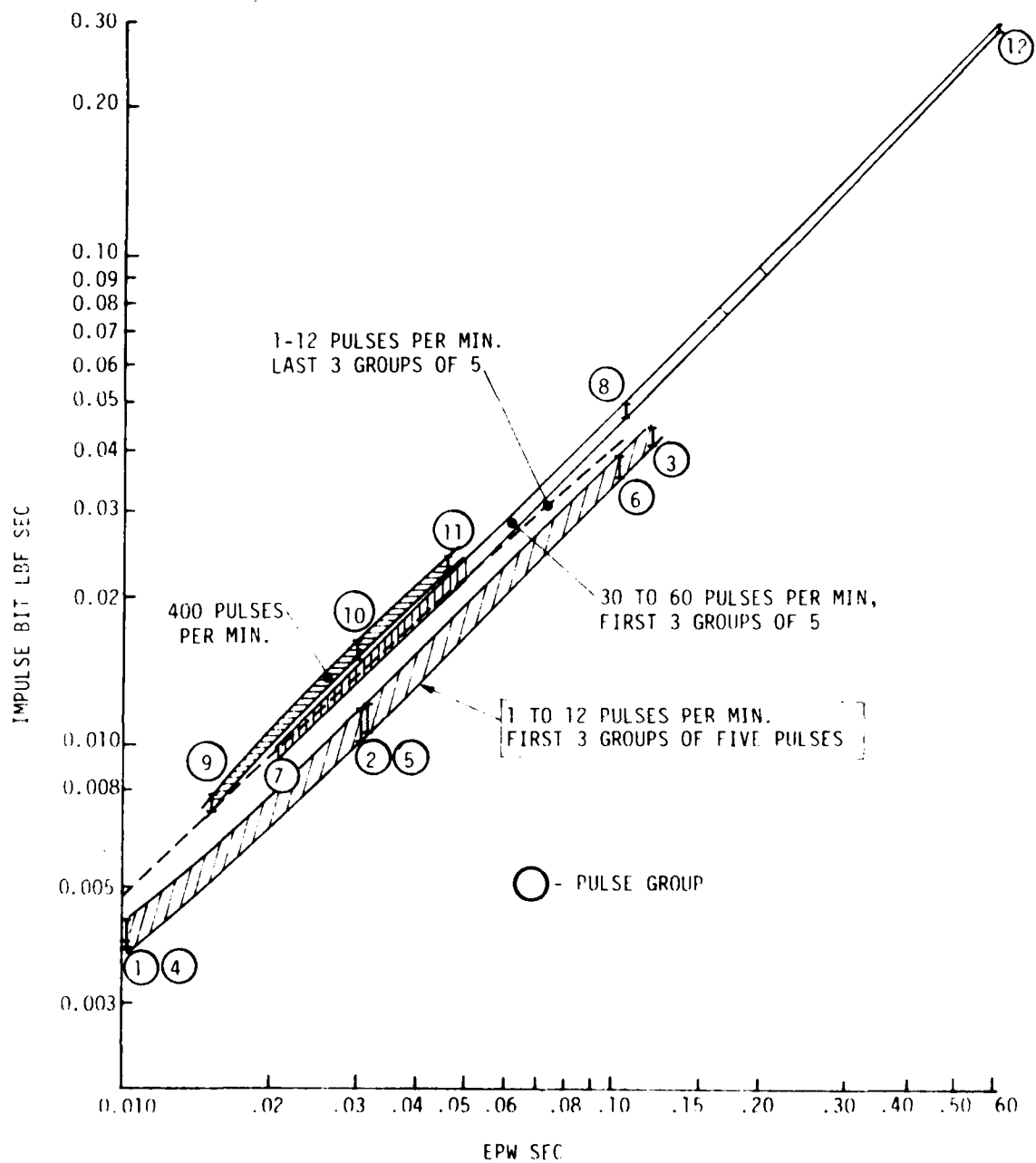


Figure 6-22. Test 512, Pulse Data Composite

6.5, Test Data Evaluation (cont.)

The dashed line in Figure 6-22 identifies the I-Bit for the last 15 pulses for the middle data band. Only a small difference between the beginning and final pulses are noted.

Figures 6-23, -24, and -25 provide the same data on 3 separate figures. The slope of the lines shows the impulse to be linear with EPW between .03 sec and .60 sec and nearly linear between .010 sec and .03 sec.

The data shown in Figures 6-26, -27 and -28 display the pulse-by-pulse I-Bit repeatability for EPW values of 0.6, .030, and .010 sec. The impulse repeatability at .6 sec EPW is $\pm 1.7\%$. The program goal of providing I-Bit capabilities of less than .005 lbf-sec with a repeatability of $\pm .0005$ is displayed in Figure 6-28. Data for pulse rates of 1 and 12 pulses per minute are shown to fall within the acceptable band.

A more complete set of plots for all pulse data, including the 15 pulses at end of the long pulse trains, is shown in Figure 6-29. The I-Bit is consistently higher for the last 15 pulses of the series than for the first 15 due to the hotter chamber wall, as discussed in the Phase II results. These differences appear to be small and predictable.

The drop in I-Bit for each successive group of 5 pulses in pulse series 1 may result from injector refrigeration caused by the vacuum evacuation of liquid propellant from the injector manifold. However, there is no data to substantiate this hypothesis.

The effect of coast time on I-Bit is displayed in Figure 6-30. Here it can be seen that faster pulsing rates provide slightly higher impulse bits for the same EPW.

The trends of the impulse data are sufficiently consistent to lend credibility to the measurements. The data indicate that the program MIB and MIB repeatability goals have been achieved.

The fact that the injector oxidizer orifice enlarged and that the P_w shifted during the pulse test is not obvious in these data. The injector failure mode did not appear to degrade the engine pulse capability.

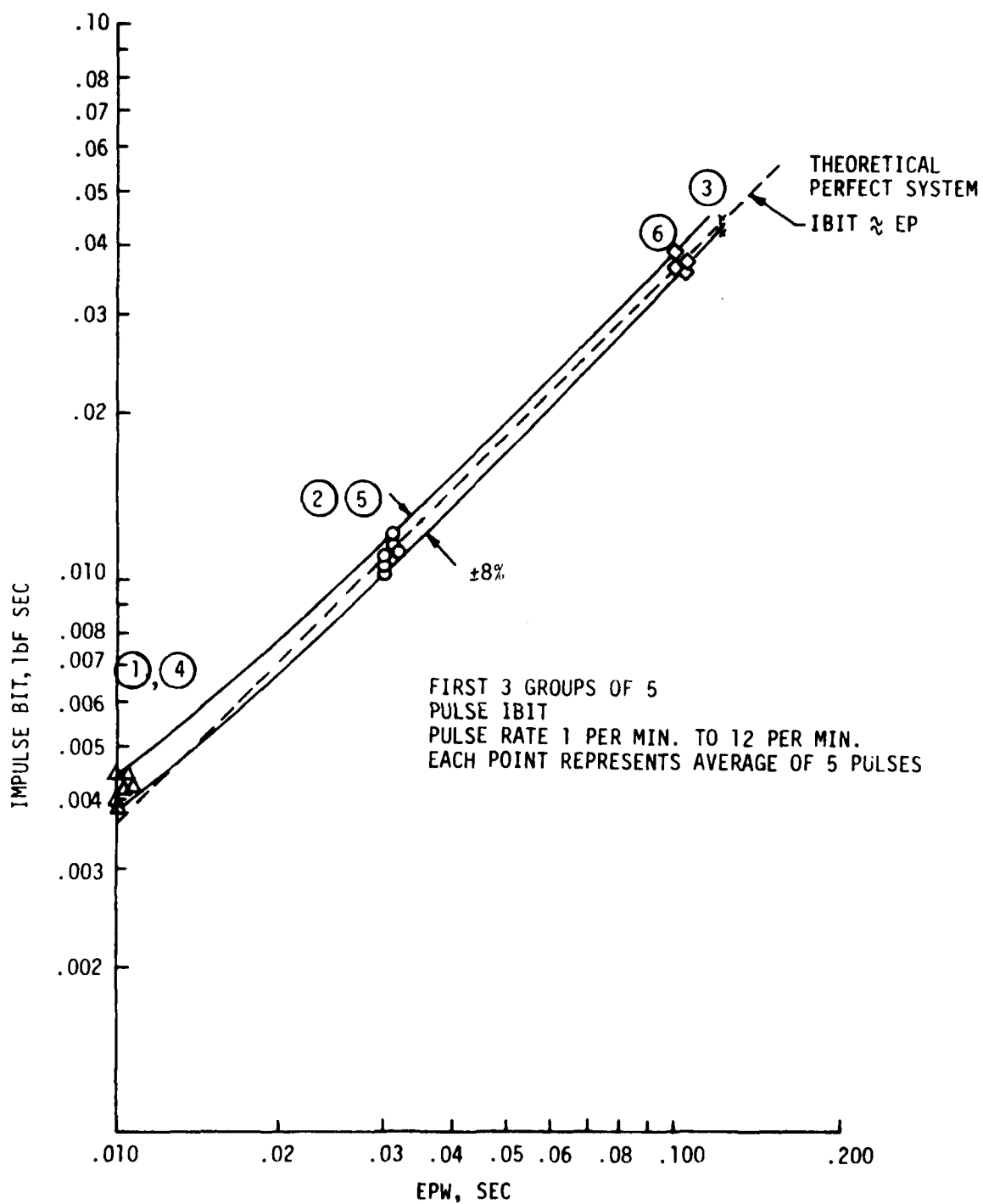


Figure 6-23. I-Bit vs EPW, First 3 Groups of 5

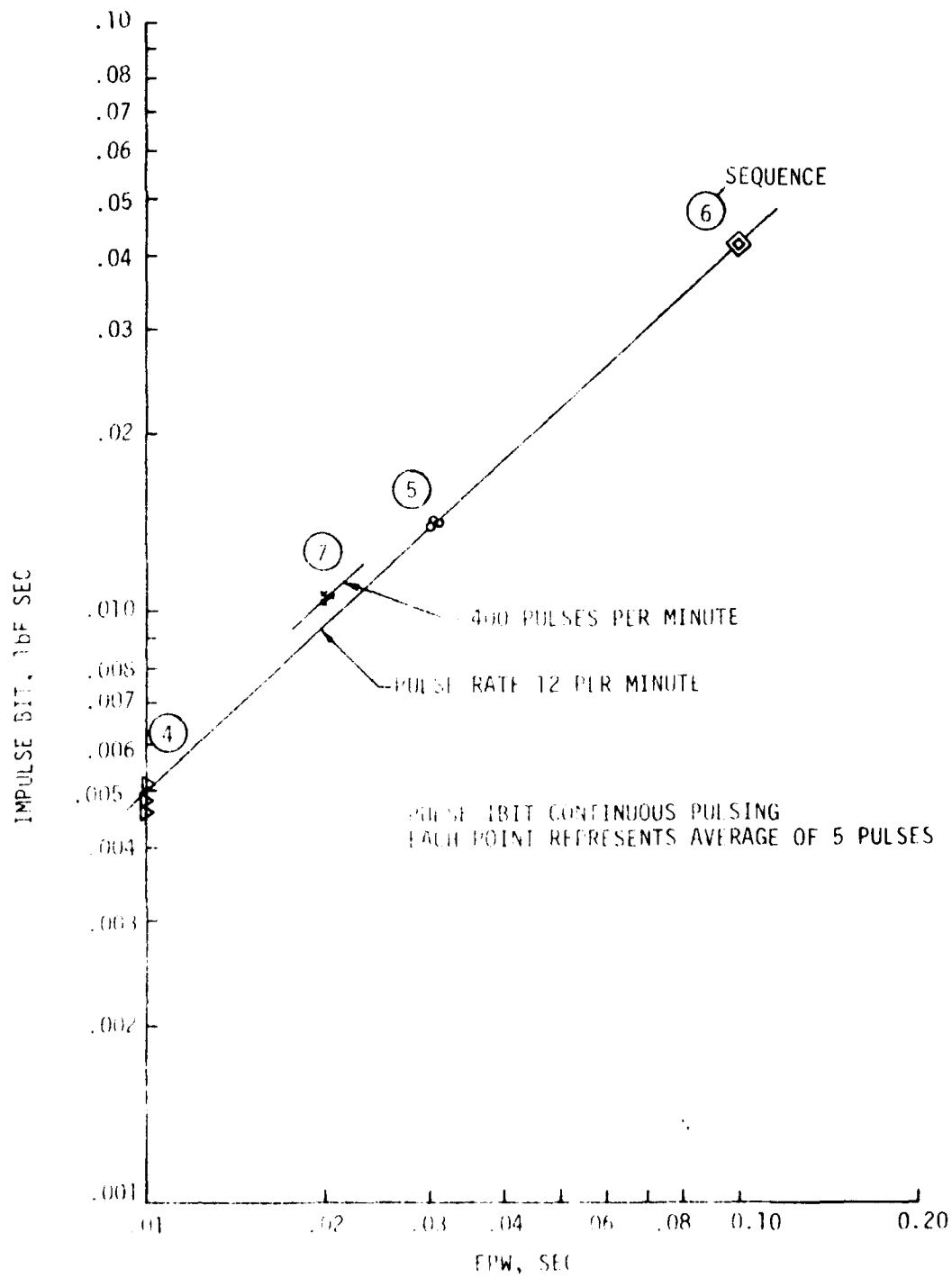


Figure 6-24. 1-Bit vs EPW, Continuous Pulsing

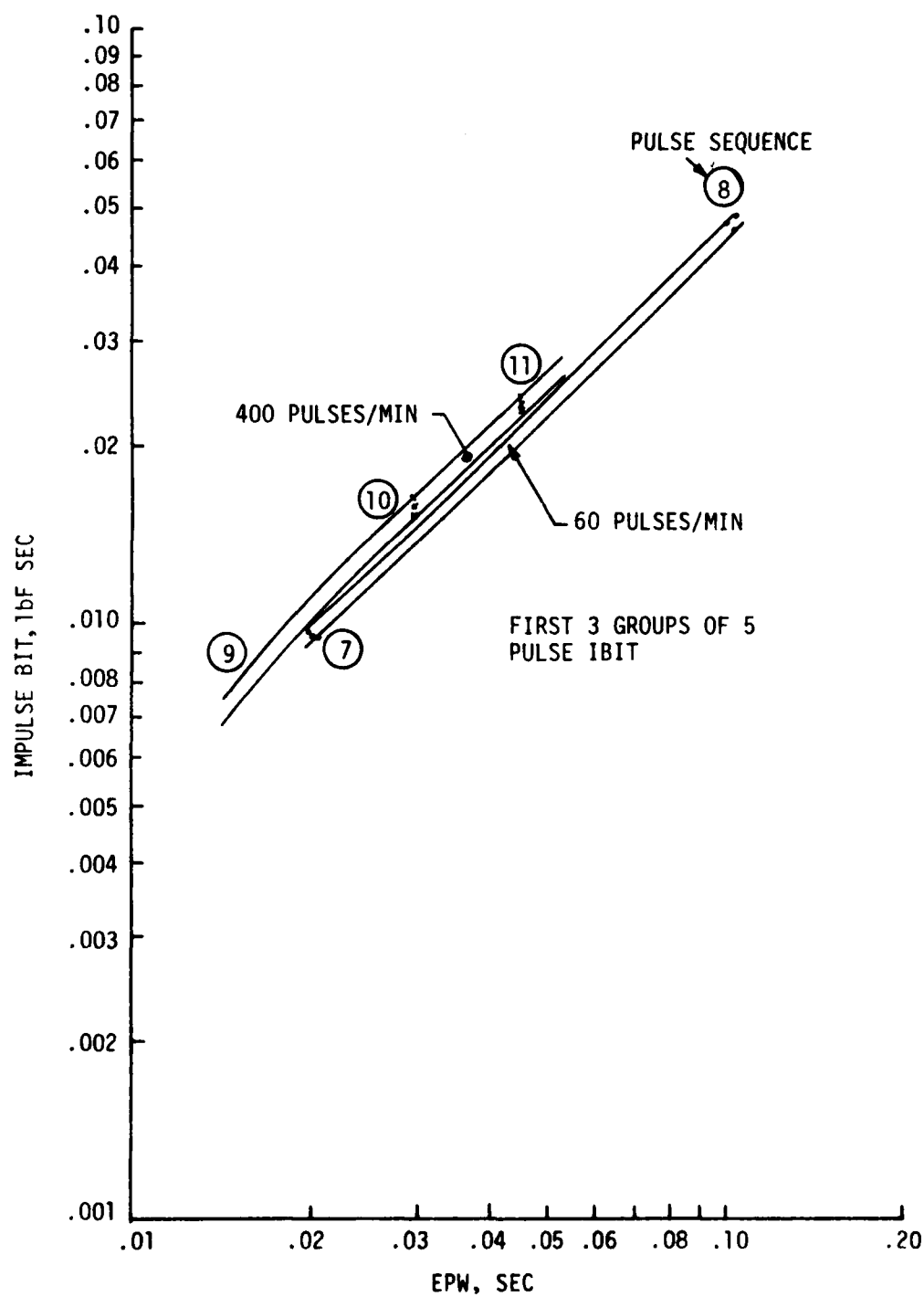


Figure 6-25. I-Bit vs EPW, First 3 Groups of 5

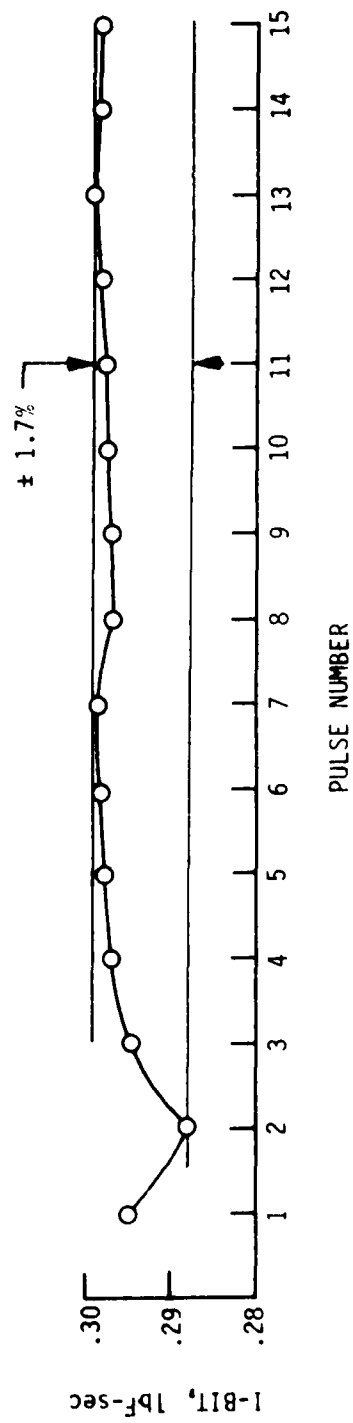


Figure 6-26. Bit Impulse Repeatability of .60 sec EPW

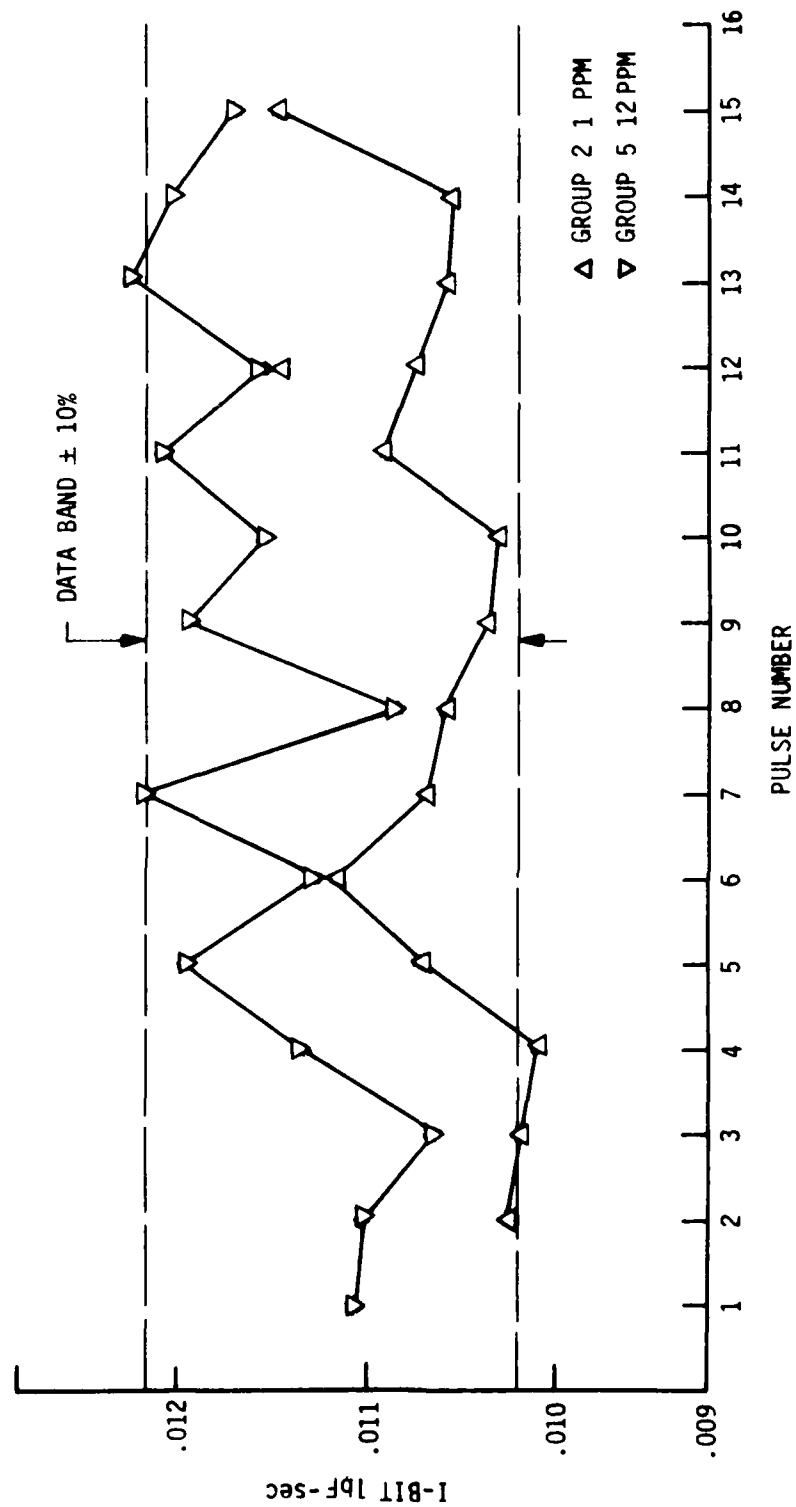


Figure 6-27. Bit Impulse Repeatability of 0.30 sec EPW

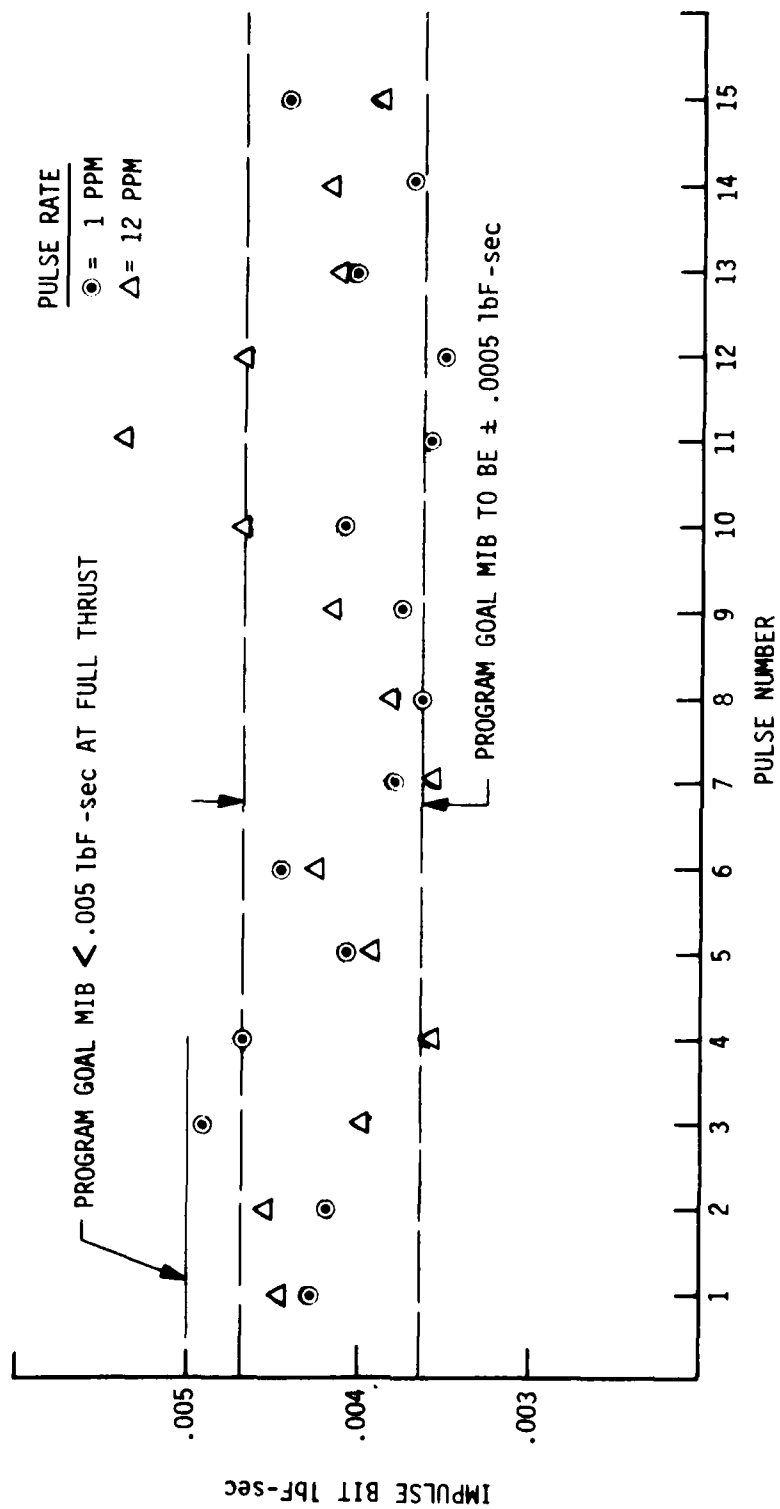


Figure 6-28. Test Data for .010 sec EPW - First 15 Pulses

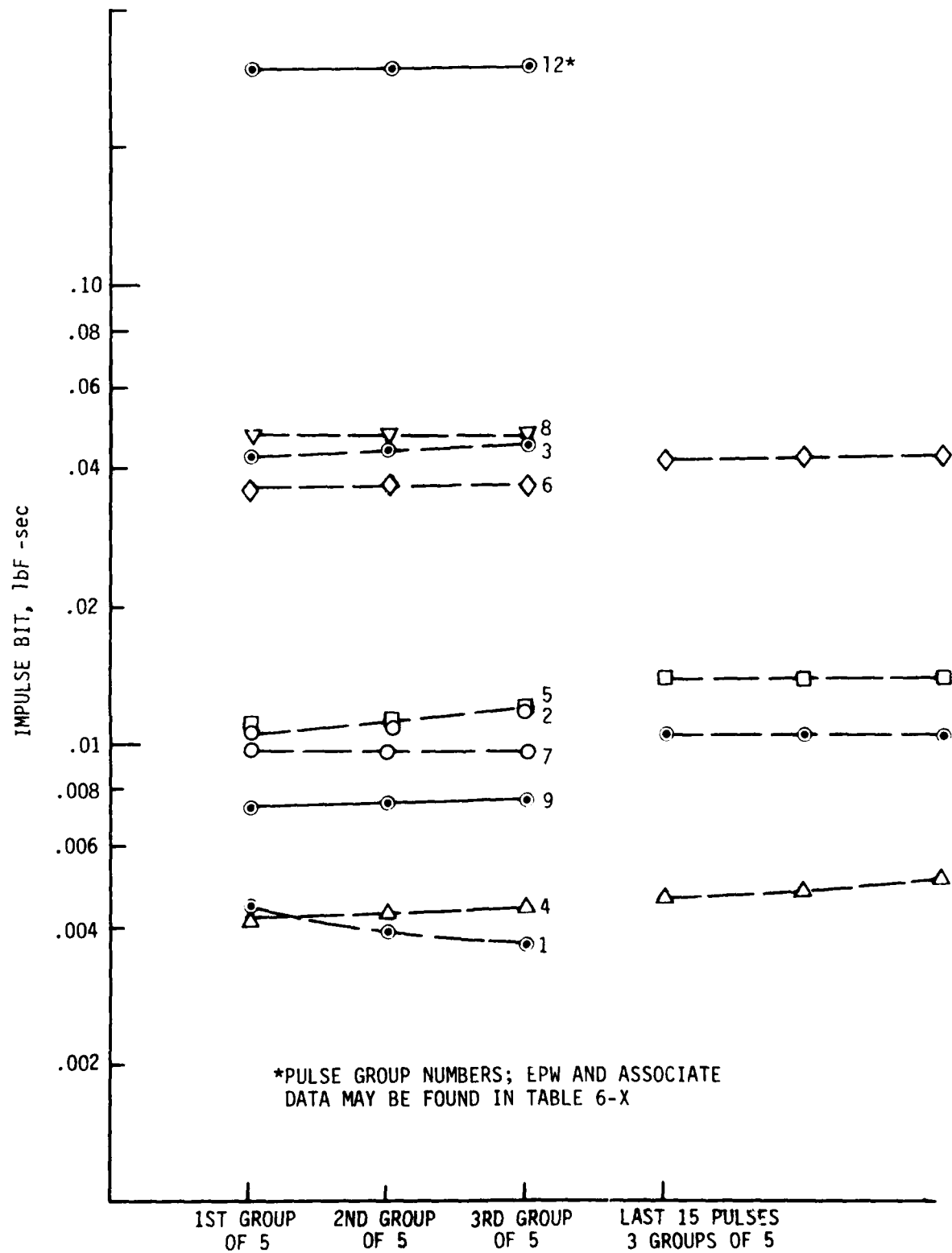


Figure 6-29. Impulse Bit Repeatability

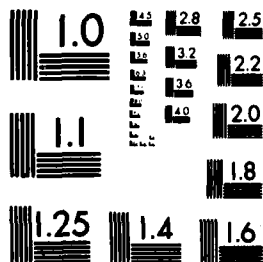
4

OF

5

AD A

091078



MICROCOPY RESOLUTION TEST CHART
NATIONAL BUREAU OF STANDARDS-1963-A

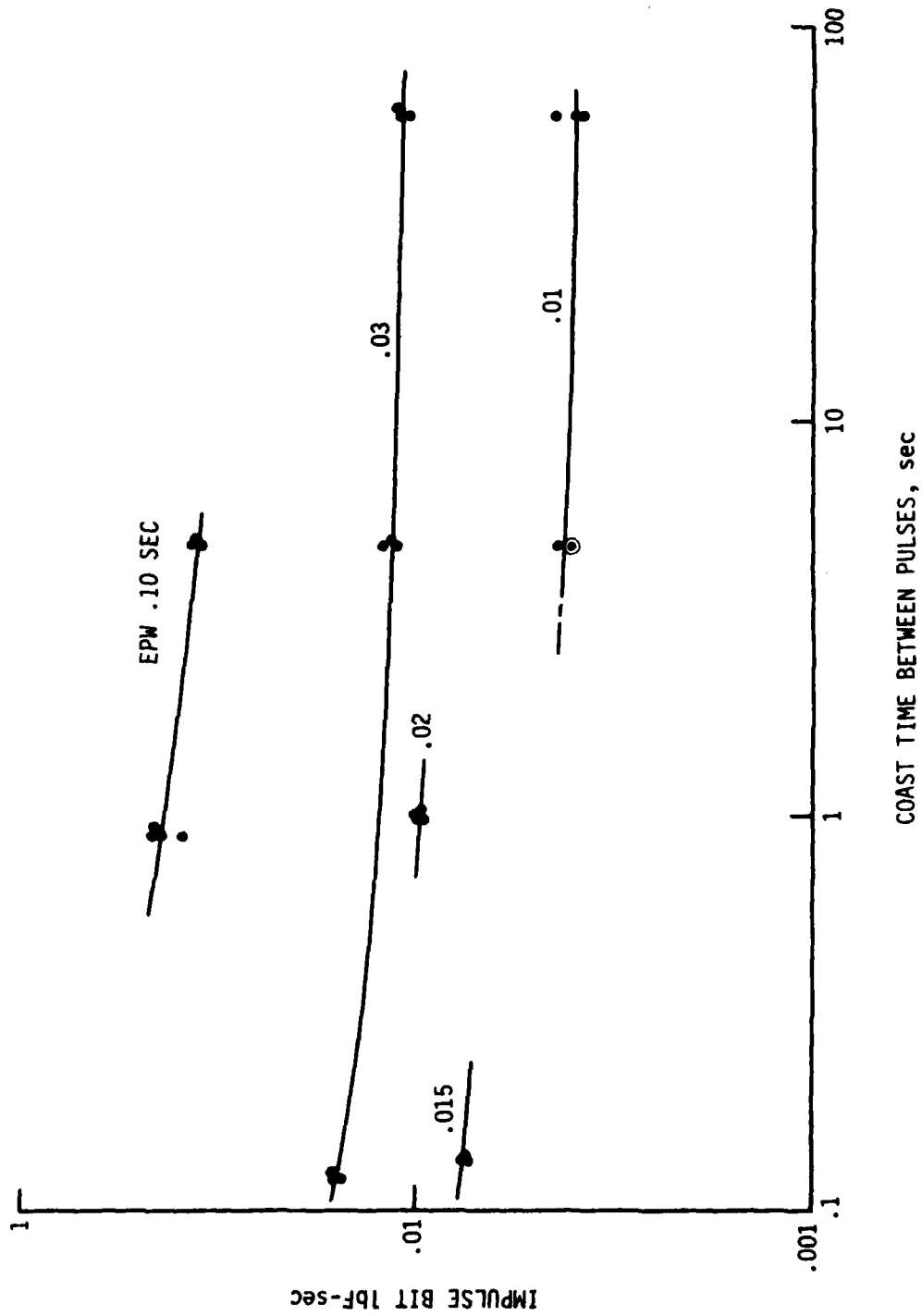


Figure 6-30. Effect of Coast Time on Impulse Bit

6.5, Test Data Evaluation (cont.)

6.5.3 Engine Specific Impulse

6.5.3.1 Steady-State

The steady-state specific impulse, C^* and C_f data were displayed in Tables 6-VII and 6-IX. The data summary periods vary from 5 sec duration in the early part of the test to 50 sec of burn duration at the end of the test. The overall test average is also shown.

No data are displayed for the first 0.5 sec as the response of the large PDFM is too slow to provide valid data. The larger data summary periods provide more accurate propellant consumption data as measured by the linear displacement of the flow measurement system.

Figure 6-31 shows the I_{sp} versus firing time for Engine SN 22. The performance is observed to increase with time at high pressures. The chamber wall heats from ambient temperatures to a steady-state value during this period. This rise in performance is due to reduced thermal losses from the hot gas to the cold wall and also the regression of the liquid film coolant length along the chamber wall as the heat is conducted from the throat to the forward end of the chamber. The data indicate that 150 to 200 seconds of burn time is required to reach maximum specific impulse.

At lower pressures, the performance decreased significantly at about 20 sec into the test. This drop in performance is apparently a thermally induced effect, since it is accompanied by a rapid rise of the head end temperature and the onset of rough combustion. The rise in head end temperature due to heat conduction along the chamber wall triggers the combustion roughness, which, in turn, causes a reduction in specific impulse.

The data of Figure 6-31 also show that higher performance levels are attained at higher operating pressure.

Figure 6-32 shows the relation between vacuum thrust and steady-state specific impulse. Three performance curves are shown for SN 21 Engine. The dashed line corresponds to the time period from 0.5 to 5 sec. The lower solid line corresponds to the full test average, using the prefire calibration and thrust "zero" position. The upper set of data corresponds to the last 20 sec of burn, when the chamber is at maximum temperature and the thrust measurement is corrected to the postfire zero. The latter is considered to be the most valid data as it eliminates thermal drift in the measurement system during the long burn periods. The correction to postfire

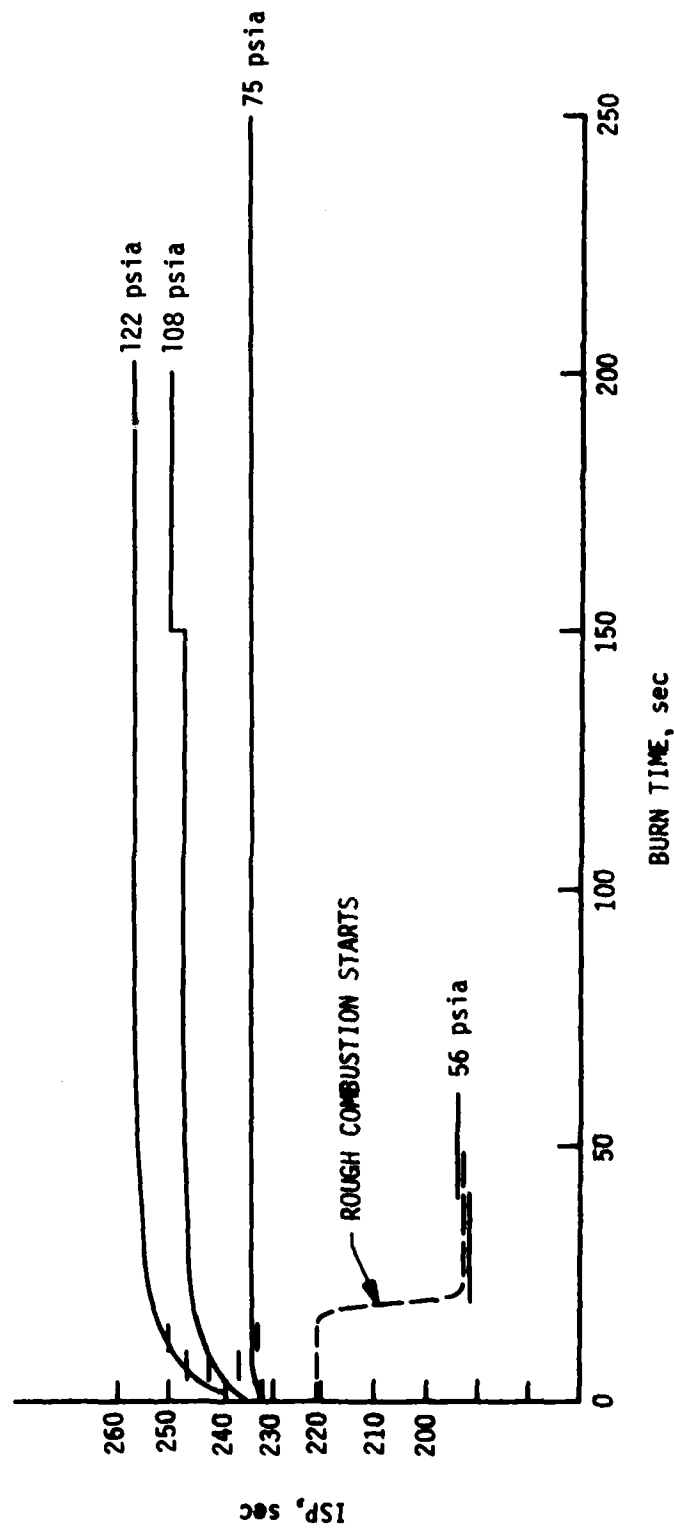


Figure 6-31. Specific Impulse vs Firing Time Engine SN 22

1-CAS INJECTOR TESTS 501-506
PROP TEMP 50 to 55°F

	MR	Pc	Kw/°F	F
501	1.55	52.7	465/363	.195
502	1.56	50.7	480/375	.200
503	1.66	73.5	472/384	.290
504	1.58	88.3	472/409	.335
505	1.70	111.6	479/399	.437
506	1.62	53.6	467/379	.208

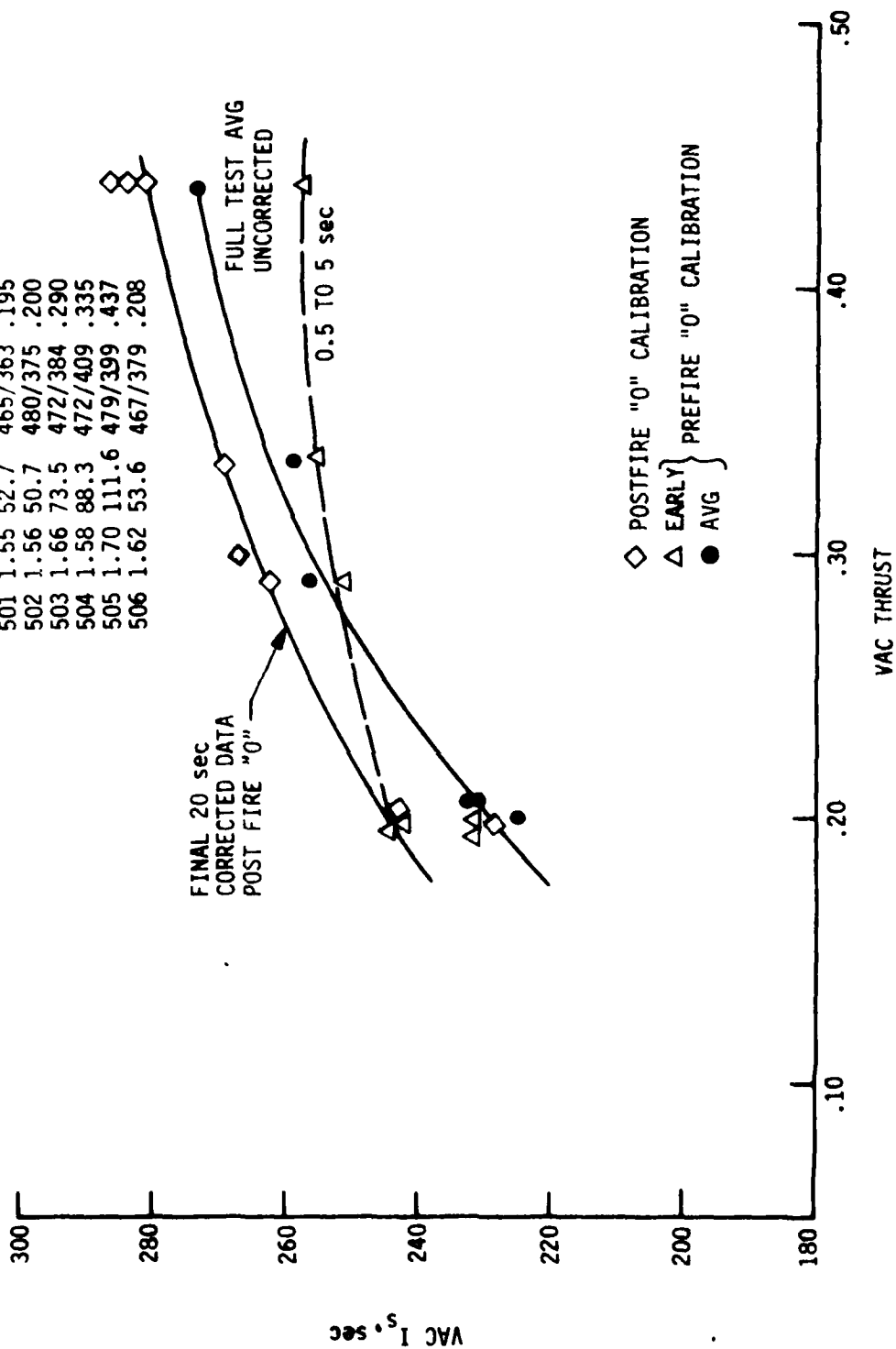


Figure 6-32. Vacuum Thrust vs Steady-State I_s

6.5, Test Data Evaluation (cont.)

zero altered the Isp performance up to 10 sec during testing of SN-21. SN 22 data showed little change in "zero" position during the long tests; thus no correction was necessary.

Figure 6-33 provides the "end-of-test" steady-state specific impulse and uncorrected C^* for the two engines tested. The pre- to postfire zero shift for the second engine testing was very small. The differences in performance of the two units, as thrust is reduced, are attributed to the injector pressure drop. The second unit has lower injection velocity.

Figure 6-33 also provides a comparison of the data obtained with radiation-cooled and insulated chambers. The insulated chambers provide higher performance because of a reduction in heat loss. Both specific impulse and C^* measurements are noted to improve when the chamber is insulated. The improvement in Isp performance, when the insulation was added, was greater on SN-21 than on SN-22. The reason for this difference cannot be identified from the limited test data. It is possible that it could be a measurement error, since the differences are within the measurement error band.

Figure 6-34 displays the Isp consistency at a given chamber pressure over mixture ratio variations from approximately 1.5 to 1.9.

The experimental nozzle C_f values, derived from selected tests, were shown in Tables 6-VII and 6-IX and are displayed in Figure 6-35. These are noted to increase with time and temperature. The dotted lines show C_f values based on the area of the heated throat, rather than on the prefire measurements. Use of the throat area, corrected to the measured temperature, tends to reduce the rise in C_f with temperature.

A boundary layer thickness change resulting from chamber wall heating provides a possible explanation for the increase in C_f with time. The data show that the experimental C_f is 88 to 90% of the theoretically predicted value, based on an assumed ODE analysis.

The maximum performance measured in this test series was at full thrust with an insulated chamber and a high pressure drop injector. The achieved Isp of 268 sec is less than the 280 sec program goal.

Analysis of the data to establish the source of the Isp loss is difficult as a result of the small size of the hardware and the dimensional changes that take place with heating. The Isp for the perfect

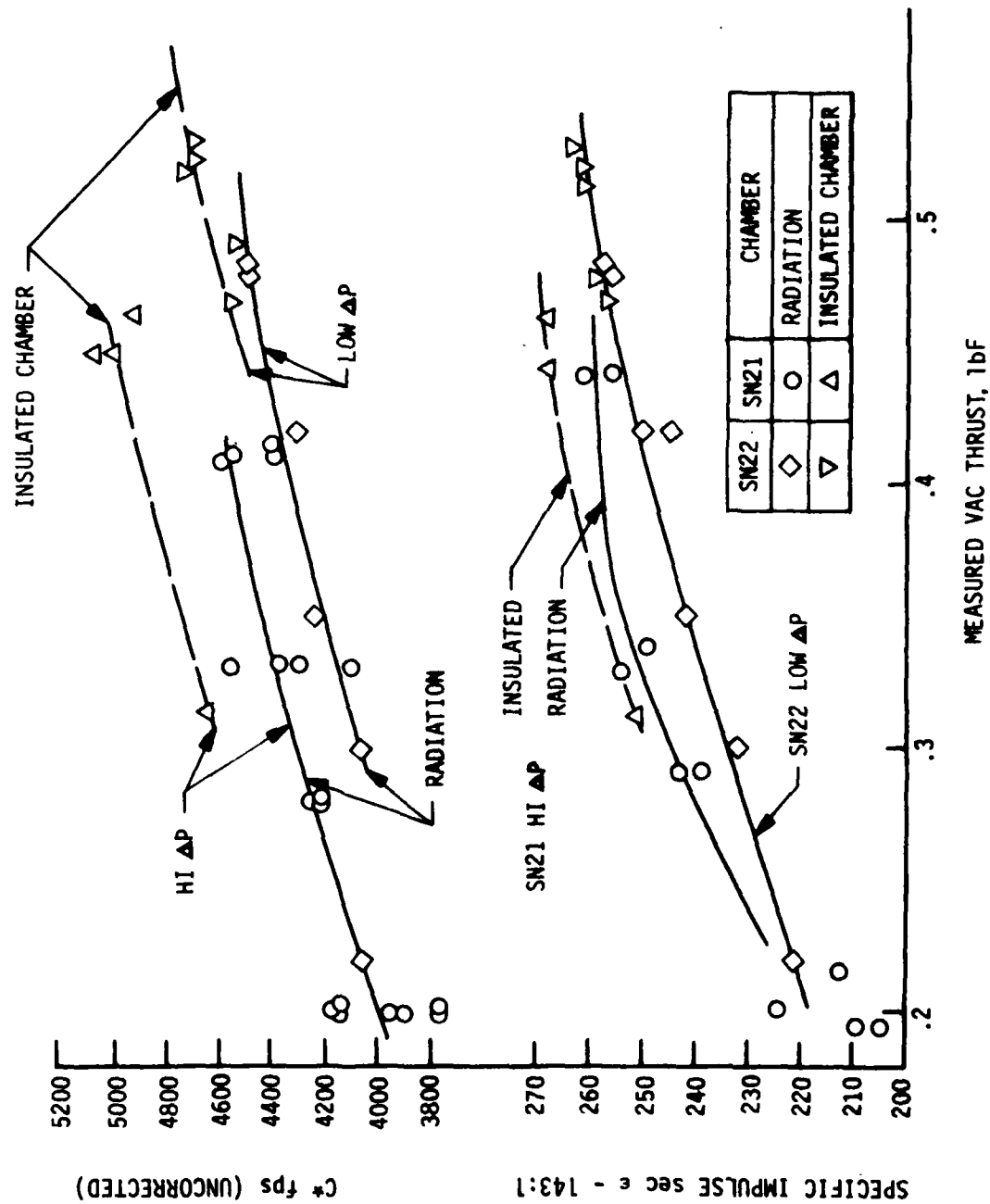


Figure 6-33. Vacuum Thrust vs I_{sp} and C^*

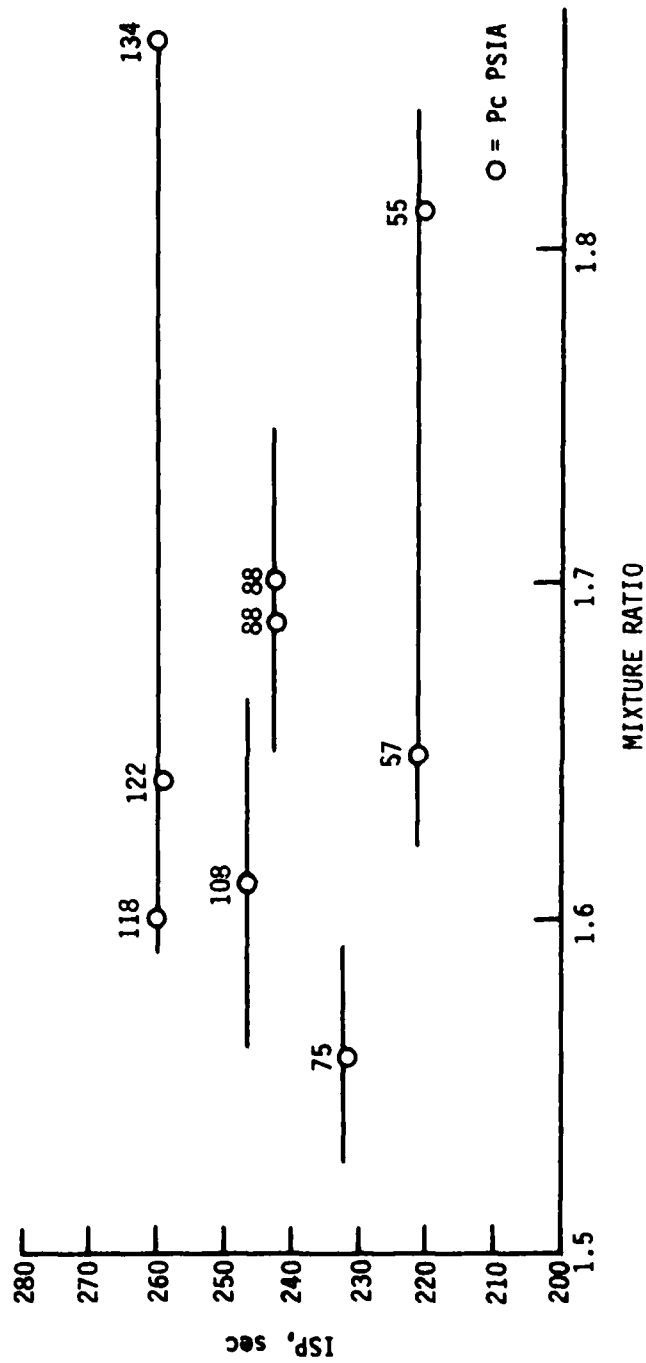


Figure 6-34. Engine SN 22 MR Sensitivity

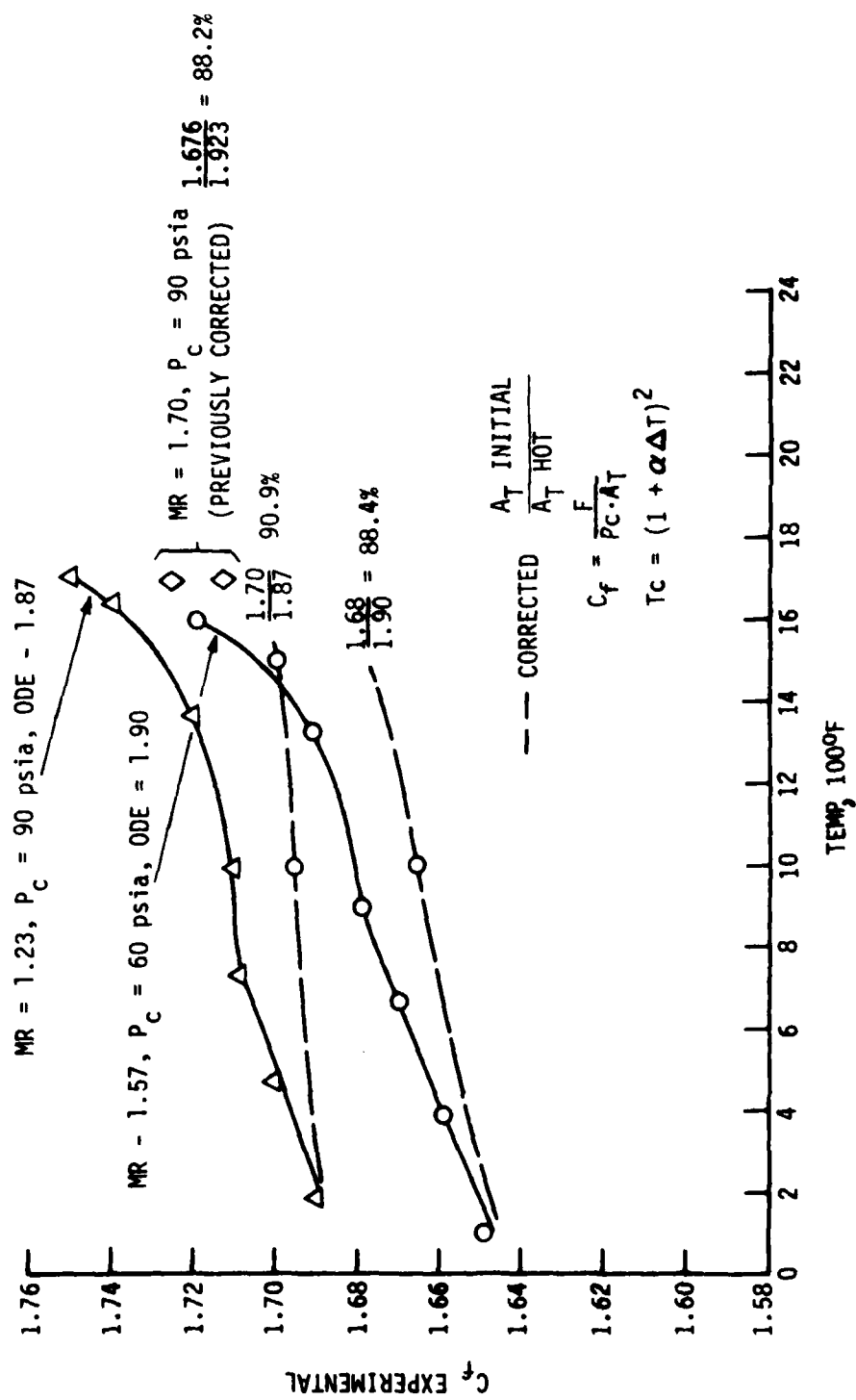


Figure 6-35. Nozzle C_f Correlation

6.5, Test Data Evaluation (cont.)

injector and an optimum 100:1 area ratio nozzle contour is 315 sec. The nozzle contour was selected by using BLIMP model analyses with adjustments to account for the predicted adiabatic wall boundary layer displacement thickness. This led to a 143:1 geometric contour in order to provide for a 100:1 area ratio aerodynamic contour. The contract testing did not provide sufficient data to validate this design assumption. If the design analysis is assumed to be correct, the performance losses in the insulated chamber at steady-state would be 3% due to nozzle and 11% due to energy release loss. The energy release loss includes both vaporization and mixture ratio maldistribution. Most of the mixture ratio maldistribution is a result of the fuel-rich condition at the wall.

A view of the axial temperature profile, leads to the conclusion that the amount of fuel in the outer stream tube of the injector is "marginal to adequate" for protecting and cooling the chamber head end and excessive for cooling the throat region. This results in a recommendation to provide additional mixing to improve the performance. Mixing can be obtained by increasing the chamber length; however, this would result in greater heat removal from the combustion gas during the thermal transients and could lower the short burn and pulsing performance. Therefore the recommended methods of improving the mixing without increasing chamber length or changing the injector design are to modify the chamber contour as shown in Figure 6-36, where various turbulence producing devices are considered.

The use of these devices could also eliminate the combustion roughness experienced at low pressure operation if the source of the roughness is the accumulation and intermittent burning of propellant which is only partially reacted due to poor injector mixing.

6.5.3.2 Pulse Performance

Phase II did not provide sufficient pulse testing data with the micro-PDFM's to allow definition of the pulse specific impulse of the Phase III design.

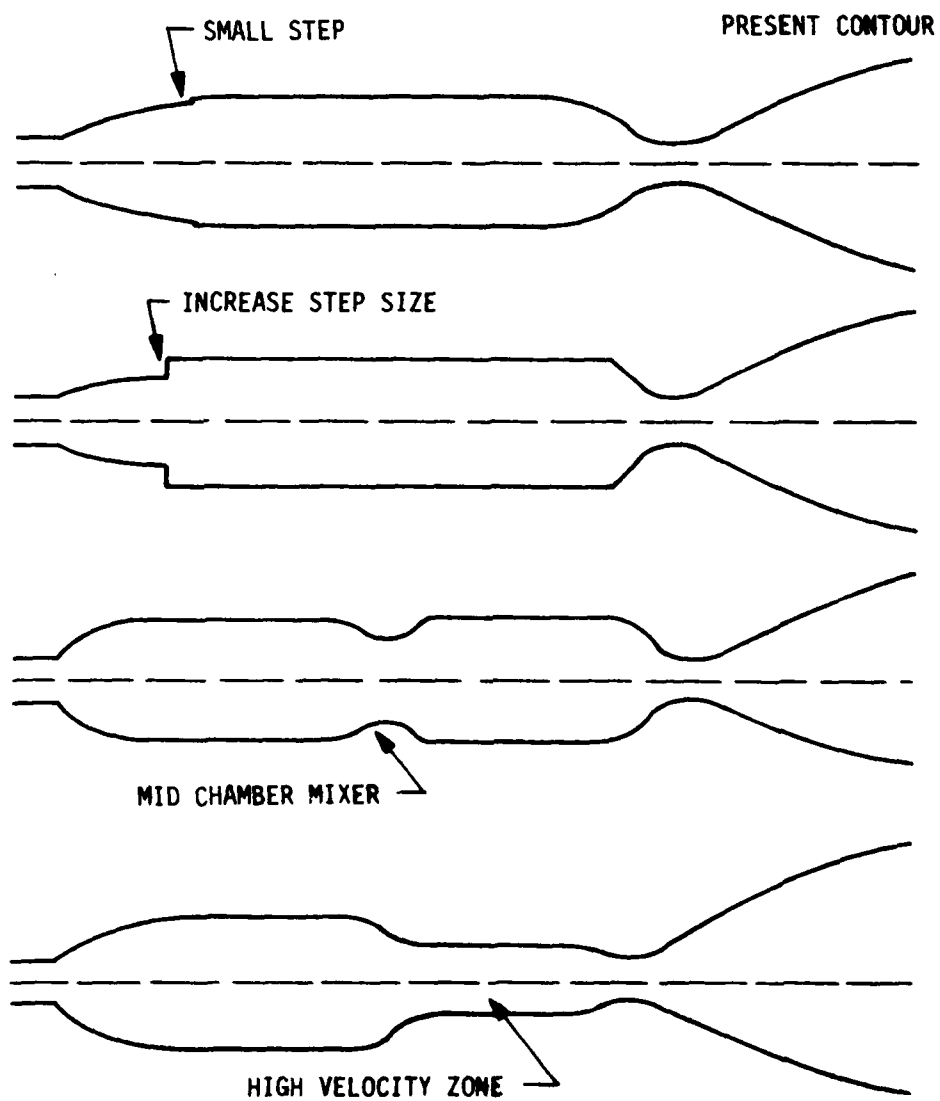


Figure 6-36. Chamber Contour Changes to Improve Mixing

6.5, Test Data Evaluation (cont.)

6.5.4 Thermal Data Evaluation

6.5.4.1 Steady-State Blowdown Thermal Characteristics

The measured engine temperatures obtained in the Phase III testing are documented in Appendix E.

The steady-state axial temperature profiles for SN 21 Engine at thrust levels of .21, .29 and .45 lb thrust are shown in Figure 6-37. The effect of insulating the chamber, as shown in the engine drawing, is to increase the temperatures about 200°F. No throat temperature measurements were made in the radiation-cooled mode on this assembly. The maximum temperature in the buried mode was slightly greater than 2000°F.

The data shown in Figure 6-37 indicate that the head end temperatures of the chamber, the valve, and the injector remain in an acceptable range. Similar data for Engine SN 22 are provided in Table 6-XI and Figure 6-38. The increase in throat temperatures, starting with Test 521, is due to the addition of insulation. Comparison of the temperature measurements for Engine SN 21 and 22 in Figure 6-39 shows the 2 units to be essentially identical in the insulated mode.

The second engine tested provided a direct throat temperature measurement in the radiation mode. The addition of insulation increased the throat temperature from 1652°F to approximately 2000°F. The throat temperatures tended to drift up over the life of the engine, reaching about 2100°F after eight hours of total burn time.

This thermal drift is believed to be caused by a change in the thermocouple junction calibration due to diffusion of the silicide coating into the junction. This effect has been reported in industry literature.

An addition of a temperature measurement at the uncooled columbium weld joint of the bimetallic transition ring and machined columbium chamber (TG 180) was made. The data obtained indicated that the uncoated columbium weld was operating at approximately 1600°F. Although this is higher than desired from an oxidation standpoint, there appeared to be no adverse reaction on the chamber exterior during the 8 hours of testing completed.

The temperature at the SS-Cb transition was about 926°F at the nominal mixture ratio of 1.65 and increased to nearly 1100°F at

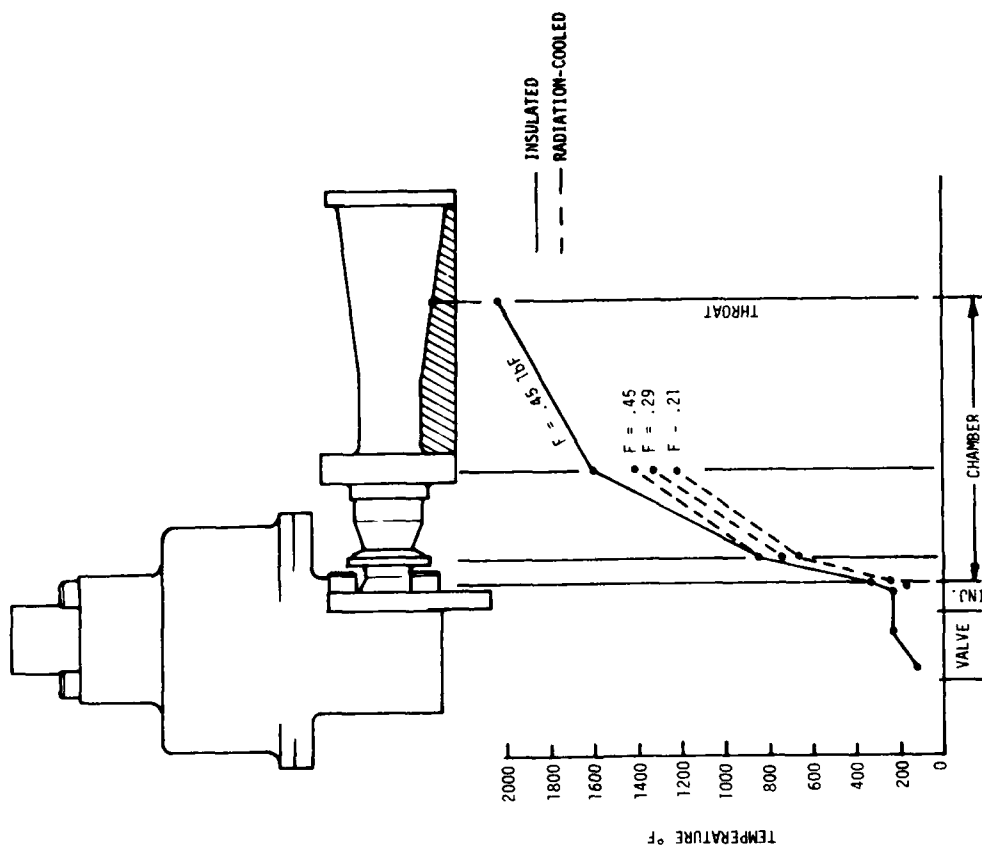


Figure 6-37. Axial Temperature Profile, Engine SN 21

TABLE 6-XI
ENGINE 22 THERMAL DATA

Test	Time Sec	TPC	TVB	TJB	Steel 90, 170, 270	TL	TVC	cb/ss 180	Trans 270	Rad fin. 217	Throat
517 Rad	250-300	144	102	203	222, 249, 238	285		897	890	1450	1390
518 Rad	200-250	140	100	198	231, 257, 249	288	155	890	883	1410	1387
519 Rad	200-217	142	100	204	244, 267, 264	296	157	903	896	1407	1478
520 Rad	150-199	157	108	226	257, 284, 276	314	181	949	945	1463	1652
521 ins	150-206	153	103	232	256, 286, 278	321	173	990	990	1794	1984
522 ins	150-181	159	107	246	267, 302, 294	394	180	1042	1073	1799	2019
523 ins	40-45	104*	94*	170	265, 301, 319	478	114*	1023	1096	1223*	1271*
524 ins	100-133	122*	87*	191	250, 275, 269	306	142	967	964	1670*	1791*
525 ins	700-744	177	114	255	259, 287, 280	325	270	962	965	1743	1945
526 ins	7100-8113	181	119	255	261, 287, 284	325	229	922	918	1748	2079
TG-180											
528 ins	2463	179	117	---	1622, 289, 286	334	228	922	928	1732	2105
529 ins	18,000	185	119	---	1519, 275, 290	354	231	853	908	1712	2117

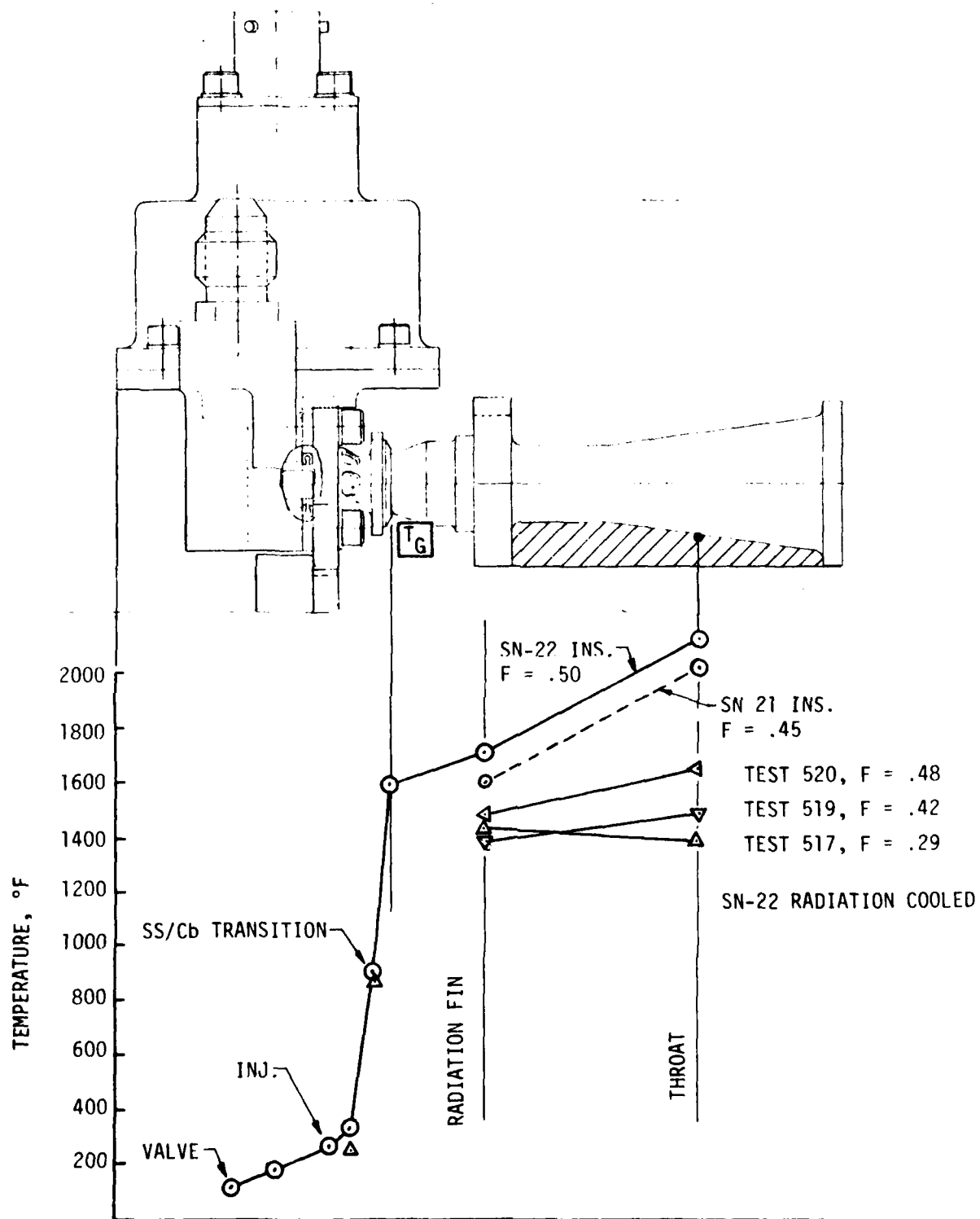


Figure 6-38. Axial Temperature Profile, Engine SN 22

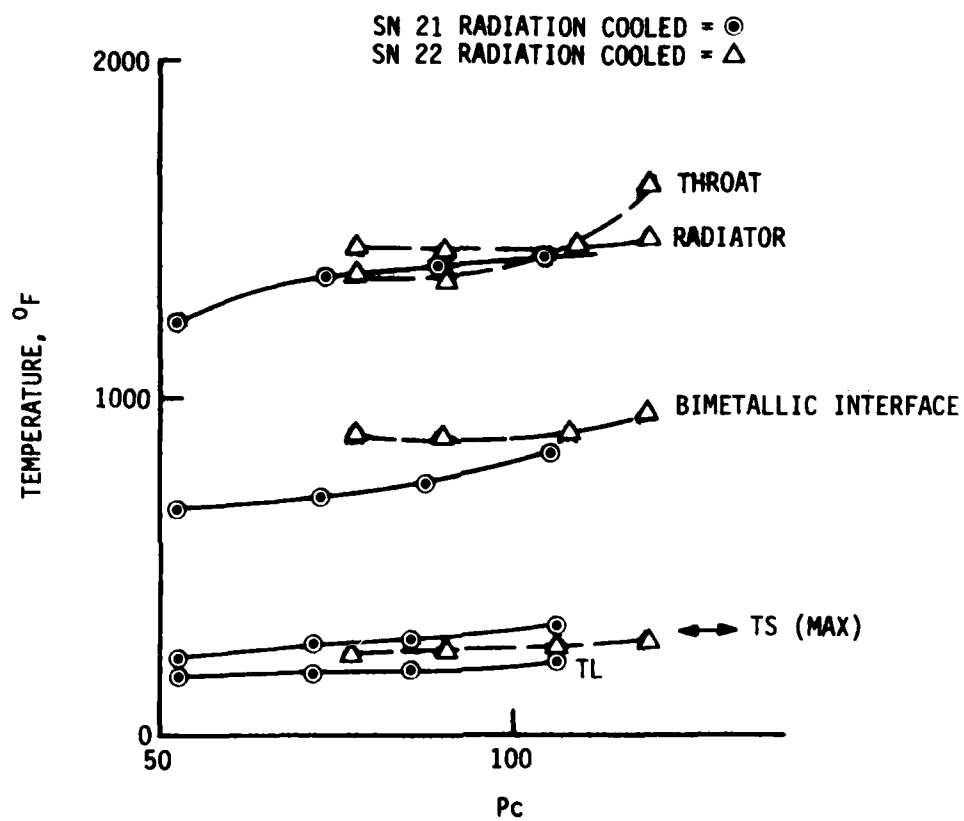


Figure 6-39. Wall Temperatures vs Pc, Engines SN 21 and SN 22

6.5, Test Data Evaluation (cont.)

a mixture ratio of 1.9 in Test 523. The predicted steady-state and soakout values at a MR of 1.65 were 616°F and 980°F, respectively. The measured soakout temperature was 1022°F, very close to the prediction. This temperature determines the thermal cyclic life of the joint. The Phase I life cycle analyses indicated that the maximum temperature of this joint is the controlling parameter on the thermal cyclic life of the engine. A temperature of 1000°F equates to approximately 1000 full thermal cycles. The limits of steady-state operation have not been defined and could best be accomplished by further testing.

The influence of chamber pressure on the steady-state operating temperature of both engines operating in the radiation-cooled mode was shown in Figure 6-39. Varying the chamber pressure between 50 psia and 120 psia has only a minor influence on the operating temperature at each location. The thermal characteristics of both engines are nearly identical.

6.5.4.2 Postfire Heat Soak

Small engines often encounter operating limitations due to the postfire heat soak from the hot chamber to the injector and valve. The chamber head end is therefore designed to provide sufficient thermal resistance to minimize the heat soakback that usually occurs after a long burn.

Test data showing the postfire heat soak under a variety of operating conditions is provided in the plots of Appendix E. These data show the following locations to experience a temperature rise on shutdown.

T Weld	=	Bimetallic interface
TS	=	Stainless steel thermal standoff
TL	=	Stainless steel structural support (leg)
TVB	=	Valve body
TPC	=	Pressure tap boss
TJB	=	Injector backside

All other locations experienced maximum operating temperatures during firing.

The time required for the chamber to reach steady-state operating temperature is approximately 100 to 150 sec. The valve body temperature continues to rise slowly for about 600 sec, and the cover reaches thermal equilibrium at about 900 sec. This is based on the data from Test 528 which was 2463 sec in duration.

6.5, Test Data Evaluation (cont.)

Table 6-XII provides a summary of Test 528 measurements, demonstrating a worst case thermal soak condition.

TABLE 6-XII

POSTFIRE HEAT SOAK FOLLOWING TEST 528
FULL-THRUST INSULATED CHAMBER

<u>LOCATION</u>	<u>STEADY-STATE TEMP. °F</u>	<u>MAX. SOAK TEMP. °F</u>	<u>TIME OF MAX. TEMP. AFTER SHUTDOWN SEC AFTER FS-2</u>
TS	288	645	20
T Weld	926	1022	10
TL	335	534	20
T Pc	180	205	86
TVB	117	160	66
TJB	255	343	20
TVC	228 Max.	228	0
Tg	1605	1605	0

None of the above soak conditions caused operational problem within the limits of testing on the program. Areas which could become limiting for a long life chamber include:

- (1) The bimetallic interface (T weld), due to the relative differences in material expansion coefficients.
- (2) TJB (the injector backside), due to creep of the Teflon valve seats with time. Since the actual time at temperature is very short, the 343 peak value may not be a problem, although this should be evaluated further.

The valve body soakout temperature of 160°F would not be a problem in a hot restart if the chamber pressure were kept above 110 psia. A worst case restart would exist at a chamber pressure below 110 psia. The N₂O₄ in the valve body at the valve body temperature of 160°F would cause the oxidizer to flash at the injector orifice. This would cause a shift in mixture ratio to a fuel-rich condition until the valve body had cooled down.

6.5, Test Data Evaluation (cont.)

Additional postfire heat soak data for the two engines tested in the radiation-cooled and insulated chamber modes is defined in Table 6-XIII.

6.5.4.3 Thermal Pulsing Characteristics

Pulsing operation is generally less severe at the high temperature region of the chamber because there is sufficient time between pulses to conduct the heat to cooler zones. The normally cooler zones in the head end of the chamber can run hotter in pulsing operation if the rate of heat soak from the throat region exceeds the rate of heat loss to the valve and structure. The valve-injector interface temperature is limited by the vapor pressure of the N_2O_4 (vapor lock) and by the Teflon shutoff element in the valve that is in contact with the injector.

The temperature of the engine at the injector inlet is normally measured by the parameter TJB; however, this measurement was non-functional on Engine SN 21. The nearest fast responding measurement was on the steel chamber sleeve (TS) about 0.3 in. away. The TS location is normally hotter than the TJB location and operates at the fuel saturation temperature (320°F at full thrust). TS 270 was selected as the critical location for evaluating the limits of safe pulsing. Starting the engine should be safe as long as TS 270 is less than 320°F.

The thermal data recorded in the pulse series Test 512 is documented in Appendix F. These data consist of plots of TS 270 versus pulse number and tables of other temperatures at the start and end of each pulse for which data were processed. The temperature TS 270/2 at the end of pulse 15 and also at the end of each pulse group is shown in Figure 6-40. This temperature is plotted versus "% Duty Cycle" (expressed as on time/time between pulse starts). During testing, all pulse tests were terminated if the TS axial station exceeded 450°F, except in Group 12, where the limit was increased to 1000°F. A number of the low duty cycle pulse groups attained thermal equilibrium temperatures which were well below 320°F.

Figure 6-38 shows that continuous pulsing is possible up to a 4% duty cycle by using a $TS \leq 320^\circ F$ criteria. The dark circles indicate where equilibrium temperatures were achieved. A minimum of 15 successive pulses could be conducted up to a duty cycle of $\approx 20\%$, if the chamber is cold at the start of testing. This observation should be confirmed by additional testing, since it represents only one engine and one test series. The number of continuous pulses required to reach 450°F for a data group is indicated in the boxes above each pulse group where temperatures continued to rise above 320°F.

TABLE 6-XIII

POSTFIRE HEAT SOAK AT VARIOUS OPERATING CONDITIONS

ENGINE SN-21

<u>Condition</u>	<u>Test</u>	<u>TS</u>	<u>T-BM</u>	<u>TL</u>	<u>TPC</u>	<u>TVB</u>	<u>TJB</u>	<u>TVC</u>	<u>Tg</u>
Rad	504	255/452	741/815	179/288	138/161**	**	*	**	*
Rad	505	276/470	793/841	221/298	140/164**	**	*	**	*
Rad	506	216/418	672/752	179/267	129/151**	**	*	**	*
<u>ENGINE SN-22</u>									
ins	521	286/605	990/	322/525	**	**	239/330	**	*
ins	522	303/653	1071/1071	395/542	148/199**	**	250/346	**	*
ins	525	286/633	960/1028	325/529	178/204	115/162	256/347	221/221	*
ins	528	288/645	926/1022	335/534	180/205	117/160	255/343	228/228	1605/Max

MAX SOAKOUT TEMPERATURE °F



Temperature at end of steady-state firing
duration 200-300 sec, °F

*data not available

**steady-state value not attained in test duration

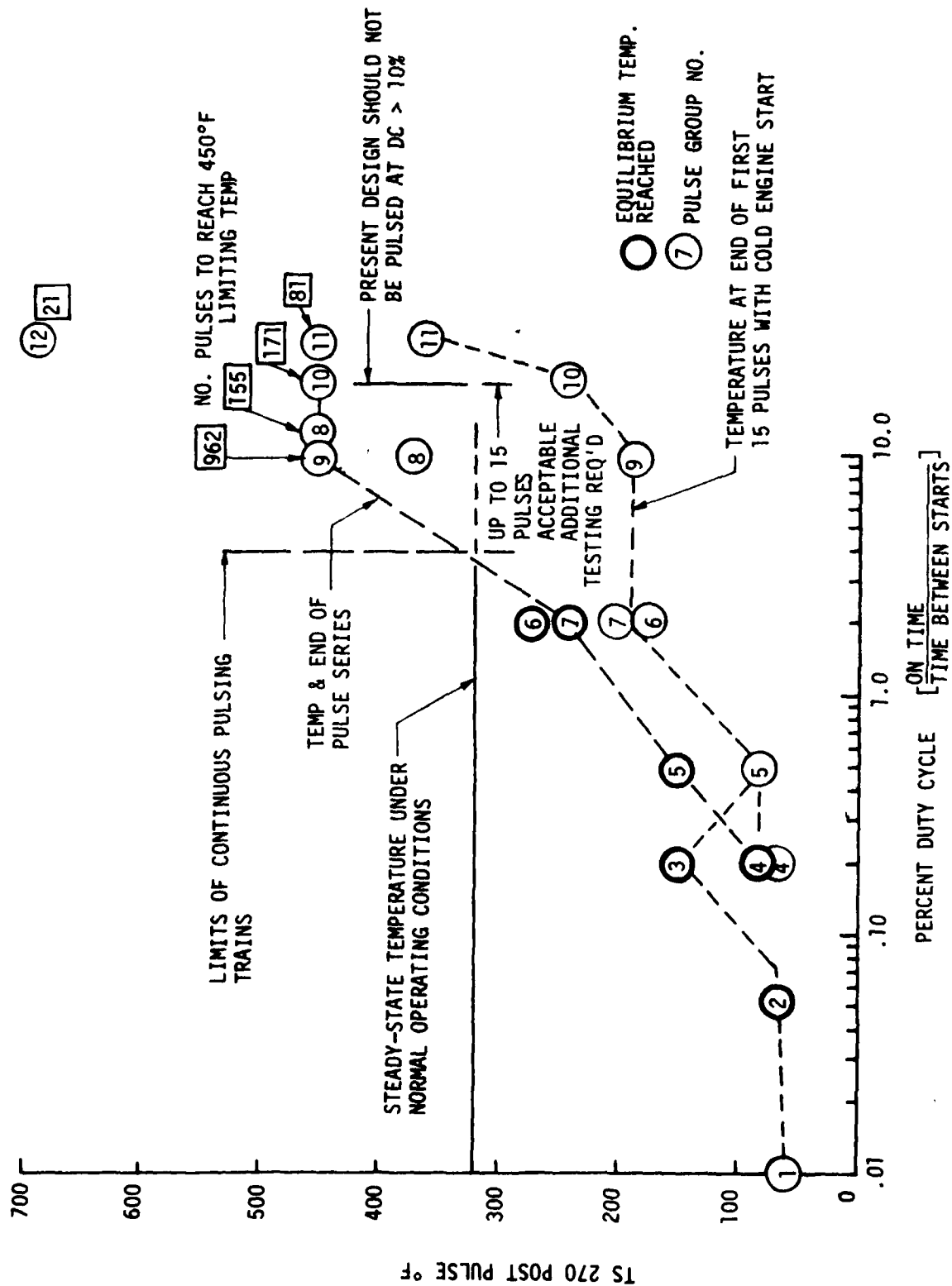


Figure 6-40. Temperatures vs Pulse Number

6.5, Test Data Evaluation (cont.)

The higher head end temperature observed in the 10% duty cycle could be the cause or result of the injector oxidizer orifice enlargement. Since the orifice enlargement increased the mixture ratio, it can be expected that the fuel film cooling will be less effective and the head end will be hotter.

Additional pulse testing is required before more specific conclusions can be drawn.

SECTION 7.0

TEST 512 DATA EVALUATION

7.0 TEST 512 DATA EVALUATION

7.1 TEST OBJECTIVES

The objectives of this test were to 1) identify potential duty cycle limitations resulting from evaporative chilling or heat pump up; 2) characterize impulse bit repeatability and minimum impulse bit capability; 3) obtain estimates of pulse performance.

7.2 TEST RESULTS

The fire testing of Engine SN 21 was intended to accumulate a total pulse quantity of 10,546, with an accumulated on-time of over 800 sec at each of the 3 tank pressure settings. The planned test program and the actual fire testing pulse quantities and durations are summarized in Table 6-VIII. The actual fire test program departed from the planned activity in the latter tests (pulse groups 8 through 12), which were limited by the overheating of the forward end of the thrust chamber. This resulted in the temperature "kill" condition of 450°F, terminating the various pulse series prior to the accumulation of the programmed pulse quantities. Table 6-VIII also displays the pulse quantities at which each pulse group terminated.

The final test of the pulse group was intended to be a three hundred second continuous burn which would have been a repeat of previously demonstrated long duration operation. This firing was terminated at about five seconds when the chamber head end temperature reached 1000°F.

7.3 TEST DATA EVALUATION

The data obtained on the pulse mode test series included: temperatures, impulse bit, propellant consumption, and, in some instances, chamber pressure. Pc data was not available on the earlier firings apparently due to a blocked .010 in. diameter port leading to the pressure transducer. The latter tests provided Pc pressure traces, since the blockage was apparently corrected by the effects of pressure and temperature.

The Pc pressure traces did not, however, provide rapid response information as they lagged measured thrust by about 0.020 sec. Thus the most useful data in the comparison of pulse-to-pulse operation was that from the highly responsive dynamic thrust measurement system. Some of these data, shown in Figure 7-1, clearly displayed transient and steady-state operation.

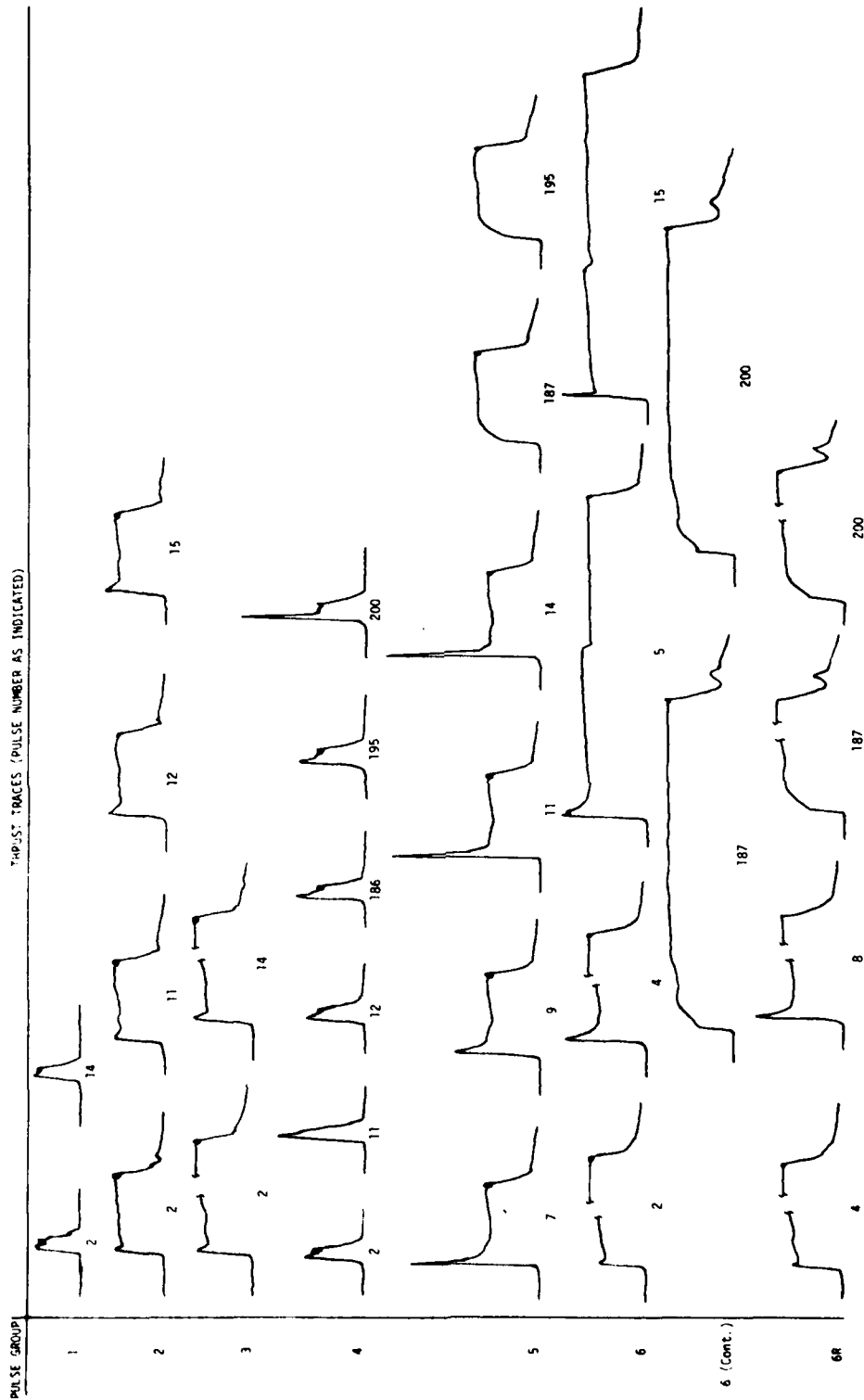


Figure 7-1. Test No. 512 Thrust Traces From Various Pulses of Each Pulse Group

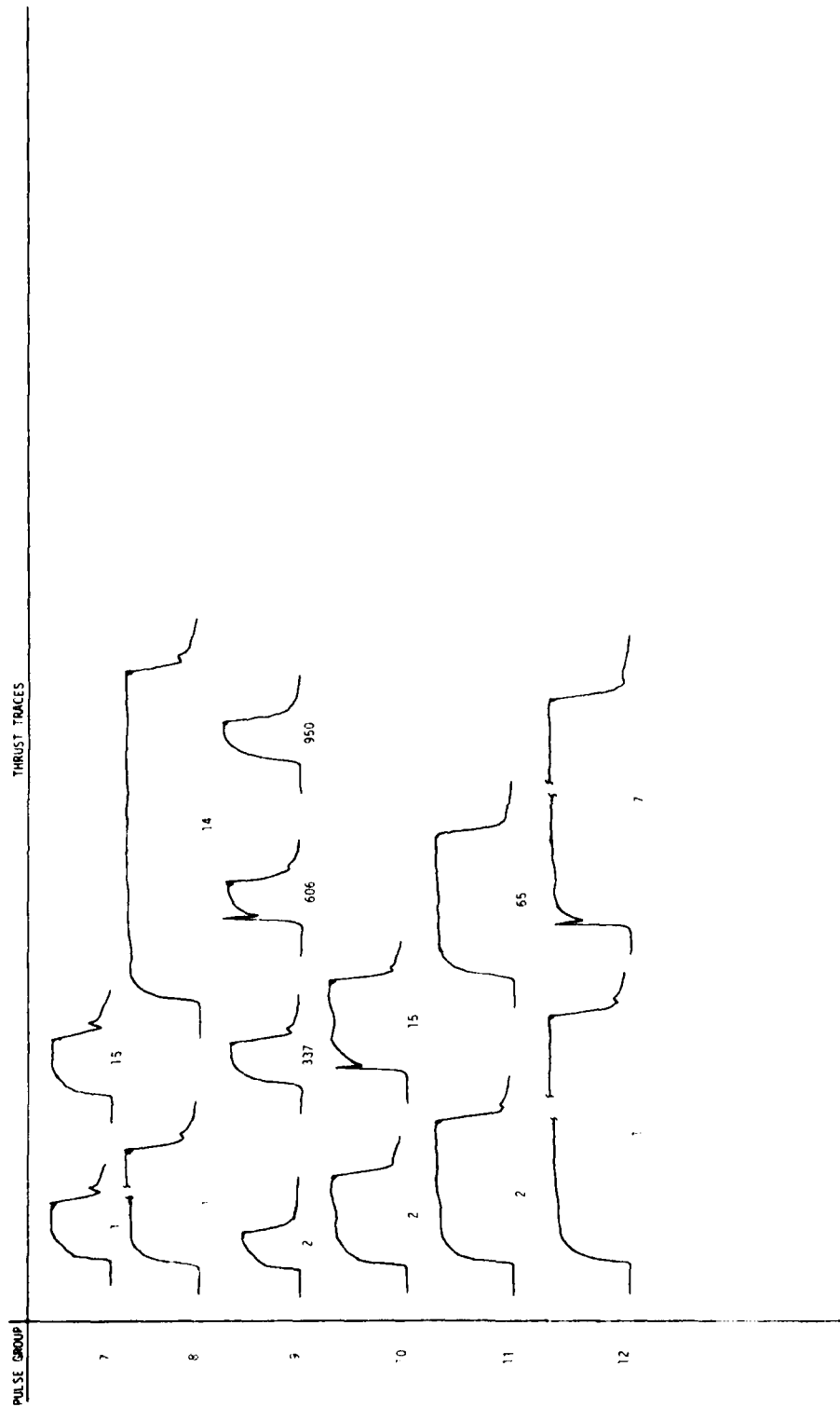


Figure 7-1. Test No. 512 Thrust Traces From Various Pulses of Each Pulse Group (Cont.)

7.3, Test Data Evaluation (cont.)

The initial Pulse Group consisted of 0.01 sec on-times with 60.0 sec coasts. Early and late pulses of this fifteen pulse series are shown in the Figure. This was followed by Pulse Group 2 with 0.03 sec on-times and 60.0 sec periods between pulses. Pulse numbers 2-2, -11, -12, and -15 are also shown. Pulses -12 and -15 show a slightly greater spike at start.

Pulse Group 3 operated with 0.12 sec on-times and 60.0 sec coasts for fifteen pulses. Early and late pulses indicate operation which is the same as the prior series. The subsequent Pulse Series 4 had 0.01 sec on-times with 5.0 sec coasts. These pulses incurred start transients with larger and more frequent start spikes. Early and later pulses in the series were very similar. These are shown by the traces of pulse numbers 4-2, -11, -12, -186, -195 and -200. The final pulse of the series (pulse No. -200) had a very large start spike which is indicated by a 300% deflection in the thrust trace.

It should be noted that only the first and last 15 pulses were monitored in each series. Thus there are no oscillograph traces for the pulses between 16 and 185.

Pulse Group 5 ran 0.03 sec on-times with 5.0 sec coasts. There were 200 pulses completed. The early pulses showed ignition spikes on about five of the fifteen pulses recorded. These are illustrated by pulses 5-5, -7, -9, -11, and -14. The subsequent pulses at the end of the series display entirely different transient characteristics, with little evidence of an ignition spike (ref. pulses 5-187 and -195). The final pulses showed a higher thrust than the early pulses of Pulse Group 5. An increase in the thrust and impulse is normally expected when the chamber is hotter, as discussed in previous sections.

Pulse Group 6 operated for on-times of 0.10 sec with 5.0 sec coasts. Two series of 200 pulses were made. The first series displayed bi-level operation on about one third of the initial 15 pulses. The final pulses had the same soft start characteristics of those seen at the end of Pulse Group 5. Pulse numbers 6-2, -4, -5 and -15 show the early firings. The subsequent firings are shown by pulses 6-187 and -200. The higher thrust portion of the bi-level tests appears to match that of the final pulses.

Pulse Group 6 was repeated following the discovery of the bi-level operation. This series is described as 6R in Figure 7-1. The repeat of Pulse Group 6 did not reproduce the bi-level operation; start transients on the early pulses were quite normal and similar to those of series 2 and 3. This is shown by traces from pulses 6R-4, -8 and -14. The traces from the

7.3, Test Data Evaluation (cont.)

final pulses of this series, 6R-187 and -200, are very similar to those of the latter part of the first Pulse Group 6. The initial conclusion during the testing was that the engine was operating normally.

Pulse Group 7 had 0.02 sec on-times with coasts of 1.0 sec. Traces from some of the first and last fifteen pulses of this 300 pulse series are also shown in Figure 7-1. Traces from pulses 7-1, -15, and -190 are typical; none show the ignition spike evident on earlier firings.

Pulse Group 8 ran 0.1 sec on-times and 0.9 sec coasts for a series of 155 pulses. The traces from pulses 8-1 and -14 are typical of this series. Testing was terminated when the TS measurement reached 450°F after pulse -155.

Pulse Group 9 ran 0.015 sec on-times and coasts of 0.135 sec. Typical traces are shown by pulses 9-2, -337, -696 and -950. Random data sampling in this series provided the traces for pulses -696 and -950. There was no evidence of an ignition spike on any of the pulses. Testing terminated after pulse -962 when TS reached 450°F.

Pulse Group 10 ran 0.030 sec on-times and coasts of 0.12 sec. Data from pulses 10-2, -15 and -169 are shown in Figure 7-1. There were several small start spikes evident, although most pulses were like those of series 9. The Pulse Group 10 series was stopped at pulse -171 (although 3000 had been planned) when the chamber head end indicated 450°F.

Pulse Series 11 had on-times of 0.045 sec with coasts of 0.105 sec. Typical traces from pulses 11-2 and -65 are shown. There was no evidence of start spikes. Again, the series was terminated due to high head end temperatures after 81 pulses.

Pulse Series 12 had on-times of 0.60 sec with coasts of 1.40 sec. It was programmed for 300 pulses but was terminated at pulse 21 due to high head end temperatures. Pulse traces 12-1 and -7 are shown. These are typical; no ignition spikes were evident.

Pulse Group 13 was to be a 300.0 sec continuous duration burn. It was terminated at 4.75 sec due to high head end temperatures.

7.4 TEST DATA INTERPRETATION

The fire testing of Injector 1-CAS SN 21 on the Test No. 512 pulse mode series disclosed normal operation on the initial three Pulse

7.4, Test Data Interpretation (cont.)

Groups. Pulse Group 4 displayed ignition spikes with a significant overshoot on the final pulse (4-200). Pulse Group 5 showed similar characteristics of the start of the series, with the unit becoming more smooth at the pulse group series completion. Pulse Group 6 displayed bi-level thrust operation on the early tests. All subsequent tests were smooth and essentially devoid of ignition spikes.

The latter pulse groups incurred higher than expected head end temperatures, higher than nominal thrusts, and a tendency toward higher MR operation. Posttest waterflow showed the injector's oxidizer ΔP to be reduced. Subsequent disassembly and visual examination showed the oxidizer orifice to be oversize and partially eroded.

The fire test data appears to indicate a progressive deterioration of the injector over Pulse Groups 4 and 5. It is unclear whether the ignition spike occurrences on these tests were the cause of, or the effect of, the deterioration. The attenuation of the P_c pressure measurement prevents the identification of "pops." The Kulite and Kistler pressure transducers located in the feed lines at the valve inlet show no evidence of manifold pops. It is possible that the ignition spikes in the thrust chamber forced minute amounts of fuel into the oxidizer manifold and that subsequent and repeated oxidizer manifold detonations caused enlargement of the oxidizer orifice. This appears to have been a self-correcting condition as the orifice enlargement either changed flow characteristics precluding subsequent ignition and/or manifold "pops" or precluded further damage to the orifice. The reduced oxidizer ΔP , however, resulted in a MR shift and/or flow change which disturbed the combustion at the upstream end of the chamber, causing an increased wall temperature.

The occurrence of ignition spikes appears to relate to the engine duty cycle. The Pulse Group 1 and 2 tests which had short on-times and long coasts provide sufficient opportunity for the manifolds to evacuate prior to the subsequent firing. The latter pulse groups with their reduced coast times and longer on-times operated with a hotter wall which reduces the ignition spike magnitude but, at the same time, will allow less time for the evacuation of the manifolds.

7.5 CONCLUSIONS

The physical changes in the engine hydraulics resulting from this test series result in an inability to perform continuous burns greater than 5 sec or to pulse at a rapid rate for extended periods. The ability to pulse at a low duty cycle without further engine degradation appears possible

7.5, Conclusions (cont.)

but has not been demonstrated. The conditions which led to the hard starts and the exact cause of the orifice enlargement require additional testing of Pulse Group 4, 5 and 6 with continuous data recording on all pulses.

SECTION 8.0

PROGRAM CONCLUSIONS AND RECOMMENDATIONS

8.0 PROGRAM CONCLUSIONS AND RECOMMENDATIONS

The development of the technology for a bipropellant thruster in the 0.5 lbF class has proven to be a challenging task in terms of design, fabricability, engine performance, and test measurement techniques for an engine with components of this minute size and low magnitude operational parameters.

8.1 CONCLUSIONS

While a 100% achievement of all contract goals has proven to be elusive significant advancements in small engine technology have been made that prove the feasibility of developing a 0.5 lbF class bipropellant engine. Encouraging results in all facets of design, fabrication and testing outweigh the problems that were encountered in the course of this program.

Steady-state durability of 8 hours of firing without failure has been demonstrated, along with a small impulse bit of $<0.005 \pm .0005$ lbF sec.

It is reasonable to predict that the same engine that ran 8 hours steady-state will be able to accomplish the 10-hour life goal based on its excellent postfire condition.

The pulsing duty cycle limitations encountered early in the 106 pulse durability test of the Phase III engine may, in fact, have been artificially created by the selection of a duty cycle that is much more rigorous than would be required in actual use. The rapid pulsing rate was selected to compress the 10-year life into a one-week time span.

Further testing is required to define the cause of hard engine starts which lead to gradual enlargement of the oxidizer orifice. Based on previous experience, there is reason to believe that simple structural reinforcement of the oxidizer orifice platelet would provide sufficient margin to preclude damage resulting from hard starts. In addition, a modified duty cycle with longer coast periods would result in a more complete evaluation of the injector, thereby minimizing hard starts.

8.1, Conclusions (cont.)

An engine performance (Isp) of 275 and 265 sec has been demonstrated in Phase II and III, respectively, of the program. These are lower than the program goal of 280 sec. Since the maximum chamber temperatures were 500°F less than allowable, further development could improve secondary mixing within the combustion chamber and raise performance. Improved secondary mixing might also attenuate the hard pulsing starts which could be caused by an accumulation of uncombusted propellant on the cold chamber wall.

Valve response, repeatability, life, engine minimum impulse bit requirements, and pulse repeatability were demonstrated on all configurations hot-fire tested.

All aspects of engine fabrication, i.e., platelets, valves, chambers, and metallurgical columbium-stainless steel assembly techniques, have been proven. Reproducibility of injectors and valves has been satisfactorily demonstrated to a degree commensurate with potential production requirements for these engines. The integration of the valve and injector, with the resultant low dribble volume required for the minimum plume contamination, has also been demonstrated. The selected valve and injector internal filtration system has been 100% successful in preventing clogging, flow decay, or other phenomena which could cause thrust reductions or mixture ratio shifts.

The unanticipated difficulties in testing, i.e., measurements of thrust and flowrates at the low flow and force ranges, have been overcome. Overall, Phase III testing has been efficient and has produced highly accurate, repeatable data.

8.2 RECOMMENDATIONS

The remaining elements for proper completion of the technology phase of the development of a 0.5 lbF class bipropellant engine are presented herein for consideration for future resource commitment.

1) Steady-state life testing on engine SN 22 should continue to provide chamber coating life data to at least 20 hours.

2) An in-depth evaluation of pulse train/duty cycle requirements must be undertaken to define minimum coasts between pulses accurately. A hot-fire test evaluation of the Phase III design, pertinent to the pulse train definition, should be systematically undertaken to determine

8.2, Recommendations (cont.)

its suitability for these requirements. If the required duty cycle cannot be achieved by this unit, further injector design upgrading would be required.

Combustion chamber configurations to create better propellant mixing should be evaluated, more so for reduction of plume contamination by unburnt propellants than for Isp increase. This, however, will be a by-product of combustion efficiency improvement. An analytical and experimental verification of theoretical nozzle losses should be undertaken to define performance potential more accurately. Testing of chambers with different area ratios (larger and smaller) and nozzle surface roughness due to the silicide coating would be useful. These data would advance the state-of-the-art in performance analysis of small bipropellant thrusters.

Execution of these recommendations would complete the technology required and ready the resulting engine for an advanced development phase.

APPENDIX A
INDUSTRY REQUIREMENTS SURVEY

Low Thrust Bipropellant Engine

1/2-POUND THRUSTER CAPABILITY SURVEY

Mission Aspects

1. After 1980, do you anticipate flying your satellites on any launch vehicles other than Space Shuttle?
If yes, which?
2. Do you expect most of your future satellites to be for commercial applications, military purposes, or scientific/applications oriented? (Please rank them 1-2-3, 1 = most, or indicate percentages, life 60% - 40% - 0%)

Commercial _____ Military _____ Scientific _____

3. How do you see the trend in mission life? With the advent of Space Shuttle, what will be the on-orbit life required? (Use the type satellite from question 2 as a basis)

- a. Will most of your missions be at altitudes above, say, 10,000 n.mi?
- b. If "yes", do you expect to use the Solid Spinning Upper Stages (SSUS-A, -D)?
- c. If "yes" to (b), would you expect to integrate apogee ΔV capability into your satellite?
- d. If "no" to (b), how would you accomplish transfer from Shuttle and circularization?
Comment?
- e. Have you considered, or are you considering, storable bipropellants for apogee ΔV ?
- f. Do you think use of storable bipropellants for apogee ΔV on your satellites is likely in the next 5 years?
- g. Do you think use of storable bipropellants for ACS on your satellites is likely in the next 5 years?
If either (f) or (g) are "no" would you care to comment?

ALRC CONCLUSIONS

50-50 Military-Commercial

3 to 6 Years
Greater than 10 Years

Today's Biprop ACS still not understood

5. Yes 2. No
Titan III, Ariane
Ten responses ranked military satellites ..
No. 1, nine responses ranked com'l satellites No. 1

Military 2 5 3
1-2 3-4 5-6
Com'l 1 2 7
5-6 7-9 10
7 10 1
Yes No Don't know
3 4
Yes No
3 Yes No
1 3
TUS Other
Integrated propulsion
16 3
Yes No
12 7
Yes No
6 12
Yes No

Low Thrust Bipropellant Engine

1/2-FOUND THRUSTER CAPABILITY SURVEY - SPACECRAFT SYSTEM CONSIDERATIONS

		ALRC CONCLUSIONS																																																																																																																																																																																																																																																																																																																																																																																																																								
1. What proportion of your new satellite designs in the next 5 years will be 3-axis stabilized versus spin stabilized?	<table border="1"> <tr> <td colspan="2">Mostly 3-axis</td> <td>17</td> </tr> <tr> <td colspan="2">About same</td> <td></td> </tr> <tr> <td colspan="2">Mostly spin</td> <td>1</td> </tr> </table>	Mostly 3-axis		17	About same			Mostly spin		1	3 Axis																																																																																																																																																																																																																																																																																																																																																																																																															
Mostly 3-axis		17																																																																																																																																																																																																																																																																																																																																																																																																																								
About same																																																																																																																																																																																																																																																																																																																																																																																																																										
Mostly spin		1																																																																																																																																																																																																																																																																																																																																																																																																																								
2. a. Do you consider plume contamination as a potential problem with hydrazine ACS?	<table border="1"> <tr> <td colspan="2">Biprop.</td> </tr> <tr> <td>Yes</td> <td>No</td> </tr> <tr> <td>1</td> <td>20</td> </tr> <tr> <td>No</td> <td>1</td> </tr> </table>	Biprop.		Yes	No	1	20	No	1	Contamination perceived to be a problem.																																																																																																																																																																																																																																																																																																																																																																																																																
Biprop.																																																																																																																																																																																																																																																																																																																																																																																																																										
Yes	No																																																																																																																																																																																																																																																																																																																																																																																																																									
1	20																																																																																																																																																																																																																																																																																																																																																																																																																									
No	1																																																																																																																																																																																																																																																																																																																																																																																																																									
b. Do you consider plume contamination as a potential problem with H_2O_2 /MMH ACS?	<table border="1"> <tr> <td colspan="2">Biprop.</td> </tr> <tr> <td>Yes</td> <td>No</td> </tr> <tr> <td>6</td> <td>5</td> </tr> <tr> <td>10</td> <td>10-20</td> </tr> <tr> <td></td> <td>>20</td> </tr> </table>	Biprop.		Yes	No	6	5	10	10-20		>20	10 watts reasonable																																																																																																																																																																																																																																																																																																																																																																																																														
Biprop.																																																																																																																																																																																																																																																																																																																																																																																																																										
Yes	No																																																																																																																																																																																																																																																																																																																																																																																																																									
6	5																																																																																																																																																																																																																																																																																																																																																																																																																									
10	10-20																																																																																																																																																																																																																																																																																																																																																																																																																									
	>20																																																																																																																																																																																																																																																																																																																																																																																																																									
3. a. If you had to use the spacecraft from thrusters a problem	<table border="1"> <tr> <td colspan="2">Biprop.</td> </tr> <tr> <td>Yes</td> <td>No</td> </tr> <tr> <td>3</td> <td>3</td> </tr> <tr> <td>6</td> <td>5</td> </tr> <tr> <td>10</td> <td>10-20</td> </tr> <tr> <td></td> <td>>20</td> </tr> </table>	Biprop.		Yes	No	3	3	6	5	10	10-20		>20	Design for Buried & Radiation																																																																																																																																																																																																																																																																																																																																																																																																												
Biprop.																																																																																																																																																																																																																																																																																																																																																																																																																										
Yes	No																																																																																																																																																																																																																																																																																																																																																																																																																									
3	3																																																																																																																																																																																																																																																																																																																																																																																																																									
6	5																																																																																																																																																																																																																																																																																																																																																																																																																									
10	10-20																																																																																																																																																																																																																																																																																																																																																																																																																									
	>20																																																																																																																																																																																																																																																																																																																																																																																																																									
b. How much heat input through conduction is acceptable from a given engine installation (in watts)?	<table border="1"> <tr> <td colspan="2">Biprop.</td> </tr> <tr> <td>Free to radiate</td> <td>Buried or insulated</td> </tr> <tr> <td>0</td> <td>0</td> </tr> <tr> <td>1</td> <td>2</td> </tr> <tr> <td>Both</td> <td></td> </tr> </table>	Biprop.		Free to radiate	Buried or insulated	0	0	1	2	Both																																																																																																																																																																																																																																																																																																																																																																																																																
Biprop.																																																																																																																																																																																																																																																																																																																																																																																																																										
Free to radiate	Buried or insulated																																																																																																																																																																																																																																																																																																																																																																																																																									
0	0																																																																																																																																																																																																																																																																																																																																																																																																																									
1	2																																																																																																																																																																																																																																																																																																																																																																																																																									
Both																																																																																																																																																																																																																																																																																																																																																																																																																										
c. How much heat input through radiation is acceptable?	<table border="1"> <tr> <td colspan="2">Biprop.</td> </tr> <tr> <td>Free to radiate</td> <td>Buried or insulated</td> </tr> <tr> <td>0</td> <td>0</td> </tr> <tr> <td>1</td> <td>2</td> </tr> <tr> <td>Both</td> <td></td> </tr> </table>	Biprop.		Free to radiate	Buried or insulated	0	0	1	2	Both																																																																																																																																																																																																																																																																																																																																																																																																																
Biprop.																																																																																																																																																																																																																																																																																																																																																																																																																										
Free to radiate	Buried or insulated																																																																																																																																																																																																																																																																																																																																																																																																																									
0	0																																																																																																																																																																																																																																																																																																																																																																																																																									
1	2																																																																																																																																																																																																																																																																																																																																																																																																																									
Both																																																																																																																																																																																																																																																																																																																																																																																																																										
d. Will ACS thruster nozzles normally be free to radiate or not?	<table border="1"> <tr> <td colspan="2">Biprop.</td> </tr> <tr> <td>Free to radiate</td> <td>Buried or insulated</td> </tr> <tr> <td>0</td> <td>0</td> </tr> <tr> <td>1</td> <td>2</td> </tr> <tr> <td>Both</td> <td></td> </tr> </table>	Biprop.		Free to radiate	Buried or insulated	0	0	1	2	Both																																																																																																																																																																																																																																																																																																																																																																																																																
Biprop.																																																																																																																																																																																																																																																																																																																																																																																																																										
Free to radiate	Buried or insulated																																																																																																																																																																																																																																																																																																																																																																																																																									
0	0																																																																																																																																																																																																																																																																																																																																																																																																																									
1	2																																																																																																																																																																																																																																																																																																																																																																																																																									
Both																																																																																																																																																																																																																																																																																																																																																																																																																										
e. Would ΔV engine nozzles normally be free to radiate or not?	<table border="1"> <tr> <td colspan="2">Biprop.</td> </tr> <tr> <td>Free to radiate</td> <td>Buried or insulated</td> </tr> <tr> <td>0</td> <td>0</td> </tr> <tr> <td>1</td> <td>2</td> </tr> <tr> <td>Both</td> <td></td> </tr> </table>	Biprop.		Free to radiate	Buried or insulated	0	0	1	2	Both																																																																																																																																																																																																																																																																																																																																																																																																																
Biprop.																																																																																																																																																																																																																																																																																																																																																																																																																										
Free to radiate	Buried or insulated																																																																																																																																																																																																																																																																																																																																																																																																																									
0	0																																																																																																																																																																																																																																																																																																																																																																																																																									
1	2																																																																																																																																																																																																																																																																																																																																																																																																																									
Both																																																																																																																																																																																																																																																																																																																																																																																																																										
4. By adding NO to H_2O_2 , the freezing point can be suppressed without appreciably affecting performance. What would be your preference for propellant temperature operating range? (MMH freezes at -62°F.)	<table border="1"> <tr> <td colspan="2">Biprop.</td> </tr> <tr> <td>+20°F to +120°F</td> <td>3</td> </tr> <tr> <td>0°F to +100°F</td> <td>7</td> </tr> <tr> <td>-20°F to +80°F</td> <td>6</td> </tr> <tr> <td>6 (4 from 1 Company)</td> <td></td> </tr> </table>	Biprop.		+20°F to +120°F	3	0°F to +100°F	7	-20°F to +80°F	6	6 (4 from 1 Company)		0° F to 100 °F preferred																																																																																																																																																																																																																																																																																																																																																																																																														
Biprop.																																																																																																																																																																																																																																																																																																																																																																																																																										
+20°F to +120°F	3																																																																																																																																																																																																																																																																																																																																																																																																																									
0°F to +100°F	7																																																																																																																																																																																																																																																																																																																																																																																																																									
-20°F to +80°F	6																																																																																																																																																																																																																																																																																																																																																																																																																									
6 (4 from 1 Company)																																																																																																																																																																																																																																																																																																																																																																																																																										
5. What is the most stringent minimum impulse bit required by your satellite control subsystems for a half-pound-class thruster (including down to 0.1 lbf thrusters)?	<table border="1"> <tr> <td colspan="2">Biprop.</td> </tr> <tr> <td>(lb-sec)</td> <td>2</td> </tr> <tr> <td>0.001</td> <td>0.001</td> </tr> <tr> <td>0.003</td> <td>0.004</td> </tr> <tr> <td>0.01</td> <td>0.01</td> </tr> <tr> <td>0.02</td> <td>0.02</td> </tr> <tr> <td>0.03</td> <td>0.03</td> </tr> <tr> <td>0.04</td> <td>0.04</td> </tr> <tr> <td>0.05</td> <td>0.05</td> </tr> <tr> <td>0.06</td> <td>0.06</td> </tr> <tr> <td>0.07</td> <td>0.07</td> </tr> <tr> <td>0.08</td> <td>0.08</td> </tr> <tr> <td>0.09</td> <td>0.09</td> </tr> <tr> <td>0.1</td> <td>0.1</td> </tr> <tr> <td>0.11</td> <td>0.11</td> </tr> <tr> <td>0.12</td> <td>0.12</td> </tr> <tr> <td>0.13</td> <td>0.13</td> </tr> <tr> <td>0.14</td> <td>0.14</td> </tr> <tr> <td>0.15</td> <td>0.15</td> </tr> <tr> <td>0.16</td> <td>0.16</td> </tr> <tr> <td>0.17</td> <td>0.17</td> </tr> <tr> <td>0.18</td> <td>0.18</td> </tr> <tr> <td>0.19</td> <td>0.19</td> </tr> <tr> <td>0.2</td> <td>0.2</td> </tr> <tr> <td>0.21</td> <td>0.21</td> </tr> <tr> <td>0.22</td> <td>0.22</td> </tr> <tr> <td>0.23</td> <td>0.23</td> </tr> <tr> <td>0.24</td> <td>0.24</td> </tr> <tr> <td>0.25</td> <td>0.25</td> </tr> <tr> <td>0.26</td> <td>0.26</td> </tr> <tr> <td>0.27</td> <td>0.27</td> </tr> <tr> <td>0.28</td> <td>0.28</td> </tr> <tr> <td>0.29</td> <td>0.29</td> </tr> <tr> <td>0.3</td> <td>0.3</td> </tr> <tr> <td>0.31</td> <td>0.31</td> </tr> <tr> <td>0.32</td> <td>0.32</td> </tr> <tr> <td>0.33</td> <td>0.33</td> </tr> <tr> <td>0.34</td> <td>0.34</td> </tr> <tr> <td>0.35</td> <td>0.35</td> </tr> <tr> <td>0.36</td> <td>0.36</td> </tr> <tr> <td>0.37</td> <td>0.37</td> </tr> <tr> <td>0.38</td> <td>0.38</td> </tr> <tr> <td>0.39</td> <td>0.39</td> </tr> <tr> <td>0.4</td> <td>0.4</td> </tr> <tr> <td>0.41</td> <td>0.41</td> </tr> <tr> <td>0.42</td> <td>0.42</td> </tr> <tr> <td>0.43</td> <td>0.43</td> </tr> <tr> <td>0.44</td> <td>0.44</td> </tr> <tr> <td>0.45</td> <td>0.45</td> </tr> <tr> <td>0.46</td> <td>0.46</td> </tr> <tr> <td>0.47</td> <td>0.47</td> </tr> <tr> <td>0.48</td> <td>0.48</td> </tr> <tr> <td>0.49</td> <td>0.49</td> </tr> <tr> <td>0.5</td> <td>0.5</td> </tr> <tr> <td>0.51</td> <td>0.51</td> </tr> <tr> <td>0.52</td> <td>0.52</td> </tr> <tr> <td>0.53</td> <td>0.53</td> </tr> <tr> <td>0.54</td> <td>0.54</td> </tr> <tr> <td>0.55</td> <td>0.55</td> </tr> <tr> <td>0.56</td> <td>0.56</td> </tr> <tr> <td>0.57</td> <td>0.57</td> </tr> <tr> <td>0.58</td> <td>0.58</td> </tr> <tr> <td>0.59</td> <td>0.59</td> </tr> <tr> <td>0.6</td> <td>0.6</td> </tr> <tr> <td>0.61</td> <td>0.61</td> </tr> <tr> <td>0.62</td> <td>0.62</td> </tr> <tr> <td>0.63</td> <td>0.63</td> </tr> <tr> <td>0.64</td> <td>0.64</td> </tr> <tr> <td>0.65</td> <td>0.65</td> </tr> <tr> <td>0.66</td> <td>0.66</td> </tr> <tr> <td>0.67</td> <td>0.67</td> </tr> <tr> <td>0.68</td> <td>0.68</td> </tr> <tr> <td>0.69</td> <td>0.69</td> </tr> <tr> <td>0.7</td> <td>0.7</td> </tr> <tr> <td>0.71</td> <td>0.71</td> </tr> <tr> <td>0.72</td> <td>0.72</td> </tr> <tr> <td>0.73</td> <td>0.73</td> </tr> <tr> <td>0.74</td> <td>0.74</td> </tr> <tr> <td>0.75</td> <td>0.75</td> </tr> <tr> <td>0.76</td> <td>0.76</td> </tr> <tr> <td>0.77</td> <td>0.77</td> </tr> <tr> <td>0.78</td> <td>0.78</td> </tr> <tr> <td>0.79</td> <td>0.79</td> </tr> <tr> <td>0.8</td> <td>0.8</td> </tr> <tr> <td>0.81</td> <td>0.81</td> </tr> <tr> <td>0.82</td> <td>0.82</td> </tr> <tr> <td>0.83</td> <td>0.83</td> </tr> <tr> <td>0.84</td> <td>0.84</td> </tr> <tr> <td>0.85</td> <td>0.85</td> </tr> <tr> <td>0.86</td> <td>0.86</td> </tr> <tr> <td>0.87</td> <td>0.87</td> </tr> <tr> <td>0.88</td> <td>0.88</td> </tr> <tr> <td>0.89</td> <td>0.89</td> </tr> <tr> <td>0.9</td> <td>0.9</td> </tr> <tr> <td>0.91</td> <td>0.91</td> </tr> <tr> <td>0.92</td> <td>0.92</td> </tr> <tr> <td>0.93</td> <td>0.93</td> </tr> <tr> <td>0.94</td> <td>0.94</td> </tr> <tr> <td>0.95</td> <td>0.95</td> </tr> <tr> <td>0.96</td> <td>0.96</td> </tr> <tr> <td>0.97</td> <td>0.97</td> </tr> <tr> <td>0.98</td> <td>0.98</td> </tr> <tr> <td>0.99</td> <td>0.99</td> </tr> <tr> <td>1.0</td> <td>1.0</td> </tr> <tr> <td>1.01</td> <td>1.01</td> </tr> <tr> <td>1.02</td> <td>1.02</td> </tr> <tr> <td>1.03</td> <td>1.03</td> </tr> <tr> <td>1.04</td> <td>1.04</td> </tr> <tr> <td>1.05</td> <td>1.05</td> </tr> <tr> <td>1.06</td> <td>1.06</td> </tr> <tr> <td>1.07</td> <td>1.07</td> </tr> <tr> <td>1.08</td> <td>1.08</td> </tr> <tr> <td>1.09</td> <td>1.09</td> </tr> <tr> <td>1.1</td> <td>1.1</td> </tr> <tr> <td>1.11</td> <td>1.11</td> </tr> <tr> <td>1.12</td> <td>1.12</td> </tr> <tr> <td>1.13</td> <td>1.13</td> </tr> <tr> <td>1.14</td> <td>1.14</td> </tr> <tr> <td>1.15</td> <td>1.15</td> </tr> <tr> <td>1.16</td> <td>1.16</td> </tr> <tr> <td>1.17</td> <td>1.17</td> </tr> <tr> <td>1.18</td> <td>1.18</td> </tr> <tr> <td>1.19</td> <td>1.19</td> </tr> <tr> <td>1.2</td> <td>1.2</td> </tr> <tr> <td>1.21</td> <td>1.21</td> </tr> <tr> <td>1.22</td> <td>1.22</td> </tr> <tr> <td>1.23</td> <td>1.23</td> </tr> <tr> <td>1.24</td> <td>1.24</td> </tr> <tr> <td>1.25</td> <td>1.25</td> </tr> <tr> <td>1.26</td> <td>1.26</td> </tr> <tr> <td>1.27</td> <td>1.27</td> </tr> <tr> <td>1.28</td> <td>1.28</td> </tr> <tr> <td>1.29</td> <td>1.29</td> </tr> <tr> <td>1.3</td> <td>1.3</td> </tr> <tr> <td>1.31</td> <td>1.31</td> </tr> <tr> <td>1.32</td> <td>1.32</td> </tr> <tr> <td>1.33</td> <td>1.33</td> </tr> <tr> <td>1.34</td> <td>1.34</td> </tr> <tr> <td>1.35</td> <td>1.35</td> </tr> <tr> <td>1.36</td> <td>1.36</td> </tr> <tr> <td>1.37</td> <td>1.37</td> </tr> <tr> <td>1.38</td> <td>1.38</td> </tr> <tr> <td>1.39</td> <td>1.39</td> </tr> <tr> <td>1.4</td> <td>1.4</td> </tr> <tr> <td>1.41</td> <td>1.41</td> </tr> <tr> <td>1.42</td> <td>1.42</td> </tr> <tr> <td>1.43</td> <td>1.43</td> </tr> <tr> <td>1.44</td> <td>1.44</td> </tr> <tr> <td>1.45</td> <td>1.45</td> </tr> <tr> <td>1.46</td> <td>1.46</td> </tr> <tr> <td>1.47</td> <td>1.47</td> </tr> <tr> <td>1.48</td> <td>1.48</td> </tr> <tr> <td>1.49</td> <td>1.49</td> </tr> <tr> <td>1.5</td> <td>1.5</td> </tr> <tr> <td>1.51</td> <td>1.51</td> </tr> <tr> <td>1.52</td> <td>1.52</td> </tr> <tr> <td>1.53</td> <td>1.53</td> </tr> <tr> <td>1.54</td> <td>1.54</td> </tr> <tr> <td>1.55</td> <td>1.55</td> </tr> <tr> <td>1.56</td> <td>1.56</td> </tr> <tr> <td>1.57</td> <td>1.57</td> </tr> <tr> <td>1.58</td> <td>1.58</td> </tr> <tr> <td>1.59</td> <td>1.59</td> </tr> <tr> <td>1.6</td> <td>1.6</td> </tr> <tr> <td>1.61</td> <td>1.61</td> </tr> <tr> <td>1.62</td> <td>1.62</td> </tr> <tr> <td>1.63</td> <td>1.63</td> </tr> <tr> <td>1.64</td> <td>1.64</td> </tr> <tr> <td>1.65</td> <td>1.65</td> </tr> <tr> <td>1.66</td> <td>1.66</td> </tr> <tr> <td>1.67</td> <td>1.67</td> </tr> <tr> <td>1.68</td> <td>1.68</td> </tr> <tr> <td>1.69</td> <td>1.69</td> </tr> <tr> <td>1.7</td> <td>1.7</td> </tr> <tr> <td>1.71</td> <td>1.71</td> </tr> <tr> <td>1.72</td> <td>1.72</td> </tr> <tr> <td>1.73</td> <td>1.73</td> </tr> <tr> <td>1.74</td> <td>1.74</td> </tr> <tr> <td>1.75</td> <td>1.75</td> </tr> <tr> <td>1.76</td> <td>1.76</td> </tr> <tr> <td>1.77</td> <td>1.77</td> </tr> <tr> <td>1.78</td> <td>1.78</td> </tr> <tr> <td>1.79</td> <td>1.79</td> </tr> <tr> <td>1.8</td> <td>1.8</td> </tr> <tr> <td>1.81</td> <td>1.81</td> </tr> <tr> <td>1.82</td> <td>1.82</td> </tr> <tr> <td>1.83</td> <td>1.83</td> </tr> <tr> <td>1.84</td> <td>1.84</td> </tr> <tr> <td>1.85</td> <td>1.85</td> </tr> <tr> <td>1.86</td> <td>1.86</td> </tr> <tr> <td>1.87</td> <td>1.87</td> </tr> <tr> <td>1.88</td> <td>1.88</td> </tr> <tr> <td>1.89</td> <td>1.89</td> </tr> <tr> <td>1.9</td> <td>1.9</td> </tr> <tr> <td>1.91</td> <td>1.91</td> </tr> <tr> <td>1.92</td> <td>1.92</td> </tr> <tr> <td>1.93</td> <td>1.93</td> </tr> <tr> <td>1.94</td> <td>1.94</td> </tr> <tr> <td>1.95</td> <td>1.95</td> </tr> <tr> <td>1.96</td> <td>1.96</td> </tr> <tr> <td>1.97</td> <td>1.97</td> </tr> <tr> <td>1.98</td> <td>1.98</td> </tr> <tr> <td>1.99</td> <td>1.99</td> </tr> <tr> <td>2.0</td> <td>2.0</td> </tr> </table>	Biprop.		(lb-sec)	2	0.001	0.001	0.003	0.004	0.01	0.01	0.02	0.02	0.03	0.03	0.04	0.04	0.05	0.05	0.06	0.06	0.07	0.07	0.08	0.08	0.09	0.09	0.1	0.1	0.11	0.11	0.12	0.12	0.13	0.13	0.14	0.14	0.15	0.15	0.16	0.16	0.17	0.17	0.18	0.18	0.19	0.19	0.2	0.2	0.21	0.21	0.22	0.22	0.23	0.23	0.24	0.24	0.25	0.25	0.26	0.26	0.27	0.27	0.28	0.28	0.29	0.29	0.3	0.3	0.31	0.31	0.32	0.32	0.33	0.33	0.34	0.34	0.35	0.35	0.36	0.36	0.37	0.37	0.38	0.38	0.39	0.39	0.4	0.4	0.41	0.41	0.42	0.42	0.43	0.43	0.44	0.44	0.45	0.45	0.46	0.46	0.47	0.47	0.48	0.48	0.49	0.49	0.5	0.5	0.51	0.51	0.52	0.52	0.53	0.53	0.54	0.54	0.55	0.55	0.56	0.56	0.57	0.57	0.58	0.58	0.59	0.59	0.6	0.6	0.61	0.61	0.62	0.62	0.63	0.63	0.64	0.64	0.65	0.65	0.66	0.66	0.67	0.67	0.68	0.68	0.69	0.69	0.7	0.7	0.71	0.71	0.72	0.72	0.73	0.73	0.74	0.74	0.75	0.75	0.76	0.76	0.77	0.77	0.78	0.78	0.79	0.79	0.8	0.8	0.81	0.81	0.82	0.82	0.83	0.83	0.84	0.84	0.85	0.85	0.86	0.86	0.87	0.87	0.88	0.88	0.89	0.89	0.9	0.9	0.91	0.91	0.92	0.92	0.93	0.93	0.94	0.94	0.95	0.95	0.96	0.96	0.97	0.97	0.98	0.98	0.99	0.99	1.0	1.0	1.01	1.01	1.02	1.02	1.03	1.03	1.04	1.04	1.05	1.05	1.06	1.06	1.07	1.07	1.08	1.08	1.09	1.09	1.1	1.1	1.11	1.11	1.12	1.12	1.13	1.13	1.14	1.14	1.15	1.15	1.16	1.16	1.17	1.17	1.18	1.18	1.19	1.19	1.2	1.2	1.21	1.21	1.22	1.22	1.23	1.23	1.24	1.24	1.25	1.25	1.26	1.26	1.27	1.27	1.28	1.28	1.29	1.29	1.3	1.3	1.31	1.31	1.32	1.32	1.33	1.33	1.34	1.34	1.35	1.35	1.36	1.36	1.37	1.37	1.38	1.38	1.39	1.39	1.4	1.4	1.41	1.41	1.42	1.42	1.43	1.43	1.44	1.44	1.45	1.45	1.46	1.46	1.47	1.47	1.48	1.48	1.49	1.49	1.5	1.5	1.51	1.51	1.52	1.52	1.53	1.53	1.54	1.54	1.55	1.55	1.56	1.56	1.57	1.57	1.58	1.58	1.59	1.59	1.6	1.6	1.61	1.61	1.62	1.62	1.63	1.63	1.64	1.64	1.65	1.65	1.66	1.66	1.67	1.67	1.68	1.68	1.69	1.69	1.7	1.7	1.71	1.71	1.72	1.72	1.73	1.73	1.74	1.74	1.75	1.75	1.76	1.76	1.77	1.77	1.78	1.78	1.79	1.79	1.8	1.8	1.81	1.81	1.82	1.82	1.83	1.83	1.84	1.84	1.85	1.85	1.86	1.86	1.87	1.87	1.88	1.88	1.89	1.89	1.9	1.9	1.91	1.91	1.92	1.92	1.93	1.93	1.94	1.94	1.95	1.95	1.96	1.96	1.97	1.97	1.98	1.98	1.99	1.99	2.0	2.0	.001-.003 Design Interval 5-pounder was on target Need for Biprops is implicit here Need for Biprops is implicit here
Biprop.																																																																																																																																																																																																																																																																																																																																																																																																																										
(lb-sec)	2																																																																																																																																																																																																																																																																																																																																																																																																																									
0.001	0.001																																																																																																																																																																																																																																																																																																																																																																																																																									
0.003	0.004																																																																																																																																																																																																																																																																																																																																																																																																																									
0.01	0.01																																																																																																																																																																																																																																																																																																																																																																																																																									
0.02	0.02																																																																																																																																																																																																																																																																																																																																																																																																																									
0.03	0.03																																																																																																																																																																																																																																																																																																																																																																																																																									
0.04	0.04																																																																																																																																																																																																																																																																																																																																																																																																																									
0.05	0.05																																																																																																																																																																																																																																																																																																																																																																																																																									
0.06	0.06																																																																																																																																																																																																																																																																																																																																																																																																																									
0.07	0.07																																																																																																																																																																																																																																																																																																																																																																																																																									
0.08	0.08																																																																																																																																																																																																																																																																																																																																																																																																																									
0.09	0.09																																																																																																																																																																																																																																																																																																																																																																																																																									
0.1	0.1																																																																																																																																																																																																																																																																																																																																																																																																																									
0.11	0.11																																																																																																																																																																																																																																																																																																																																																																																																																									
0.12	0.12																																																																																																																																																																																																																																																																																																																																																																																																																									
0.13	0.13																																																																																																																																																																																																																																																																																																																																																																																																																									
0.14	0.14																																																																																																																																																																																																																																																																																																																																																																																																																									
0.15	0.15																																																																																																																																																																																																																																																																																																																																																																																																																									
0.16	0.16																																																																																																																																																																																																																																																																																																																																																																																																																									
0.17	0.17																																																																																																																																																																																																																																																																																																																																																																																																																									
0.18	0.18																																																																																																																																																																																																																																																																																																																																																																																																																									
0.19	0.19																																																																																																																																																																																																																																																																																																																																																																																																																									
0.2	0.2																																																																																																																																																																																																																																																																																																																																																																																																																									
0.21	0.21																																																																																																																																																																																																																																																																																																																																																																																																																									
0.22	0.22																																																																																																																																																																																																																																																																																																																																																																																																																									
0.23	0.23																																																																																																																																																																																																																																																																																																																																																																																																																									
0.24	0.24																																																																																																																																																																																																																																																																																																																																																																																																																									
0.25	0.25																																																																																																																																																																																																																																																																																																																																																																																																																									
0.26	0.26																																																																																																																																																																																																																																																																																																																																																																																																																									
0.27	0.27																																																																																																																																																																																																																																																																																																																																																																																																																									
0.28	0.28																																																																																																																																																																																																																																																																																																																																																																																																																									
0.29	0.29																																																																																																																																																																																																																																																																																																																																																																																																																									
0.3	0.3																																																																																																																																																																																																																																																																																																																																																																																																																									
0.31	0.31																																																																																																																																																																																																																																																																																																																																																																																																																									
0.32	0.32																																																																																																																																																																																																																																																																																																																																																																																																																									
0.33	0.33																																																																																																																																																																																																																																																																																																																																																																																																																									
0.34	0.34																																																																																																																																																																																																																																																																																																																																																																																																																									
0.35	0.35																																																																																																																																																																																																																																																																																																																																																																																																																									
0.36	0.36																																																																																																																																																																																																																																																																																																																																																																																																																									
0.37	0.37																																																																																																																																																																																																																																																																																																																																																																																																																									
0.38	0.38																																																																																																																																																																																																																																																																																																																																																																																																																									
0.39	0.39																																																																																																																																																																																																																																																																																																																																																																																																																									
0.4	0.4																																																																																																																																																																																																																																																																																																																																																																																																																									
0.41	0.41																																																																																																																																																																																																																																																																																																																																																																																																																									
0.42	0.42																																																																																																																																																																																																																																																																																																																																																																																																																									
0.43	0.43																																																																																																																																																																																																																																																																																																																																																																																																																									
0.44	0.44																																																																																																																																																																																																																																																																																																																																																																																																																									
0.45	0.45																																																																																																																																																																																																																																																																																																																																																																																																																									
0.46	0.46																																																																																																																																																																																																																																																																																																																																																																																																																									
0.47	0.47																																																																																																																																																																																																																																																																																																																																																																																																																									
0.48	0.48																																																																																																																																																																																																																																																																																																																																																																																																																									
0.49	0.49																																																																																																																																																																																																																																																																																																																																																																																																																									
0.5	0.5																																																																																																																																																																																																																																																																																																																																																																																																																									
0.51	0.51																																																																																																																																																																																																																																																																																																																																																																																																																									
0.52	0.52																																																																																																																																																																																																																																																																																																																																																																																																																									
0.53	0.53																																																																																																																																																																																																																																																																																																																																																																																																																									
0.54	0.54																																																																																																																																																																																																																																																																																																																																																																																																																									
0.55	0.55																																																																																																																																																																																																																																																																																																																																																																																																																									
0.56	0.56																																																																																																																																																																																																																																																																																																																																																																																																																									
0.57	0.57																																																																																																																																																																																																																																																																																																																																																																																																																									
0.58	0.58																																																																																																																																																																																																																																																																																																																																																																																																																									
0.59	0.59																																																																																																																																																																																																																																																																																																																																																																																																																									
0.6	0.6																																																																																																																																																																																																																																																																																																																																																																																																																									
0.61	0.61																																																																																																																																																																																																																																																																																																																																																																																																																									
0.62	0.62																																																																																																																																																																																																																																																																																																																																																																																																																									
0.63	0.63																																																																																																																																																																																																																																																																																																																																																																																																																									
0.64	0.64																																																																																																																																																																																																																																																																																																																																																																																																																									
0.65	0.65																																																																																																																																																																																																																																																																																																																																																																																																																									
0.66	0.66																																																																																																																																																																																																																																																																																																																																																																																																																									
0.67	0.67																																																																																																																																																																																																																																																																																																																																																																																																																									
0.68	0.68																																																																																																																																																																																																																																																																																																																																																																																																																									
0.69	0.69																																																																																																																																																																																																																																																																																																																																																																																																																									
0.7	0.7																																																																																																																																																																																																																																																																																																																																																																																																																									
0.71	0.71																																																																																																																																																																																																																																																																																																																																																																																																																									
0.72	0.72																																																																																																																																																																																																																																																																																																																																																																																																																									
0.73	0.73																																																																																																																																																																																																																																																																																																																																																																																																																									
0.74	0.74																																																																																																																																																																																																																																																																																																																																																																																																																									
0.75	0.75																																																																																																																																																																																																																																																																																																																																																																																																																									
0.76	0.76																																																																																																																																																																																																																																																																																																																																																																																																																									
0.77	0.77																																																																																																																																																																																																																																																																																																																																																																																																																									
0.78	0.78																																																																																																																																																																																																																																																																																																																																																																																																																									
0.79	0.79																																																																																																																																																																																																																																																																																																																																																																																																																									
0.8	0.8																																																																																																																																																																																																																																																																																																																																																																																																																									
0.81	0.81																																																																																																																																																																																																																																																																																																																																																																																																																									
0.82	0.82																																																																																																																																																																																																																																																																																																																																																																																																																									
0.83	0.83																																																																																																																																																																																																																																																																																																																																																																																																																									
0.84	0.84																																																																																																																																																																																																																																																																																																																																																																																																																									
0.85	0.85																																																																																																																																																																																																																																																																																																																																																																																																																									
0.86	0.86																																																																																																																																																																																																																																																																																																																																																																																																																									
0.87	0.87																																																																																																																																																																																																																																																																																																																																																																																																																									
0.88	0.88																																																																																																																																																																																																																																																																																																																																																																																																																									
0.89	0.89																																																																																																																																																																																																																																																																																																																																																																																																																									
0.9	0.9																																																																																																																																																																																																																																																																																																																																																																																																																									
0.91	0.91																																																																																																																																																																																																																																																																																																																																																																																																																									
0.92	0.92																																																																																																																																																																																																																																																																																																																																																																																																																									
0.93	0.93																																																																																																																																																																																																																																																																																																																																																																																																																									
0.94	0.94																																																																																																																																																																																																																																																																																																																																																																																																																									
0.95	0.95																																																																																																																																																																																																																																																																																																																																																																																																																									
0.96	0.96																																																																																																																																																																																																																																																																																																																																																																																																																									
0.97	0.97																																																																																																																																																																																																																																																																																																																																																																																																																									
0.98	0.98																																																																																																																																																																																																																																																																																																																																																																																																																									
0.99	0.99																																																																																																																																																																																																																																																																																																																																																																																																																									
1.0	1.0																																																																																																																																																																																																																																																																																																																																																																																																																									
1.01	1.01																																																																																																																																																																																																																																																																																																																																																																																																																									
1.02	1.02																																																																																																																																																																																																																																																																																																																																																																																																																									
1.03	1.03																																																																																																																																																																																																																																																																																																																																																																																																																									
1.04	1.04																																																																																																																																																																																																																																																																																																																																																																																																																									
1.05	1.05																																																																																																																																																																																																																																																																																																																																																																																																																									
1.06	1.06																																																																																																																																																																																																																																																																																																																																																																																																																									
1.07	1.07																																																																																																																																																																																																																																																																																																																																																																																																																									
1.08	1.08																																																																																																																																																																																																																																																																																																																																																																																																																									
1.09	1.09																																																																																																																																																																																																																																																																																																																																																																																																																									
1.1	1.1																																																																																																																																																																																																																																																																																																																																																																																																																									
1.11	1.11																																																																																																																																																																																																																																																																																																																																																																																																																									
1.12	1.12																																																																																																																																																																																																																																																																																																																																																																																																																									
1.13	1.13																																																																																																																																																																																																																																																																																																																																																																																																																									
1.14	1.14																																																																																																																																																																																																																																																																																																																																																																																																																									
1.15	1.15																																																																																																																																																																																																																																																																																																																																																																																																																									
1.16	1.16																																																																																																																																																																																																																																																																																																																																																																																																																									
1.17	1.17																																																																																																																																																																																																																																																																																																																																																																																																																									
1.18	1.18																																																																																																																																																																																																																																																																																																																																																																																																																									
1.19	1.19																																																																																																																																																																																																																																																																																																																																																																																																																									
1.2	1.2																																																																																																																																																																																																																																																																																																																																																																																																																									
1.21	1.21																																																																																																																																																																																																																																																																																																																																																																																																																									
1.22	1.22																																																																																																																																																																																																																																																																																																																																																																																																																									
1.23	1.23																																																																																																																																																																																																																																																																																																																																																																																																																									
1.24	1.24																																																																																																																																																																																																																																																																																																																																																																																																																									
1.25	1.25																																																																																																																																																																																																																																																																																																																																																																																																																									
1.26	1.26																																																																																																																																																																																																																																																																																																																																																																																																																									
1.27	1.27																																																																																																																																																																																																																																																																																																																																																																																																																									
1.28	1.28																																																																																																																																																																																																																																																																																																																																																																																																																									
1.29	1.29																																																																																																																																																																																																																																																																																																																																																																																																																									
1.3	1.3																																																																																																																																																																																																																																																																																																																																																																																																																									
1.31	1.31																																																																																																																																																																																																																																																																																																																																																																																																																									
1.32	1.32																																																																																																																																																																																																																																																																																																																																																																																																																									
1.33	1.33																																																																																																																																																																																																																																																																																																																																																																																																																									
1.34	1.34																																																																																																																																																																																																																																																																																																																																																																																																																									
1.35	1.35																																																																																																																																																																																																																																																																																																																																																																																																																									
1.36	1.36																																																																																																																																																																																																																																																																																																																																																																																																																									
1.37	1.37																																																																																																																																																																																																																																																																																																																																																																																																																									
1.38	1.38																																																																																																																																																																																																																																																																																																																																																																																																																									
1.39	1.39																																																																																																																																																																																																																																																																																																																																																																																																																									
1.4	1.4																																																																																																																																																																																																																																																																																																																																																																																																																									
1.41	1.41																																																																																																																																																																																																																																																																																																																																																																																																																									
1.42	1.42																																																																																																																																																																																																																																																																																																																																																																																																																									
1.43	1.43																																																																																																																																																																																																																																																																																																																																																																																																																									
1.44	1.44																																																																																																																																																																																																																																																																																																																																																																																																																									
1.45	1.45																																																																																																																																																																																																																																																																																																																																																																																																																									
1.46	1.46																																																																																																																																																																																																																																																																																																																																																																																																																									
1.47	1.47																																																																																																																																																																																																																																																																																																																																																																																																																									
1.48	1.48																																																																																																																																																																																																																																																																																																																																																																																																																									
1.49	1.49																																																																																																																																																																																																																																																																																																																																																																																																																									
1.5	1.5																																																																																																																																																																																																																																																																																																																																																																																																																									
1.51	1.51																																																																																																																																																																																																																																																																																																																																																																																																																									
1.52	1.52																																																																																																																																																																																																																																																																																																																																																																																																																									
1.53	1.53																																																																																																																																																																																																																																																																																																																																																																																																																									
1.54	1.54																																																																																																																																																																																																																																																																																																																																																																																																																									
1.55	1.55																																																																																																																																																																																																																																																																																																																																																																																																																									
1.56	1.56																																																																																																																																																																																																																																																																																																																																																																																																																									
1.57	1.57																																																																																																																																																																																																																																																																																																																																																																																																																									
1.58	1.58																																																																																																																																																																																																																																																																																																																																																																																																																									
1.59	1.59																																																																																																																																																																																																																																																																																																																																																																																																																									
1.6	1.6																																																																																																																																																																																																																																																																																																																																																																																																																									
1.61	1.61																																																																																																																																																																																																																																																																																																																																																																																																																									
1.62	1.62																																																																																																																																																																																																																																																																																																																																																																																																																									
1.63	1.63																																																																																																																																																																																																																																																																																																																																																																																																																									
1.64	1.64																																																																																																																																																																																																																																																																																																																																																																																																																									
1.65	1.65																																																																																																																																																																																																																																																																																																																																																																																																																									
1.66	1.66																																																																																																																																																																																																																																																																																																																																																																																																																									
1.67	1.67																																																																																																																																																																																																																																																																																																																																																																																																																									
1.68	1.68																																																																																																																																																																																																																																																																																																																																																																																																																									
1.69	1.69																																																																																																																																																																																																																																																																																																																																																																																																																									
1.7	1.7																																																																																																																																																																																																																																																																																																																																																																																																																									
1.71	1.71																																																																																																																																																																																																																																																																																																																																																																																																																									
1.72	1.72																																																																																																																																																																																																																																																																																																																																																																																																																									
1.73	1.73																																																																																																																																																																																																																																																																																																																																																																																																																									
1.74	1.74																																																																																																																																																																																																																																																																																																																																																																																																																									
1.75	1.75																																																																																																																																																																																																																																																																																																																																																																																																																									
1.76	1.76																																																																																																																																																																																																																																																																																																																																																																																																																									
1.77	1.77																																																																																																																																																																																																																																																																																																																																																																																																																									
1.78	1.78																																																																																																																																																																																																																																																																																																																																																																																																																									
1.79	1.79																																																																																																																																																																																																																																																																																																																																																																																																																									
1.8	1.8																																																																																																																																																																																																																																																																																																																																																																																																																									
1.81	1.81																																																																																																																																																																																																																																																																																																																																																																																																																									
1.82	1.82																																																																																																																																																																																																																																																																																																																																																																																																																									
1.83	1.83																																																																																																																																																																																																																																																																																																																																																																																																																									
1.84	1.84																																																																																																																																																																																																																																																																																																																																																																																																																									
1.85	1.85																																																																																																																																																																																																																																																																																																																																																																																																																									
1.86	1.86																																																																																																																																																																																																																																																																																																																																																																																																																									
1.87	1.87																																																																																																																																																																																																																																																																																																																																																																																																																									
1.88	1.88																																																																																																																																																																																																																																																																																																																																																																																																																									
1.89	1.89																																																																																																																																																																																																																																																																																																																																																																																																																									
1.9	1.9																																																																																																																																																																																																																																																																																																																																																																																																																									
1.91	1.91																																																																																																																																																																																																																																																																																																																																																																																																																									
1.92	1.92																																																																																																																																																																																																																																																																																																																																																																																																																									
1.93	1.93																																																																																																																																																																																																																																																																																																																																																																																																																									
1.94	1.94																																																																																																																																																																																																																																																																																																																																																																																																																									
1.95	1.95																																																																																																																																																																																																																																																																																																																																																																																																																									
1.96	1.96																																																																																																																																																																																																																																																																																																																																																																																																																									
1.97	1.97																																																																																																																																																																																																																																																																																																																																																																																																																									
1.98	1.98																																																																																																																																																																																																																																																																																																																																																																																																																									
1.99	1.99																																																																																																																																																																																																																																																																																																																																																																																																																									
2.0	2.0																																																																																																																																																																																																																																																																																																																																																																																																																									
6. How do you see the trend in spacecraft size and weight, say from 1000 on?	<table border="1"> <tr> <td colspan="2">Biprop.</td> </tr> <tr> <td>Up to 25% heavier</td> <td>3</td> </tr> <tr> <td>More than 25% heavier</td> <td>2</td> </tr> <tr> <td>More than 50% heavier</td> <td>6</td> </tr> <tr> <td>More than 75% heavier</td> <td>8</td> </tr> </table>	Biprop.		Up to 25% heavier	3	More than 25% heavier	2	More than 50% heavier	6	More than 75% heavier	8																																																																																																																																																																																																																																																																																																																																																																																																															
Biprop.																																																																																																																																																																																																																																																																																																																																																																																																																										
Up to 25% heavier	3																																																																																																																																																																																																																																																																																																																																																																																																																									
More than 25% heavier	2																																																																																																																																																																																																																																																																																																																																																																																																																									
More than 50% heavier	6																																																																																																																																																																																																																																																																																																																																																																																																																									
More than 75% heavier	8																																																																																																																																																																																																																																																																																																																																																																																																																									
7. How do you see the trend in spacecraft propulsion total impulse, from 1000 on?	<table border="1"> <tr> <td colspan="2">Biprop.</td> </tr> <tr> <td>(lb-sec)</td> <td>1</td> </tr> <tr> <td>50,000</td> <td>4</td> </tr> <tr> <td>50K-100K</td> <td>6</td> </tr> <tr> <td>100K-250K</td> <td>7</td> </tr> <tr> <td>>250K</td> <td>7</td> </tr> </table>	Biprop.		(lb-sec)	1	50,000	4	50K-100K	6	100K-250K	7	>250K	7																																																																																																																																																																																																																																																																																																																																																																																																													
Biprop.																																																																																																																																																																																																																																																																																																																																																																																																																										
(lb-sec)	1																																																																																																																																																																																																																																																																																																																																																																																																																									
50,000	4																																																																																																																																																																																																																																																																																																																																																																																																																									
50K-100K	6																																																																																																																																																																																																																																																																																																																																																																																																																									
100K-250K	7																																																																																																																																																																																																																																																																																																																																																																																																																									
>250K	7																																																																																																																																																																																																																																																																																																																																																																																																																									

Low Thrust Bipropellant Engine

1/2-POUND THRUSTER CAPABILITY SURVEY - PROPULSION SUBSYSTEM REQUIREMENTS

Propulsion Subsystem Requirements		ALRC CONCLUSIONS
1. What is your personal preference for propellant acquisition devices?	Screens/Capillaries: <u>17</u> Nonmetallic Bladders: <u>4</u> Metallic Bladders: <u>1</u>	Screens/Capillaries preferred
2. a. Do you expect your satellite propulsion to operate in a blowdown or regulated mode in the next several years?	Blowdown: <u>14</u> Both <u>3</u> Regulated: <u>1</u>	Blowdown Mode Most Used
b. If blowdown, would you prepressurize the propellant tanks, or carry onboard pressure bottles? What is a typical tank blowdown ratio?	Prepress: <u>12</u> Onboard bottles: <u>3</u> Both <u>2</u> <u>14</u> <u>4</u> <u><3:1</u> <u>3:1</u> <u>>3:1</u> <u>3</u> <u>6</u> Yes No	Pressurized Tanks 3:1 Blowdown Meets Most Needs
c. If regulated, do you require a quad-redundant regulator?	<u>14</u> <u>3</u> Yes No if cost tradeoff favorable	Higher Performance Desired if Cost Effective
3. Since regulated pressure systems result in higher performance (but cost more) would you consider using a regulated system (assuming you now prefer blowdown), if total reliability, with quad-redundant regulator, were equivalent?	<u>14</u> <u>3</u> Yes No if cost tradeoff favorable	Monopropellant Most Preferred
4. What is your personal preference for ACS thruster propellant/gases?	<u>11</u> <u>5</u> <u>2</u> Monoprop Biprop Cold Gas	Tank Pressures Seldom Exceed 350 psia
5. What propellant tank pressure do you expect to use normally? (Initial pressure, if blowdown mode is assumed.)	<u>1</u> <u>6</u> <u>7</u> <u>2</u> <u><250</u> <u>>300</u> <u>>350</u> <u>>400</u> (psia) Other? <u>1 @ 500 psia</u>	

Low Thrust Bipropellant Engine

1/2-POUND THRUST CAPABILITY SURVEY - THRUSTER REQUIREMENTS

ALRC CONCLUSIONS	
Freezing Depression is Worth Looking at	
500,000 pulses reasonable	
Demonstrate 2 x above for Qual.	
2 hour burn OK	
10 hrs life OK at 5 lbf	
>10 hrs Life Needed for 0.5 lbf	
<10% desired	
See Q. 10	

- Since N₂O₄ and MMH both have freezing points below 20°F, they thus require little, if any, heating.
Is this 5 A big plus 5
13 Some advantage 13
1 Trivial
- a. what number of mission total pulses do you think will be required for:
o the five-pound-class thruster? 5 100,000-250,000 8 >250,000 4
o the half-pound-class thruster? 2 250,000-500,000 2 >500,000 4
b. If possible, please provide us a copy of a recent duty cycle definition, for a program that you would consider representative of its satellite class.
- For a flight qualification program, what multiplier would you apply to 2.a?
1.25 - 1.49 3 1.50 - 1.74 6
1.75 - 2.00 7 Other? 10 x 1
- What single-burn duration do you think would be required for the
a. five-pound-class thruster?
b. half-pound-class thruster?
c. what thruster valve power drain per hour is acceptable during these long single burns?
<2 hr 15 2-4 hr 3 >4 hr —
<2 hr 13 2-4 hr 2 >4 hr 3
4 3 6 2
24 5-7 8-10 Other, 11-20
watts watts watts (Please Specify)
- What total firing life do you think would be required for the
a. five-pound-class thruster?
b. half-pound-class thruster?
<5 hr 8 5-10 hr 7 >10 hr 3
<5 hr 7 5-10 hr — >10 hr 10
- What value of thrust or impulse repeatability do you require.
a. run-to-run on a given engine?
b. from engine to engine?
<10% 14 10-20% 4 >20% —
<10% 14 10-20% 4 >20% —
- What is your maximum allowable thruster valve leakage (scch/hr, G₀ @ max feed system pressure)
<2.5 9 2.5-5 4 6-10 1 >10

Low Thrust Bipropellant Engine

1/2-POUND THRUST CAPABILITY SURVEY - THRUSTER REQUIREMENTS (cont.)

Thruster Requirements (cont.)		ALRC CONCLUSIONS	
1. Do you require a chamber pressure transducer on a. five-pound-class thrusters? b. half-pound-class thrusters?	Yes <u>3</u> No <u>14</u> Yes <u>1</u> No <u>15</u>	Don't know <u>1</u> Don't know <u>1</u>	Pc taps not required for flight
2. Would redundant thermocouples be acceptable as an alternate means of indicating thruster response?	Yes <u>8</u> No <u>7</u>	Not Sure <u>9</u>	Valve redundancy required Seats & coil
3. Do you require redundancy on engine valves such as dual coils, dual seats or dual cut-off elements?	Yes <u>15</u> No <u>1</u>	May in future <u>1</u>	Biprops perceived to be less mature and less reliable
4. How do you view biprop reliability and maturity compared to monoprops?	Equivalent <u>4</u>	Less <u>9</u> Much <u>5</u> Less	
5. Would you care to comment on additional requirements or what you may perceive as deficiencies in bipropellant propulsion subsystems for future satellites? We would appreciate candid remarks, particularly as they pertain to reasons why you would not baseline bipropellants in your next satellite propulsion design.	<p>Small passages & obstructions Low life High heat rejection No proven Insufficient data or blow down Exhaust plume time required Lower reliability, higher cost and complexity State of development not comparable to monoprops</p>		
			Users & SPOs need to be educated

APPENDIX B

SUPPORTING VALVE CYCLE LIFE ANALYSIS

FLEXURE SLEEVE STRESS ANALYSIS

The stress level at any point in the flexure sleeve is the combination of three separately induced stresses:

σ_a = Bending stress due to armature rotation

σ_b = Bending stress due to flapper wind up

σ_p = Axial stress due to internal pressure

The maximum stress level is assumed to be a linear combination of the maximum values of each of the above stresses.

$$\sigma_{\max} = (\sigma_a + \sigma_b + \sigma_p)_{\max}$$

Force Analysis

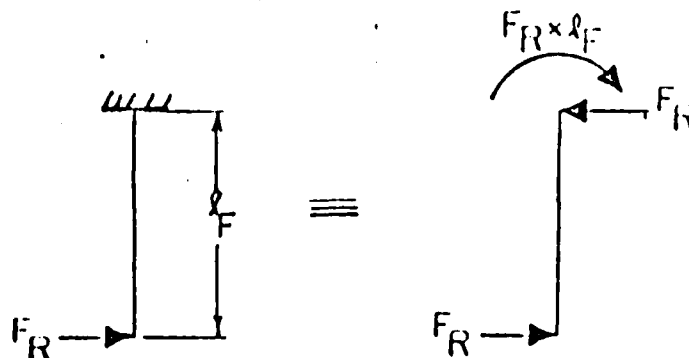
Forces are exerted on the flexure sleeve by the armature, the flapper and the system pressure.

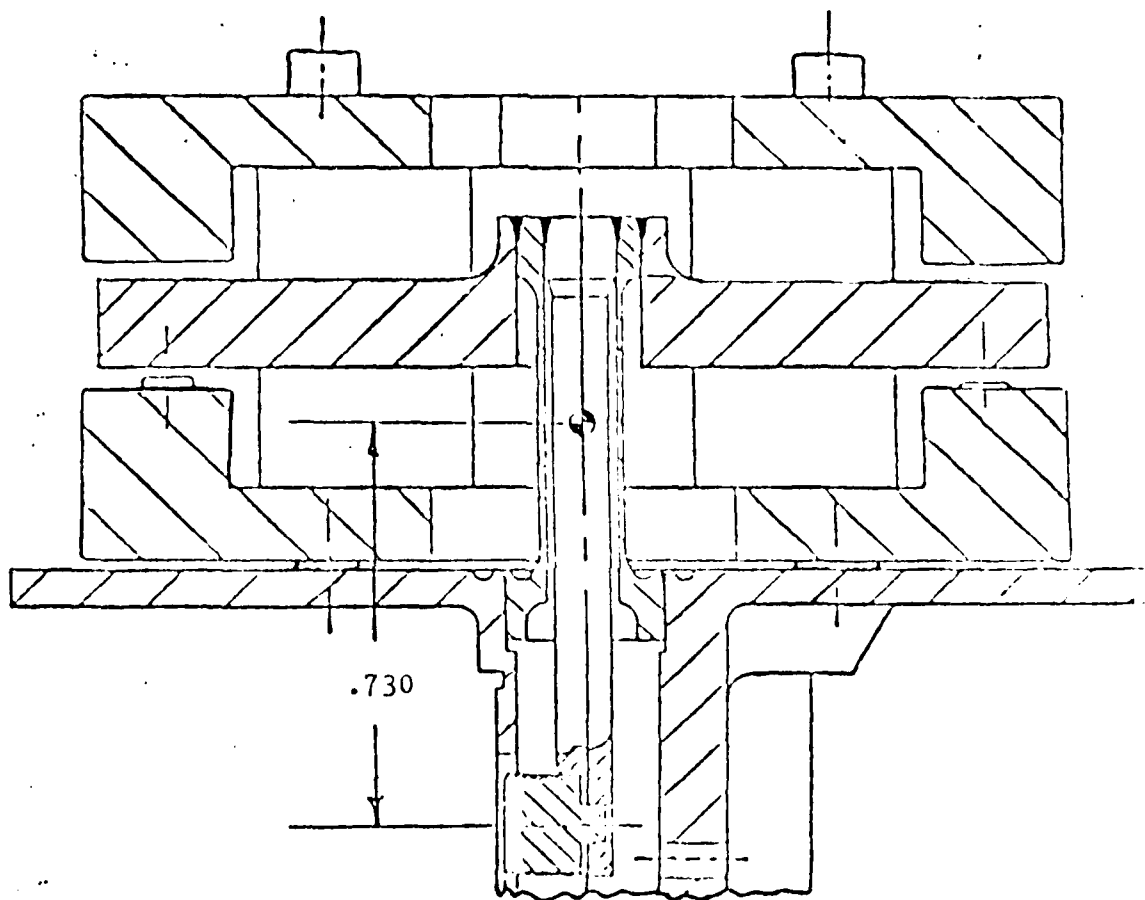
a. Armature Forces

The armature produces a moment M_a on the flexure sleeve which is constant along the length of the flexure sleeve. M_a is calculated by determining the angular rotation of the armature. The armature rotation must be sufficient to produce the required hydraulic stroke X plus the required seat preload. The magnitude of the armature rotation is governed by the geometry of the torque motor (see Figure 1). It is assumed that the armature possesses infinite stiffness.

b. Flapper Forces

Forces due to the flapper occur only when flapper "wind up" is produced by contact with the seat (or stop pins). When this occurs, the flapper is considered to be loaded as follows:

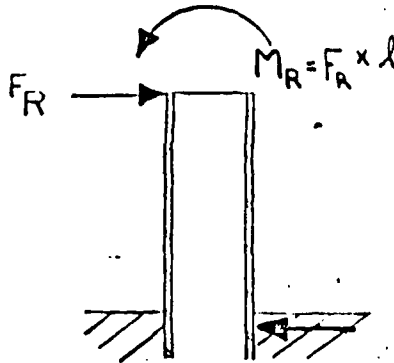




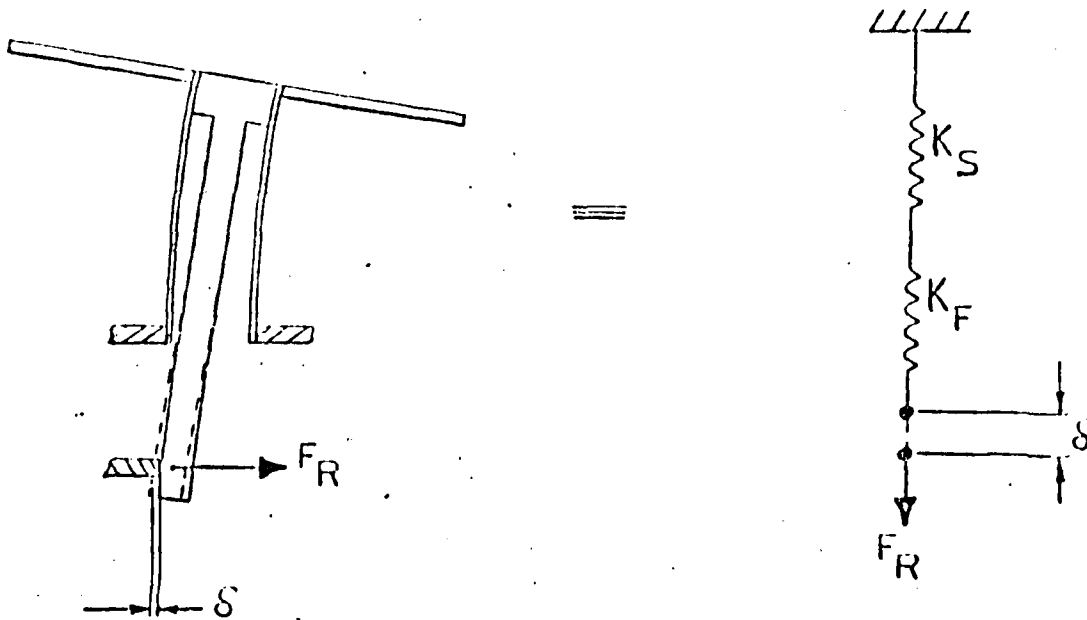
● Center of Rotation

Figure 1 - Center of Rotation for Model 51-101A Bipropellant Valve

This results in the following reaction forces on the flexure sleeve.



Force F_R due to flapper "wind up" is calculated by assuming that the flapper and flexure sleeve can be modeled as two springs in series.



Where K_f = stiffness of flapper
 K_s = stiffness of flexure sleeve
 δ = flapper "wind up" on seat or stop pin

The total stiffness of the flapper and flexure sleeve is:

$$K_t = \frac{K_f K_s}{K_f + K_s}$$

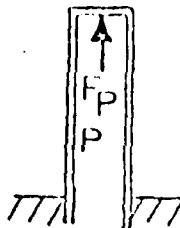
Therefore,

$$F_R = K_t \delta$$

The moment, M_R , can be lumped with the armature moment, M_a , to give the net moment which rotates the armature until contact is made with the armature stops. i.e. $M = M_a - M_R$

c. Pressure Forces

For the purpose of this analysis, only the axial force due to pressure is considered. The flexure sleeve is modeled as a tube closed at one end.



Therefore,

$$F_P = PA$$

Where

A = Area of end of tube

Maximum Rotation of the Armature

The armature is designed to rotate symmetrically about its zero stress position. The maximum displacement of the button from the zero stress position is:

$$X_t = \frac{1}{2} S + \delta^*$$

* " δ " determined from seat and torque motor geometry $\delta_{\max} = 0.003$

Where

S = Hydraulic Stroke

δ = Flapper "wind up"

$$x_t = 1/2 (.006) + .003$$

$$= .006$$

Therefore

$$\theta_a = \frac{.006}{.730} = 0.0082 \text{ Radians}$$

The stress produced by this displacement is calculated using the following equations.

$$\theta_a = \frac{Ml}{EI} \quad \text{and} \quad \sigma_a = \frac{Mc}{I}$$

Where

M = Armature moment producing displacement

c = Stress radius

I = Moment of inertia of flexure sleeve

l = Flexure sleeve length

Combining the above equations gives

$$\sigma_a = \frac{Ec\theta_a}{l}$$

$$\sigma_a = \frac{(29.5 \times 10^6) (.0557) (.0082)}{.360}$$

$$= 37,514 \text{ psi}$$

Bending Stress Due to F_R

$$K_t = \frac{K_f K_s}{K_f + K_s}$$

$$= 262 \text{ lbs/in}$$

$$F_R = K_t \delta$$

$$= .785 \text{ lbs.}$$

$K_f = 298 \text{ lbs/in}$
 $K_s = 2135 \text{ lbs/in}$

The maximum stress will occur where the bending moment is a maximum, i.e. at the body end of the flexure sleeve.

$$\begin{aligned}\sigma_{\max} &= \frac{F k_F C}{I} \\ &= \frac{(.785) (.360) (.0557)}{1.125 \times 10^{-6}} \\ &= 13,992 \text{ psi}\end{aligned}$$

Axial Stress Due to Internal Pressure

The axial stress due to system pressure is calculated as follows.

$$\sigma_P = \frac{P \pi/4 D_1^2}{4 \pi/4 (D_o^2 - D_1^2)}$$

Where

$$P = 300 \text{ psi (25 atms)}$$

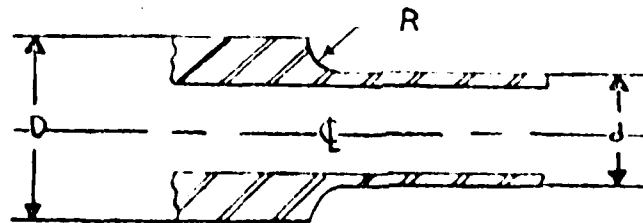
$$D_o = .1114$$

$$D_1 = .1070$$

$$\sigma_P = 3574 \text{ psi}$$

Stress Concentration

Since the flexure sleeve does have stepped diameters, stress concentration should be considered. Stress concentration factors have been derived for the flexure sleeve for tension and for bending using data obtained from Reference 1.



$$d = .1114$$

$$D = .2500$$

$$R = .015$$

$$\text{Tension } K_c = 1.67$$

$$\text{Bending } K_c = 1.54$$

Corrected Stresses

	k_c	Stress (psi)	Corrected Stress (psi)
Bending (M_a)	1.54	37,514	57,772
Bending (F_R)	1.54	13,992	21,546
Tension (P)	1.54	3,574	5,969

Total Corrected Stress 85,288 psi

Discussion of Stress Analysis Results

Figure 2 shows that the preferred flexure sleeve material 17-7 (RH 950) will perform satisfactorily for the required cyclic life of 10^6 cycles.

¹ Peterson, R. E., Stress Concentration Design Factors

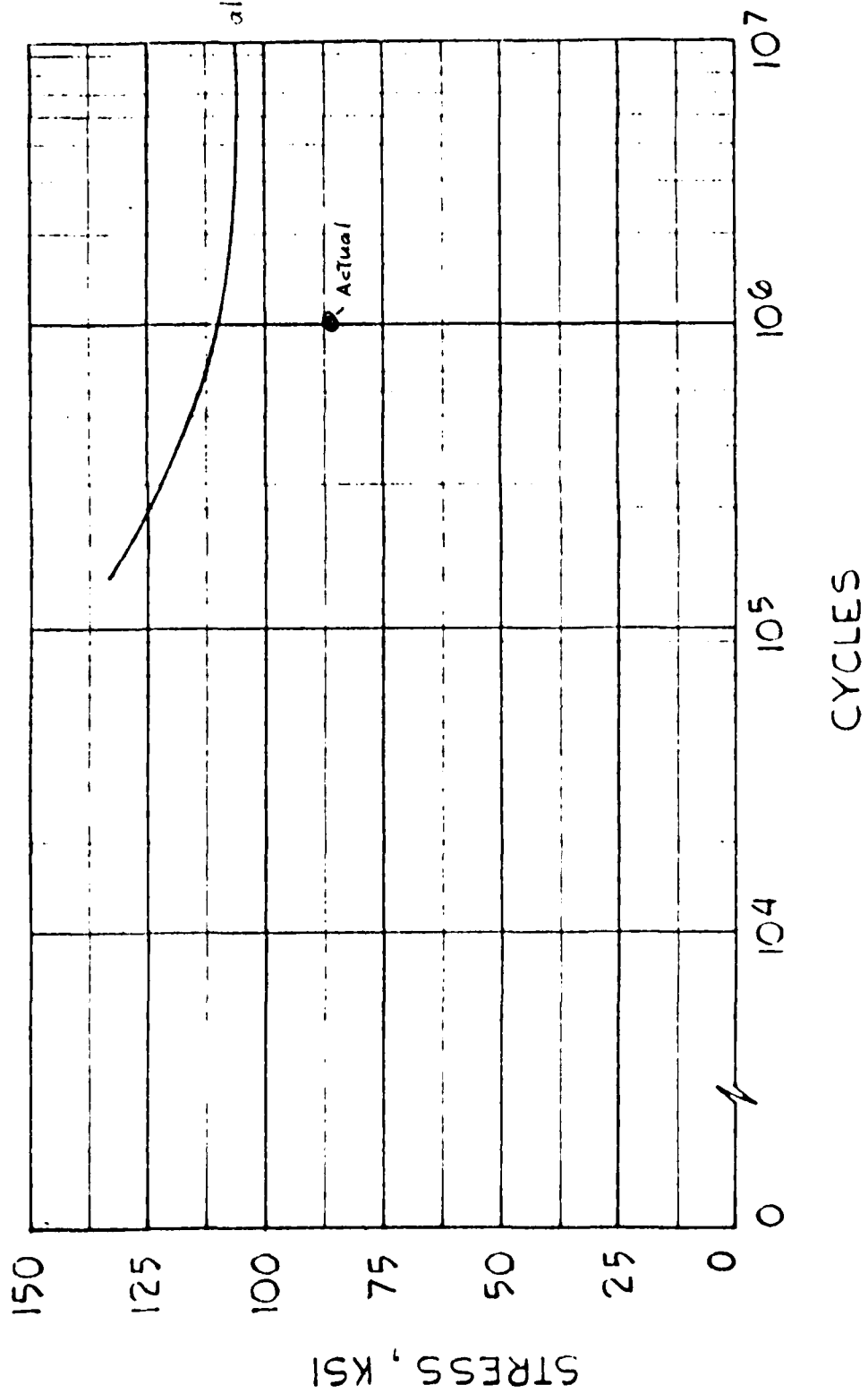


FIGURE 2 S-N CURVE FOR 17-7PH (RH 950)

APPENDIX C

INJECTOR DIMENSIONAL AND FLOW DATA

A. DESIGN

The hydraulic design of injector PN 1188746 was based upon super scale (10X) cold flow data discussed in Section 4. The expected 1:1 scale Kw's for the fuel and ox circuit and the resulting measured values are as follows:

	EXPECTED	H ₂ O FLOW	ACTUAL PROPELLANT FLOW
Fuel	4.77×10^{-5}	3.1 to 3.6×10^{-5}	3.2×10^{-5}
Ox	6.41×10^{-5}	4.9 to 6.9×10^{-5}	6.5×10^{-5}

B. DETAILED PRESSURE DROP INVESTIGATION

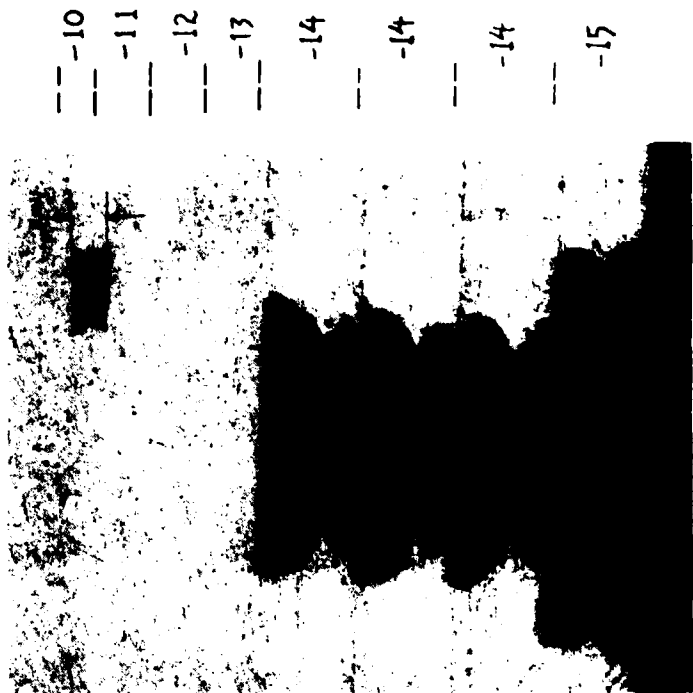
The following diagnostic testing was conducted to establish the causes of the high pressure drop in the fuel circuit.

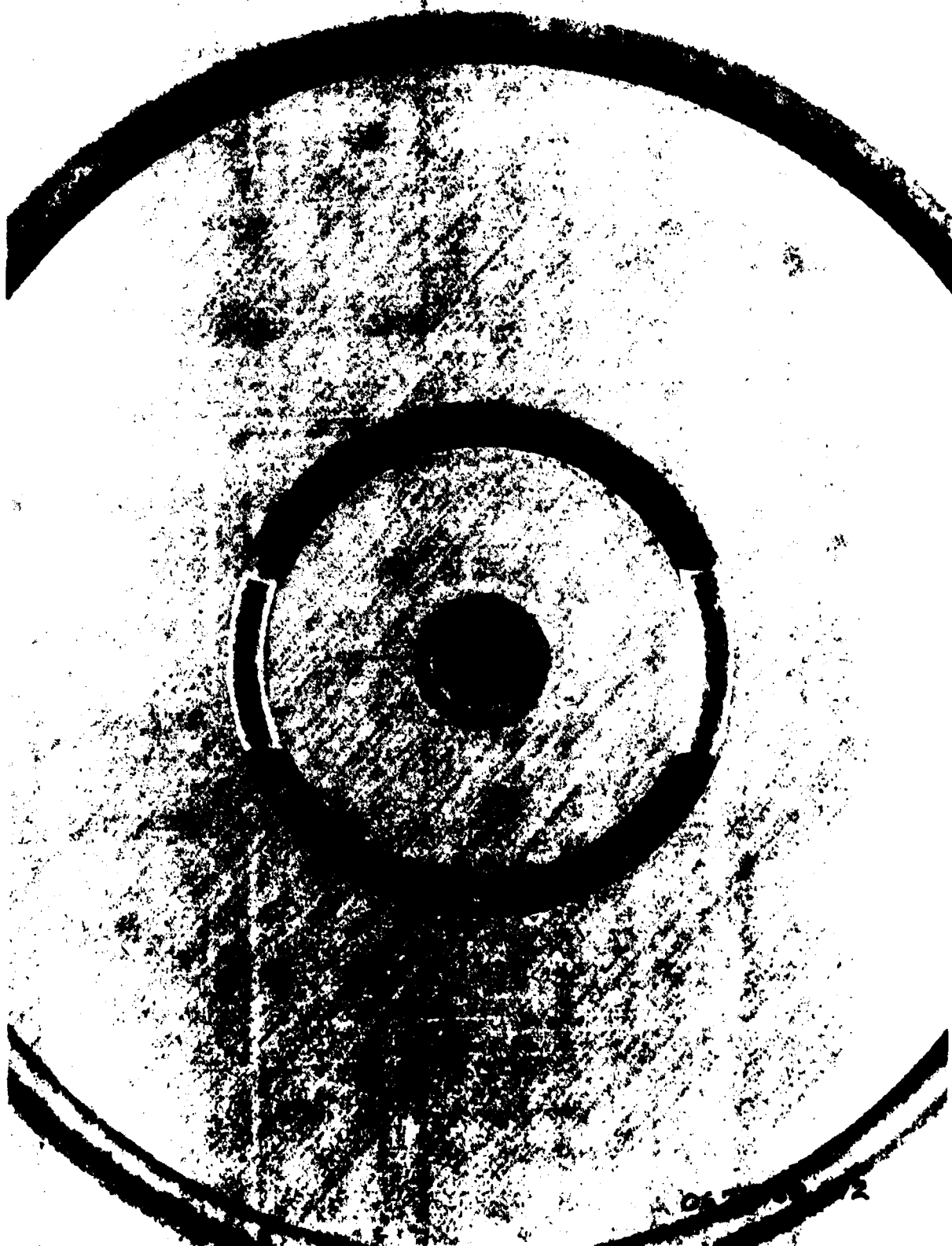
1) Did critical passage sizes change during bonding? The minimum fuel passage size by design is .0037 wide by .002 high. A 100x section through injector SN 7 (see Figure 1) shows the actual passage size to be equal to or larger than the required size.

	HEIGHT	WIDTH
Required	.002	.0037
Actual	.002	.0045

2) Is misalignment in the manifold plates 1 through 12 due to either design or fabrication a problem? Non alignment of approximately .001 to .0015 in. can be observed from Figure 2. In order to isolate the down flow manifold from the cross flow section the fuel manifold of injector SN 7 was cut open such that the flow from the .007 mil hole in the dash 12 plate discharges to atmosphere rather than enter the .004 x .008 in. cross feed manifold.

0.5 lbf INJECTOR S/N 7 FEATURE SIZE

[illegible]



C-3

Figure 2

The resulting Kw's for this condition are as follows:

Experimental Kw

Fuel ΔP Psi	Kwf 10^{-5}
10	9.16
20	8.21
40	8.90
80	9.42
Experimental Kw At Rated Flow	$9.2 \cdot 10^{-5}$

The above results compare favorably with the following predicted ΔP 's at the rated fuel flow of $6.75 \cdot 10^{-4}$ lb/sec.

Inlet	5.3 psi
8 Filter Plates	24.5 psi
2 Dash 16 Transition	28.7 psi
Axial Friction	9.8 psi
ΔP	68
Predicted Kw	$8.75 \cdot 10^{-5}$

The experimental fuel Kw was very close to the predicted values for these plates. The full flow pressure drop for these manifold plates is 62 psi vs a predicted value of 68.3. Note, however, most plates were over etched.

3) The possibility of misalignment or other losses in the manifold and/or swirler legs, plates dash nos. 10, 11 and 13 was evaluated.

Loose stacks of plates were assembled on the valve simulator block in the following sequence to identify the location of the high pressure loss.

- a) baseline configuration
- b) one extra dash 10 plate
- c) one extra each dash 13, 11 and 10
- d) repeat of b (removed extra dash 13 and 11)
- e) modified plates (build 10A Table I)

TABLE I. HISTORY OF 1/2 LB - 1 CAS INJECTOR BUILD

Dash	Original Print Req'd	SN 9 Hot Test	SN 10 Loose Stack One-10/Two-10	SN 10A Modified Parts Bonded
15	.042	.0395	.042	N/C
14	.032	.033	.0323	N/C
14	.032	.0325	.0322	N/C
14	.032	.0325	.0321	N/C
13	.020	.0210	.0196 .0193	N/C
12	.013	.0140	.0125	Fuel DC INC. to .0080 - .0084 Center = .0134
11	.013/.006	.0133/.0063	.0124/.005	"C" ring .0055 x .0032, DC = .0091 Center INC. to .0133
10	.0037 .0037	.0041 .0045	.0032/.0036 .0035/.0034	.0043/.0042 } 1 .0046/.0042 } 2 Two used
8	.008	.0072	.0083	N/C

TABLE I. HISTORY OF 1/2 LB - 1 CAS INJECTOR BUILD (CONT.)

<u>Dash</u>	<u>Original Print Req'd</u>	<u>SN 9 Hot Test</u>	<u>SN 10 Loose Stack One-10/Two-10</u>	<u>SN 10A Modified Parts Bonded</u>
7	.005	.0055	.0050	INC. to .0057, fuel DC .0095
6	.010	.0105	.0103	N/C
6	.010	.0100	.0101	N/C
7	.004	.00440	.0038	N/C
		.00415	.0038	
5	.004	.00350	.0043	N/C
		.00470	.0044	
5	.004	.0045	.0043	N/C
		.0042	.0047	
4		.0114	.0113	N/C
		.0095	.0093	
16			One extra plate used (3)	
3	.007		.0064 Min,	
			.0078 Max	
2			.0082 Min,	N/C
			.0090 Max	
1			.0091 deep	Seat flat .010

TABLE II. 1-CAS INJECTOR Kw

Configuration	ΔP	Fuel Kw 10^{-5}	Ox Kw 10^{-5}
Baseline SN 10 Table I	150	2.76 2.80	4.97 5.09
One Extra - 10 Plate	100	4.33	
One Extra Each -10, 11 & 13	100	4.85	5.11
	150	4.85	
	250	5.06	
One Extra - 10 Reflow	150	4.19	
	250	4.27	
	50	3.95	
One Extra - 10 } Modified to 10A	50	4.33	6.23
One Extra - 16	100	4.65	6.24
And	150	4.80	6.10
Ox Orifice Increased To .0057	200	4.85	6.06
	250	4.95	-

The results of these tests are documented in Table II.

The data of Table II clearly shows that;

a) one dash 10 plate increases the ΔP by a factor of 2.3 over two -10 plates. This was not predicted by analysis. [$\Delta P \propto (Kw)^2$]

b) The addition of one each additional dash 11 and 13 plates only reduces the ΔP by 25% over the addition of the extra -10.

c) The 10A configuration provides the proper ΔP in the fuel and ox circuits for equal tank pressure of 360 psi at 1/2 lb thrust.

4) Etching Considerations

Table I and III provide a record of the critical dimensions of all units built and flowed to date.

Table III shows that nearly all features of the first lot of 9 injectors were over etched as compared to the nominal print dimensions. Thus the higher ΔP values cannot be associated with under etched parts.

The large chevrons of Figure II (Injector SN 7) are not consistent with an over etched condition. Over etching usually produces a straight wall. This suggests our etch factors are incorrect or a problem existed with the etchant properties for the lot of parts. The latter is the most likely cause.

The desired stacking pin holes are $0.1200 + .0004/- .0000$. A number of the holes are noted to be .001 over size. The dash 14 plates in particular were too big to allow reaming, indicating an improper etch factor. A good number of stacking holes come close to the $+ .0004/- 0.0000$ goal.

5) Data Correlation and Additional Data

Table IV provides a record of the design analysis and the resulting cold flow data. A systematic re-analysis of the design using the test results as a guide would be useful in future design changes.

C. CORRECTION OF HIGH FUEL CIRCUIT ΔP

The solution to the high ΔP problem was obtained empirically for unit 10A. The fabrication of injectors SN 20 and 21 in Task III demonstrated the hydraulic reproducibility of the design of the 1-CAS injector within the limits of the following data:

	OX Kw 10^{-5}	Fuel Kw 10^{-5}
10A	5.7	4.2
20	5.6	4.6
22	5.8	4.6

D. "V" DOUBLET INSPECTION DATA

Dimensional data for this injector is documented in Table V.

TABLE III
DIMENSIONAL INSPECTION OF 1-CAS INJECTORS

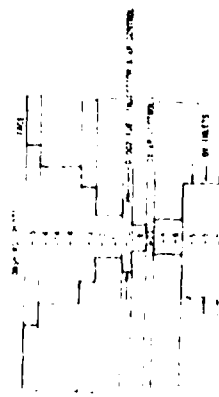
Injector SN	1	2	3	4	5	6	7	8	9	REQUIRED DIMENSION	AVERAGE DIMENSION 1-9	DEVIATION FROM REQ'D ±	NOTE P=REAMED N=NOT REAMED	DEVIATION HOLE 1	DEVIATION HOLE 2
Plate No. -15	0.040	0.039	0.039	0.0425	0.0425	0.040	0.040	0.040	0.0395	.042	.0403	-.0018		+.0005	+.0005
-14	0.033	0.033	0.0335	0.0325	0.0325	0.033	0.0325	0.033	0.033	.032	.03255	+.00055	N	+.001	+.0015
-14	0.0325	0.0325	0.0335	0.0325	0.0325	0.0325	0.032	0.0325	0.0325	.032	.0325	+.0005	N	+.0015	+.0005
-14	0.0325	0.0325	0.0320	0.0320	0.0330	0.0330	0.0325	0.0325	0.0325	.032	.0325	+.0005	N	+.001	+.001
-13	0.0200	0.0200	0.0200	0.0200	0.0205	0.0210	0.0200	0.0210	0.0210	.020	.0203	+.0003		+.0005	+.001
-12	0.0135	-	0.0130	0.0135	0.014	0.0135	0.0145	0.0135	0.014	.013	.0137	+.0007		+.0005	+.0005
-11	0.0129	0.013	0.0134	0.0130	0.0132	0.0129	0.0130	0.0130	0.0133	.013	.0131	+.0001		+.0001	+.0001
-107 B	0.0043	0.0045	0.0035	0.0043	0.0045	0.0038	0.00415	0.0045	0.0041	.0037	.0042	+.0005		-	-
	0.0043	0.0044	0.0035	0.00445	0.0041	0.0038	0.00420	0.0044	0.0045	.0037	.0042	+.0005		-	-
-8	0.0035	0.0070	0.0070	0.0065	0.0065	0.0070	0.0065	0.0065	0.0072	.008	.0067	-.0013		+.0005	+.001
-7	0.00515	0.0056	0.0039	0.0051	0.0054	0.0059	0.0047	0.0056	0.0055	.005	.0052	+.0002		+.0006	+.0005
-6	0.0105	0.0105	0.0100	0.0100	0.0100	0.0100	0.0100	0.0100	0.0105*	.010	.0102	+.0002		+.0005	+.001
-5	0.0045	0.0046	-	0.0045	0.0041	0.0042	0.0100*	0.0095	0.0100	.010	.0039	-.0001		+.0005	+.0005
-5	0.0045	0.0047	-	0.0045	0.0041	0.0042	-	-	0.0044	.004	.0042	+.0002		+.0005	+.0003
-5	0.0053	0.0045	0.0045	0.00430	0.0044	0.0046	-	-	0.00415	.004	.0043	+.0002		+.0005	-
-5	0.0042	0.0055	0.0045	-	0.0044	-	-	-	0.0035	.004	.0045	+.0005		+.0005	+.0005
-5	0.00425	0.0042	0.00429	-	0.0044	-	-	-	0.0037	.004	.0046	+.0006		+.0006	+.0005
-5	0.00425	0.0042	0.0042	-	0.0047	-	-	-	0.0045	.004	.0044	+.0004		+.0004	+.0004
-5	0.00410	0.0036	0.0036	-	0.0049	-	-	-	0.0042	.004	.0041	+.0001		+.0001	+.0001

*Griffice not round.

- No inspection

T = Top Leg

B = Bottom Leg



1-12 1-13 1-14 1-15 1-16 1-17 1-18 1-19 1-20 1-21 1-22 1-23 1-24 1-25 1-26 1-27 1-28 1-29 1-30 1-31 1-32 1-33 1-34 1-35 1-36 1-37 1-38 1-39 1-40 1-41 1-42 1-43 1-44 1-45 1-46 1-47 1-48 1-49 1-50 1-51 1-52 1-53 1-54 1-55 1-56 1-57 1-58 1-59 1-60 1-61 1-62 1-63 1-64 1-65 1-66 1-67 1-68 1-69 1-70 1-71 1-72 1-73 1-74 1-75 1-76 1-77 1-78 1-79 1-80 1-81 1-82 1-83 1-84 1-85 1-86 1-87 1-88 1-89 1-90 1-91 1-92 1-93 1-94 1-95 1-96 1-97 1-98 1-99 1-100 1-101 1-102 1-103 1-104 1-105 1-106 1-107 1-108 1-109 1-110 1-111 1-112 1-113 1-114 1-115 1-116 1-117 1-118 1-119 1-120 1-121 1-122 1-123 1-124 1-125 1-126 1-127 1-128 1-129 1-130 1-131 1-132 1-133 1-134 1-135 1-136 1-137 1-138 1-139 1-140 1-141 1-142 1-143 1-144 1-145 1-146 1-147 1-148 1-149 1-150 1-151 1-152 1-153 1-154 1-155 1-156 1-157 1-158 1-159 1-160 1-161 1-162 1-163 1-164 1-165 1-166 1-167 1-168 1-169 1-170 1-171 1-172 1-173 1-174 1-175 1-176 1-177 1-178 1-179 1-180 1-181 1-182 1-183 1-184 1-185 1-186 1-187 1-188 1-189 1-190 1-191 1-192 1-193 1-194 1-195 1-196 1-197 1-198 1-199 1-200 1-201 1-202 1-203 1-204 1-205 1-206 1-207 1-208 1-209 1-210 1-211 1-212 1-213 1-214 1-215 1-216 1-217 1-218 1-219 1-220 1-221 1-222 1-223 1-224 1-225 1-226 1-227 1-228 1-229 1-230 1-231 1-232 1-233 1-234 1-235 1-236 1-237 1-238 1-239 1-240 1-241 1-242 1-243 1-244 1-245 1-246 1-247 1-248 1-249 1-250 1-251 1-252 1-253 1-254 1-255 1-256 1-257 1-258 1-259 1-260 1-261 1-262 1-263 1-264 1-265 1-266 1-267 1-268 1-269 1-270 1-271 1-272 1-273 1-274 1-275 1-276 1-277 1-278 1-279 1-280 1-281 1-282 1-283 1-284 1-285 1-286 1-287 1-288 1-289 1-290 1-291 1-292 1-293 1-294 1-295 1-296 1-297 1-298 1-299 1-300 1-301 1-302 1-303 1-304 1-305 1-306 1-307 1-308 1-309 1-310 1-311 1-312 1-313 1-314 1-315 1-316 1-317 1-318 1-319 1-320 1-321 1-322 1-323 1-324 1-325 1-326 1-327 1-328 1-329 1-330 1-331 1-332 1-333 1-334 1-335 1-336 1-337 1-338 1-339 1-340 1-341 1-342 1-343 1-344 1-345 1-346 1-347 1-348 1-349 1-350 1-351 1-352 1-353 1-354 1-355 1-356 1-357 1-358 1-359 1-360 1-361 1-362 1-363 1-364 1-365 1-366 1-367 1-368 1-369 1-370 1-371 1-372 1-373 1-374 1-375 1-376 1-377 1-378 1-379 1-380 1-381 1-382 1-383 1-384 1-385 1-386 1-387 1-388 1-389 1-390 1-391 1-392 1-393 1-394 1-395 1-396 1-397 1-398 1-399 1-400 1-401 1-402 1-403 1-404 1-405 1-406 1-407 1-408 1-409 1-410 1-411 1-412 1-413 1-414 1-415 1-416 1-417 1-418 1-419 1-420 1-421 1-422 1-423 1-424 1-425 1-426 1-427 1-428 1-429 1-430 1-431 1-432 1-433 1-434 1-435 1-436 1-437 1-438 1-439 1-440 1-441 1-442 1-443 1-444 1-445 1-446 1-447 1-448 1-449 1-450 1-451 1-452 1-453 1-454 1-455 1-456 1-457 1-458 1-459 1-460 1-461 1-462 1-463 1-464 1-465 1-466 1-467 1-468 1-469 1-470 1-471 1-472 1-473 1-474 1-475 1-476 1-477 1-478 1-479 1-480 1-481 1-482 1-483 1-484 1-485 1-486 1-487 1-488 1-489 1-490 1-491 1-492 1-493 1-494 1-495 1-496 1-497 1-498 1-499 1-500 1-501 1-502 1-503 1-504 1-505 1-506 1-507 1-508 1-509 1-510 1-511 1-512 1-513 1-514 1-515 1-516 1-517 1-518 1-519 1-520 1-521 1-522 1-523 1-524 1-525 1-526 1-527 1-528 1-529 1-530 1-531 1-532 1-533 1-534 1-535 1-536 1-537 1-538 1-539 1-540 1-541 1-542 1-543 1-544 1-545 1-546 1-547 1-548 1-549 1-550 1-551 1-552 1-553 1-554 1-555 1-556 1-557 1-558 1-559 1-560 1-561 1-562 1-563 1-564 1-565 1-566 1-567 1-568 1-569 1-570 1-571 1-572 1-573 1-574 1-575 1-576 1-577 1-578 1-579 1-580 1-581 1-582 1-583 1-584 1-585 1-586 1-587 1-588 1-589 1-590 1-591 1-592 1-593 1-594 1-595 1-596 1-597 1-598 1-599 1-600 1-601 1-602 1-603 1-604 1-605 1-606 1-607 1-608 1-609 1-610 1-611 1-612 1-613 1-614 1-615 1-616 1-617 1-618 1-619 1-620 1-621 1-622 1-623 1-624 1-625 1-626 1-627 1-628 1-629 1-630 1-631 1-632 1-633 1-634 1-635 1-636 1-637 1-638 1-639 1-640 1-641 1-642 1-643 1-644 1-645 1-646 1-647 1-648 1-649 1-650 1-651 1-652 1-653 1-654 1-655 1-656 1-657 1-658 1-659 1-660 1-661 1-662 1-663 1-664 1-665 1-666 1-667 1-668 1-669 1-670 1-671 1-672 1-673 1-674 1-675 1-676 1-677 1-678 1-679 1-680 1-681 1-682 1-683 1-684 1-685 1-686 1-687 1-688 1-689 1-690 1-691 1-692 1-693 1-694 1-695 1-696 1-697 1-698 1-699 1-700 1-701 1-702 1-703 1-704 1-705 1-706 1-707 1-708 1-709 1-710 1-711 1-712 1-713 1-714 1-715 1-716 1-717 1-718 1-719 1-720 1-721 1-722 1-723 1-724 1-725 1-726 1-727 1-728 1-729 1-730 1-731 1-732 1-733 1-734 1-735 1-736 1-737 1-738 1-739 1-740 1-741 1-742 1-743 1-744 1-745 1-746 1-747 1-748 1-749 1-750 1-751 1-752 1-753 1-754 1-755 1-756 1-757 1-758 1-759 1-760 1-761 1-762 1-763 1-764 1-765 1-766 1-767 1-768 1-769 1-770 1-771 1-772 1-773 1-774 1-775 1-776 1-777 1-778 1-779 1-780 1-781 1-782 1-783 1-784 1-785 1-786 1-787 1-788 1-789 1-790 1-791 1-792 1-793 1-794 1-795 1-796 1-797 1-798 1-799 1-800 1-801 1-802 1-803 1-804 1-805 1-806 1-807 1-808 1-809 1-810 1-811 1-812 1-813 1-814 1-815 1-816 1-817 1-818 1-819 1-820 1-821 1-822 1-823 1-824 1-825 1-826 1-827 1-828 1-829 1-830 1-831 1-832 1-833 1-834 1-835 1-836 1-837 1-838 1-839 1-840 1-841 1-842 1-843 1-844 1-845 1-846 1-847 1-848 1-849 1-850 1-851 1-852 1-853 1-854 1-855 1-856 1-857 1-858 1-859 1-860 1-861 1-862 1-863 1-864 1-865 1-866 1-867 1-868 1-869 1-870 1-871 1-872 1-873 1-874 1-875 1-876 1-877 1-878 1-879 1-880 1-881 1-882 1-883 1-884 1-885 1-886 1-887 1-888 1-889 1-890 1-891 1-892 1-893 1-894 1-895 1-896 1-897 1-898 1-899 1-900 1-901 1-902 1-903 1-904 1-905 1-906 1-907 1-908 1-909 1-910 1-911 1-912 1-913 1-914 1-915 1-916 1-917 1-918 1-919 1-920 1-921 1-922 1-923 1-924 1-925 1-926 1-927 1-928 1-929 1-930 1-931 1-932 1-933 1-934 1-935 1-936 1-937 1-938 1-939 1-940 1-941 1-942 1-943 1-944 1-945 1-946 1-947 1-948 1-949 1-950 1-951 1-952 1-953 1-954 1-955 1-956 1-957 1-958 1-959 1-960 1-961 1-962 1-963 1-964 1-965 1-966 1-967 1-968 1-969 1-970 1-971 1-972 1-973 1-974 1-975 1-976 1-977 1-978 1-979 1-980 1-981 1-982 1-983 1-984 1-985 1-986 1-987 1-988 1-989 1-990 1-991 1-992 1-993 1-994 1-995 1-996 1-997 1-998 1-999 1-1000 1-1001 1-1002 1-1003 1-1004 1-1005 1-1006 1-1007 1-1008 1-1009 1-1010 1-1011 1-1012 1-1013 1-1014 1-1015 1-1016 1-1017 1-1018 1-1019 1-1020 1-1021 1-1022 1-1023 1-1024 1-1025 1-1026 1-1027 1-1028 1-1029 1-1030 1-1031 1-1032 1-1033 1-1034 1-1035 1-1036 1-1037 1-1038 1-1039 1-1040 1-1041 1-1042 1-1043 1-1044 1-1045 1-1046 1-1047 1-1048 1-1049 1-1050 1-1051 1-1052 1-1053 1-1054 1-1055 1-1056 1-1057 1-1058 1-1059 1-1060 1-1061 1-1062 1-1063 1-1064 1-1065 1-1066 1-1067 1-1068 1-1069 1-1070 1-1071 1-1072 1-1073 1-1074 1-1075 1-1076 1-1077 1-1078 1-1079 1-1080 1-1081 1-1082 1-1083 1-1084 1-1085 1-1086 1-1087 1-1088 1-1089 1-1090 1-1091 1-1092 1-1093 1-1094 1-1095 1-1096 1-1097 1-1098 1-1099 1-1100 1-1101 1-1102 1-1103 1-1104 1-1105 1-1106 1-1107 1-1108 1-1109 1-1110 1-1111 1-1112 1-1113 1-1114 1-1115 1-1116 1-1117 1-1118 1-1119 1-1120 1-1121 1-1122 1-1123 1-1124 1-1125 1-1126 1-1127 1-1128 1-1129 1-1130 1-1131 1-1132 1-1133 1-1134 1-1135 1-1136 1-1137 1-1138 1-1139 1-1140 1-1141 1-1142 1-1143 1-1144 1-1145 1-1146 1-1147 1-1148 1-1149 1-1150 1-1151 1-1152 1-1153 1-1154 1-1155 1-1156 1-1157 1-1158 1-1159 1-1160 1-1161 1-1162 1-1163 1-1164 1-1165 1-1166 1-1167 1-1168 1-1169 1-1170 1-1171 1-1172 1-1173 1-1174 1-1175 1-1176 1-1177 1-1178 1-1179 1-1180 1-1181 1-1182 1-1183 1-1184 1-1185 1-1186 1-1187 1-1188 1-1189 1-1190 1-1191 1-1192 1-1193 1-1194 1-1195 1-1196 1-1197 1-1198 1-1199 1-1200 1-1201 1-1202 1-1203 1-1204 1-1205 1-1206 1-1207 1-1208 1-1209 1-1210 1-1211 1-1212 1-1213 1-1214 1-1215 1-1216 1-1217 1-1218 1-1219 1-1220 1-1221 1-1222 1-1223 1-1224 1-1225 1-1226 1-1227 1-1228 1-1229 1-1230 1-1231 1-1232 1-1233 1-1234 1-1235 1-1236 1-1237 1-1238 1-1239 1-1240 1-1241 1-1242 1-1243 1-1244 1-1245 1-1246 1-1247 1-1248 1-1249 1-1250 1-1251 1-1252 1-1253 1-1254 1-1255 1-1256 1-1257 1-1258 1-1259 1-1260 1-1261 1-1262 1-1263 1-1264 1-1265 1-1266 1-1267 1-1268 1-1269 1-1270 1-1271 1-1272 1-1273 1-1274 1-1275 1-1276 1-1277 1-1278 1-1279 1-1280 1-1281 1-1282 1-1283 1-1284 1-1285 1-1286 1-1287 1-1288 1-1289 1-1290 1-1291 1-1292 1-1293 1-1294 1-1295 1-1296 1-1297 1-1298 1-1299 1-1300 1-1301 1-1302 1-1303 1-1304 1-1305 1-1306 1-1307 1-1308 1-1309 1-1310 1-1311 1-1312 1-1313 1-1314 1-1315 1-1316 1-1317 1-1318 1-1319 1-1320 1-1321 1-1322 1-1323 1-1324 1-1325 1-1326 1-1327 1-1328 1-1329 1-1330 1-1331 1-1332 1-1333 1-1334 1-1335 1-1336 1-1337 1-1338 1-1339 1-1340 1-1341 1-1342 1-1343 1-1344 1-1345 1-1346 1-1347 1-1348 1-1349 1-1350 1-1351 1-1352 1-1353 1-1354 1-1355 1-1356 1-1357 1-1358 1-1359 1-1360 1-1361 1-1362 1-1363 1-1364 1-1365 1-1366 1-1367 1-1368 1-1369 1-1370 1-1371 1-1372 1-1373 1-1374 1-1375 1-1376 1-1377 1-1378 1-1379 1-1380 1-1381 1-1382 1-1383 1-1384 1-1385 1-1386 1-1387 1-1388 1-1389 1-1390 1-1391 1-1392 1-1393 1-1394 1-1395 1-1396 1-1397 1-1398 1-1399 1-1400 1-1401 1-1402 1-1403 1-1404 1-1405 1-1406 1-1407 1-1408 1-1409 1-1410 1-1411 1-1412 1-1413 1-1414 1-1415 1-1416 1-1417 1-1418 1-1419 1-1420 1-1421 1-1422 1-1423 1-1424 1-1425 1-1426 1-1427 1-1428 1-1429 1-1430 1-1431 1-1432 1-1433 1-1434 1-1435 1-1436 1-1437 1-1438 1-1439 1-1440 1-1441 1-1442

TABLE IV

OTHER SUPPORTING COLD FLOW DATA

A-1

ΔP fuel vs number of filter plates

# Plates	ΔP at full fuel flow
4	33.5
6	29.7
* 8	24.5

A-2

ΔP vs number of - 16 transfer plates

0	159.6
* 2	28.7
4	15.1

* Number selected for Injector SN 1 - 9

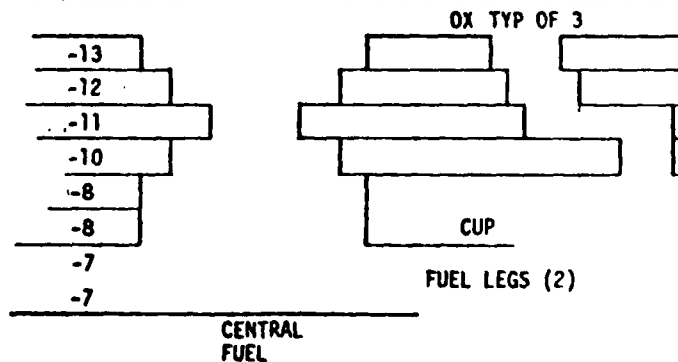
TABLE V

3-VDS INSPECTION DATA OF CRITICAL DIMENSIONS

Plate	Injector SN								
	1	2	3	4	5	6	7	8	9
- 7 T	4.5	4.5	4.5	4.5	4.5	4.0	3.5	4.5	4.5
B	4.5	4.5	4.0	4.5	4.5	4.0	3.5	4.0	4.5
- 7 T	4.5	4.5	4.5	4.5	4.5	5.0	3.5	4.5	5.0
B	4.5	4.5	4.5	4.5	4.5	4.5	3.0	4.5	4.5
- 8	14.0	14.5	14.5	14.5	14.0	14.5	14.5	14.5	14.0
	14.0	14.5	14.5	15.0	14.5	14.5	14.5	14.5	14.5
-10 C	11.5	11.0	11.0	11.5	11.0	11.0	11.0	11.0	11.5
Holes									
1	3.0/3.0	3.0/3.0	3.5/3.0	4.0/4.0	3.5/3.5	3.5/4.0	3.0/3.5	3.0/3.0	3.5/4.0
2	3.0/3.0	3.5/3.5	3.5/3.0	3.5/3.5	3.5/4.0	3.5/3.5	3.0/3.5	3.0/3.5	3.5/4.0
3	3.0/3.0	3.5/3.0	3.0/3.5	3.5/3.0	4.0/3.5	3.5/3.5	3.5/3.5	3.0/3.0	4.0/3.5
-11 C	8.0	8.0	8.0	8.0	8.0	8.0	8.0	8.0	8.0
V	3.5/3.0	4.0/3.5	3.0/3.0	3.5/3.5	3.5/3.0	3.5/3.5	3.5/3.5	3.0/3.0	3.5/3.5
-11 C	8.5	8.0	9.0	8.0	8.0	8.5	8.0	8.0	8.5
V	4.0/3.5	3.5/3.5	3.5/4.0	4.0/4.0	OK	4.0/4.0	4.0/4.0	4.0/4.0	4.0/4.0
-12 C	13.0	13.0	12.5	13.0	12.5	13.0	13.0	13.0	13.0
Orifice									
Typ of 3	3.60	3.00	2.10	3.75	3.05	3.10	3.35	3.50	3.30
-13									
(1)	4.0	4.0	4.5	4.5	Sealed	4.5	4.0	4.5	4.5
(2)	4.5	4.5	4.0	4.5	Sealed	4.5	4.5	4.0	4.0

C = Center Hole
T = Top leg of swirler
B = Bottom leg of swirler
V = V, doublet feed legs

NOTE: All dimensions Mils



APPENDIX D

PHASE III VALVE ACCEPTANCE TEST DATA, MOOG
MODEL 51E112, SN 004 and 005

Phase III valve

ACCEPTANCE TEST DATA PACKAGE

0.5 lb_f TORQUE MOTOR BIPROPELLANT VALVE

Moog Model 51E112
Moog Part Number A24461
Moog Serial Number 004

Test Data Prepared by: Samuel E. Gill Date 1-4-80
Approved by: A. Phillips Date 1-4-80

MODEL 51E112

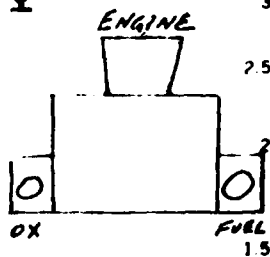
S/N 004

Test Description	Limits	Data Value
1.0 Examination of Product		
1.1 Inspection for drawing compliance	(Mark OK)	OK
1.2 S/N Identification	Check ATDP documentation and unit marking (Mark OK)	OK
1.3 Weight (with injector)		251.5 gms
2.0 Dielectric Strength at 500 VAC, 60 Hz for 60 seconds	$\leq 100 \mu A$	1.0 μA
3.0 Insulation Resistance at 500 VDC for 60 seconds	≥ 100 megohms	9,000 megohms
4.0 Coil Resistance	177 \pm 15 ohms	179.8 ohms 75 of
5.0 Proof Pressure at 800 psi GN ₂ for 3 minutes	No visible damage (Mark OK)	OK
6.0 Pull-In Current at 400 psi GN ₂		72 ma
7.0 Drop-Out Current at 400 psi GN ₂		43 ma
8.0 Valve Response	$\leq .005$ sec	
Opening & Closing Response	Inlet Pressure	Voltage
	350"	24, 28, 32
	400"	24, 28, 32
		(See Photographs RESPONSE SHEET)
9.0 PRESSURE DROP	(SEE GRAPH)	

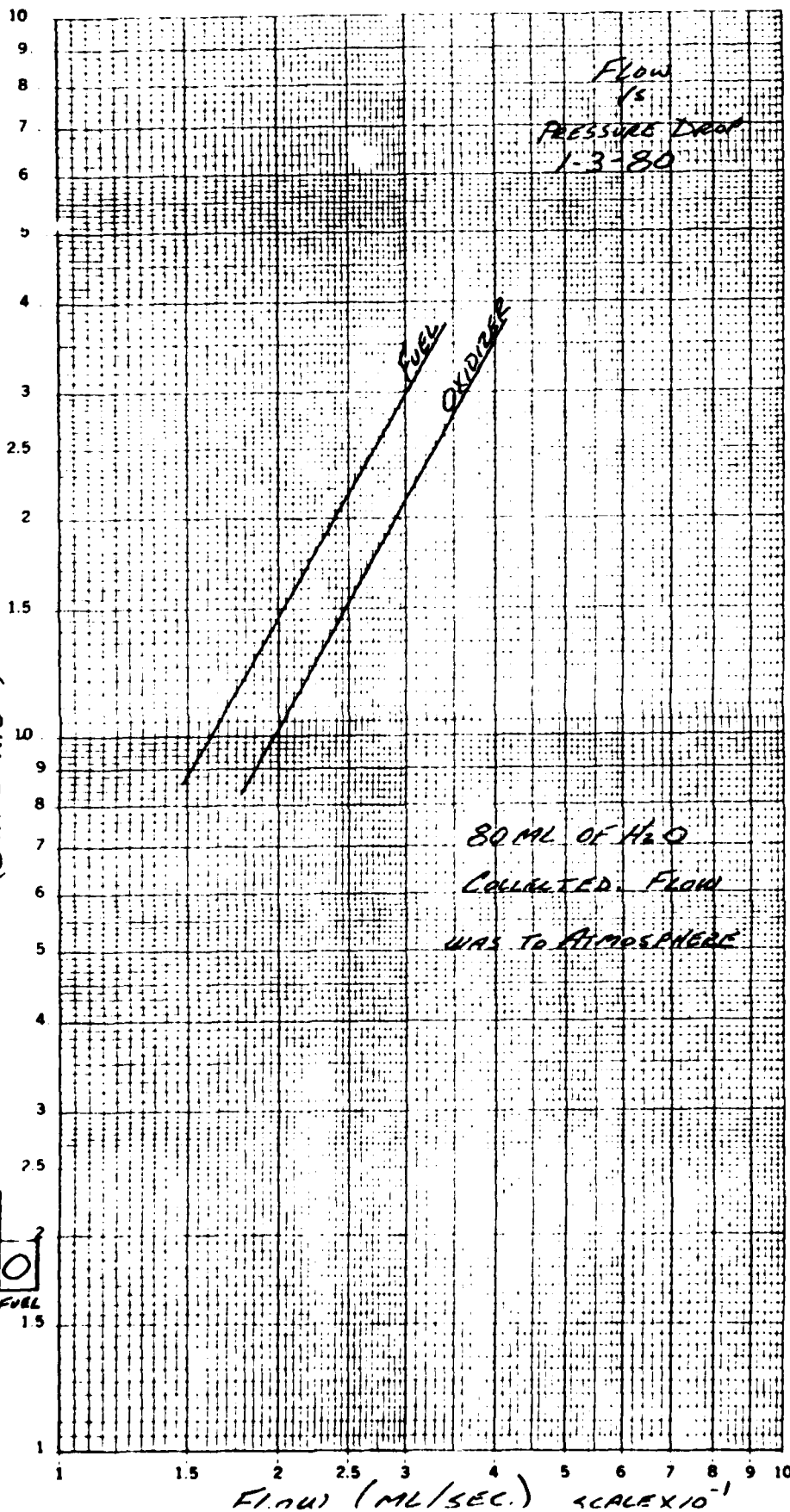
Test Description	Limits	Data Value						
9.0 Flush and Purge and Vacuum Dry for 1 hour at 120°F	Isopropyl Alcohol and GN ₂ , 100 cycles min. (Mark OK)	OK						
10.0 Internal Leakage at 50 psi at 400 psi	<2.3 sec/hr GN ₂	<table border="0"> <tr> <td>Fuel</td> <td>Ox.</td> </tr> <tr> <td>0.0 sec/hr</td> <td>0.0 sec/hr</td> </tr> <tr> <td>0.0 sec/hr</td> <td>0.0 sec/hr</td> </tr> </table>	Fuel	Ox.	0.0 sec/hr	0.0 sec/hr	0.0 sec/hr	0.0 sec/hr
Fuel	Ox.							
0.0 sec/hr	0.0 sec/hr							
0.0 sec/hr	0.0 sec/hr							
11.0 External Leakage at 50 psi at 400 psi	<2.3 sec/hr GN ₂	<table border="0"> <tr> <td>0.0 sec/hr</td> </tr> <tr> <td>0.0 sec/hr</td> </tr> </table>	0.0 sec/hr	0.0 sec/hr				
0.0 sec/hr								
0.0 sec/hr								

46 7083

K&E LOGARITHMIC 2 X 1 CYCLES
KEUFFEL & ESSER CO. MADE IN U.S.A.



PRESSURE DROP (INLET PRESS.)
(SCALE $\times 10^{-2}$)



51E112
S/N 004

FLOW TO ATMOSPHERE
INLET PRESSURE

TIME TO COLLECT 80ML H₂O
FLOW RATE

<u>PSI</u>	<u>FUEL</u>	<u>OXIDIZER</u>
<u>100</u>	494.0 SEC. .162 ML/SEC.	406.6 SEC. .197 ML/SEC.
<u>200</u>	332.3 SEC. .241 ML/SEC.	271.5 SEC. .295 ML/SEC.
<u>300</u>	266.6 SEC. .300 ML/SEC.	219.8 SEC. .364 ML/SEC.

RESPONSE

~~300~~ PSI H₂O
350

OPEN

CLOSING

24.0 VDC

4.5 ms.

0.6 ms.

28.0 VDC

3.6 ms.

0.6 ms.

32.0 VDC

3.0 ms.

0.6 ms.

400 PSI H₂O

24.0 VDC

4.8 ms.

0.6 ms.

28.0 VDC

3.8 ms.

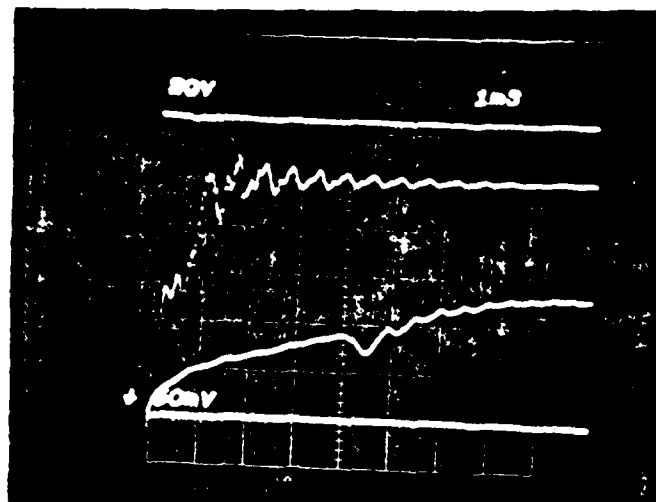
0.6 ms.

32.0 VDC

3.2 ms.

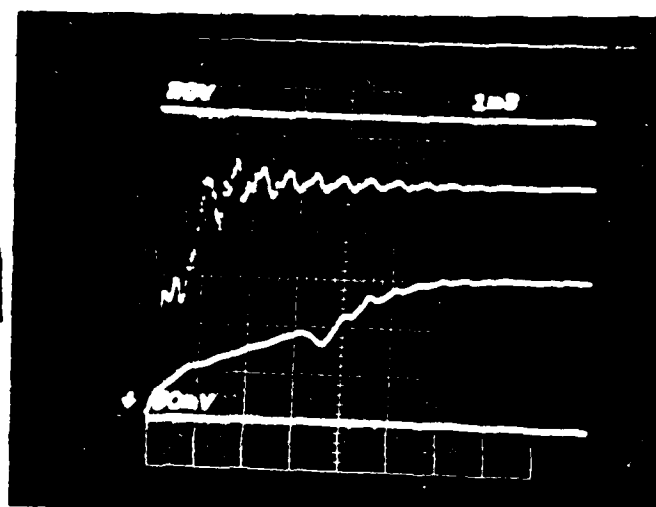
0.6 ms.

RESPONSE @ 350 PSI

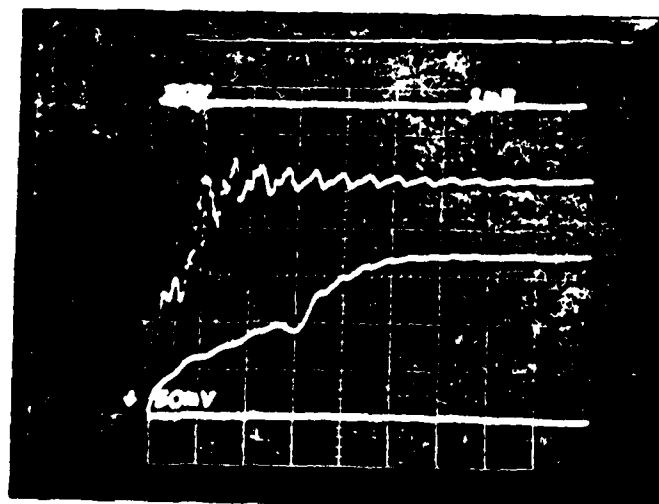


after shut down
voltage

240VDC
CURRENT

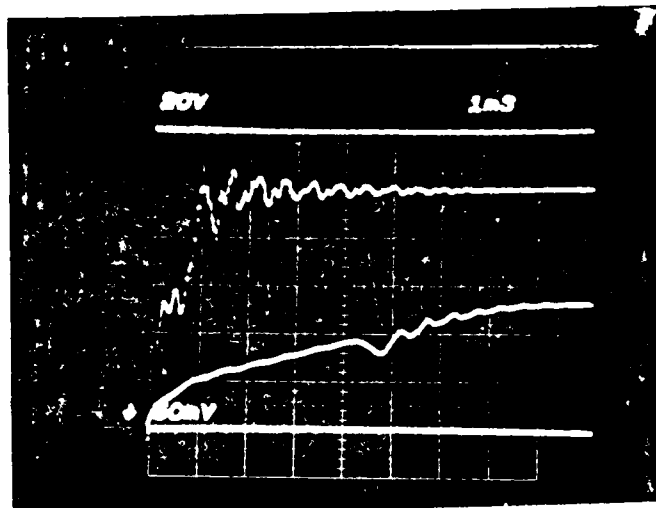


280VDC

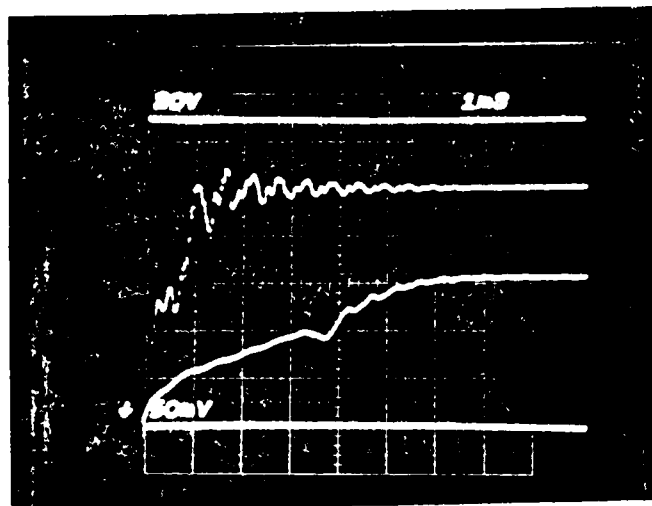


320VDC

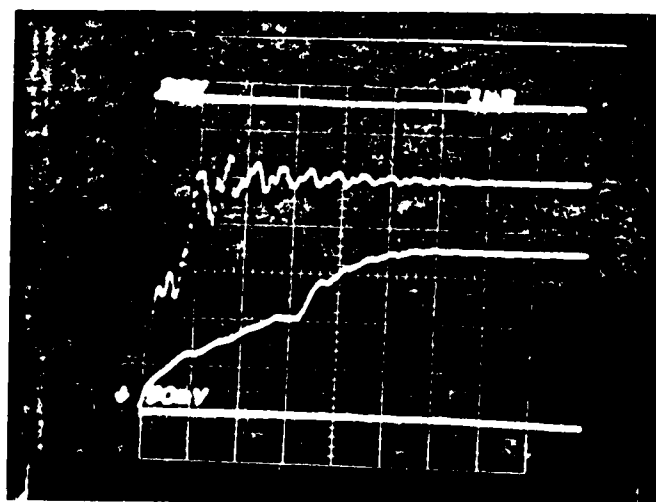
RESPONSE @ 400 PSI



24.0VDC



28.0VDC



32.0VDC

Phase III

ACCEPTANCE TEST DATA PACKAGE

0.5 lb_f TORQUE MOTOR BIPROPELLANT VALVE

Moog Model 51E112
Moog Part Number A24461
Moog Serial Number 005

Test Data Prepared by: Daniel J. East Date 1-14-80
Approved by: Arthur Phillips Date 1-14-80

MODEL 51F112

S/N 005

Test Description	Limits	Data Value
1.0 Examination of Product 1.1 Inspection for drawing compliance	(Mark OK)	<u>OK</u>
1.2 S/N Identification	Check ATDP documentation and unit marking (Mark OK)	<u>OK</u>
1.3 Weight (with injector)		<u>250.4</u> gms
2.0 Dielectric Strength at 500 VAC, 60 Hz for 10 seconds	≤ 1000 V	<u>1.0</u> uA
3.0 Insulation Resistance at 500 VDC for 60 seconds	≥ 100 megohms	<u>400,000</u> megohms
4.0 Coil Resistance	177 ± 15 ohms	e <u>180.2</u> ohms <u>78</u> °F
5.0 Proof Pressure at 800 psi GN ₂ for 3 minutes	No visible damage (Mark OK)	<u>OK</u>
6.0 Pull-In Current at 400 psi GN ₂		<u>70</u> ma
7.0 Drop-Out Current at 400 psi GN ₂		<u>33</u> ma
8.0 Valve Response	≤ 1.005 sec	
Opening & Closing Response	Inlet Pressure	Voltage
	350 400 500	24, 28, 32 24, 28, 32 24, 28, 32
		(See Photographs AND RESPONSE SHEET
9.0 Pressure Drop	(See Graph)	

<u>Test Description</u>	<u>Limits</u>	<u>Data Value</u>
9.0 Flush and Purge and Vacuum Dry for 1 hour at 120°F	Isopropyl Alcohol and GN ₂ , 100 cycles min. (Mark OK)	<u>OK</u>
10.0 Internal Leakage at 50 psi at 400 psi	<2.3 scc/hr GN ₂	Fuel Ox. <u>0.0</u> scc/hr <u>0.0</u> scc/hr <u>0.0</u> scc/hr <u>0.0</u> scc/hr
11.0 External Leakage at 50 psi at 400 psi	<2.3 scc/hr GN ₂	<u>0.0</u> scc/hr <u>0.0</u> scc/hr

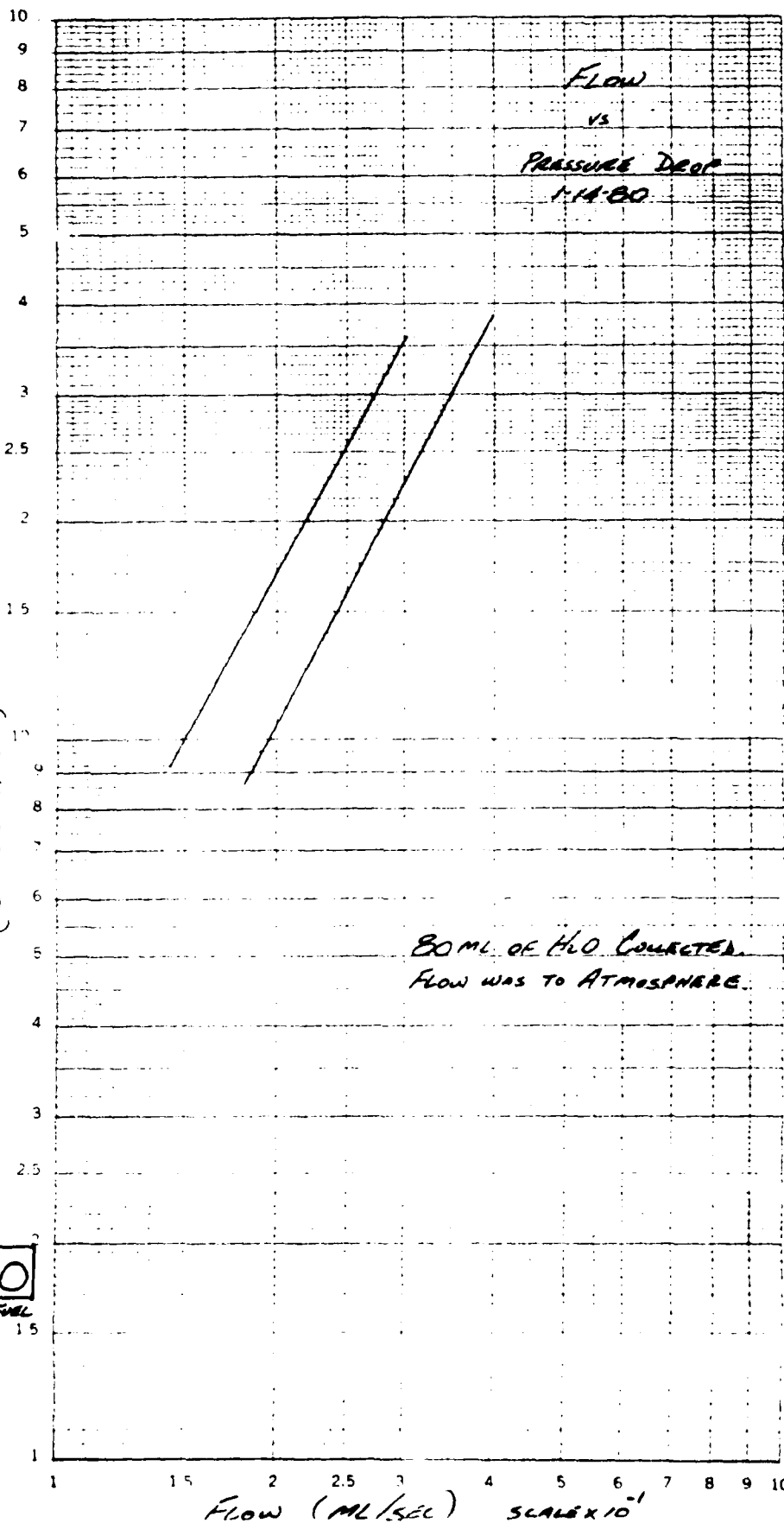
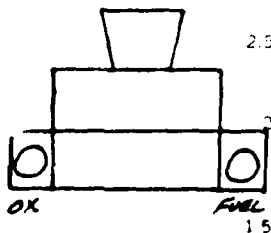
46 7083

K-E LOGARITHMIC 2 X 1 CYCLES
KEUFFEL & ESSER CO. MIN. N.Y.

PRESSURE DROP : INLET PRESSURES

(SCALE $\times 10^{-2}$)

ENGINE



51E112

5/N 005

FLOW TO ATMOSPHERE

TIME TO COLLECT 80 ML H₂O

INLET PRESSURE

FLOW RATE

PSI

FUEL

OXIDIZER

100

537.1 SEC.

408.0 SEC.

.149 ML/SEC.

.196 ML/SEC.

200

361.1 SEC.

287.0 SEC.

.222 ML/SEC.

.279 ML/SEC.

300

294.7 SEC.

220.9 SEC.

.271 ML/SEC.

.349 ML/SEC.

RESPONSE

350 PSI H₂O

	<u>OPEN</u>	<u>CLOSING</u>
24.0 VDC.	4.6 ms	0.7 ms.
28.0 VDC.	3.7 ms.	0.7 ms.
32.0 VDC.	3.1 ms.	0.7 ms.

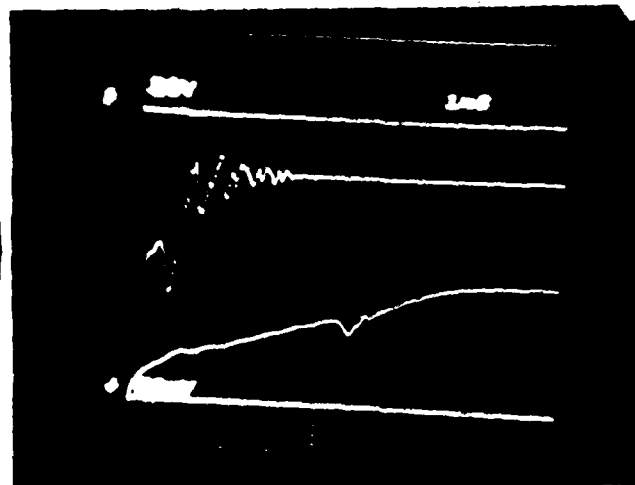
400 PSI H₂O

24.0 VDC.	4.9 ms	0.7 ms.
28.0 VDC.	4.0 ms.	0.7 ms.
32.0 VDC.	3.4 ms.	0.7 ms.

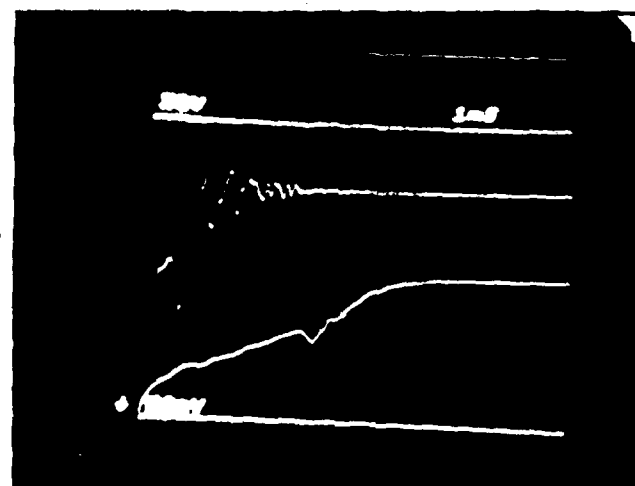
500 PSI H₂O

24.0 VDC.	6.2 ms.	0.7 ms.
28.0 VDC.	4.8 ms.	0.7 ms.
32.0 VDC.	3.9 ms.	0.7 ms.

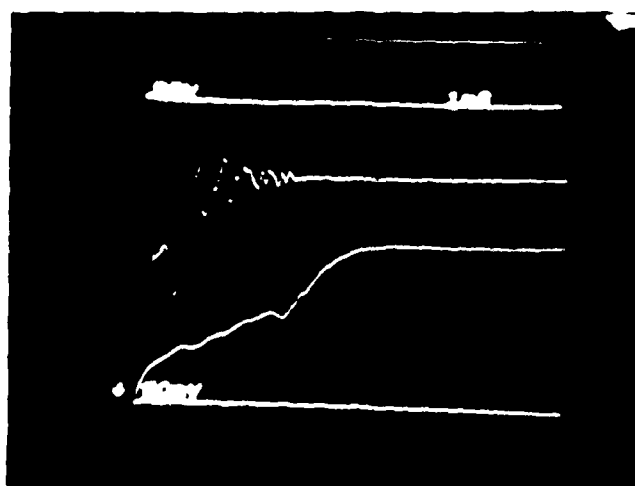
RESPONSE @ 350 PSI H₂O



24.0 VDC.

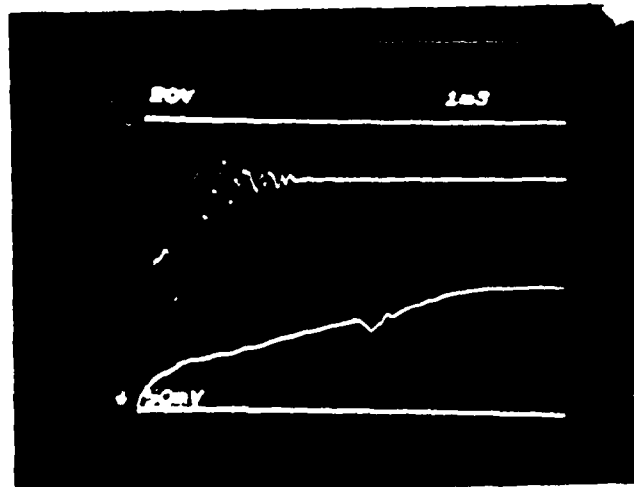


28.0 VDC.

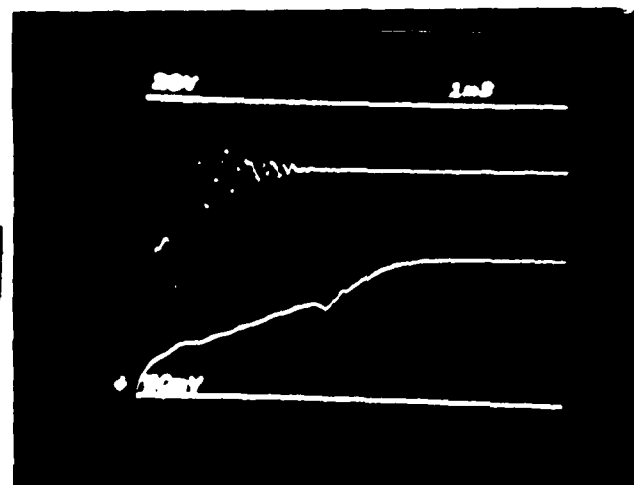


32.0 VDC.

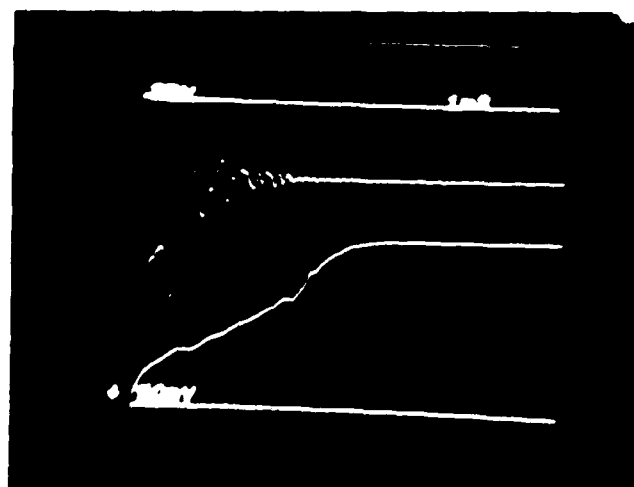
RESPONSE @ 400 PSI H₂O



24.0VDC.

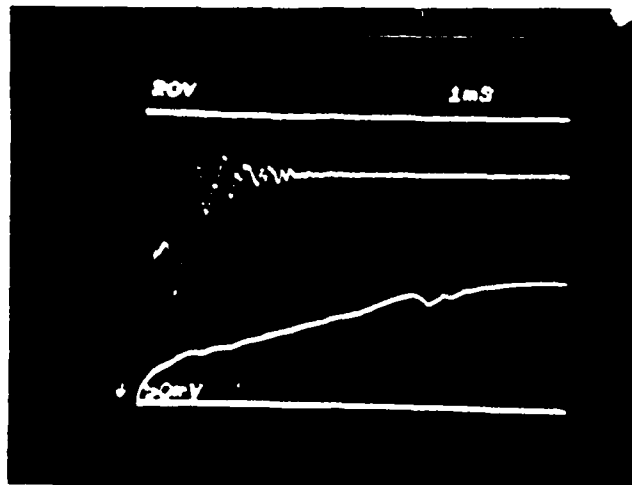


28.0VDC.

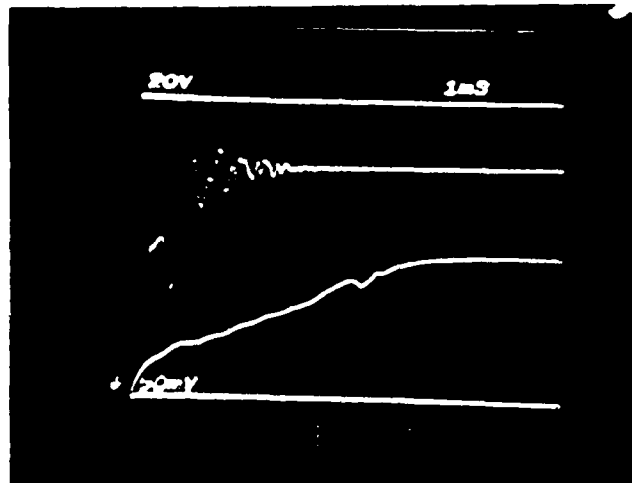


32.0VDC.

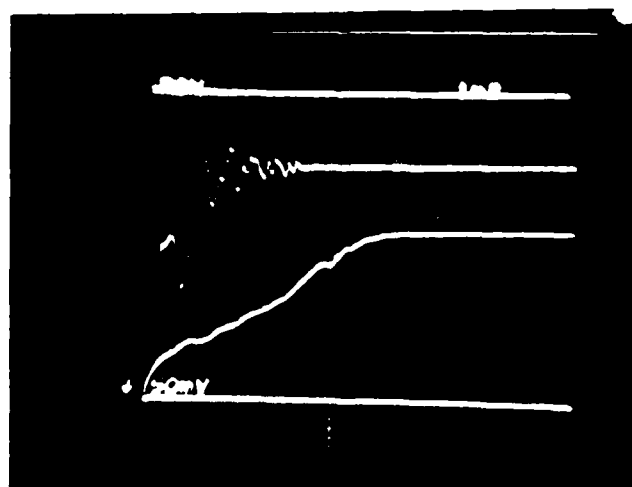
RESPONSE @ 500 PSI H₂O



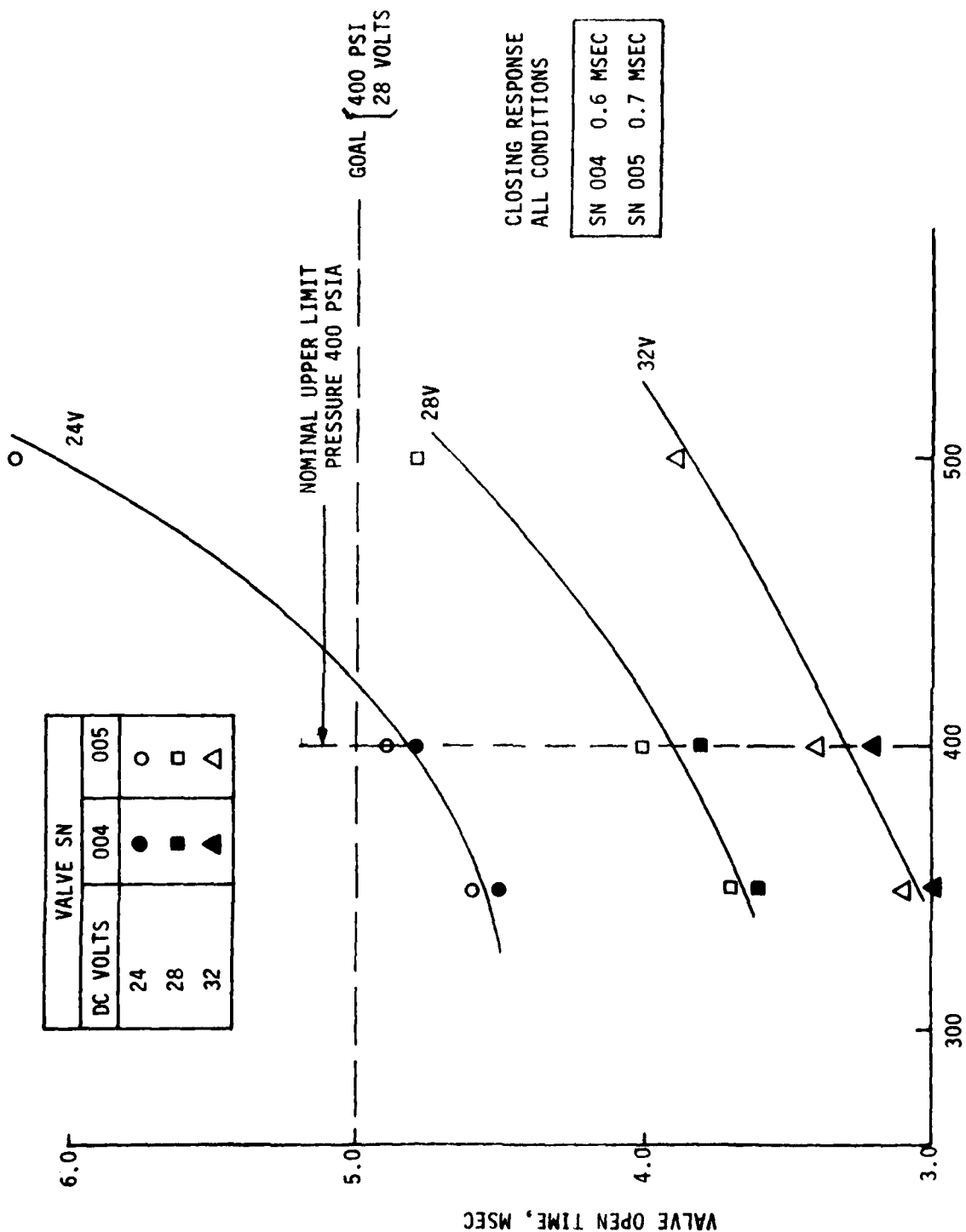
24.0 VDC.



28.0 VDC.



32.0 VDC.



VALVE INLET PRESSURE, PSIA

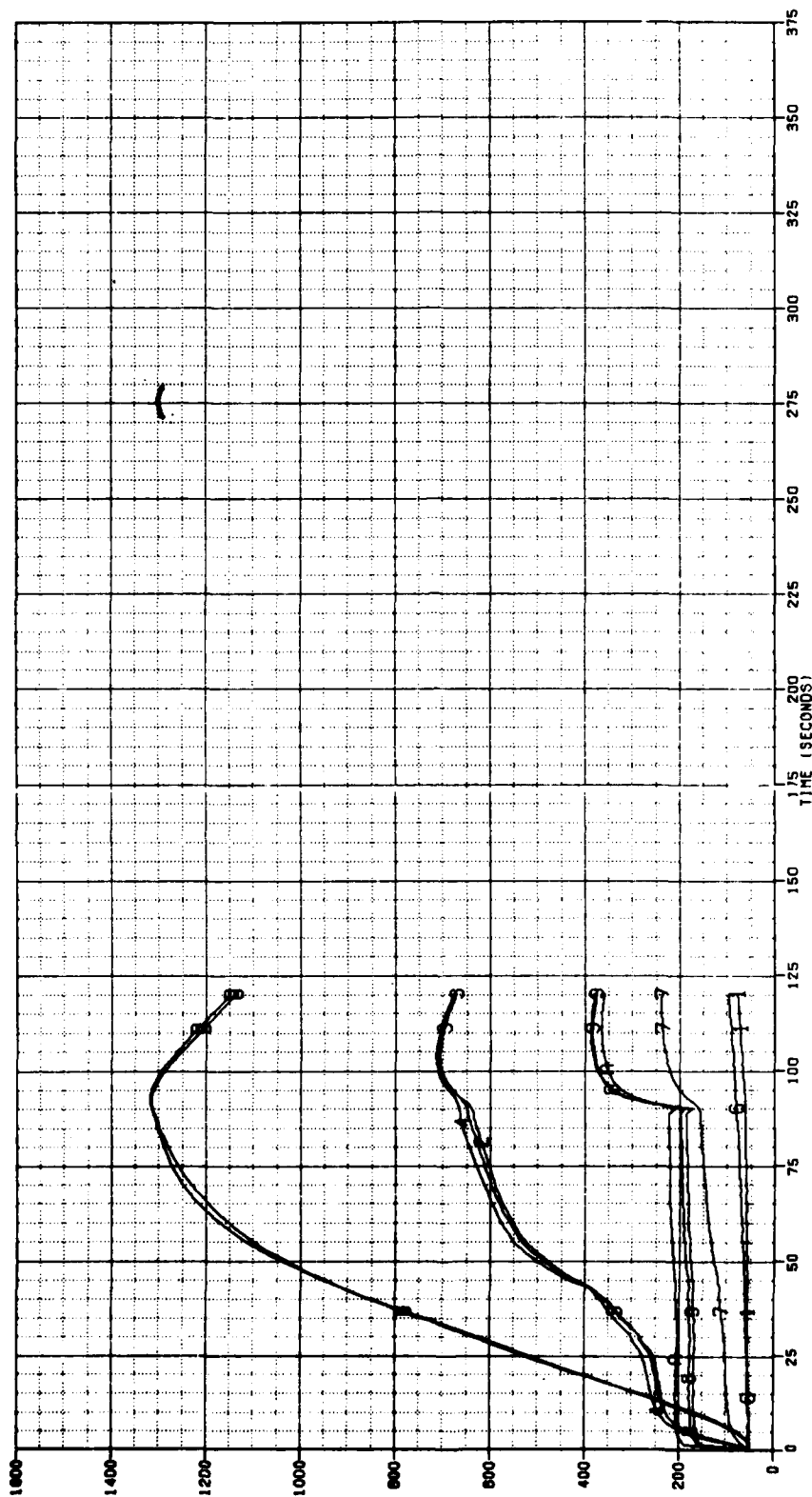
Response versus Voltage and Feed System Pressure

APPENDIX E

PHASE III STEADY-STATE DURABILITY TEST DATA

NOTES:

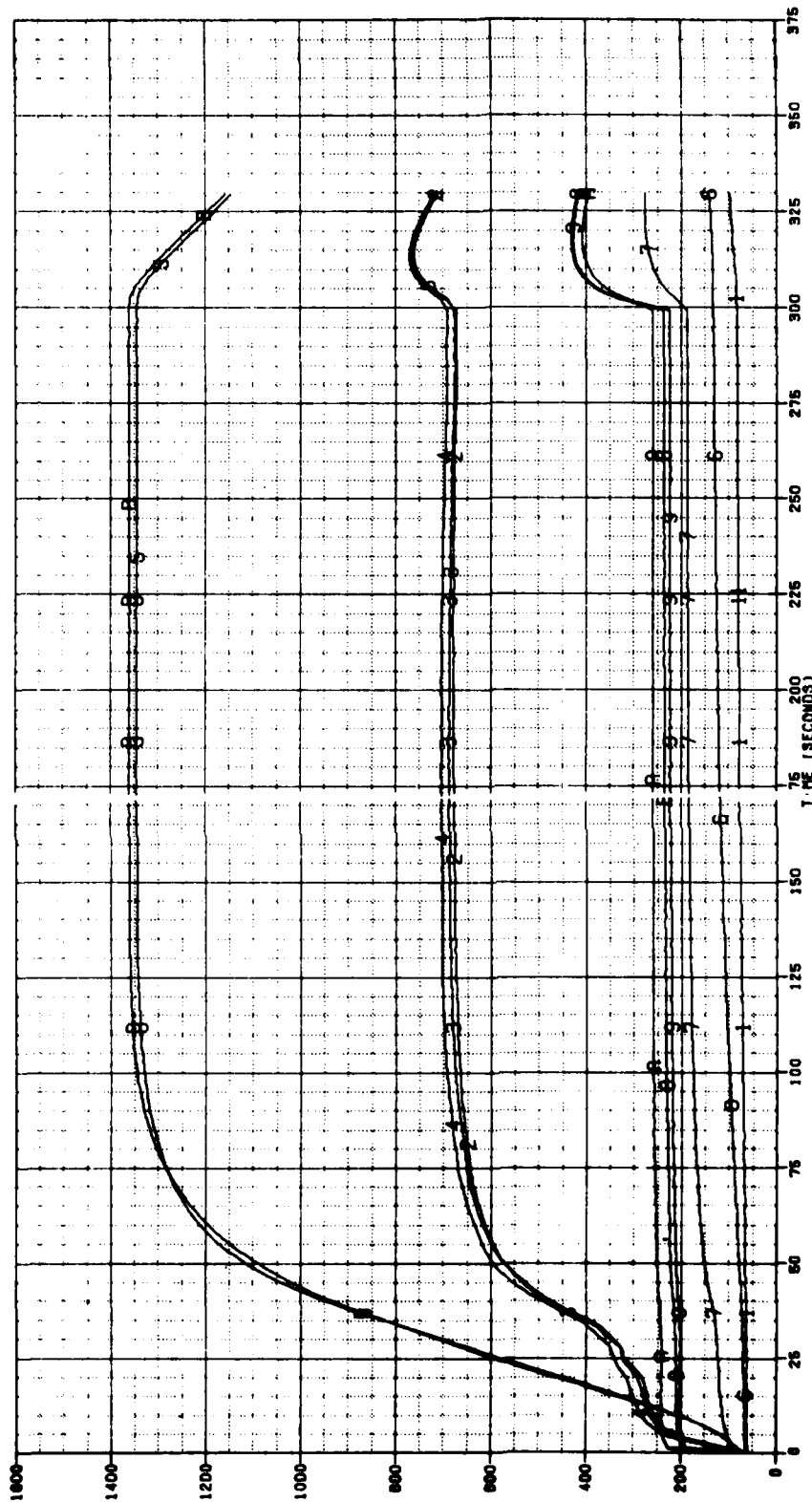
1. Thermocouple locations of the data presented in this appendix were noted in Figure 6-15.
2. Flowrates quoted are in 10^{-3} lb of water per sec. The paddle wheel flow meters have accuracy limitations that limit their usefulness to reflect changes in flow-rate, not absolute value.
3. The value of "F STAT" (thrust) shown is raw data without stand bias or exit pressure correction. The stand bias is approximately 1.26 at the start of the test. Changes in thrust are due to a combination of vacuum cell press change, thrust load cell heating, and tank pressure drifts during the tests. The first thrust record of the test is not valid due to the slow response of the hydraulically damped stand mass.



TEMPERATURES VS TIME TEST STAND A-2
 .581-698-502

TEST DATE 01-31-80

REPOJET LIQUID ROCKET COMPANY, SACRAMENTO, CALIFORNIA

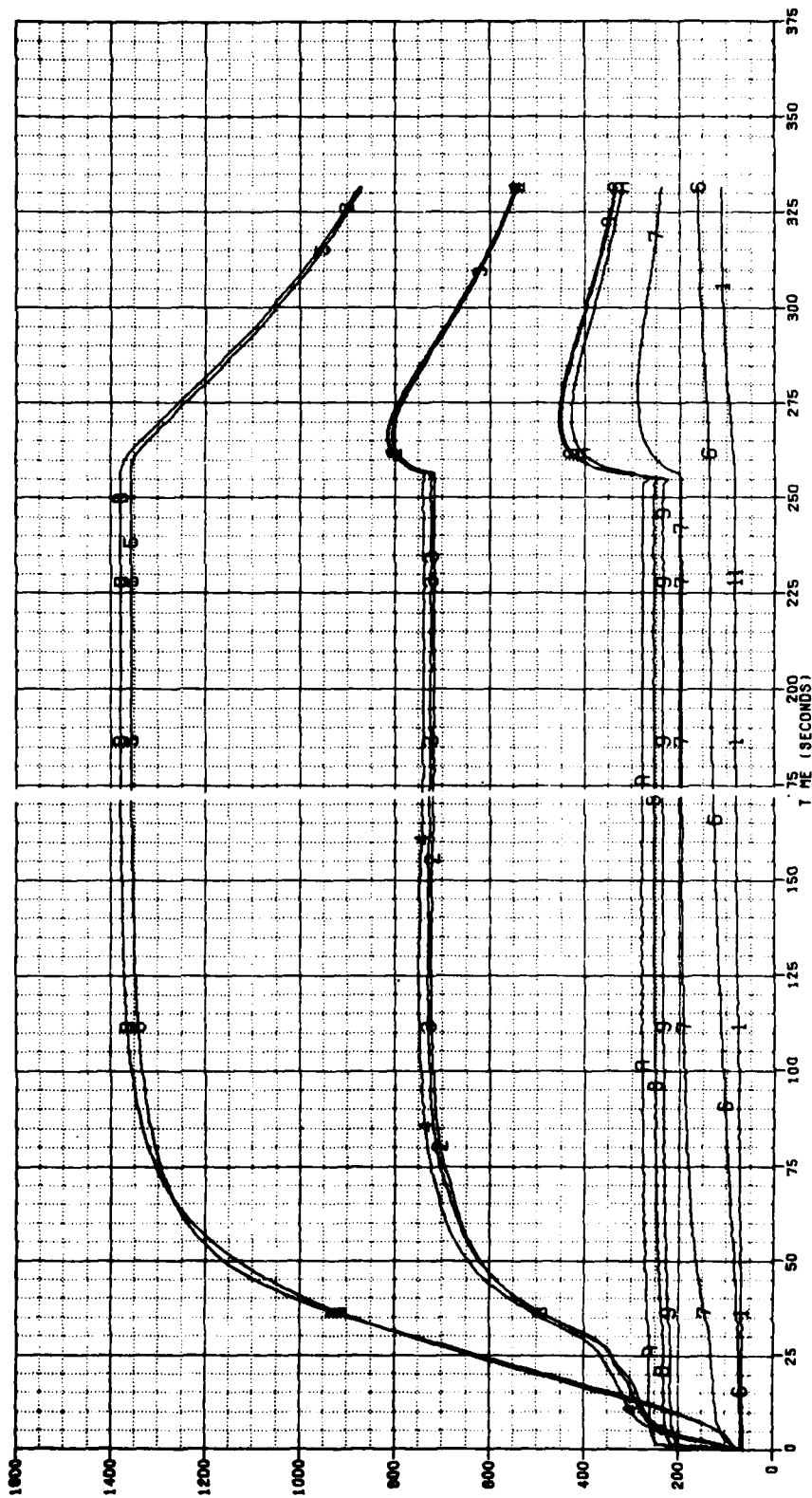


TEMPERATURES VS TIME
 .581-698-503 TEST STAND A-2

TEST DATE 01-31-80

AEROJET LIQUID ROCKET COMPANY, SACRAMENTO, CALIFORNIA

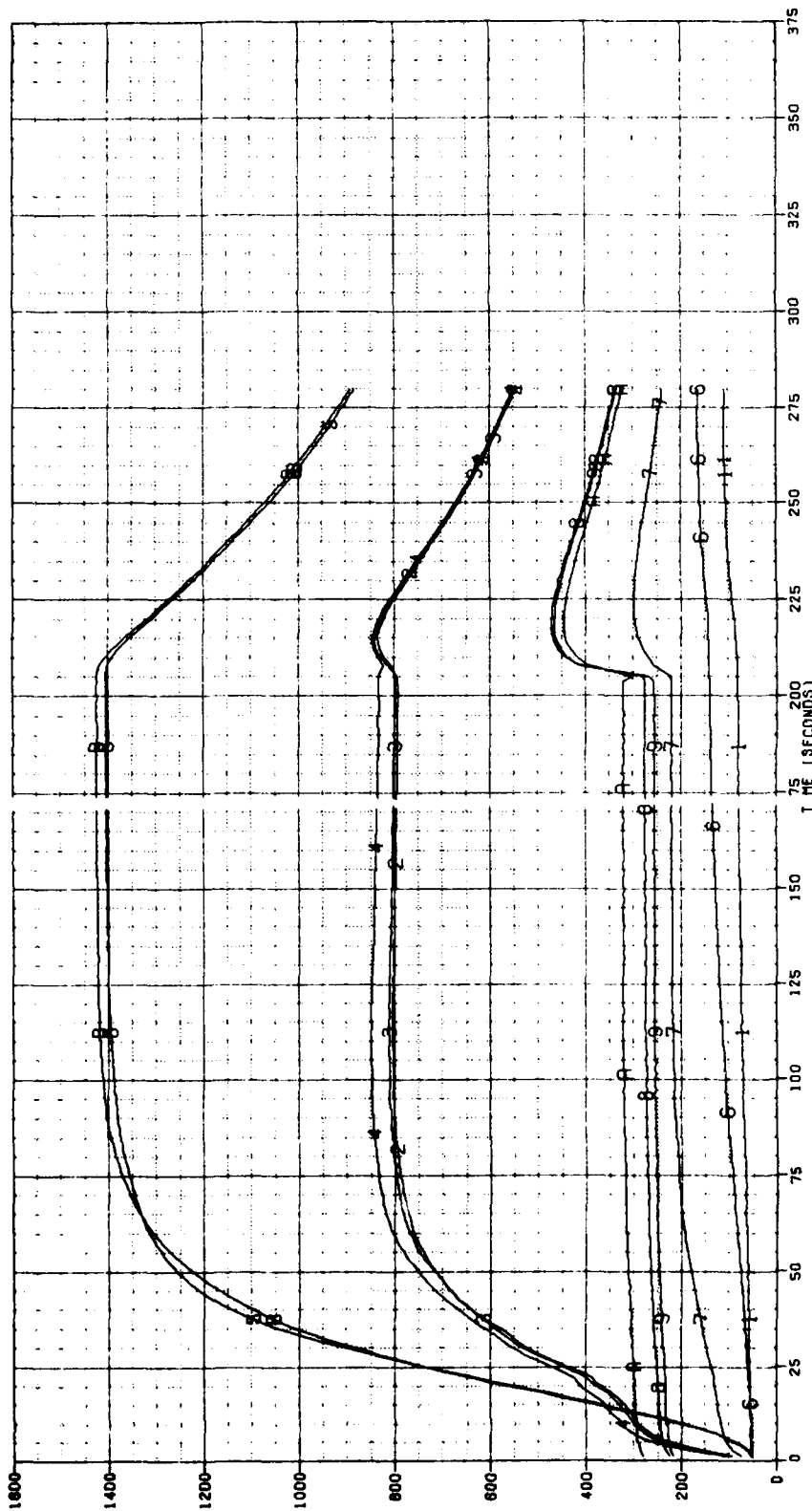
1	TV8	DEG F	7	TL	DEG F
2	TMLO-090	DEG F	8	TS-090	DEG F
3	TMLO-180	DEG F	9	TS-170	DEG F
4	TMLO-270	DEG F	A	TS-270	DEG F
5	TCR-000	DEG F	B	TR-217	DEG F
6	TPC	DEG F			



TEST DATE 01-31-80

HEROJET LIQUID ROCKET COMPANY, SACRAMENTO, CALIFORNIA

- | | | | |
|-------------|-------|-----------|-------|
| 1 TVB | DEG F | 7 TL | DEG F |
| 2 TWELD-090 | DEG F | 8 TS-090 | DEG F |
| 3 TWELD-180 | DEG F | 9 TS-170 | DEG F |
| 4 TWELD-270 | DEG F | 10 TS-270 | DEG F |
| 5 TCR-000 | DEG F | 11 TR-217 | DEG F |
| 6 TPC | DEG F | | |

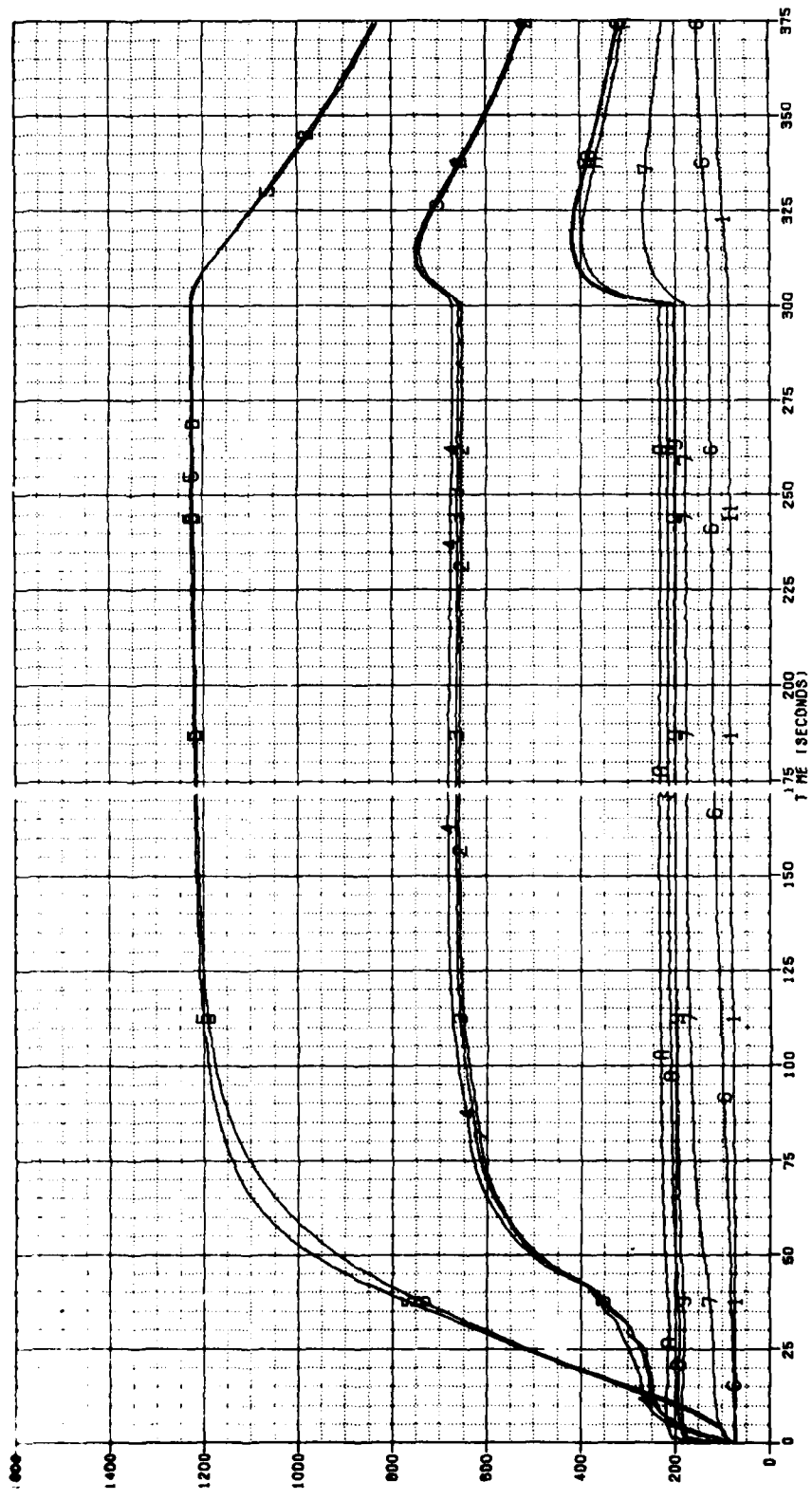


TEMPERATURES VS TIME PLOT A
 .581-698-505 TEST STAND A-2

TEST DATE 01-31-80

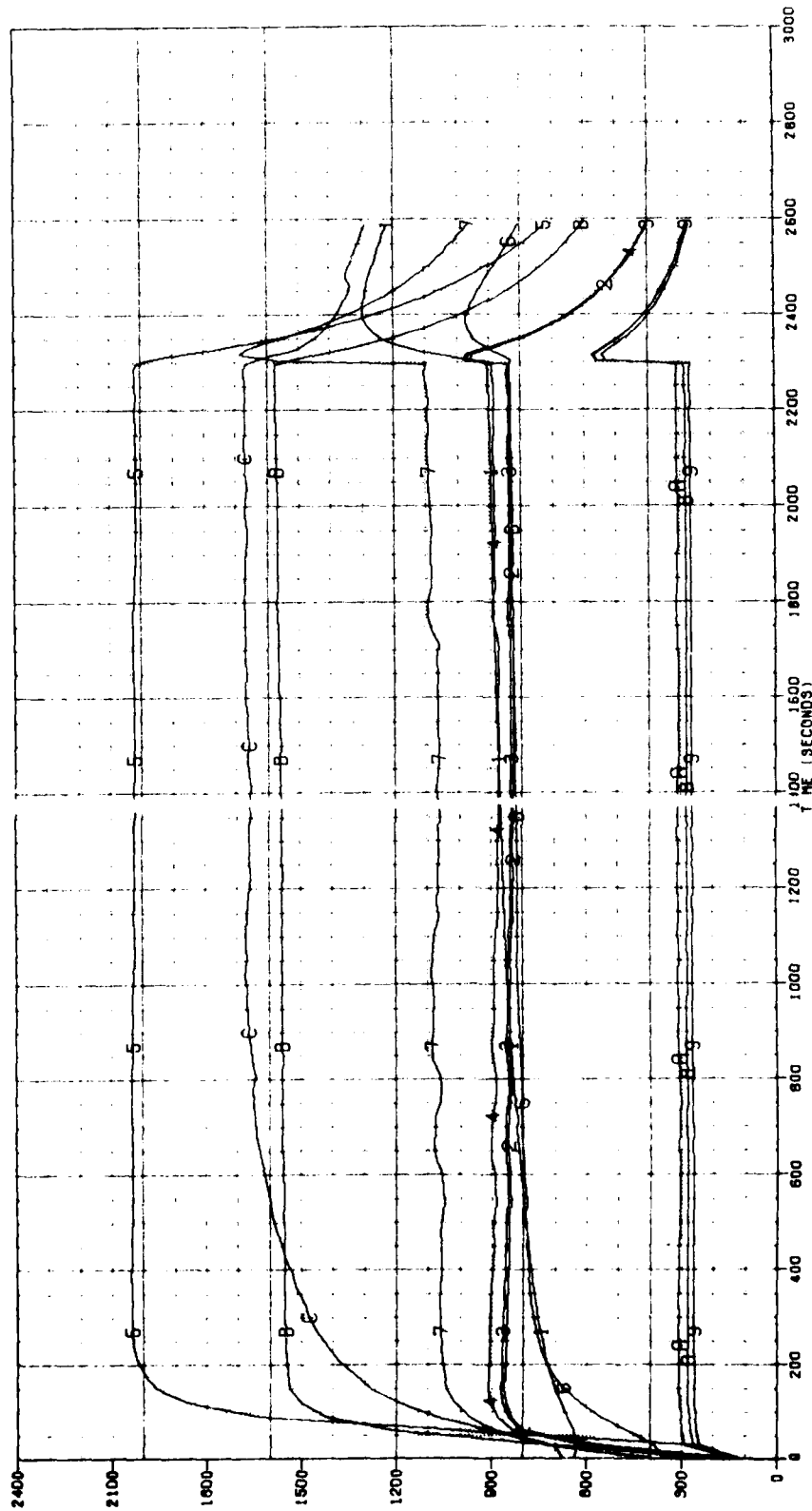
AEROJET LIQUID ROCKET COMPANY, SACRAMENTO, CALIFORNIA

- | | | | |
|-------------|-------|-----------|-------|
| 1 TV8 | DEG F | 7 TL | DEG F |
| 2 TWELD-090 | DEG F | 8 TS-090 | DEG F |
| 3 TWELD-180 | DEG F | 9 TS-170 | DEG F |
| 4 TWELD-270 | DEG F | 10 TS-270 | DEG F |
| 5 TCR-000 | DEG F | 11 TR-217 | DEG F |
| 6 TPC | DEG F | | |



TEMPERATURES VS TIME
 .581-698-506
 TEST DATE 01-31-80
 AEROJET LIQUID ROCKET COMPANY, SACRAMENTO, CALIFORNIA

- | | | | |
|-------------|-------|-----------|-------|
| 1 TVB | DEG F | 7 TL | DEG F |
| 2 TWELD-090 | DEG F | 8 TS-090 | DEG F |
| 3 TWELD-180 | DEG F | 9 TS-170 | DEG F |
| 4 TWELD-270 | DEG F | 10 TS-270 | DEG F |
| 5 TCR-000 | DEG F | 11 TR-217 | DEG F |
| 6 TPC | DEG F | | |

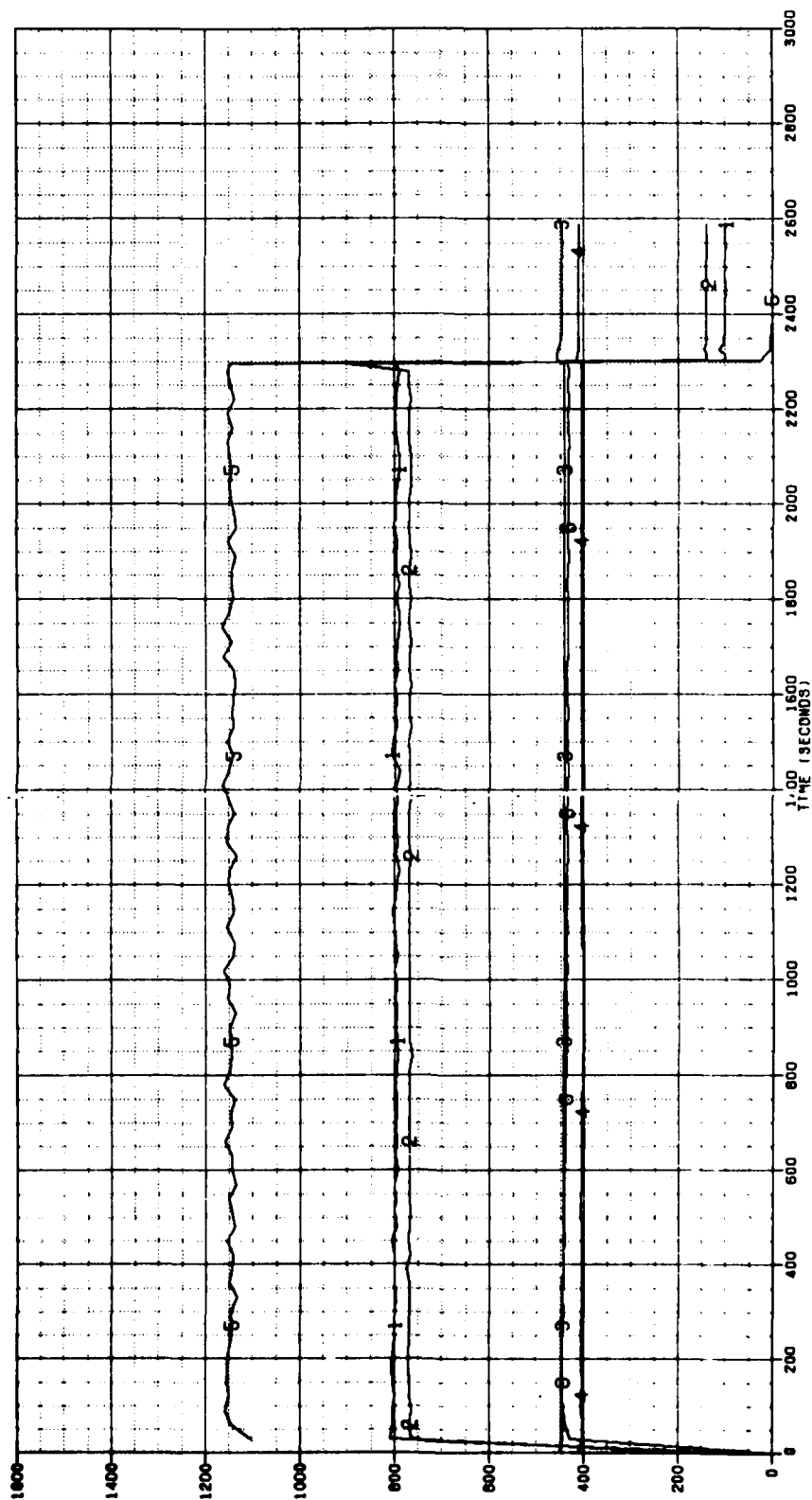


TEMPERATURES VS TIME PLOT A
 .581-698-510 TEST STAND A-2

TEST DATE 02-06-80

AEROJET LIQUID ROCKET COMPANY, SACRAMENTO, CALIFORNIA

1	TVB (MV)	DEG F
2	TMELD-990	DEG F
3	TMELD-180	DEG F
4	TMELD-270	DEG F
5	TT-090	DEG F
6	TPC	DEG F
7	TL	DEG F
8	TS-090	DEG F
9	TS-170	DEG F
10	TS-270	DEG F
11	TT-217	DEG F
12	TVL	DEG F

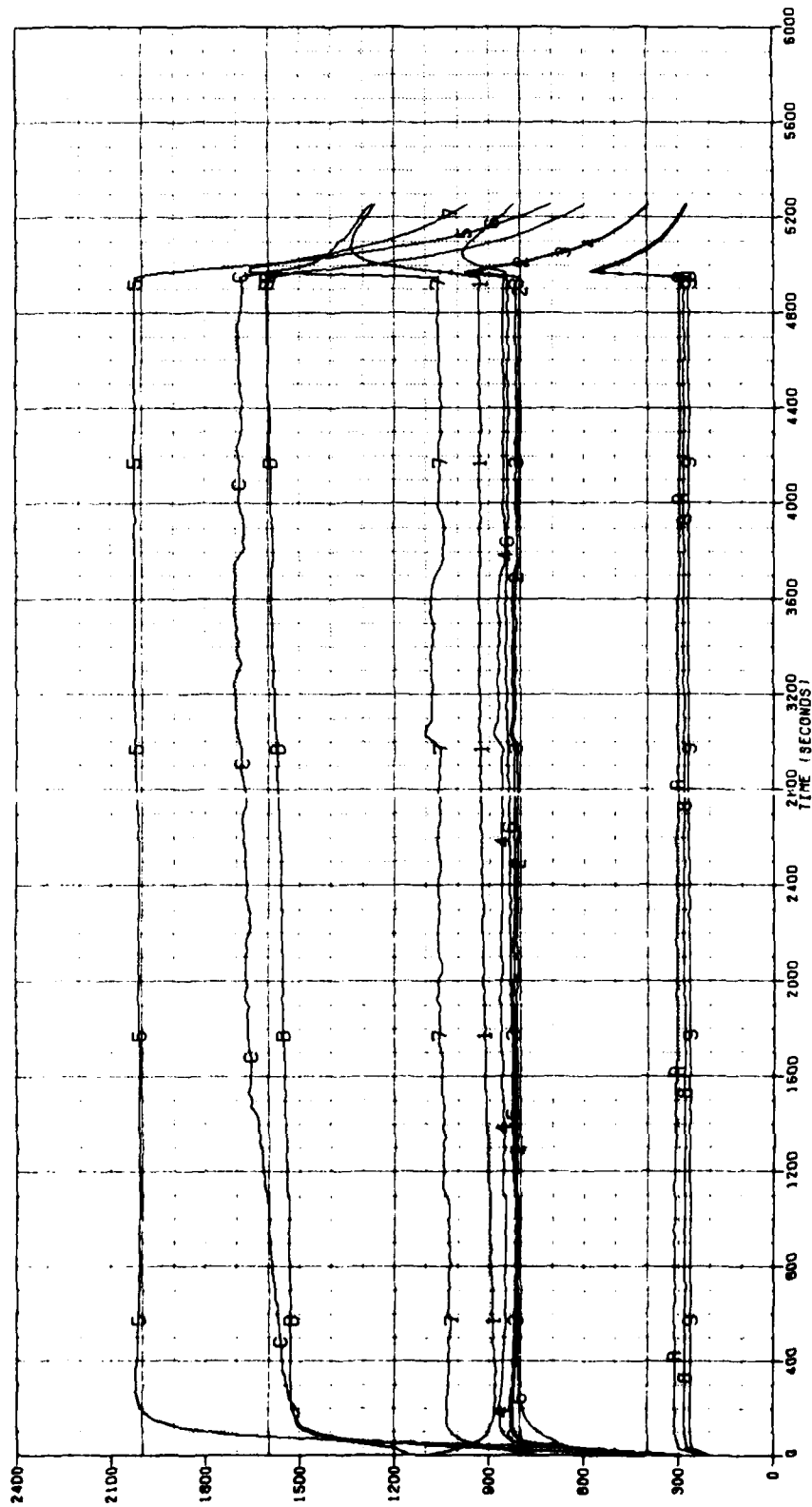


- 1 MO-1X1-E6 LB-W
- 2 MF-1X1-E8 LB-W
- 3 POL PSIA-AP
- 4 PFL PSIA-AP
- 5 PC X10. PSIA-AP
- 6 FSTAT X1000.LBS

[illegible]

THIS PAGE IS BEST QUALITY PRACTICABLE
FROM COPY OF ORIGINAL

E-12

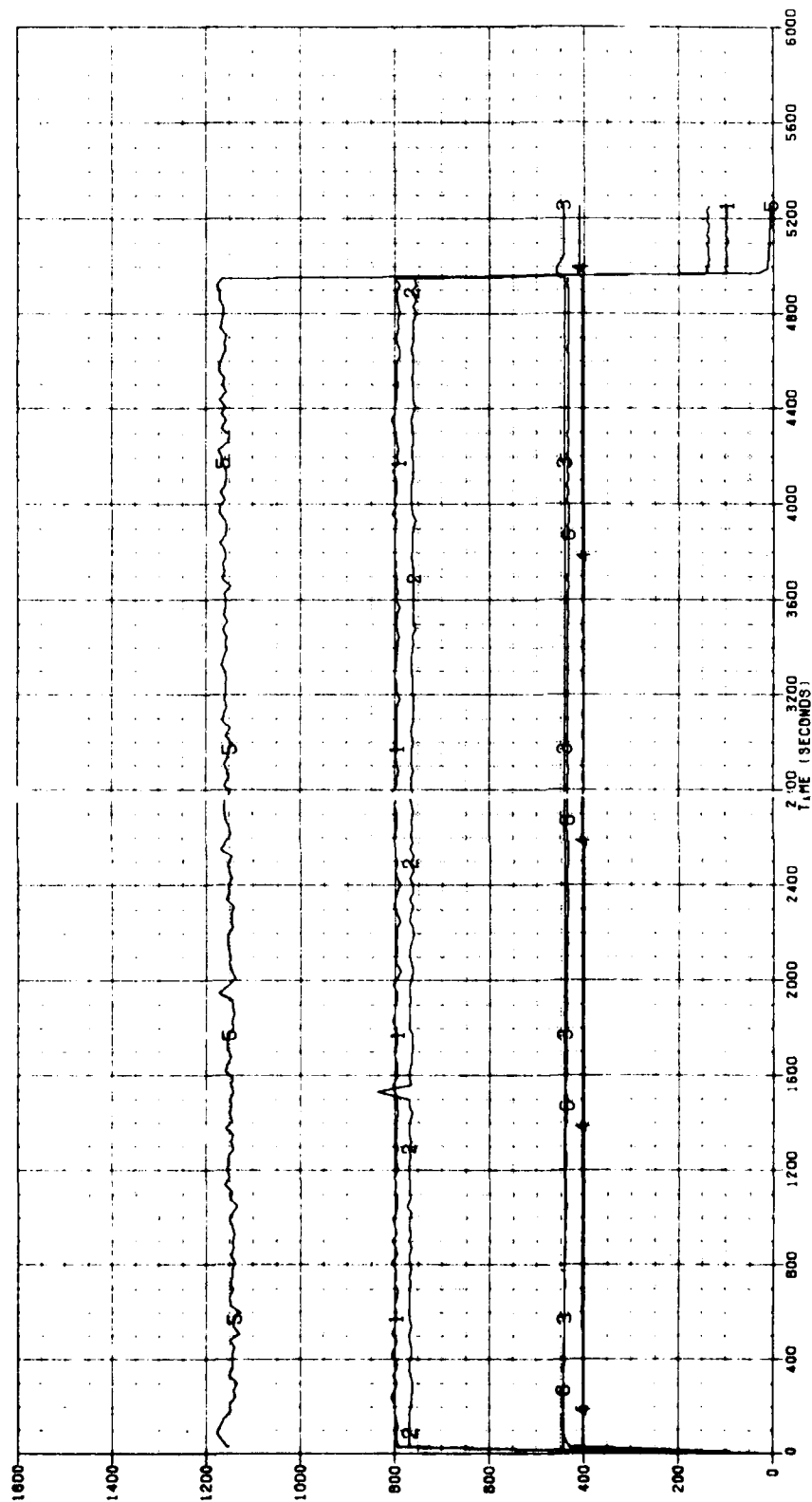


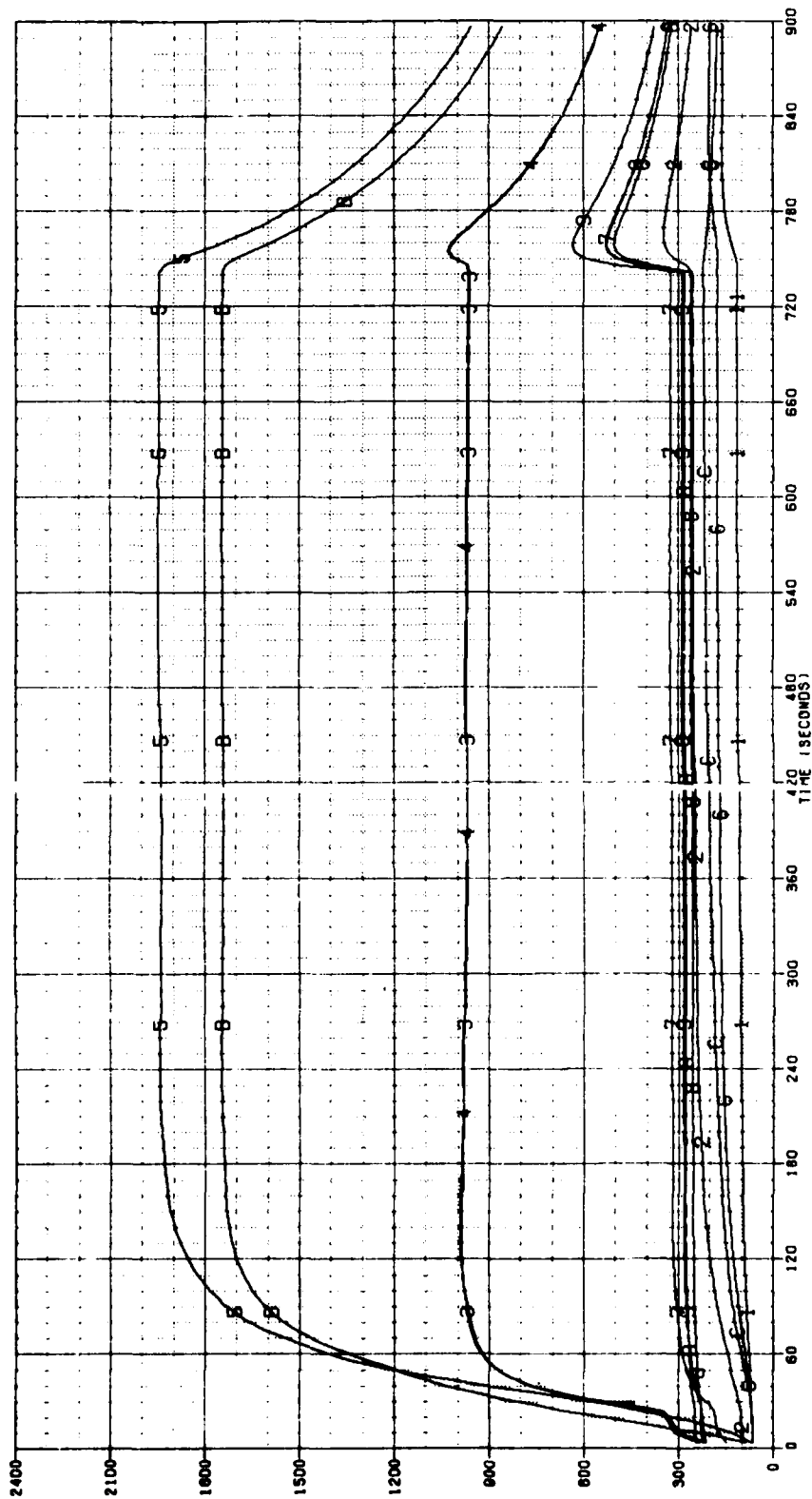
TEMPERATURES VS TIME TEST STAND A-2
 .581-698-511

TEST DATE 02-06-80

ROCKET LIQUID ROCKET COMPANY, SACRAMENTO, CALIFORNIA

1 TV8 INJECT	DEG F	7 TL	DEG F
2 TMELD-090	DEG F	8 TS-090	DEG F
3 TMELD-180	DEG F	9 TS-170	DEG F
4 TMELD-270	DEG F	A TS-270	DEG F
5 TT-090	DEG F	B TR-217	DEG F
6 TPC	DEG F	C TVC	DEG F



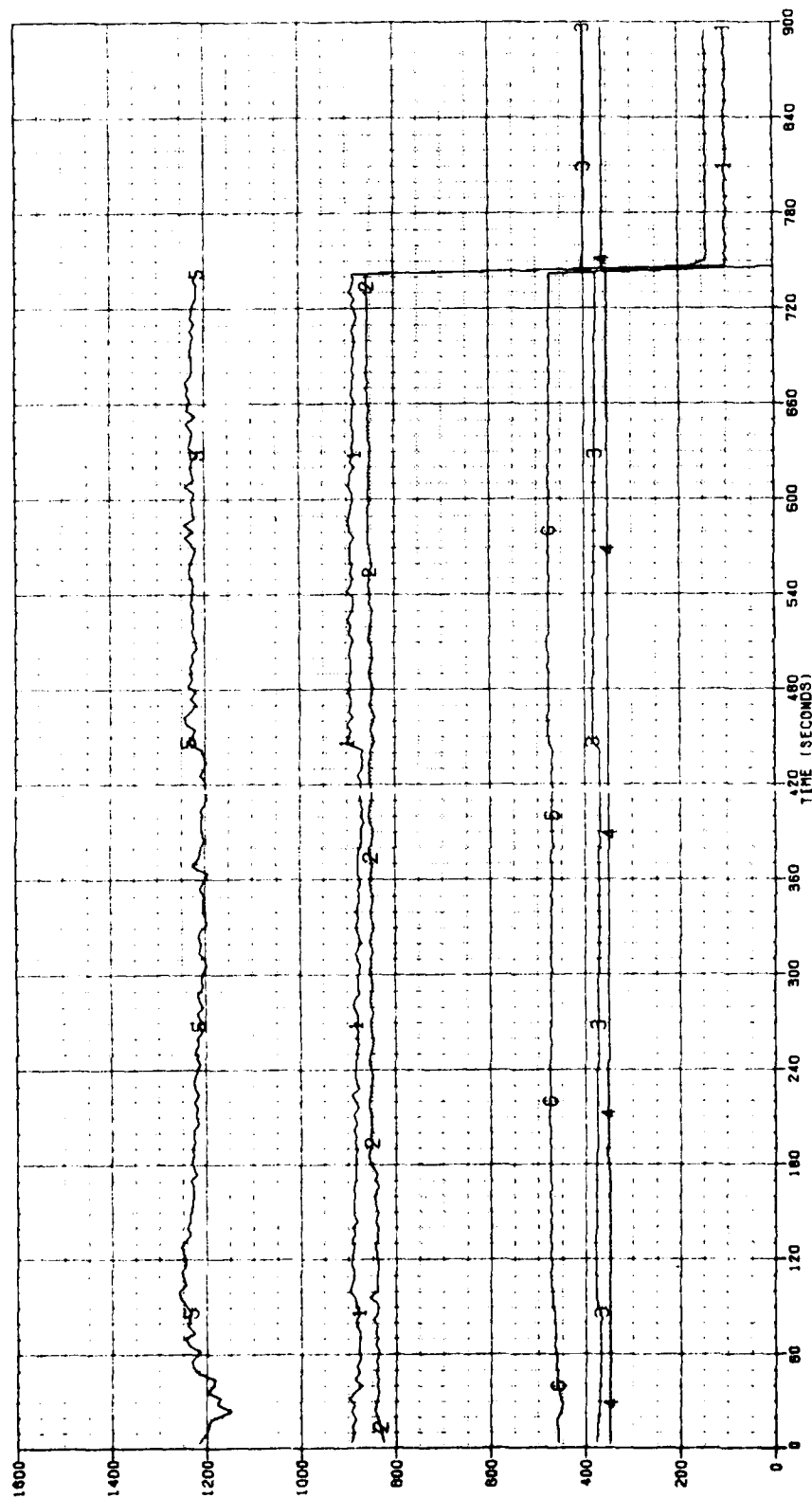


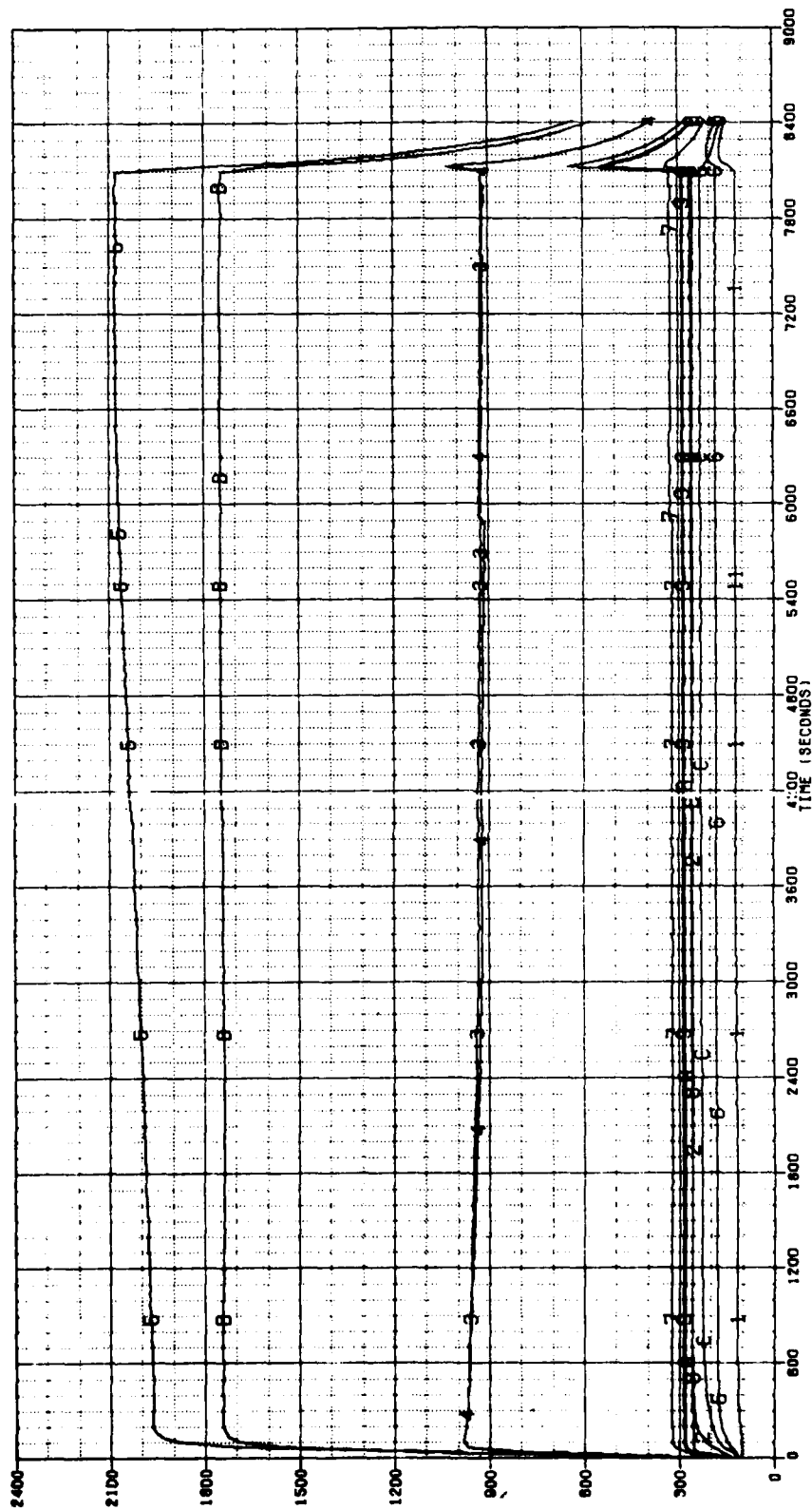
TEMPERATURES VS TIME TEST STAND A-2
PLOT A

TEST DATE 02-20-80

AEROJET LIQUID ROCKET COMPANY, SACRAMENTO, CALIFORNIA

1 TVB	DEG F	7 TL	DEG F
2 TWELD-090	DEG F	8 TS-090	DEG F
3 TWELD-180	DEG F	9 TS-170	DEG F
4 TWELD-270	DEG F	A TS-270	DEG F
5 TT-090	DEG F	B TR-217	DEG F
6 TPC	DEG F	C TVC	DEG F



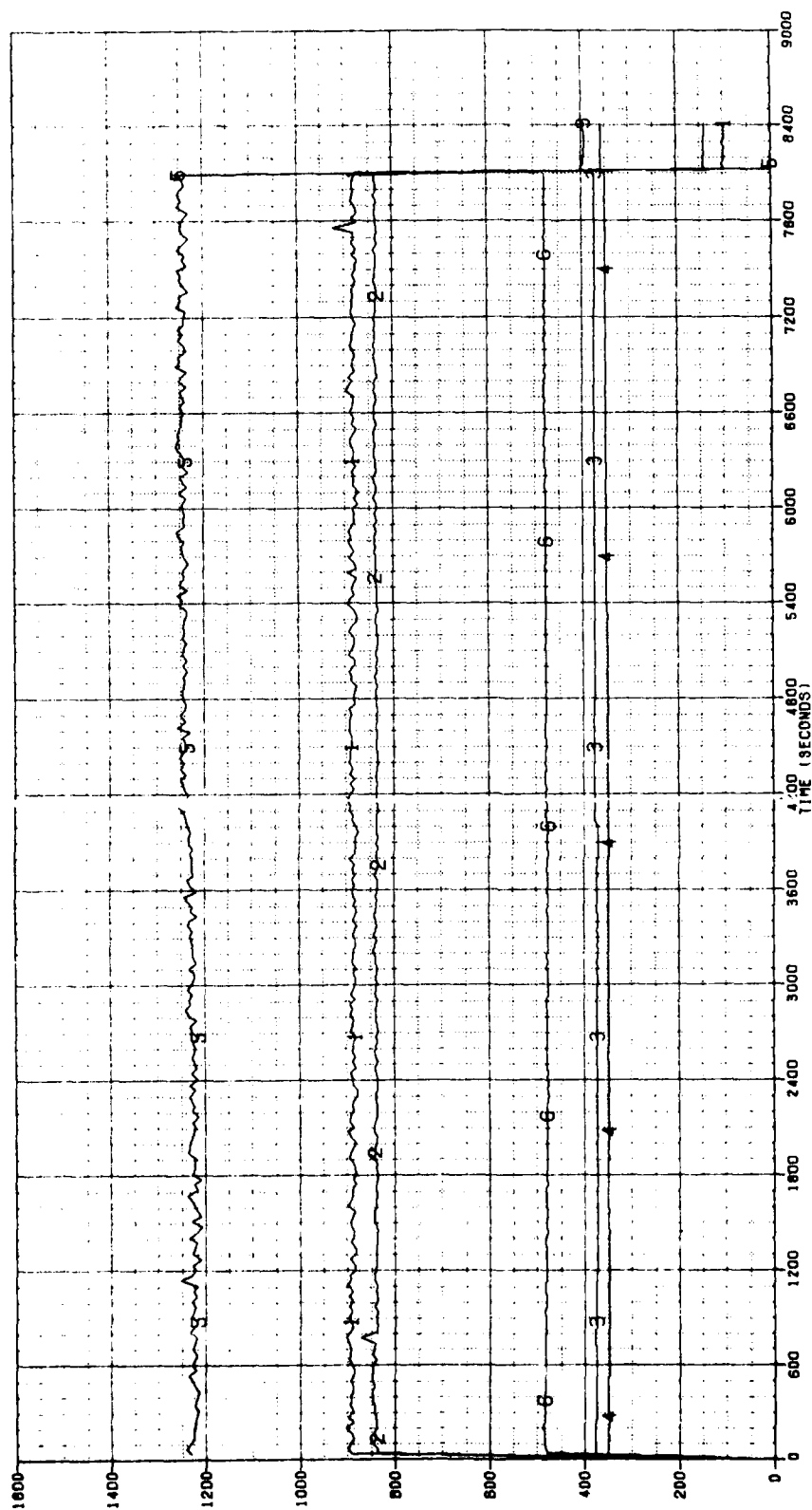


TEMPERATURES VS TIME
 .SB1-698-526 TEST STAND A-2

TEST DATE 02-20-80

HEADJET LIQUID ROCKET COMPANY, SACRAMENTO, CALIFORNIA

1	TVB	DEG F	7	TL	DEG F
2	TWELD-090	DEG F	8	TS-090	DEG F
3	TWELD-180	DEG F	9	TS-170	DEG F
4	TWELD-270	DEG F	10	TS-270	DEG F
5	TT-090	DEG F	11	TR-217	DEG F
6	TPC	DEG F		C	TVC



MEASURED PARAMETERS VS TIME PLOT B
 .581-698-526 TEST STAND A-2

TEST DATE 02-20-80

AEROJET LIQUID ROCKET COMPANY, SACRAMENTO, CALIFORNIA

- 1 MO-1X1.E6 LB-W
- 2 MF-1X1.E8 LB-W
- 3 POL PSIA-AP
- 4 PFL PSIA-AP
- 5 PC X10. PSIA-AP
- 6 FSTAT <1000.LBS

AD-A091 078

AEROJET LIQUID ROCKET CO SACRAMENTO CA
LOW-THRUST BI-PROPELLANT ENGINE TECHNOLOGY.(U)
AUG 80 L SCHOENMAN, R L FRIEDMAN

F/6 21/9.1

F04611-77-C-0053

UNCLASSIFIED

AFRPL-TR-80-47

NL

5.5

12.8

12.8

END

DATE

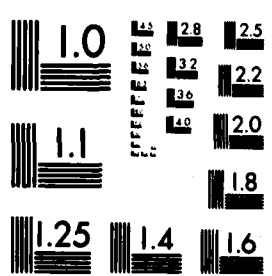
12-80

DTIC

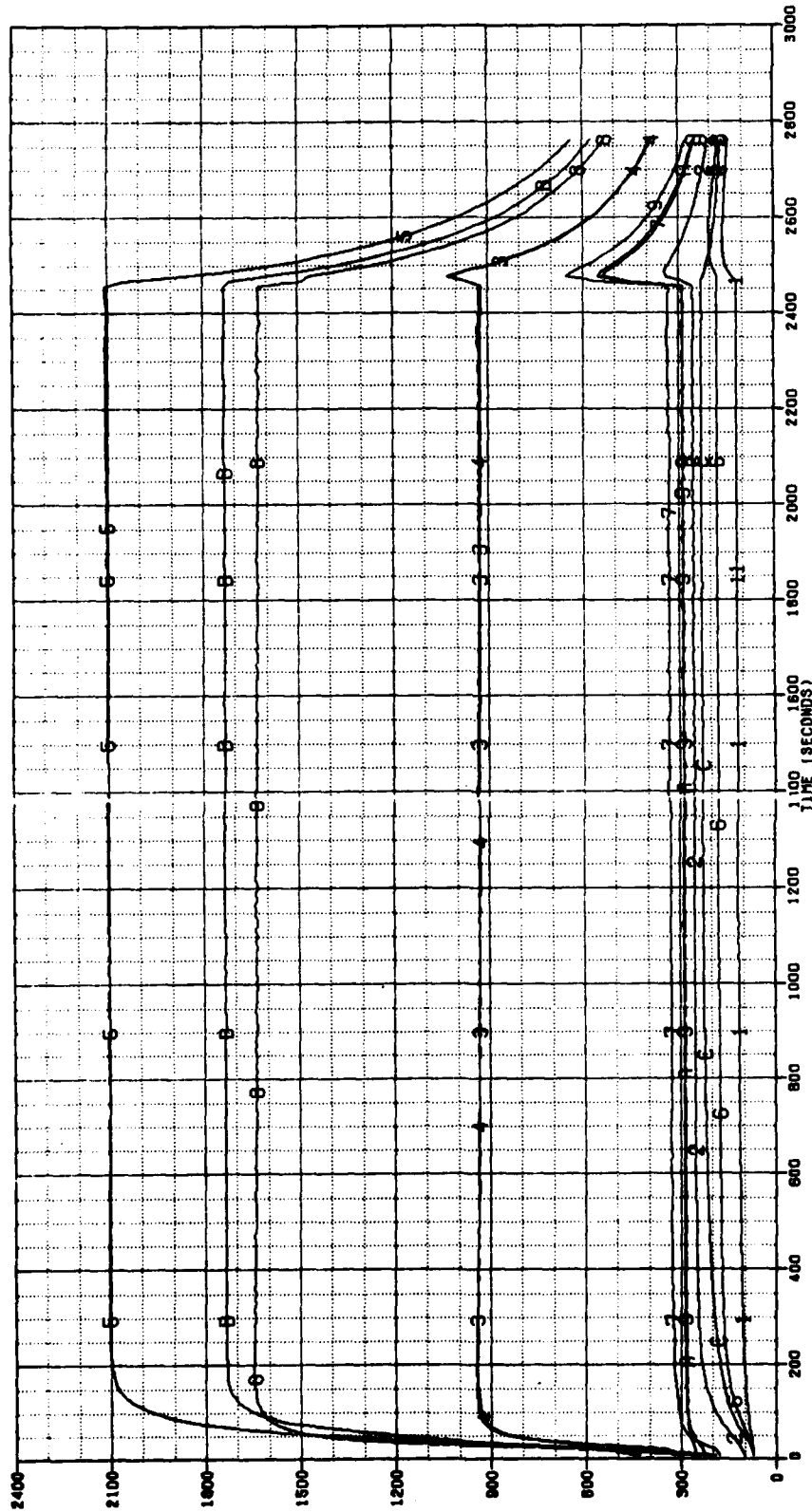
5 OF 5

AD. A

091078



MICROCOPY RESOLUTION TEST CHART
NATIONAL BUREAU OF STANDARDS-1963-A



TEMPERATURES VS TIME

TEST DATE 02-28-80

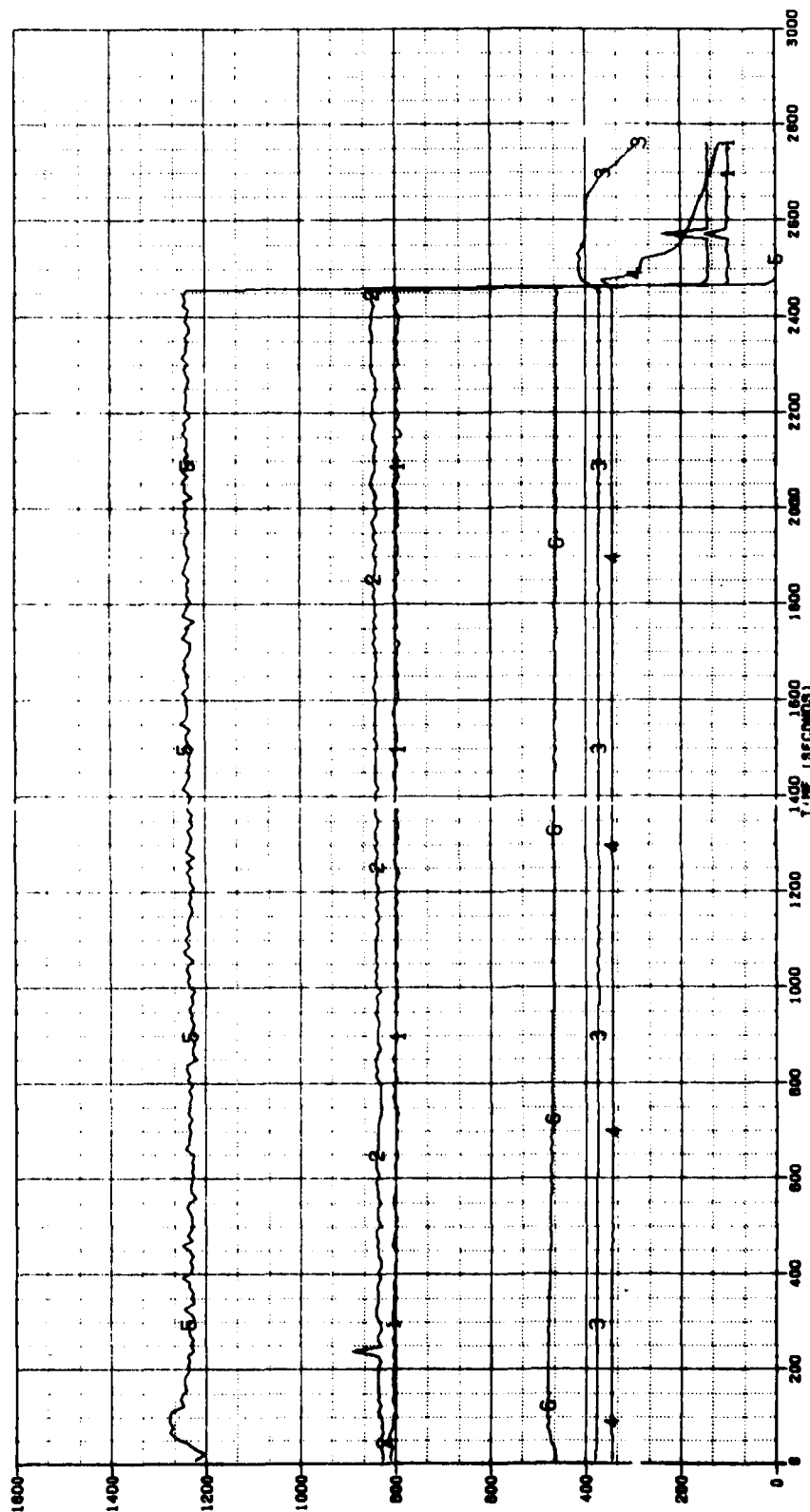
TEST STAND A-2

PLLOT A

TEMPERATURE (DEG F)

TIME (SECONDS)

1 TL
2 TO-180
3 TS-170
4 TS-270
5 TR-217
6 TVC
7 TVC
8 TVC
9 TVC
10 TVC
11 TVC



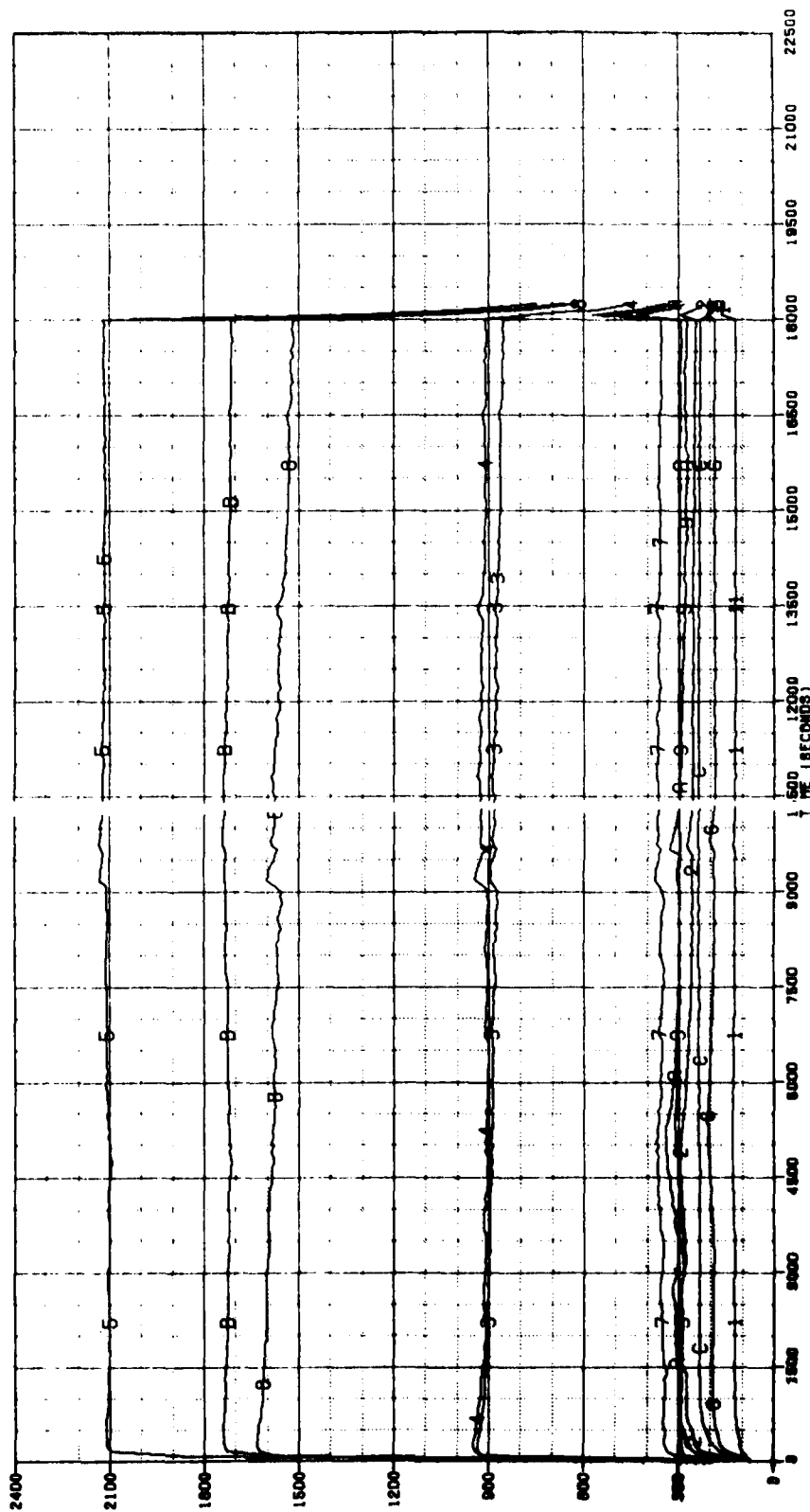
MEASURED PARAMETERS VS TIME PLOT B
 .581-698-528 TEST STAND A-2

TEST DATE 02-20-68

REJOJET LIQUID ROCKET COMPANY, SACRAMENTO, CALIFORNIA

Survey	Station	Time	Lat	Long	Alt	Temp	Wind	Dir	Bar	Hum	Vis	Cloud	Notes
131	13120-050	7400	36° 50' 30" N	156° 50' 00" W	1000	50.0	10	100	1010.0	95	10	000	13120-050
132	13120-050	7401	36° 50' 30" N	156° 50' 00" W	1000	50.0	10	100	1010.0	95	10	000	13120-050
133	13120-050	7402	36° 50' 30" N	156° 50' 00" W	1000	50.0	10	100	1010.0	95	10	000	13120-050
134	13120-050	7403	36° 50' 30" N	156° 50' 00" W	1000	50.0	10	100	1010.0	95	10	000	13120-050
135	13120-050	7404	36° 50' 30" N	156° 50' 00" W	1000	50.0	10	100	1010.0	95	10	000	13120-050
136	13120-050	7405	36° 50' 30" N	156° 50' 00" W	1000	50.0	10	100	1010.0	95	10	000	13120-050
137	13120-050	7406	36° 50' 30" N	156° 50' 00" W	1000	50.0	10	100	1010.0	95	10	000	13120-050
138	13120-050	7407	36° 50' 30" N	156° 50' 00" W	1000	50.0	10	100	1010.0	95	10	000	13120-050
139	13120-050	7408	36° 50' 30" N	156° 50' 00" W	1000	50.0	10	100	1010.0	95	10	000	13120-050
140	13120-050	7409	36° 50' 30" N	156° 50' 00" W	1000	50.0	10	100	1010.0	95	10	000	13120-050
141	13120-050	7410	36° 50' 30" N	156° 50' 00" W	1000	50.0	10	100	1010.0	95	10	000	13120-050
142	13120-050	7411	36° 50' 30" N	156° 50' 00" W	1000	50.0	10	100	1010.0	95	10	000	13120-050
143	13120-050	7412	36° 50' 30" N	156° 50' 00" W	1000	50.0	10	100	1010.0	95	10	000	13120-050
144	13120-050	7413	36° 50' 30" N	156° 50' 00" W	1000	50.0	10	100	1010.0	95	10	000	13120-050
145	13120-050	7414	36° 50' 30" N	156° 50' 00" W	1000	50.0	10	100	1010.0	95	10	000	13120-050
146	13120-050	7415	36° 50' 30" N	156° 50' 00" W	1000	50.0	10	100	1010.0	95	10	000	13120-050
147	13120-050	7416	36° 50' 30" N	156° 50' 00" W	1000	50.0	10	100	1010.0	95	10	000	13120-050
148	13120-050	7417	36° 50' 30" N	156° 50' 00" W	1000	50.0	10	100	1010.0	95	10	000	13120-050
149	13120-050	7418	36° 50' 30" N	156° 50' 00" W	1000	50.0	10	100	1010.0	95	10	000	13120-050
150	13120-050	7419	36° 50' 30" N	156° 50' 00" W	1000	50.0	10	100	1010.0	95	10	000	13120-050
151	13120-050	7420	36° 50' 30" N	156° 50' 00" W	1000	50.0	10	100	1010.0	95	10	000	13120-050
152	13120-050	7421	36° 50' 30" N	156° 50' 00" W	1000	50.0	10	100	1010.0	95	10	000	13120-050
153	13120-050	7422	36° 50' 30" N	156° 50' 00" W	1000	50.0	10	100	1010.0	95	10	000	13120-050
154	13120-050	7423	36° 50' 30" N	156° 50' 00" W	1000	50.0	10	100	1010.0	95	10	000	13120-050
155	13120-050	7424	36° 50' 30" N	156° 50' 00" W	1000	50.0	10	100	1010.0	95	10	000	13120-050
156	13120-050	7425	36° 50' 30" N	156° 50' 00" W	1000	50.0	10	100	1010.0	95	10	000	13120-050
157	13120-050	7426	36° 50' 30" N	156° 50' 00"									

THIS PAGE IS BEST QUALITY PRACTICABLE
FROM JUNE FORWARDED TO HQ

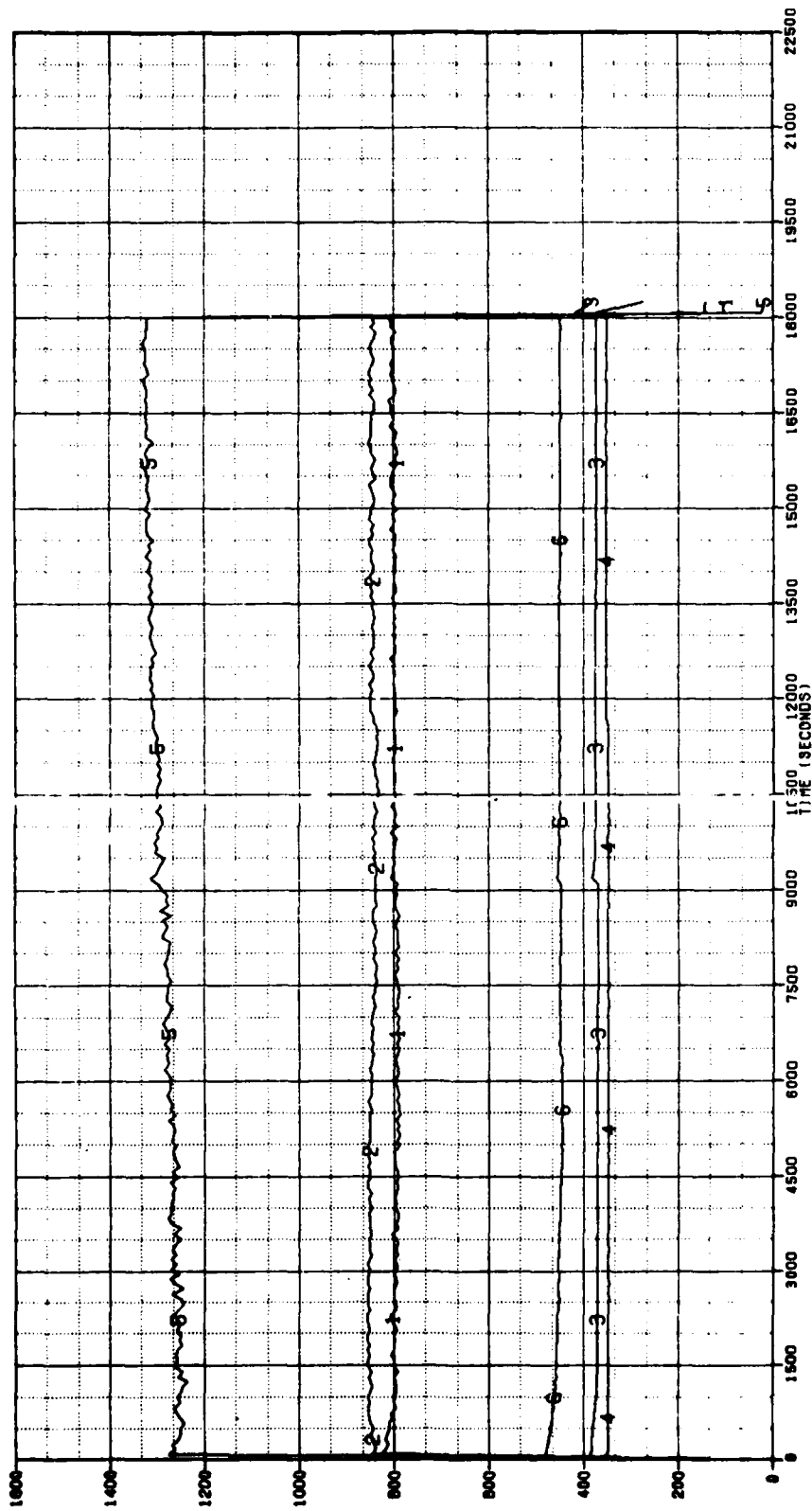


TEMPERATURES VS TIME PLOT A
 .581-698-529 TEST STAND A-2

TEST DATE 02-28-80

REDOJET LIQUID ROCKET COMPANY, SACRAMENTO, CALIFORNIA

1	TL	DEG F
2	TO-180	DEG F
3	TS-170	DEG F
4	TS-270	DEG F
5	TR-217	DEG F
6	TVC	DEG F
7	TL	DEG F
8	TO-180	DEG F
9	TS-170	DEG F
10	TS-270	DEG F
11	TR-217	DEG F
12	TVC	DEG F



APPENDIX F

PHASE III PULSE DATA, TESTS 698-512-1 THROUGH -11,
IMPULSE BIT AND REPEATABILITY

PULSE GROUP 1, 0.01 SEC EPW, 60 SEC COAST

TEST IDENT .581-698-512-1										TEST STAND A-2				DATE 02-08-80				TIME 1200			
FUNCTION		TR-217/2				TCOOL-RET/2				TAMR/2				EPW				COAST IMP.			
UNITS		TCOOL-RET		TAMR		TCOOL-RET/2		TAMR		GROUP NO.		RTT IMPULSE		F POST		F POST		F POST			
CHAN NO	DEG F	195	156	158	157	159	222	223	224	225	226	227	228	229	230	231	232	233	234		
LAG TIME	.0000	.0009	.0008	.0008	.0008	.0008	.0006	.0006	.0006	.0007	.0007	.0007	.0007	.0007	.0007	.0007	.0007	.0007	.0007		
1.0043	57.37	55.11	55.25	55.32	55.32	55.32	1.	.010357	.004334	.000103											
2.0043	57.37	55.05	55.11	55.26	55.26	55.26	2.	.010347	.004121	.000026											
3.0043	57.37	55.25	55.28	55.28	55.32	55.32	3.	.010437	.004921	.000026											
4.0043	57.37	55.14	55.25	55.28	55.32	55.32	4.	.010435	.004737	.000042											
5.0043	57.94	55.14	55.25	55.32	55.41	55.41	5.	.010445	.004062	.000040											
6.0043	58.22	55.05	55.16	55.29	55.35	55.35	1.	.010357	.004084	.000015											
7.0043	58.78	55.08	55.16	55.28	55.38	55.38	2.	.010445	.003830	.000008											
8.0043	59.50	55.08	55.16	55.41	55.40	55.40	3.	.010348	.003667	.000042											
9.0043	59.34	55.14	55.16	55.35	55.38	55.38	4.	.010348	.003743	.000011											
10.0043	60.05	55.05	55.14	55.23	55.26	55.26	5.	.010347	.004135	.000043											
11.0043	60.19	55.16	55.28	55.26	55.32	55.32	1.	.010435	.003585	.000032											
12.0043	60.47	55.14	55.16	55.38	55.38	55.38	2.	.010357	.003530	.000041											
13.0043	61.87	55.14	55.28	55.26	55.53	55.53	3.	.010347	.004065	.000013											
14.0043	62.86	55.14	55.37	55.38	55.41	55.41	4.	.010437	.003700	.000042											
15.0043	61.03	55.14	55.25	55.38	55.38	55.38	5.	.010437	.004452	.000051											

NOTE: Pages F-1 through F-6
TCOOL-RET = Test fixture coolant temperature

PULSE GROUP 2, 0.030 SEC EPW, 60 SEC COAST

TEST IDENT ,SB1-698-512-2 TEST STAND A-2 DATE 02-08-80 TIME 1200

FUNCTION		TR-217/2		TCOOL-RET/2		TAMR/2		GROUP NO.		EPW		RTT IMPULSE		COAST IMP.	
UNITS	DEG F	TCOOL-RET	DEG F	TCOOL-RET	DEG F	TAMR	DEG F	DEG F	SEC	SEC	LB, SEC	LB, SEC	LB, SEC	LB, SEC	
CHAN NO	195	156	158	157	159	159	159	222	223	224	225	226	226	226	
LAG TIME	.0000	-.0009	-.0008	-.0008	-.0008	-.0008	-.0008	.0006	.0006	.0006	.0007	.0007	.0007	.0007	
INVERTED															
1.0003	57.51	55.74	55.40	55.32	55.34	55.34	55.34	1.	.030424	-.00212	.000026	-.00212	-.00212	-.00212	
2.0003	60.05	55.52	55.34	55.34	55.34	55.34	55.34	2.	.030451	.010195	.000099	-.00071	-.00071	-.00071	
3.0003	62.15	55.40	55.37	55.41	55.34	55.34	55.34	3.	.030424	.010121	.000111	-.00032	-.00032	-.00032	
4.0003	64.12	55.28	55.16	55.38	55.26	55.26	55.26	4.	.030431	.010036	.000062	-.00025	-.00025	-.00025	
5.0003	66.36	55.28	55.25	55.26	55.22	55.22	55.22	5.	.030512	.010740	.000086	-.00030	-.00030	-.00030	
6.0003	68.64	55.49	55.25	55.35	55.32	55.32	55.32	1.	.030522	.011207	.000083	-.00040	-.00040	-.00040	
7.0003	68.33	55.49	55.49	55.41	55.34	55.34	55.34	2.	.030424	.010649	.000052	-.00039	-.00039	-.00039	
8.0003	69.45	55.37	55.34	55.47	55.44	55.44	55.44	3.	.030522	.010570	.000074	-.00035	-.00035	-.00035	
9.0003	70.15	55.49	55.49	55.35	55.34	55.34	55.34	4.	.030522	.010244	.000104	-.00032	-.00032	-.00032	
10.0003	71.13	55.49	55.40	55.34	55.34	55.40	55.40	5.	.030451	.010251	.000095	-.00032	-.00032	-.00032	
11.0003	71.27	55.40	55.28	55.34	55.32	55.32	55.32	1.	.030461	.010915	.000111	-.00031	-.00031	-.00031	
12.0003	72.52	55.52	55.52	55.47	55.44	55.44	55.44	2.	.030542	.011522	.000170	-.00043	-.00043	-.00043	
13.0003	72.38	55.52	55.49	55.26	55.23	55.23	55.23	3.	.030454	.010543	.000077	-.00050	-.00050	-.00050	
14.0003	73.64	55.49	55.49	55.35	55.34	55.34	55.34	4.	.030451	.010519	.000100	-.00034	-.00034	-.00034	
15.0003	75.32	55.52	55.49	55.37	55.41	55.41	55.41	5.	.030542	.011519	.000057	-.00049	-.00049	-.00049	

PULSE GROUP 3, 0.120 SEC EPW, 60 SEC COAST

TEST IDENT .581-69A-512-3				TEST STAND A-2				DATE 02-08-80				TIME 1200			
FUNCTION		TR-217/2		TCOOL-RET/2		TAMH/2		GROUP NO.		EPW		COAST IMP.			
UNITS	DEG F	TCOOL-RET	DEG F	TAMH	DEG F	DEG F	DEG F			LA, SEC	LA, SEC	LA, SEC	F POST		
CHAN NO	195	156	158	157	154	154	222	223	224	225	225	225	225		
LAG TIME	.0000	.0009	.0008	.0008	.0008	.0008	.0006	.0006	.0006	.0007	.0007	.0007	.0007		
1.0043	66.36	55.72	55.57	55.47	55.40	55.40	1.	.120335	.040999	.000244	.000244	.000244	.0129		
2.0043	75.32	55.72	55.72	55.53	55.38	55.38	2.	.124565	.037622	.000165	.000165	.000165	.0091		
3.0043	81.17	55.72	55.72	55.41	55.28	55.28	3.	.123230	.040825	.000202	.000202	.000202	.0063		
4.0043	87.01	55.71	55.72	55.40	55.47	55.47	4.	.120426	.043155	.000220	.000220	.000220	.0070		
5.0043	93.10	55.52	55.72	55.56	55.50	55.50	5.	.120366	.042056	.000241	.000241	.000241	.0067		
6.0043	95.87	55.71	55.72	55.40	55.44	55.44	1.	.120501	.041262	.000224	.000224	.000224	.0070		
7.0043	99.45	55.71	55.72	55.50	55.38	55.38	2.	.124531	.043054	.000172	.000172	.000172	.0082		
8.0043	102.90	55.72	55.72	55.53	55.38	55.38	3.	.123404	.046104	.000187	.000187	.000187	.0077		
9.0043	105.74	55.72	55.72	55.56	55.38	55.38	4.	.120414	.043619	.000239	.000239	.000239	.0072		
10.0043	108.26	55.81	55.71	55.59	55.44	55.44	5.	.124734	.043292	.000189	.000189	.000189	.0080		
11.0043	111.13	55.72	55.72	55.47	55.41	55.41	1.	.123097	.047188	.000202	.000202	.000202	.0085		
12.0043	112.78	55.71	55.75	55.46	55.34	55.34	2.	.124471	.044695	.000179	.000179	.000179	.0076		
13.0043	114.83	55.75	55.75	55.47	55.32	55.32	3.	.123060	.044426	.000205	.000205	.000205	.0076		
14.0043	116.34	55.81	55.75	55.57	55.38	55.38	4.	.120278	.042124	.000247	.000247	.000247	.0069		
15.0043	117.57	55.72	55.75	55.53	55.38	55.38	5.	.120256	.039681	.000252	.000252	.000252	.0060		

PULSE GROUP 4, 0.010 SEC EPW, 5 SEC COAST

TEST IDENT .581-698-512-4 TEST STAND A-2 DATE 02-08-80 TIME 1200 F

FUNCTION		TR-217/2		TCOOL-RET/2		TAMR/2		EPW		COAST 1MP	
UNITS		TCOOL-RET		TAMR		TAMR/2		HIT IMPULSF		F POST	
CHAN NO	DEG F	156	157	158	159	222	223	224	225	226	227
LAG TIME	.0000	.0009	.0008	.0008	.0008	.0008	.0006	.0006	.0007	.0007	.0007
1.0003	85.06	55.81	55.63	55.68	55.68	1.	.010444	.004477	.001460	-.0124	
2.0003	85.06	55.93	55.57	55.74	55.74	2.	.010345	.004567	.000022	-.0025	
3.0003	85.20	55.87	55.56	55.56	55.56	3.	.010355	.003996	.000033	-.0017	
4.0003	85.62	55.98	55.87	55.53	55.56	4.	.010444	.003618	.000038	-.0023	
5.0003	86.31	55.93	55.46	55.56	55.56	5.	.010345	.003936	.000033	-.0053	
6.0003	86.87	55.81	55.56	55.56	55.56	1.	.010434	.004262	.000042	-.0015	
7.0003	87.42	56.04	55.98	55.62	55.62	2.	.010050	.005593	.000014	-.0010	
8.0003	88.67	55.87	55.93	55.59	55.59	3.	.010044	.004823	.000023	-.0012	
9.0003	89.23	55.98	55.98	55.62	55.62	4.	.010355	.004189	.000038	-.0013	
10.0003	89.50	55.87	55.59	55.59	55.59	5.	.010345	.004726	.000053	-.0022	
11.0003	90.06	55.87	55.53	55.53	55.59	1.	.010444	.005342	.000046	-.0012	
12.0003	90.75	55.93	55.50	55.53	55.53	2.	.010355	.004699	.000064	-.0028	
13.0003	90.81	55.98	55.63	55.62	55.62	3.	.010434	.004156	.000035	-.0011	
14.0003	91.44	55.98	55.65	55.64	55.64	4.	.010050	.004207	.000039	-.0017	
15.0003	93.10	55.98	55.65	55.63	55.63	5.	.010355	.003940	.000042	-.0015	
16.0003	130.78	55.96	55.65	55.63	55.63	1.	.010345	.004698	.000056	-.0012	
17.0003	130.64	55.98	55.75	55.75	55.75	2.	.010434	.004971	.000055	-.0017	
18.0003	130.64	56.04	55.56	55.56	55.56	3.	.010434	.004863	.000042	-.0033	
19.0003	131.19	55.98	55.56	55.56	55.56	4.	.010434	.003981	.000021	-.0001	
20.0003	131.19	55.98	55.53	55.53	55.53	5.	.010345	.003604	.000034	-.0003	
21.0003	131.32	55.96	55.54	55.54	55.54	1.	.010044	.004974	.000031	-.0000	
22.0003	131.32	56.04	55.57	55.53	55.53	2.	.010444	.005040	.000039	-.0009	
23.0003	131.73	55.98	55.59	55.59	55.59	3.	.010355	.005068	.000052	-.0010	
24.0003	131.19	56.04	55.54	55.54	55.54	4.	.010444	.004650	.000030	-.0002	
25.0003	131.46	55.93	55.53	55.53	55.53	5.	.010044	.004222	.000044	-.0004	
26.0003	131.19	55.98	55.62	55.62	55.62	1.	.010444	.004833	.000044	-.0055	
27.0003	131.32	55.87	55.65	55.65	55.71	2.	.010355	.004524	.000036	-.0004	
28.0003	131.86	56.04	55.57	55.57	55.62	3.	.010345	.005622	.000037	-.0004	
29.0003	131.73	55.87	55.59	55.59	55.59	4.	.010355	.004505	.000054	-.0012	
30.0003	131.32	55.96	55.56	55.56	55.63	5.	.010444	.006285	.000039	.0002	

PULSE 186 TO 200

PULSE GROUP 5, 0.030 EPW, 5 SEC COAST

TEST IDENT 581-698-512-5			TEST STAND A-2			DATE 02-04-80			TIME 1200		
FUNCTION		TR-217/2		TCOUL-RET/2		TAMH/2		FPK		COAST IMP.	
UNITS	DEG F	TCOUL-RET	TAMH	DEG F	DEG F	DEG F	DEG F	GROUP NO.	W11 IMPULSF	F POST	
CHAN NO	195	156	158	157	159	222	223	224	225	226	
LAG TIME	.0000	.0009	.0008	.0008	.0008	.0006	.0006	.0006	.0007	.0007	
1.0043	87.42	56.22	56.22	55.53	55.44	1.	.030436	.011028	.000114	-.0014	
2.0043	88.67	56.19	56.22	55.47	55.40	2.	.030426	.011037	.000141	-.0012	
3.0043	90.33	56.04	56.19	55.53	55.56	3.	.030430	.010477	.000104	-.0000	
4.0043	93.10	56.19	56.04	55.50	55.46	4.	.030426	.011345	.000127	-.0011	
5.0043	95.45	56.04	56.19	55.53	55.53	5.	.030525	.012063	.000105	-.0020	
6.0043	98.35	56.22	56.22	55.53	55.53	1.	.030436	.011291	.000098	-.0009	
7.0043	101.93	56.04	56.22	55.53	55.53	2.	.030525	.012304	.000124	-.0021	
8.0043	103.54	55.98	56.19	55.56	55.59	3.	.030525	.010472	.000109	-.0011	
9.0043	106.33	56.19	56.04	55.62	55.56	4.	.030426	.012023	.000114	-.0010	
10.0043	108.26	56.22	55.98	55.63	55.65	5.	.030436	.011636	.000129	-.0017	
11.0043	111.13	55.98	55.93	55.62	55.47	1.	.030416	.012214	.000130	-.0049	
12.0043	112.78	56.19	56.22	55.64	55.59	2.	.030426	.011606	.000141	-.0040	
13.0043	115.52	56.22	56.22	55.59	55.53	3.	.030426	.012000	.000126	-.0055	
14.0043	117.16	56.19	56.22	55.62	55.53	4.	.030426	.012215	.000143	-.0002	
15.0043	120.84	56.28	56.22	55.69	55.59	5.	.030426	.011224	.000134	-.0055	
16.0043	303.01	56.07	56.06	55.79	55.74	1.	.030604	.013497	.000225	-.0020	
17.0043	303.01	55.96	55.96	55.71	55.63	2.	.030514	.013846	.000160	-.0061	
18.0043	303.01	55.98	56.07	55.65	55.64	3.	.030525	.013979	.000149	-.0020	
19.0043	303.29	56.06	56.07	55.68	55.64	4.	.030514	.013452	.000163	-.0020	
20.0043	303.65	56.06	56.10	55.62	55.66	5.	.030525	.013400	.000181	-.0014	
21.0043	304.42	56.06	56.06	55.63	55.62	1.	.030525	.014014	.000209	-.0020	
22.0043	305.40	56.06	56.07	55.65	55.71	2.	.030525	.014168	.000156	-.0017	
23.0043	304.98	55.96	56.06	55.63	55.65	3.	.030614	.014456	.000160	-.0017	
24.0043	305.96	56.06	55.96	55.62	55.71	4.	.030504	.013784	.000162	-.0016	
25.0043	306.25	56.06	55.96	55.69	55.64	5.	.030514	.014110	.000187	-.0021	
26.0043	306.67	56.07	56.06	55.71	55.57	1.	.030515	.013999	.000184	-.0010	
27.0043	306.95	56.07	56.07	55.71	55.64	2.	.030515	.014571	.000167	-.0013	
28.0043	307.51	56.06	56.06	55.65	55.63	3.	.030514	.014235	.000201	-.0020	
29.0043	307.93	56.07	56.06	55.79	55.71	4.	.030525	.014162	.000172	-.0020	
30.0043	308.36	55.98	56.07	55.82	55.82	5.	.030525	.013999	.000135	-.0014	

PULSE GROUP 6 (FIRST DATA SET), 0.10 SEC EPW, 5 SEC COAST

TEST IDENT .SRI-698-512-6										TEST STAND A-2				DATE 02-11-80				TIME 1200							
TR-217/2										TCOOL-RET/2				TAMH/2				EPW				COAST IMP.			
FUNCTION		TCOOL-RET		TAMH		TCOOL-RET/2		TAMH/2		GROUP NO.		HIT IMPULSF		F POST											
UNITS		DEG F		DEG F		DEG F		DEG F		SEC.		LA, SEC		LA, SEC		LMS									
CHAN NO		195		156		157		159		222		223		224		225									
LAG TIME		.0000		.0009		.0008		.0008		.0006		.0006		.0006		.0007									
1.0043		43.24		47.15		47.26		45.74		45.68		1.		100504		.030444		.000121				-.0132			
2.0043		46.35		47.31		47.37		45.65		45.61		2.		100504		.033472		.000191				-.0070			
3.0043		53.12		47.37		47.26		45.77		45.68		3.		100523		.041163		.000162				-.0073			
4.0043		62.69		47.26		47.31		45.74		45.62		4.		100574		.036484		.000184				-.0049			
5.0043		72.22		47.34		47.37		45.59		45.59		5.		100564		.039278		.000178				-.0055			
6.0043		81.98		47.37		47.34		45.71		45.68		1.		100532		.036719		.000223				-.0039			
7.0043		91.13		47.38		47.54		45.80		45.71		2.		100584		.041618		.000203				-.0059			
8.0043		101.62		47.37		47.38		45.61		45.65		3.		100594		.036002		.000247				-.0024			
9.0043		119.00		47.38		47.38		45.74		45.74		4.		67.1224		.25.687		.00060				.3402			

ALOC JOB 0003

1/2 LA PULSE ENGINE PERFORM

TEST IDENT 581-000-512-7

TEST STAND A-2

DATE 02-11-60

TIME 1200

FUNCTION		TR-217/2		TCOOL-RET/2		TAMB/2		EPM		COAST IMP.	
UNIT		TCOOL-RET		TAMB		GROUP NO.		HIT IMPULSE		F POST	
CHAN NO		DEG F	DEG F	DEG F	DEG F	222	223	LB SEC	LB SEC	224	226
LAG TIME		0.0000	0.0000	0.0000	0.0000	0.0000	0.0000	0.0000	0.0000	0.0007	0.0007
1.0003	76.02	48.07	48.21	47.69	47.69	1.	100503	032610	000297		0037
2.0003	75.34	48.08	48.08	47.69	47.63	2.	100553	034705	000201		0013
3.0003	75.19	47.90	48.07	47.63	47.54	3.	100503	036043	000243		0000
4.0003	86.42	48.04	48.07	47.60	47.57	4.	100477	035948	000252		0014
5.0003	93.62	48.07	48.08	47.60	47.60	5.	100537	036415	000252		0002
6.0003	101.62	48.07	48.07	47.63	47.57	1.	100466	036757	000253		0013
7.0003	102.00	48.08	48.08	47.75	47.69	2.	100553	036159	000227		0025
8.0003	116.71	48.08	48.08	47.74	47.69	3.	100594	037108	000230		0044
9.0003	122.25	48.08	48.21	47.78	47.75	4.	100543	037070	000240		0045
10.0003	136.07	48.04	48.08	47.75	47.75	5.	100583	036691	000284		0000
11.0003	137.38	48.04	48.08	47.81	47.75	1.	100523	036536	000273		0055
12.0003	143.36	48.07	48.07	47.69	47.69	2.	100563	037053	000277		0063
13.0003	149.28	48.30	48.08	47.75	47.75	3.	100517	036958	000309		0062
14.0003	155.49	48.08	48.24	47.84	47.75	4.	100506	037135	000351		0063
15.0003	160.74	48.08	48.08	47.84	47.72	5.	100487	037362	000344		0053
16.0003	401.97	48.45	48.51	48.58	48.52	1.	100562	042740	000212		0062
17.0003	401.97	48.51	48.51	48.52	48.58	2.	100561	042645	000207		0057
18.0003	401.97	48.51	48.45	48.61	48.61	3.	100619	041751	000219		0057
19.0003	403.91	48.45	48.42	48.52	48.52	4.	100629	042040	000231		0062
20.0003	403.91	48.45	48.54	48.55	48.61	5.	100629	042170	000233		0056
21.0003	403.91	48.42	48.51	48.61	48.61	1.	100629	041943	000257		0059
22.0003	404.18	48.54	48.51	48.66	48.55	2.	100619	042052	000224		0060
23.0003	404.46	48.55	48.54	48.72	48.61	3.	100649	041769	000254		0064
24.0003	404.73	48.51	48.54	48.63	48.69	4.	100561	042064	000225		0059
25.0003	405.01	48.51	48.54	48.61	48.63	5.	100521	042097	000240		0061
26.0003	405.36	48.51	48.54	48.61	48.66	1.	100562	042179	000225		0059
27.0003	405.86	48.51	48.42	48.66	48.61	2.	100531	041987	000245		0062
28.0003	405.98	48.45	48.54	48.63	48.72	3.	100531	042099	000254		0059
29.0003	406.39	48.45	48.51	48.72	48.63	4.	100571	041926	000221		0058
30.0003	406.45	48.32	48.32	48.75	48.74	5.	100620	042566	000200		0062
31.0003	467.58	48.30	48.32	48.61	48.72	1.	020480	009472	000145		0000
32.0003	467.58	48.54	48.55	48.63	48.66	2.	020490	009549	000141		0019
33.0003	467.22	48.51	48.54	48.58	48.63	3.	020392	009765	000128		0019
34.0003	466.67	48.51	48.48	48.56	48.66	4.	020480	009841	000129		0013
35.0003	467.50	48.54	48.55	48.63	48.72	5.	020480	009585	000114		0012
36.0003	467.22	48.51	48.55	48.66	48.72	1.	020568	009489	000134		0016
37.0003	466.95	48.55	48.55	48.75	48.72	2.	020480	009638	000146		0017
38.0003	466.95	48.55	48.55	48.74	48.74	3.	020568	009548	000134		0008
39.0003	467.22	48.54	48.55	48.66	48.75	4.	020480	009693	000139		0014
40.0003	467.22	48.55	48.55	48.72	48.75	5.	020568	009714	000126		0016
41.0003	467.08	48.55	48.55	48.69	48.61	1.	020480	009558	000125		0013
42.0003	467.08	48.55	48.55	48.78	48.78	2.	020480	009476	000111		0014
43.0003	467.22	48.55	48.55	48.75	48.63	3.	020490	009561	000136		0015
44.0003	467.22	48.55	48.55	48.72	48.66	4.	020490	009629	000137		0020
45.0003	467.50	48.55	48.54	48.75	48.63	5.	020480	009621	000116		0011
46.0003	567.00	48.51	48.54	49.02	49.16	1.	020402	018765	000134		0016
47.0003	567.00	48.55	48.55	49.16	49.09	2.	020490	010620	000111		0020
48.0003	569.07	48.55	48.55	49.16	49.02	3.	020480	010660	000108		0014
49.0003	569.07	48.55	48.55	49.16	49.16	4.	020480	010670	000113		0025
50.0003	569.07	48.56	48.55	49.05	49.16	5.	020490	010550	000116		0014
51.0003	569.34	48.55	48.55	49.16	49.16	1.	020392	010645	000140		0014
52.0003	569.34	48.55	48.55	49.02	49.05	2.	020402	010403	000127		0015
53.0003	569.61	48.55	48.55	49.16	49.16	3.	020480	010997	000115		0013
54.0003	569.66	48.55	48.55	49.16	49.16	4.	020490	010406	000131		0017
55.0003	569.66	48.55	48.55	49.16	49.16	5.	020392	010757	000126		0017
56.0003	570.42	48.55	48.55	49.16	49.16	1.	020480	010774	000124		0020
57.0003	570.69	48.45	48.74	49.16	49.16	2.	020402	010672	000113		0017
58.0003	570.97	48.45	48.74	49.16	49.16	3.	020402	010554	000131		0026
59.0003	571.31	48.55	48.55	49.16	49.16	4.	020392	010411	000134		0021
60.0003	571.74	48.56	48.55	49.16	49.16	5.	020480	010910	000107		0004
61.0003	571.31	48.51	48.54	49.16	49.16	1.	100441	004283	000164		0081
62.0003	572.49	48.54	48.51	49.16	49.16	2.	100442	004449	000170		0042
63.0003	573.41	48.54	48.45	49.16	49.02	3.	100502	004250	000162		0014
64.0003	574.49	48.54	48.51	49.16	49.16	4.	100432	004434	000196		0022
65.0003	576.12	48.45	48.55	49.22	49.16	5.	100422	004274	000204		0042
66.0003	578.29	48.54	48.51	49.16	49.05	1.	100411	004791	000197		0044
67.0003	580.06	48.54	48.54	49.22	49.16	2.	100509	004507	000173		0041
68.0003	583.08	48.49	48.54	49.22	49.16	3.	100431	004400	000183		0044
69.0003	586.42	48.55	48.54	49.16	49.16	4.	100431	004455	000192		0047
70.0003	589.04	48.55	48.55	49.16	49.16	5.	100529	004374	000194		0044
71.0003	593.73	48.55	48.55	49.16	49.16	1.	100431	004676	000180		0044
72.0003	598.06	48.45	48.54	49.16	49.16	2.	100509	004702	000175		0047
73.0003	601.65	48.54	48.55	49.16	49.16	3.	100431	004695	000167		0041
74.0003	606.17	48.55	48.54	49.16	49.16	4.	100431	047782	000204		0040
75.0003	610.46	48.55	48.55	49.16	49.16	5.	100431	049748	000166		0043

PULSE GROUP 6 (REPEAT), 0.100 SEC EPM, 5 SEC COAST, PULSES 1-15 AND 186-200

PULSE GROUP 7, 0.020 SEC EPM, .90 SEC COAST, PULSES 1-15 AND 286-300

PULSE GROUP 8, 0.100 SEC EPM, .90 SEC COAST, PULSES 1-15

PULSE GROUP 9, 0.015 SEC EPW, .135 SEC COAST

TEST IDENT .581-698-512-A TEST STAND A-2 DATE 02-11-80 TIME 1200

FUNCTION		TR-217/2		TCNOL-RET		TCNOL-RET/2		TAMH		TAMH/2		EPW		GROUP NO.		HIT IMPULSE		COAST IMP.	
CHAN NO	DEG F	195	156	158	157	159	222	223	224	225	226	227	228	229	230	231	232	233	234
LAG TIME	.0000	.0009	.0008	.0008	.0008	.0008	.0008	.0008	.0008	.0008	.0007	.0007	.0007	.0007	.0007	.0007	.0007	.0007	.0007
1.0043	162.49	48.80	48.92	48.97	49.02	49.07	49.12	49.17	49.22	49.27	49.32	49.37	49.42	49.47	49.52	49.57	49.62	49.67	49.72
2.0043	162.49	48.97	49.02	49.07	49.12	49.17	49.22	49.27	49.32	49.37	49.42	49.47	49.52	49.57	49.62	49.67	49.72	49.77	49.82
3.0043	162.49	49.02	49.07	49.12	49.17	49.22	49.27	49.32	49.37	49.42	49.47	49.52	49.57	49.62	49.67	49.72	49.77	49.82	49.87
4.0043	161.28	49.02	49.07	49.12	49.17	49.22	49.27	49.32	49.37	49.42	49.47	49.52	49.57	49.62	49.67	49.72	49.77	49.82	49.87
5.0043	162.49	49.02	49.07	49.12	49.17	49.22	49.27	49.32	49.37	49.42	49.47	49.52	49.57	49.62	49.67	49.72	49.77	49.82	49.87
6.0043	161.14	49.02	49.07	49.12	49.17	49.22	49.27	49.32	49.37	49.42	49.47	49.52	49.57	49.62	49.67	49.72	49.77	49.82	49.87
7.0043	162.49	49.21	49.33	49.37	49.42	49.47	49.52	49.57	49.62	49.67	49.72	49.77	49.82	49.87	49.92	49.97	50.02	50.07	50.12
8.0043	162.49	49.02	49.27	49.27	49.32	49.37	49.42	49.47	49.52	49.57	49.62	49.67	49.72	49.77	49.82	49.87	49.92	49.97	50.02
9.0043	162.49	49.21	49.02	49.02	49.07	49.12	49.17	49.22	49.27	49.32	49.37	49.42	49.47	49.52	49.57	49.62	49.67	49.72	49.77
10.0043	162.49	49.15	49.02	49.02	49.07	49.12	49.17	49.22	49.27	49.32	49.37	49.42	49.47	49.52	49.57	49.62	49.67	49.72	49.77
11.0043	162.49	49.21	49.21	49.21	49.21	49.21	49.21	49.21	49.21	49.21	49.21	49.21	49.21	49.21	49.21	49.21	49.21	49.21	49.21
12.0043	162.49	49.02	49.02	49.02	49.02	49.02	49.02	49.02	49.02	49.02	49.02	49.02	49.02	49.02	49.02	49.02	49.02	49.02	49.02
13.0043	161.14	49.15	49.21	49.21	49.21	49.21	49.21	49.21	49.21	49.21	49.21	49.21	49.21	49.21	49.21	49.21	49.21	49.21	49.21
14.0043	162.49	49.15	49.21	49.21	49.21	49.21	49.21	49.21	49.21	49.21	49.21	49.21	49.21	49.21	49.21	49.21	49.21	49.21	49.21
15.0043	162.49	49.02	49.21	49.21	49.21	49.21	49.21	49.21	49.21	49.21	49.21	49.21	49.21	49.21	49.21	49.21	49.21	49.21	49.21

PULSE GROUP 10, 0.030 SEC EPW, .120 SEC COAST

EST IDENT .581-698-512-9										TEST STAND A-2										DATE 02-11-80										TIME 1200																																							
TR-217/2										TCOOL-RET/2										TAMH/2										EPW										GROUP NO.										HIT IMPULSE										COAST IMP.									
FUNCTION					UNITS					TCOOL-RET					TCOOL-RET/2					TAMH					DEG F					DEG F					DEG F					SEC.					LBS.					LBS.					F POST														
CHAN NO					DEG F					DEG F					DEG F					DEG F					DEG F					DEG F					SEC.					LBS.					LBS.					F POST																			
LAG TIME					.0000					-.0009					-.0008					-.0008					-.0008					-.0008					.0006					.0006					.0007					.0007																			
1.0043					172.18					49.3A					49.3A					51.11					51.05					1.					.030320					.014046					.000170					-.0025																			
2.0043					171.91					49.3A					49.21					51.17					51.19					2.					.025052					.014824					.000101					-.5542																			
3.0043					171.91					49.3A					49.33					51.05					51.11					3.					.030424					.015097					.000187					-.0449																			
4.0043					171.64					49.38					49.44					51.11					51.11					4.					.030504					.015552					.000190					-.0000																			
5.0043					171.91					49.44					49.3A					51.11					51.05					5.					.030408					.015428					.000202					.0004																			
6.0043					171.91					49.44					49.44					51.08					51.17					1.					.030504					.015591					.000179					-.0001																			
7.0043					171.64					49.44					49.44					51.11					51.19					2.					.030504					.015718					.000184					-.0032																			
8.0043					172.1A					49.44					49.47					51.14					51.14					3.					.030416					.015035					.000161					.0004																			
9.0043					171.91					49.44					49.44					51.14					51.14					4.					.030416					.015017					.000100					.0002																			
10.0043					172.05					49.44					49.47					51.17					51.19					5.					.030426					.015904					.000186					.0004																			
11.0043					172.18					49.38					49.47					51.11					51.22					1.					.030426					.016309					.000178					.0004																			
12.0043					172.45					49.3A					49.47					51.22					51.22					2.					.030416					.016113					.000185					.0002																			
13.0043					172.45					49.38					49.3A					51.17					51.11					3.					.030416					.015904					.000190					-.0039																			
14.0043					172.99					49.44					49.44					51.22					51.22					4.					.030514					.016950					.000148					-.0001																			
15.0043					173.53					49.38					49.27					51.17					51.11					5.					.030408					.016275					.000177					.0004																			

PULSE GROUP 11, 0.045 SEC EPW, .105 SEC COAST

TEST IDENT .5B1-69A-51210										TEST STAND A-2				DATE 02-11-80				TIME 1200			
FUNCTION		TR-217/2				TCOOL-RET/2				TAMR/2				GROUP NO.		EPW		COAST IMP.			
UNITS	DEG F	TCOOL-RET	DEG F	TCOOL-RET	DEG F	TAMR	DEG F	TAMR	DEG F	DEG F	DEG F	DEG F	DEG F		SEC.	LA.SEC	LB.SEC	F POST	LBS		
CHAN NO	195	156	158	157	159	222	223	224	225	226	227	228	229								
LAG TIME	.0000	-.0009	-.0008	-.0008	-.0008	.0006	.0006	.0006	.0007	.0007	.0007	.0007	.0007								
1.0043	225.91	49.47	49.47	51.52	51.52	51.52	1.	.045362	.022028	.000201	-.0030										
2.0043	226.04	49.73	49.44	51.46	51.46	51.46	2.	.040523	.022013	.000110	-.5574										
3.0043	225.91	49.85	49.49	51.46	51.52	51.52	3.	.045105	.023310	-.00034	-.2098										
4.0043	225.91	49.73	49.73	51.55	51.49	51.49	4.	.045362	.023158	.000183	-.0055										
5.0043	225.64	49.79	49.73	51.52	51.43	51.43	5.	.045450	.023591	.000188	-.0014										
6.0043	225.64	49.91	49.73	51.58	51.52	51.52	1.	.042720	.029937	-1.7163	-15601										
7.0043	225.91	49.79	49.62	51.52	51.52	51.52	2.	.045450	.023739	.000172	.0012										
8.0043	225.91	49.73	49.64	51.61	51.54	51.54	3.	.045362	.024200	.000170	-.0014										
9.0043	225.64	49.73	49.85	51.58	51.61	51.61	4.	.045450	.023792	.000176	-.0003										
10.0043	226.18	49.85	49.85	51.61	51.64	51.64	5.	.045372	.023750	.000178	-.0014										
11.0043	226.18	49.79	49.64	51.58	51.58	51.58	1.	.045450	.023605	.000170	-.0059										
12.0043	225.91	49.79	49.85	51.64	51.61	51.61	2.	.045450	.023093	.000174	-.0013										
13.0043	226.72	49.79	49.64	51.64	51.58	51.58	3.	.045450	.023271	.000175	-.0013										
14.0043	227.27	49.85	49.85	51.61	51.64	51.64	4.	.045450	.022530	.000161	-.0007										
15.0043	227.54	49.91	49.85	51.66	51.69	51.69	5.	.045450	.022858	.000164	-.0015										

PULSE GROUP 12, 0.60 SEC EPW, 1.40 SEC COAST

TEST IDENT .581-69A-51211				TEST STAND A-2				DATE 02-11-80				TIME 1200			
FUNCTION		TR-217/2		TCOOL-RET		TCOOL-RET1/2		TAMH		TAMH/2		GROUP NO.		EPW	
UNITS	DEG F	DEG F	DEG F	DEG F	DEG F	DEG F	DEG F	DEG F	DEG F	DEG F	DEG F	HIT IMPULSE	COAST IMP.	F POST	F POST
CHAN NO	195	156	157	159	222	223	224	225	226	227	228	229	230	231	232
LAG TIME	.0000	-.0009	-.0008	-.0008	-.0008	-.0008	-.0008	-.0008	-.0008	-.0008	-.0008	-.0008	-.0008	-.0008	-.0008
1.0043	221.02	49.85	49.95	51.72	51.72	51.72	51.72	51.72	51.72	51.72	51.72	1. .601697	.295222	.000183	-.0320
2.0043	225.64	49.94	50.08	51.72	51.72	51.72	51.72	51.72	51.72	51.72	51.72	2. .600712	.295222	.000009	-.0143
3.0043	241.19	49.94	50.08	51.72	51.72	51.72	51.72	51.72	51.72	51.72	51.72	3. .600702	.295396	.000120	-.0244
4.0043	268.19	49.94	50.20	51.75	51.75	51.75	51.75	51.75	51.75	51.75	51.75	4. .601762	.297218	.000123	-.0270
5.0043	304.32	50.14	50.14	51.75	51.75	51.75	51.75	51.75	51.75	51.75	51.75	5. .600672	.297832	.000122	-.0274
6.0043	347.69	49.95	49.95	51.72	51.72	51.72	51.72	51.72	51.72	51.72	51.72	1. .600672	.298084	.000130	-.0275
7.0043	392.65	49.94	49.91	51.78	51.78	51.78	51.78	51.78	51.78	51.78	51.78	2. .600657	.298745	.000151	-.0283
8.0043	441.19	50.08	50.20	51.84	51.84	51.84	51.84	51.84	51.84	51.84	51.84	3. .600634	.297832	.000110	-.0280
9.0043	490.38	49.95	50.26	51.99	51.99	51.99	51.99	51.99	51.99	51.99	51.99	4. .600631	.297687	.000132	-.0285
10.0043	536.40	50.14	50.20	51.99	51.99	51.99	51.99	51.99	51.99	51.99	51.99	5. .600690	.297810	.000133	-.0291
11.0043	582.36	50.14	50.14	51.84	51.84	51.84	51.84	51.84	51.84	51.84	51.84	1. .600690	.297996	.000123	-.0295
12.0043	626.14	50.14	50.14	51.99	51.99	51.99	51.99	51.99	51.99	51.99	51.99	2. .600719	.298821	.000148	-.0308
13.0043	667.56	50.08	50.14	51.99	51.99	51.99	51.99	51.99	51.99	51.99	51.99	3. .600647	.299195	.000156	-.0312
14.0043	704.24	50.20	50.20	51.99	51.99	51.99	51.99	51.99	51.99	51.99	51.99	4. .601687	.298827	.000131	-.0314
15.0043	738.67	50.14	50.14	51.99	51.99	51.99	51.99	51.99	51.99	51.99	51.99	5. .600669	.298708	.000150	-.0318

APPENDIX G

PHASE III PULSING THERMAL DATA

ALOC 100 0003		1 1 2		1 1 3		1 1 4		1 1 5		1 1 6		1 1 7		1 1 8		1 1 9		1 2 0		1 2 1		1 2 2		1 2 3		1 2 4		1 2 5		1 2 6		1 2 7		1 2 8		1 2 9		1 3 0		1 3 1		1 3 2		1 3 3		1 3 4		1 3 5		1 3 6		1 3 7		1 3 8		1 3 9		1 4 0		1 4 1		1 4 2		1 4 3		1 4 4		1 4 5		1 4 6		1 4 7		1 4 8		1 4 9		1 5 0		1 5 1		1 5 2		1 5 3		1 5 4		1 5 5		1 5 6		1 5 7		1 5 8		1 5 9		1 6 0		1 6 1		1 6 2		1 6 3		1 6 4		1 6 5		1 6 6		1 6 7		1 6 8		1 6 9		1 7 0		1 7 1		1 7 2		1 7 3		1 7 4		1 7 5		1 7 6		1 7 7		1 7 8		1 7 9		1 8 0		1 8 1		1 8 2		1 8 3		1 8 4		1 8 5		1 8 6		1 8 7		1 8 8		1 8 9		1 9 0		1 9 1		1 9 2		1 9 3		1 9 4		1 9 5		1 9 6		1 9 7		1 9 8		1 9 9		2 0 0		2 0 1		2 0 2		2 0 3		2 0 4		2 0 5		2 0 6		2 0 7		2 0 8		2 0 9		2 1 0		2 1 1		2 1 2		2 1 3		2 1 4		2 1 5		2 1 6		2 1 7		2 1 8		2 1 9		2 2 0		2 2 1		2 2 2		2 2 3		2 2 4		2 2 5		2 2 6		2 2 7		2 2 8		2 2 9		2 3 0		2 3 1		2 3 2		2 3 3		2 3 4		2 3 5		2 3 6		2 3 7		2 3 8		2 3 9		2 4 0		2 4 1		2 4 2		2 4 3		2 4 4		2 4 5		2 4 6		2 4 7		2 4 8		2 4 9		2 5 0		2 5 1		2 5 2		2 5 3		2 5 4		2 5 5		2 5 6		2 5 7		2 5 8		2 5 9		2 6 0		2 6 1		2 6 2		2 6 3		2 6 4		2 6 5		2 6 6		2 6 7		2 6 8		2 6 9		2 7 0		2 7 1		2 7 2		2 7 3		2 7 4		2 7 5		2 7 6		2 7 7		2 7 8		2 7 9		2 8 0		2 8 1		2 8 2		2 8 3		2 8 4		2 8 5		2 8 6		2 8 7		2 8 8		2 8 9		2 9 0		2 9 1		2 9 2		2 9 3		2 9 4		2 9 5		2 9 6		2 9 7		2 9 8		2 9 9		3 0 0		3 0 1		3 0 2		3 0 3		3 0 4		3 0 5		3 0 6		3 0 7		3 0 8		3 0 9		3 1 0		3 1 1		3 1 2		3 1 3		3 1 4		3 1 5		3 1 6		3 1 7		3 1 8		3 1 9		3 2 0		3 2 1		3 2 2		3 2 3		3 2 4		3 2 5		3 2 6		3 2 7		3 2 8		3 2 9		3 3 0		3 3 1		3 3 2		3 3 3		3 3 4		3 3 5		3 3 6		3 3 7		3 3 8		3 3 9		3 4 0		3 4 1		3 4 2		3 4 3		3 4 4		3 4 5		3 4 6		3 4 7		3 4 8		3 4 9		3 5 0		3 5 1		3 5 2		3 5 3		3 5 4		3 5 5		3 5 6		3 5 7		3 5 8		3 5 9		3 6 0		3 6 1		3 6 2		3 6 3		3 6 4		3 6 5		3 6 6		3 6 7		3 6 8		3 6 9		3 7 0		3 7 1		3 7 2		3 7 3		3 7 4		3 7 5		3 7 6		3 7 7		3 7 8		3 7 9		3 8 0		3 8 1		3 8 2		3 8 3		3 8 4		3 8 5		3 8 6		3 8 7		3 8 8		3 8 9		3 9 0		3 9 1		3 9 2		3 9 3		3 9 4		3 9 5		3 9 6		3 9 7		3 9 8		3 9 9		4 0 0		4 0 1		4 0 2		4 0 3		4 0 4		4 0 5		4 0 6		4 0 7		4 0 8		4 0 9		4 1 0		4 1 1		4 1 2		4 1 3		4 1 4		4 1 5		4 1 6		4 1 7		4 1 8		4 1 9		4 2 0		4 2 1		4 2 2		4 2 3		4 2 4		4 2 5		4 2 6		4 2 7		4 2 8		4 2 9		4 3 0		4 3 1		4 3 2		4 3 3		4 3 4		4 3 5		4 3 6		4 3 7		4 3 8		4 3 9		4 4 0		4 4 1		4 4 2		4 4 3		4 4 4		4 4 5		4 4 6		4 4 7		4 4 8		4 4 9		4 5 0		4 5 1		4 5 2		4 5 3		4 5 4		4 5 5		4 5 6		4 5 7		4 5 8		4 5 9		4 6 0		4 6 1		4 6 2		4 6 3		4 6 4		4 6 5		4 6 6		4 6 7		4 6 8		4 6 9		4 7 0		4 7 1		4 7 2		4 7 3		4 7 4		4 7 5		4 7 6		4 7 7		4 7 8		4 7 9		4 8 0		4 8 1		4 8 2		4 8 3		4 8 4		4 8 5		4 8 6		4 8 7		4 8 8		4 8 9		4 9 0		4 9 1		4 9 2		4 9 3		4 9 4		4 9 5		4 9 6		4 9 7		4 9 8		4 9 9		5 0 0		5 0 1		5 0 2		5 0 3		5 0 4		5 0 5		5 0 6		5 0 7		5 0 8		5 0 9		5 1 0		5 1 1		5 1 2		5 1 3		5 1 4		5 1 5		5 1 6		5 1 7		5 1 8		5 1 9		5 2 0		5 2 1		5 2 2		5 2 3		5 2 4		5 2 5		5 2 6		5 2 7		5 2 8		5 2 9		5 3 0		5 3 1		5 3 2		5 3 3		5 3 4		5 3 5		5 3 6		5 3 7		5 3 8		5 3 9		5 4 0		5 4 1		5 4 2		5 4 3		5 4 4		5 4 5		5 4 6		5 4 7		5 4 8		5 4 9		5 5 0		5 5 1		5 5 2		5 5 3		5 5 4		5 5 5		5 5 6		5 5 7		5 5 8		5 5 9		5 6 0		5 6 1		5 6 2		5 6 3		5 6 4		5 6 5		5 6 6		5 6 7		5 6 8		5 6 9		5 7 0		5 7 1		5 7 2		5 7 3		5 7 4		5 7 5		5 7 6		5 7 7		5 7 8		5 7 9		5 8 0		5 8 1		5 8 2		5 8 3		5 8 4		5 8 5		5 8 6		5 8 7		5 8 8		5 8 9		5 9 0		5 9 1		5 9 2		5 9 3		5 9 4		5 9 5		5 9 6		5 9 7		5 9 8		5 9 9		6 0 0		6 0 1		6 0 2		6 0 3		6 0 4		6 0 5		6 0 6		6 0 7		6 0 8		6 0 9		6 1 0		6 1 1		6 1 2		6 1 3		6 1 4		6 1 5		6 1 6		6 1 7		6 1 8		6 1 9		6 2 0		6 2 1		6 2 2		6 2 3		6 2 4		6 2 5		6 2 6		6 2 7		6 2 8		6 2 9		6 3 0		6 3 1		6 3 2		6 3 3		6 3 4		6 3 5		6 3 6		6 3 7		6 3 8		6 3 9		6 4 0		6 4 1		6 4 2		6 4 3		6 4 4		6 4 5		6 4 6		6 4 7		6 4 8		6 4 9		6 5 0		6 5 1		6 5 2		6 5 3		6 5 4		6 5 5		6 5 6		6 5 7		6 5 8		6 5 9		6 6 0		6 6 1		6 6 2		6 6 3		6 6 4		6 6 5		6 6 6		6 6 7		6 6 8		6 6 9		6 7 0		6 7 1		6 7 2		6 7 3		6 7 4		6 7 5		6 7 6		6 7 7		6 7 8		6 7 9		6 8 0		6 8 1		6 8 2		6 8 3		6 8 4		6 8 5		6 8 6		6 8 7		6 8 8		6 8 9		6 9 0		6 9 1		6 9 2		6 9 3		6 9 4		6 9 5		6 9 6		6 9 7		6 9 8		6 9 9		7 0 0		7 0 1		7 0 2		7 0 3		7 0 4		7 0 5		7 0 6		7 0 7		7 0 8		7 0 9		7 1 0		7 1 1		7 1 2		7 1 3		7 1 4		7 1 5		7 1 6		7 1 7		7 1 8		7 1 9		7 2 0		7 2 1		7 2 2		7 2 3		7 2 4		7 2 5		7 2 6		7 2 7		7 2 8		7 2 9		7 3 0		7 3 1		7 3 2		7 3 3		7 3 4		7 3 5		7 3 6		7 3 7		7 3 8		7 3 9		7 4 0		7 4 1		7 4 2		7 4 3		7 4 4		7 4 5		7 4 6		7 4 7		7 4 8		7 4 9		7 5 0		7 5 1		7 5 2		7 5 3		7 5 4		7 5 5		7 5 6		7 5 7		7 5 8		7 5 9		7 6 0		7 6 1		7 6 2		7 6 3		7 6 4		7 6 5		7 6 6		7 6 7		7 6 8		7 6 9		7 7 0		7 7 1		7 7 2		7 7 3		7 7 4		7 7 5		7 7 6		7 7 7		7 7 8		7 7 9		7 8 0		7 8 1		7 8 2		7 8 3		7 8 4		7 8 5		7 8 6		7 8 7		7 8 8		7 8 9		7 9 0		7 9 1		7 9 2		7 9 3		7 9 4		7 9 5		7 9 6		7 9 7		7 9 8		7 9 9		8 0 0		8 0 1		8 0 2		8 0 3		8 0 4		8 0 5		8 0 6		8 0 7		8 0 8		8 0 9		8 1 0		8 1 1		8 1 2		8 1 3		8 1 4		8 1 5		8 1 6		8 1 7		8 1 8		8 1 9		8 2 0		8 2 1		8 2 2		8 2 3		8 2 4		8 2 5		8 2 6		8 2 7		8 2 8		8 2 9		8 3 0		8 3 1		8 3 2		8 3 3		8 3 4		8 3 5		8 3 6		8 3 7		8 3 8		8 3 9		8 4 0		8 4 1		8 4 2		8 4 3		8 4 4		8 4 5		8 4 6		8 4 7		8 4 8		8 4 9		8 5 0		8 5 1		8 5 2		8 5 3		8 5 4		8 5 5		8 5 6		8 5 7		8 5 8		8 5 9		8 6 0		8 6 1		8 6 2		8 6 3		8 6 4		8 6 5		8 6 6		8 6 7		8 6 8		8 6 9		8 7 0		8 7 1		8 7 2		8 7 3		8 7 4		8 7 5		8 7 6		8 7 7		8 7 8		8 7 9		8 8 0		8 8 1		8 8 2		8 8 3		8 8 4		8 8 5		8 8 6		8 8 7		8 8 8		8 8 9		8 9 0		8 9 1		8 9 2		8 9 3		8 9 4		8 9 5		8 9 6		8 9 7		8 9 8		8 9 9		9 0 0		9 0 1		9 0 2		9 0 3		9 0 4		9 0 5		9 0 6		9 0 7		9 0 8		9 0 9		9 1 0		9 1 1		9 1 2		9 1 3		9 1 4		9 1 5		9 1 6		9 1 7		9 1 8		9 1 9		9 2 0		9 2 1		9 2 2		9 2 3		9 2 4		9 2 5		9 2 6		9 2 7		9 2 8		9 2 9		9 3 0		9 3 1		9 3 2		9 3 3		9 3 4		9 3 5		9 3 6		9 3 7		9 3 8		9 3 9		9 4 0		9 4 1		9 4 2		9 4 3		9 4 4		9 4 5		9 4 6		9 4 7		9 4 8		9 4 9		9 5 0		9 5 1		9 5 2		9 5 3		9 5 4		9 5 5		9 5 6		9 5 7		9 5 8		9 5 9		9 6 0		9 6 1		9 6 2		9 6 3		9 6 4		9 6 5		9 6 6		9 6 7		9 6 8		9 6 9		9 7 0		9 7 1		9 7 2		9 7 3		9 7 4		9 7 5		9 7 6		9 7 7		9 7 8		9 7 9		9 8 0		9 8 1		9 8 2		9 8 3		9 8 4		9 8 5		9 8 6		9 8 7		9 8 8		9 8 9		9 9 0		9 9 1		9 9 2		9 9 3		9 9 4		9 9 5		9 9 6		9 9 7		9 9 8		9 9 9		1 0 0 0	
---------------	--	-------	--	-------	--	-------	--	-------	--	-------	--	-------	--	-------	--	-------	--	-------	--	-------	--	-------	--	-------	--	-------	--	-------	--	-------	--	-------	--	-------	--	-------	--	-------	--	-------	--	-------	--	-------	--	-------	--	-------	--	-------	--	-------	--	-------	--	-------	--	-------	--	-------	--	-------	--	-------	--	-------	--	-------	--	-------	--	-------	--	-------	--	-------	--	-------	--	-------	--	-------	--	-------	--	-------	--	-------	--	-------	--	-------	--	-------	--	-------	--	-------	--	-------	--	-------	--	-------	--	-------	--	-------	--	-------	--	-------	--	-------	--	-------	--	-------	--	-------	--	-------	--	-------	--	-------	--	-------	--	-------	--	-------	--	-------	--	-------	--	-------	--	-------	--	-------	--	-------	--	-------	--	-------	--	-------	--	-------	--	-------	--	-------	--	-------	--	-------	--	-------	--	-------	--	-------	--	-------	--	-------	--	-------	--	-------	--	-------	--	-------	--	-------	--	-------	--	-------	--	-------	--	-------	--	-------	--	-------	--	-------	--	-------	--	-------	--	-------	--	-------	--	-------	--	-------	--	-------	--	-------	--	-------	--	-------	--	-------	--	-------	--	-------	--	-------	--	-------	--	-------	--	-------	--	-------	--	-------	--	-------	--	-------	--	-------	--	-------	--	-------	--	-------	--	-------	--	-------	--	-------	--	-------	--	-------	--	-------	--	-------	--	-------	--	-------	--	-------	--	-------	--	-------	--	-------	--	-------	--	-------	--	-------	--	-------	--	-------	--	-------	--	-------	--	-------	--	-------	--	-------	--	-------	--	-------	--	-------	--	-------	--	-------	--	-------	--	-------	--	-------	--	-------	--	-------	--	-------	--	-------	--	-------	--	-------	--	-------	--	-------	--	-------	--	-------	--	-------	--	-------	--	-------	--	-------	--	-------	--	-------	--	-------	--	-------	--	-------	--	-------	--	-------	--	-------	--	-------	--	-------	--	-------	--	-------	--	-------	--	-------	--	-------	--	-------	--	-------	--	-------	--	-------	--	-------	--	-------	--	-------	--	-------	--	-------	--	-------	--	-------	--	-------	--	-------	--	-------	--	-------	--	-------	--	-------	--	-------	--	-------	--	-------	--	-------	--	-------	--	-------	--	-------	--	-------	--	-------	--	-------	--	-------	--	-------	--	-------	--	-------	--	-------	--	-------	--	-------	--	-------	--	-------	--	-------	--	-------	--	-------	--	-------	--	-------	--	-------	--	-------	--	-------	--	-------	--	-------	--	-------	--	-------	--	-------	--	-------	--	-------	--	-------	--	-------	--	-------	--	-------	--	-------	--	-------	--	-------	--	-------	--	-------	--	-------	--	-------	--	-------	--	-------	--	-------	--	-------	--	-------	--	-------	--	-------	--	-------	--	-------	--	-------	--	-------	--	-------	--	-------	--	-------	--	-------	--	-------	--	-------	--	-------	--	-------	--	-------	--	-------	--	-------	--	-------	--	-------	--	-------	--	-------	--	-------	--	-------	--	-------	--	-------	--	-------	--	-------	--	-------	--	-------	--	-------	--	-------	--	-------	--	-------	--	-------	--	-------	--	-------	--	-------	--	-------	--	-------	--	-------	--	-------	--	-------	--	-------	--	-------	--	-------	--	-------	--	-------	--	-------	--	-------	--	-------	--	-------	--	-------	--	-------	--	-------	--	-------	--	-------	--	-------	--	-------	--	-------	--	-------	--	-------	--	-------	--	-------	--	-------	--	-------	--	-------	--	-------	--	-------	--	-------	--	-------	--	-------	--	-------	--	-------	--	-------	--	-------	--	-------	--	-------	--	-------	--	-------	--	-------	--	-------	--	-------	--	-------	--	-------	--	-------	--	-------	--	-------	--	-------	--	-------	--	-------	--	-------	--	-------	--	-------	--	-------	--	-------	--	-------	--	-------	--	-------	--	-------	--	-------	--	-------	--	-------	--	-------	--	-------	--	-------	--	-------	--	-------	--	-------	--	-------	--	-------	--	-------	--	-------	--	-------	--	-------	--	-------	--	-------	--	-------	--	-------	--	-------	--	-------	--	-------	--	-------	--	-------	--	-------	--	-------	--	-------	--	-------	--	-------	--	-------	--	-------	--	-------	--	-------	--	-------	--	-------	--	-------	--	-------	--	-------	--	-------	--	-------	--	-------	--	-------	--	-------	--	-------	--	-------	--	-------	--	-------	--	-------	--	-------	--	-------	--	-------	--	-------	--	-------	--	-------	--	-------	--	-------	--	-------	--	-------	--	-------	--	-------	--	-------	--	-------	--	-------	--	-------	--	-------	--	-------	--	-------	--	-------	--	-------	--	-------	--	-------	--	-------	--	-------	--	-------	--	-------	--	-------	--	-------	--	-------	--	-------	--	-------	--	-------	--	-------	--	-------	--	-------	--	-------	--	-------	--	-------	--	-------	--	-------	--	-------	--	-------	--	-------	--	-------	--	-------	--	-------	--	-------	--	-------	--	-------	--	-------	--	-------	--	-------	--	-------	--	-------	--	-------	--	-------	--	-------	--	-------	--	-------	--	-------	--	-------	--	-------	--	-------	--	-------	--	-------	--	-------	--	-------	--	-------	--	-------	--	-------	--	-------	--	-------	--	-------	--	-------	--	-------	--	-------	--	-------	--	-------	--	-------	--	-------	--	-------	--	-------	--	-------	--	-------	--	-------	--	-------	--	-------	--	-------	--	-------	--	-------	--	-------	--	-------	--	-------	--	-------	--	-------	--	-------	--	-------	--	-------	--	-------	--	-------	--	-------	--	-------	--	-------	--	-------	--	-------	--	-------	--	-------	--	-------	--	-------	--	-------	--	-------	--	-------	--	-------	--	-------	--	-------	--	-------	--	-------	--	-------	--	-------	--	-------	--	-------	--	-------	--	-------	--	-------	--	-------	--	-------	--	-------	--	-------	--	-------	--	-------	--	-------	--	-------	--	-------	--	-------	--	-------	--	-------	--	-------	--	-------	--	-------	--	-------	--	-------	--	-------	--	-------	--	-------	--	-------	--	-------	--	-------	--	-------	--	-------	--	-------	--	-------	--	-------	--	-------	--	-------	--	-------	--	-------	--	-------	--	-------	--	-------	--	-------	--	-------	--	-------	--	-------	--	-------	--	-------	--	-------	--	-------	--	-------	--	-------	--	-------	--	-------	--	-------	--	-------	--	-------	--	-------	--	-------	--	-------	--	-------	--	-------	--	-------	--	-------	--	-------	--	-------	--	-------	--	-------	--	-------	--	-------	--	-------	--	-------	--	-------	--	-------	--	-------	--	-------	--	-------	--	-------	--	-------	--	-------	--	-------	--	-------	--	-------	--	-------	--	-------	--	-------	--	-------	--	-------	--	-------	--	-------	--	-------	--	-------	--	-------	--	-------	--	-------	--	-------	--	-------	--	-------	--	-------	--	-------	--	-------	--	-------	--	-------	--	-------	--	-------	--	-------	--	-------	--	-------	--	-------	--	-------	--	-------	--	-------	--	-------	--	-------	--	-------	--	-------	--	-------	--	-------	--	-------	--	-------	--	-------	--	-------	--	-------	--	-------	--	-------	--	-------	--	-------	--	-------	--	-------	--	-------	--	-------	--	-------	--	-------	--	-------	--	-------	--	-------	--	-------	--	-------	--	-------	--	-------	--	-------	--	-------	--	-------	--	-------	--	-------	--	-------	--	-------	--	-------	--	-------	--	-------	--	-------	--	-------	--	-------	--	-------	--	-------	--	-------	--	-------	--	-------	--	-------	--	-------	--	-------	--	-------	--	-------	--	-------	--	-------	--	-------	--	-------	--	-------	--	-------	--	-------	--	-------	--	-------	--	-------	--	-------	--	-------	--	-------	--	-------	--	-------	--	-------	--	-------	--	-------	--	-------	--	-------	--	-------	--	-------	--	-------	--	-------	--	-------	--	-------	--	-------	--	-------	--	-------	--	-------	--	-------	--	-------	--	-------	--	-------	--	-------	--	-------	--	-------	--	-------	--	-------	--	-------	--	-------	--	-------	--	-------	--	-------	--	-------	--	-------	--	-------	--	-------	--	-------	--	-------	--	-------	--	-------	--	-------	--	-------	--	-------	--	-------	--	-------	--	-------	--	-------	--	-------	--	-------	--	-------	--	-------	--	-------	--	-------	--	-------	--	-------	--	-------	--	-------	--	-------	--	-------	--	-------	--	-------	--	-------	--	-------	--	-------	--	-------	--	-------	--	-------	--	-------	--	-------	--	-------	--	-------	--	-------	--	-------	--	-------	--	-------	--	-------	--	-------	--	-------	--	-------	--	-------	--	-------	--	-------	--	-------	--	-------	--	-------	--	-------	--	-------	--	-------	--	-------	--	-------	--	-------	--	-------	--	-------	--	-------	--	-------	--	-------	--	-------	--	-------	--	-------	--	-------	--	-------	--	-------	--	-------	--	-------	--	-------	--	-------	--	-------	--	-------	--	-------	--	-------	--	-------	--	-------	--	-------	--	-------	--	-------	--	-------	--	-------	--	-------	--	-------	--	-------	--	-------	--	-------	--	-------	--	-------	--	-------	--	-------	--	-------	--	-------	--	-------	--	-------	--	-------	--	-------	--	-------	--	-------	--	-------	--	-------	--	-------	--	-------	--	-------	--	-------	--	-------	--	-------	--	-------	--	-------	--	-------	--	-------	--	-------	--	-------	--	-------	--	-------	--	-------	--	-------	--	-------	--	-------	--	-------	--	-------	--	-------	--	-------	--	-------	--	-------	--	-------	--	-------	--	-------	--	-------	--	-------	--	-------	--	-------	--	-------	--	-------	--	-------	--	-------	--	-------	--	-------	--	-------	--	-------	--	-------	--	-------	--	-------	--	-------	--	-------	--	-------	--	-------	--	-------	--	-------	--	-------	--	-------	--	-------	--	-------	--	-------	--	-------	--	-------	--	-------	--	-------	--	-------	--	-------	--	-------	--	-------	--	-------	--	-------	--	---------	--

G-4

ALOC JNA 0003									
TEST IDENT 501-0000512-5									
TEST STATION A02 DATE 12-08-60 TIME 1200 EST-052									
TEST IDENT 501-0000512-5									
FUNCTION	DEC F	TS-0000	TL	TL/2	TS-0000/2	TS-170	TS-170/2	TS-270	TS-270/2
UNITS	DEC F	DEC F	DEC F	DEC F	DEC F	DEC F	DEC F	DEC F	DEC F
CHN NO	170	170	170	170	170	170	170	170	170
LAS TIME	0000	0000	0000	0000	0000	0000	0000	0000	0000
1-0039	77.10	77.10	65.72	65.72	65.72	65.72	65.72	65.72	65.72
2-0039	79.06	79.06	65.72	65.72	65.72	65.72	65.72	65.72	65.72
3-0039	81.03	81.03	65.72	65.72	65.72	65.72	65.72	65.72	65.72
4-0039	83.00	83.00	65.72	65.72	65.72	65.72	65.72	65.72	65.72
5-0039	85.00	85.00	65.72	65.72	65.72	65.72	65.72	65.72	65.72
6-0039	87.00	87.00	65.72	65.72	65.72	65.72	65.72	65.72	65.72
7-0039	89.00	89.00	65.72	65.72	65.72	65.72	65.72	65.72	65.72
8-0039	91.00	91.00	65.72	65.72	65.72	65.72	65.72	65.72	65.72
9-0039	93.00	93.00	65.72	65.72	65.72	65.72	65.72	65.72	65.72
10-0039	95.00	95.00	65.72	65.72	65.72	65.72	65.72	65.72	65.72
11-0039	97.00	97.00	65.72	65.72	65.72	65.72	65.72	65.72	65.72
12-0039	99.00	99.00	65.72	65.72	65.72	65.72	65.72	65.72	65.72
13-0039	101.00	101.00	65.72	65.72	65.72	65.72	65.72	65.72	65.72
14-0039	103.00	103.00	65.72	65.72	65.72	65.72	65.72	65.72	65.72
15-0039	105.00	105.00	65.72	65.72	65.72	65.72	65.72	65.72	65.72
16-0039	107.00	107.00	65.72	65.72	65.72	65.72	65.72	65.72	65.72
17-0039	109.00	109.00	65.72	65.72	65.72	65.72	65.72	65.72	65.72
18-0039	111.00	111.00	65.72	65.72	65.72	65.72	65.72	65.72	65.72
19-0039	113.00	113.00	65.72	65.72	65.72	65.72	65.72	65.72	65.72
20-0039	115.00	115.00	65.72	65.72	65.72	65.72	65.72	65.72	65.72
21-0039	117.00	117.00	65.72	65.72	65.72	65.72	65.72	65.72	65.72
22-0039	119.00	119.00	65.72	65.72	65.72	65.72	65.72	65.72	65.72
23-0039	121.00	121.00	65.72	65.72	65.72	65.72	65.72	65.72	65.72
24-0039	123.00	123.00	65.72	65.72	65.72	65.72	65.72	65.72	65.72
25-0039	125.00	125.00	65.72	65.72	65.72	65.72	65.72	65.72	65.72
26-0039	127.00	127.00	65.72	65.72	65.72	65.72	65.72	65.72	65.72
27-0039	129.00	129.00	65.72	65.72	65.72	65.72	65.72	65.72	65.72
28-0039	131.00	131.00	65.72	65.72	65.72	65.72	65.72	65.72	65.72
29-0039	133.00	133.00	65.72	65.72	65.72	65.72	65.72	65.72	65.72
30-0039	135.00	135.00	65.72	65.72	65.72	65.72	65.72	65.72	65.72

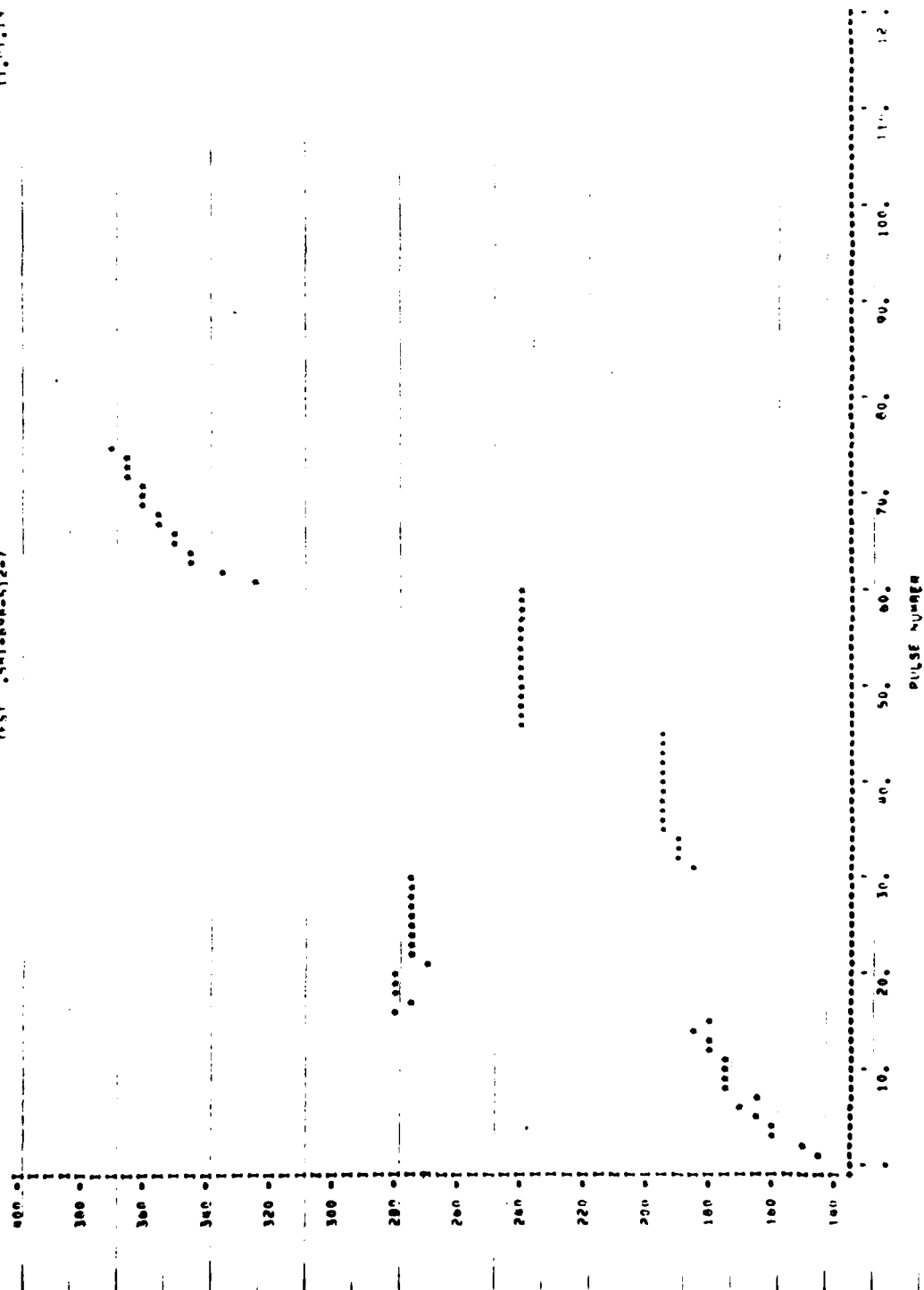
02-10-60 00:37:36

10. 175
02-10000
11. 1.15

172 LR PULSES ENGINE PERFORMANCE

TEST 541-000-512-7

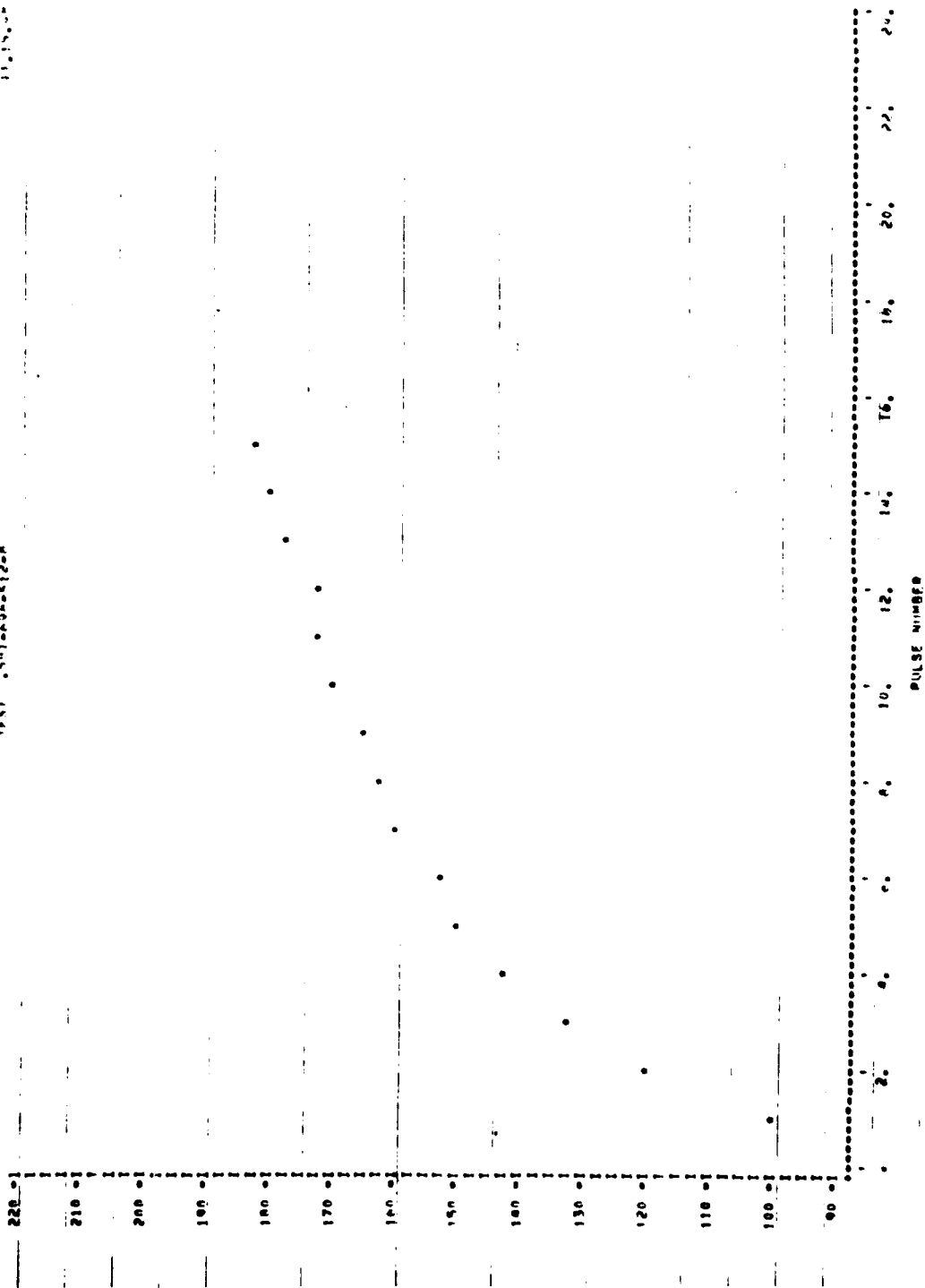
19-27022 DFC 8



100 175
100 175
100 175

1 2 3 4 5 6 7 8 9 10 11 12 13 14 15 16 17 18 19 20 21 22 23 24
1957 AUGUST 28

15-270/2 DEC 5



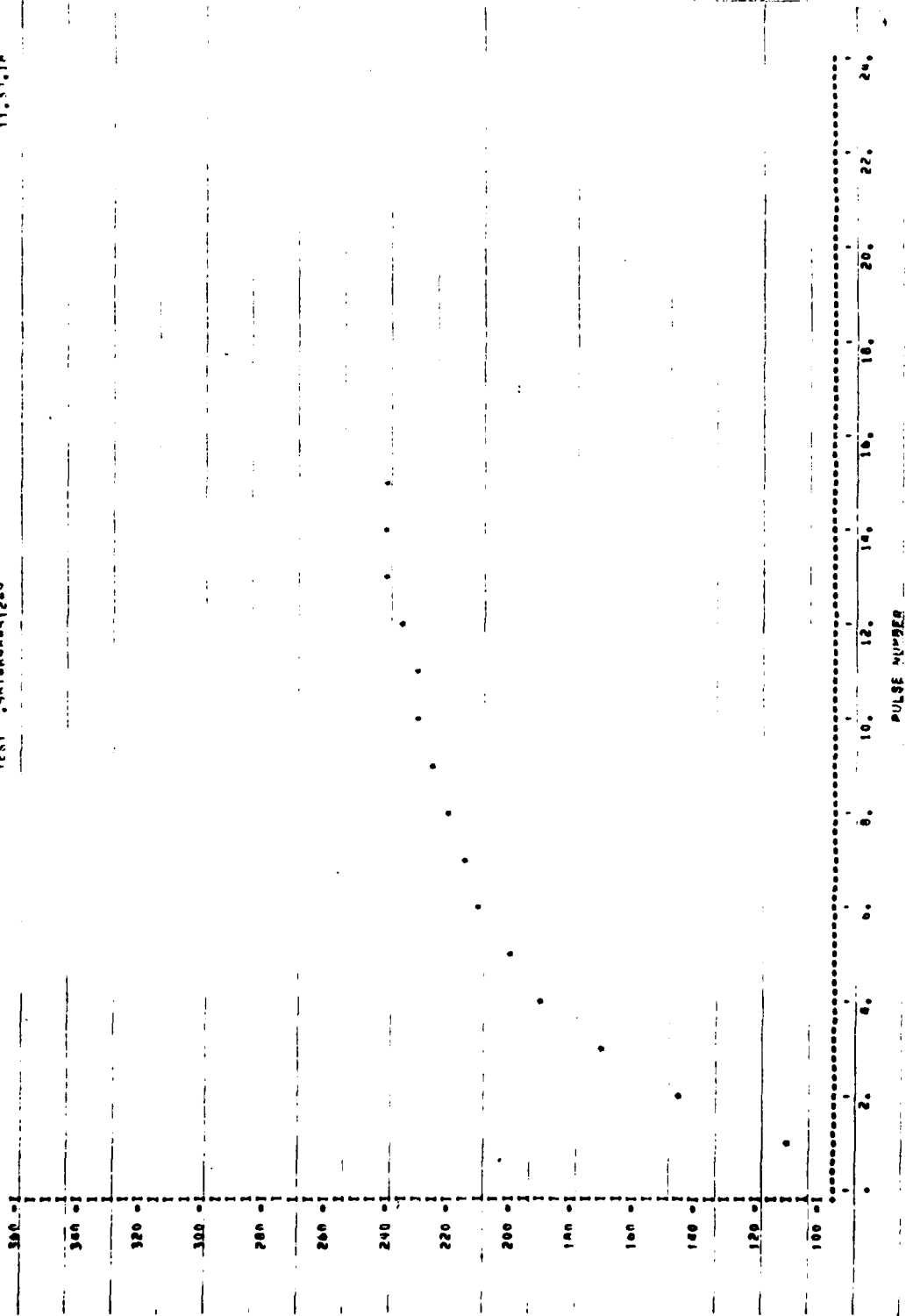
ALBC JNR 0003									
TEST INSTR .531-0000-51200									
TEST STATION 100 DATE 02-11-68 TIME 1200 PSI-FSP									
FUNCTION TL 71/2 TS-000 TS-000/2 TS-170 TS-210 TS-270/2									
UNITS DEG F DEG F DEG F DEG F DEG F DEG F DEG F DEG F DEG F									
CHAN NO 170 171 172 173 174 175 176 177 178									
LAG TIME .0000 .0000 .0000 .0000 .0000 .0000 .0000 .0000 .0000									
1.0030	125.72	125.72	125.72	125.72	125.72	125.72	125.72	125.72	125.72
2.0030	125.72	125.72	125.72	125.72	125.72	125.72	125.72	125.72	125.72
3.0030	125.72	125.72	125.72	125.72	125.72	125.72	125.72	125.72	125.72
4.0030	125.72	125.72	125.72	125.72	125.72	125.72	125.72	125.72	125.72
5.0030	125.72	125.72	125.72	125.72	125.72	125.72	125.72	125.72	125.72
6.0030	125.72	125.72	125.72	125.72	125.72	125.72	125.72	125.72	125.72
7.0030	125.72	125.72	125.72	125.72	125.72	125.72	125.72	125.72	125.72
8.0030	125.72	125.72	125.72	125.72	125.72	125.72	125.72	125.72	125.72
9.0030	125.72	125.72	125.72	125.72	125.72	125.72	125.72	125.72	125.72
10.0030	125.72	125.72	125.72	125.72	125.72	125.72	125.72	125.72	125.72
11.0030	125.72	125.72	125.72	125.72	125.72	125.72	125.72	125.72	125.72
12.0030	125.72	125.72	125.72	125.72	125.72	125.72	125.72	125.72	125.72
13.0030	125.72	125.72	125.72	125.72	125.72	125.72	125.72	125.72	125.72
14.0030	125.72	125.72	125.72	125.72	125.72	125.72	125.72	125.72	125.72
15.0030	125.72	125.72	125.72	125.72	125.72	125.72	125.72	125.72	125.72

100-1173
(2-1-60)
11, 5, 18

1/2 IN PULSE PULSING PERFORMANCE

TEST 5M1-000-512-0

15-27072 DEC F



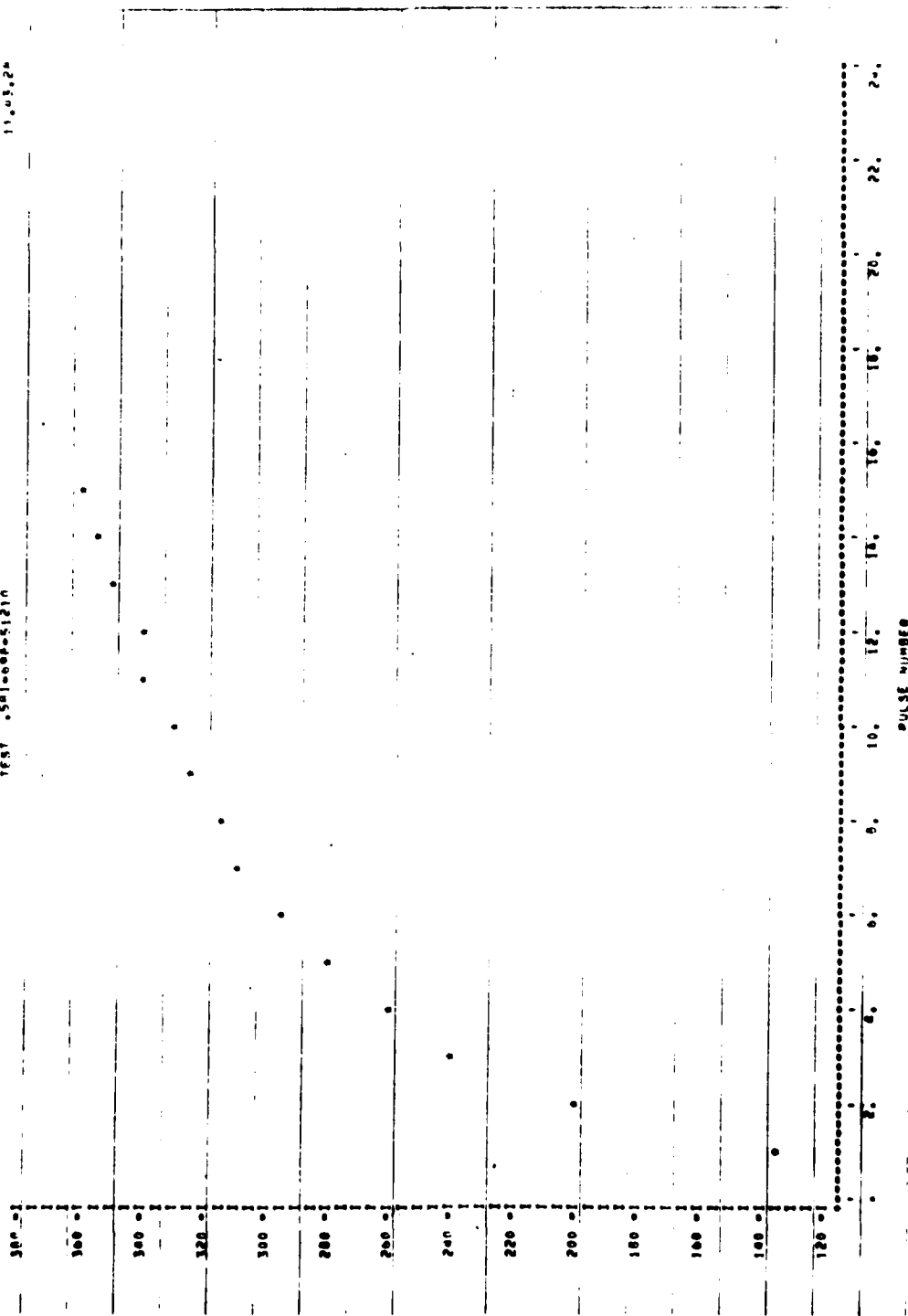
PULSE NUMBER

10-11A
10-11B
10-11C

1/2 IN PULSE ENGINE PERFORMANCE

TEST 501-000-51210

10-27022 DEC 1



100 175
250000
11,500

172 IN 0158 ENGINE PERFORMANCE
TEST 541000-51211

78-270-2 REC 1

